PLIO-QUATERNARY SEDIMENTATION AND GEOMORPHOLOGY WITHIN AN ACTIVE FORE-ARC: MESSENIA AND EASTERN LAKONIA PENINSULAE, SOUTHERN PELOPONNESE, GREECE

NIKOLAOS KOURAMPAS

Thesis submitted for the degree of Doctor of Philosophy, University of Edinburgh

EDINBURGH 2001

ABSTRACT

This work focuses on the sedimentation and geomorphology of the Messenia and Eastern Lakonia Peninsulae (S Peloponnese, Greece) during the Pliocene-Quaternary (last ca. 5 Ma). Shallow-marine and subaerial sediments and landforms are described and interpreted in terms of tectonic and sea level controls. The S Peloponnese underwent regional uplift since the Middle Miocene. Normal faulting in directions parallel and transverse to the Aegean Arc led to the formation of horsts and grabens, on scales varying from <1 to >20 km. Sea level cyclicity resulted in deposition of shallow-marine to subaerial sequences separated by unconformities. Changing climatic conditions since the Middle-Late Miocene influenced subaerial erosion and sedimentation and also the facies/fauna of marine and marginal marine deposits. Pliocene-Quaternary landforms and sediments in the two areas studied reflect the interplay between the above controls.

In both the Messenia and Eastern Lakonia Peninsulae, Late Tertiary surfaces of subaerial erosion and Quaternary marine sediments and terraces are present at progressively lower altitudes with decreasing age as a result of uplift and forced regression. Maximum numbers of terraces are present in fault-bounded areas of maximum Quaternary uplift, in the NW parts of each peninsula, where uplift rate since the early Pleistocene (last ca.1 Ma) was 0.08-0.35 m/ka.

Pliocene (only in the Messenia Peninsula) and Quaternary shallow-marine sediments (in both Peninsulae) are subdivided into informal units, correlated with 3rd or higher-order sea level cycles. The Pleistocene part of the stratigraphy, present in both Peninsulae, is resolved into two 3rd order sequences, of early and middle-late Pleistocene age, respectively. The middle-late Pleistocene sequence is further divided into middle Pleistocene, Eutyrrhenian and Neotyrrhenian units, correlated with higher order late Pleistocene sea level cycles.

Shallowing-up units (sequences/parasequences) were deposited during sea level highstands and the early stages of sea level fall. Shallow-marine sequences exhibit a progradational architecture, with transition from offshore-lower shoreface to foreshore-backshore facies up-section, coupled with diagenetic evidence for transition from submarine to suaberial conditions. Lithological types include detrital and bioconstructed carbonates and mixed carbonate-siliciclastic facies. Facies within each sequence were also influenced by the palaeogeography of each site, largely fault controlled. These units are separated by unconformities/disconformities correlated with sea level fall and lowstands. Valley incision, alluvial fan deposition and caliche formation also took place during periods of low relative sea level. Alluvial fan progradation was markedly more extensive within the Eastern Lakonia Peninsula, reflecting more closely spaced fault pattern.

The Plio-Quaternary stratigraphy of the Messenia and the Eastern Lakonia Peninsulae can be correlated with other areas within the Aegean fore-arc (e.g. Crete, Rhodes), Cyprus and Sicily, and also with the back-arc Corinth-Patras graben. Despite local differences in the timing of the Late Pliocene-Quaternary forced regression, a similar number of shallow-marine to terrestrial sequences are present within all these areas, demonstrating that short-term sea level cyclicity, combined with long-term regional uplift, were the principal controls on Plio-Quaternary deposition.

ACKNOWLEDGEMENTS

This thesis would have never been completed without the help of so many people, both in Edinburgh and elsewhere. I am grateful to Alastair Robertson, for his supervision both in the field and in Edinburgh, his correction of draft after draft, his suggestions for numerous improvements and his gentle supervisory approach. John Dixon, my second supervisor, contributed very useful comments on earlier versions of some chapters. John Miller was interested and encouraging throughout; his advice on petrological techniques and sedimentary environments is gratefully acknowledged. Khalil Al Riyami has been a close friend and flatmate and also a colleague with whom I had numerous stimulating discussions. Timur Ustaömer, Sukru Ersoy (both in Istanbul) and Erhan Akay (Izmir) offered me both their friendship and advise, same as Taniel Danelian (now in Paris), Noah Jaffey, Anna Augusti and Erika Angerer. I am grateful to Peder Aspen and Ian Parsons for their help with the microscopic photographs. The staff in the *Image Processing Centre* (JCMB) were extremely helpful with the preparation of some images. I am particularly indebted to Dimitris Frydas and Stella Tsaila-Monopolis (both in Patras), who agreed to identify nannoplankton and foraminifera, respectively and also offered invaluable practical help, hospitality and support during my time in their department. Theodoros Doutsos, Leonidas Stamatopoulos and Abraham Zelilidis (also in Patras) showed keen interest in my project, discussed the neotectonics and sediments of the area and guided me through the Greek literature. It goes without saying that I am solely responsible for any omissions and mistakes.

Work for this thesis was supported by the Greek Institute of State Scholarships (I.K.Y.) (grant no. 95104/88: *Geodynamic Evolution during the Quaternary*). Yiorgos Migiros (Athens) contributed suggestions and ideas for the formulation of the project.

I am indebted to people I met during the fieldwork in Greece and whose generosity, kindness and sense of humour made my time there deeply enjoyable: Babis in Martahopolis, the Koilakos family in Marathia, the German travellers near Finikounta, the people in the *Gykovrisi Camping* and many others. Eleni Tsirogoti made my stay in Eastern Lakonia really memorable. I am grateful to Vasilis Panayiotou for his company in the field during the summer of 1998. His efforts to raise my political awareness and cultivate my literary taste under the scorching July sun were remarkable, albeit fruitless. Christina Souyoultzi, Panayis Travlos, Vangelis Panayiotou, and Maria Gartzonika always made me welcome and allowed me to catch up with their lives after long periods of absence.

My debt to Penny Travlou is inestimable; I cannot thank her enough for her patience, understanding and generosity during some bitter times and for her influence, inspiration and challenge. Selen Etingü, with her unique way of looking at things, helped me much more than she realised; her friendship changed me deeply. Gregoris Gregoriadis, Nadja Kanelopeoulou, Spiros Livas, Vangelis Makrigiannakis, Clare Middleton, Maria Priovolou, Tania and Rachel Stuart and Hristos Zographos have been the nicest friends I could aspire to have. The warmth of their company has kept me going. I am particularly grateful to Nadja and Hristos for their help with printing and photocopying this thesis. My friends and flatmates Barbara Buckinx and Çahit Oz have been extremely supportive and understanding during the (long) final stages of this work. My family, Kleopatra Chronaki and Lambros and Ilias Kourampas, are deeply thanked for being who they are, for all the support they provided and for bearing the strain of our separation with magnanimity.

CONTENTS

LIST OF FIGURES

CHAPTER 3 **Page**

CHAPTER 4 **Page**

CHAPTER 5 **Page**

CHAPTER 6 **Page**

CHAPTER 7 **Page**

CHAPTER 8 **Page**

LIST OF TABLES

CHAPTER 1: THE QUATERNARY OF THE SOUTHERN PELOPONNESE

1.1 INTRODUCTION

This study focuses on the sedimentary and tectonic evolution of the Messenia and Eastern Lakonia Peninsulae (Southern Peloponnese, Greece) during the Pliocene-Quaternary (last ca. 5 Ma). These two areas (Figs. 1.1, 1.2) were selected for the following reasons:

1) They are situated within a critical tectonic setting of the Aegean fore-arc, just behind the western (Ionian) sector of the Hellenic Trench, where active subduction of Mediterranean oceanic crust beneath the Aegean Arc (Eurasian margin) takes place (McKenzie, 1978; Le Pichon and Angelier, 1979; Jacobshagen et al., 1978; Robertson et al., 1995; see Figs. 1.1, 1.2). A SW-NE oriented transect, perpendicular to the strike of Messenia and Eastern Lakonia Peninsulae, allows comparison between an "external", near-trench setting, that of the Messenia Peninsula, and an "internal" setting, that of the Eastern Lakonia, closer to the back-arc Aegean Sea (Fig. 1.1). The southern Peloponnese is the only area of the Aegean Arc that allows onland observations to be made along transects perpendicular to the arc, of length greater than 100 km.

2) The areas of study can be compared with other, well documented areas of similar geotectonic setting within the Eastern Mediterranean, e.g. Crete and Rhodes (Meulenkamp et al., 1988; Hanke, 1999) along the Hellenic fore-arc, Cyprus (Poole, 1992; Poole and Robertson, 1991), Calabria and Sicily (Pedley and Grasso, 1993; Buttler et al., 1995; Pedley, 1996a,b) (see Fig. 1.2).

3) The Messenia and Eastern Lakonia Peninsulae, as in the Southern Peloponnese as a whole, exhibit a prominent coastal topography, with evidence of vertical land movements, in the form of uplifted marine terraces and surfaces of subaerial erosion (Keraudren, 1970, 1971; Dufaure, 1977; Kelletat et al., 1977, 1978; Kowalczyk et al., 1992). Various sea level indicators were previously investigated by many researchers of the regional neotectonics (see below).

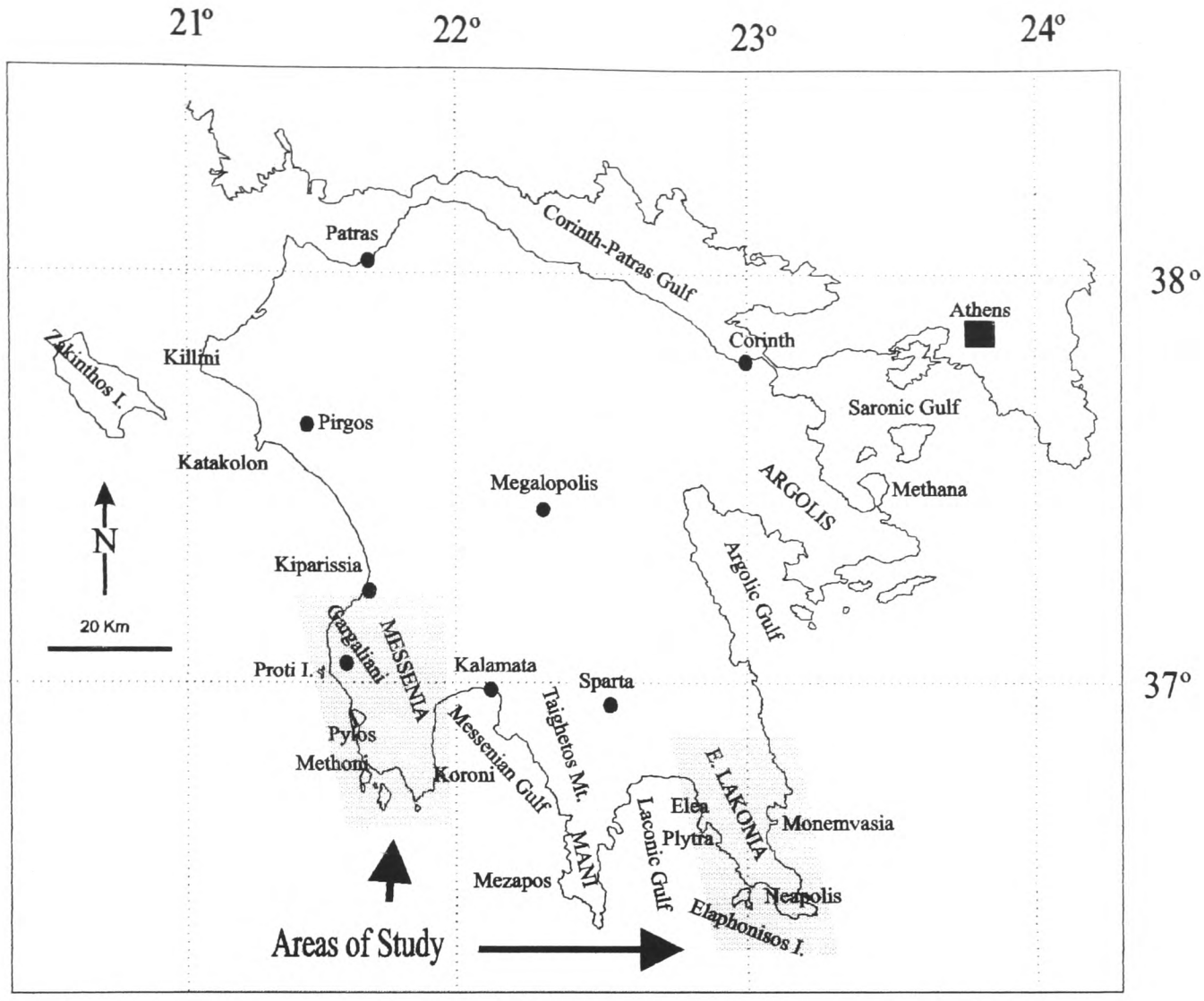

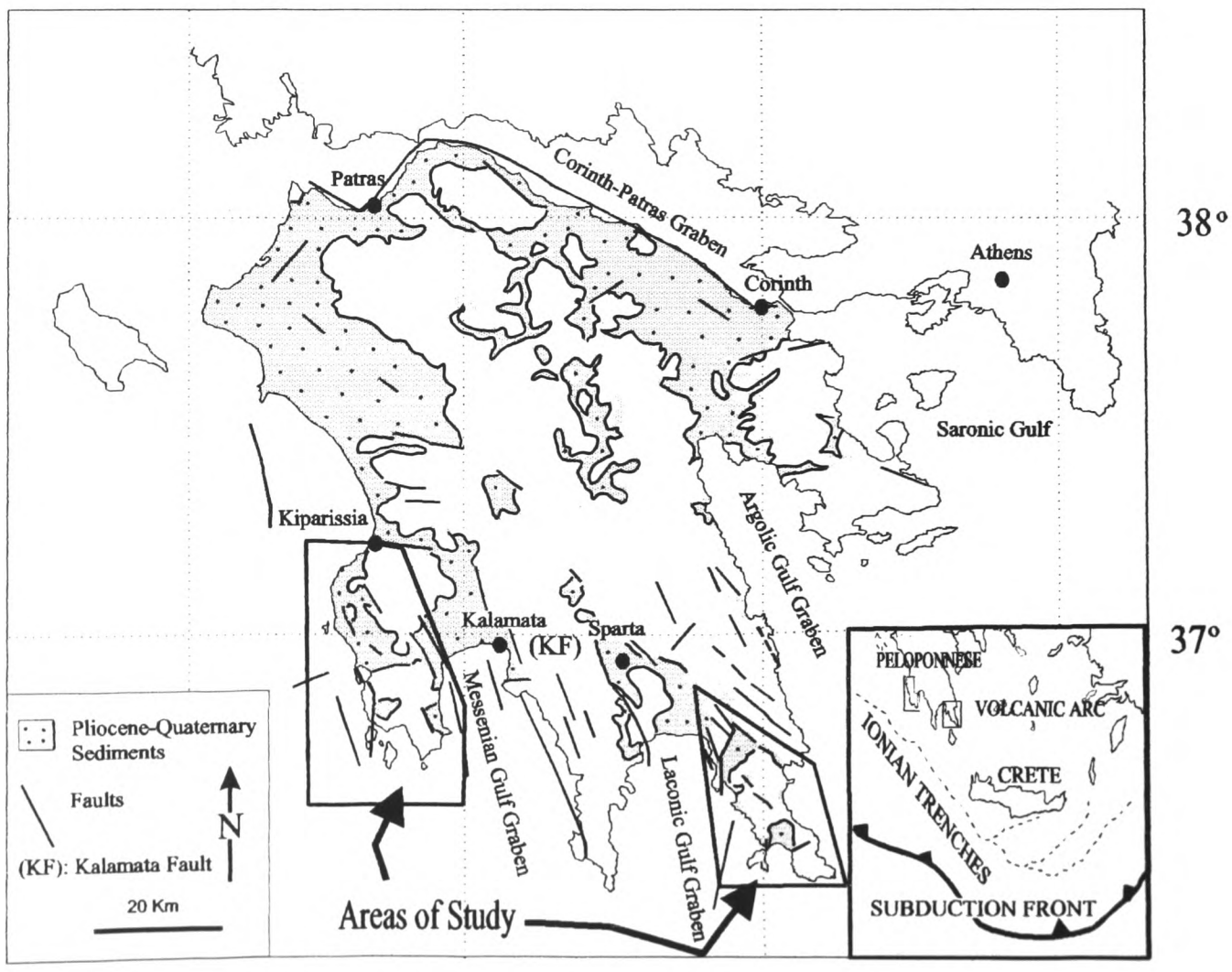

Figure 1.1: The Peloponnese and the areas of study (Messenia and Eastern Lakonia Peninsulae). **a)** Map of main place names referred in the text. **b) Geological map of** the Peloponnese. **Insert:** The Aegean Arc.

1.2 REGIONAL GEOTECTONIC SETTING OF THE AEGEAN ARC

The Peloponnese, a large southward continuation of the Greek mainland, is situated just behind the western sector of the Hellenic Trench, where active subduction of the north-eastward moving Ionian (relative to a stable Aegean) takes place (Figs. 1.1, 1.2). The geodynamic setting of the wider Eastern Mediterranean area is complex, as evidenced by the plethora of proposed models (e.g. McKenzie, 1978; Dewey and Sengör, 1979; Le Pichon and Angelier, 1979; Angelier et al., 1982; Rotstein, 1985; Taymaz et al., 1991). The fundamental physiographic characteristics of the region, that also coincide with the major foci of geodynamic activity, are the following (from the S-SW to the N-NE; Figs. 1.1, 1.2):

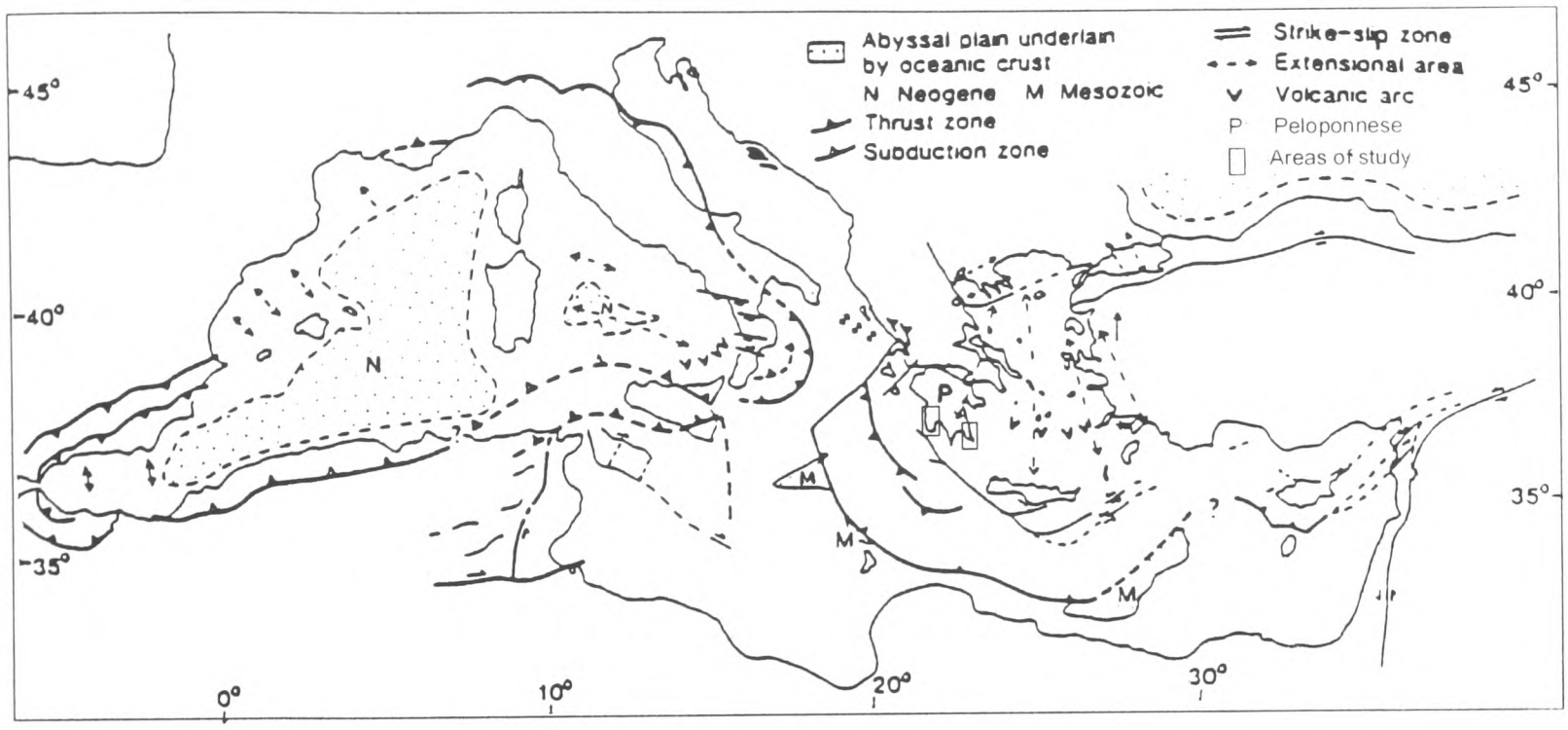

Figure 1.2: Plio-Quaternary geotectonic setting of the Eastern Mediterranean (Robertson and Grasso, 1995).

1.2.1 The Mediterranean Ridge; a swell at the bottom of the Eastern Mediterranean Sea, follows the curvature of the arc and is interpreted as an accretionary wedge (Kastens et al., 1993; Chaumillon and Mascle, 1995; Robertson and Grasso, 1995b), at various stages of collision along different sectors of the active continental margin (Robertson et al., 1995). Deformation style in the Mediterranean Ridge, as revealed by seismic reflection and drilling, is consistent with horizontal compression (Vittori et al., 1981; Mascle et al., 1982; Kastens et al., 1993; Robertson and Grasso, 1995b). This interpretation is also supported by earthquake focal mechanisms in close vicinity of the Mediterranean Ridge (McKenzie, 1978; Rotstein, 1985). The system continues offshore of Cyprus, as an arcuate convergent front (Robertson and Grasso, 1995b; Robertson et al., 1995; Robertson, 1998).

1.2.2 The Hellenic Trench System; a complex set of narrow depressions, that begin offshore of western Peloponnese, with a NNW-SSE to NW-SE strike (Ionian Trough, Matapan Trough) and then bends offshore of western Crete, to split into several, roughly parallel, WSW-ENE troughs offshore of central-eastern Crete (Pliny Trench, Strabo Trench). The bending point that marks the tip of the Aegean Arc is, thus, defined by the ca. 110° angle between the two intersecting trench sectors (Fig. 1.2). This tip of the arc is not merely a geometrical feature, since the inferred geodynamic conditions differ on each side. Thus, while active subduction of Eastern Mediterranean crust and orthogonal shortening of the arc takes place along the eastern, NW-SE striking sector, left-lateral strike-slip movement prevails along the western, ENE-WSW striking sector (McKenzie, 1978; Le Pichon and Angelier, 1979; Mascle et al., 1982; Angelier et al., 1982; Meulenkamp et al., 1988; Armijo et al., 1992; Chaumillon and Mascle, 1995). This was interpeted as resulting from "*side arc collision*" of the subducted slab with the deeper sectors of continental crust (Rotstein, 1985). The Hellenic Trench System continues eastwards offshore of Rhodes, with ENE-WSW strike (Figs. 1.1, 1.2).

1.2.3 The Hellenic Orogenic Arc comprises the most external parts of the Hellenides mountain belt. In mainland Greece and the Peloponnese, the latter follows the '*Dinaric*', NNW-SSE direction as a result of the last stages of the Tethyan orogenesis. Through the Kythera-Antikythera ridge (Lyberis et al., 1982), the Hellenic Orogenic Arc passes into western Crete, where it acquires a roughly E-W strike, followed by a SW-NE strike, passing through the islands of Karpathos and Rhodes to the Turkish mainland (Fig. 1.2). The present strike of the Hellenic Orogenic Arc at its southernmost part (Crete) has resulted from inferred outward (southward) movement of that region ('roll-back'), since the initiation of the Aegean Arc, sometime after the Early Miocene. Estimations of that time vary from ca. 5 Ma (McKenzie, 1978), ca. 13 Ma (Le Pichon and Angelier, 1979; Angelier et al., 1982), to ca. 26 Ma (Meulenkamp et al., 1988). The Hellenic Orogenic Arc is dissected by a fault network directed radially and parallel to its curvature (Mascle et al., 1982; Angelier et al., 1982; Lyberis et al., 1982; Armijo et al., 1992), detected both onland and offshore. This fault fabric is consistent with a pattern of peripheral and radial trajectories of horizontal extension, as deduced by microtectonic analyses (Le Pichon and Angelier, 1979; Angelier et al., 1982) and earthquake focal mechanisms (McKenzie, 1978; Lyon-Caen et al., 1988; Armijo et al., 1992), considerable local discrepancies notwithstanding (Rotstein, 1985). Oblique-slip activity of arc-parallel faults accounts for the shortening of the external part of the arc in perpendicular directions, as, e.g., in the Kythera Strait and, probably, in its 'mirror image', between the Eastern Crete and Rhodes (Lyberis et al., 1982; Armijo et al., 1992; see

Figs. 1.1, 1.2). This style of deformation permitted the outward 'expansion' of Crete since the beginning of the 'neotectonic' geodynamic regime in Middle Miocene-Pliocene (Jacobschagen et al., 1978; Angelier et al., 1982). Many authors attribute the latter process to gravity tectonics, in response to collapse of the Tethyan orogen in the South Aegean region (e.g. Makris, 1978, 1985; Angelier et al., 1982).

1.2.4 The Sea of Crete, further north (Figs, 1.1, 1.2), is the area with the most extented crust in the whole Aegean (Makris, 1978; McKenzie, 1978; Le Pichon and Angelier, 1979; Angelier et al., 1982) and, consequently, with the greatest recorded depths (>1200 m locally). Estimates of the actual amount of stretching depend largely on the particular computational approach (e.g. contrast McKenzie, 1978 with Le Pichon and Angelier, 1979; Angelier et al., 1982).

1.2.5 The Aegean Volcanic Arc, northwards, is a belt of Plio-Quaternary calc-alkaline volcanism (inculding andesite, basalt, rhyolite; Fytikas et al., 1984), and associated geothermal activity, that follows the general curvature of the arc (Figs. 1.1, 1.2). The Aegean volcanic arc starts from Methana Volcano in the Saronic Gulf, then passes through the major volcanic centres of Milos and Santorini (and nine other sites) and becomes difficult to follow east of Nisyros Island.

1.2.6 The back-arc region of the central and northern Aegean Sea and the Greek mainland, further north, also experienced extension during the Late Teriary-Quaternary (Figs. 1.1, 1.2). Many authors argue that this is controlled by the westward movement (and possible rotation; Rotstein, 1985) of Anatolia along the sinistral North Anatolia Fault system (McKenzie, 1978; Dewey and Sengör, 1979; Papazachos, 1991; Taymaz et al., 1991; Meijer, 1995). This movement is interpreted as a response ('escape') triggered from compression along the Zagros collisional zone, further east (Fig. 1.2). The northern Aegean trough system, a complex linear feature of NE-SW strike, together with several similar features in the central Aegean, are interpreted as westward continuations of the North Anatolia Fault system, with a considerable dip-slip component. This interpretation entails that the North Anatolia Fault, instead of maintaining its localised configuration, characteristic of its onland sector in NW Turkey, splits into several branches beneath the northern-central Aegean Sea. The latter interpretation is supported by earthquake focal mechanisms in the vicinity of the northern Aegean trough system (McKenzie, 1978; Jackson et al., 1985; Taymaz et al., 1991). The uncertain continuation of these structures on the Greek mainland, however, remains an unsolved problem of regional neotectonics, directly related to the accommodation of stresses

responsible for horizontal movement. A model by Taymaz et al. (1991) suggests that slabs of brittle upper crust could rotate clockwise and extend in a N-S direction, forced by the westward motion of Turkey. The extension of the Greek mainland, therefore, as well as the overthrusting of the Aegean over the Eastern Mediterranean crust in the Ionian Sea, are interpreted as a result of the westward drift of Anatolia. Alternative interpretations attribute these phenomena to back-arc extension, triggered by roll-back of the subduction zone during the last ca. 26 Ma (e.g. Meulenkamp et al., 1988, 1994).

Geomechanical interpretations of the Aegean region range from the 'continuum tectonics model', according to which the entire Aegean crust is deformable in a continuous, 'plastic' manner, with the deformation accommodated not at specific boundaries lines, but as a dense network of discontinuities (e.g. Rostein, 1985), to a microplate configuration suggested by McKenzie (1978). According to the latter, deformation is accommodated along the boundaries of rigid microplates. These boundaries are prominent zones of discontinuity that take up the motion of largely undeformable parts. There are also intermediate views, like that of Flemming (1978), suggesting that the Aegean crust is dissected into small (50×50 to 25×50) blocks, decoupled from each other and behaving semi-independently. The dimensions of these tectonic blocks correlate well with the maximum length of basin-bounding fault segments in central Greece (Roberts and Jackson, 1991). Taymaz et al. (1991) suggested a model involving continuous behaviour of the lower crust and discontinuous, rigid-block segmentation of the upper crust, where the bulk of the deformation is taken up by major seismic faults. This model is favoured by recent workers.

1.3 THE QUATERNARY

The Quaternary is the last period of the history of the Earth (Fig. 1.3), with fauna and flora largely similar to the present (Harland et al., 1982). The Quaternary was a time of pronounced environmental change (see below). The major part of human evolution took place during this period; the environmental effects of human activity became markedly more evident during the later part of the Quaternary (Williams et al., 1993).

On formal stratigraphic terms, the Quaternary System (chronostratigraphic unit) / Period (geochronological unit) is divided into two series (epochs): the Pleistocene, from the begining of the Quaternary to ca. 10,000 years before present, and the Holocene, covering the last 10,000 years (Lyell, 1839; Desnoyres, 1929; Bonifay, 1975; North American Stratigraphic Code, 1983; Haq et al., 1988) (Fig. 1.3). The date of the begining of the

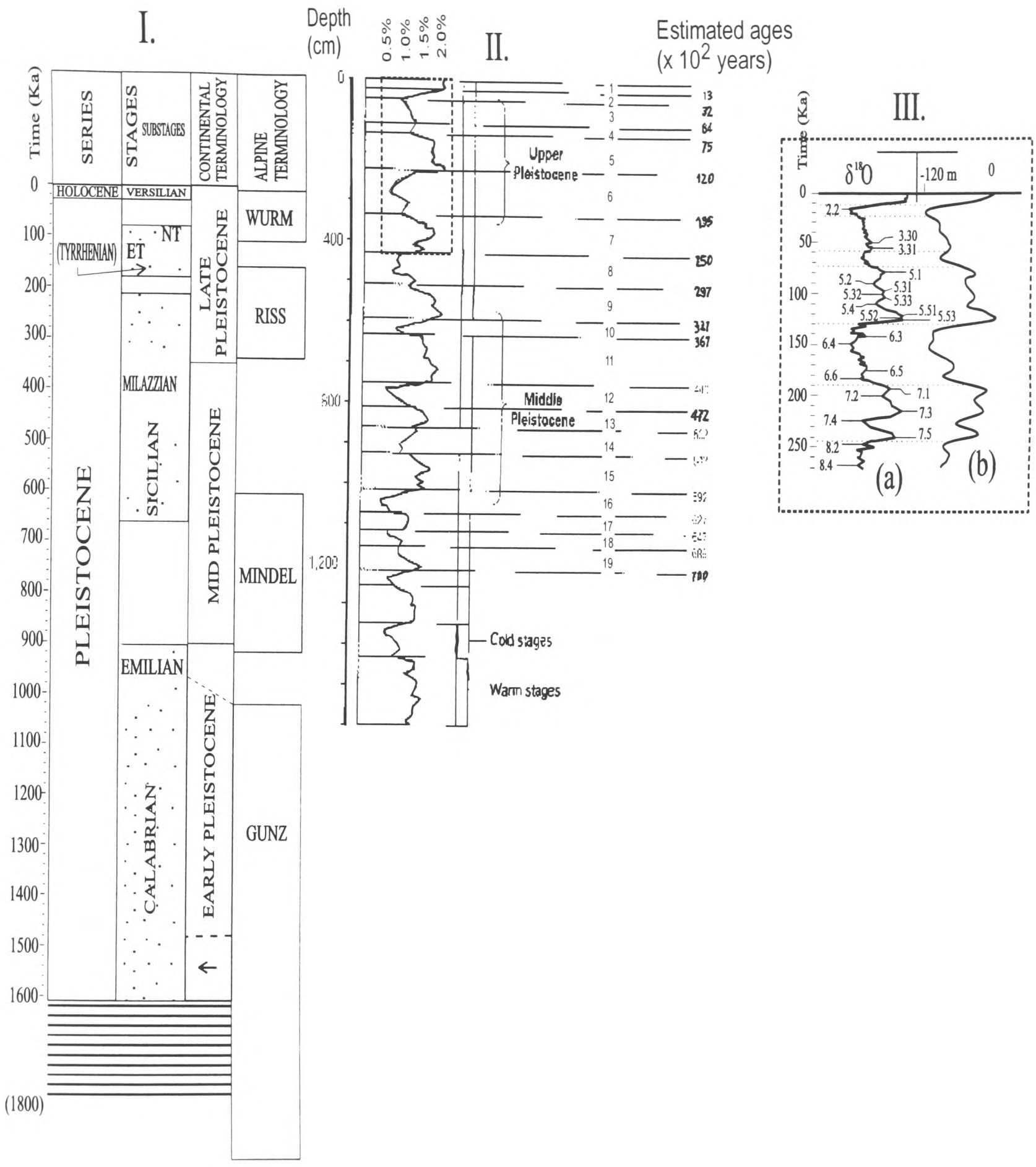

Figure 1.3: Quaternary stratigraphy. **I:** Traditional stratigraphic nomeclature (Bonifay, 1975). **II:** Oxygen-isotope curve during the last ca. 700 ka (Shackleton, 1987). **III:** Oxygen-isotope curve (**a:** Imbrie et al., 1984) and eustatic sea level curve (**b:** Martinson et al., 1985), during the last ca. 250 ka (late Quaternary).

Quaternary is still debated; estimates range from 2 ±0.1 Ma (Selli et al., 1977), to 1.8 Ma (Sibrava, 1978; Nikiforova, 1978), to 1.6 Ma (Haq et al., 1977, 1988) (for a discussion see Bonifay, 1975; Harland et al., 1982; Williams et al., 1993).

1.3.1 Mediterranean Quaternary stratigraphy: In circum-Mediterranean areas, marine Quaternary sediments are dated biostratigraphically on the basis of index fossils or faunal assemblages, including calcareous nannoplankton, planktic and benthic foraminifera and bivalves (Martini, 1971; Keraudren, 1970, 1971; Bonifay, 1975; Frydas, 1990, 1992; Frydas and Bellas, 1994; Haq et al., 1988). Terrestrial Quaternary sediments are dated on the basis of mammalian fauna and flora (Kourtin, 1969; Sauvage, 1978, 1979) (Table 1.1).

TABLE 1.1

Marine organisms:	**Nannoplankton** (Frydas, 1990, 1993; Frydas and Bellas, 1994)
	Pseudoemiliana lacunosa, *Gephyrocapsa*
	Planktic Foraminifera (Blanc-Vernet, 1969)
	Globorotalia trunctulinoides (presence indicates a Pleistocene age)
	Benthic Foraminifera (Keraudren, 1970, 1971; Frydas 1990, 1993)
	Hyalinea balthica (appeared in the Mediterranean in early Pleistocene, later than *Globorotalia truncatulinoides*)
	Mollusks (Keraudren, 1970, 1971)
	Arctica islandica (early Pleistocene), *Chlamys tigrina* (Pleistocene), *Strombus bubonius* (migrated from the west African coast during the Last Interglacial).
Terrestrial Organisms:	**Large Mammals** (Kurtin, 1969)
	Archidiscodon meridionalis, Palaeoloxodon antiquus, Dicerorhinus etruscus, Hippopotamus major, Equus stenonis, Bos primigenius (all suggesting warm climatic conditions), *Mammonteus primigenius, M. trogontherii, Coelodonta antiquitatis, Bison priscus, Ovibos moschatus, Rangifer tarandus* (all suggesting cool climatic conditions), *Ursus spelaeus, U. arctos, Canis lupus, Crocuta sp., Sus scrofa, Capra sp.* (all suggesting Pleistocene age).
	Micromammals
	Several rodent assemblages indicate cool or warm climatc conditions

	Arthropods (Coope, 1970, 1975) Coleoptera (beatle) fauna can be used to infer climatic conditions in great detail.
	Plants (Sauvage, 1978, 1979) Pollen evidence allows identification of distinct plant communities, thus leading to inference of climatic conditions.
Human remains:	**Human fossils** (Fagan, 1989) The only forms present in the northern coast of the Mediterranean are transitional between the *Homo erectus* and *H. sapiens*, of late-middle Pleistocene age (ca. 250 ka), the late Pleistocene *H. sapiens neaderthalensis* and the late Pleistocene-Holocene *H. sapiens sapiens*.
	Tool Technology (Williams et al., 1993) Acheulian (early and middle Pleistocene), Mousterian (early late Pleistocene), Levalois (early late Pleistocene), Aurignacian, Gravetian, Solutrian, Magdalenian (late Pleistocene, successively younger), Mesolithic and Neolithic (Holocene).

Table 1.1: Faunal, floral and archaeological evidence used to infer Quaternary stratigraphy and palaeoenvironments.

The Quaternary has been a period of marked environmental change, characterised by periods of low temperature, glaciation and lower sea level, alternating with periods of high temperature, deglaciation and higher sea level (Daly, 1924; Bonifay, 1975). This environmental cyclicity underpins both the terrestrial and marine stratigraphic record, thus forming the basis of any detailed chronostratigraphy of the Quaternary period. Traditionally, the marine Quaternary is divided into four to five major stages (ages), each one corresponding to a major sea level cycle of transgression, highstand and regression (Harland et al., 1982). Although nomeclature and terminology vary between different authors and regions of application, a subdivision applied to circum-Medditerranean regions commonly distinguishes between the **Calabrian**, **Sicilian**, **Tyrrhenian** and **Versilian** stages (Bonifay, 1975; see Fig. 1.3). The continental Quaternary of Europe is traditionally divided into four periods of glaciation: namely **Günz**, **Mindel**, **Riss** and **Würm**, and four interglacial periods: namely **Günz-Mindel**, **Mindel-Riss**, **Riss-Würm** and **post-Würm**

(Fig. 1.3). The stratigraphic subdivision outlined above is based on the independent definition of marine and continental Quaternary stages, as has resulted from investigations in the 19th-early 20th centuries (Aggassiz, 1840; Daly, 1924). Most authors correlate the marine stages, marked by warm water fauna and high sea level, with continental interglacials, marked by retreat of the ice sheets and warm to temperate terrestrial fauna and flora. The assumption of glacio-eustasy (Tooley, 1990) is implicit in any proposed correlation between marine and continental depositional systems. During glacial periods water is stored in ice sheets in the form of ice and, thus, removed from the hydrological cycle. This causes the level of the global ocean to drop. Global warming, during interglacials, by contrast, facilitates melting of the ice sheets and release of melt-water to the ocean, in turn causing global sea level to rise. Bonifay (1975) proposed a correlation of Quaternary high sea levels with interglacial periods (Fig. 1.3). This model also accounts for the dynamic response of marine depositional systems to changing sea level, i.e. periods of sea level rise and fall, that marked the beginning and the end of interglacial periods, respectively. This model, by predicting the response of depositional systems to changing sea level, can accommodate principles of sequence-stratigraphy, as introduced later (Van Wagooner et al., 1988; Milton and Myers, 1992). A modified version of this chronostratigraphic scheme (Bonifay, 1975) is used in this work (Chapters 3, 5, 7).

1.3.1.1 Terrestrial Quaternary: The applicability of the central European nomenclature to the terrestrial Quaternary of circum-Mediterranean regions is not generally accepted. Most authors, however, recognise at least one late Pleistocene glaciation in the eastern Mediterranean mountains. This is manifested by geomorphological evidence (Dufaure, 1977; Vavliakis, 1981; Vavliakis and Psilovikos, 1982/83, Palmentola, 1994), alluviation triggered from inferred 'rhexistatic' conditions (i.e. pronounced erosion due to diminution of vegetation cover during a colder climate; Dufaure, 1977; Psilovikos, 1981; Smith et al., 1994, Brousoulis and Yiakkoupis, 1994) and presence of 'cold' mammalian fauna in open air and cave sites (Melentis, 1967; Tsoukala, 1989). This cold period in the late Pleistocene is tentatively correlated with the Würm glaciation in central Europe and the Alps (Figs. 1.3, 1.4). Earlier cold periods, correlative with the Riss and Mindel glaciations in the central European Quaternary stratigraphy, are also recognised by some authors (Bonifay, 1975; Dufaure, 1977; Smith et al., 1994). In circum-Mediterranean areas, the Pliocene-Quaternary boundary is marked by red beds with 'Vilafrancian' mammalian faunas, transitional between the 'typical' Pliocene and the 'typical' Pleistocene faunas. For instance, Mastodons, typical of the Pliocene period, co-existed with the Pleistocenic elephant, *Archidiscodon meridionalis* at the beginning of the 'Vilafrancian' and became extinct by its end (Bonifay,

1975; Koufos et al., 1989). Along the northern coast of the Mediterranean Sea, the 'Vilafrancian' climate is characterised by a relatively cool period with 'Pretiglian' flora, including pine trees, followed by a warmer period with 'Tiglian' flora, including *Tsuga*, *Carya*, *Pterocarya* (Sauvage, 1978, 1979). In agreement with their transitional character, 'Tiglian' floras also included relict plant taxa of typically Pliocene age (Sauvage, 1978, 1979). The development of these, characteristically transitional, biota coincided with the establishment of a seasonally fluctuating climate of Mediterranean type, probably initiated ca. 2.3 Ma ago (Suc, 1984).

1.3.1.2 Marine Quaternary: The cyclic alternations of colder and warmer climatic conditions during the Quaternary is also evident in marine sediments and fauna of the circum-Mediterranean region (Blanc-Vernet, 1969; Keraudren, 1970, 1971; Bonifay, 1975). Periods of high sea level were, thus, characterised by warm-temperate faunas, which, gradually came to include emigrant species from the warm Atlantic coasts of Africa ('*Senegalese faunas*'), as the Quaternary advanced. The gastropod, *Strombus bubonius*, believed to have migrated into the Mediterranean Sea during the warm Tyrrhenian stage, in the late Pleistocene (ca. 120 ka), is a typical example (Keraudren, 1970, 1971; Bonifay, 1975). These species were replaced by cool-temperate species during cooler periods of lower sea level. The appearance of the bivalve *Arctica islandica* in the Mediterranean in the earliest Pleistocene is inferred to correlate with lower water temperature during that time, associated with glaciation in central Europe and the Alps (Keraudren, 1970, 1971).

1.3.2 Oxygen isotope evidence: Alternating cold and warm periods during the Quaternary affected the composition of ocean water relative to the two isotopes 16O and 18O. The lighter isotope 16O escapes preferentially during evaporation of ocean waters. During glaciations, water is removed from the water cycle and stored as ice, mainly within continental ice sheets. The water of these ice sheets is enriched in 16O; correspondingly, the ocean water during glacial stages is enriched in the heavier 18O. During deglaciations, 16O returns to the ocean in the form of meltwater and the 16O/18O ratio is increased (Shackleton, 1987). Assuming that the 16O/18O ratio in tests of benthic foraminifera reflects the isotopic composition and temperature of the ambient water during their life-time, oxygen isotope records are used as a proxy of Quaternary climate change (Shackleton, 1987; Williams et al., 1993). Imbrie et al. (1984) compiled an oxygen isotope curve that covers the last ca. 800 ka (Fig. 1.3.II). This curve shows 21 alternating cold and warm stages, correlated with glacial and interglacial periods, respectively.

1.3.3 Quaternary environmental change: The Quaternary has been a period of rapid climate change. The changing global extent and distribution of ice sheets affected the global sea level and organic communites and triggered isostatic movemnts of the crust (Daly, 1924; Lambeck, 1991; Williams et al., 1993; see below). The significance and the extent of Quaternary glaciations were first appreciated by Agassiz (1840; after Imbrie, 1988). Four major glaciations were first recognised, each followed by periods of warmer climate and glacial retreat (Geikie, 1874). Today, with the aid of high-resolution oxygen isotope records, more than 22 Pleistocene glacial episodes are recognised (Bowen, 1991). The Quaternary glaciations are viewed as the culmination of climatic phenomena that started earlier, in Tertiary time. In the Southern Hemisphere ice begun to accumulate in Antarctica ca. 20 Ma ago; whereas, in the Northern Hemisphere the first regional ice sheets were formed ca. 2.4 Ma ago (Kennett, 1982). A cyclical pattern of glaciation and deglaciation was well established by the beginning of the Quaternary. Climatic cyclicity had a periodicity of ca. 41 Ka during the early Quaternary (up to ca. 0.9 Ma ago); since then the periodicity rose to ca. 100 Ka, and the amplitude of climatic cycles increased (Ruddiman and Raymo, 1988). This latter periodicity, of ca. 100 Ka, falls well within the '*Milankovitch band*' (10-400 Ka; Imbrie, 1985), matching the period of orbital change in eccentricity (Williams et al., 1993). Several hypotheses were advanced to explain the forcing mechanism(s) of Quaternary climatic change and the striking periodicity of 100 Ka during the middle-late Quaternary (Bowen, 1978; Imbrie, 1985; Williams et al., 1993). These hypotheses involve either interference of separate periodicities in the orbit of the Earth, which would produce periodic changes in the degree of the Earth's insolation (Imbrie, 1985), or isostatic readjustment of the crust under the load of glaciers, which, by lowering the elevation of the crust, would cause ablation of ice sheets to dominate over ice accumulation (see Williams et al., 1993 for a review).

A major effect of Quaternary glaciations and deglaciations was global sea level change. Storage of water in land ice during glaciations resulted into global sea level fall, whereas release of meltwater to the oceans during deglaciations resulted into global sea level rise (Daly, 1934; Williams et al., 1993). Glacio-eustatic sea level change is a rapid process; sea level is believed to fall at the rate of 1-5 m/ka during glaciations and to rise even faster, at the rate of 5-10 m/ka during deglaciations (Williams et al., 1993). The absolute amount of eustatic sea level drop reached 120-150 m during the Last Glacial Maximum (ca. 12 Ka before present; Williams et al., 1993). Furthermore, redistribution of mass between the oceans and continents during Quaternary glaciations/deglaciations produced glacio-isostatic and hydro-isostatic effects, which, through redistribution of mass in the asthenosphere

(viscous flow), could have affect areas far removed from the foci of former ice sheets (Mörner, 1987; Lambeck, 1991; Williams et al., 1993). The amplitude of such isostatic effects was significant, reaching a value of 300 m locally (e.g. Scandinavia; Mörner, 1976, 1987).

A good record of Quaternary sea levels over the last ca. 400 ka (middle and late Pleistocene-Holocene) has been derived from flights of marine terraces in rapidly uplifting areas (e.g. the Huon Peninsula, Papua New Guinea- Chappel, 1974; Aharon, 1984; Barbados- Bard et al., 1990), calibrated with the oxygen isotope record of marine organisms (Imbrie et al., 1984; Martinson et al., 1984; Chappel and Shackleton, 1987). For the older part of the Quaternary, glacio-eustatic sea level change is inferred from oxygen isotope ratios of benthic organisms (e.g. Imbrie et al., 1984; see Fig. 1.3.II).

1.4 THE QUATERNARY OF THE PELOPONNESE: A REVIEW OF PREVIOUS WORK.

Works concerning the morphological, sedimentological and neotectonic development of the Peloponnese as a whole, during Pliocene-Quaternary, include those by Dufaure (1965, 1969, 1977), Kelletat et al. (1976, 1978), Berckhemer and Kowalczyk (1978), Mariolakos et al. (1985). The last two works attempted large-scale geodynamic modelling. Keraudren's (1970, 1971) work on the marine Quaternary of Greece and the Aegean coasts of Turkey includes detailed sedimentological and palaeontological data from many Peloponnesian sites. Flemming (1972) and Kraft et al. (1975, 1977) focused on the late Holocene evolution of coastal areas in the Peloponnese. Lambeck (1995) reinterpreted their results, also taking into account isostatic movements since the last deglaciation. Geophysical and seismological data were published by various authors, e.g. Leydecker et al. (1978), Makris (1977; 1978), Hetzfeld et al. (1989, 1990), Jackson et al. (1992), Meijer (1995). Numerous other works deal with sedimentation, neotectonics and geomorpholoy of particular areas in the Peloponnese (Table 1.2).

1.4.1 GEOGRAPHY AND FAULTS

The Peloponnese, situated within 36°20' 25"-38° 20' 25" N latitude and 21° 06' 30" E longitude, is the southernmost peninsula of the European Continent. Its total area is 21,441 square km and its average altitude is 543 m (Mariolakos, 1975). Mountains of NW-SE general direction, parallel to the typical strike of the Dinaric-Hellenic mountain belt, and of altitude reaching 2407 m (Taighetos), lie besides plains and basins of tectonic origin (Fig. 1.1). The mountainous relief extends seawards in the form of peninsulae, separated by gulfs and their onland continuation as alluvial plains.

The southern part of the Peloponnese exhibits the most prominent coastal configuration (Fig. 1.1). The three peninsulae of Messenia, Mani, and Eastern Laconia (from west to east) are the seaward continuations of elevated terrestrial areas (mountains of Kiparissia, Taighetos, Parnon), with the Messenian and Laconic Gulfs in between. At the heads of these gulfs, the rivers Pammisos and Eurotas formed the alluvial plains of Kalamata-Messini and Sparti-Githion, respectively. On a smaller scale, numerous small bays, extended sandy beaches and rocky cliffs resulted from an interplay between surface processes and active tectonics.

The Peloponnese is dissected by a dense network of major normal faults, as depicted on maps of 1:500,000 scale (I.G.M.E., 1978). The dominant strikes of Km- to 10's of Km-long fault systems in the Peloponnese depends on location. The northern and western regions are cut by generally E-W (from ENE-WSW to ESE-WNW) striking faults, whereas the southern and eastern regions are mainly cut by NNW-SSE (to N-S) striking faults (Fig. 1.1). Mariolakos et al. (1985) suggested that these two sectors with different fault strikes can be separated by a NE-SW trending imaginary line, extending from Corinth in the north to Pylos in the south (Fig. 1.1).

1.4.2 PRESENT-DAY TECTONICS: EARTHQUAKE DISTRIBUTION, HORIZONTAL MOVEMENTS AND STRESS/STRAIN PATTERN

1.4.2.1 Distribution of earthquake epicentres: As mentioned in the introduction, the Peloponnese, situated at the western part of the Aegean fore-arc (Fig. 1.2), is one of its most tectonically active areas.

1.4.2.1.1 Shallow earthquakes: The majority of events recorded in microearthquake surveys (Leydecker et al., 1978; Hetzfeld et al., 1989, 1990) comprise shallow earthquakes (focal depth: <40 km). The densest sets of epicentres occur in the western and northern parts of the Peloponnese, offshore of the Messenia Peninsula and around the Corinth-Patras Gulf, respectively (Fig. 1.7). The maximum density of earthquake epicentres is located around the Corinth-Patras Gulf (Leydecker et al., 1978; Berckhemer and Kowalczyk, 1978; Mariolakos et al., 1985; Hatzfeld et al., 1989, 1990).

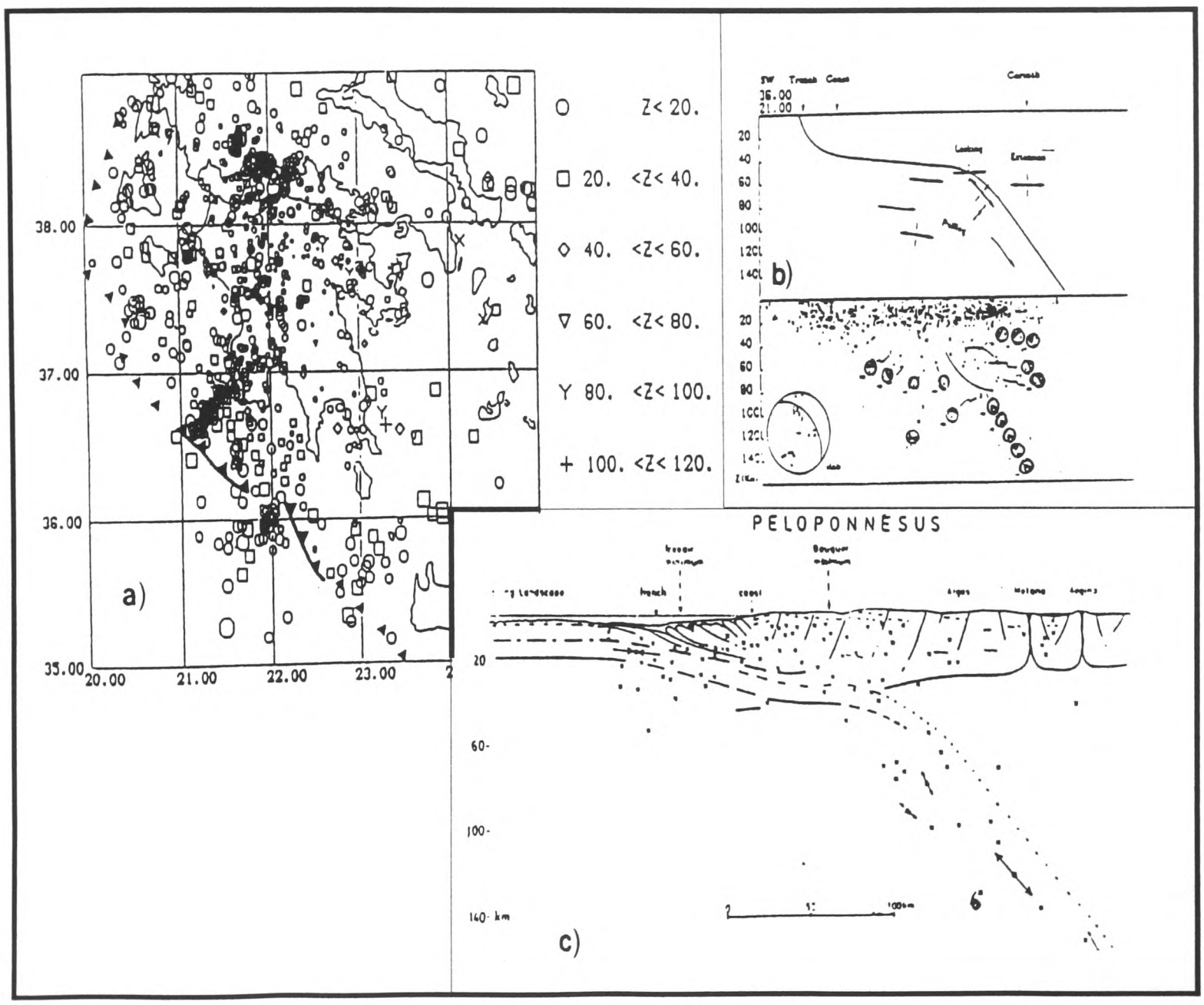

Figure 1.4: a) Distribution of earthquake epicentres in the Peloponnese (Hatzfeld et al., 1989). **b)** Vertical distribution of earthquake foci and proposed interpretation (Hatzfeld et al., 1989). **c)** Geodynamic model of the Peloponnese (Berkhemer and Kowalczyc, 1978).

Hatzfeld et al. (1989, 1990) concluded that the distribution of earthquake epicentres is diffuse, defining clusters of activity rather than distinct faults. One of the major clusters, located offshore of Messenia (SW Peloponnese), was attributed by the same authors to a local locking of a subduction zone beneath.

The vertical distribution of shallow earthquakes, by contrast, appears to be uniform, suggesting that the crust of the Peloponnese is deeply fractured (Hatzfeld et al., 1989, 1990; Fig. 1.4). The same authors identified a westward-deepening of the brittle-ductile transition and attributed this to an increase in strain westwards, due to collision of the Ionian crust with the Peloponnese. No abnormal seismicity was detected around Kalamata, even though Hatzfeld et al.'s (1989, 1990) microearthquake survey was conducted just two months before the destructive earthquake of 1986.

1.4.2.1.2 Earthquakes of intermediate depth: Earthquakes deeper than 40 km occur under the Argolis Peninsula (Figs. 1.1, 1.4), eastward of 22° E longitude (Leydecker et al., 1978; Berckhemer and Kowalczyk, 1978; Hatzfeld et al., 1989). The foci of these earthquakes define a plane dipping at ca. 45°, broadly to the east, although its exact direction of dip is poorly constrained (Hatzfeld et al., 1989). This plane possibly extends until a depth of ca. 180 km. Berckhemer and Kowalczyk (1978) interpreted this pattern of focal distributions as a Benioff zone, corresponding to the upper, brittle part of the subducting Ionian slab. The relatively abrupt deepening of earthquake foci under the Argolis Peninsula was found to coincide with a zone of roughly horizontal P-axis (maximum compression), where the subduction zone is thought to be locked (Hetzfeld et al., 1989). Deeper than this zone, the T-axes (maximum extension) are oriented parallel with the inferred subducting slab. This is interpreted as a slab-pulling effect, activated by the cold, subducting lithosphere (Hetzfeld et al., 1989), or as a result of high-pressure mineral transformation (Berckhemer and Kowalczyk, 1978).

1.4.2.2 Stress/strain pattern: Focal mechanisms after a microearthquake survey of the Peloponnese (Hetzfeld et al., 1989), indicate N-S extension in the area of Corinth-Patras Gulf and NE-SW compression in the area of the Hellenic Trench. In the Southern Peloponnese, the T-axes (maximum extension) are directed NW-SE to N-S, different from the direction of motion of Africa relative to the Aegean (NE-SW), but very similar to the relative motion between Africa and Europe (Hetzfeld et al., 1989). This contradicts the results of Lyon-Caen et al. (1988) and Armijo et al. (1992), suggesting that E-W direction, oblique to the Aegean Arc, during Quaternary (Pleistocene-Holocene), replaced the older,

Pliocene regime of N-S extension. The latter results, deduced from focal mechanisms of the 1986 Kalamata earthquakes and by microtectonic analysis of Holocene normal faults in southern Peloponnese, respectively, are in agreement with stress pattern over the Aegean during "*Recent Quaternary*", as proposed by Angelier et al. (1982; Fig. 1.8). A recent microtectonic analysis in the areas of Kyparissia (Messenia Peninsula) and Kythera Island (offshore of the SE Peloponnese; Fig. 1.1) (Meijer, 1995) indicated horizontal extension of directions ranging from ENE-WSW to NNW-SSE. This result is similar with the stress pattern inferred for central Crete (Angelier et al., 1982); the latter was interpreted as resulting from maximum and intermediate horizontal stress of comparable absolute magnitudes (i.e. $\sigma 1 \approx \sigma 2$). Meijer (1995) concluded that this stress pattern persisted over the south Peloponnese since the middle Pleistocene.

1.4.2.3 "Shallow underthrusting": The distribution of earthquake foci beneath and around the Peloponnese suggests shallow underthrusting of the Ionian slab in the west, and abrupt subduction east of 22° E longitude (Berckhemer and Kowalczyk, 1978). This model is also supported by further geophysical evidence, namely the position and orientation of a prominent seismic reflector, interpreted as corresponding to the crust-mantle boundary, as well as the great thickness of the crust beneath western Peloponnese (ca. 45 km; Makris, 1978, 1985; pers. com. 1998) and its gradual decrease towards the east. A similar model of shallow underthrusting beneath the Peloponnese was also suggested by Hatzfeld et al. (1989). According to a more recent interpretation (Backman, 1991; Backman et al., 1993, after Meijer, 1995) the subducted slab detaches further eastwards.

1.4.2.4 Horizontal movements: The spatial variation of horizontal seismic strain indicates a general southwestward movement of the Peloponnese relative to Africa (Jackson et al., 1992). The exact direction of movement differs between the NE and SW parts of region, in consistency with clockwise rotation of the Aegean. The rate of this movement was found to be at the order of 20 mm/yr (Jackson et al., 1992); this result is in agreement with the value of 31 mm/yr of southwestward movement of the SW Peloponnese, derived from satellite laser ranging (WEGENER/MEDLAS project; Robbins et al., 1992; Noomen et al., 1993 - from Meijer, 1995).

Longer-term trends of horizontal movement, during the last century, were inferred from comparison of the results of three triangulation surveys on the National Triangulation Network, established in 1899 (Stiros, 1993). The rotational (clockwise) character of horizontal deformation was confirmed, consistent with the inferred deformation over

Pliocene-Quaternary time (Angelier et al., 1982) and the present-day (Jackson et al., 1992; Meijer, 1995). Stiros (1993) concluded that these geodetic data suggest "*important changes in the strain pattern over the time-scale of 30 years*".

1.4.3 LONG-TERM FAULTING AND UPLIFT

Dufaure (1977) distinguished two major periods in the neotectonic development of the Peloponnese. A first period of Pliocene-earliest Pleistocene extension controlled the development and degradation of piedmont landscapes in the Peloponnese (see below). A second period of extension, active until the present, resulted in uplift, evidenced by relative sea level fall, formation of consequent rivers, and underground tapping of karstic drainage. Pleistocene neotectonic activity is documented by fault scarps, and friable "rock-walls" with trapezoid facets wherever the faults cut through poorly consolidated Plio-Pleistocene deposits. The style of faulting and fault scarp preservation differ locally (Dufaure, 1969). The same author (1977) classified the major "*neotectonic systems*" of the Peloponnese into '*tilted fault blocks*', '*fault-angle troughs*' and '*neotectonic coasts*'. The effect of Quaternary climatic fluctuations was superimposed on the effects of tectonic activity, as an additional control on sedimentation processes (Dufaure, 1977).

Kelletat et al. (1976, 1978) synthesised the Pliocene-Quaternary evolution of the Peloponnese, based on study of its coastal regions. The present and former sea levels were used to infer vertical movements. Key features for deciphering the regional history were the following (Fig. 1.5):

1) Distribution of marine Neogene deposits: These tend to be more widespread and at higher altitudes in the northern and northwestern parts of the Peloponnese (Fig. 1.1) as compared with the eastern parts; their altitude decreases gradually towards the south. A similar spatial pattern is repeated within each of the southern peninsulae (Messenia, Mani and Eastern Lakonia).

2) Distribution of pediment and pediment-like plains: These surfaces, interpreted as roughly corresponding to the sea level during the Pliocene-Quaternary boundary, follow a pattern almost identical to that followed by the Neogene sediments (Fig. 1.5.B).

3) Distribution of pre-Tyrrhenian terraces: These terraces are almost completely absent from areas covered by friable Neogene deposits, probably due to erosion, with the exception of the Corinth- Xylokastron area. They are, however, preserved on hard bedrock in the southern peninsulae. Pre-Tyrrhenian terraces occur in great numbers and at higher altitudes

in the western and northwestern flanks of the Messenia and Eastern Lakonia Peninsulae, with their number and altitude decreasing towards the south and east (Fig. 1.5.B).

4) Distribution of the Tyrrhenian terraces: These terraces were divided into two separate stages, the "Eutyrrhenian", corresponding to the Eem-Ipswich Interglacial (ca. 10 ka) and the "Neotyrrhenian", inferred to correspond to the Wurm I-II Interstadial (ca. 30 ka) (see also Keraudren, 1970, 1971; Bonifay, 1975; Kowalczyk et al., 1992). At lower elevations, these terraces tend to follow the same spatial pattern as the older Pleistocene terraces (Fig. 1.5.A).

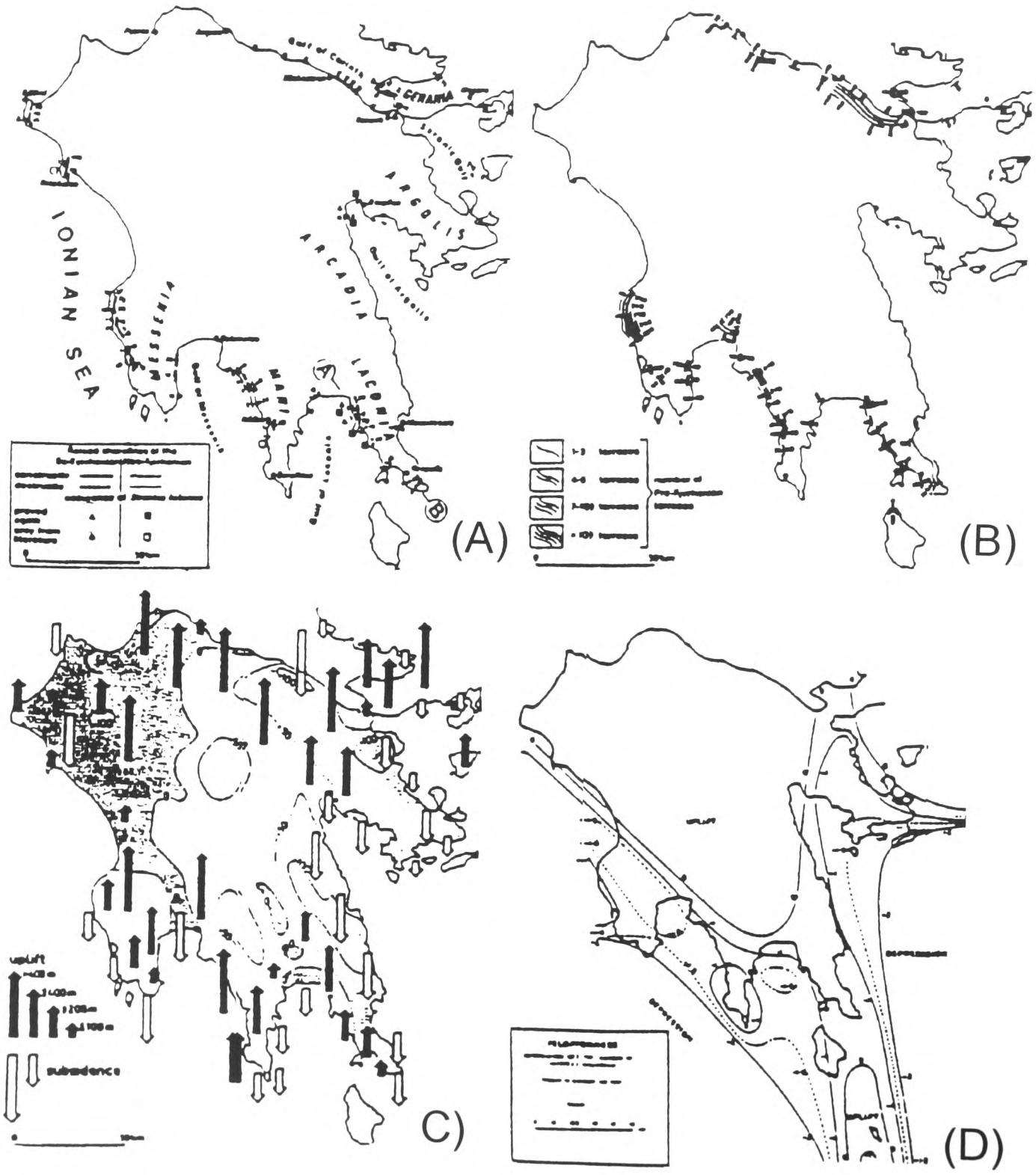

Figure 1.9: Quaternary uplift of the Peloponnese **(A, B: Kelletat et al., 1975; C:** Berckhemer and Kowalczyk, 1978; **D:** Flemming, 1978). **A: Distribution of uplifted** Tyrrhenian terraces. **B:** Distribution of uplifted **pre-Tyrrhenian terraces and Plio-**Quaternary pediments. **C:** The regional pattern of uplift and subsidence, **correlated with** free-air gravity anomalies. **D:** Pattern of Holocene deformation in Peloponnese.

Based on the above evidence, Kelletat et al. (1976, 1978) proposed a pattern of vertical movements for the entire Peloponnese (Fig. 1.5.C). Briefly, their model infers uplift of the northern and western Peloponnese, contrasting with subsidence of the eastern Peloponnese. In the south, the Messenia, Mani and Eastern Lakonia Peninsulae are characterised by alternating areas of uplift and subsidence, striking roughly parallel to the long axes of the peninsulae. This pattern was found to correlate well with the pattern of free-air gravity anomalies (Berckhemer and Kowalczyk, 1978). The model outlined by the above authors is, currently, the most comprehensive synthesis of Quaternary deformation in the Peloponnese.

1.4.5 PREVIOUS WORK ON COASTAL AREAS OF THE PELOPONNESE

The following section is an outline of published information concerning each of the main coastal areas of the Peloponnese. Only works dealing with Pliocene-Quaternary sedimentation and neotectonics of relatively large areas and of relatively broad interpretative scope are summarised here; numerous other works that deal with descriptions and dating of local outcrops are referred to in relevant chapters (Chapters 3, 5).

1.4.5.1 Corinth-Patras Gulf: The area of the Corinth-Patras Gulf is considered as the most seismically active of the whole Peloponnese (Dufaure, 1965, 1977; Mariolakos et al., 1985), as also manifested by the seismological data referred to above (Berckhemer and Kowalczyk, 1978; Leydecker et al., 1978; Hatzfeld et al., 1989, 1990) (see Fig. 1.7). The recurrence time of large (> 6.5 R) earthquakes in the area ranges between 80 to 1690 years (Doutsos and Poulimenos, 1992). This area is cut by ESE-WNW major faults, of accumulated throws probably >2000 m (Dufaure, 1977). Mariolakos (1975) inferred a maximum value of 1759 m of differential uplift during the Quaternary for the central sector of the southern flank of the Corinth-Patras Gulf (Fig. 1.1). Kelletat et al. (1976, 1978) concluded that Quaternary movement ranged from >400-100 m (Fig. 1.5.C). The neotectonics of the area are among the most thoroughtly researched in Greece, as shown by the number of references (e.g. Jackson et al., 1982; Jackson and McKenzie, 1983; Mariolakos et al., 1985; Vita-Finzi, 1987; Collier, 1990; Doutsos and Piper, 1990; Collier and Dart, 1991; Leeder et al., 1991; Collier et al., 1992; Doutsos and Poulimenos, 1992; Leeder and Jackson, 1993; Poulimenos et al., 1993). Quaternary geomorphology and sedimentation processes were controlled by major normal faults of E-W strike that bound the Corinth-Patras Gulf. These listric faults are segmented into sectors of 20 km maximum length (Roberts and Jackson, 1993). Dextral (Berckhemer and Kowalczyk, 1978; Jackson et al., 1982; Mariolakos et al., 1985) and sinistral (Stiros, 1993) components of horizontal movement along these faults were also

inferred. Listric faulting, with the dip of the fault- plane decreasing with depth, can be attributed to rheological variations of the crust with depth, the need for accommodation of rotation, or reactivation of older thrust planes under an extensional stress field (Jackson and McKenzie, 1983). Listric faulting was evoked to explain the asymmetry of the Corinth-Patras Gulf and inversions in the direction of movement, responsible for the uplift of Plio-Pleistocene marine sediments in the southern flank of the gulf (Mariolakos, 1975; Jackson and McKenzie, 1983). Mariolakos (1975) proposed a model of '*tectonic dipoles*' in order to explain the asymmetrical uplift of each side of the Corinth-Patras Gulf. According to this model, updated with seismological and geophysical data (Mariolakos et al., 1985), most of the movement was accommodated, not by individual fault blocks, but by larger-scale blocks, bounded by fault zones of great extent (>10-20 km). Movement at the edges of these units differed in direction and/or rate, resulting in relative uplift of one segment in relation to the other and monoclinal tilting of the deformed units. This style of deformation is inferred to prevail in the whole of the northern Peloponnese, as a result of transtension.

The sedimentary record of the Corinth-Patras area comprises uplifted and tilted Quaternary fluvio-lacustrine sequences (progradational fan-deltas; Doutsos and Piper, 1990; trapezoidal fan-deltas, Poulimenos et al., 1993) and several marine terraces superimposed on the latter. Opinions about the exact number and significance of these terraces vary. Keraudren and Sorel (1987) referred to 20 distinct terraces, inferred to record eustatic sea level variations during the last 500 ka, whereas Doutsos and Piper (1990) interpreted most of the terrace-like morphologic features as the result of normal faulting of the same deltaic surface. According to the latter workers, only the lowermost surfaces correspond to real marine terraces, of late Pleistocene (Tyrrhenian) age.

Information about the present-day rate of vertical movements is derived from studies of co-seismic or near-seismic deformation around the Corinth-Patras Gulf. Jackson et al. (1982) studied the macroseismic effects of the 1981 earthquake sequence (magnitudes: 6.7, 6.4, 6.4). These include coastline uplift and subsidence, of a pattern consistent with theoretical predictions of listric normal faulting. Throws of up to 150 cm were observed, with their maximum values located in the central parts of the fault segments active during the earthquakes. However, Stiros (1986), based on geodetic monitoring of post-seismic displacement (order of magnitude: ca. 1-2 cm), also inferred a component of horizontal movement. Correlation of this displacement with the fault pattern of the area suggests that the present-day vertical movements are a continuation of the Quaternary graben-formating processes (as above).

TABLE 1.2

PREVIOUS WORK ON THE QUATERNARY OF THE PELOPONNESE

Author(s):	Subject:
Dufaure, 1965, 1969, 1977	Geomorphology, Sedimentation, Neotectonics
Area:	**Peloponnese**
Dating:	Flora (continental deposits) Molluscs, foraminifera (marine deposits)
Age:	Pliocene-Pleistocene
Kelletat et al., 1976, 1978	Geomorphology, Neotectonics
Area:	**Peloponnese** (Coastal areas)
Dating:	Molluscs in marine terraces (Tyrrhenian) Foraminifera, nannoplankton (Plio-Pleistocene marine sediments) Lithic industries (marine terraces of Eastern Lakonia) C14 dates (Corinth-Patras Gulf)
Age:	Quaternary
Keraudren, 1970, 1971	Sedimentation, Stratigraphy, Palaeontology
Area:	**Corinth, Elia, Argolis, Lakonia**
Dating:	Mollusc fauna, foraminifera, lithic industries
Age:	Quaternary
Flemming, 1968, 1972, 1978	Sea level change, Neotectonics
Area:	Peloponnese (Coastal Areas)
Dating:	Archaeological sites
Age:	Middle-late Holocene
Kraft et al., 1975, 1977	Sedimentation, Geoarchaeology
Area:	**Messenia, Lakonia, Argolis** (Coastal plains)
Dating:	7 C14 dates Pottery and other archaeological dating
Age:	Late Holocene
Mariolakos et al., 1985	Neotectonics, Morphotectonics, Geophysics
Area:	**Peloponnese**
Age:	Pliocene-Quaternary
Vita-Finzi, 1987	Neotectonics
Area:	**Gulf of Corinth**
Dating:	9 C14 dates on corals (ca. 30,000 yrs BP) Archaeological evidence
Age:	Latest Pleistocene-Holocene
Collier, 1990; **Collier et al.**, 1991, 1993	Sedimentation, Neotectonics, Sea level change
Area:	**Gulf of Corinth**
Dating:	3 U-series dates of *Acropora* corals (> 350,000-205,000 yrs BP)
Age:	Late Pleistocene

Table 1.2

Frydas et al., 1995	Sedimentary environments, biostratigraphy
Area:	**Gulf of Corinth**
Dating:	Nannoplancton (*Gephyrocapsids*)
	3 U-series dates on corals (ca. 400,000 yrs BP)
Age-span:	Middle-late Pleistocene
Keraudren and Sorel, 1987	Sedimentation, Sea level change, Neotectonics
Area:	Gulf of Corinth
Dating:	Nannoplankton (Gephyrocapsids), correlation of terraces with peaks of the δ O18 curve.
Age:	Late Quaternary (the last 450,000 years)
Pirazzoli et al., 1994	Seismotectonics
Area:	**Gulf of Corinth (Perachora Peninsula)**
Dating:	6 C14 dates on bivalves, gastropods, barnacles
Age:	Late Holocene (4440 B.C. to 540 A.D.)
Zelilidis, 1988; **Zelilidis and Doutsos**, 1992 **Zelilidis and Kontopoulos**, 1994, **Zelilidis and Frydas**, 1994	Sedimentation, Neotectonics
Area:	**Messenia (Kalamata Graben)**
Dating:	Planktic foraminifera, nannoplankton
Age:	Pliocene-Pleistocene
Frydas, 1990:	Nannoplankton biostratigraphy
Area:	**Messenia**
Dating:	Nannoplankton, foraminifera
Age:	Early Pliocene-Pleistocene
Frydas, 1993	Nannoplankton biostratigraphy
Area:	**Mani, Eastern Lakonia**
Dating:	Nannoplankton
Age-span:	Late Pliocene-Early Pleistocene
Petrochilou, 1963	Speleology, geomorphology
Area:	**Mani**
Dating:	Submerged archaeological sites
Age-span:	Pleistocene-Holocene
Theodoropoulos, 1973	Geomorphology, Neotectonics
Area:	**Eastern Lakonia (Neaolis Voion)**
Age:	Neogene-Quaternary

Table 1.2: Previous work on the Pliocene-Quaternary of the Peloponnese.

Sediments in the southern coast of the Corinth-Patras Gulf are the best dated in the Peloponnese with radiometric techniques (Table 1.3). Radiocarbon dating of marine sediments (King and Vita-Finzi, 1985, after Vita-Finzi, 1987) revealed a pattern of differential uplift, with rates ranging between 0.01-2.93 mm/yr. Radiocarbon dating of marine notches in the Perahora Peninsula (Pirazzoli et al., 1994) quantified late Holocene deformation, interpreted as coseismic. U-Th disequilibrium dating of coral from middle and late Pleistocene marine terraces (Collier, 1990) suggested minimum uplift rates of the order of 0.3 mm/yr throughout the Late Pleistocene-Holocene.

Other approaches to the chronostratigraphy of the Pleistocene marine deposits in the area included the correlation of inferred marine terraces with peaks of the oxygen isotope curve (Keraudren and Sorel, 1987) and the high-resolution calcareous nannoplancton biochronozones (Keraudren and Sorel, 1987; Frydas et al., 1994). The bostratigraphic results of the latter workers are consisted with the results of U-series dating.

Flemming's (1972, 1978) results from statistical analysis of displaced archaeological sites suggested a general uplift of the south coast of the Corinth-Patras Gulf during the late Holocene (Fig. 1.5.D). Lambeck (1995), taking isostatic effects into account, inferred rates of Holocene uplift as high as 1.5 mm/yr.

1.4.5.2 NW Peloponnese: The main normal faults in the NW Peloponnese strike N-S, E-W, and NE-SW (I.G.M.E.,1978; Mariolakos et al., 1991; see Fig. 1.1). Kelletat et al. (1976, 1978) divided the broader region into areas of Quaternary subsidence and uplift (Fig. 1.5.C). Possible inversion in the direction of movement was inferred for the southernmost sector, north of Kiparissia (Fig. 1.1). The present altitude of the base of Late Pliocene sediments indicates that the western pediment of the Erimanthos Mountain was uplifted by >400 m (possibly 700 m) during the Quaternary (Kelletat et al., 1976). The area between Pirghos and Kato Achaia (Fig. 1.1), by contrast, probably subsided since Miocene. Late Pleistocene terraces occur only locally, at altitudes of >100m in the area of Killini (Fig. 1.1). Their relative altitudes in the latter area were interpreted as suggesting that faulting of the "Eutyrrhenian" terraces took place before deposition of the younger "Neo-Tyrrhenian" terraces. The high altitude of the Kilini terraces, as compared with the rest of the Pleoponnese (Fig. 1.5) was attributed to diapirism of Triassic gypsum, (Kelletat et al., 1976, 1978; Mariolakos et al., 1991). The timing of diapirism is debatable. Kelletat et al. (1976, 1978) inferred a succession of phases of "*salt-tectonics*", that started in the Miocene and

continued until the Early Quaternary, at a reducing rate. Mariolakos et al. (1991) suggested that this 'diapirism' was in part responsible for late Pleistocene uplift of "Tyrrhenian" deposits, at the rate of 1.8 mm/yr locally. Intercalation of continental (colluvial) facies with Palaeolithic tools with late Pleistocene marine terrace deposits allows an archaeological dating of local outcrops (Keraudren, 1970, 1971).

Holocene vertical movements in the NW Peloponnese included both uplift and subsidence. Beach-rock emergence, at an altitude of ca. 2 m, is attributed to co-seismic deformation (Mariolakos et al., 1991; Lekkas et al., 1991). The macroseismic effects of the 1988 earthquake at Killini (magnitude: 5.5), included faulting with throws of 5-20 cm and uplift of beach-rocks by >15-20 cm locally. Flemming (1972, 1978) also characterised the area as uplifting during late Holocene, with the exception of the western tip of the Killini Peninsula and the coast north of Kiparissia (Figs. 1.1, 1.5.D). This interpetation of late Holocene archaeological evidence is consistent with longer-term results of Quaternary uplift (Kelletat et al., 1976, 1978). Tide-gauge records of 15 years (Flemming and Woodworth, 1988) show a very high rate of relative subsidence in the area of Katakolon (ca: 3.5 mm/yr) (Fig. 1.1).

1.4.5.3 Argolis Peninsula: The Argolic Gulf (Fig. 1.1) is bounded by NNW-SSE trending normal faults, cut by normal or transcurrent, mainly left-lateral ENE-WSW faults (Van Andel et al., 1993; Papanikolaou et al., 1994). The SE tip of the Argolis Peninsula is cut by ENE-WSW to E-W normal faults, that separate Idhra Island from the Peloponnesian mainland (Van Andel et al., 1993). An absence of uplifted marine terraces led Kelletat et al. (1976, 1978) to conclude that the Argolis Peninsula, together with the entire eastern coast of the Peloponnese, underwent long-lasting subsidence, with the exception of some 'stable' areas around Monemvasia (Fig. 1.1).

Plio-Pleistocene sedimentation in the the Argolic Gulf is well documented (Van Andel and Lianos, 1984; Van Andel et al., 1990, 1993; Papanikolaou et al., 1994). Based on submarine seismic profiles, Van Andel et al. (1993) inferred that coastal subsidence around the head of the gulf is younger than 500 ka. Flemming (1972, 1978) suggested that late Holocene uplift took place onland of the head of the Argolic Gulf, whereas maximum subsidence took place along a NW-SE trending imaginary line within the Argolis Peninsula (Fig. Felemming model). However, Van Andel et al. (1993) deduced a pattern of southward increasing subsidence that also affected areas considered by Flemming as uplifting. Estimated rates of subsidence vary between 1-2 mm/yr (Flemming, 1972) and 0.5-1 mm/yr (Van Andel et al.,

1993). By contrast, Kraft et al. (1977), interpreting evidence from onland drilling and radiometric dating, concluded that the Argolis Plain is a relatively stable area, undergoing regression due to floodplain progradation. This result is in agreement with models that take into account the isostatic contribution to the apparent sea level change (Lambeck, 1995).

1.4.5.4 Messenia Peninsula: This area, in the SW part of the Peloponnese and proximal to the Hellenic Trench (Figs. 1.1, 1.2), is less studied than the areas in the vicinity of the Corinth-Patras Gulf. The Messenia Peninsula is cut by NNW-SSE to N-S and ENE-WSW normal faults (I.G.M.E., 1980a,b; Mariolakos et al., 1985), also identified from offshore evidence (Vittori et al., 1980, 1981; Angelier et al., 1982; Mascle et al., 1982). These faults were thought to control the deposition within troughs that constitute the Hellenic Trench, southwest of the Messenia Peninsula (Vittori et al. 1981). N-S faults are interpreted as resulting from E-W oriented Quaternary extension over the Aegean fore-arc; a consequence of the continental collision of the African margin with the Aegean crust and the southwestward expansion of the latter over the more easily subductable Ionian crust (Lyon-Caen et al., 1988; Taymaz et al., 1991; Armijo et al., 1992). Local variations, however, must have been considerable, since recent microtectonic analysis in Kiparissia (Fig. 1.1) suggested a N-S direction of maximum extension (Meijier, 1995).

The spatial distribution of Plio-Quaternary morphological surfaces (pediments, marine terraces) suggests that Messenia Peninsula comprises alternating areas of uplift and subsidence, including the subdued southwestern sector of Proti Island-Pylos-Sphacteria Island, the uplifting sector of western Messenia, and the subsiding sector of the Pamissos fluvial plain (Kelletat et al., 1976; 1978) (see Fig. 1.5.C).

Evidence from the area of Filiatra (NW Messenia; Figs. 1.1, M.1: back-pocket) was used to infer Late Pliocene subsidence, at an estimated rate of 0.19 mm/yr, followed by upplift since the middle Pleistocene, at an estimated rate of 0.62 mm/yr (Marcopoulou-Diacantoni et al., 1991). Late Pliocene-early Pleistocene subsidence was also inferred from the Kalamata-Pamisos graben, a structure controlled by N-S to NNE-SSW trending faults (Zelilidis and Kontopoulos, 1994), which propagated during the early Pleistocene and modified "*the configuration of pre-existing graben margins*" (p. 653). This resulted in the formation of asymmetrical basins, with eastward increasing depth that accommodated prograding deltaic systems (e.g. Messenian Gulf; Fig. 1.1). Fan deltas were deposited near the fault-controlled eastern margin of the basin (Zelilidis and Kontopoulos, 1994). Pliocene and early

Pleistocene sediments of the Messenia Peninsula were dated biostratigraphically, using planktic and benthic foraminifera and nannoplankton (Frydas 1990; Frydas and Bellas, 1994; Marcopoulou-Diakantoni et al., 1991).

In areas emergent during the Pliocene-Quaternary boundary, a characteristic pediment surface was formed, followed by Pleistocene terraces at lower altitudes (Keraudren, 1970, 1971; Kelletat et al., 1976, 1978; Dufaure, 1977). Kelletat et al. (1976, 1978) distinguished more than 10 distinct terraces locally (NW Messenia). Faulting and tilting of pediment and terraces took place, with throws decreasing with decreasing altitude/age of the surfaces (Kelletat et al., 1976). Possible inversions in the direction of movement were inferred from the area NE of Kalamata, bounded by the active (Lyon-Caen, 1988) Kalamata Fault (Fig. 1.1). Fault throws in the young (ca. 120 Ka), Tyrrhenian terraces are generally <1m (Kelletat et al., 1976). A decreasing altitude of Tyrrhenian terraces towards the south was interpreted as indicating southward tilting of the entire western coast of the Messenia Peninsula (Kelletat et al. 1976, 1978).

A southward titling of the Messenia Peninsula during the late Holocene was inferred from the distribution of submergent archaeological sites (Flemming, 1972, 1978). Statistical analysis of the latter suggested that late Holocene subsidence of the Messenia Peninsula followed a NW-SE trending pattern (Fig. 1.5.C). These results contradict the pattern of vertical movement inferred for the whole Quaternary, that comprises alternating areas of uplift and subsidence and persistent directions of movement for each block (Kelletat et al., 1972, 1978; see Fig. 1.9). Kraft et al. (1975, 1977), based on sedimentological data from the Pamisos Plain (Fig. 1.1), supplemented by of C14 and pottery dating, inferred an abrupt relative sea level rise ca. 5.5 ka (Late Neolithic). This distinguishes the Pamisos Plain from other coastal plains in the Peloponnese, characterised by smoothly rising Holocene sea level curves. This abrupt relative sea level rise could, thus, be attributed to local tectonics (Kraft, 1975, 1977). Tide gauge data, during a period of 15 years before the 1986 Kalamata earthquake, also suggest subsidence of the head of the Messenian Gulf ('*Kalamata Station*'), at a very high rate of 9.2 mm/yr (Flemming and Woodworth, 1988). A more recent model, however, that also considers isostatic readjustment of the crust since the last deglaciation (Lambeck, 1995), inferred that Holocene subsidence of the Pamisos Plain resulted from isostatic rather than tectonic effects.

The present-day tectonics of the Messenia Peninsula is evidenced by the macroseismic effects of numerous earthquakes (Galanopoulos, 1947, 1955; Lyon-Caen et al., 1988;

Mariolakos et al., 1990). The recent 1986 Kalamata earthquake (M =5.5 or 5.8) is the best studied. This earthquake is attributed to a segment of a NNW-SSE striking *en echelon* fault system, of ca. 1000 m minimum accumulated throw during the Quaternary (Lyon-Caen et al., 1988; see Fig. 1.1). The event, resulting from E-W oriented axis of maximum horizontal extension ($\sigma 3$), was accompanied by co-seismic displacements of up to 150 cm.

1.4.5.5 Mani Peninsula: The Mani Peninsula is the seaward prolongation of the NNW-SSE striking Taighetos mountain range, a 'megahorst' that neighbours the Megalopolis Graben further NW (Dufaure, 1965) (Fig. 1.1). These two units are bounded by a NNW-SSE striking normal fault, that dips to the NE along the Taighetos mountain front and towards the SW further north, along the Megalopolis Basin margin (Mariolakos et al., 1985). This fault geometry was interpreted as scissor-faulting, (Mariolakos et al., 1985), similar to major basin-bounding faults in the central Greece and the Corinth area (Roberts and Jackson, 1993). Fytrolakis (1991) inferred a scissor-fault geometry of smaller NNW-SSE faults further south, in the central part of the Mani Peninsula. Kelletat and Gassert (1975, after Kelletat et al., 1976, 1978), located an area of maximum uplift in the NW part of the Mani Peninsula, with >400 m accumulated Quaternary uplift (Fig. 1.9.d). Southward submergence of Pleistocene terraces was interpreted as suggesting inversion in the direction of movement, with uplift succeeded by subsidence during late Quaternary time. The same authors, based on the pattern of terrace deformation, inferred eastward tilting and gradual southward subsidence of the Mani Peninsula. This can be visualised as the result of eastward rotation around a southward-dipping axis, parallel to the long axis of the peninsula (Kelletat et al., 1976). By contrast, Mariolakos et al. (1985), based on morphotectonic evidence, infered westward tilting of the peninsula. The Mani Peninsula is cut by penninsula-parallel (N-S and NNW-SSE) and cross-peninsular normal faults (E-W to ENE-WSW), that partly controlled the deposition of Pleistocene fanglomerates and breccias (Dufaure, 1977; I.G.M.E., 1980b). Cross-peninsular, E-W faults in the central-western part of the peninsula were interpreted as younger than the NNW-SSE to NNE-SSW faults (Fytrolakis, 1991). Armijio et al. (1992), however, interpreted the N-S faults as active during the Holocene; these faults were thought to be responsible for the destructive Sparta earthquake of 464 BC. The same workers inferred slip rates ranging from 0.1 to 2-3 mm/yr along these faults. The focal mechanism of the 1986 Kalmata earthquake further east (Lyon-Caen et al., 1988), as well as regional neotectonic syntheses (Angelier et al., 1982), suggests E-W oriented maximum horizontal extension during the Pleistocene-Holocene, that activated N-S normal faults.

A pediment surface is very well preserved in the western-northwestern parts of the Mani Peninsula. This surface was correlated with the Pliocene-Pleistocene boundary by Kelletat et al. (1976, 1978), whereas Dufaure (1977) interpreted it as Late Miocene (Pontian) in origin. Pleistocene marine terraces in the Mani Peninsula were researched by various workers (Petrochilos, 1953; Kelletat et al., 1976, 1978; Dufaure, 1977; Fytrolakis, 1991; Bassiakos, 1993). Their number varies locally, depending on the vertical movements of individual fault-bounded blocks (Kelletat et al., 1976, 1978; Dufaure, 1977, Fytrolakis, 1991). Most Pleistocene terraces in the Mani Peninsula are erosive, so their dating and correlation are tentative.

Despite the relative scarcity of terrace-covering sediments, a potential record of Pleistocene relative sea level change may be present in the numerous caves of the Mani Peninsula, one of the most intensely karstified areas in Greece. The Dhiros cave complex, in particular, the biggest known in Greece, evolved in close association with Quaternary sea level change (Petrochilou, 1964; Bassiakos, 1993). Many caves and rock-shelters in the Mani Peninsula accommodated human activity during Palaeolithic and Neolithic (Pisios, 1989).

A list of submerged archaeological sites was published by Petrochilou (1964). Flemming (1968b, 1972, 1978), also based on archaeological data, concluded that Mani Peninsula subsided *en masse* during late Holocene time. Contours of equal subsidence follow a NNW-SSE oriented pattern, consistent with the main fault trend in the area (Fig. 1.5.D).

1.4.5.6 Eastern Lakonia Peninsula: Kelletat et al. (1976, 1978) interpreted this peninsula (Figs. 1.1, M.2: back-pocket) as comprising alternating, NNW-SSE trending areas of Quaternary uplift and subsidence (Fig. 1.5.C). Starting from the east, the Eurotas Plain is described as subdued relative to its surroundings, although uplifted in absolute terms. The western coast of the Eastern Lakonia Peninsula was uplifted, whereas the eastern coast subsided continuously during the Quaternary. The Eastern Lakonia Peninsula is viewed as been gradually inclined to the S "*but neither with constant tilt, nor as a uniform fault block*" (Kelletat et al., 1976, p.458).

The Eastern Lakonia Peninsula is cut by NW-SE and NE-SW (up to ENE- WSW) striking faults (I.G.E.Y., 1970; Kelletat et al., 1976, 1978; I.G.M.E., 1980; Mariolakos et al., 1985). The same fault directions are present within Kythera Island (Lyberis et al., 1982; see Fig. 1.1) and in the NNW-SSE trending, submarine Kythera-Antikythera Ridge (Vittori et al.,

1981; Angelier et al., 1982; Lyberis et al., 1982; Mascle et al., 1982). These normal faults dissect the Eastern Lakonia Peninsula into distinct blocks that evolved semi-independently. The northern part of the peninsula underwent continuous uplift during the Pleistocene, whereas the southern part underwent minor uplift and possibly temporary subsidence (Kelletat et al., 1976). The overall pattern of Quaternary deformation is similar to that of the Mani Peninsula, but more complicated (Fig. 1.5.C). The above authors inferred fold-like deformation in the area near Neapolis-Elaphonisos (Fig. 1.1).

The uppermost erosional surface is prominent in many of the uplifted parts in the western coast of the Eastern Lakonia. This surface was dated as Late Pliocene-early Pleistocene by Kelletat et al. (1976, 1978), although Theodoropoulos (1973) and Dufaure (1977) inferred a Late Miocene age. The absence of this surface from southern areas (e.g. Neapolis, Elaphonisos) was taken to imply that these areas were submerged during the Late Pliocene-early Pleistocene (Calabrian) (Kelletat et al., 1976). Offshore facies in the Eastern Lakonia Peninsula contain well dated early Pleistocene fauna and nannoplankton (Keraudren, 1970, 1971; Frydas, 1993), including the bivalve, *Arctica islandica,* characteristic of an early Pleistocene age (Table 1.1). As in the other peninsuale of the Southern Peloponnese, the maximum accumulated Quaternary uplift is observed in the NW part of the Eastern Lakonia Peninsula (Kelletat et al., 1976, 1978; see Fig. 1.5.C).

Late Quaternary terraces are well preserved in the Eastern Lakonia Peninsula, intercalated with subaerial deposits (Keraudren, 1970, 1971; Kelletat et al., 1976, 1977; Kowalczyk et al., 1992). Two distinct "Tyrrhenean" terraces are present, correlated with the "Eutyrrhenian" and the "Neotyrrhenian" sea level cycles, respectively. Descriptions of the sedimentology and mollusc fauna of these deposits that commonly include the characteristic gastropod, *Strombus bubonius* (see Table 1.1), were published by Keraudren (1970, 1971) and Kowalczyk et al. (1992). Alluvia intercalated between "Eutyrrhenian" and "Neotyrrhenian" deposits were dated with lithic technologies (Kowalczyk et al., 1992).

According to Theodoropoulos (1973), the Holocene development of the area is characterised by a "*Flandrian transgression*" (p. 466) and subsequent sea level oscillations. Uplifted sea level markers, of inferred Holocene age are abundant, including marine notches (Keraudren, 1970, 1971) and conglomerates (Kowalczyk et al., 1992). Flemming (1968b, 1972, 1978) concluded that the Eastern Lakonia Peninsula subsided during the late Holocene, however, at a slower rate in comparison with the neighbouring Peninsulae (Mani, Argolis). The inferred spatial pattern of late Holocene subsidence in the Eastern Lakonia Peninsula was

also different compared with the neighbouring peninsulae (Mani, Argolis). Equal subsidence contours are oriented in a N-S direction, influenced by the uplifting Antikythera Range, farther south (Flemming, 1972, 1978; see Fig. 1.5.D). The Antikythera Island moved independently of the Southern Peloponnese and in connection with the western Crete during the late Holocene (Early Byzantine times; Pirazzoli et al., 1982). Kraft et al. (1977) deduced a gently sloping relative sea level curve for Eurotas Plain, indicative of a smooth Holocene sea level rise. This was interpreted as suggesting that the latter area was tectonic 'stable'. Lambeck's (1995) results, after consideration of the isostatic effect of the last deglaciation, agree with the latter interpretation.

1.5 THIS STUDY

As mentioned in the introduction, this study focuses on the sedimentation and landscape evolution of Messenia and Eastern Lakonia Peninsulae (Fig. 1.1) during Pliocene-Quaternary time. Sedimentological and geomorphological evidence is presented and analysed with reference to glacio-eustatic, tectonic, and climatic controls. The following section introduces some basic concepts that underlie the approach followed.

1.5.1 SEA LEVEL INDICATORS AND RELATIVE SEA LEVEL CHANGE

1.5.1.1 Sea level indicators: Sea levels of the past (before instrumental recording) can be inferred by various sea level indicators, i.e. characteristic markers of a former sea surface, or other associated surfaces. Numerous types of sea level indicators have been proposed; some are correlated with the mean sea level, or with other characteristic levels within the tidal range, whereas others allow the correlation of a site with a distinct sub-environment of the shoreface zone (Van de Plassche, 1986a). Sea level indicators can be divided into the following categories:

1.5.1.1.1 Biological/ecological indicators: e.g. barnacles (Van de Plassche, 1986a), ostracods (Van Harten, 1986), boring bivalves, with the *Lithophaga* as a characteristic example (Stiros et al., 1992), other marine molluscs (Petersen, 1986), vermetid gastropods (Laborel, 1986), coralline algae (Adey, 1986), coral reefs (Hopley, 1986b), terrestrial vegetation (Van de Plassche, 1986a), and many others.

1.5.1.1.2 Sedimentological indicators: e.g. Beachrocks (Alexandersson, 1972; Hopley, 1986a), clastic foreshore facies (Kraft et al., 1975, 1977; Postma and Nemec, 1990), characteristic diagenetic features (Land, 1970; Longman, 1980; Coudray and Montaggioni, 1986; Pirazzoli et al., 1982, 1989), ooids (Kump and Hine, 1986).

1.5.1.1.3 Erosional features: e.g. marine terraces and abrasion surfaces (numerous references), marine notches (Pirazzoli, 1986; Pirazzoli et al., 1982, 1989; Stiros et al., 1992).

1.5.1.1.4 Anthropogenic indicators, usually, but not exclusively, of Holocene palaeoshores, e.g. shell middens accumulated by human consumers (Martin et al., 1986), constructions for accommodation of human activities related to the sea, or positioned in relation to past sea levels (Flemming, 1968b, 1972, 1978; Dermitzakis, 1972; Kraft et al., 1975, 1978; Kambouroglou, 1989; Stiros, 1988).

The above categories are not mutually exclusive, since all processes that operate in the coastal zone influence each other within the same dynamic system; this makes the study of former sea levels a multidisciplinary subject. Table 1.3 lists some commonly used sea level indicators (with the exception of anthropogenic ones):

1.5.1.2 Relative sea level change: Any relative sea level change is the net result of many functions that possibly operate contemporaneously. The isolation of distinct components and the assessment of their relative contribution to relative sea level change is difficult, especially when based on incomplete evidence. As a general rule, high-frequency low-amplitude components (e.g. meteorological, hydrological, oceanographic) are excluded from studies with a geological time scale. These studies, instead, focus on longer-term components of relative sea level change, i.e. 'eustasy' (absolute change of global sea level) and 'tectonics' (sea level change resulting from land movement). Isostatic effects, although present during the whole of the Quaternary, can be taken into account only in studies of latest Pleistocene-Holocene sea levels. This is because the growth and melting history of large glaciers, which exercised the major control on isostatic readjustment on a global scale, are relatively well constrained only in respect to the last glacial cycle (Lambeck, 1995).

1.5.2 METHODOLOGY

The following procedures were followed during this study:

1) Field mapping and logging of Pliocene-Pleistocene sediments and terraces: Standard sedimentological techniques were applied for logging and sampling of sections and collection of palaeocurrent evidence (Tucker, 1992). Sediments were also sampled for coral, initially expected to yield precise geochronological results (U-series techniques). However, the original aragonite of all collected samples was recrystallised to low Mg-calcite, rendering them unsuitable for U-series dating.

2) Altimetric and geomorphological evidence (erosion, soil coverage, etc.) was also gathered. Analysis of the 1:50,000 H.A.M.G.S. topographical maps of the area was carried out, using standard geomorphological techniques (e.g. Defontaines and Chorowicz, 1991; Defontaines et al., 1994; Keller and Pinter, 1996; Ahnert, 1998).

3) Data on neotectonic faults and joints were collected, using standard techniques of microtectonic analysis (McClay, 1988).

4) Laboratory studies involved examination of thin sections of Plio-Quaternary sedimentary rocks, mineralogical analysis of bulk rock samples and coral (X-ray diffraction).

5) Planktic and benthic foraminifera and nannoplankton were also sampled and identified, for dating and palaeobathymetric information (Blank-Vernet, 1969; Murray, 1973; Amorosi et al., 1998). The biostratigraphic part of the study was carried out in the University of Patras (foraminifera: S. Tsaila; nannoplankton: D. Frydas).

This study synthesises sedimentological, petrological, biostatigraphic, neotectonic and geomorphological evidence towards a new interpretation of the sedimentary and tectonic evolution of the Messenia and Eastern Lakonia Peninsulae during the Pliocene-Quaternary. A relative stratigraphy is proposed independently for Messenia and Eastern Lakonia, based on the interpretation of the Plio-Quaternary sedimentary record in terms of sea level and tectonic controls (Kourampas and Robertson, 2000). This facilitated a correlation between the two peninsuale; the first such correlation scheme proposed since the late 70's (Kelletat et al., 1976; Dufaure, 1977; see above) and the first to incorporate a sequence-stratigraphic approach on the Quaternary of the Southern Peloponnese.

1.6 STRUCTURE OF THE THESIS

Chapter 2 focuses on the neotectonics and geomorphology of the Messenia Peninsula. The main fault sets are introduced and their control on the relief of the peninsula is discussed. The main generations of Late Tertiary-Quaternary surfaces of subaerial erosion and marine terraces are also described, together with the drainage of the peninsula and its relation to neotectonic faulting and other controls. A model of drainage evolution is proposed, taking into account the normal faulting and Plio-Quaternary sea level change.

Chapter 3 describes and interprets Plio-Quaternary suaberial and shallow-marine sediments of the Messenia Peninsula. The biostratigraphic, geological, sedimentological and geomorphological evidence that supports the dating scheme adopted in this work is explained. Detailed descriptions of represenative outcrops of each recognised stratigraphic unit are them given, followed by their paleoenvironmental interpretation. The chapter concludes with a synthesis of the sedimentary and tectonic evolution of the Messenia Peninsula during the Pliocene-Quaternary, linking sedimentological evidence with geomorphological and neotectonic evidence presented in Chapter 2.

Chapter 4 focuses on the neotectonics and geomorphology of the Eastern Lakonia Peninsula. The structure of this follows closely that of Chapter 2, starting with the description of the main neotectonic fault sets in the Eastern Lakonia, then discussing their control on the relief (i.e. fault-bounded blocks). Late Tertiary-Quaternary surafces of subaerial erosion and marine terraces are then described and examples of morphological differences between fault-bounded blocks are given. The drainage of the Eastern Lakonia Peninsula is also described, with the emphasis on its response to normal faulting and relative sea level change.

Chapter 5 describes and interprets Pliocene-Pleistocene suaberial and shallow-marine sediments from the Eastern Lakonia Pensinsula. As in Chapter 3, evidence for relative dating is given first and detailed descriptions of identified stratigraphic units follow, including a palaeonevironmental interpretation. This chapter concludes with a synthesis of the Pliocene-Quaternary sedimentary and tectonic evolution of the Eastern Lakonia Peninsula, incorporating evidence presented in this and in the preceding chapter.

Chapter 6 focuses on the petrology and diagenesis of Pleistocene shallow-marine and subaerial sediments and soils from both the Messenia and Eastern Lakonia Peninsulae. The main microfacies present in both areas are described and interpreted in terms of depositional

environments and diagenesis. A synthesis of the diagenetic evolution of shallow-marine sediments is then presented, correlating the successive diagenetic stages with the relative sea level history of Quaternary shorelines. The main types of caliche present in the areas of study are described and discussed in relation to the relative age of the host sediment/surface and the indicated palaeoclimate. A relative stratigraphy of main caliche types in the Messenia and Eastern Lakonia Peninsulae is proposed.

Chapter *7* starts with a correlation between the two peninsulae, synthesising evidence presented in the previous chapters. The marine terraces are interpreted in terms of relative sea level controls and characteristic shallow-marine successions are correlated with particular stages of relative sea level change. The rates of uplift of the Messenia and Eastern Lakonia Peninsulae are discussed in the context of limitations posed by the lack of firm chronostratigraphic control. The chapter finishes with a model for the evolution of both the Messenia and Eastern Lakonia Peninsulae during the Pliocene-Pleistocene. This model highlights similarities resulting from common background controls (regional uplift of the fore-arc, eustatic sea level change) and differences, resulting from the location of each peninsula in relation to the active plate boundary, and local faulting.

Chapter 8 compares the Messenia and Eastern Lakonia Peninsulae with areas of similar tectonic setting within the Eastern and Central Mediterranean. These include Crete and Rhodes (central and eastern part of the Hellenic fore-arc), Cyprus, and Calabria-Sicily (Tyrrhenian Arc). The areas of study are also compared and contrasted with the well-studied graben of the Corinth Gulf, further north, a back-arc area that has experienced high rates of extension during the Late Pliocene-Quaternary.

Finally, ***Chapter 9*** lists the main conclusions of this work, followed by some suggestions for further study.

CHAPTER 2: GEOMORPHOLOGY OF THE MESSENIA PENINSULA

2.1 INTRODUCTION

This chapter focuses on the Late Tertiary-Quaternary faulting and landforms in the Messenia Peninsula. The fault pattern and the segmentation of the peninsula into fault-bounded blocks are described first, followed by the principal morphological surfaces and the drainage. At last, controls of normal faulting, Pliocene-Quaternary sea level change and the influence of climate on the development of these landforms are discussed.

2.1.1 Regional plate tectonic setting: The Messenia Peninsula, situated ca. 60 km NE of the western segment of the Hellenic Trench (Ionian trenches), forms part of the forearc of the northward-dipping Aegean subduction system (e.g. McKenzie, 1978; Le Pichon and Angelier, 1979; Figs. 1.1, 1.2). To the west lies the westerly extension of the Mediterranean Ridge, interpreted as an accretionary prism created by subduction of deep-sea sediments of the African plate beneath the Eurasian plate (Kastens et al., 1993; Chaumillon and Mascle, 1995, Robertson and Kopf, 1998; see Chapter 1, Figures 1.1, 1.2). In keeping with this regional trend, compression apparently continued until the end of Early Pliocene time within a few kilometres offshore from the Western Peloponnese (e.g. Strophades Islands; Lyberis and Bizon, 1981; L.H. Royden, pers. comm., 1998), but later in the Plio-Quaternary the plate boundary shifted to the Mediterranean Ridge further offshore (Kastens et al., 1993; Chaumillon and Muscle, 1995; Robertson and Kopf, 1998).

During the Plio-Quaternary, the Messenia Peninsula underwent regional uplift, as part of the Peloponnese as a whole (Dufaure, 1977; Kelletat et al., 1976; see Chapter 1). This uplift is thought to relate to underplating of the overriding Eurasian plate margin by buoyant accreted sediments (Le Pichon and Angelier, 1979), or to result from changes in the angle of underthrusting of the Peloponnese by the subducting slab (Berkchemer and Kowalczyk, 1978; Hatzfeld et al., 1989), or both processes. Normal faulting, related to generally E-W extension in the western segment of the Aegean Arc (Armijio et al, 1979; Lyon-Caen et al., 1988), is superimposed on regional uplift of the Peloponnese.

Today, the area remains seismically active (e.g. Galanopoulos, 1947), as shown by the 1986 Kalamata earthquake (Hatzfeld et al., 1990; see Figure 1.4.a).

1.2 Tethyan Basement: The Tethyan bedrock of the Messenia Peninsula comprises the 'External Hellenides' zones of Tripolis and Pindos (Fytrolakis, 1971; Jacobschangen et al., 1978; I.G.M.E., 1980a,b; see Figure 2.1). The thrust-contact of the Pindos Zone over the Tripolis Zone is a prominent NNW-SSE trending tectonic lineament (Figs. 2.1, 2.2): Ribbon-radiolarite, thin-bedded pelagic limestone and 'flysch' constitute the Pindos Zone nappes, thrusted over Upper Eocene-Oligocene 'flysch' and Eocene nummulitic limestone of the Tripolis Zone. The latest thrusting, of Middle Miocene age (Jacobschangen et al., 1978; Mariolakos et al., 1994), also affected clast-supported conglomerates ("*Messenian Conglomerate*"), of presumably Late Oligocene age, interpreted as a "molasse", deposited in the foreland of advancing Pindos thrust-sheets (see Chapter 3).

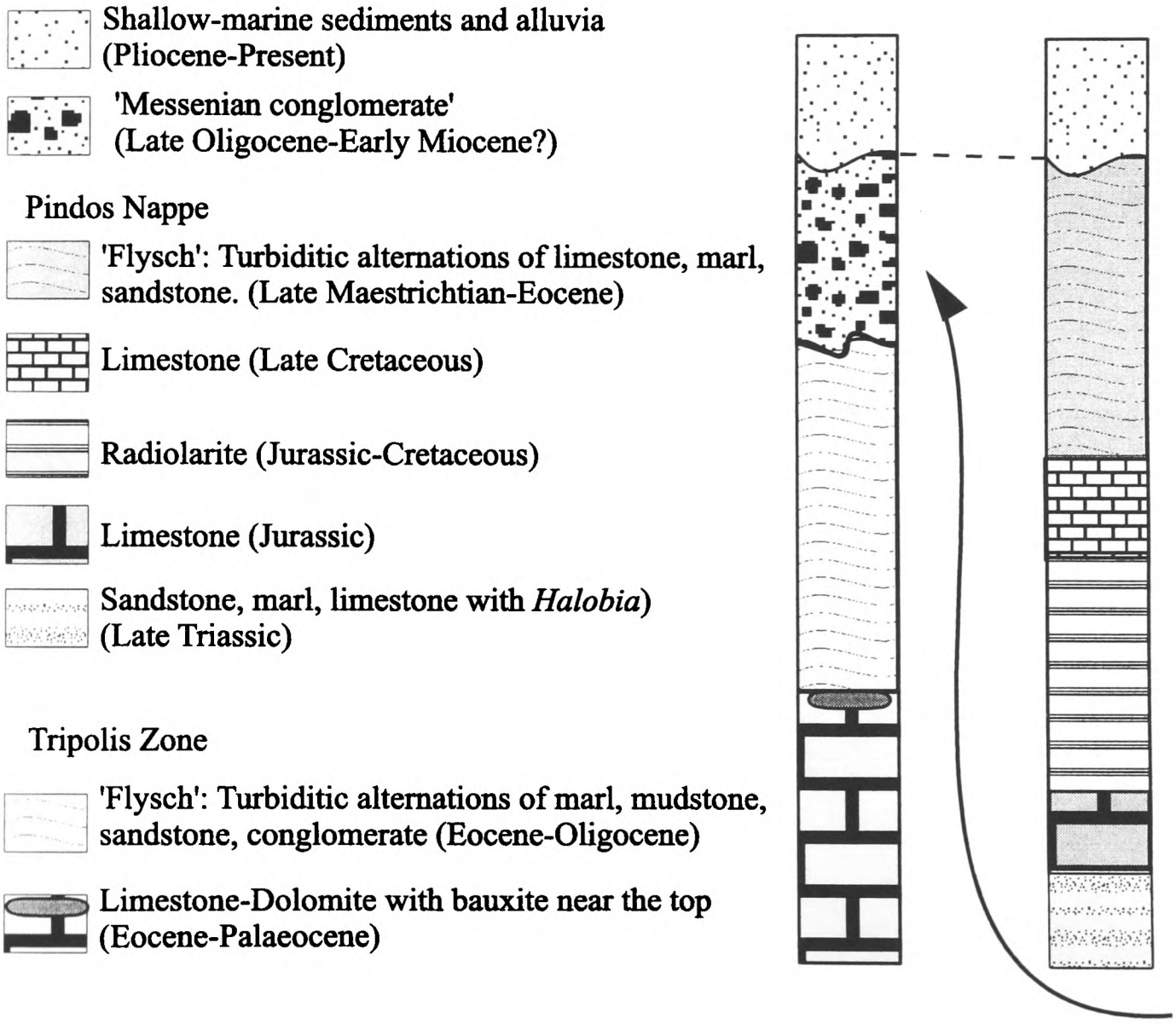

Figure 2.1: Outline stratigraphic column of the Messenia Peninsula, with the emphasis on the Tethyan bedrock underlying the Pliocene-Quaternary sediments. The Tethyan bedrock comprises lithologies of the Tripolis Zone (neritic carbonates, turbiditic alternations of mudstone/sandstone), and lithologies of the Pindos Zone (Pindos thrust sheets: pelagic limestones, radiolarites, turbidites). The Pindos zone thrust sheets were thrusted over the Tripolis Zone in Early-Middle Miocene time. Sources: Fytrolakis (1971), Jacobschangen et al. (1978), I.G.M.E. (1980a,b), Degnan and Robertson (1994).

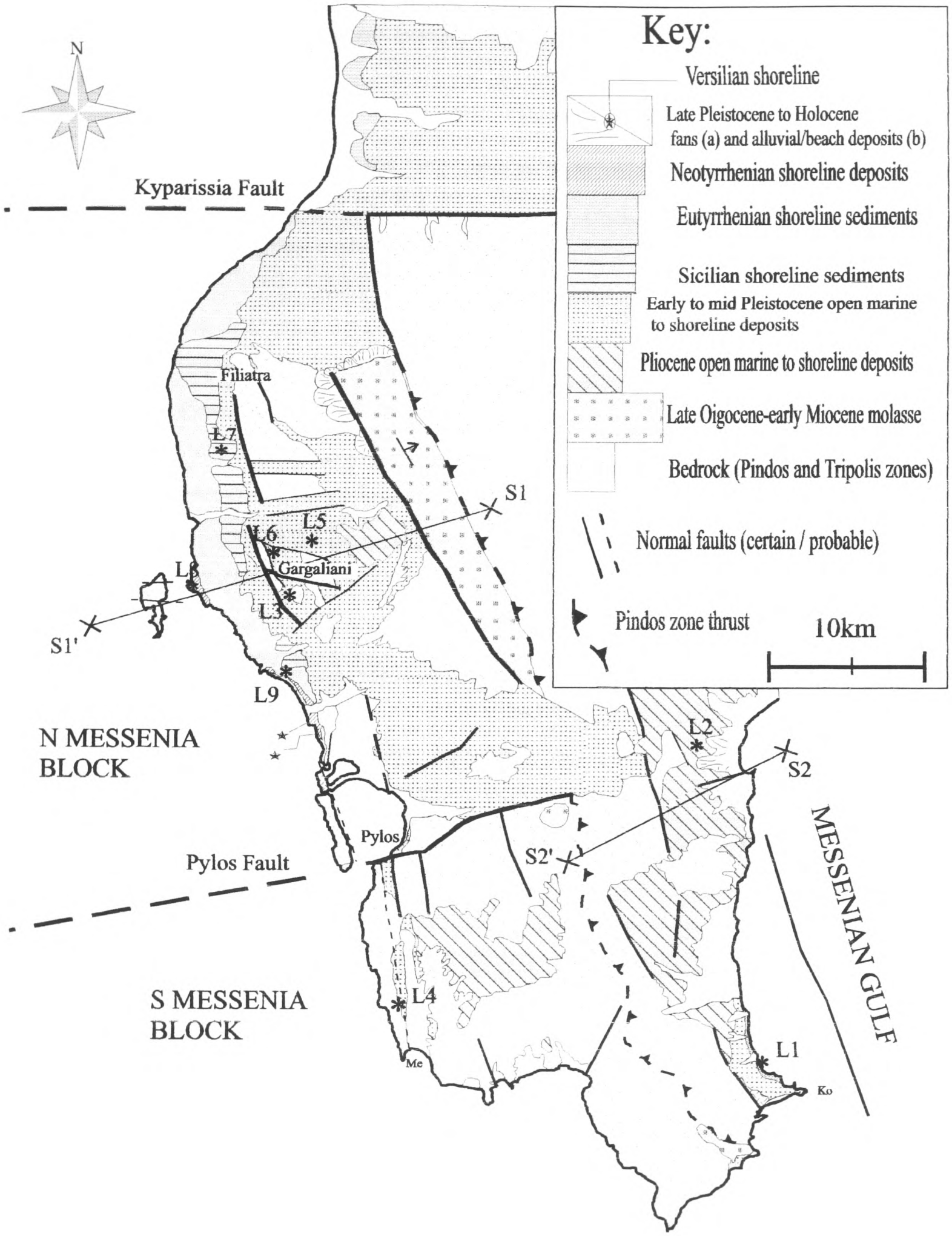

Figure 2.2: Outline geological map of the Messenia Peninsula. Note the subdivision of the area into two tectonic-geomorphological segments, the Northern and the Southern Messenia Blocks.

2.2 NEOTECTONIC STRUCTURE

The Messenia Peninsula is cut by several mappable sets of faults (Fig. 2.2), as indicated on the I.G.M.E. maps (1980a,b). During this work, previously published information was supplemented by regional and local mapping and collection of outcrop-scale kinematic data on fault orientation, displacement and sense of movement (Fig. 2.3). The main fault trends are as follows:

2.2.1 NNW-SSE faults: These long, parallel faults, with the greatest observed cumulative throw (up to >120 m for the Gargaliani-Filiatra Fault; Figs. 2.2, 2.3, M.1), are oriented parallel to the regional strike of pre-existing Tethyan structures (thrusts, fold-axes), and are also parallel to a major graben within the Kalamata-Messenia Gulf to the east (Fig. 1.1). The major NNW-SSE fault trends are inferred to re-activate zones of weakness within the Tethyan basement. However, there is no evidence of reactivation of the major NNW-SSW, Tethyan, Pindos thrust front (Figs. 2.2, M.1) as a Plio-Quaternary extensional lineament. The NNW-SSE faults commonly comprise left-stepping *en echelon* sets, which can be grouped together into up to 20 km-long fault zones (Figs. 2.2, M.1). Principal fault zones in Messenia coincide with major geomorphic boundaries, in the form of scarps that bound pediment systems (see below; Figures 2.6, 2.7, 2.8). Mesoscopic faults and joints of the NNW-SSE fault set (average strike: 175°) are the dominant in bedrock and late Pleistocene sediments (Fig. 2.3). Their relative abundance is reduced in early Pleistocene sediments. Given the dominance of this set in Late Pliocene sediments of the Kalamata Basin, east of the area of study (Zelilidis and Doutsos, 1991; see Figure 1.1), their origin was probably pre-Pleistocene. In accordance with these observations, dominant NNW-SSE faulting in late Pleistocene sediments can be attributed to reactivation of deeper, pre-existing structures. As indicated by striated fault scarps, faults of this set were also activated by oblique slip (Fig. 2.3.d); however, the time of their activation cannot be determined, since striated scarps were found exclusively in pre-Pliocene bedrock (commonly nereitic limestone of the Tripolis Zone).

2.2.2 ENE-WSW (to E-W) faults (e.g. Kiparissia and Pylos Faults; Figs. 2.2, M.1): These faults divide the Messenia Peninsula into two contrasting tectonic-morphological blocks: the northern boundary of each block is defined by the Kiparissia Fault and the Pylos Fault, respectively (see below; Figure 2.2). The large ENE-WSW faults, up to 5-7 km long (e.g. Pylos Fault), are seen as major transverse structures, related to cross-strike segmentation of the Neogene Aegean Arc (although these, too, might reactivate older, Tethyan structures). In NW Messenia, the dominant NNW-SSE fault trend is offset by E-W to ENE-WSW trending

faults (Figs. 2.2, M.1). Large ENE-WSW faults in bedrock were probably formed in pre-Pliocene time (see below), but these faults were active throughout the Quaternary (see Figure 2.16).

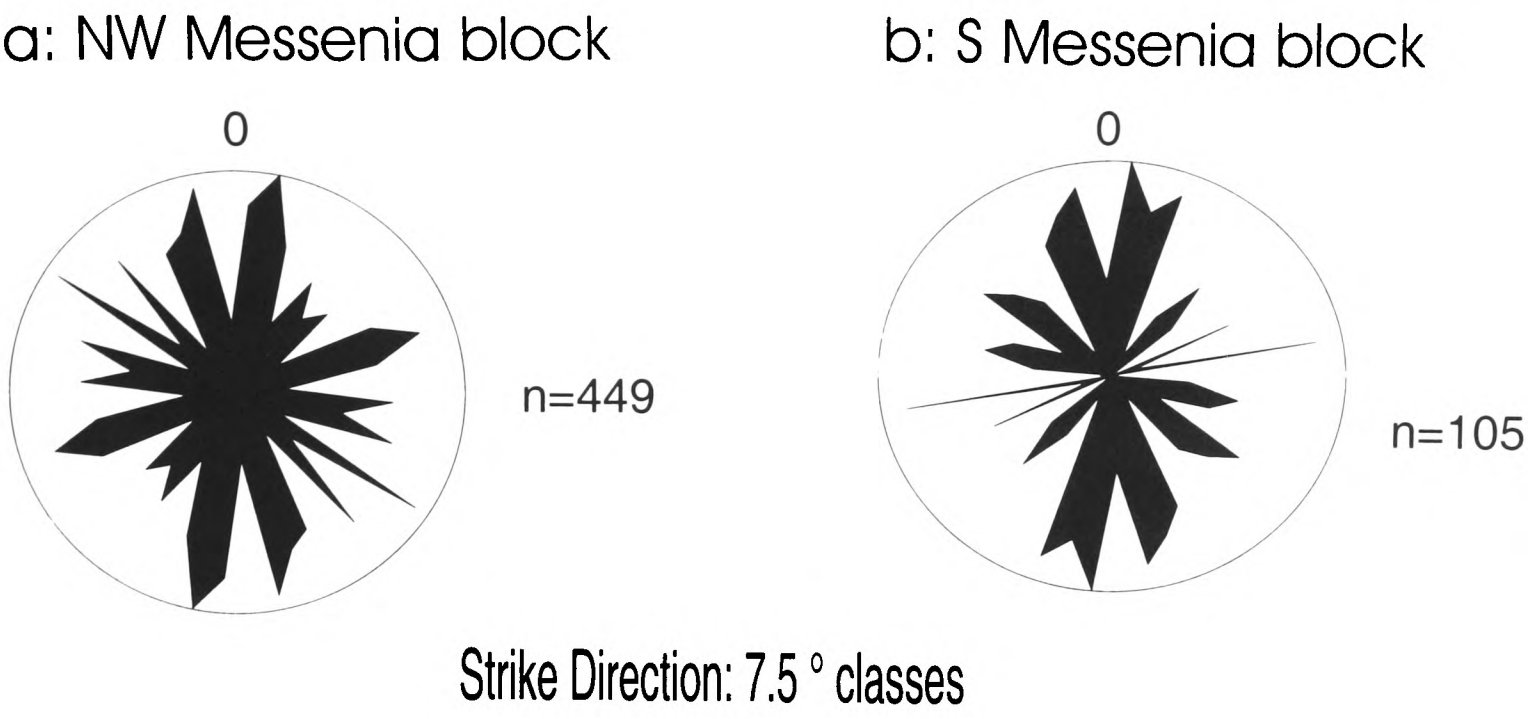

Figure 2.3: Stereoplots of fault data from the Messenia Peninsula. **a)** Strike directions of faults in the Northern Messenia Block. Note the variable directions, with predominant ca. N-S (peninsula-parallel, from NNW-SSE to NNE-SSW) and ca. E-W (cross-peninsular, from ENE-WSW to ESE-WNW) trends. **b)** Strike directions of faults in the Southern Messenia Block. The main fault trends are the same as in the Northern Messenia Block, but here near N-S faults are more prominent. **c)** Planes (great circles) and poles (crosses) of normal faults from the Messenia Peninsula. Arrows show trend and plunge of measured slicknsides. The measured fault trends correspond to the mapped N-S and E-W transverse faults (Fig. 2.2). The slickenside data indicate that oblique slip took place along both N-S and E-W faults (see text).

In addition, there are many smaller (up to 1-2 km) "transverse" faults that cut both Pliocene-Pleistocene sediments and bedrock, accommodating local extensional stress variations (e.g. between Filiatra and Gargaliani; Figures. 2.2, M.1). "Tyrrhenian" sediments in the Strophades Islands (a few kms offshore the Western Peloponnese: see Fig. 1.2) are cut by faults of this set (Lyberis and Bizon, 1981). As indicated by a few low-angle slickensides, ENE-WSW faults were also reactivated by oblique slip (Fig. 2.3.c), but the timing of their reactivation remains uncertain, since striated fault-scarps are found in bedrock limestone. These faults are still potentially active under oblique slip, as the present-day regime is generally E-W extension (Lyon-Caen et al., 1988; Hatzfeld et al., 1989, 1990; Armijio et al., 1992).

2.2.3 NNE-SSW faults: These faults, with 15° average strike, are the commonest outcrop-scale faults in early to middle Pleistocene sediments within the Messenia Peninsula (Fig. 2.3), as well as in the Kalamata-Avramio Basin further east (Zelilidis and Doutsos, 1992) (see Fig 1.1). Most of these faults are too small to show on a regional map of the area (Figs. 2.2, M.1). NNE-SSW faults also occur within longer NNW-SSE *en echelon* systems, often associated with earthquake activity (e.g. Kalamata Fault on the eastern flanks of the Kalamata graben; Lyon-Caen et al., 1988; Fig. 1.1). The seismically active NNE-SSW faults apparently constitute the youngest fault-population in the area (Zelilidis 1988; Zelilidis and Doutsos, 1992). These faults can be related to Quaternary-Recent extension of the SW Hellenic Arc (Lyon-Caen et al., 1988; Hatzfeld et al., 1990; Armijio et al., 1992). Only a few mesoscopic faults of this set were reactivated by oblique slip (Fig. 2.3.c). Probably as a result of their younger age, these faults exercise a weaker control on the landscape as compared with faults of other sets (see below).

2.2.4 ESE-WNW faults, generally at right angles to faults of the previous set, are also common in Quaternary sediments and bedrock, on both mesoscopic and macroscopic scales (Figs. 2.2, 2.3, M.1). These faults were also activated by oblique slip, as indicated by striated fault scarps (Fig. 2.3.c). "Tyrrhenian" sediments in the Strophades Islands (Lyberis et Bizon, 1981) and the Kiparissia-Kalo Nero Graben, north of the area studied (Fountoulis and Moraiti, 1994) are affected by faults of this set.

2.2.5 Stress pattern in the Messenia Peninsula: Figure 2.3.c shows plots of slickensided mesoscopic faults in the Messenia Peninsula. Most of these faults cut Tripolis Zone limestone bedrock, but few also affect early Pleistocene sediments. The distribution of slickensides indicates a complex pattern of deformation, involving oblique slip reactivation of faults of all the above sets. It seems possible that this pattern results from transtensional deformation, as suggested by Mariolakos et al. (1985, 1997). Such an effect could also result from axes of minimum and intermediate compression of almost equal value ($\sigma 2 \cong \sigma 3$), similar to that inferred in the fore-arc area of western Crete by Angelier et al. (1982). A recent neotectonic analysis in the areas of Kiparissia, very close to the area of study (Meijier, 1995), concluded that horizontal extension since the middle Pleistocene ranged from ENE-WSW to NNW-SSE. Such a stress field would account for the activation of any fault set in the area. In any case, faults of all the above directions can be considered as geologically coeval over the time scale of Late Tertiary-Quaternary, since they mutually cut each other (Caputo, 1995) (see Fig. M.1). It is possible that occurrence of oblique slickensides on fault-scarps of any of the principal directions reflects internal deformation of faulted blocks, not necessarily consistent with an external applied stress-field.

Caputo (1995) proposed a mechanism for the evolution of coeval extensional joints that could probably be also applied to the evolution of extensional fault systems. As deformation progresses within a fractured block of rock, movement of faults directed perpendicular to $\sigma 3$ (minimum compression) would reduce tension along the latter fault-set; such movement would probably cause faults parallel to $\sigma 3$ to move by oblique slip. A drop of tension across faults perpendicular to $\sigma 3$, however, would increase the relative tension on faults directed perpendicular to $\sigma 2$ (intermediate compression), thus causing them to slip as normal faults; such movement would probably entail oblique slip of faults perpendicular to $\sigma 2$ (see Fig. 2.6). Such temporary swap between the $\sigma 3$ and $\sigma 2$ could reflect the progress of deformation within an extended mass of rock, rather than changes in the external stress field; such changes are highly improbable over the time scale of the last 2-1 Ma (Late Pliocene-Pleistocene; Caputo, 1995).

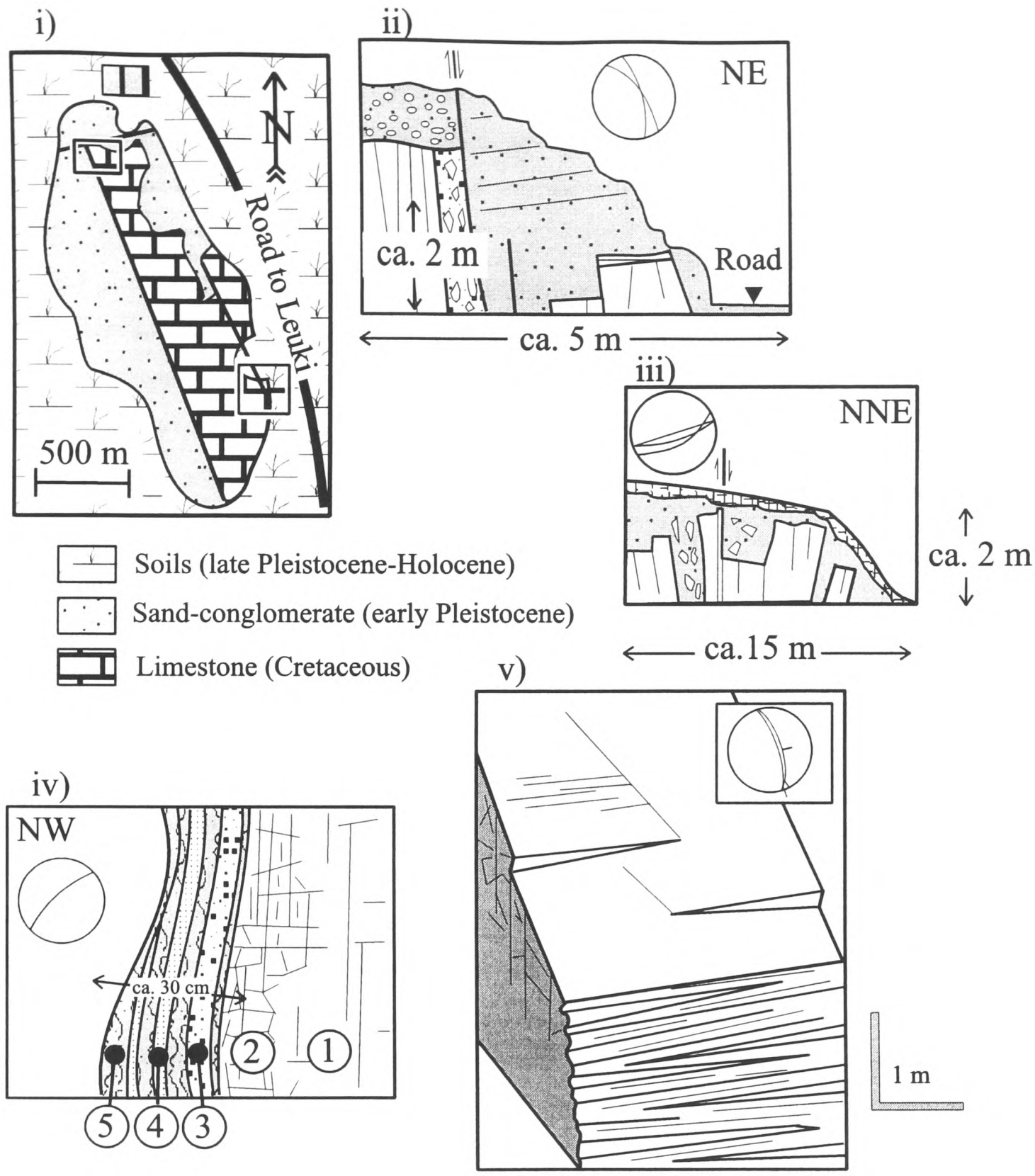

Figure 2.4: Examples of Pleistocene faulting in the Gargaliani area, Northern Messenia Block (for location see Figures 2.6, M.1). **i)** Sketch map of a hill near Gargaliani. Early Pleistocene marine sediments are both in transgressive and faulted contacts with bedrock limestone. Both NNW-SSE faults were active during the Pleistocene. **ii, iii)** Sections across the contact of early Pleistocene marine sediments and bedrock (for location see sketch map). **iv, v)** Faults of uncertain age of activity, but preserving evidence of successive reactivation. **iv:** Schematic section across a NE-SW fault scarp from site (B) (see sketch map). Three successive layers of cemented tectonic breccia (3) and fragmented travertine (4) indicate slip along the fault scarp. These alternate with flowstone carapaces (5), deposited in periods between faulting events. A zone of heavily brecciated bedrock (2) lies between the fault scarp and the bedrock limestone (1). **v:** Sketch of NNW-SSE fault scarps with evidence of normal and oblique slip. The scarp higher up dips at 70° to the ENE and preserves evidence for normal slip (steps) and oblique slip (striations; pitch: 170-160° to the SSE). The scarp in the lower part of the section dips at ca. 80° to the ENE and preserves evidence of oblique slip, in the form of striations (pitch: 174° to the SW). Oblique slip was probably the latest movement along these surfaces.

2.3 SURFACES OF SUBAERIAL EROSION AND MARINE TERRACES

The Messenia Peninsula exemplifies a piedmont benchland (*sensu* Ahnert, 1995), with a series of successively younger surfaces at successively lower altitudes, from the internal mountain range to the present-day coastline (Figs. 2.5, 2.6, 2.7, 2.8, 2.9). From older to younger, the following main surfaces were distinguished in the northern part of the Messenia Peninsula, where the morphological profiles are best preserved (Kourampas and Robertson, 2000):

1) Uplifted pediments and pediplains, of Late Tertiary age,
2) Pediments of Late Pliocene age,
3) Marine terraces of early and early-middle Pleistocene age,
4) Marine terraces of middle and late Pleistocene age,
5) Marine abrasion platforms of Holocene age.

2.3.1 Uplifted surfaces of subaerial erosion (Late Miocene-Pliocene)

The number of these surfaces varies locally within the Messenia Peninsula, in relation to intensity of normal faulting, uplift, denudation and fluvial erosion since their formation. These surfaces are best preserved on Pindos Zone limestone and Late Oligocene-Early Miocene "*Messenian Conglomerate*" (Figs. 2.6, 2.7, 2.8, 2.9). The highest surfaces are elevated up to 1200 m in the northern part of the Messenia Peninsula; in the southern part of the peninsula, however, their elevation is <500 m (Figs. 2.5, 2.7, 2.8). In the central parts of the Messenia Peninsula these surfaces are commonly preserved as narrow ridges (width: ca. 500-1000 m) of broadly NNW-SSE strike, parallel to the principal tectonic grain (Tethyan fold axes and thrusts, neotectonic faults; see Figs. 2.2, 2.4, 2.9, 2.10) and isolated from each other by deep fluvial incision, locally reaching ca. 500 m in the northern part of Messenia (Fig. 2.8; see below). Lower down, a series of up to 5 uplifted pediments are separated from each other by steep cliffs, locally controlled by NNW-SSE faults (e.g. Kiparissia Mountain Front), as evidenced by the presence of triangular facets, separated by V- shaped incised valleys (Fig. 2.7, 2.10; photograph of the Kiparissia mountian front). Inselbergs occur in the centre of the Messenia Peninsula (e.g. Handrinos; Fig. 2.4, 2.7, M.1), commonly formed on 'Miocene Conglomerate'. These marginal inselbergs are correlated with lower members of the pediment flight further inland (Fig. 2.7). The pattern of incision, with a dense network of steep, deep valleys differentiates this from areas of younger (Late Pliocene-Pleistocene) relief. These uplifted surfaces are incised by multiphase valleys that generally start from the level of the Late Pliocene surface (Figs. 2.10, M.1).

Figure 2.5: Relief of the Messenia Peninsula (3D model of maximum altitudes; contour interval 100 m). The different generations of relief and the segmentation of the Peninsula into a northern and a southern block are shown.

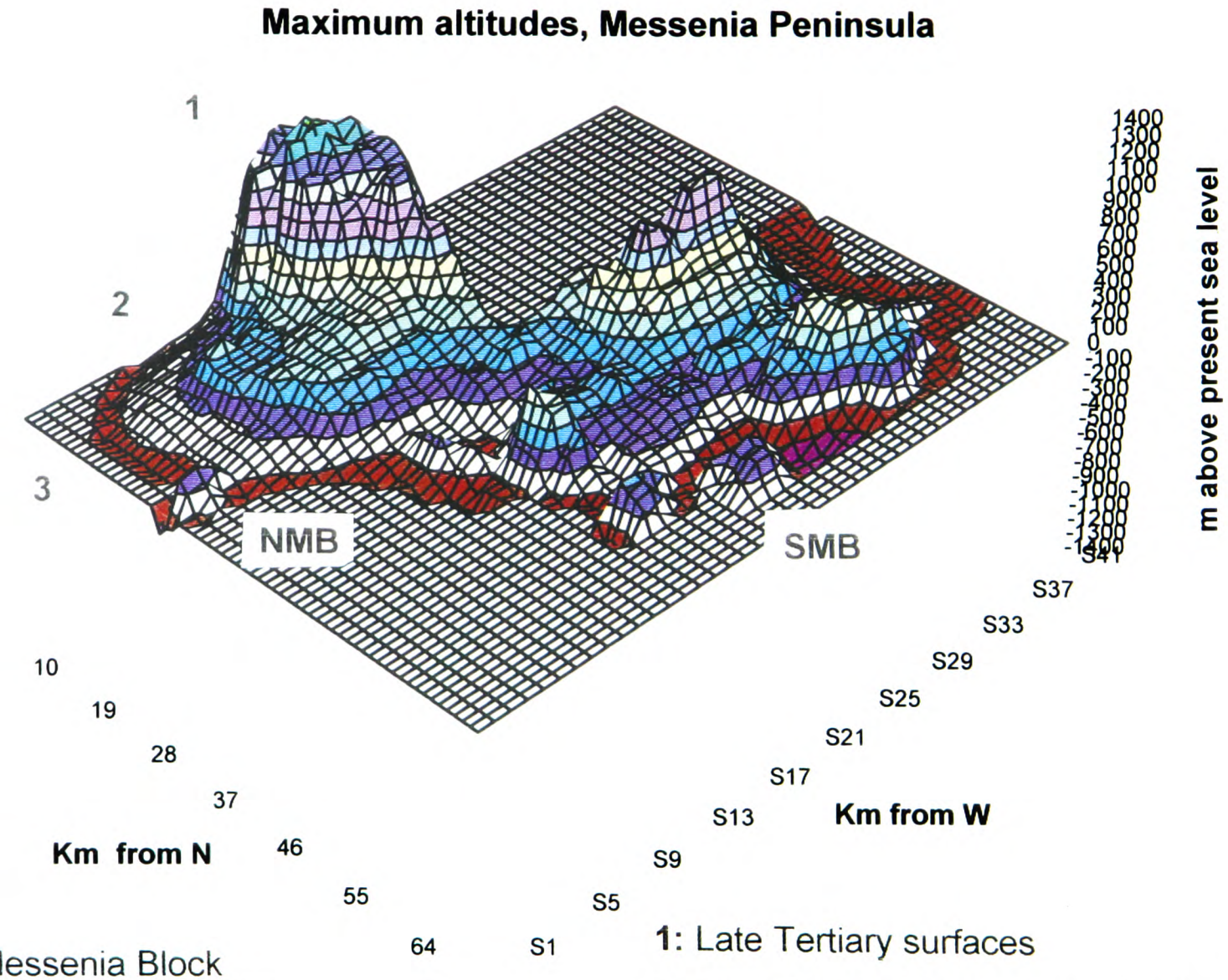

NMB: Northern Messenia Block

SMB: Southern Messenia Block

1: Late Tertiary surfaces

2: Late Pliocene pediment-early Pleistocene terraces

3: Middle-late Pleistocene terraces

Long, broad (up to 500 m), U-, or open V-shaped, valleys ran across the uplifted pediment relief in the NW and western parts of the Southern Messenia (see below; Fig. 2.9, M.1), with valley bottom elevation at ca. 740 m (NW Messenia), probably resulting from pre-Quaternary fluvial incision. These streams were later captured by headward erosion of the Quaternary drainage (see below).

Previous workers suggested a Miocene-Pliocene age for the uplifted pediments/pediplains of the Peloponnese (Dufaure, 1976). These surfaces (including the inselberg relief) can be correlated with similar Miocene-Pliocene surfaces in the central Peloponnese (Arcadia; Riedl, 1977), the Cyclades Islands (Riedl et al., 1982) and northern Greece (Vavliakis, 1981; Psilovikos and Vavliakis, 1982/83; Weingartner and Hejl, 1994), also dated as Late Miocene-Pliocene.

2.3.2 Late Pliocene pediment-early Pleistocene terrace

2.3.2.1 Description: These two surfaces are discussed together because it is not always possible to distinguish them, especially where both are formed on bedrock (Kelletat et al., 1976). These are the most extensive surfaces in the Messenia Peninsula. They are particularly well preserved in the NW Messenia, where they stretch for ca. 27 km, attaining a maximum width of ca. 11km across. In the Southern Messenia, these surfaces are best developed along the eastern coast, stretching for ca. 20 km and with a width of generally <6-7 km (Figs 2.5, 2.7, 2.8, 2.9). Early Pleistocene terraces reach a maximum altitude of ca. 320-350 m in the NW Messenia, whereas in the Southern Messenia, their maximum altitude is ≤ cM.180-200 m (Figs. 2.7, 2.8). The landward boundaries of early Pleistocene terrace(s) and Late Pliocene pediments coincide with the steep cliffs of the Late Miocene-Pliocene pediments (Figs. 2.5, 2.7, 2.9). In areas of typical development (e.g. NW Messenia, near Gargaliani; see Figs. 2.5, 2.7, 2.9), their seaward boundaries coincide with a steep cliff, up to 120-130 m high, eroded in early Pleistocene sediments and bedrock limestone. Elsewhere (e.g. southern and eastern parts of the Messenia Peninsula), early Pleistocene surfaces dip gently down to present sea level, locally interrupted by a few cliffs and terraces (Figs. 2.5, 2.8, 2.9).

The inner parts of this composite surface, correlated with the Late Pliocene pediment, form a gently concave morphology (Figs. 2.6, 2.9), eroded on bedrock limestone and ''flysch'' (Tripolis and Pindos Zones). The outer parts of the composite surface, correlated with the early Pleistocene marine terrace(s), were generally formed on shallow-marine sediments of Late Pliocene-early Pleistocene age (Units 1.5, 1.6, 2.1, 2.2, 2.4; see Chapter 3) and locally

on carbonate bedrock (e.g. Gargaliani area; Figs. 2.3, 2.7). Locally, two or more distinct surfaces of inferred early Pleistocene age are present (e.g. Gargaliani; Fig. 2.6, 2.9, 2.11), separated from each other by low (generally <15-20 m), relatively degraded cliffs. The Late Pliocene pediment and the early Pleistocene terrace(s) are difficult to differentiate, since cliffs that separate them, where present, are generally low, degraded and inconspicuous, with the possible exception of the central part of the Messenia Peninsula (from Pylos to Rhizomilos; see Figs. 2.6, 2.9, A1). There, the altimetric difference between an extensive, inferred Late Pliocene pediplain, and surfaces formed on shallow-marine sands, of inferred early Pleistocene age, is ca. 50-70 m (Fig. 2.6). In most other parts of the Messenia Peninsula, however, these two generations of surfaces cannot be separated. This suggests that the Late Pliocene pediplain was affected by the Latest Pliocene-early Pleistocene marine transgression.

2.3.2.2 Soil cover: The composite Late Pliocene pediment-early Pleistocene terrace(s) are covered with subaerial sediments and soils, suggesting that these surfaces functioned as pediments after their emergence, in early, to early-middle, Pleistocene time. Coalescent alluvial fans, of early Pleistocene, to Holcecene age (Units 3.4, 3.5, 3.8; see Chapter 3), are present locally, in the inland fringes of the surface, especially near normal faults (e.g. east of Gargaliani-Filiatra, west of Petalidhi; see Figs. 2.2, 2.6, 2.9, M.1); fluvial sediments are also widespread. Soils comprise various types of caliche, developed mainly on early Pleistocene shallow-marine carbonates, terra rosa and a red siliceous soil, widespread in the inland fringes of the surface in NW Messenia (see also Chapters 3, 6). The presence of the latter soil type suggests that, after the emergence of the early Pleistocene marine terrace, the climate of the area was humid tropical, favouring extensive leaching (Fitz-Patrick, 1980).

2.3.2.3 Fluvial incision: Fluvial incision of the Late Pliocene pediment-early Pleistocene terrace ranges in depth from 60-140 m (Figs. 2.7, 2.12, M.1), commonly comprising multi-phase valleys, with alluvial terraces at their flanks. The Lagouvardhos Gorge, near Valta, incised across the cliff that rims the early Pleistocene terrace(s) in NW Messenia (Figs. 2.7, 2.12), preserves evidence for at least two successive stages of incision. The older one resulted in a relatively shallow (ca. 20-30 m), broad valley, of gentle U-shaped profile. The younger incision, down to the level of the middle Pleistocene terrace and below, gave rise to a deep (ca. 80 m), narrow (<30 m), V-shaped gorge. Similar V-shaped gorges, cut across cliffs that bound early Pleistocene terrace(s), are present in many areas of Messenia (e.g. Xerias Rema; see Fig. M.1).

2.3.2.4 Faulting: The early Pleistocene terrace(s) are cut by a dense set of mesoscopic faults and joints (Figs. 2.2, 2.3, 2.4, 2.9). Throws across individual faults are generally <10 m, but the combined effect of parallel faulting led to displacements of the order of 100 m (Kelletat et al., 1976, 1978; Zelilidis, 1989). Throws of the order of ca. 20 m occur along NNE-SSW faults in the area of Palionero, in Southern Messenia (Fig. M.1).

2.3.3 Middle Pleistocene Terraces

Marine terraces situated lower than the early Pleistocene terrace and higher than the Eutyrrhenian terrace are correlated with middle Pleistocene sea levels (Kelletat et al., 1976, 1978). In general, marine terraces of inferred middle Pleistocene age were eroded in sediments of inferred early Pleistocene age (e.g. Gargaliani area; Figs. 2.7, 2.9) and bedrock (e.g. Methoni area; Fig. M.1). These terraces occur as narrow marine abrasion platforms or notches, at altitude varying from 20-280 m. Their exact number varies in different areas of the Messenia Peninsula and their lateral discontinuity, narrow development and absence of distinct sediment cover makes their correlation difficult. Kelletat et al. (1976) identified a maximum of 6 middle Pleistocene terraces in the area of Gargaliani (see Fig. 1.5.B).

A constructive marine terrace of inferred late middle Pleistocene ('Sicilian') age is preserved in the area of Filiatra (NW Messenia; see Figs. 2.2, 2.7, 2.9), at an average altitude of ca. 60 m. This terrace was formed above algal boundstone and sandstone/conglomerate (Unit 3.1; see Chapter 3). The terrace surface bears a variety of small karst forms ('*karren*') and is covered with terra rossa and brown soil; its carbonate substartum is calichified extensively. The Lagouvardhos Rema ravine was incised into this terrace, as an entrenched meander with a U-shaped valley profile (Figs. 2.7, M.1).

2.3.4 "Eutyrrhenian" terrace

This terrace is widespread in NW Messenia (see also Kelletat et al., 1976, 1978), formed above shallow-marine sediments of inferred Eutyrrhenian age (ca. 120 ka), middle and early Pleistocene sediments and bedrock, at an average altitude of 10-20 m. In the western coast of the Southern Messenia, erosional terraces and marine notches at altitudes <10 m can be tentatively correlated with the Eutyrrhenian stage (Fig. 2.14). The same terrace level is generally absent from the eastern coast with the exception of a marine abrasion platform at ca. 17 m, at Koroni (Figs. 2.8, 2.15). The age-specific gastropod, *Strombus bubonius*, characteristic of the Mediterranean Tyrrhenian stage(s) (see Chapter 1) was, in the past, reported from sediments associated with this terrace level (Kelletat et al., 1976), but was not encountered during the course of this study.

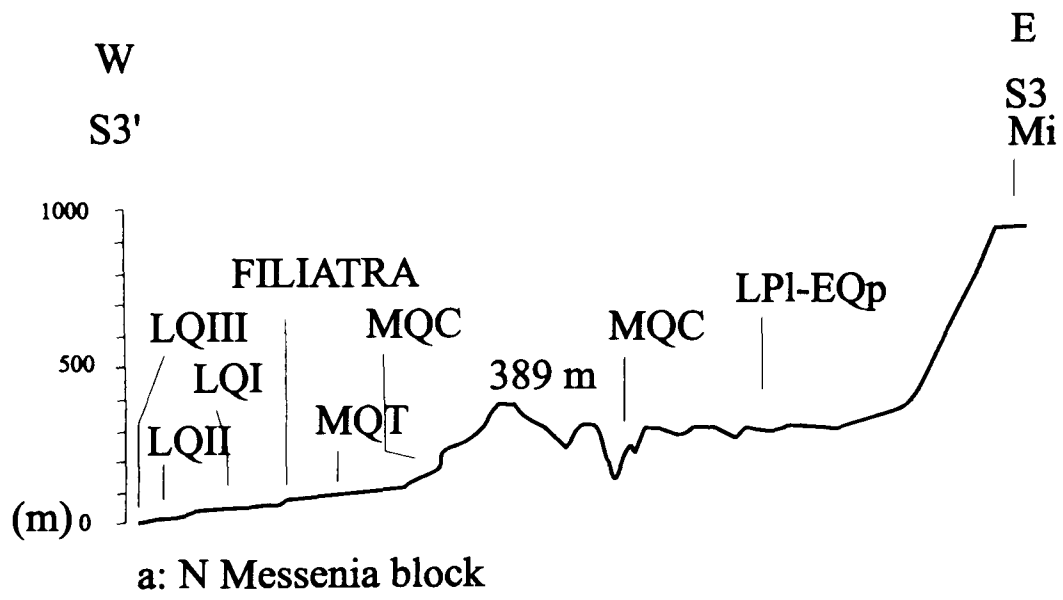

Key:

Mi: Miocene surface

LPl-EQp: Late Pliocene-early Quaternary pediment / pediplain

MQC: Mid-Quaternary cliffs and incised valleys

MQT: Mid-Quaternary terrace (Sicilian)

LQ: Late Quaternary terraces (I: Eutyrrhenian / II: Neotyrrhenian / III: Holocene)

M-LQ: Mid- to late Quaternary terraces (undifferentiated)

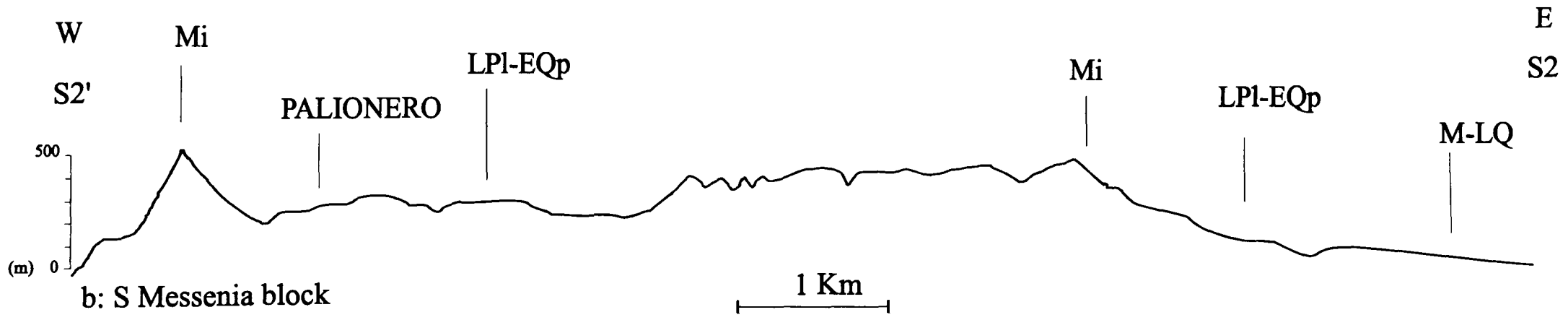

Figure 2.6: Morphological profiles. **a)** Northern Messenia Block, **b)** Southern Messenia Block. Inland, the topography is mainly fault-controlled, whereas near the coast marine terracing is the dominant influence. See Fig. M.1 (back pocket) for locations of profiles.

The Eutyrrhenian terrace is covered with alluvia, fluvial sediments and soils, including terra rossa and brown soils. Tens of cm thick horizons of chalky caliche formed on the sediment substratum of this terrace (e.g. Mati coast; Figs. 2.7, M.1; see also Chapters 3, 6). Fluvial incision resulted to V-shaped valleys of linear course, probably corresponding to base level lower than the present one. Local normal faulting of this terrace surface (e.g. Mati coast) attained throws <2 m; however, Kelletat et al. (1976) reported displacements of the Eutyrrhenian terrace at the order of 10 m, accumulated over a multitude of normal faults.

2.3.5 'Neotyrrhenian' terrace

Kelletat et al. (1976, 1978) reported the presence of the Neotyrrhenian terrace in several locations of the Messenia Peninsula; however, this is unambiguous only in the NW part of the peninsula, at an altitude of ca. 2-5 m (e.g. Marathopolis, Romanos; Figs. 2.2, 2.7, 2.13, M.1). There, the Neotyrrhenian terrace was formed on detrital shoreline facies of inferred 'Neotyrrhenian' age (Unit 3.3; see Chapter 3). Marine abrasion platforms are present elsewhere within the Messenia Peninsula at similar elevations, but their correlation with the 'Neotyrrhenian' sea level cycle is only tentative.

On the Marathopolis and Romanos coasts, this terrace is covered with aeolianites and related backshore facies, with well preserved dune morphology in places (Figs. 2.13, M.1). The inland parts of the terrace are covered with pebbly terra rossa that was probably reworked. Other soil types include *Rhizocretion* caliche in aeolianites and red caliche carapaces along the walls of extensional joints in the underlying Neotyrrhenian sediment substratum (see Chapter 6). Karstification resulted in the formation of cylindrical cavities, of depth extending below present sea level. Assuming that local subsidence did not take, the presence of these karstic sinkholes suggests that relative sea level fell below the present one during the latest Pleistocene.

2.3.6 Holocene terrace ('Versilian' or Historical)

The lowest terrace level, at 1.5 m, was interpreted as 'Versilian' by Kelletat et al. (1976, 1978). In most areas this occurs as a marine abrasion platform, eroded in Neotyrrhenian and older sediments. In Romanos coast (Fig. M.1), the Holocene terrace is associated with encrustations of Vermetid gastropods (Unit 3.5; see Chapter 3) and beach-rocks; rock pools and other foreshore erosion features are common in the later surface (Fig. 2.13). Similar terraces in Greece and Turkey, including the Eastern Lakonia Peninsula (Keraudren, 1970, 1971; Theodoropoulos, 1973; Kellletat et al., 1976, 1978; Kowalczyk et al., 1992; see Chapter 4) were correlated with the 'Versilian' stage of the Holocene (ca. 6000 a),when

eustatic sea level was slightly higher than the present one (Labeyrie et al., 1987; Kambouroglou, 1989). On the other hand, the Holocene terrace in the Messenia Peninsula could be much younger, correlated with shorelines uplifted during the "*Early Byzantine tectonic paroxysm*" (*sensu* Pirazzoli, 1986) all over the Eastern Mediterranean (see Chapter 1).

2.4 GEOMORPHOLOGICAL-TECTONIC SEGMENTS

As a whole, the Messenia Peninsula can be viewed as an uplifted area, between the Ionian Sea on the west and the Messenian Gulf on the east (Fig. 1.1). On the basis of relative altitude, structural, geomorphological and stratigraphic features, the Messenia Peninsula can be subdivided into two segments on a scale of 30-40 km, termed the *Northern Messsenia Block* and the *Southern Messenia Block* (Kourampas and Robertson, 2000) (see Figures 2.2, 2.5, M.1). The dimensions of these blocks make them comparable to the *"1st order neotectonic macrostructures"* of Mariolakos et al. (1994). In addition, both blocks are segmented into grabens and half-grabens on a 5-7 km-scale (Figs. 2.2, 2.5, 2.6, 2.7, 2.8, 2.9, A1). The two blocks are separated by the important Pylos Fault, across which the relief and sedimentary record differ markedly. Segmentation on this large scale (comparable to the depth of the seismogenic layer of the crust), is known elsewhere, including central Greece (Roberts and Jackson, 1991). Each fault-bounded morphological block of the Messenia Peninsula is discussed below:

2.4.1 Northern Messenia Block

2.4.1.1 Faults: This block extends from the uplifted area of Kiparissia in the north, to the low-relief (alluvial plain/lagoon) areas north of Pylos, in the south (Figs. 2.2, 2.5, M.1). A southward tilting of the NW Messenia block is, thus, discernible. The deformation was taken up by the dense network of parallel and transfer faults (Figs. 2.2, M.1). The Northern Messenia block is characterised by a regionally extensive cover of post-Tethyan sediments (Fig. 2.2). The earliest dated marine deposits of the area (Frydas, 1990; Frydas and Bellas, 1994) were correlated with the NN 18 biochronozone *sensu* Martini (1971) (Piacenzian, Late Pliocene, ca. 2.0-1.6 Ma; see Chapter 3). These sediments are correlated with the sea level cycle 3.8 *sensu* Haq et al. (1986). The fault fabric within the Northern Messenia Block comprises NNW-SSE and NNE-SSW faults, predominately synthetic, but also antithetic to the morphology; ENE-WSW transfer faults are also present (Figs. 2.2, 2.7, 2.9). Faults of all

these sets were active during the Quaternary. Parallel faults controlled Pleistocene shorelines, whereas transfer grabens were occupied by drainage (above sea level) and embayments (below sea level), perpendicular to the general trend of the palaeocoast. This fault-pattern affected the pattern of deposition of Pleistocene deltaic facies, that locally correspond with transfer fault zones (see also Chapter 3).

The morphotectonic fabric of the Northern Messenia Block can be described as an alteration of relatively closely-spaced horsts and grabens (average width: ca. 6.5 km), in an overall step-like succession (Fig. 2.6, 2.7, 2.9). Along a section from Proti Island in the west to the summit-range of the Kiparissia Mountains in the east, the Marathopolis graben, where middle-late Pleistocene deposition took place, is bounded by the synthetic Gargaliani Fault (dipping to the west). An elongate ridge of bedrock limestone (Gargaliani-Filiatra Ridge), on the footwall of the Gargaliani Fault, crops out as a horst between Pleistocene sediments (Figs. 2.7, 2.9). This is a faulted anticlinal structure (I.G.M.E., 1981a), cut by a network of closely-spaced normal faults. The Valta Graben, further inland, is bounded by the eastward dipping faults of the Gargaliani-Filiatra Ridge (antithetic) and the composite faults of the Kiparissia Mountain Front (synthetic). The latter separates an area of strongly uplifted bedrock, Late Oligocene molasse ("*Messenian Conglomerate*": Unit 1.1; see Chapter 3) and deeply dissected Miocene peneplains (erosion depth: up to 500 m) from an area of Late Pliocene(?)- middle Pleistocene marine and terrestrial sediments and well preserved marine terraces (Figs. 2.2, 2.5, 2.6, 2.7, 2.9).

To the south, the Northern Messenia Block terminates in a half-graben controlled by ENE-WNW faults (Figs. 2.2, 2.5), partly transgressed by the sea in Holocene times (Kraft et al., 1975). Its subaerial part extends over Yialova-Petrohori, Voidokilia Lagoon and further eastwards (Fig. M.1). Latest Pleistocene or Holocene activity within this graben is possibly indicated by subsidence of latest Pleistocene aeolianites and soils in the coast of Petrohori.

Figure 2.7 (following page): Geomorphological sketch-map of the Gargaliani-Filiatra area, Northern Messenia Block. Three principal relief segments are distinguished: namely uplifted remnants of Late Tertiary surfaces (on bedrock), Late Pliocene pediment and early Pleistocene terraces and late-middle to late Pleistocene terraces and Holocene coastal plains (on Pleistocene sediments and bedrock). These are separated by cliffs (Kiparissia Mountain Front, of Late Tertiary age, and Gragaliani Escarpment, of middle Pleistocene age) that coincide with NNW-SSE trending fault systems (Kiparissia Mountains Fault and Gargaliani Fault, respectively). The major cliffs are incised by streams transverse to the morphological-tectonic grain (e.g. Lagouvardhos and Filiatrino Rema). Note that the Filiatrino Rema stream captured NNW-SSE flowing streams east of the Kyparissia Mountain Front. A centre of uplift, around which stream courses diverge, is located east of Gargaliani.

21 31′

21° 45′

37° 10′

Late Tertiary surfaces (on bedrock)

Quaternary terraces (on sediment)

Quaternary terraces (on bedrock)

Mountain front

Steep cliffs

Incised valleys

Normal faults

Pindos thrust

Centre of uplift

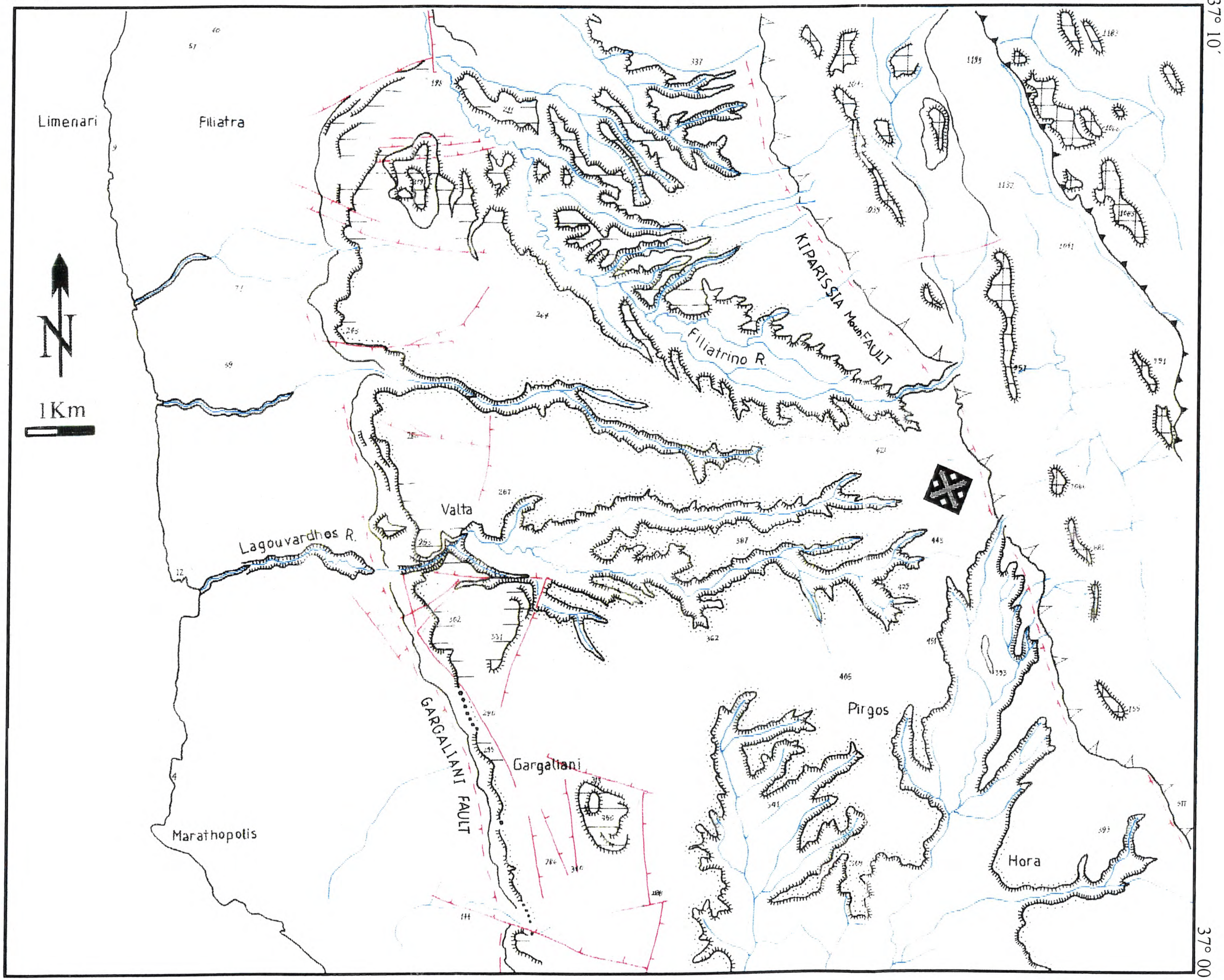

37° 00′

21° 31′

21° 45′

2.4.1.2 Surfaces and terraces: A series of 4-5 pre-Quaternary surfaces of subarial erosion and 8-9 Quaternary terraces were identified in the Northern Messenia Block (Figs. 2.6, 2.7, 2.9). The maximum number of marine terraces observed in the Southern Peloponnese occurs within this block, as already noted by Kelletat et al. (1976), who, however, identified up to 11 Quaternary terrace levels. Five of the Quaternary terraces correspond to regionally correlative depositional stages, with preserved transgressive and highstand system tracts (see Chapter 3). The remainder are erosional terraces. Definite identification of the latter as marine abrasion surfaces is possible only in seaward, relatively distal parts of the terrace surfaces. These erosional terraces are not regionally correlative. Their high number possibly resulted from high uplift rates of the Northern Messenia Block (see Chapter 7) and, locally, by the effects of faulting parallel to the peninsula. Normal faulting of a few marine-abrasion levels to produce larger number of morphological terraces in the Eleophito Basin (southern part of the Northern Messenia Block; see Fig. M.1) was also envisaged by Zelilidis (1988).

2.4.2 Southern Messenia Block

2.4.2.1 Faults and sediments: The Southern Messenia Block is bounded to the north by the ENE-WSW trending, northward dipping Pylos Fault; however, no sharp tectonic boundaries are distinguished to the south (Figs. 2.2, 2.5, 2.8, M.1). The eastern boundary of the Southern Messenia Block coincides with NNW-SSE to N-S, eastward dipping faults that downthrow the Kalamata-Messenian Gulf graben to the east (Figs. 2.2, 2.8, 2.9, M.1). Submarine scarps of generally N-S direction and considerable throw (100's of m; Mascle et al., 1982) probably correspond to the western boundaries of the block (Fig. 2.2). This tectonic fabric delineates an uplifted area of broadly N-S morphological strike. Normal faults within the Southern Messenia Block are as in the Northern Messenia Block, i.e. NNW-SSE to N-S faults, parallel to the elongation of the peninsula and fewer ENE-WSW transfer faults (Figs. 2.2, 2.3).

Figure 2.8 (following page): Geomorphological sketch-map of the Koroni-Finikounta area, Southern Messenia Block. An area of uplifted Late Tertiary surfaces runs along the axis of the Messenia Peninsula, bordered by the Pindos Thrust to the west and NNW-SSE normal faults to the east. The early Pleistocene terraces (on Plio-Quaternary shallow-marine sediments) developed extensively in the eastern part of the area (Koroni-Kombi-Vounaria). In the western part of the area, north of Finikounta, early (to middle ?) Pleistocene surfaces (on bedrock and Plio-Quaternary sediments) deep to the south (sea). Note the lower altitudes of this area as compared with Figure 2.7, indicative of an overall southward tilting of the Messenia Peninsula.

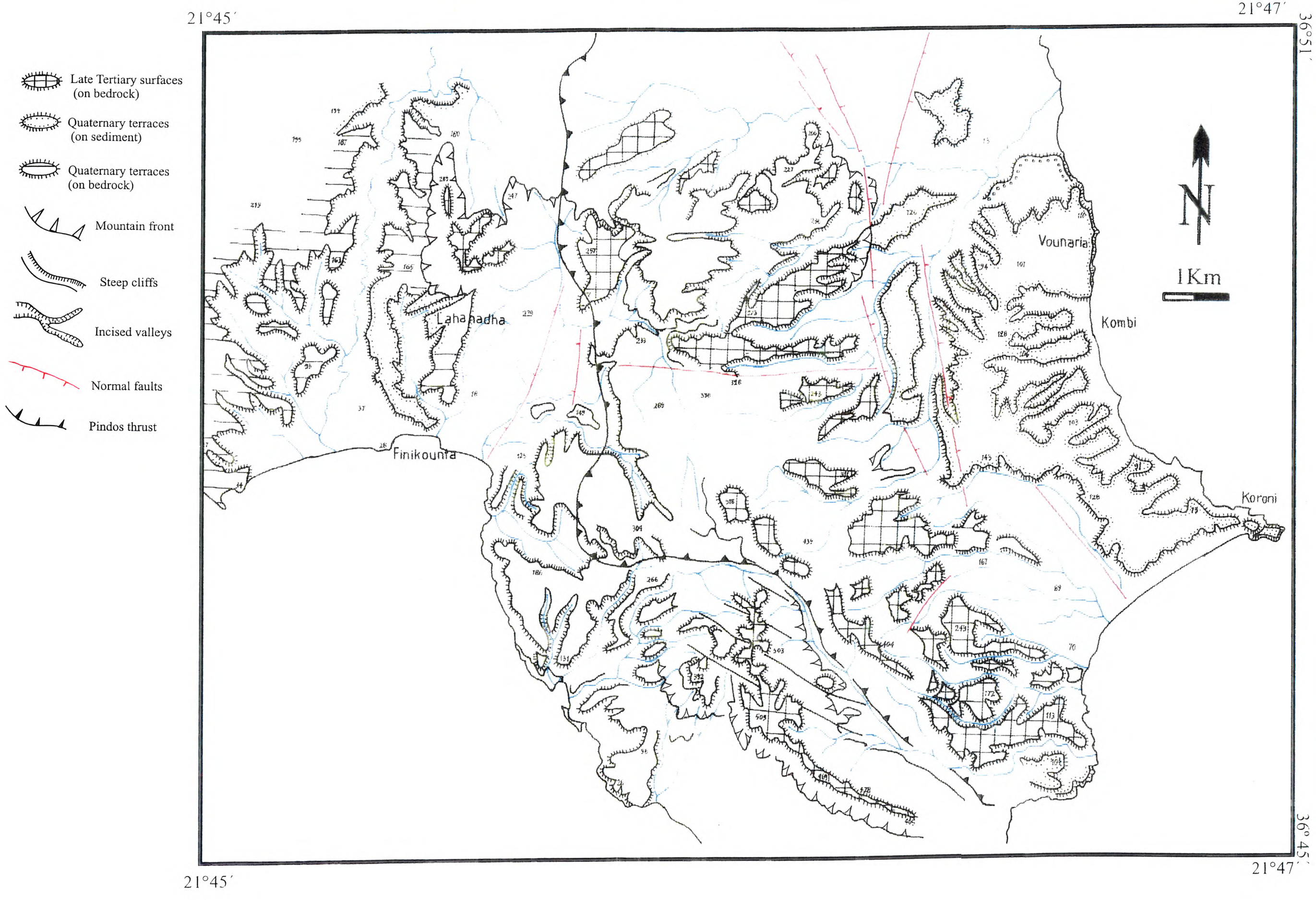
21°45′
21°47′
36°51′
36° 45′
Late Tertiary surfaces (on bedrock)
Quaternary terraces (on sediment)
Quaternary terraces (on bedrock)
Mountain front
Steep cliffs
Incised valleys
Normal faults
Pindos thrust
N
1Km
Lahanadha
Finikounta
Vounaria
Kombi
Koroni

In the Southern Messenia Block, Plio-Quaternary deposits are less widespread as compared with the Northern Messenia Block (Figs. 2.2, M.1). Plio-Quaternary sediments are mostly preserved along the eastern coast of the peninsula that coincides with the uplifted flanks of the Kalamata-Messenian Gulf graben (Figs. 2.2; 2.10). The oldest dated marine sediments in the area ("*Falanthi section*", Frydas, 1990; Frydas and Bellas, 1994) were correlated with the NN 13 biochronozone *sensu* Martini (1971) (middle Lower Pliocene, Zanclean, ca. 5-4.2 Ma; see Chapter 3). These sediments, thus, correspond with the sea level cycle 3.4 *sensu* Haq et al. (1986). The maximum altitude of Plio-Quaternary sediments is ca. 300 m and ca.220 m, along the eastern and western coast of the Southern Messenia Block, respectively (Figs. 2.4, 2.7, 2.11).

2.4.2.2 Terraces and fluvial incision: Four pre-Quaternary surfaces of subaerial erosion and 4 to 6 Quaternary terraces are distinguished within the Southern Messenia Block (Figs. 2.6, 2.8, 2.9). The highest surfaces are either incised karstic pediplains with inselberg relief, as in the northern sector, or conical hills with uniform slopes to the pediment of the oldest Plio-Quaternary surface (Figs. 2.5, 2.6, 2.8, 2.9). In the northern part of the Southern Messenia Block distinction between the lowest Late Tertiary surface and the early Pleistocene terrace is unclear. An extensive surface with inselbergs is, instead, covered with subaerial sediments in its central parts and shallow-marine sediments near its margins (Figs. 2.2, M.1). The latter are correlated with the early Pleistocene Unit 2.4 (see Chapter 3). This coincidence of a Late Tertiary surface with the early Pleistocene terrace suggests that Late Pliocene-early Pleistocene uplift, widespread elsewhere in Messenia (see below), was of lower intensity in the northern part of the Southern Messenia Block. In the eastern areas of the Southern Messenia Block, by contrast, Late Tertiary and early Quaternary surfaces are separated by steep cliffs (Figs. 2.2, 2.5, 2.6, 2.8, 2.9). These cliffs commonly coincide with normal faults that bound the Kalamata-Messenian Gulf Graben. In the NE part of the Southern Messenia Block, the height of these cliffs (minimum accumulated throw of the graben-bounding faults) is ca. 500-600m. The two highest pre-Quaternary surfaces are tilted at about 2.22% (ca. 2.5°) to the west.

Similar to features described in the Northern Messenia Block, U-shaped, dry valleys following NNW-SSE directions were incised into all the pre-Quaternary surfaces, down to the level of the Late Pliocene pediment (Figs. 2.8, 2.10, M.1). The bases of these pre-Quaternary valleys in the Southern Messenia Block are at lower altitudes than in the Northern Messenia Block (ca. 50-150 m, as compared with ca. 300-400 m). Such differences in altitude probably resulted from Pleistocene normal faulting, possibly along the ENE-

WSW Pylos Fault that separates the two sectors. In the NW area of the Southern Messenia Block (Palioneron area; see Fig. M.1), a pre-Quaternary valley was infilled with shallow-marine carbonates of inferred early Pleistocene age (Unit 2.4; see Chapter 3) and was subsequently rejuvenated in middle-late Pleistocene time.

2.5 DRAINAGE OF THE MESSENIA PENINSULA

The Messenia Peninsula is mainly drained by streams of mixed, dendritic-parallel pattern, with local presence of trellis and parallel patterns (Fig. M.1). A drainage divide runs parallel to the long axis of the peninsula, from NNW to SSE. No streams of order >6 are present within the Messenia Peninsula. As shown in Figure M.1, there is a marked decrease in stream density with increasing stream order. Drainage density varies with varying bedrock lithology, with maximum values on Tripolis Zone 'flysch' and Pindos Zone 'flysch' and radiolarite and minimum drainage densities on Tripolis Zone limestone (Fig. M.1). Pliocene-Pleistocene sediments are characterised by low drainage density and immature, 1^{st}-2^{nd} order streams. Normal faulting partly controlled the orientation of streams within the Messenia Peninsula, with the majority of streams flowing parallel to the main fault and joint strikes (Fig. M.1), as expected in any highly faulted area (Ahnert, 1995). On a finer scale, drainage characteristics differ across the two main Northern and Southern Messenia fault-bounded blocks:

2.5.1 Northern Messenia Block

The drainage of the Northern Messenia Block is of a mixed, dendritic-parallel pattern (Fig. M.1). The longest streams, of 4^{th}-3^{rd} order, drain across the horst and graben structure, from the coast to the Kiparissia Mountains. Although these streams are transverse to the topography overall, parts of their courses are axial (e.g. Filiatrino Rema; see Fig. M.1). The footwalls of small, <5 km-scale normal faults are drained by small, straight, 1^{st}-2^{nd} order streams. Streams that drain exclusively middle-late Pleistsocene sediments are also of 1^{st}-2^{nd} order.

2.5.1.1 Stream divergence: Stream branches in the Northern Messenia Block diverge around a loosely defined centre, located in the area of Gargaliani-Hora, on the Late Pliocene pediment-early Pleistocene terrace surface (Figs. 2.7, M.1). North and south of this centre of divergence, streams flow towards the NW and the SW, respectively.

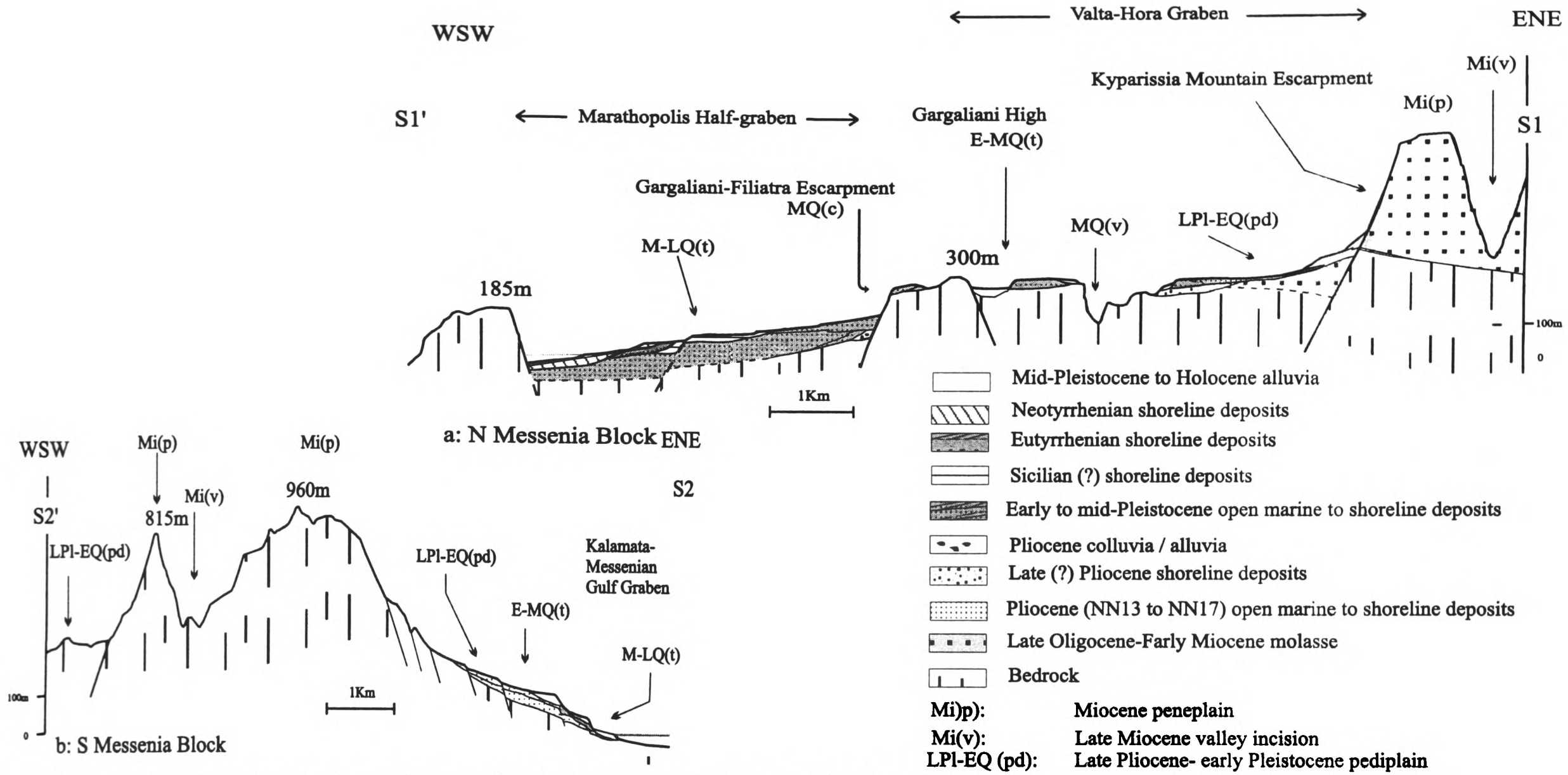

Fig. 2.9: Representative cross-sections of **a)** the Northern Messenia Block, and **b)** the Southern Messenia Block: **a)** Section in the Northern Messenia block from the mountain front westwards. Note that the topography is controlled by horsts and grabens. **b)** Section in the Southern Messenia block from the mountain front eastwards. Note the fault-controlled topography, stepping down to the Messenia Gulf Graben. In both areas, older sediments are generally preserved at higher altitudes (see Figure 2.2 for locations of the cross-sections).

Since this centre of stream divergence does not correspond with any mapped morphological high or any lithological unit resistant to erosion, it was concluded that it coincides with a centre of maximum Pleistocene uplift (Mariolakos et al., 1991). The latter authors mapped this centre of uplift as an axis extending E-W, across the morphological grain of the Messenia Peninsula and the uplifted Late Pliocene pediment-early Pleistocene terrace, and interpreted it as an axis of neotectonic folding. However, given the poor topographical resolution of this centre of uplift and the general absence of outcrop-scale neotectonic folding from the Messenia Peninsula, alternative interpretations could be suggested (e.g. tilting related to normal faulting, possible presence of unmapped, closely-spaced faults, etc.).

2.5.1.2 Longitudinal stream profiles: The northern part of the Messenia Peninsula is an area of well developed benchland relief, with a step-like succession of morphological surfaces, from higher to lower altitudes (see above and Figs. 2.5, 2.6, 2.7, 2.9). Streams of 4^{th}-3^{rd} order, that transverse this benchland morphology, have step-like longitudinal profiles (Fig. 2.10). For instance, Filiatrino Rema (Figs. 2.7, M.1), typifies the main stages of valley development in the area. From its lower to its upper reaches, four main sectors are distinguished along the course of this stream (Fig. 2.10). The lowest sector, from present sea level to 60 m, follows a meandering course from W to E and drains late-middle and late Pleistocene sediments (Figs. 2.9, M.1). This stream exhibits a gentle longitudinal profile, with gradients ranging from ca. 0.006% along its lower reaches, to ca. 0.025% along its upper reaches (Fig. 2.12). A convex knick point at 80 m separates this from the second sector, that flows from SE to NW, draining early and middle Pleistocene sediments. For a large part of its course this sector is oblique, to axial, to the early Pleistocene terrace(s) and the Late Pliocene pediment (Figs. 2.9, M.1). The lower reaches of this sector are high-frequency meanders, with stream gradients ranging from 0.012-0.023%, whereas its upper parts are low-frequency meanders to straight streams, with incised valleys and stream gradients from 0.031-0.133%. This is separated from the third higher sector by a convex knick point at 400 m (Fig. 2.10). This sector, with a stream gradient ca. 0.019%, also flows from E/ENE to W/WSW, draining Pleistocene alluvial fans and bedrock on the uplifted Late Pliocene pediment (Figs. 2.7, 2.10). At least three convex knick points, from 700 to 740 m, coincide with the incised Kiparissia Mountains escarpment (Figs. 2.10, M.1). The ca. 140 m deep valley incised across this escarpment is very steep, with stream gradients from 0.2-0.5%. Upstream of the 740 m knick point, the stream changes course, flowing to the S, almost perpendicular to the flow of the lower sectors and parallel to the tectonic-

morphologic grain of the Messenia Peninsula (Figs. 2.2, M.1). This sector drains Late Oligocene-Early Miocene conglomerate and Oligocene 'flysch' (Tripolis Zone) and flows in a mature, broad, U-shaped valley, incised into uplifted Late Miocene pediments/pediplains (see above). The stream gradient of this sector is low, ranging from 0.018-0.033% (Fig. 2.12).

The longitudinal profile of the 4th order Laghouvardhos Rema stream (Figs. 2.9, M.1), that flows across the Northern Messenia benchland, allows the resolution of several Late Pliocene-Pleistocene base levels, all correlative with the fourth and the second stream levels of the Filiatrino Rema stream (see above). Starting from the present river mouth, the stream follows a shallow valley, incised in middle and late Pleistocene sediments, with stream gradients from 0.01-0.023% (Fig. 2.12). Profiles of this valley are open V-shaped along the lower reaches and U-shaped along the upper reaches. No knick point separating these different valley types is resolved on the 1:50,000 topographical map (H.A.G.S., 1984). Field observations, however, showed that the transition from a V-shaped to a U-shaped valley coincides with the cliff between the late Pleistocene ("Tyrrhenian") terraces (on detrital carbonate) and the late-middle Pleistocene ("Sicilian") terrace (on algal boundstone). This knick point is, thus, located at ca. 30-40 m. Upstream of the latter knick point, a steep sector of the profile coincides with the ca. 120 m deep Lagouvardhos Gorge, incised into the Gargaliani Escarpment (Fig. 2.9). Upstream of the 220 m knick point, Lagouvardhos Rema follows a loosely meandering course, draining the early Pleistocene terrace (Figs. 2.9, M.1). Incision along this sector is generally <30 m; rejuvenation took place in at least two stages, as indicated by the presence of two paired bedrock terraces in its lower reaches (in and directly upstream of the Lagouvardhos Gorge). The longitudinal profile of this sector is mature, gently concave (Fig. 2.12).

Figure 2.10 (following page): Longitudinal profiles of streams in the Messenia Peninsula. Two types of streams are distinguished: **1)** Steams of very steep profile are widespread along both the western and eastern coast of the peninsula, commonly associated with NNW-SSE faults in bedrock and Pleistocene sediments. **2)** Streams of step-like profile, combine smooth, concave, low-gradient segments with narrower, seep segments bounded by knick points. Low-gradient valley segments are correlated with Late Tertiary, Late Pliocene, early Pleistocene and middle-late Pleistocene-Holocene surfaces of subaerial erosion and marine terraces. Steep valley segments are correlated with Pliocene, early Pleistocene and middle Pleistocene cliffs, commonly controlled by NNW-SSE faults (e.g. Kiparissia Mountain Front, Gargaliani Escarpment). The longest of these polycyclic valleys occur along the western coast of the Peninsula (e.g. **FR:** Filiatrino Rema). An overall eastward tilting of the Messenia Peninsula is indicated by the higher altitude of valley heads and correlative valley segments of streams flowing towards the west. **LR:** Lagouvardhos Rema.

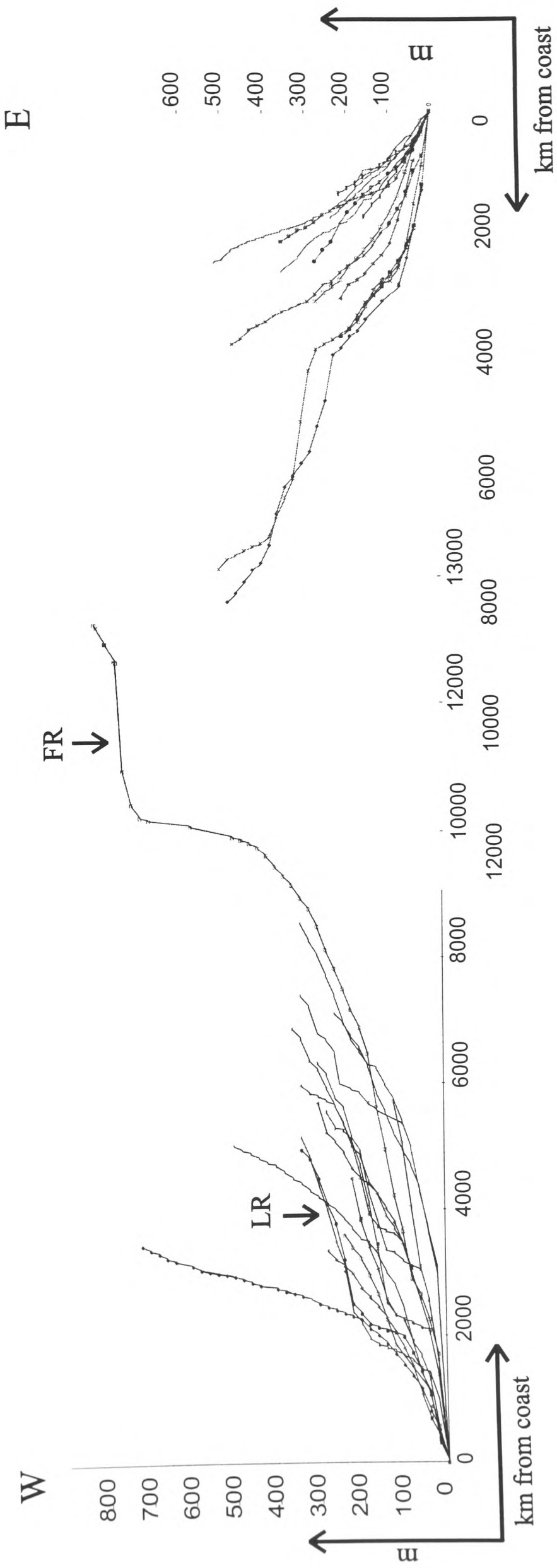
E
-600
-500
-400
-300
-200
-100
0
m
km from coast
2000
4000
6000
8000
10000
12000
13000
FR
W
800
700
600
500
400
300
200
100
0
m
LR
km from coast
2000
4000
6000
8000
10000
12000

2.5.2 Southern Messenia Block

The Southern Messenia Block is characterised by less extensive Plio-Quaternary sediment cover and lower average altitudes, compared to the Northern Messenia Block (see above; Figs. 2.2, 2.5). The Pindos Thrust, that runs along the long axis of the Southern Messenia Block, forms the boundary between two drainage domains (Figs. 2.2, M.1). West of the Pindos Thrust, streams drain mainly Tripolis Zone carbonates and 'flysch' and relatively small outcrops of Plio-Quaternary sediments. These streams follow generally N-S courses, parallel to the morphological grain of the Messenia Peninsula and the fault-bounded horst and graben structures. Locally, streams that drain NNW-SSE trending grabens allow a distinction between axial trank streams (up to 5th order), flowing parallel to the long axes of the grabens, and tributaries (up to 3rd order) that drain the uplifted footwalls on the flanks of the grabens (e.g. Xerias Rema; see Fig. M.1).

East of the Pindos Thrust, streams drain the lithologicaly variable Pindos Zone bedrock ('flysch', radiolarites, pelagic carbonates) and extensive outcrops of Plio-Quaternary sediments (Figs. 2.1, 2.2, M.1). Streams in that area flow to the west (sea), transverse to the morphological grain of the Messenia Pensinsula and the principal faults of the area. A distinction can be made between short 1st-2nd order streams that drain exclusively Plio-Quaternary sediments, and longer, up to 5th order dendritic streams that drain both Plio-Quaternary sediments and Pindos Zone bedrock. The former streams are of Quaternary age, whereas the latter probably date back to Pliocene time (age of the oldest drained relief).

The longitudinal profiles of streams in the Southern Messenia Block are generally steeper compared to streams of the Northern Messenia Block. As in the Northern Messenia Block, knick points reflect lithologic heterogeneity of the drained substratum, the presence of terraced relief and probably Quaternary activity of NNW-SSE and NNE-SSW normal faults (see Fig. 2.10).

2.5.3 Drainage and faulting

Two principal drainage directions are distinguished, in relation to fault-pattern and fault-controlled relief features (Figs. 2.7, 2.8, M.1):

2.5.3.1 Drainage parallel to the tectonic/morphologic grain: follow NNW-SSE to N-S directions and drain areas of incised Late Tertiary relief, east of the Late Pliocene Kiparissia Mountain Front, in the Northern Messenia Block, and south of Pylos, in the Southern

Messenia Block (Figs. 2.7, 2.8, M.1). These streams follow the dominant grain of NNW-SSE, compressional (thrusts, fold axes) and extensional (normal faults) tectonic elements and the long morphologic axis of Messenia Peninsula. The same streams are transverse to ENE-WSW transfer faults. Deep (maximum depth: ca. 500 m), narrow valleys, incised in the Late Tertiary surfaces, are drained by streams of this group (Fig. 2.7). These are polycyclic valleys that underwent more than three stages of incision, alternating with stages of lateral erosion, as evidenced by the surviving bedrock terraces flanking the valleys (Fig. 2.7). Since many of these valleys correspond to the base level of the Late Pliocene pediment (see above), their final incision probably took place in Late Pliocene time. Parallel streams were captured by headward erosion of transverse streams (see bellow).

2.5.3.2 Drainage transverse to the tectonic/morphologic grain (*sensu* Ahnert, 1998): These generally follow E-W (ENE-WSW to ESE-WNW) directions, transverse to the dominant tectonic grain and the long axis of the Messenia Peninsula. Streams of this group are parallel to, and commonly follow, ENE-WSW transfer faults (Figs. 2.7, 2.8, M.1). Control by transfer faults is particularly evident on transverse streams that cross the Gargaliani Escarpment (e.g. Lagouvardhos Rema; see Fig. 2.7). Transverse streams drain the area west of the Kiparissia Mountain Front, from the Late Pliocene pediment upstream, to the latest Pleistocene marine terraces and Holocene alluvial plains downstream (Fig. M.1). Streams of this group are of a mixed, parallel-dendritic type, reflecting the gentle morphological dip of the drained relief (Fig. M.1). In many cases, headward erosion cut "water gaps" through the Kiparissia Mountain Front and streams of NNW-SSE direction, parallel to the tectonic/morphologic grain of the peninsula, were captured (e.g. Filiatrino Rema; see Fig. M.1). Multiphase incision of the Gargaliani Escarpment by transverse streams (e.g. Lagouvardhos Rema; see Fig. 2.7) resulted in a series of fluvial terraces, tentatively correlative with marine terraces of the Northern Messenia Block. The deepest incision, that resulted in the 80m deep Lagouvardhos Gorge (see Fig. 2.12), is correlated with the middle-late Pleistocene (between Sicilian and Tyrrhenian) relative sea level lowstand, that also resulted in the ca. 120 m high cliff that separates early-middle from late Pleistocene marine terraces in the same area (Figs. 2,7, 2.9, 2.10, 2.11). Fluvial terraces preserved along the downstream course of transverse streams are correlated with rising sea level during the Eutyrrhenian and the Holocene (see Chapter 3).

2.5.3.3 'Antecedent' and 'superimposed' streams: West-flowing streams of the Northern Messenia Block transverse a step-like relief (Figs. 2.5, 2.6, 2.7, 2.9) that resulted from three causative factors:

1) Formation of marine terraces, due to superposition of eustatic sea level cyclicity on regional land uplift.

2) Activity of shore-parallel, synthetic faults (NNW-SSE to NNE-SSW directions), that resulted in step-like dislocation of gentle relief segments.

3) Fault-induced lithologic heterogeneity across the Gargaliani-Filiatra Ridge. NNW-SSE faults, both synthetic and antithetic, juxtaposed easily eroded 'flysch' with more resistant neretic limestone (I.G.M.E., 1980a; see Fig. 3.6). Higher denudation rates on 'flysch' probably resulted in relatively more rapid lowering of the surface, which further enhanced the fault-controlled step-like configuration of the relief.

The largest transverse streams are both '*antecedent*' to and '*superimposed*' on the step-like morphology of the Northern Messenia Block. Relief development, controlled by faulting and relative sea level change, as well as progression of drainage over land newly emergent due to regional uplift, both took place diachronously during the Quaternary. Large streams (e.g. Lagouvardhos and Filiatrino Rema) were superimposed upon major relief features such as Gargaliani Escarpment and the Kiparissia Mountain Front (Figs. 2.7, M.1), that probably originated in Late Tertiary times (see above). However, convex knick points along the long profiles of the same valleys (Fig. 2.10) suggest that normal faults transversed by Lagouvardhos and Filitrino Rema were active during the Quaternary. Furthermore, the presence of marine terraces demonstrates that the relief of the area was substantially modified as a result of Pleistocene sea level change. In conclusion, the terms '*antecedence*' and '*superposition*' of streams seem to have little relevance in situations of dynamically evolving relief, subject to land movement and sea/base level cyclicity, as is the case in the Messenia Peninsula.

2.5.4 Drainage evolution in the Messenia Peninsula

The two drainage groups probably are not of the same age: The parallel drainage group, oriented NNW-SSE, is probably older, as shown by its association with a Late Tertiary relief. Streams of this group flow in deep, U-shaped intramountain valleys, with mature slopes, incised into Late Miocene-Pliocene surfaces (see above). Since these valleys generally correspond to the level of the Late Pliocene pediment, their evolution (and that of the corresponding drainage) probably took place between the Middle Miocene (time of

emergence of the area after the Tethyan orogenensis; Jacobschangen et al., 1978; Mariolakos et al., 1991) and the Late Pliocene. Streams of this drainage group were subsequently captured by branches of the transverse, E-W drainage. Transverse streams drain the Late Pliocene pediment and the entire Quaternary terrace flight. Some streams of this group probably originated from streams that drained the Late Pliocene pediplain, prior to the first Plio-Quaternary marine transgression. Other transverse streams, however, do not extend inland of the late Pleistocene terraces (Fig. M.1). The development of the transverse drainage group, therefore, spanned the time from Late Pliocene to Present.

The timing of drainage development reflects the neotectonic and morphologic evolution of the Messenia Peninsula during the Late Tertiary-Quaternary. A change in drainage orientation, from NNW-SSE, parallel to the axis of the peninsula, to E-W, transverse to the axis of the peninsula, took place sometime in the Pliocene (possibly towards the Late Pliocene). This change in drainage orientation could be explained as a result of the interplay between activity of different fault-groups and relative sea level change, probably of glacio-eustatic origin. The origin of the peninsula-parallel drainage, during Late Miocene-Pliocene time, required a NNW-SSE directed topographic gradient. This could have resulted from the tilting of fault-bounded blocks. Given the segmentation of the Messenia Peninsula across its strike by ENE-WSW faults, it is reasonable to suggest that tilting to NNW-SSE directions (perpendicular to the fault strike) resulted from ENE-WSW to E-W faulting. The oldest dated marine sediments in the nearby Kiparissia-Kalo Nero Basin (a half-graben bordered to the south by the E-W striking Kiparissia faults; see Figs. 2.2, M.1) are of early Zanclean age (i.e. basis of the Pliocene) (Fountoulis and Moraiti, 1994). This probably reflects high subsidence rates along E-W faults around the Miocene-Pliocene boundary, the significance of eustatic sea level rise notwithstanding.

As noted above, areas of Late Miocene relief (e.g. east of the Kiparissia Mountain Front) are mainly drained by parallel streams. The absence of transverse, E-W directed drainage during Late Miocene to Pliocene time probably reflects a palaeogeographic setting different from the present one. The present-day coastline configuration, with the sea (base level of erosion) located west of the peninsular mountain range, creates an E-W topographical gradient; the latter favours the development of E-W drainage. This coastal topography is largely controlled by a series of NNW-SSE, mainly synthetic faults. From this it follows that the development of NNW-SSE drainage, during Late Miocene-Pliocene time, took place within a different geographic configuration, with a more 'inland' setting of the drained area and no

westward topographical gradient. This geographic configuration would be favoured by two conditions:

1) Reduced activity of the NNW-SSE faults, so that a westward topographical gradient was not generated.

2) A relative sea level low, combined with the previous condition, that further enhanced the 'inland' character of the area and removed the grading effect of the proximity of the sea (base level).

The origin of the transverse drainage during Late Pliocene-early Quaternary time was associated with the initiation of an E-W topographical gradient, a prerequisite for this drainage to develop. This change was possibly controlled by activity of NNW-ESE normal faults, which have influenced the Messenian coastline configuration ever since. In NW Messenia, a series of west-dipping, NNW-SSE faults downthrow their hangingwall blocks, thus bringing the sea level (base level of erosion) to the west of the Messenian uplands. Ancestral streams of the transverse group probably drained the Late Pliocene pediplain of the Kiparissia Mountains. The latter was inundated by the (Latest Pliocene?)-early Pleistocene sea and was then re-emergent and subjected to subaerial processes in early to middle Pleistocene time. The early stages of development of tranverse streams, therefore, were probably correlated with a peak of the relative sea level curve (i.e transgression of the pediplain, subsequent regression and progression of drainage over the marine sediments). Relative sea level rise itself probably enhanced the effect of fault-induced relief-steepening, by allowing the sea to encroach on the peninsula. Ongoing transgression of irregular relief would favour the development of drainage in directions transverse to the retrograding coastline. Given a fault-induced shoreward gradient, streams would select the shortest course, perpendicular to the shore.

The evolution of transverse streams, after their initiation in Late Pliocene time and their advance over marine deposits of the first Quaternary sea level cycle, was accomplished through their gradual advance over land emerging due to regional uplift of the peninsula. This process was punctuated by periods of gradient reduction, alluviation and landward stream retreat, probably coinciding with sea level highs of the Quaternary eustatic cycles. Although speculative for early and middle Pleistocene stages, correlation of late Pleistocene sea level highs with alluviation further inland is suggested by the altitudinal correlation of Eutyrrhenian marine deposits and alluvia in the NW Messenia (e.g. Lagouvardhos Stream; Kourampas and Robertson, 2000). Similar models were proposed for Pleistocene marine and alluvial terraces in Cyprus (Poole, 1991; Poole and Robertson, 1990, 1998).

2.6 SUMMARY-CONCLUSIONS

- Normal faults that cut Plio-Pleistocene sediments within the Messenia Peninsula follow the following trends:: 1) NNW-SSE, 2) ENE-WSW, 3) NNE-WSW, 4) ESE-WNW. Cross-peninsular faults are interpreted as transfers to faults parallel to the morphological-tectonic grain of the Messenia Peninsula.
- Faults of all the above sets mutually cut each other. Also, faults of all sets experienced oblique slip. This points to the coeval activity of all the fault-sets during the Plio-Quaternary.
- The following generations of surfaces are recognised within the Messenia Peninsula: 1) Late Miocene-Pliocene pediments, 2) Late Pliocene pediment, 3) Early to early middle Pleistocene marine terrace(s), 4) Middle Pleistocene ("Sicilian") marine terrace, 5) Late Pleistocene ("Eutyrrhenian" and "Neotyrrhenian") marine terraces, 6) Holocene ("Versilian" or Historical) marine abrasion platform.
- In NW Messenia, high (>80 m) cliffs separate Late Miocene-Pliocene from Late Pliocene and younger surfaces and early to early-middle Pleistocene from middle Pleistocene and younger marine terraces.
- ENE-WSW faults divide the Messenia Peninsula into blocks at a scale of 30-40 km: i.e. the Northern Messenia and the Southern Messenia Blocks. The number and altitude of surfaces of subaerial erosion and marine terraces and also the extent of Pliocene-Pleistocene sediments differ between the Northern and the Southern Messenia Blocks. NNW-SSE faults define horsts and grabens within each block.
- The Northern Messenia Block is the more elevated and retains a relatively complete Pleistocene stratigraphy relative to the Southern Messenia Block, which is subdued and dips beneath the sea the to the south. Both blocks are flanked by an extensional fore-arc to the west, while the Southern Messenia Block is bordered by the Messenia Gulf graben to the east. On a regional scale, the Messenia Peninsula, thus, represents, a large segmented horst within a regionally extending area.
- The Northern Messenia Block preserves the most complete succession of Pleistocene marine terraces, in decreasing altitude with decreasing age. Absolute altitudes of marine terraces are also highest within this block.
- The drainage of the Messenia Peninsula is mixed dendritic-parallel, with local presence of trellis or parallel types. Stream order is $\leq 6^{th}$.
- Drainage was controlled by lithology, normal faulting and relative sea level change.

- A focus of stream divergence is present in the area of Gargaliani-Hora (Northern Messenia Block). This was previously interpreted as a result of neotectonic folding; however, alternative interpretations could also be proposed (e.g. ENE-WSW faulting).
- Longitudinal profiles of streams suggest segmentation into three principal sectors, each one correlated with a principal group of subaerial surfaces or marine terraces (i.e. Late Tertiary, Late Pliocene-early Pleistocene, middle Pleistocene-Holocene surfaces). Other knick points are correlated with cliffs of individual terraces among these larger groups, or with normal faults and lithological boundaries.
- In relation to the tectonic grain, the drainage of the Messenia Peninsula is distinguished into parallel and transverse groups.
- Parallel drainage was probably formed in the Pliocene, controlled by ENE-WSW faults. Transverse drainage, that locally captures the previous one, was formed in Late Pliocene-Early Pleistocene time, and evolved throughout the Quaternary, controlled by NNW-SSE faults.

Figure 2.11: Erosive terraces correlated with early Pleistocene sea levels. In the background, the extensive coastal plain comprises middle and late Pleistocene terraces. Valta, looking SW.

Figure 2.12: A narrow, V-shaped gorge, incised into the early Pleistocene terraces. Such gorges and correlative cliffs correspond to a middle Pleistocene relative sea level fall.
Laghouvardhos Gorge, Valta.

Figure 2.13: The Neotyrrheinian terrace, covered by recent dunes is visible in the background. A Holocene beachrock is present within the small bay, indicating recent emergence. Romanos Coast.

Figure 2.14 (left): A marine notch of inferred Eutyrrhenian age, at altitude ca. 7 m, formed on the scarp of a NNW-SSE trending fault. Pylos Port.

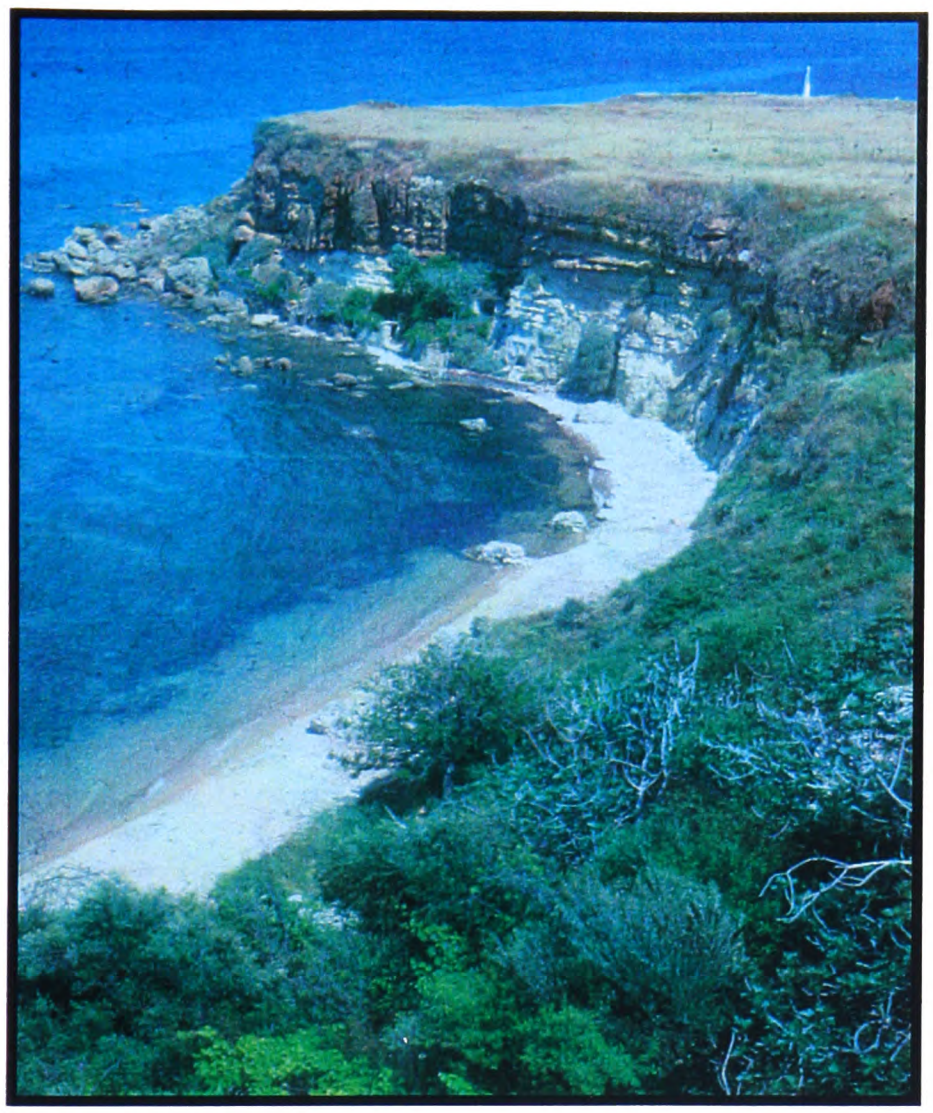

Figure 2.15: Marine terrace at ca. 17-20 m, formed on progradational clinoforms of inferred late Pleistocene (Eutyrrhenian) grainstone (brown). The latter sediment is unconformable above Early Pliocene mud (pale). Koroni

Figure 2.16: ENE-WSW trending fault brings into contact early Pleistocene packstone (left) with brecciated bedrock limestone (right). Gargaliani. This is one of the faults shown in Figure 2.4.

CHAPTER 3: PLIO-QUATERNARY SEDIMENTS OF THE MESSENIA PENINSULA: STRATIGRAPHY AND SEDIMENTARY ENVIRONMENTS

3.1 INTRODUCTION

In this chapter, well exposed Plio-Quaternary (Early Pliocene to Holocene) shallow-marine and terrestrial sediments from the Messenia Peninsula are described and interpreted in terms of potential controls, including regional tectonic uplift, eustatic sea level change, uplift and subsidence related to local faulting, climate and autocyclic (normal) sedimentary processes. Geological, sedimentological and palaeontological evidence are synthesised into a new stratigraphic model for the Plio-Quaternary of the Messenia Peninsula, that takes into account sea level cyclicity and land uplift during the last ca. 5 Ma. A model for the geological evolution of the Messenia Peninsula during the Pliocene-Quaternary is then proposed (Kourampas and Robertson, 2000).

Previous work in the area focused on the geomorphology of marine terraces (Kelletat et al., 1976; Mariolakos et al., 1994), the sedimentology and the neotectonics of selected areas (Zelilidis, 1988; Zelilidis et al., 1988, Zelilidis and Doutsos, 1992; see Chapter 1). In this study an integrated approach is adopted, drawing on the sedimentology and structural evidence, in addition to geomorphology (Chapter 2), to deduce the Plio-Quaternary geological history of the region.

3.2 AGE CONSTRAINS:

Up to five Late Tertiary erosion surfaces (without sediments) and seven Quaternary (L:ate Pliocene, Pleistocene and Holocene) terraces (with sediments) are identified within the Northern Messenia Block (Figs. 2.5, 2.6.a, 2.7, 2.9.a), representing the maximum number of terraces found in the S Peloponnese (see Chapter 2). Terraces and sediments associated with the Southern Messenia Block are less well developed and, thus, difficult to correlate (Figs. 2.5, 2.6.b, 2.8, 2.9.b; see Chapter 2). Nevertheless, the Pliocene stratigraphy is well preserved in the Southern Messenia Block.

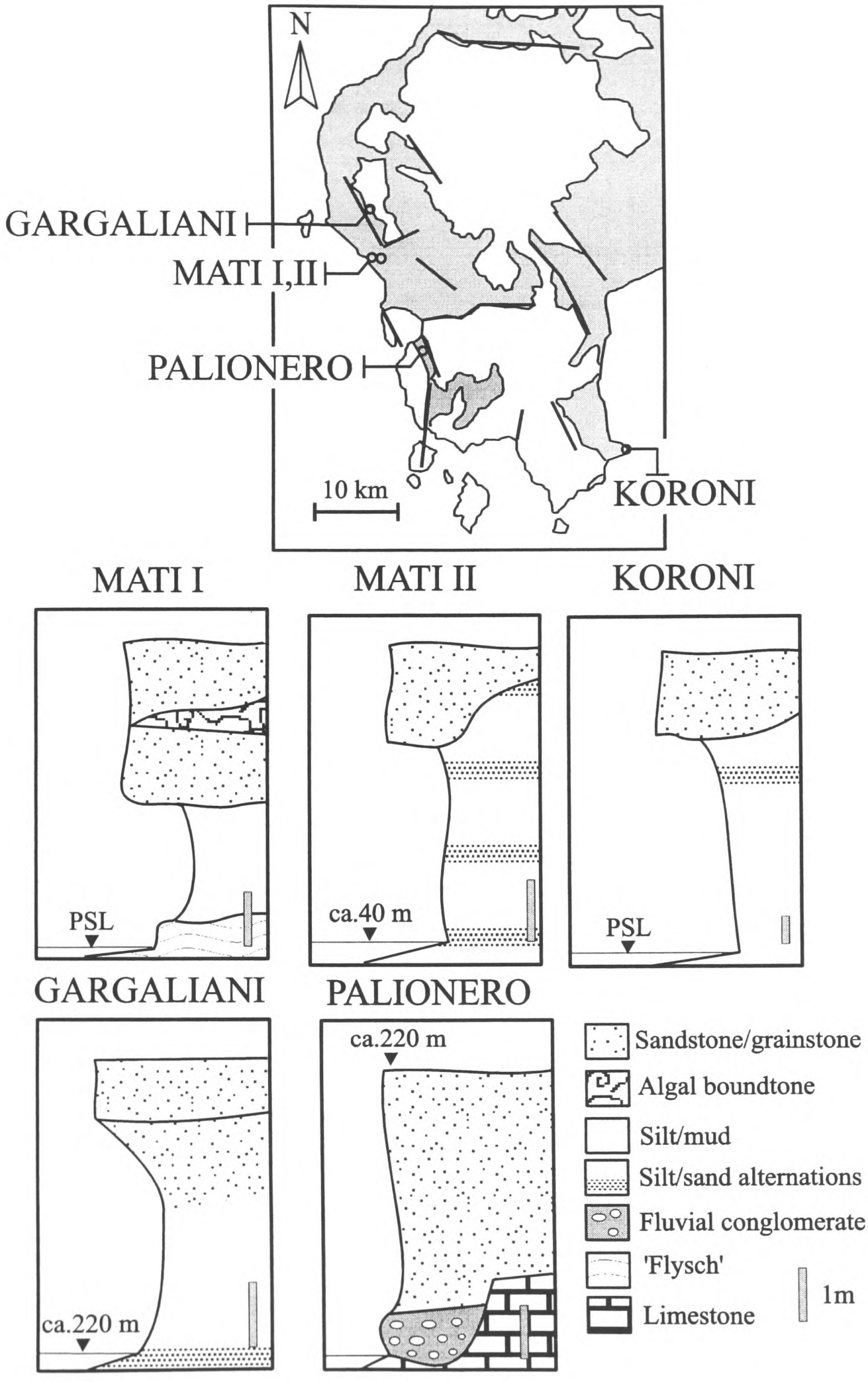

Figure 3.1: Evidence for stratigraphic subdivision of Plio-Quaternary sediments in the Messenia Peninsula. Schematic logs of sections that provide the evidence for stratigraphic subdivision into informal units proposed here. White: Shallow-marine facies; Grey: Subaerial facies.

3.2.1 Dating: During this study, Early Pleistocene sediments were dated biostratigraphically (identifications by D. Frydas, Patras University). Also Pliocene to early Pleistocene sediments were correlated with adjacent dated sequences (Berckhemer and Kowalczyk, 1978; Frydas, 1990; Frydas and Bellas, 1994). Attempts at U-series dating of solitary corals were unsuccessful, as all the material collected was recrystallised to calcite (see Chapter 6).

However, two late Pleistocene marine terraces can be correlated with the "Eutyrrhenian" and "Neotyrrhenian" substages of the "Tyrrhenian" sea level cycle (Bonifay, 1975), as determined in the Peloponnese (Keraudren, 1970, 1971; Kelletat et al., 1976; Kowalczyk et al., 1992) and other areas of the Mediterranean (e.g. Sicily, Calabria, Cyprus). In addition, an uplifted shoreline of Holocene age is correlated with the "Versilian" stage of the classical Mediterranean chronostratigraphy (Keraudren, 1970, 1971; Bonifay, 1975). Correlations are based on relative altitude, geomorphology, lateral extent and detailed sedimentary facies.

3.2.2 Sea level correlation: In an attempt to further constrain the age of Pliocene to Holocene sediments and terraces a sequence-stratigraphic approach has been adopted (Figs. 3.3, 3.4). Regionally extensive maximum flooding surfaces and unconformities observed in the field are interpreted to relate to global eustatic sea level highstands and lowstands, respectively. The marine sedimentary record can, thus, be tentatively linked to a relatively well constrained sea level history (see Figures 3.1, 3.2, 3.3).

3.2.2.1 Late Pleistocene-Holocene terraces: The five terraces younger than early Pleistocene are assigned provisional ages, as follows (Fig. 3.3): Both late Pleistocene marine terraces identified as "Eutyrrhenian" and "Neotyrrhenian" can be correlated with the 4th order isotopic stage 5 (Last Interglacial) in the global eustatic sea level curve, constructed from oceanic oxygen isotope evidence (Imbrie et al., 1984, Martinson et al., 1987; see Chapter 1). Following this correlation, each of these terraces corresponds to a higher order substage within the 4th order isotopic stage 5 (*sensu* Martinson et al., 1987). Given the lack of absolute dating of these two terraces in Messenia Peninsula, correlation with particular substages is arbitrary. Nevertheless, a correlation of the "Eutyrrhenian" with the isotopic substage 5.5 and the "Neotyrrhenian" with the isotopic substages 5.3+5.1 is favoured, for the following reasons: 1) The "Eutyrrhenian" is traditionally defined as the "transgressive maximum" of the "Tyrrhenian" (Last Interglacial) sea level cycle (Bonifay, 1975). According to isotopic evidence, this transgressive maximum took place ca. 120 ka before Present, during isotopic substage 5.5, when the eustatic sea level probably exceeded the present one by a few metres (Imbrie et al., 1984; Labeyrie et al., 1987).

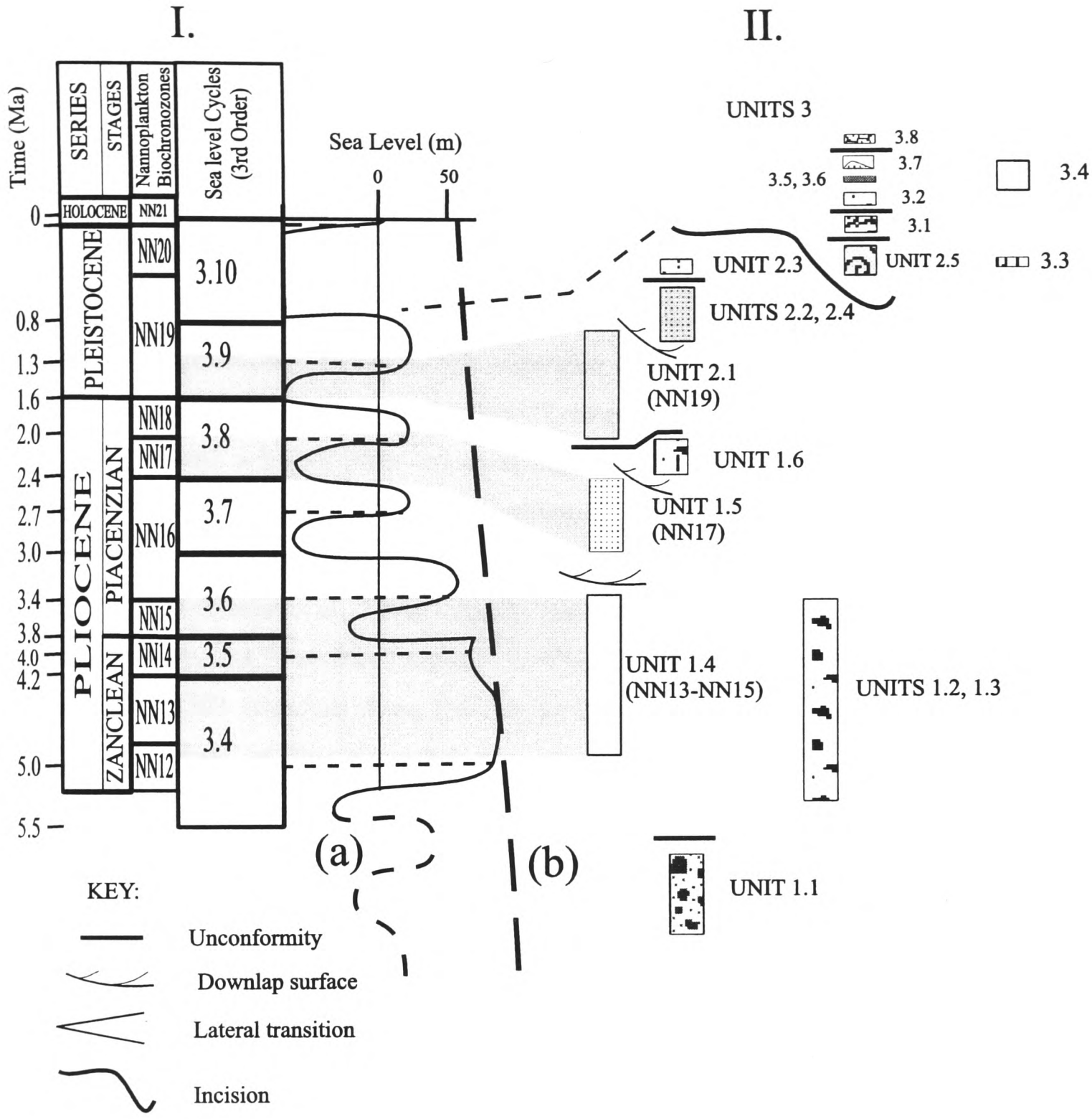

Figure 3.2: Age model for the Plio-Quaternary sediments of the Messenia Peninsula: Plio-Quaternary time scale (the last 5.5 Ma). **i)** Global eustatic sea level curves (**a:** 3rd order cycles; **b:** 2nd order cycle), correlated with nannoplankton biochronozones (Haq et al., 1988); **ii)** Simplified logs of sedimentary successions from Messenia. Maximum intact sequences are shown as log segments. Correlation with the eustatic sea level curve is based on nannofossil dating for the Pliocene-early Pleistocene (Frydas, 1990; pers. comm., 1998; Frydas and Bellas, 1994). Transgressive-regressive shallow-marine sequences of Pliocene to early Pleistocene age correlate with 3rd order eustatic highs of the global sea level curve.

2) The "Neotyrrhenian" is traditionally defined as the later part of the "Tyrrhenian" (Last Interglacial) sea level cycle, when 4th order sea level fall was punctuated by short-lived sea level highstands (Bonifay, 1975). Isotopic evidence suggests that the later part of isotopic stage 5 (Last Interglacial) was punctuated by higher order sea level cyclicty. The isotopic substages 5.3 (ca. 100 ka) and 5.1 (ca. 80 ka) correspond to higher order highstands during a period of falling sea level (Labeyrie et al., 1987; Martinson et al. 1987; Fig. 3.3.II, III), conforming with the definition of the "Neotyrrhenian" substage (Bonifay, 1975). The presence of both substages 5.3 and 5.1 in Messenia Peninsula cannot be proved without geochronological evidence. However, field evidence suggests that the "Neotyrrhenian" terrace comprises two stacked marine sequences separated by soil (see Fig. 3.5 and below). The "Versilian" terrace, above the two "Tyrrhenian" (Last Interglacial) terraces, can be correlated with a higher order sea level highstand, after the Last Glacial Maximum, but before the eustatic sea level reached its present-day level (Bonifay, 1975). Geochronological evidence from the western Mediterranean (Gulf of Lions, France; Labeyrie et al., 1976) and the Red Sea (Plaziat et al., 1996) suggests that a sea level highstand occurred at ca. 5-7 ka. Alternatively, this "Versilian" deposit could be correlated with coastal features of historic age (1700-1500 years) all along the Aegean Arc (from Antikythera to Crete), S Turkey, Syria and Israel, uplifted as a result of a regional tectonic event ca. 1530-1550 years ago ("*Early Byzantine tectonic paroxysm*") (Pirazzoli, 1986, 1987; Kelletat, 1991).

3.2.2.2 Early and middle Pleistocene terraces: The two remaining marine terraces (Units 2.3 to 2.5; see Fig. 3.3) are tentatively correlated with early to middle and middle Pleistocene eustatic highstands, respectively, although with marked uncertainty in view of multiple highstands within the latter.

Fig. 3.3 (following page): Age model for the Quaternary sediments of the Messenia Peninsula: Pleistocene-Holocene time scale (the last 1.6 Ma). A Pleistocene stratigraphic scheme (modified from Bonifay, 1975) is shown on the left **(I)**. The beginning of the Pleistocene is set at 1.6 Ma. The easily identifiable "Versilian", "Euthyrrhenian"/"Neotyrrhenian" terraces in **(III)** (Units 3.8, 3.1 and 3.2, respectively) are correlated with the high-resolution oxygen-isotope curve (**II a**; Martinson et al., 1987) and the corresponding eustatic sea level curve (**II b**; Imbrie et al., 1984). In addition, the terraces between the dated early Pleistocene (Unit 2.1) and correlated "Euthyrrhenian"/"Neotyrrhenian" terraces (i.e. late "Calabrian"/"Sicilian": Units 2.1 to 2.5; see **III**) are assumed to relate to intervening eustatic highs (column **I**), although with major uncertainties owing to the presence of unresolved, multiple eustatic sea level highs. Key to sediments as in Figure 3.2.

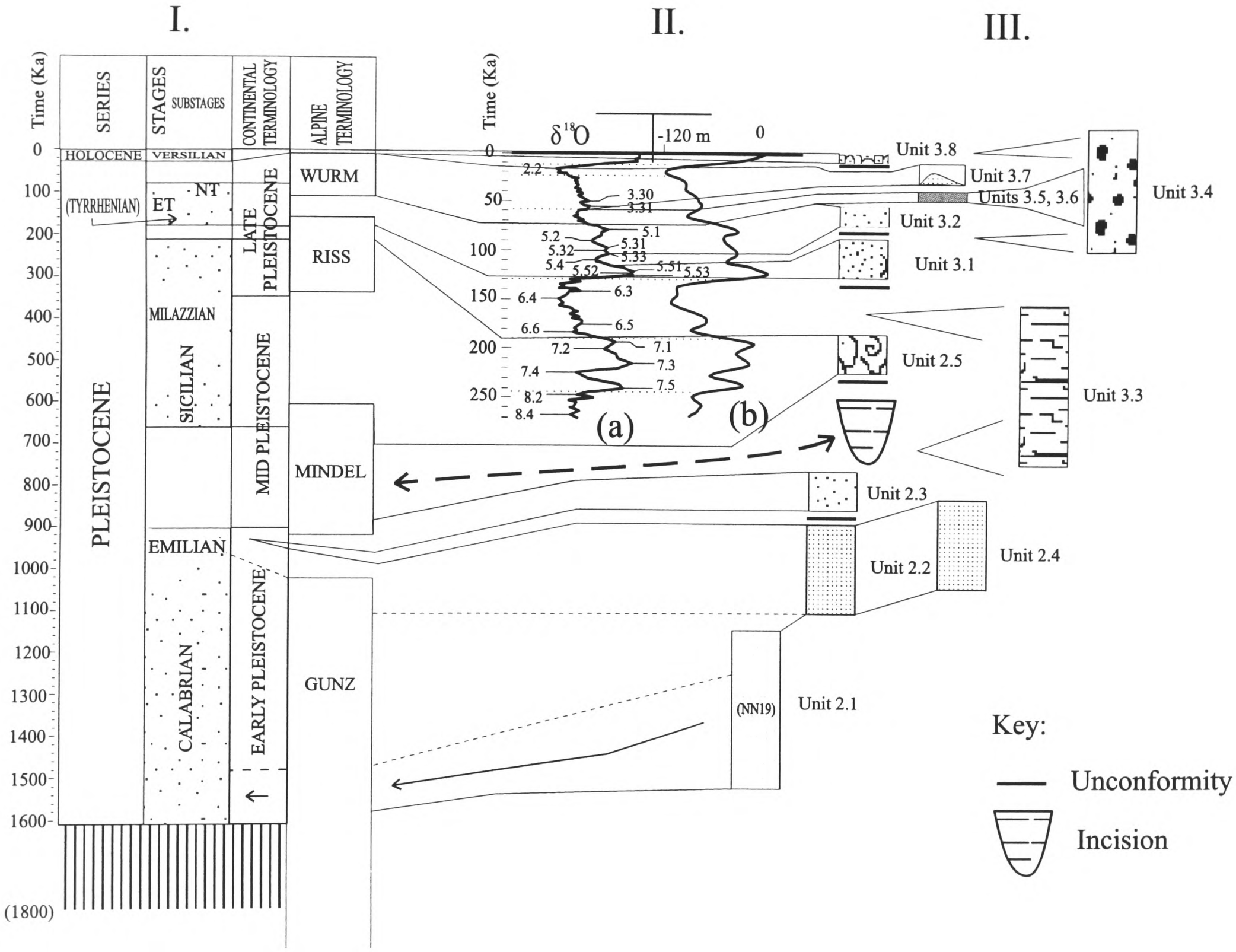
I.
II.
III.
Time (Ka)
SERIES
STAGES
SUBSTAGES
CONTINENTAL TERMINOLOGY
ALPINE TERMINOLOGY
HOLOCENE
VERSILIAN
(TYRRHENIAN)
ET
NT
MILAZZIAN
SICILIAN
EMILIAN
CALABRIAN
PLEISTOCENE
LATE PLEISTOCENE
MID PLEISTOCENE
EARLY PLEISTOCENE
WURM
RISS
MINDEL
GUNZ
δ18O
-120 m
0
2.2
3.30
3.31
5.1
5.2
5.31
5.32
5.33
5.4
5.51
5.52
5.53
6.3
6.4
6.5
6.6
7.1
7.2
7.3
7.4
7.5
8.2
8.4
(a)
(b)
Unit 3.8
Unit 3.7
Units 3.5, 3.6
Unit 3.4
Unit 3.2
Unit 3.1
Unit 2.5
Unit 3.3
Unit 2.3
Unit 2.2
Unit 2.4
(NN19)
Unit 2.1
Key:
Unconformity
Incision

The first marine terrace topographically above the "Eutyrrhenian" (Unit 2.5) is attributed to the multiple "Sicilian" highstand, which, according to the classical chronostratigraphic scheme (Bonifay, 1975), spans the time from ca. 450-200 ka (Fig. 3.3). The latest of these cycles corresponds to isotopic stage 7, with a transgressive maximum at ca. 210 ka (*sensu* Martinson et al., 1987; Fig. 3.3). Field evidence also suggests that in Messenia Peninsula the "Sicilian" terrace comprises more than one amalgamated marine sequence (see Fig. 3.4 and below), but ages remain uncertain. A further terrace (Unit 2.5), unconformably overlying the early Pleistocene (late "Calabrian") terrace, could correspond to any isotopic stage earlier than stage 7, possibly including higher order "intra-Calabrian" sea level cyclicity. The second alternative is favoured, as field evidence suggests that this terrace predates a major pre-late Pleistocene phase of cliff cutting (Figs. 3.3, 3.4). Assuming that the latter feature corresponds to the "Mindel" sea level lowstand (Bonifay, 1975), this terrace is probably late Early Pleistocene (latest "Calabrian") in age. Finally, Unit 2.4 from southern Messenia is younger than the lower "Calabrian" Unit 2.1, dated biostratigraphicaly. Unit 2.4 could, thus, be correlated with either of the upper "Calabrian" units 2.2 or 2.3 in NW Messenia. The first alternative is favoured on the basis of similar facies, sedimentary architecture and stratigraphic position.

Using a sequence stratigraphic approach, constrained by available micropalaeontological data, the Pliocene to Holocene sequences in Messenia are, thus, correlated with stages in the classical Mediterranean Pleistocene stratigraphy (Bonifay, 1975). In the NW Messenia block, where the Pleistocene stratigraphic record is more complete, six successive 4^{th} (or higher) order depositional sequences correlate with marine terraces, located at progressively lower elevations. Our correlation suggests a minimum uplift rate of ca. 0.1 m/ka since the "Eutyrrhenian" (last ca. 120 ka), assuming constant uplift rate (see Chapter 7). The minimum uplift rate since the end of the "Calabrian" (last ca. 900 ka) was between 0.23-0.33 m/ka, depending on the correlation of the "Sicilian" terrace with middle Pleistocene isotopic stages (see Chapter 7). These rates are similar to the radiometrically constrained minimum uplift rate in the Corinth area, N Peloponnese (ca. 0.3m/ka; Collier, 1990).

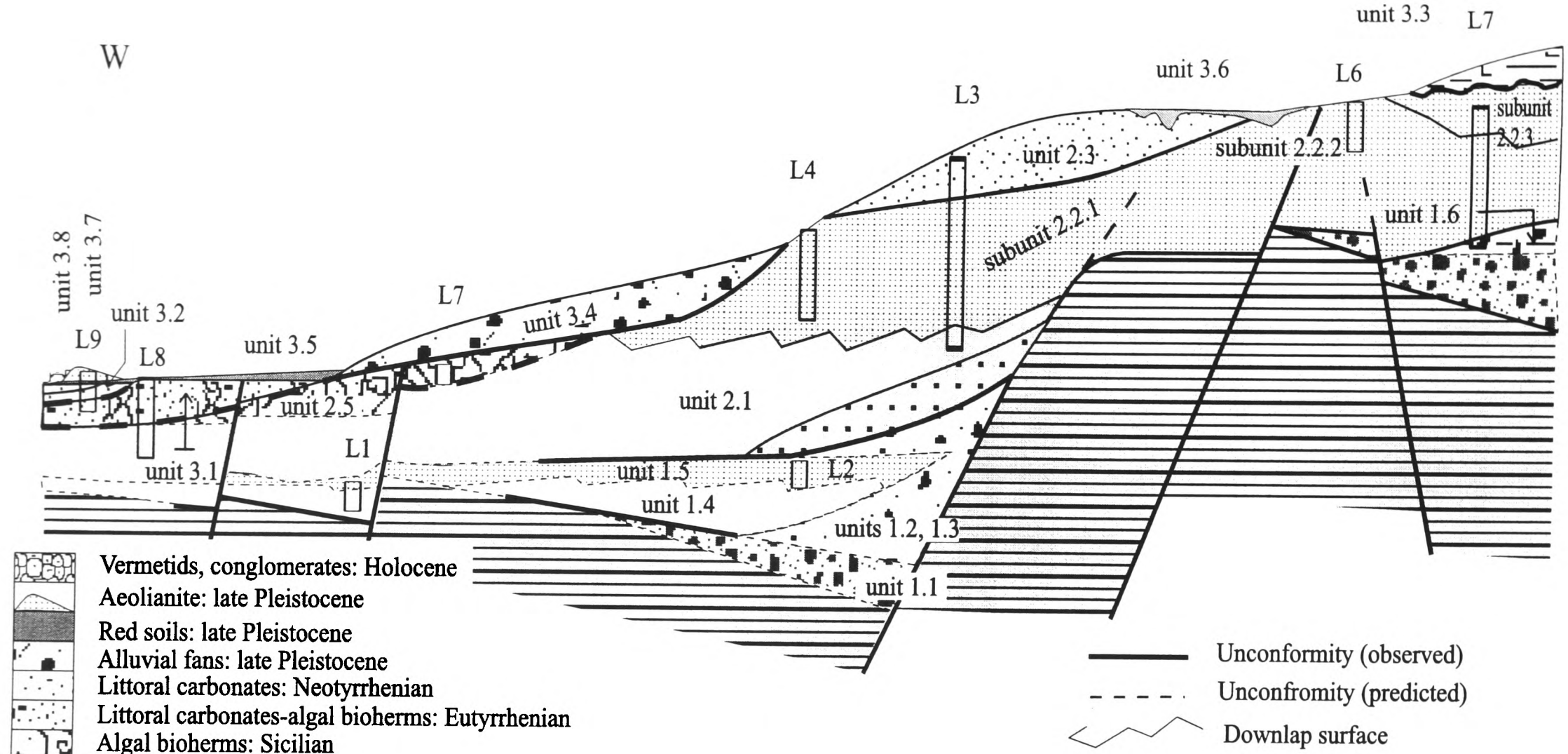

Figure 3.4: Tectonic-stratigraphic diagram showing the relative positions of the Plio-Pleistocene units discussed in the text. The figure illustrates the relationships of each of the units described and is *not* intended as an accurate cross-section, as the logs are projected onto a simplified E-W traverse (approximate horizontal scale: ca. 7 km across). The figure is mainly applicable to the Northern Messenia Block, where the stratigraphy is more complete, than in the Southern Messenia Block. Individual logs are shown in detail in subsequent figures.

3.3 PLIO-PLEISTOCENE SEDIMENTS OF THE MESSENIA PENINSULA

In this section Pliocene-Pleistocene sedimentary successions in the Messenia Peninsula are described and interpreted, on the basis of individual outcrop relations. A striking feature of the Messenia Peninsula is the presence of the well-developed flight of marine terraces along the western coastal area (Kelletat et al., 1976; Zelilidis, 1988) (Figs. 2.6, 2.9, 3.4). Up to eleven Pleistocene terraces were recognised by Kelletat et al. (1976), whereas during this study up to six Pleistocene-Holocene terraces were mapped, all with preserved shallow-marine sediments, at least locally. In addition, correlative marginal marine (e.g. lagoonal) and non-marine (terrestrial) sediments are locally present (Figs. 3.6, 3.6). Within individual areas, local short successions (generally tens of metres of less) can be recognised, based on sedimentary facies and the identification of unconformites/disconformities (Figs. 3.1, 3.4). These local successions contain a sufficient number of distinctive features to allow lateral correlation of the main Plio-Quaternary marine units throughout the Messenia Peninsula. Such correlations take account of proximal-distal facies variation within single depositional packages.

3.3.1 Stratigraphy of the Messenia Peninsula: In the Messenia Peninsula, marine sedimentation began in the Early Pliocene (Zanclian; ca. 5 Ma) and continued until the Holocene, interrupted by periods of emergence, subaerial erosion, alluviation and pedogenesis. The Pliocene-Holocene sedimentary record of the Messenia Peninsula is resolved into 19 informal units. Marine sediments are resolved into 9 distinct depositional units, bounded by unconformities. Subaerial sediments (10 units) are distinguished on the basis of their relation to marine sediments, major landforms (e.g. river valleys, erosional surfaces) and facies. However, at least some of the suabaerial units may be contemporaneous, reflecting differences of depositional environment.

The Pleistocene-Holocene sedimentary record of the Messenia Peninsula (last ca. 1,6 Ma), is grouped into two 3rd-order depositional sequences, namely: MQ1, of early Pleistocene age, correlated with the sea level cycle 3.9 *sensu* Haq et al. (1988) and MQ2, of middle Pleistocene-Holocene age, correlated with the sea level cycle 3.10. Sequence MQ1 was deposited on Late Pliocene subaerial relief (pediment, palaeovalleys) and terminates upwards with soils. The early Pleistocene marine terrace(s) were formed above sediments of Sequence MQ1. Sequence MQ2 was deposited on middle Pleistocene subaerial relief (cliffs, pediments) that locally reach ca. 120 m. This sequence terminates upwards with soils and aeolianites. The middle and late Pleistocene terraces and the Holocene marine abrasion platform were formed above sediments of Sequence MQ2. The post-middle Pleistocene

sequence MQ2 is resolved into at least three 4th-order 'sequences' (formally parasequences), bounded by unconformities, namely: "Sicilian", "Tyrrhenian" and Holocene. These are correlated with 4th-order sea level cycles that reflect glacio-eustatic sea level change. The "Tyrrhenian" is further subdivided into "Eutyrrhenian" and "Neotyrrhenian" units, reflecting higher frequency glacio-eustatic cyclicity within isotopic stage 5. The early Pleistocene Sequence MQ1 is resolved into at least two higher-order 'sequences', also bounded by unconformities. The earliest 'sequence' is correlated with the regressive "Calabrian" stage of the early Pleistocene. The latest 'sequence' can be correlated with either an intra-"Calabrian", 4th or higher-order sea level cycle (by comparison with the 4th-order 'sequences' present within Sequence MQ2), or with an early middle Pleistocene sea level cycle, predating emergence and cliff-cutting.

A relative stratigraphy was erected for the entire area, including twenty informal units, correlated with 3rd and 4th order sea level cycles, as discussed above (Figs. 2.1, 3.4). In addition, various sub-units were recognised, representing 4th, or higher-order cycles that could not be resolved, or lateral facies variations within a given chronostratigraphic unit. Each of the units is shown on a schematic tectono-stratigraphic diagram (Fig. 3.4), most applicable to the North Messenia Block, where the sedimentary record is best preserved. Representative measured sedimentary logs for the marine units are shown on Figures logs. The key to all logs is in Figure 3.8.

3.3.2 PRE-PLEISTOCENE SEDIMENTARY SEQUENCES

3.3.2.1 Unit 1.1 (Late Oligocene-Early Miocene ?): conglomerate

Successions are dominated by well cemented clast-supported polymict conglomerates that exhibit east-dipping tabular cross-bedding. These conglomerates contain well-rounded, mostly rod-shaped, imbricate clasts of basement lithologies (limestone, turbiditic sandstone, radiolarian chert and pelagic limestone), in a matrix of medium- to coarse-grained sandstone. This unit, >200m thick, crops out widely west of the Pindos thrust in N. Messenia and as small, patchy outcrops in S. Messenia (Figs. 2.1, 3.5, 3.6). A typical section is exposed a few kilometres east of Hora, towards Kalamata (Figs. 2.1, 3.5). This exposure was mapped by Fytrolakis (1971) as the uppermost, most proximal facies of the Tripolis zone "flysch", of Late Oligocene(?) age. Alternatively, I.G.M.E. (1980 a,b) mapped this sedimentary unit ("Messenian Conglomerate") as Late Oligocene to Early Miocene, affected by "*late-orogenic folding*". This unit was also correlated with the "*Late Miocene (or older)*" "*Rahes Formation*" of the "Kyparissia-Kalo Nero Basin" by Fountoulis and Moraiti (1994).

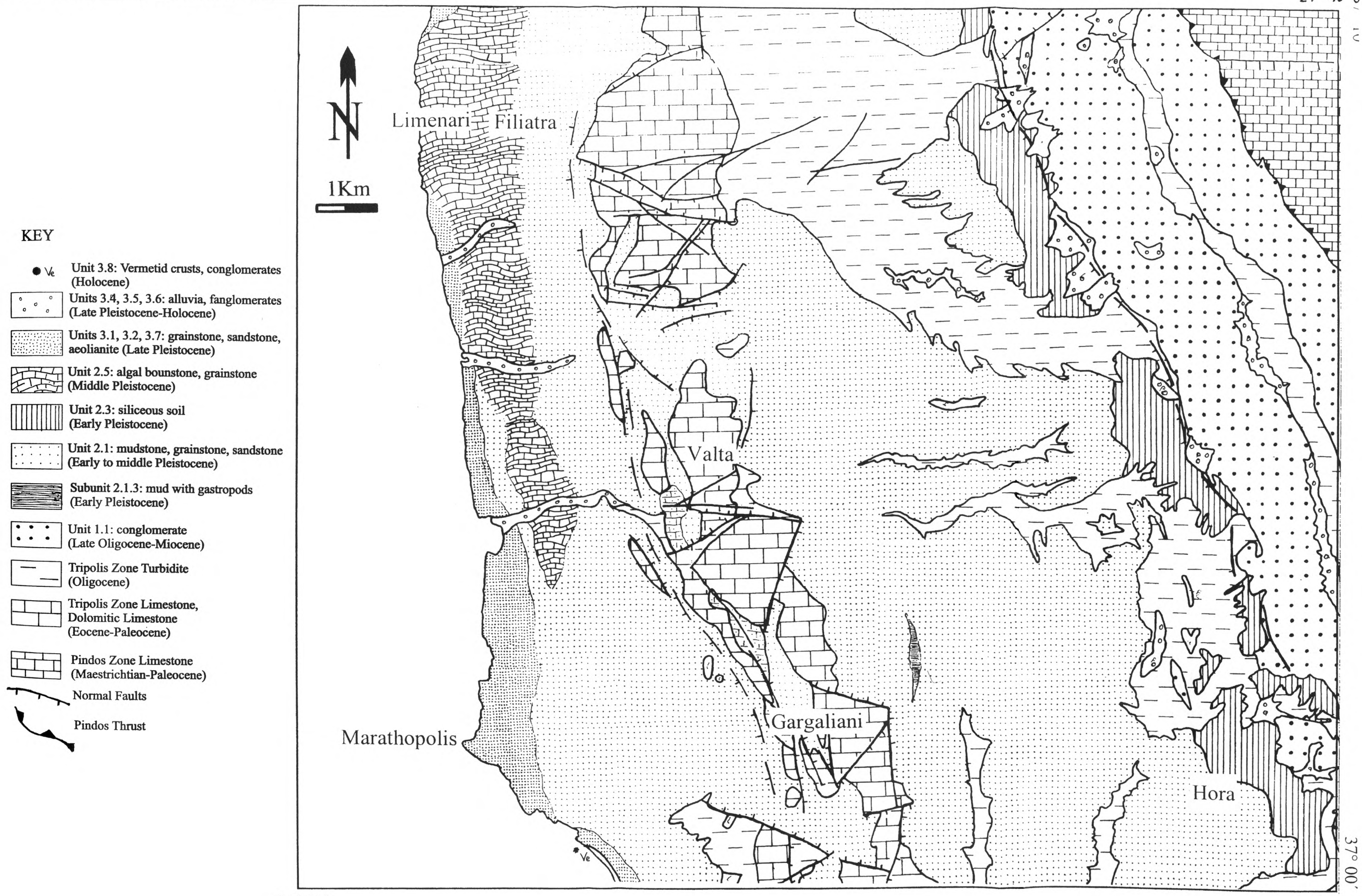

Figure 3.5: Geological map of the Garagliani-Filiatra area, Northern Messenia Block.

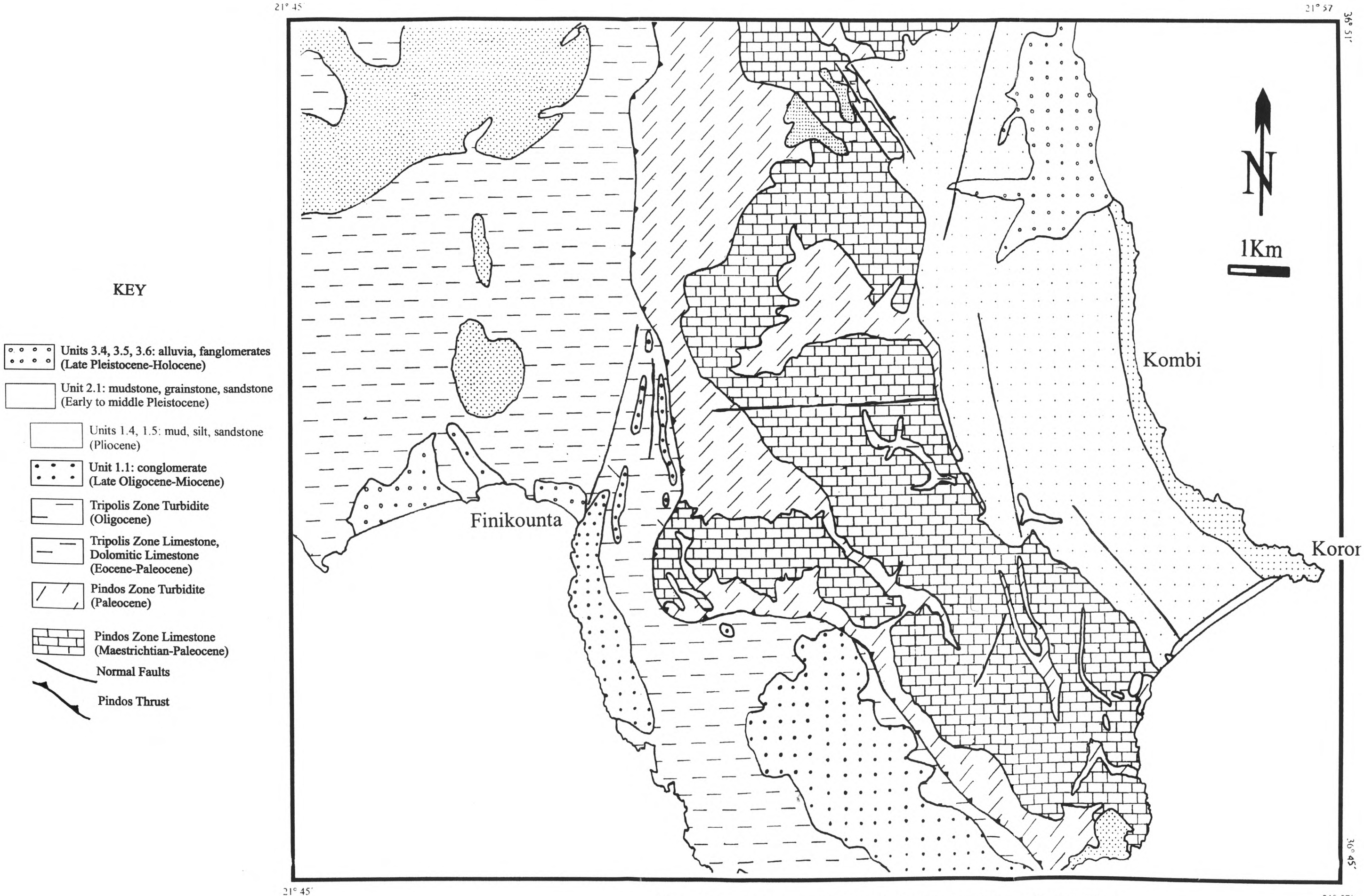

Figure 3.6: Geological map of the Koroni-Vounaria area, Southern Messenia Block.

Reconnaissance during this study suggests that this conglomeratic unit represents fluvial clastic sediments deposited within a flexural foreland during, or soon after, the latest stage of thrusting (Late Oligocene(?)-Early Miocene) of the Pindos zone over the Tripolis zone foreland. This unit was subaerially exposed, eroded and peneplanated, probably during the Late Miocene.

3.3.2.2 Unit 1.2 (Pliocene?): fluvial conglomerate

This unit, with a maximum exposed thickness of only 1-2 m, consists of local outcrops of well indurated clast-supported, polymict conglomerates, set in a red siltstone matrix. Individual clasts (3-7 cm) are commonly rod-shaped. The best exposure is seen within a N-S trending palaeovalley on the road from Pylos to Methoni (near the village of Palioneron; S Messenia; see Fig. M.1). This unit is unconformably overlain by shallow-marine sediments of inferred early to mid-Pleistocene age (Unit 2.4; see below; Figs. 3.2, 3.3. 3.4).

Interpretation: The conglomerate is interpreted as the fluvial infill of a N-S trending paleovalley. Such paleovalleys in the Messenia Peninsula are commonly correlated with Late Tertiary drainage (see Chapter 2). This, together with the very well-cemented state of the deposit and its stratigraphic position below shallow-marine sediments of inferred early Pleistocene age (Unit 2.4) suggest a Late (?) Pliocene age for the Unit 1.2 fluvial conglomerate.

3.3.2.3 Unit 1.3 (Late Pliocene?): breccia

This unit is composed of well cemented, red, monomict limestone breccias that crop out locally at an altitude of ca. 210 m, parallel to a prominent NW-SE-trending escarpment, near Gargaliani (Figs. 3.5, 3.6, 3.8). The breccia includes marine fossils (bivalves, corals) and reworked clasts of grainstone/packstone and is unconformably overlain by early to mid-Pleistocene shallow-marine sediments (Unit 2.2; see below; Fig. 3.2). Where locally exposed, these sediments are strongly jointed, but not faulted.

Interpretation: The red breccias are interpreted as colluvium, partly resulting from weathering and erosion of earlier marine terrace(s) developed along the margins of an elevated area (Gargaliani), west of the Gargaliani-Filiatra escarpment. Exposure is insufficient to determine whether, or not, the Gargaliani-Filiatra fault was active during, or after accumulation of this unit. The age of the breccias could correspond to one of the sea-level lowstands prior to the early Pleistocene deposition of Unit 2.1.

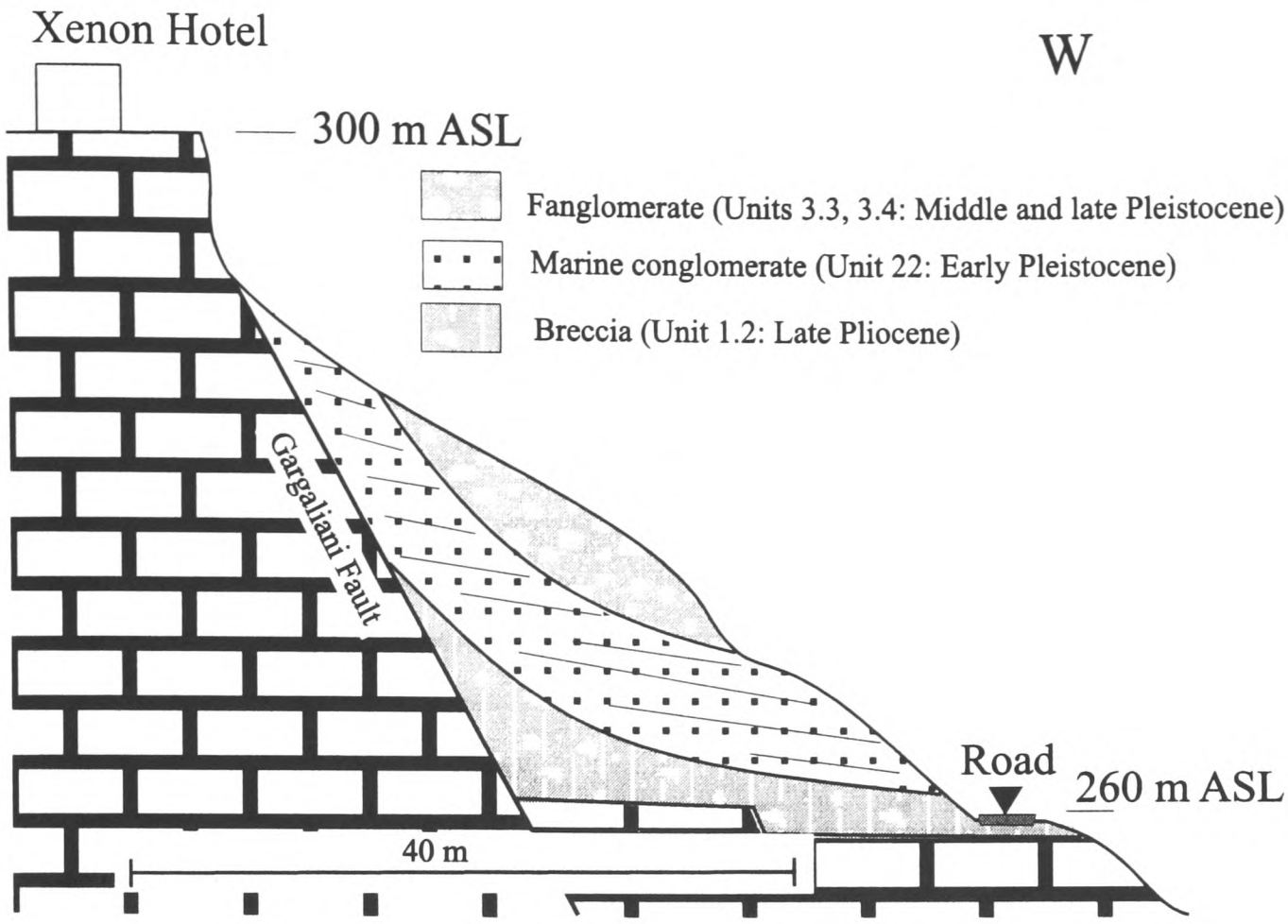

Figure 3.7: Cross-section across the Gargaliani cliff (for location see Figure 3.5): Late Pliocene subaerial colluvia (Unit 1.3) drape the NNW-SSE trending Gargaliani fault scarp. These are covered unconfromably by early Pleistocene shallow-marine conglomerates (base of Unit 2.1), followed by middle and late Pleistocene fanglomerates (Units 3.3, 3.4; see text).

3.3.2.4 Unit 1.4 (Early Pliocene; Zanclean): shallow-marine sandstone-mud

The upper part of this unit is well exposed in SE Messenia, in coastal cliffs north of Koroni (Figs. 2.1, 3.9: log 1). This unit comprises very bioturbated medium-to thick-bedded, muddy sandstones (0.50-1.50 m thick), alternating with beds (10-20 cm thick) composed of imbricate shells and shell fragments, set in a muddy matrix. A high-density fauna includes mud-dwelling bivalves, commonly still articulated and in life position, together with some gastropods. The shell-rich beds are sharp-based, locally with an undulating microrelief (1-3 cm). The lower parts of individual beds consist of imbricated shells set in a muddy matrix, coarsening upwards into fine micaceous, laminated silty sandstone, with local symmetrical ripples and scattered shells. The microfauna of this unit were described by Frydas (1990).

Similar muddy sediments that commonly include sharp based beds with dense accumulations of bivalves and gastropods are exposed in coastal cliffs all along the eastern coast of the S Messenia Peninsula, from Koroni to Vounaria (see Figs. 2.15, 3.6, 3.16, M.1).

Sandstone / grainstone-packstone

Conglomerate

Mud / marl

Algal boundstone

Caliche (chalky / duricrust)

Red soil

Nodular caliche

Lenticular caliche

Low angle planar cross-lamination (-bedding)

Trough cross-lamination (-bedding)

Hummocky cross-stratification

Slumps, disrupted bedding

Convolute lamination

Current scours

Pectenidae

Ostrea

Glycimeris

Gastropods

Vermetidae

Scaphopods

Brachiopods

Echinoids

Thyssanopods (Balanus sp.)

Scleractenian corals (Cladocora caespitosa)

Branching bryozoa

Encrusting bryozoa

Serpulid worms

Rhodoliths

Mammalian bone-fragments

Scolithos

Diplocraterion

Cruziana

Bivalve escape-traces

Rhizocretion

Figure 3.8: Key to all measured logs in this chapter.

Interpretation: This facies is interpreted as a storm-influenced upper offshore environment, with shell beds prograding over muds, deposited below the fair-weather wave-base. Previously, some sections of Unit 1.4 were dated as Early Pliocene (Koutsouveli, 1987) and correlated with the NN13, NN14 and NN15 biochronozones (*sensu* Martini 1971), spanning the entire Early Pliocene (Zanclean) (Frydas, 1990). This unit correlates with sea-level cycles 3.4, 3.5 and 3.6 *sensu* Haq et al. (1986) (ca. 5.0-3.4 Ma) (Fig. 3.3). No sequence boundaries that could allow further subdivision were observed in the field. No equivalent unit is found in NW Messenia; however, lower Zanclean (NN13 *sensu* Martini, 1971) deposits are known in the Kiparissia-Kalo Nero half-graben, north of the studied area (Fountoulis and Moraiti, 1994). Similar offshore facies of early Pleistocene age are also known from other areas of the Hellenic forearc (e.g. Rhodes; "*Kritika Formation*" -Bromley et al., 1996, Crete; Dermitzakis, 1972, Meulenkamp et al., 1988).

3.3.2.5 Unit 1.5 (Early-Late Pliocene; Zanclean-Piacenzian): shallow-marine conglomerate-sand

This unit comprises trough cross-stratified, matrix- to clast-supported polymict conglomerate, well exposed near Rhizomilos village (Zelilidis, 1988; Figs. 2.1, M.1, 3.9, log 2). The exposed base of the sequence consists of tangential bedsets (50 cm thick) composed of well-sorted, fine sandstone and conglomerate, dipping N/NE at 18-22°. Clasts are well-rounded, and can be correlated with lithologies of the Pindos zone (e.g. chert, pelagic limestone, turbiditic sandstone). The sequence passes upwards into polymict conglomerates with low-angle, N/NE dipping, tabular beds, alternating with well-sorted, tabular-planar beds of well-sorted yellow sandstone, up to 20 cm thick, with a shallow-water fauna of bivalves and benthic foraminifera (Table 3.1). An erosion surface above Unit 1.5 is located at 60 m ASL.

Interpretation: Trough cross-bedded conglomerates near the base correspond to fill of distributory channels, whilst alternating conglomerates and sands above represent prograding delta-front deposits of a coastal marine delta. The whole section thus corresponds to a progradational fan-delta, in view of the coarse grain size and the steep, largely fault-controlled morphological gradients in the source areas further west (Postma, 1990) (see Figs. 2.7.b, 2.11.b). Frydas and Bellas (1994) correlated sediments from the same locality (10-20 m N) with the NN17 biochronozone (*sensu* Martini, 1971) of the L:ate Pliocene, Piacenzian stage (ca. 3.4-3.0 Ma). In sequence stratigraphic terms, Unit 1.5, can be attributed to the highstand systems tract of sea-level cycle 3.6 *sensu* Haq et al. (1986;

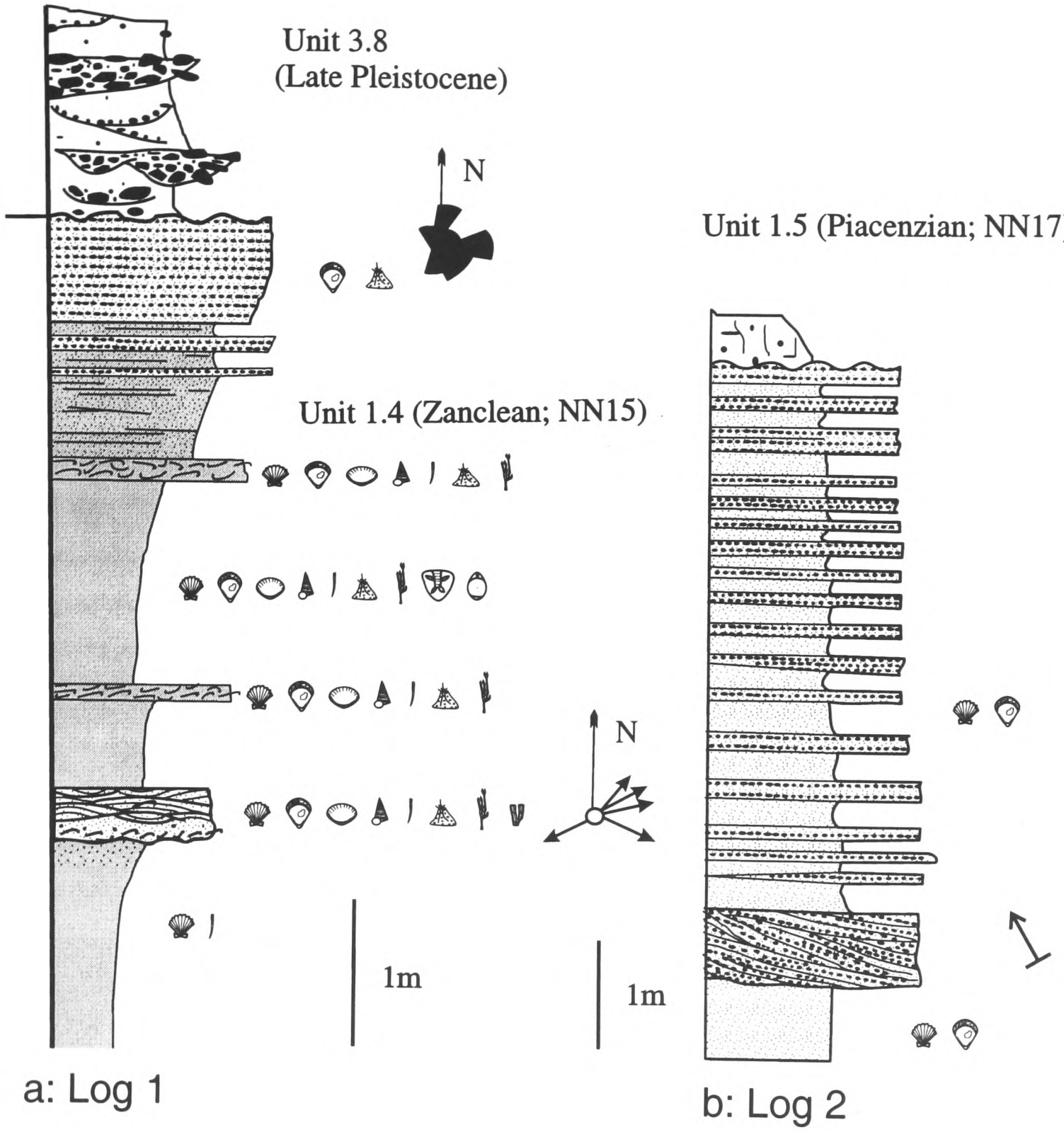

Fig. 3.9: Representative sedimentary logs of Pliocene and younger sequences (logs 1 & 2): **a)** Early Pliocene shallow-marine sediments (Zanclean; Unit 1.4), unconformably overlain by late Pleistocene alluvia (Unit 3.4); note palaeocurrent data; Kombi. **b)** Early to Late Pliocene (Zanclean-Piacenzian; Unit 1.5) from Rhizomilos (see Figures 3.6, M.1 for locations).

Fig. 3.2). In the Kiparissia-Kalo Nero Basin, NW of the area of study, sediments equivalent to the Early Pliocene Unit 1.4 (see above) are capped by fluvial conglomerate, of inferred Late Pliocene age (Fountoulis and Moraiti, 1994). The deltaic conglomerates of Unit 1.5 could represent more distal counterparts of these fluvial conglomerates further north.

3.3.2.6 Unit 1.6 (Late (?) Pliocene): sandstone-conglomerate

This is a well cemented, extensively karstified unit, only 2-3 m thick, that crops out on the road near the exit from Gargaliani towards Valta (Figs. 2.1, 3.5). It consists of well-sorted lithic greywacke, containing numerous grains of radiolarian chert of Pindos zone origin. There are also interbeds of clast- or matrix-supported conglomerate, with well-rounded clasts, correlated with Tripolis limestone. A shallow-marine, intralittoral and circumlittoral fauna of bivalves and foraminifera (Table 3.1) are present. This deposit is unconformably overlain by the inferred early Pleistocene Unit 2.2 (Figs. 3.3, 3.4, 3.5).

Interpretation: This is interpreted as a clastic shoreline deposit, adjacent to a deltaic system, based on the circum-littoral benthic foraminiferal fauna, the presence of terrigenous sediment and proximity to the Kiparissia Mountain front. There is no direct age evidence. However, the relatively high altitude (ca. 300 m ASL) and well cemented diagenetic state are suggestive of a Pliocene age. Similar, well cemented conglomerates separate Early Pliocene from early Pleistocene shallow-marine sediments in the Kiparissia-Kalo Nero half-graben further north (Fountoulis and Moraiti, 1994). Unit 1.6 probably represents a more distant, submarine equivalent of this latter, probably Late Pliocene unit.

3.3.3 EARLY TO MIDDLE PLEISTOCENE SEDIMENTS

3.3.3.1 Unit 2.1 (Early Pleistocene; «Lower Calabrian»): bioturbated mud

This unit comprises parallel-bedded carbonate muds, rich in planktic and benthic foraminifera and exhibiting extensive *Thalassinoides* bioturbation (Fig. 3.17). Typical outcrops are seen in cliffs (<10m high) above Pylos port in W Messenia (Figs. 2.1, M.1). Rich microfauna of benthic and planktic foraminifera are present (Table 3.1). Facies equivalents in NW Messenia (near Filiatrino Rema; see Fig. 3.5) are represented by marl with shallow-marine foraminifera, including *Hyalinea balthica* and *Globorotalia truncatulinoides*, together with mollusks and bryozoa (Marcopoulou-Diakantoni et al., 1991).

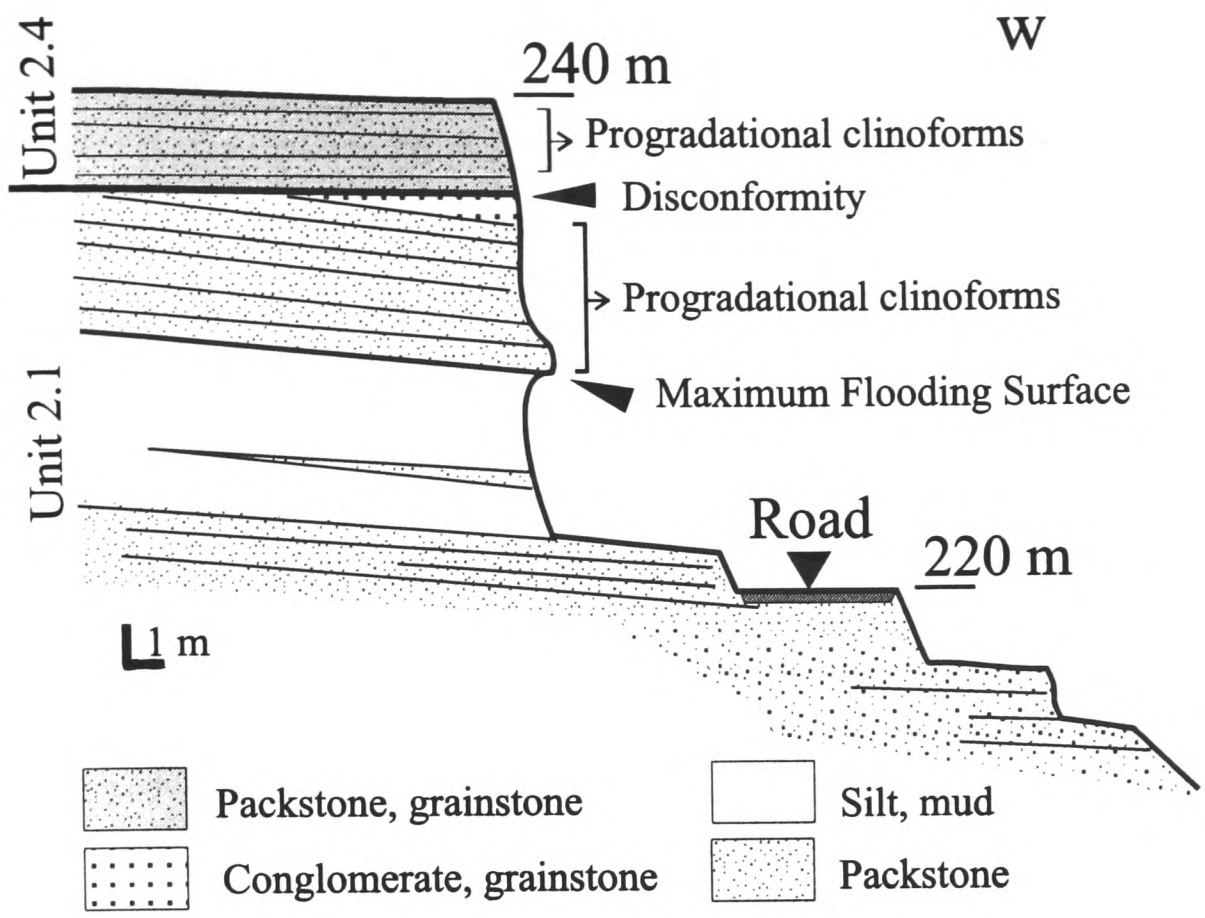

Figure 3.10: Cross-section in Pylos (for location see Fig. 3.5): Early Pleistocene shallow-marine sediments, with well-developed progradational architecture towards the top (Unit 2.1) are followed by packstone of early-middle Pleistocene age (Unit 2.4; see text).

Interpretation: The benthic foraminifera fauna present in the succession (including *Uvigerina peregrina*), suggest deposition within the offshore, below 90 m (Blanc-Vernet, 1969; Murray, 1973; Amorosi et al., 1998), thus making this unit the deepest early Pleistocene facies known in the Messenia Peninsula. Nannoplankton identification by D. Frydas (pers. comm., 1998) suggests that these sediments belong to the NN19 biochronozone, *sensu* Martini (1971), of early Pleistocene, «Calabrian» age (ca. 1600-900 ka). This unit can, thus, be correlated with the transgressive part of eustatic cycle 3.6 *sensu* Haq et al. (1988; see Figure 3.2), corresponding to the «Emilian» substage in the classical chronostratigraphy (Bonifay, 1975). Nannoplankton within similar facies in the Kiparissia-Kalo Nero half-graben further north ("*Miros Formation*") were also assigned to the NN19 biochronozone (Fountoulis and Moraiti, 1994). Unit 2.1 in the Messenia Peninsula was deposited in a narrow asymmetrical offshore graben, defined by NNW-SSE normal faulting (Figs. 2.9, 3.5). No indications of syn-depositional faulting were found; however, the unit is cut by antithetic faults, suggesting a long-history of fault movement. Similar offshore facies of early Pleistocene age are present in Crete (Dermitzakis, 1972, Meulenkamp et al., 1988) and Rhodes ("*Lindos Bay Clay*"; Bromley et al., 1991; Hansen, 1999) (see Fig. 1.2); such sediments in Rhodes were also correlated with an early Pleistocene relative sea level highstand.

3.3.3.2 Unit 2.2 Early to mid-Pleistocene («Upper Calabrian»)

This unit comprises a very extensive overall transgressive-regressive sequence in NW Messenia (e.g. near Gargaliani; Figs. 2.1, 3.4, 3.5). The transgressive base of the sequence is exposed only locally, as clast-supported polymict conglomerate forming steep clinoforms. These are deposited directly on bedrock and cemented colluvia/breccia (Unit 1.3) along the Gargaliani-Filiatra escarpment (Figs. 3.4, 3.7). The regressive part of the sequence is widely exposed near the western margin of the Gargaliani-Filiatra High further E (Figs. 3.5, 3.10.a, 3.11.b). Details of the individual outcrops are as follows:

3.3.3.2.1 Subunit 2.2.1: lithic packstone to pebbly-silty calcareous sandstone (Figs. 3.5, 3.10.a, log 3):

This sequence consists of foresets of lithic packstone to pebbly-silty calcareous sandstone, alternating with bioturbated mudstone. A typical outcrop (180-240 m ASL) occurs ca. 300 m S of Gargaliani (Fig. 3.5), where a fining-upwards, then coarsening-upward trend is observed. The lower beds are rich in carbonate skeletal grains, whilst the terrigenous content increases upwards. The uppermost beds comprise well-sorted, matrix-free, coarse-grained sandstone to granular conglomerate, with very well-rounded pebbles, alternating with laminated calcareous sandstone. Foresets (10-40 cm thick) dip WNW at 7-18° (Fig 3.10.a, log 3). Individual beds are commonly sharp-based, normally graded (low in the sequence), or coarsen upwards to pebbly sandstone/matrix-supported conglomerate. Disc- and rod-shaped clasts are relatively common in the upper parts of the sequence. Pebbles, including rounded, bored limestone, are correlated with the Tripolis zone basement, whereas angular granule-sized grains of red chert were derived from the Pindos zone. Many pebbles are bored by *Lithophaga* sp., barnacles, and *Clionid* sponges. A small proportion of the calcareous sandstone clasts were reworked from older terraces located around the periphery of the Gargaliani High (e.g. Unit 1.6). A shallow-marine fauna of molluscs, bryozoa, barnacles and echinoids are present, locally forming shell beds. Bioclast density decreases upwards and the uppermost, terrigenous-rich beds contain only a few thick-shelled macrofossils (e.g. *Ostrea* sp.).

Associated muddy units (up to 2.20 m thick) contain a diverse fauna of non-abraded bivalves, together with moderately abraded and fragmented barnacles, gastropods, corals, echinoids and bryozoa. The sediment is commonly well mixed as a result of bioturbation. Sharp-based, coarse, shelly sandstone beds, with a dense and diverse fauna of thin-shelled bivalves and scaphopods (<1-2 cm in size) occur in the upper parts of the muddy intervals.

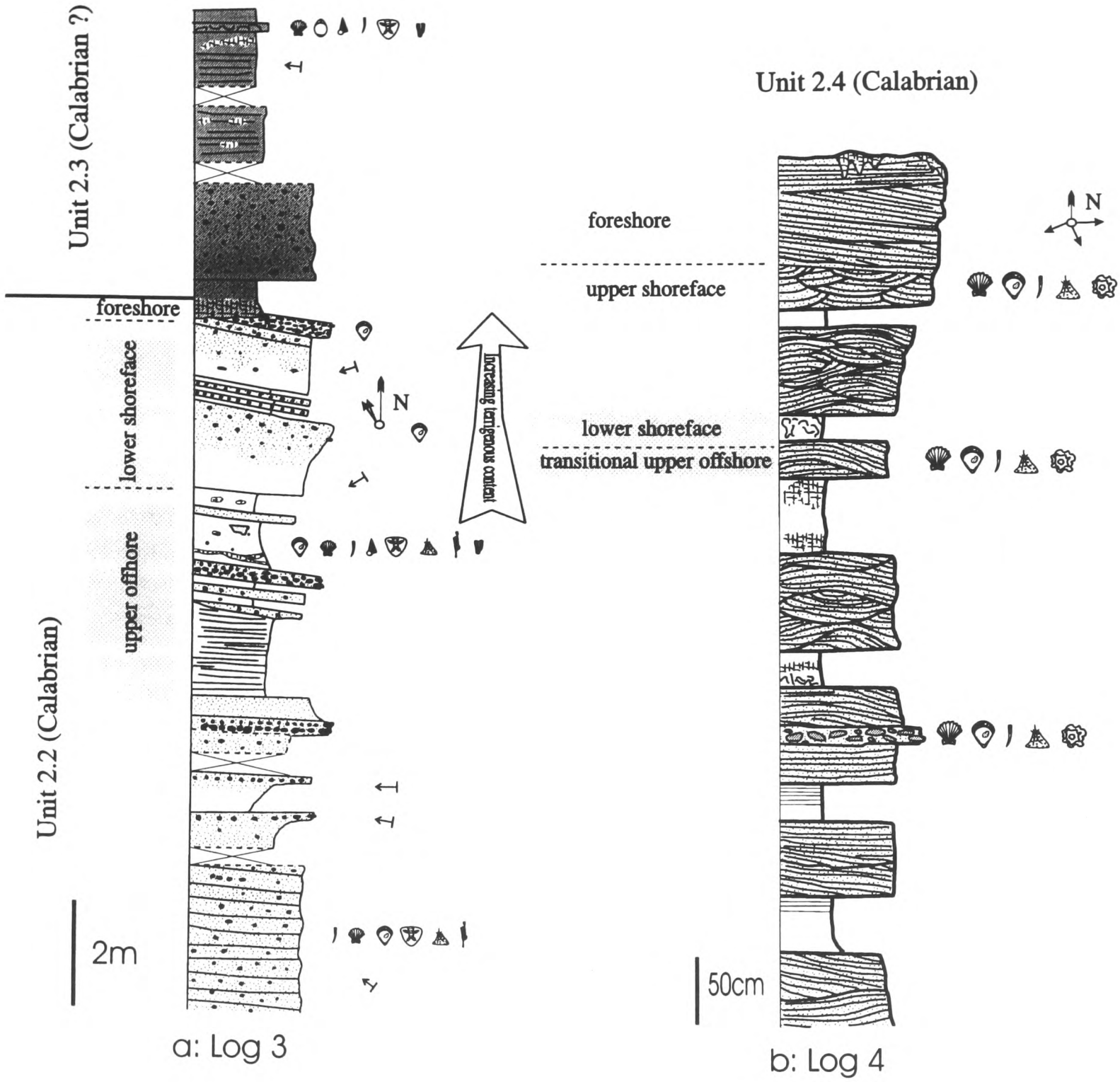

Figure 3.11: Representative sedimentary logs of early (to middle ?) Pleistocene sequences (logs 3 & 4): **a)** Subunit 2.2.1 (Calabrian) overlain unconformably by Unit 2.3 (Upper Calabrian ?), Gargaliani. This section may indicate intra-Calabrian sea level cyclicity. Alternatively, the Unit 2.3 may correspond to some early middle Pleistocene sea level highstand. **b)** Unit 2.4, Ayios Vasilios (see Figures 3.6, M.1 for locations). Palaeocurrent evidence is included from Unit 2.4.

Most of the bivalve shells are convex side upwards; some are imbricated. Triangular scours (ca. 7 cm wide × ca. 5 cm deep) were infilled with well-sorted, very coarse, bioclastic sand (largely scaphopod fragments). A diverse microfauna is present in the muddy intervals (Table 3.1), whereas coarser-grained beds contain relatively few, mainly epiphtytic foraminifera.

Interpretation: This overall shallowing-up succession is interpreted as prograding deltaic/inner shelf deposits. The benthic microfauna are of mixed shallow marine-bathyal origin (Blanc-Vernet, 1969; Murray, 1973; Amorosi et al., 1998), probably indicating deposition in the upper bathyal zone, but are not age diagnostic. Delta-influenced clinoforms prograded into a shallow sea west of the Gargaliani-Filiatra escarpment. Clinoform progradation was interrupted by periods of lower-energy, finer-grained muddy deposition. Accumulation of sand-size sediment was influenced by longshore drift, as indicated by NNW-SSE palaeocurrents parallel to the inferred palaeo-shoreline (Fig. 3.5). Muddy sediments accumulated below the fair-weather wave base, but above storm-wave base, as indicated by palaeo-water depth, storm-wave scouring and pervasive bioturbation. Terrigenous-rich foresets high in the sequence are interpreted as lower shoreface deposits, probably in a deltaic/clastic shoreline setting. The pebble content probably reflects storm-wave reworking of beach deposits: rod-and blade-shaped pebbles are common in the lower beach zone (Reading and Collision, 1996). Bored pebbles probably derived from storm-reworking of adjacent rocky cliffs and pebbly beaches along the Gargaliani Escarpment. The uppermost, laminated, matrix-free sandstone/conglomerate is interpreted as an upper shoreface-foreshore deposit.

3.3.3.2.2 Subunit 2.2.2: sand-conglomerate (Figs. 3.4, 3.11.b, log 6):

This subunit comprises steep, matrix-supported conglomerate foresets dipping at 30° to the W/WNW, passing upwards into lower angle (ca. 8-10°), poorly sorted pebbly sand, well exposed in quarries ca. 1 km N of Gargaliani and at an altitude of ca. 270-290 m (Fig. 3.5) and in Eleophyton (Fig. 3.15). The contact between steep foresets and gentle topsets is transitional, with a gradual decrease in dip. The bedset geometry is sigmoidal; individual bedset-bounding surfaces can be traced from fore- to topsets in single longitudinal sections. Bounding surfaces are locally truncated by reactivation surfaces. The sediment is poorly sorted and strongly bimodal, with both medium-grained sand and pebbles/granules. Pebbles include well-rounded, heavily bored limestone and chert, correlated with Tripolis and Pindos zone lithologies, respectively. Fauna include barnacles, molluscs, scaphopods and

benthic foraminifera. Rich accumulations of articulated *Ostrea* sp. occur as banks within topset units.

Interpretation: This subunit is interpreted as a proximal, shallow marine equivalent of the prograding offshore/coastal unit above (Subunit 2.2.1) that accumulated behind (east of) the Gargaliani-Filiatra escarpment. A proximal delta-front/delta-top setting (of partly Gilbert type), is inferred from the terrigenous nature, sedimentary structure and poor sorting (Orton and Reading, 1993). The characteristic sigmoidal architecture and presence of reactivation surfaces indicate wave influence (Colella, 1988).

3.3.3.2.3 Subunit 2.2.3: heterogeneous terrigenous sediments (Figs. 3.4, 3.11.a, log 5): This begins with dark grey, sandy, relatively homogenous mud, with local sub-horizontal lamination. A typical outcrop is located E (inland) of the two subunits described above, were it unconformably overlies Late(?) Pliocene sediments (Unit 1.6), at an altitude of 280-290 m ASL. This mud is spectacularly fossiliferous, with a very dense and diverse macrofauna, including gastropods (e.g. *Cerithids*), bivalves, scaphopods, occasional arthropod remnants and carbonised sea-grass, all in excellent state of preservation (Fig. 3.18). Gastropods outnumber bivalves, but the relative abundance of the latter increases upwards. Many of the bivalve shells are still articulated. The microfauna exclusively consist of benthic foraminifera and ostracods (Table 3.1).

The mudstone is succeeded by brown marl with a very high-density, monospecific, macrofauna of *Cardium edule* and an oligospecific microfauna, including *Ammonia tepida* (Table 3.1). Well-sorted, matrix-free, fine quartzose sand sharply overlies the brown marl. Sedimentary structures in this sand include millimetre-scale festoon and tangential ripple cross-lamination, planar cross-lamination, symmetrical and asymmetrical ripples and reactivation surfaces that define larger-scale ripple-sets. Palaeocurrent directions are both WSW (offshore) and N and S (shore-parallel) (Fig. 3.12.a, log 5). Bioturbation is restricted to a few *Skolithos*-like burrows. The sand is succeeded by alternating planar cross-beds (3-7 cm thick) of conglomerate and well-sorted, ripple cross-laminated sand. The basal beds of this interval consist of coarsening-upward, matrix-supported conglomerate, passing into well-sorted, trough cross-laminated sand, with planar, clast-supported, normally graded and imbricated conglomerate towards the top. The maximum clast size increases upwards from 1 to 7 cm. The clasts (Tripolis limestone and Pindos chert) are moderately-rounded, commonly disc- and rod-shaped. Planar bedsets dip NNW at ca. 10°. Imbrication, ripple

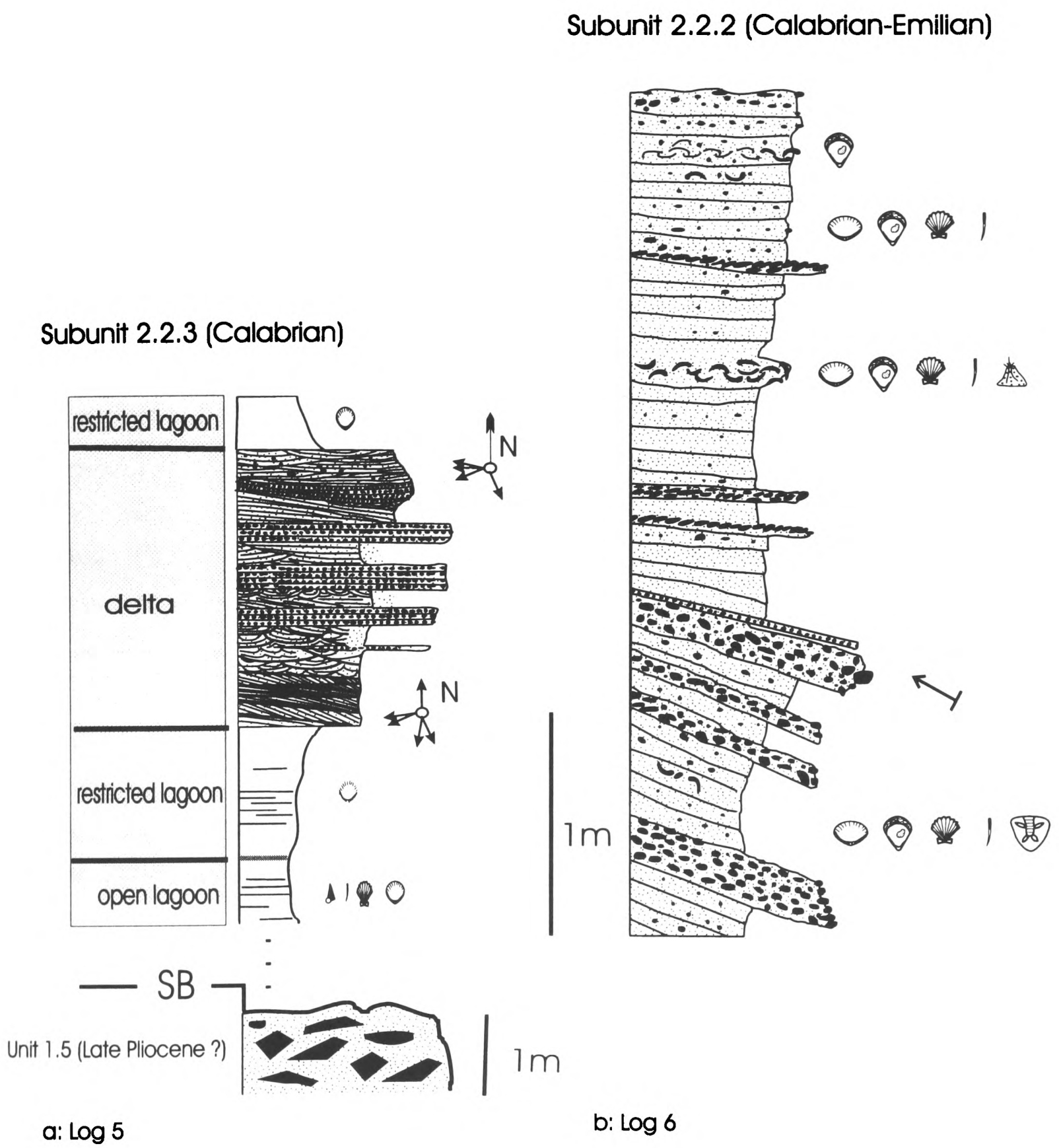

Figure 3.12: Representative sedimentary logs of late (?) Pliocene and early Pleistocene sequences (logs 5 & 6): **a,** Shallow marine Unit 1.5 (possibly late Pliocene) overlain unconformably by marginal marine Subunit 2.2.3 (Early Pleistocene); road from Gargaliani to Valta. **b,** Subunit 2.2.2 (Early Pleistocene) from Gargaliani (see Figures 3.7, M.1 for locations).

cross-lamination and trough cross-bedding indicate a NW direction of transport. Above this, brown mud (intervals 1.5-2 m), similar to the mud lower in the succession, contains a monospecific fauna of *Cardium edule*.

Interpretation: The lower parts of the sequence (grey mud with a mixed *Cerithid* gastropod and bivalve fauna) was deposited in a low-energy, shallow-marine environment of reduced salinity, as indicated by the presence of hyposaline species (e.g. *A. tepida)* (Fernandez-Gonzalez et al., 1994; Amorosi et al., 1998). Oxygen depletion below the sediment-water interface is suggested by excellent preservation of organic matter (Pemberton et al., 1992). The low-diversity benthic fauna may reflect stressful ecological conditions. The most probable setting is a lagoon behind a barrier, but with an open-marine connection in view of the fully marine macrofauna present. The upward incoming of the dominantly brackish mollusc *Cardium edule* may indicate brackish-water conditions in a more restricted lagoonal environment. The overlying coarsening-upward sand/conglomerate intervals are interpreted as a Gilbert-type delta ("*Hjulstrüm-type*" delta of Postma, 1990) that prograded into the lagoon. The overall sequence is interpreted as progradational, with an increase in the thickness of deltaic facies toward the top, representing a proximal equivalent of more westerly offshore unit discussed above (Subunits 2.2.1 and 2.2.2) (Fig. 3.5).

3.3.3.2.4 Interpretation of Unit 2.2: The prograding sediments of Unit 2.2. probably correspond to a prominent highstand systems tract over the maximum flooding deposits of Unit 2.1 (inferred «Calabrian», ca. 1600-800 ka; Figs. 3.3, 3.4). A late «Calabrian» age (ca. 1300-800 ka) is, thus, plausible, corresponding to the later, highstand part of eustatic cycle 3.10 *sensu* Haq et al. (1986) (Fig. 3.3). A similar age was assigned to sediments elsewhere in NW and in S. Messenia by Frydas (1990). A shallowing-up trend is observed in early Pleistocene sediments of NW Messenia, from offshore mud (Unit 2.1) to shoreface-foreshore packstone/snadstone/conglomerate (Subunits 2.2.1 and 2.2.2), then lagoonal mud and fluvial sand (Subunit 2.3.3). The upper part of the early Pleistocene succession is also characterised by prominent progradational depositional architecture. These characteristics reflect shoreline progradation during the highstand and early stages of sea level fall of the sea level cycle 3.9 (*sensu* Hag et al., 1998).

3.3.3.3 Unit 2.3 (Lower Pleistocene ?): shallow-water carbonates (Figs. 2.1, 3.5, 3.6, 3.10.a, log 3)

This unit rests on a sharp erosional surface at the top Unit 2.2.1, near Gargaliani, at an altitude of ca. 280 m. It begins with packstone/wackestone that accumulated on the underlying Unit 2.2, over a minor erosional relief (5-10 cm). This sequence passes upwards into coarser-grained bioclastic packstone/grainstone, with a few intervals of fine-grained carbonate. Scoured surfaces are overlain by pebbly lags. The lower, fine-grained parts of the sediment are very porous and almost unconsolidated, with widespread bivalve-moldic porosity after small bivalves and gastropods. The preserved fauna are restricted to small fragments of thin-shelled bivalves. The upper, coarser-grained beds are parallel bedded (20-45 cm thick) and dip to the SSW (190 - 200°) at ca. 10°. The sediment is very bioclastic, with abundant (but not age diagnostic) fragments of molluscs, gastropods, echinoids, brachiopods, scaphopods and coral. Common bioturbation includes vertical burrows (7-9 cm long x 2 cm deep).

Interpretation: This unit accumulated in a current- or wave-swept shallow-marine setting. Assuming that the directly underlying sediments (Unit 2.2, Fig. 3.10.a) are of upper Calabrian age, Unit 2.3 could record high-frequency (4^{th} order) "intra-Calabrian" sea level cyclicity, within the 3^{rd} order sea level cycle 3.9 (Haq et al., 1988; Fig. 3.3). This interpretation is further supported by the fact that a prominent cliff of inferred early mid-Pleistocene age (Gargaliani-Filiatra Escarpment; see Fig. 2.9) post-dates the deposition of the Unit 2.3. However, a possible early mid-Pleistocene age (beginning of the sea level cycle 3.10) cannot be excluded.

3.3.3.4 Unit 2.4 (Early-Middle Pleistocene ?): shallow-marine carbonates-siliciclastics (Figs. 2.1, 3.10.b: log. 4, 3.20)

Calcareous mudstone, at the base of the exposed sections, grade upwards into grainstone/packstone with occasional algal boundstone bioherms and low-angle, trough cross-laminated calcareous sandstone. The unit crops out in the Southern Messenia block, over Pliocene(?) subaerial sediments (e.g. Unit 1.2) and bedrock (Tripolis zone limestone). Good exposures are seen along the road from Pylos to Methoni in S Messenia (e.g. Palioneron, Ayios Vassilios; see Figs 2.1; 3.12, M.1). Locally (Palioneron), this unit was deposited on the hangingwall of a NNW-SSE normal fault (with ca. 60 m of minimum accumulated Quaternary throw; see Fig. 3.12). A coarsening-upward sequence drapes a fluvial channel incised into pre-Quaternary fluvial conglomerate (Unit 1.2).

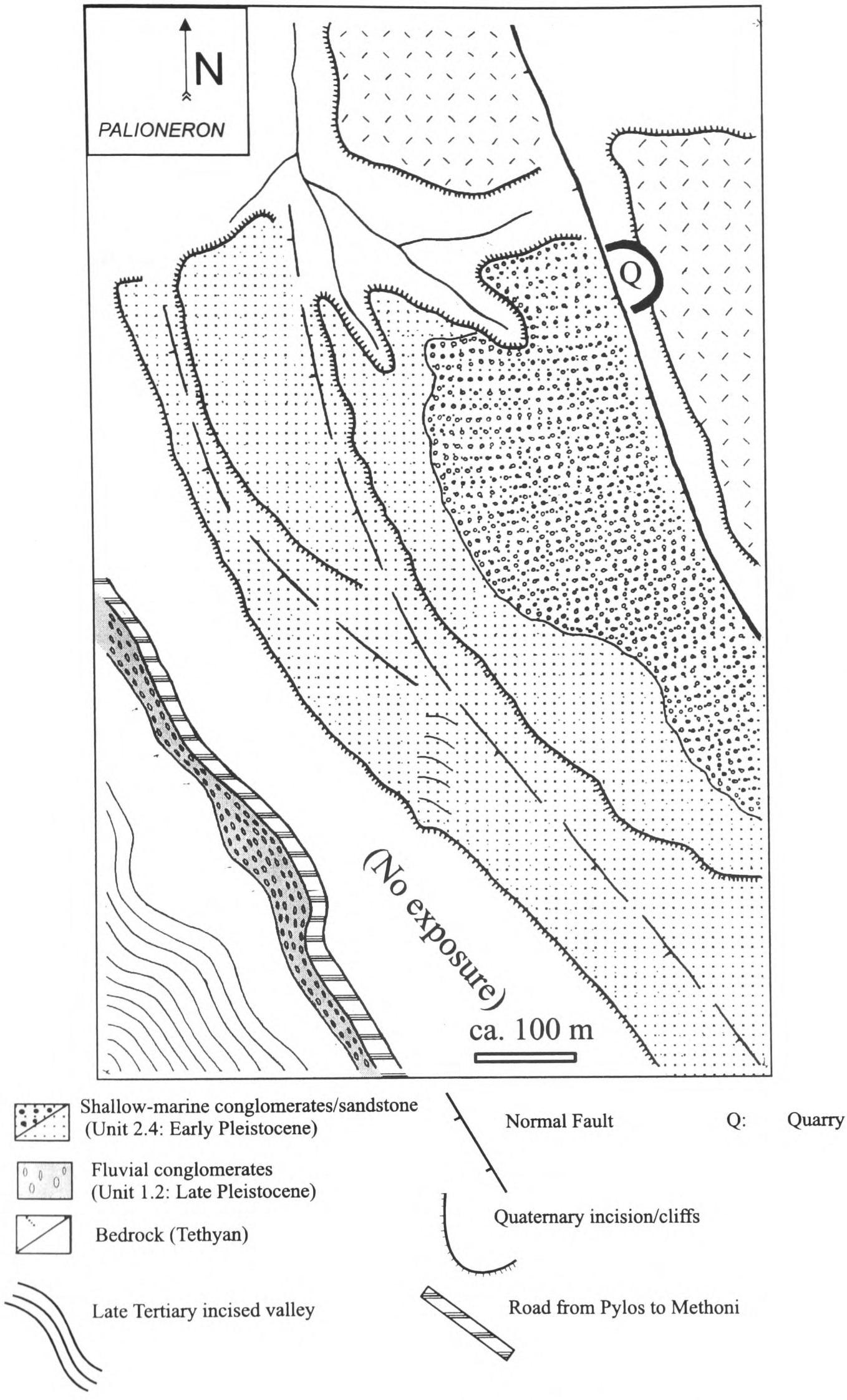

Figure 3.12: Field sketch of Palionero, Southern Messenia Block (for location see Figure M.1). Early Pleistocene shallow-marine sediments were deposited in a NNW-SSE palaeovalley, of inferred Late Tertiary age, on the hangingwall of a NNW-SSE fault in bedrock. The Pleistocene terrace was cut by NNW-SSE faults.

The upper parts of Unit 2.4 comprise planar cross-laminated calcareous sandstone/conglomerate, with well-rounded and bored Tripolis limestone pebbles, together with bivalves and worm-burrows (Fig. 3.20). Further inland, toward the NNW-SSE fault, the sediment passes upwards into clast-supported, bouldery conglomerate with a calcareous siltstone matrix. Clasts are very well-rounded, commonly spherical, including *Lithophaga*-bored bedrock limestone boulders and a few, commonly discoidal, chert pebbles. Post-depositional faulting with a N-S strike and a throw of ca. 20 m is coupled with intense jointing.

Elsewhere in the Southern Messenia (e.g. Ayios Vassilios: Figs. 2.1, M.1. 3.10.b: log 4), the sequence begins with intensively karstified and calcified calcareous mudstone/siltstone, deposited above a ravinement surface on Tripolis zone limestone. This facies contains a poorly preserved microfauna (Table 3.1). Up-sequence, beds of sharp-based, hummocky cross-stratified calcareous sandstone, or lithic packstone/grainstone alternate with calcareous mudstone. This is followed by coarse calcareous sandstone with, first, trough cross-bedding, then low-angle planar cross-lamination, accompanied by an increase in bed-thickness and degree of amalgamation. Mollusks, scaphopods, barnacles, red and green algae and diverse foraminifera (Table 3.1) are abundant in sandstones and grainstones. Many bioclasts are micritised, or surrounded by micritic envelopes. Micritic envelopes also surround non-carbonate grains (e.g. Pindos zone chert). The benthic foraminifera in upper levels are of mixed shallow-marine/upper bathyal type (Blanc-Vernet, 1969; Murray, 1973).

Interpretation: The first-mentioned sequence (Palionero: Figs. 2.1, M.1, 3.12) is interpreted as a transition through the following environments: upper offshore (lower mudstone with storm-deposited packstone interbeds), middle-upper shoreface (trough cross-laminated sandstone), and then upper shoreface/foreshore (planar cross-laminated sandstone), probably all indicative of overall coastal progradation. The conglomerate facies close to the fault-scarp is interpreted as a rocky foreshore deposit, probably resulting from wave-reworking of scarp colluvium.

The second sequence (Ayios Vassilios) is also interpreted to reflect a transition from shoreface to foreshore environments, as above. Most of the carbonate grains originated as micritised allochems, probably derived from *Thalassia* banks, as shown by the presence of 'constructive' micritic envelopes (Perry, 1997; see also Chapter 6). In the lower part of the section, the high content of *Textulariidae*, together with presence of *Lagenidae*, probably indicate a water depth of >50 m (Blanc-Vernet, 1969; Murray, 1973). The mixing of

shallow-marine and upper bathyal benthic foraminifera is suggestive of storm influence. The trough cross-bedding in the upper parts of the sequence is attributed to storm-generated bar and trough morphology in the foreshore-upper shoreface zone (Kumar, 1976; Reading and Collinson, 1996).

Unit 2.4 is in the same relative stratigraphic position (and probably of the same age) as Unit 2.2 in the Northern Messenia Block and is, therefore, interpreted as corresponding to the highstand of early Pleistocene (upper «Calabrian») age (sea level cycle 3.10 *sensu* Haq et al., 1988), prograding over more basinal (maximum flooding) facies of lower «Calabrian» age, represented by Unit 2.1 (Figs. 3.2, 3.5).

3.3.3.5 Unit 2.5: («Sicilian»?): boundstone and clastic sediments (Figs. 2.1, 3.4, 3.5, 3.13.a: log. 7, 3.19)

This unit crops out between Gargaliani and Filiatra (Figs. 2.1, 3.5), forming a prominent terrace surface (altitude 40-70 m) in the Northern Messenia block. Its contact with the earlier Pleistocene units is not visible. Unit 2.5 consists of extensively karstified and bioeroded red algal boundstone (Fig. 3.19), passing up into a thin interval of lithic grainstone and conglomerate. Algal limestone below is separated from clastic sediments above by a sharp surface (with centimetre-scale erosional relief). The limestone facies includes porous algal boundstone, rhodolithic rudstone and packstone. Typical encrusting organisms are crustose coralline algae, bryozoa, foraminifera and gastropods, with a lower abundance of articulating coralline algae. Diverse non-encrusting benthic foraminifera occur, in addition (Table 3.1). Erect bryozoa taxa are also present, together with a few ostracods and common rhodoliths. *Polychaetae* worms burrows are common in wackestones. *Cladocora cespitosa* corals are locally abundant, either as *in situ* colonies, or as fragments in coral-mollusc lags. Molluscs comprise bivalves and gastropods (including *Astrea rugosa*), while echinoids are very common. The overlying grainstone is matrix-free, with well-rounded grains, derived mainly from the Pindos zone.

Interpretation: This boundstone lithofacies is interpreted as an algal reef deposited in the high-energy shoreface zone, away from fluvial influence (James, 1983; Poole and Robertson, 1991, 2000). The benthic assemblage indicates shallow-marine deposition. The gastropod *Astrea rugosa* is a common component of warm Mediterranean faunas during interglacial periods (Keraudren, 1970, 1971; Poole and Robertson, 1991, 2000). The unit is correlated with the mid-Pleistocene «Sicilian» stage (Bonifay, 1975), since it is younger

than the early mid-Pleistocene cliffs (Gargaliani-Filiatra Escarpment), but older than the "Eutyrrhenian", further west (Fig. 3.4). The overlying matrix-free grainstone is interpreted as a foreshore deposit. The succession probably records "intra-Sicilian" sea-level cyclicity (of 4th- or higher-order; see Fig. 3.3), with an erosive relief on the algal boundstone resulting from relatively short-lived emergence, prior to resumed sea level rise and progradation of lithic grainstone.

3.3.4 LATE PLEISTOCENE-HOLOCENE SEDIMENTS

3.3.4.1 Unit 3.1 («Eutyrrhenian»): littoral carbonates (Figs. 2.1, 2.13, 3.4, 3.5, 3.6, 3.13.b: log 8, 3.16, 3.23)

This unit, extensively developed in the Northern Messenia Block (Figs. 2.1, 3.5), can be split into a mixed clastic-carbonate lower part and a carbonate, to terrigenous, upper part.

This sequence overlies a relatively smooth (but locally undulating) ravinement surface, cut into offshore muds of the early Pleistocene Unit 2.1, or Tripolis zone bedrock (mainly sandstone), as seen in NW Messenia (Mati-Vromoneri coast; Figs. 2.1, 3.4, 3.5). The subunit begins with oligomict, poorly-sorted, clast-supported, intraformational conglomerate (including slab-shaped clasts of calcareous sandstone), or with polymict conglomerate with well-rounded, to disc- and rod-shaped clasts of Tripolis limestone, Pindos zone-derived chert and calcareous sandstone, with abraded bivalve shells. Relatively well-sorted, fine sand with *pectenidae* is succeeded by an alternation of well-sorted, medium-bedded calcareous sand with low-angle planar cross-lamination and small, mound-shaped red algal bioherms (20-60 cm across × 30 cm, <2m high). Lamination is commonly disrupted by load-structures, slumps and other liquefaction features (Fig. 3.23). A poorly expressed cyclicity was observed, with cemented, laminated calcareous sandstone alternating with well-sorted, trough cross-laminated, uncemented sand. A gradual transition from calcareous sand, to fine sand with reactivation surfaces and longitudinal scours was commonly observed. SW (offshore)-directed palaeocurrents are indicated from measurements of cross-bedding (Fig. 3.13.b: log 8). The discontinuous, red algal bioherms comprise closely bound boundstone and packstones with a high content of entrapped terrigenous grains. In general, the boundstone becomes more abundant/closely-spaced, to locally amalgamated upwards. The sequence is capped by latest Pleistocene terra rossa and caliche of Unit 3.6 (see below). Sediments of this unit are cut by closely-spaced, NNW-SSE faults, with throws ca. 3-5m.

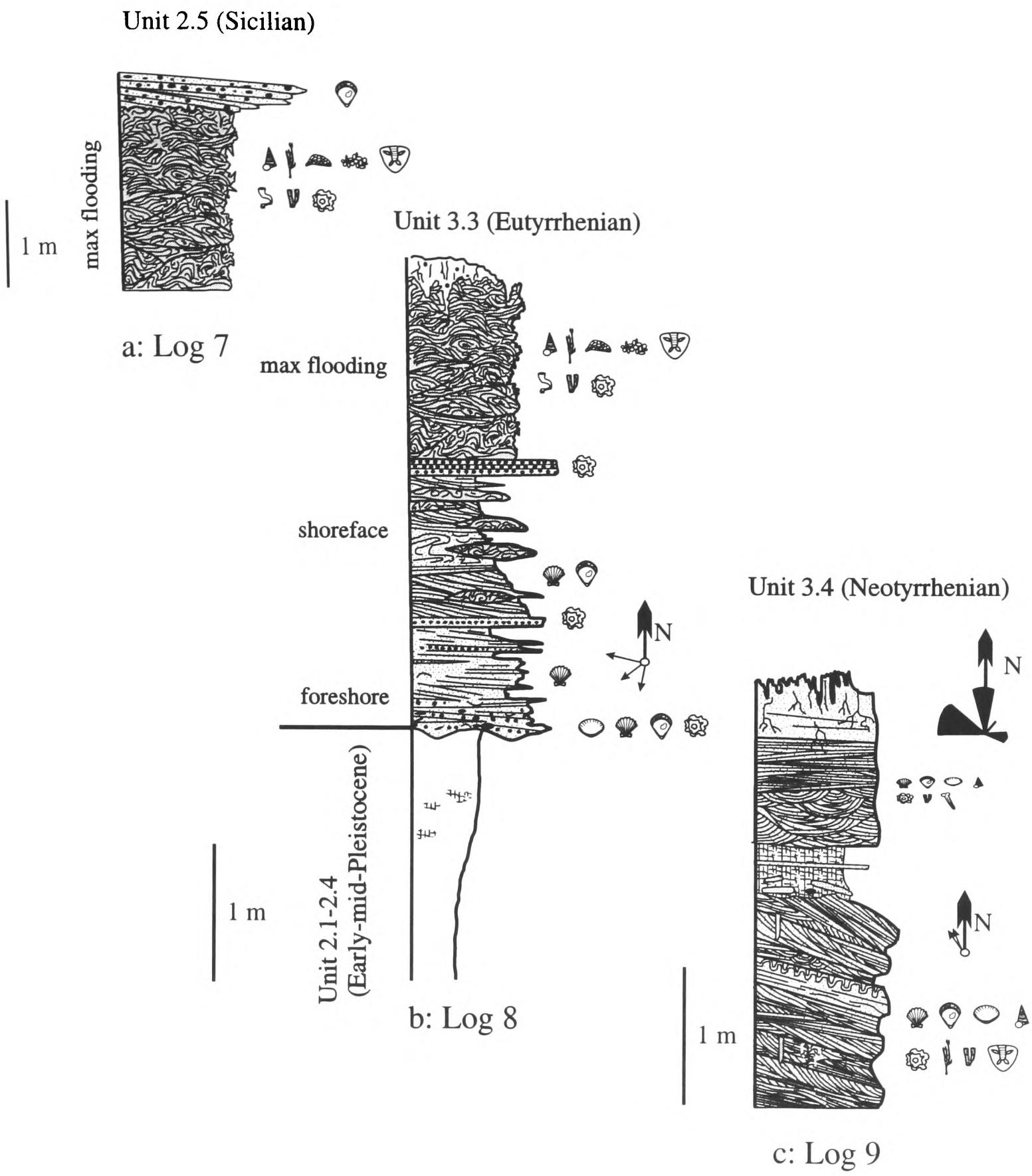

Figure 3.13: Representative sedimentary logs of middle and late Pleistocene sequences (logs 7, 8, 9). **a:** Sicilian (Unit 2.5) from near Filiatra. The sharp contact between the algal bioherm below and the detrital sediment above may reflect high order intra-Sicilian sea level cyclicity (see also Fig. 3.3) **b:** Eutyrrhenian (Unit 3.1), unconformably over early (to middle ?) Pleistocene (Units 2.1-2.3); Mati Coast. Note the gradual development of algal bioherms up sequence. **c:** Neotyrrhenian (Unit 3.2); Note palaeocurrent data; Marathopolis (see Figures 2.1, 3.5, M.1 for locations).

Interpretation: This sequence is interpreted as part of the «Eutyrrhenian» marine transgression (isotopic stage 5e; ca. 120 ka; Imbrie et al., 1987; Martinson et al., 1987; see Figure 3.3) The uneven ravinement surface with the coarse clasts and intraclasts is interpreted as a buried plunge step on a palaeo-foreshore (Dabrio et al., 1990). The calcareous sandstone is interpreted as beachrock that underwent storm-reworking and redeposition as lags. Slump and liquefaction events were probably triggered by syn-sedimentary seismic activity, consistent with ubiquitous faulting. The terrigenous composition indicates shoreline reworking and redeposition of fluvially derived sediment. The overlying finer-grained sand is indicative of high-energy upper shoreface sediments, marked by offshore-directed scour structures. Above this, the algal bioherms required high-energy conditions and low clastic sedimentation input to form (Martindale, 1976; James, 1983); these were possibly controlled by autocyclic (i.e. 'normal' sedimentary) processes. However, the dominance of algal bioherms high in the succession probably reflects maximum flooding conditions, when deltas were in retreat, as also inferred for "Tyrrhenian" equivalent in southern Cyprus (Poole and Robertson, 1991, 2000).

Shallow-marine carbonates correlated with the "Eutyrrhenian" sea level cycle are generally scarce within the Southern Messenia Block. An outcrop of inferred "Eutyrrhenian" age occurs near Koroni Castle, at an altitude of ca. 17-20 m (Figs. 2.15, 3.6, 3.16). The Eutyrrhenian sediment comes above a ravinement surface eroded into offhsore muds of Early Pliocene age (Unit 1.4; see above). It comprises coarse-grained lithic grainstone with an abundance of abraded bivalve fragments, shells of thick shelled bivalves (mainly *Ostrea* sp., *Arca* sp.) and rhodoloths. The microfauna comprise mainly epiphytic benthic foraminifera of intralittoral habitat (Table 3.1). The sediment has a progradational architecture, with 10-25 cm thick clinofroms that dip seawards (E) at 10-15° (Fig. 2.15).

Interpretation: The deposit of the Koroni Castle terrace is interpreted as a carbonate shoreface deposit, on the basis of grain-size, microfacies and fauna (Wilson, 1975; Flügel, 1982; Tucker and Wright, 1990; Hansen, 1999). Shoreface progradation is suggested by the depositional architecture; this probably took place during the highsrtand and early stages of sea level fall of the Eutyrrheinan sea level cycle (isotopic stage 5e; ca. 120 ka).

Unit 3.1 is similar, both in facies and relative altitude, to Eutyrrhenian (isotopic stage 5e) deposits from the Peloponnese (e.g. Corinth area: Keraudren, 1970, 1971; Doutsos and Piper, 1990; Collier and Dart, 1991; Elis: Keraudren, 1970, 1971; Streif, 1978; Mariolakos et al., 1991; Mani: Petrohilos, 1953; Eastern Lakonia: Symeonidis, 1969; Theodoropoulos,

1973; Kowalczyk et al., 1992; Chapter 5, this study), other areas of the Aegean forearc (e.g. Crete: Keraudren, 1970, 1971; Angelier et al., 1976, Papapetrou-Zamanis, 1971; Dermitzakis, 1972; Rhodes: Keraudren, 1970, 1971; Bromley et al., 1991), Cyprus (Poole, 1991: Poole and Robertson, 1991, 2000) and the Red Sea (Arvidson et al., 1994; El Moursi et al., 1994; El Asmar, 1997; Plaziat et al., 1998). The main characteristics of the Mediterranean "Tyrrhenian" deposits are summarised by Pirazzoli (1987).

3.3.4.2 Unit 3.2 («Neotyrrhenian»): mainly littoral carbonates (Figs. 2.13, 3.3, 3.5, 3.13.c: log 9; 3.21)

This unit is dominated by shallow-marine carbonates with a distinctive intercalation of red palaeosol. This unit was mapped as «Neotyrrhenian» by Kelletat et al. (1976) in NW Messenia, but depositional terraces of this age were not identified in S Messenia during this study. Where exposed (near Marathopolis; Figs. 2.1, 3.5), the unit unconformably overlies «Eutyrrhenian» (Unit 3.1) or earlier Pleistocene sediments.

In Marathopolis, the lower part of the unit consists of steep (ca. 30-32°) planar-tabular bedsets of rhodolitic grain/packstone (30-100 cm thick) dipping to the WSW. Prograding clinoforms are internally cross-laminated with normally graded, tangential cross-laminae (0.2-3 cm thick). Measured palaeocurrents are mainly offshore, but shore-parallel trends were also noted (Fig. 3.13.c: log 9). The uppermost beds consist of calcirudite with large (up to 7 cm) fossil fragments, clasts of bedrock limestone (<3 cm in size), algal boundstone (derived from Unit 3.1, 2.5) and tabular intraclasts of matrix-free grainstone. The fauna include bivalves, gastropods, large asymmetrical echinoids (in life-position), solitary corals and rhodoliths (up to 3 cm in diameter). Foraminifera are mainly benthic forms of shoreline habitat and a few non-age-diagnostic planktic taxa (Table 3.1). The sediment is intensively bioturbated, with *Cruziana, Diplocraterion* and *Skolithos* burrows (i.e. *Cruziana* ichnofacies; see Pemberton et al., 1992), also bivalve escape-traces (Fig. 3.21). The relative abundance of molluscs, rhodoliths, trace fossils and matrix decreases towards the top of the unit.

The red soil layer consists of sandy-pebbly caliche (hardpan) that overlies the littoral grainstones with a marked erosional relief. Numerous slab-shaped, angular intraclasts (<60 cm long) were derived from the directly subjacent calcarenite. *Rhizocretion* bioturbation is abundant. Elsewhere, this red interval consists of multiple caliche crusts, alternating with layers of normal- or reverse-graded, calcified grainstone, up to three cm-thick.

Above the caliche comes trough cross-laminated grainstone and shell concentrates (2.5-3 m thick) with bivalves, gastropods, a few rhodoliths, *Cladocora cespitosa* fragments and rare mammalian bone-fragments. Shells are mostly convex side-upwards. Almost horizontal trough cross-bedded bedsets (up to 20 cm thick) exhibit internal trough and festoon cross lamination (0.2-3 cm thick). Individual laminae are normal and reverse graded. Current directions, determined from imbricated bivalves and trough cross lamination, are both WNW (offshore) and NNE (shore-parallel) (Fig. 3.13.c). Low-angle planar cross-laminated predominates higher up, with laminae dipping in both offshore and onshore directions. Locally, along the Marthopolis coast (Fig. 3.5) the red soil is directly overlain by small *in situ* colonies of *Cladocora cespitosa*.

Interpretation: The lower part of this unit is interpreted to reflect progradation of shoreface sand-waves over quiet, shoreface areas stabilised by *Thalassia*. The tabular calcarenite intraclasts in the uppermost bedsets are interpreted as beachrock clasts, reworked by storms from the foreshore. This unit is, therefore, thought to represent transgression during the «Neotyrrhenian» sea level cycle (Fig. 3.3). This lower part is, thus, correlated with the substage 5.3 of the isotopic stage 5 (Last Interglacial; ca. 100 ka; Martinson et al., 1987; Fig. 3.3). Above, the red interval indicates subaerial exposure and soil formation during an "intra-Neotyrrhenian" sea-level fall, possibly corresponding to the substage 5.2 (ca. 90 ka; Martinson et al., 1987). The multiple caliche crusts may record storm-induced? backshore deposition (i.e. autocyclic effects). Alternatively, they could reflect very high order sea-level cyclicity during the substage 5.2 lowstand. The overlying upper interval is interpreted as a barrier located within a middle to upper shoreface, to foreshore setting. This feature developed during a resumed Latest Pleistocene sea-level rise, that possibly corresponded to substage 5.1 (ca. 80 ka; Martinson et al., 1987; Fig. 3.3). Well-sorted peloidal grainstone with spherical, blue-green algae/microbia-encrusted grains is locally preserved ca. 4-5 m onshore from the above facies. As this occurs at the same elevation this sediment is interpreted as a small, restricted lagoon behind a coastal barrier. Further S (Romanos; Figs. 2.1, M.1), this unit is represented by siliciclastic foreshore-backshore facies (Fig. 2.13). Alternatively, the above stratigraphy could reflect even higher-order, intra-substage sea level variation at time thousands of years-time scale (e.g. the multiple substage 5.3.3+5.3.1 *sensu* Martinson et al., 1987).

3.3.4.3 Unit 3.3 (middle to late Pleistocene ?): palaeosols

The unit comprises purple-red siliceous soil overlying detrital carbonates and sandstones of Unit 2.2 (Figs. 3.2. 3.3, 3.4). The siliceous content mainly consists of angular, corroded grains of red chert of Pindos zone origin. This unit is widely exposed within the Northern Messenia Block, on an elevated, relatively level area, west of the Kiparissia Mountain front (Fig. 3.5).

Interpretation: This unit is interpreted as an extensively hydrolysed krasnozerm soil, locally reworked into sandier, arenosol facies (*sensu* FitzPatrick, 1971). Its formation was probably favoured by a relatively flat topography. Extensively hydrolysed soils are formed in wet, to dry, tropical conditions of mean annual temperature, ideally >25°C, associated with a vegetation ranging from semi-deciduous forest to savannah (FitzPatrick, 1971). Identical palaeosols further north, in the Kiparissia-Kalo Nero Basin ("*Kalo Nero Formation*") post-date early Pleistocene sediments, and are overlain by calcarenites of probable «Tyrrhenian» age (Fountoulis and Moraiti, 1994).

3.3.4.4 Unit 3.4 (Middle to late Pleistocene): fluvial conglomerate (Figs. 2.1, M.1, 3.6, 3.9: log 1)

Red, clast-supported fluvial conglomerates form a number of fluvial terraces, well exposed on the eastern coast of S Messenia (Paniperi-Petalidi and Koroni areas; Figs. 2.1, 3.6, M.1). In the Kombi area (Fig. 3.6), the upper part of this clastic unit comprises fluvial conglomerates, inferred overbank deposits and reworked terra rossa that post-date apparent equivalents of littoral carbonates in Unit 3.1 (see above). In NW Messenia, this clastic unit is restricted to Profitis Ilias Hill near Filiatra (Fig. 3.5), and also to the Eleophyton-Iklena area (see Fig. M.1), discussed previously (Zelilidis, 1988; Zelilidis et al., 1988). This unit unconformably overlies sediments equivalent to Units 2.4, 2.5, or older, and was assigned a mid- to late Pleistocene age by Fytrolakis (1971) and I.G.M.E. (1980 b), although it is probably diachronous.

3.3.4.5 Unit 3.5 (Latest Pleistocene): terra rossa (Fig. 3.24)

This unit consists of terra rossa, often associated with chalky caliche. It covers "Neotyrrhenian" shallow-marine sediments (Unit 3.2) in NW Messenia (Marathopolis and Petrohori; Figs. 3.5, M.1). The unit is considered to be a time equivalent of the upper parts of the Unit 3.4 (Figs. 3.4, 3.5).

3.3.4.6 Unit 3.6 (Late Pleistocene ?): terra rossa (Fig. 3.23)

This unit comprises a karstic cavity-fill in the topsets of Subunit 2.2.2, as seen in and around Gargaliani Quarry (Fig. 3.5). It consists of reworked sandy terra rossa with bovine and micro-mammal bone fragments and lithic tools. Fluvial reworking is indicated by the nature of grading, pebble and fossil imbrication. This deposit may also be Holocene in age.

3.3.4.7 Unit 3.7 (Latest Pleistocene): aeolianite (Figs. 3.4, 3.13: log 9; 3.24)

Neotyrrhenian sediments (Unit 3.2) are overlain by well-sorted, fine to medium-grained, trough cross-laminated, or massive grainstone, extensively calichified, with *Rhizocretion*. This unit is interpreted as aeolianite, probably derived by reworking of sand from an exposed offshore shelf during the Last Glacial Maximum sea level low (Fig. 3.3). Deep solution wells penetrate this sediment to below present-day sea level, suggesting that the water table fell beneath present-day levels, as expected during sea-level lowstands (assuming no significant tectonic subsidence during the Holocene).

3.3.4.8 Unit 3.8 («Versilian» or younger ?): bioconstructions

Vermetid bioconstructions ("*trottoires*") occur at an altitude of ca. 1-1.5 m along the coast of NW Messenia (Romanos; Figs. 2.1, M.1, 3.4), associated with an abrasion platform cut into «Neotyrrhenian» sediments (Unit 3.2). This unit can be attributed to the «Versilian» highstand, of Holocene age, as elsewhere in Greece (e.g. Keraudren, 1970, 1971). The age of this high-order highstand is radiometricaly constrained at ca. 5-7 ka (e.g. Red Sea; Plaziat et al., 1996). Alternatively, this unit could be correlated with other similar foreshore deposits of the Aegean Arc (Crete), S Turkey (Alanya), Syria, Lebanon and Israel (Pirazzoli, 1986, 1987; Kelletat, 1991). Radiometric dating of these deposits suggests that they were uplifted ca. 1550-1530 years ago, as a result of a tectonic event of regional significance ("*Early Byzantine tectonic paroxysm*"; Pirazzoli, 1986). Holocene beachrocks occur locally in NW Messenia a few centimetres above present sea level, but still within the intertidal zone (<20-30 cm). Their present position is interpreted as resulting from localised uplift, probably fault-controlled.

3.3.4.9 Unit 3.9: Modern sediments

Modern sedimentation is represented by beaches, active and inactive dunes, ephemeral lagoons, fluvial sediments and various soils (Figs. 2.1, 3.5, 3.6, M.1). Present-day sedimentation in the Messenia Peninsula is mainly controlled by a combination of climate

and the inherited geomorphic setting of particular areas (Kraft et al., 1975, 1977), largely fault-controlled.

3.4 DISCUSSION: PLIO-QUATERNARY TECTONIC-SEDIMENTARY EVOLUTION OF THE MESSENIA PENINSULA

Eleven main stages in the post-Miocene depositional/tectonic history of the Messenia Peninsula are recognised, as follows (Kourampas and Roberston, 2000):

3.4.1 Pliocene (Fig. 3.14.a.1)

Following 'late orogenic' compressional tectonics in Late Oligocene-Early Miocene time, a long period of Miocene subaerial erosion culminated in peneplanation, followed by valley incision. Faulting into the two tectonic-geomorphological blocks (Northern Messenia and Southern Messenia Blocks) probably began by this time, with activation of ENE-WSW to E-W normal faults, transverse to the inherited Neotethyan tectonic grain. These transverse faults were active by Late Miocene-Early Pliocene time, as shown by evidence from the Kiparissia-Kalo Nero half graben further north (Fountoulis and Moraiti, 1994). In SE Messenia, NNW-SSE faults that bound the Messenian Gulf graben were clearly active in Early Pliocene, controlling deposition of offshore sediments (Unit 1.4). By contrast, in W Messenia, west of the Kyparissia Mountain front, colluvial wedges (Unit 1.2) and fluvial conglomerates (Unit 1.1) accumulated. This suggests that although extensional faulting was already taking place in W Messenia in Pliocene times, the subsidence rate was inadequate to allow marine transgression. In NW Messenia, the earliest reported marine sediments, of latest Pliocene (late Piacenzian) age (Frydas, 1990), are associated with fault activity within NNW-SSE to N-S grabens and half-grabens (e.g. Gargaliani-Filiatra half-graben; see also Zelilidis and Doutsos, 1994).

3.4.2 Early to mid-Pleistocene (Fig. 3.14.a.2)

Relative sea-level rise, starting in the Early Pliocene in SE Messenia, culminated in extensive progradation of shallow-marine clinoforms (e.g. Unit 2.2) over offshore mud, now preserved mainly within narrow, NNW-SSE to N-S grabens (e.g. Unit 2.1, Pylos). The rate of fault-induced basinal subsidence was locally high enough to allow deposition of offshore facies at water depths of > 90 m. These facies represent the maximum marine transgression during the early Pleistocene («Emilian» *sensu* Bonifay, 1975) and shoreline progradation during the subsequent highstand (sea-level cycle 3.10 *sensu* Haq et al., 1988). Mixed detrital

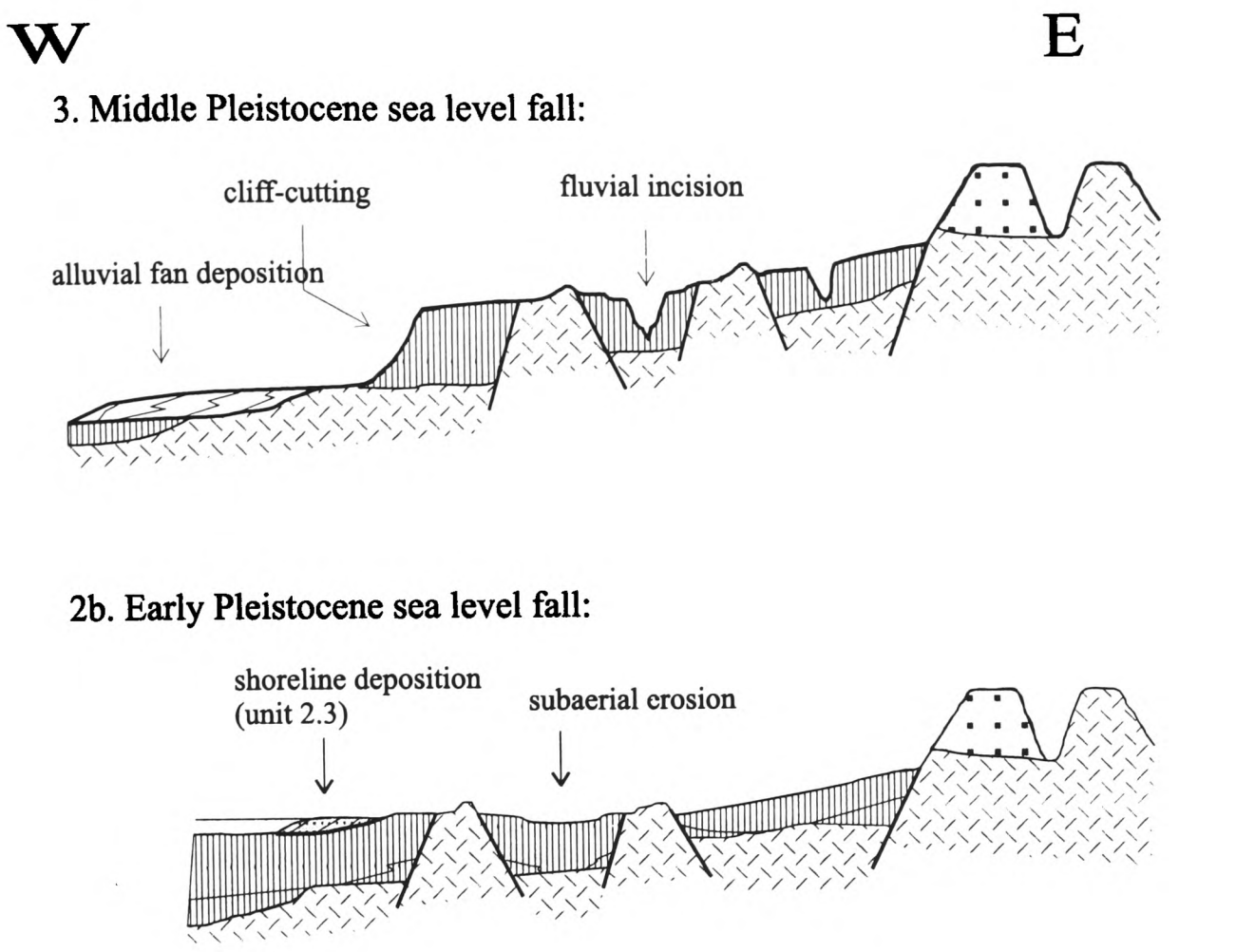

Figure 3.14 a,b: Interpretative cross-sections showing the recognisable stages in the Pliocene-Holocene development of the Messenia Peninsula. These are applicable mainly to the Northern Messenia Block, where the sedimentary record is nearly complete. The dominant control on sedimentation was regional tectonic uplift, with marine terraces and associated shallow-marine sediments being related to marine transgressions and eustatic sea level highs. Additional accommodation space was mainly provided by localised subsidence along the hanging walls of extensional faults that are inferred to have remained mainly collectively active. See text for details.

W E

7. Late Pleistocene sea level low II and Versilian sea level high:

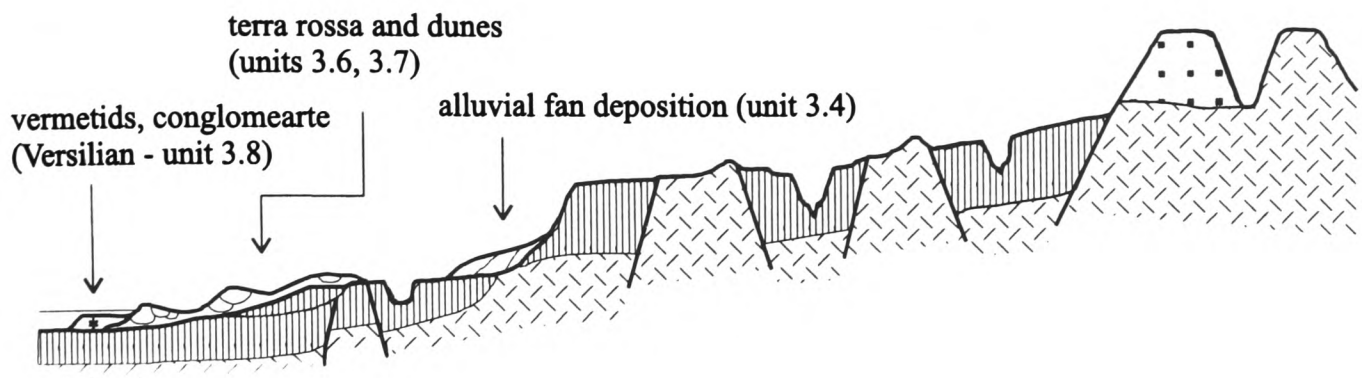

6. Eutyrrhenian and Neotyrhenian sea level high:

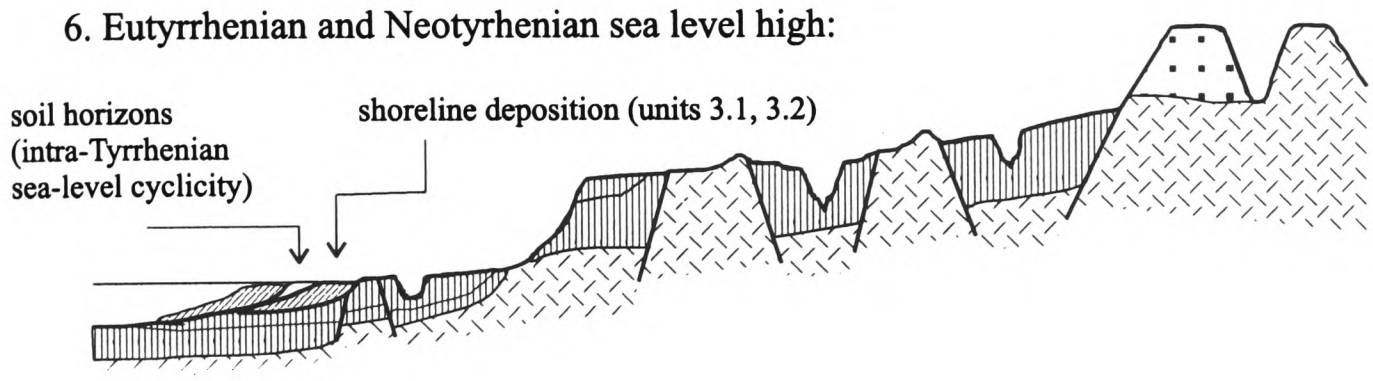

5. Late Pleistocene sea level low I:

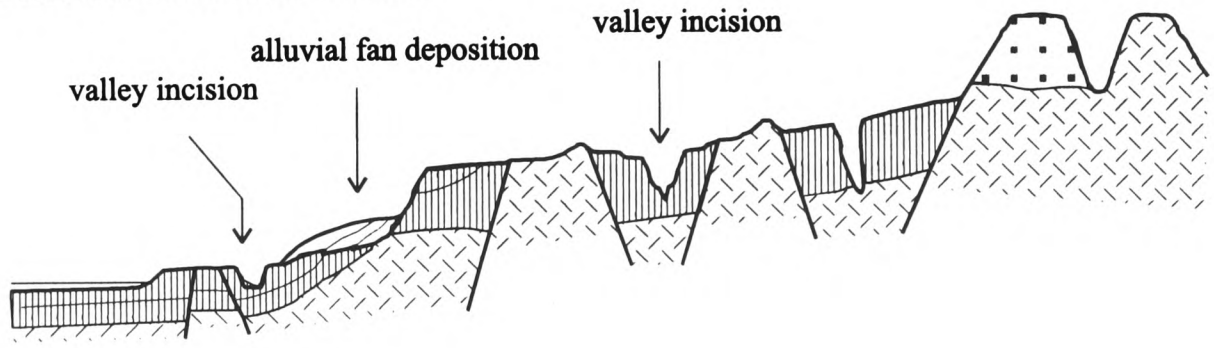

4. Sicilian sea level high:

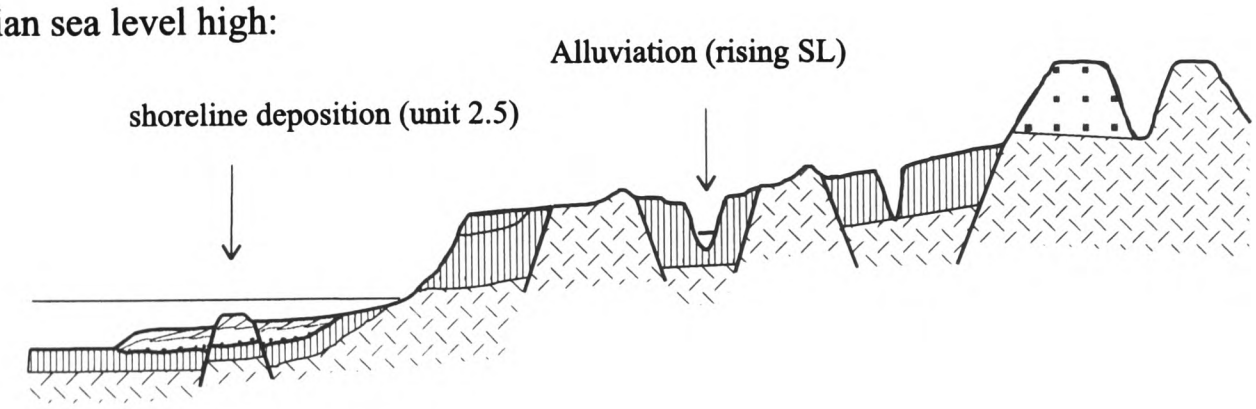

Key:

- Alluvial-backshore sediments
- Eutyrrhenian-Neotyrrhenian shoreline sediments
- Sicilian shoreline sediements
- Early Pleistocene (Calabrian) shallow marine sediments
- Pliocene shallow marine sediments
- Late Oligocene-early Miocene "molasse"
- Bedrock

carbonate/terrigenous clinoforms developed away from areas of fluvial input (e.g. Subunit 2.2.1), whereas deltaic sands/conglomerates were deposited close to river mouths (e.g. Subunit 2.2.2). Areas of high fluvial discharge commonly coincided with the ENE-WSW to E-W transverse fault lineaments that were exploited by drainage transverse to the regional N-S tectonic grain. Brackish lagoonal and braided stream deposits (e.g. Subunit 2.2.3) correspond to back-barrier settings that prograded over shoreline sediments. This was followed by relative sea level fall that allowed cliff-cutting and fluvial incision of marine sediments and bedrock. This relative sea-level fall may be explained as high-order, intra-«Calabrian» sea-level cyclicity. Resumed relative sea-level rise during the late Early (to mid-?) Pleistocene then resulted in deposition of detrital carbonate shoreline clinoforms (e.g. Unit 2.3) over a ravinement surface cut into «Calabrian» shoreline to offshore facies.

3.4.3 Mid-Pleistocene lowstand (Fig. 14.a.3)

Important relative sea-level fall took place during mid Pleistocene time. In NW Messenia, a major cliff (Gargaliani Escarpment; Figs. 2.9, 2.11, 3.5) separates early/mid (?) Pleistocene from late Pleistocene terraces. The minimum magnitude of relative sea-level fall in that area equals the height of the cliff (ca. 120 m). Relative sea level fall probably resulted from combination of eustatic sea-level fall, regional uplift and possibly footwall uplift related to the Gargaliani-Filiatra fault (assuming that the latter was active). The regional extent of cliffs and incised valleys, together with the observation that pre- and post-cliff marine terraces are relatively closely-spaced, suggest that much of the Quaternary uplift of the Messenia Peninsula took place after the early Pleistocene, prior to, or during, this phase of major downcutting. Assuming a late middle Pleistocene age for the succeeding "Sicilian" terrace (i.e. correlated with oxygen-isotopic stage 7), a long time interval (~ 400-500 ka) separates the early and late Pleistocene marine terraces.

The above inferred mid-Pleistocene lowstand corresponds to the Mindel sea level fall (beginning of the mid-Pleistocene) in Bonifay's (1975) chronostratigraphic scheme (Fig. 6 b). However, final (present day) incision could be the cumulative effect of downcutting during both the Mindel and the Riss (begining of the late Pleistocene) lowstands. Karstic dissolution of early Pleistocene carbonates and further freshwater diagenesis/pedogenesis took place during this stage. Alluvial fans related to the intense downcutting probably bypassed the present coastal zone and were deposited further offshore. Two notable exceptions are alluvial fans preserved on the flanks of the Kalamata-Messenian Gulf Graben (Paniperi-Petalidhi; Figs. 2, 3, 4b), and associated with a small graben elsewhere (Eleophyton area). Some of the older/higher fanglomerates of the Unit 3.4 (diachronous?)

may correspond to the mid-Pleistocene low-stand. Reworked terra rossa of unit 3.5 was deposited at this time, or later. Fanglomerate deposition probably indicates a climate characterized by strongly seasonal rainfall.

3.4.4 «Sicilian» (Fig. 3.14.b.4)

During the «Sicilian» stage (*sensu* Bonifay, 1975, Figs. 1.3, 3.3), the sea level rose to the level of the piedmont west of the Gargaliani-Filiatra escarpment (at a present altitude of 40-60 m). Algal boundstone bioherms were deposited (e.g. Unit 2.5), probably recording maximum transgression and delta retreat. "Intra-Sicilian" relative sea level cyclicity is suggested by erosional contact of underlying algal boundstones and prograding detrital shoreline sediments; the latter were probably formed during a later «Sicilian» highstand. Pronounced sea-level cyclicity during the mid-Pleistocene is suggested by correlation with oxygen-isotope curves (Imbrie et al., 1987; Martinson et al., 1987; Fig. 3.3).

2.4.5 «Sicilian-Tyrrhenian» Lowstand (Fig. 3.14.b.5)

The sea level fell after the «Sicilian» (at about 180 ka), triggering fluvial incision and cliff cutting. U-shaped meanders were entrenched into «Sicilian» algal boundstone in the Northern Messenia Block (e.g. middle reaches of the Lagouvardos gorge; see Figs. 2.6, 2.12, 3.5). This stage, associated with subaerial diagenesis and calichification of the previous marine deposits, possibly corresponds to the isotopic stage 6 lowstand (ca. 180-130 ka; Martinson et al., 1987), equivalent to the «Riss» lowstand, *sensu* Bonifay (1975) (Figs. 1.3, 3.3).

2.4.6 «Eutyrrhenian» (Fig. 3.14.b. 6)

During the «Eutyrrhenian» (isotopic stage 5.5; ca. 120 ka; Martinson et al., 1987) the sea-level rose again, to the level of c. 20 m (present altitude). In the Northern Messenia block, sediments corresponding to the Eutyrrhenian marine transgression (Unit 3.1) were deposited over a ravinement surface cut into offshore facies of early (or middle ?) Pleistocene age (Figs. 3.1, 3.6). The lower part of the transgressive sequence is characterised by detrital sediments (terrigenous or carbonates, according to proximity to fluvial discharge), whereas algal bioherms characterise higher parts, interpreted as a maximum flooding horizon. The highstand is characterized by clinoforms of detrital carbonates/conglomerates, locally capped by deltaic, to fluvial deposits. By contrast, with the exception of the coast of Koroni (Fig. 3.6), no unambiguous «Eutyrrhenian» deposits were found in the Southern Messenia Block (c.f. Kelletat et al., 1976).

3.4.7 Late Pleistocene Lowstand I (Fig. 3.14.b. 6)

Sea level fell after the «Eutyrrhenian» and valley incision and cliff-cutting took place (substage 5.4; ca. 110 ka; Martinson et al., 1987). Alluvial fan progradation probably occurred in NE areas of the Southern Messenia Block (e.g. lower/younger fans of Unit 3.4), representing an area of intense normal faulting along the uplifting flanks of the Messenian Gulf graben. Elsewhere, alluvial fan progradation was minimal. Intense calichification of «Eutyrrhenian» carbonates, accompanied by karstic dissolution and cementation took place during this first "post-Eutyrrhenian" lowstand.

3.4.8 «Neotyrrhenian» (Fig. 3.14.b. 6)

Sea-level rose again during the «Neotyrrhenian» (substages 5.3+5.1; ca. 100-80 ka; Martinson et al., 1987) and detrital sediments were deposited over a karstified and bio-eroded relief of previous «Eutyrrhenian» deposits in NW Messenia (Unit 3.2). Only very proximal sediments are exposed (upper shoreface to foreshore). Higher order, "intra-Neotyrrhenian", sea level cyclicity is possibly indicated by thin caliche horizons intercalated with shallow-marine sediments. Tectonic activity was locally intense, as indicated by dense jointing of «Neotyrrhenian» deposits. Extensional joints follow well established trends in the bedrock and demonstrate that «Neotyrrhenian»/post-«Neotyrrhenian» tectonic activity involved reactivation of older, buried extensional fault lineaments (Chapter 2). By contrast, in S Messenia, low (1-5m ASL) marine abrasion platforms without sediment may not be of «Neotyrrenian» age despite their low altitude, but could instead reflect diminished uplift (or even subsidence), leaving older Pleistocene terraces near (or below) sea level in this area.

3.4.9 Late Pleistocene Lowstand II (Fig. 3.14. b.7)

Sea-level fell again after the «Neotyrrhenian» and during the Last Glacial Maximum lowstand, resulting in further valley incision, cliff-cutting and karstic dissolution (isotopic stages 4 and 2; ca. 60-12 ka, respectively; Martinson et al., 1987; equivalent to the «Würm» lowstand, *sensu* Bonifay, 1975). Alluvial fan progradation was restricted to areas of inferred active normal faulting, coinciding with major tectonic boundaries (e.g. lowest/youngest parts of diachronous Unit 3.4). Elsewhere, in most parts of the peninsula, red terra rossa soils, locally associated with chalky caliche horizons, covered a karstified relief of «Neotyrrhenian» and older sediments (e.g. Unit 3.5). Emergence of inner shelf areas during the maximum regression exposed uncemented littoral carbonate sand that was reworked into sand dunes (e.g. Unit 3.6) that drape «Neotyrrhenian» foreshore facies and terra rossa attributed to Late Pleistocene Lowstand II (Units 3.1, 3.5). A similar model was proposed for late Pleistocene aeolianites in southern Cyprus (Poole and Robertson, 1991, 2000).

Aeolianites are widespread along the exposed western coast of the Messenia Peninsula, facing the open Ionian Sea, but are almost absent from the eastern coast, facing the Messenian Gulf. Palaeowind directions from inferred late "Pleistocene lowstand II" aeolianites (Fig. 3.13.b: log 8) are generally eastwards, similar to the present-day prevailing wind direction. Co-existence of calichification with sub-surface karstic dissolution is suggestive of a semi-arid climate, with alternating wet/dry periods. Rainfall possibly increased towards the end of this period to early Holocene (prior to the maximum of the Holocene transgression in the «Versilian»), allowing deep solution holes in coastal aeolianite to penetrate deeper that the present sea level.

3.4.10 «Versilian» (Fig. 3.14b.7)

Eustatic sea-level rose after the Last Glacial Maximum, reaching the present, or a slightly higher level at ca. 6 ka (Kraft et al., 1975; Labeyrie et al., 1976; Kambouroglou, 1989; Plaziat et al., 1996). As a result, cemented Pleistocene deposits were transgressed and subjected to marine abrasion and bioerosion (e.g. Romanos and Petrohori coasts). A short-lived marine transgression/regression event in the Kalamata-Messenian Gulf Graben (Pamissos Plain) at around this time (Kraft et al., 1975) can be attributed either to the «Versilian» sea-level cycle, or to local tectonic subsidence. Deposits formed during the short-lived «Versilian» sea level highstand were either Vermetid bioconstructions (e.g. Romanos coast, Figs. 3.3, M.1), or pebbly-beach sediments deposited on a ravinement surface over aeolianite of the latest Pleistocene lowstand stage (e.g. Petrohori coast). These deposits could also be of an even younger (historical ?) age, uplifted during the "Early Byzantine tectonic paroxysm" (*sensu* Pirazzoli, 1986).

3.4.11 Later Holocene to Recent

Since regional relative sea level change after the «Versilian» is well documented (e.g. Kraft et al., 1975), local deviations from the regional sea level curve is assumed to relate to faulting (Flemming, 1968, 1978), combined with the effects of possible regional isostatic readjustment after the last glaciation (Lambeck, 1995). The Messenia Peninsula has been constantly inhabited since Neolithic times and human activity has influenced geomorphic and sedimentary processes. An example of noticeable geomorphic change in the peninsula since Mycaenean times is the ca. 3 km of delta/flood-plain progradation in the S part of the Northern Messenia Block (Yialova area) (Fig. M.1).

3.5 SUMMARY-CONCLUSIONS:

- The Plio-Pleistocene sedimentary and record of the Messenia Peninsula, SW Peloponnese, is very well preserved, shedding light on the tectonic-sedimentary evolution of a forearc area adjacent to the Ionian subduction zone, along the western part of the Hellenic arc. The results supplement observations from an area between the better known Corinth-Patras and Cretan areas to the north and south, respectively.
- The Plio-Quaternary marine sediments are dated using nannofossils for the Pliocene-early Pleistocene time interval. In addition, late Pleistocene sediments are correlated with the well known «Euthyrrenian» (isotopic stage 5.5; ca. 120 ka) and «Neotyrrhenian» (isotopic stages 5.3+5.1; ca. 100-80 ka) deposits elsewhere in Greece and other Mediterranean areas (e.g. Cyprus). A sequence-stratigraphic approach, involving correlation of successive marine terraces with known, dated, global sea-level highs is used to infer possible ages for the "Calabrian" and "Sicilian" stages (although with uncertainties resulting from unresolved multiple sea-level highs).
- Within the N Messenia Block six main Quaternary (Pleistocene-Holocene) terraces with overlying shallow marine sediments are present (Early Pleistocene (<200-340 m), late Early (to middle) Pleistocene (ca. 240 m), «Sicilian» (40-60 m), «Eutyrrhenian» (15-20 m), «Neotyrrhenian» (2-4 m) and «Versilian» (0.2-1.5 m). Some of the marine successions are backed by correlative non-marine (e.g. lagoonal), to terrestrial deposits.
- Within the North Messenia Block younger marine terraces occur at successively lower levels. This implies that at time scales of the order of 1-2 Ma (L:ate Pliocene to Holocene) regional tectonic uplift, punctuated by glacio-eustatic sea level change, exercised the dominant control over shallow-marine sedimentation. On the time scale of the last 1 Ma the uplift rate (assumed to be constant), ranges from 0.33-0.23 m/ka, comparable with that that inferred for the Gulf of Corinth region further north (ca. 0.3 m /ka; Collier, 1990).
- Local extensional faulting controlled some deposition (notably of early Pleistocene offshore sediments within narrow asymmetrical grabens). As a result, on an outcrop scale, the preserved sediments mainly document the interplay between the effects of regional tectonic uplift, glacio-eustatic sea-level change and footwall uplift (or hangingwall subsidence) related to local extensional faults.
- On a regional scale, an east to west progression of graben formation through time is confirmed. In the east (vicinity of Messenian Gulf graben), subsidence rates were high enough to allow deposition of offshore sediments in Early Pliocene time, whereas in the west subsidence was delayed until latest Pliocene-early Pleistocene time. This migration of deformation towards the west through time is attributed to "roll-back" of the

subducting North African plate (possibly accompanied with gravity spreading of the overriding crust).

Table 3.1: Benthic and planktic foraminifera fauna from Plio-Pleistocene sediments of the Messenia Peninsula. Environmental information from **1:** Amorosi et al. (1998), **2:** Blanc-Vernet (1969), **3:** Fernadez-Gonzales at al (1994), **4:** Murray (1973).

UNITS

Foraminifera	1.5	1.6	2.1	2.2.1	2.2.2	2.2.3	2.3	2.4	2.5	3.1	3.2	3.8	**Environment**
Ammonia becarii	+	+		+	+	+	+	+	+	+	+		**15-<100m, high energy, normal-slightly hyposaline, coastal lagoons (1, 2)**
A. tepida						+							**10-30 m, hyposaline, fluvial runoff (1, 2, 4)**
A. spp.			+		+		+	+	+				
Angulogerina angulosa			+										
Asterigerinata mamila			+	+	+		+		+	+			
Brizalina spathulata			+										
Br. spp.			+										
Bulimina marginata			+										**60-150m, oxygen deficiency, fluvial runoff (1, 2)**
Bl. spp.			+										**>20m (4)**
Carpenteria utricularis									+				
Cassidulina crassa			+										
Cibicides lobatulus	+		+	+	+		+	+	+	+			
C. refulgens			+	+	+		+			+			
C. ungerianus-pseudungerianus	+		+										
C. spp.								+			+		
Discorbis sp.		+		+			+	+		+			
Elphidium acculeatum			+										
E. advenum			+	+									

E. complanatum			+	+									
E. crispum	+	+		+	+	+	+	+	+	+			**10-75 m, commonly epiphytic (1, 2, 3)**
E. jenseni				+									
E. macellum	+			+	+					+			**10-75 m, commonly epiphytic (1, 2, 3, 4)**
E. spp.	+	+			+	+	+	+	+	+	+		
Gladulina sp.			+										
Globocassidulina subglobosa			+										
Hanzawaia sp.			+										
Homotrema rubrum									+	+			
Lagena orbignyana			+										
other Lagenidae								+					
Nonion depressulum				+									**10-40 m, normal-slightly hyposaline (1)**
N. incrassatum				+									
Nonionella sp.			+										
Planorbulina mediterranensis			+						+	+			**infralittoral, epiphytic (2, 4)**
Planulina ariminensis			+										
Quinqueloculina spp.									+	+	+		**Infralittorla, epiphytic (1, 2, 4)**
Reophacidae									+				
Reussella spinulosa			+										
Robertina bradyii			+										**Infralittoral. Epiphytic (2, 4)**
Rosalina utricularis									+				**Infralittoral, epiphytic (2, 4)**
Sphaeroidina bulloides			+										
Spiroloculina sp.									+	+	+		**Infralittoral, epiphytic (2, 4)**

Textularia sagitula			+										**>50m, inner shelf (3)**
T. spp.			+					+	+				**-//- (3)**
Triloculina sp.									+	+	+		
Uvigerina(meditarranea)			+										**>90 m , rich in organic matter (1, 2, 3)**
Valvulinidae				+									
Globigerina bulloides			+										
G. falconensis			+										
G. venezuellana (*)				+									
Globigerinella aequilaterallis			+	+									
Globigerinoides ruber			+								+		**Warm water (2)**
Gb. Obliguus Extremus			+										**-//- (2)**
Neogloboquadrina humerosa			+	+									**-//- (2)**
Orbulina universa			+										**-//- (2)**
Globigerinidae,		+						+	+		+		
Globorataliidae								+	+				

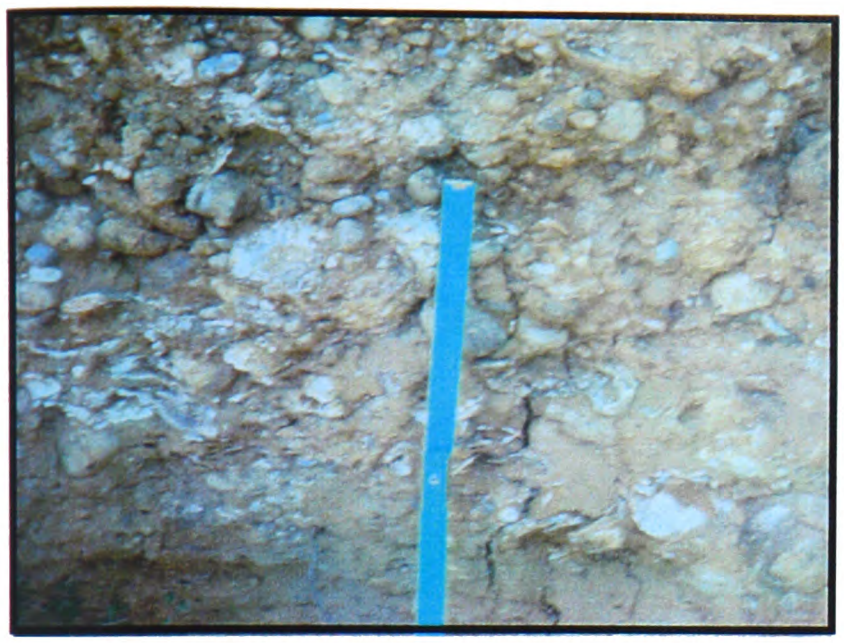

Figure 3.15: Upper parts of Unit 2.2 (early Pleistocene). Conglomerate with well rounded pebbles and *Ostrea* sp. in a fine-grained sandstone matrix. Eleophyton.

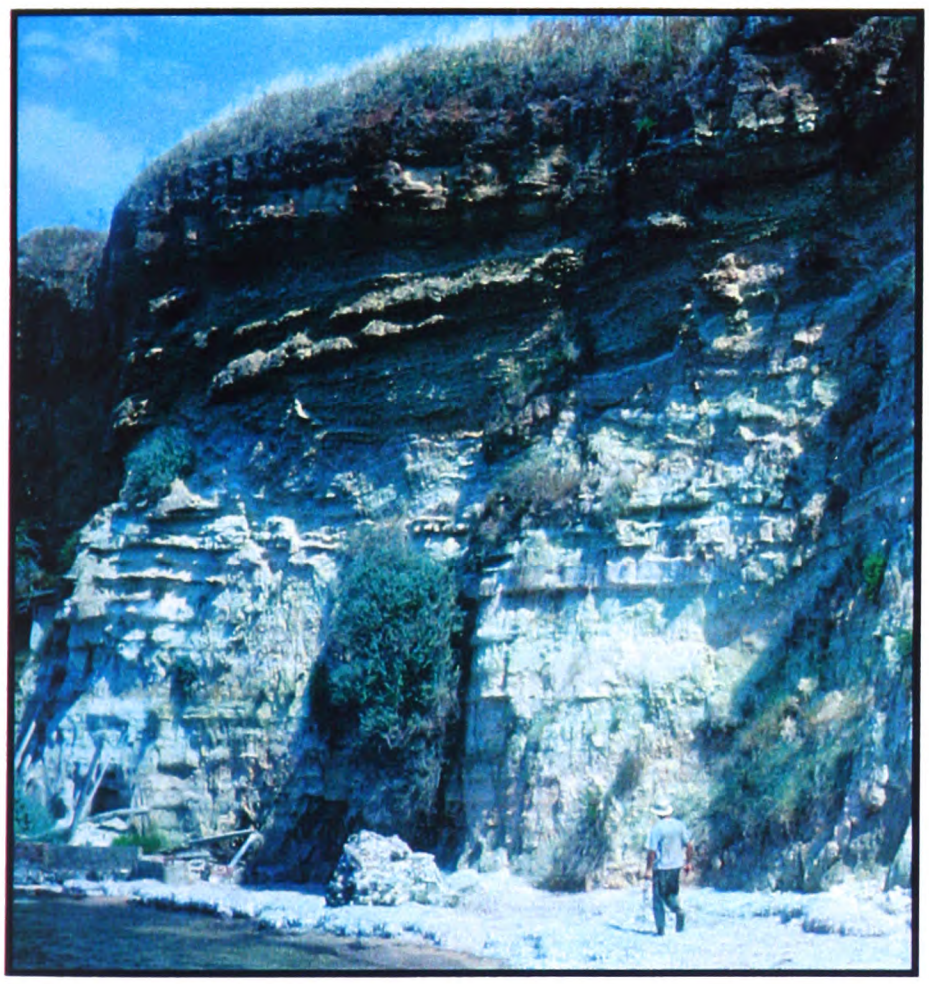

Figure 3.16 (left): Unconformity between Early Pliocene (Zanclian) offshore mud Unit 1.4) below and late Pleistocene (Eutyrrhenian) shoreface carbonates (Unit 3.1) above. Note that the Eutyrrhenian deposit exhibits a progradational architecture, with steep foresets passing up to almost horizontal topsets. Koroni Castle.

Figure 3.17: Offshore carbonate mud of early Pleistocene (NN 19a) age (Unit 2.1). Note bioturbation, with mainly horizontal burrows. These sediments were deposited in a narrow, NNW-SSE striking graben. Pylos Port.

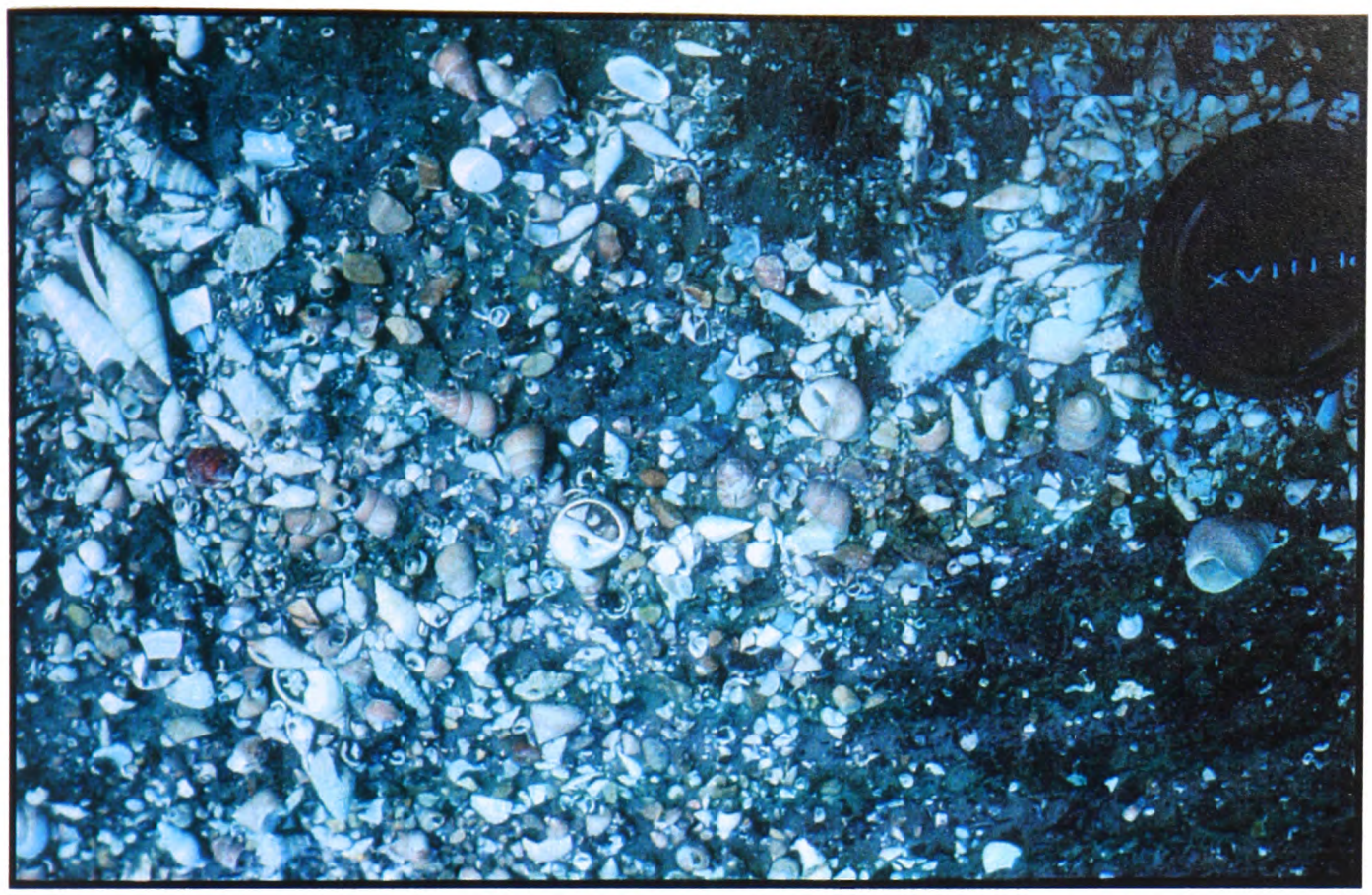

Figure 3.18: A dense accumulation of Cerithid and other gastropods and bivalves in black mud. Note the exceptional preservation of the shells (including colour) and the predominance of gastropods in the fauna. The depositional environment is interpreted as a restricted brackish lagoon. Early Pleistocene, road from Gargaliani to Valta

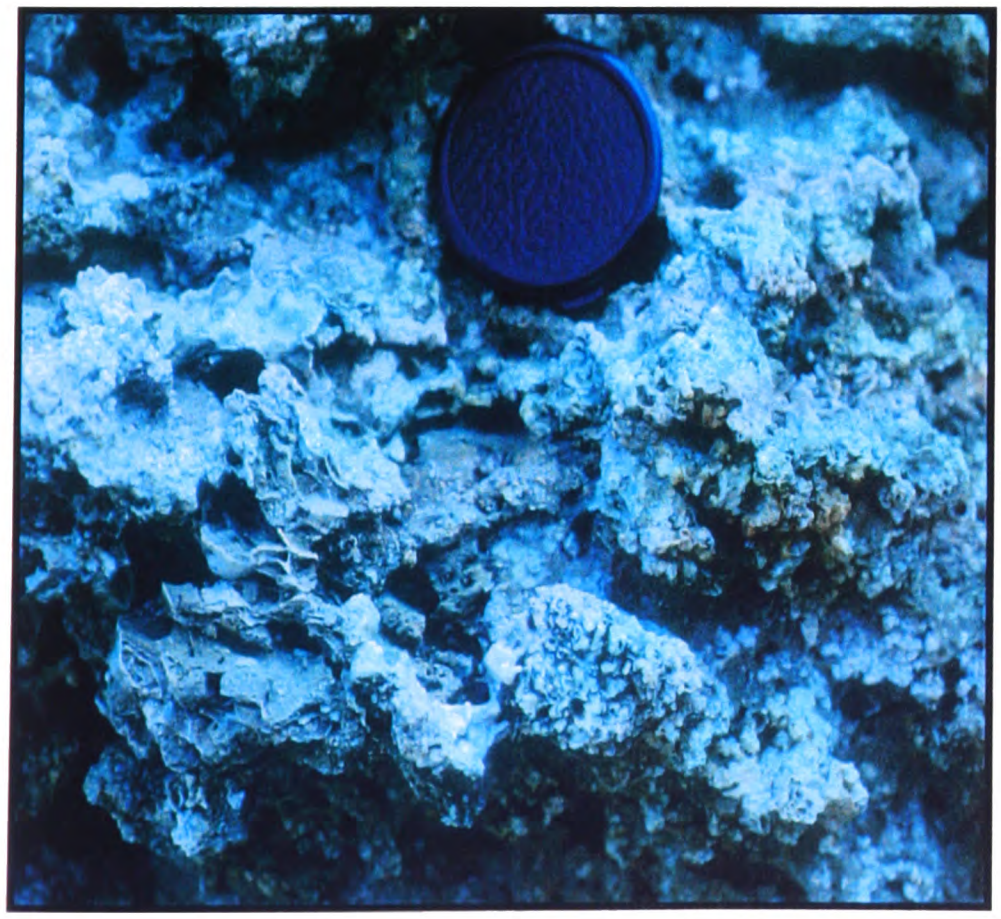

Figure 3.19: Red algal boundstone of middle Pleistocene age (Unit 2.5). Note the high primary porosity and the presence of rhodoliths. Limenari.

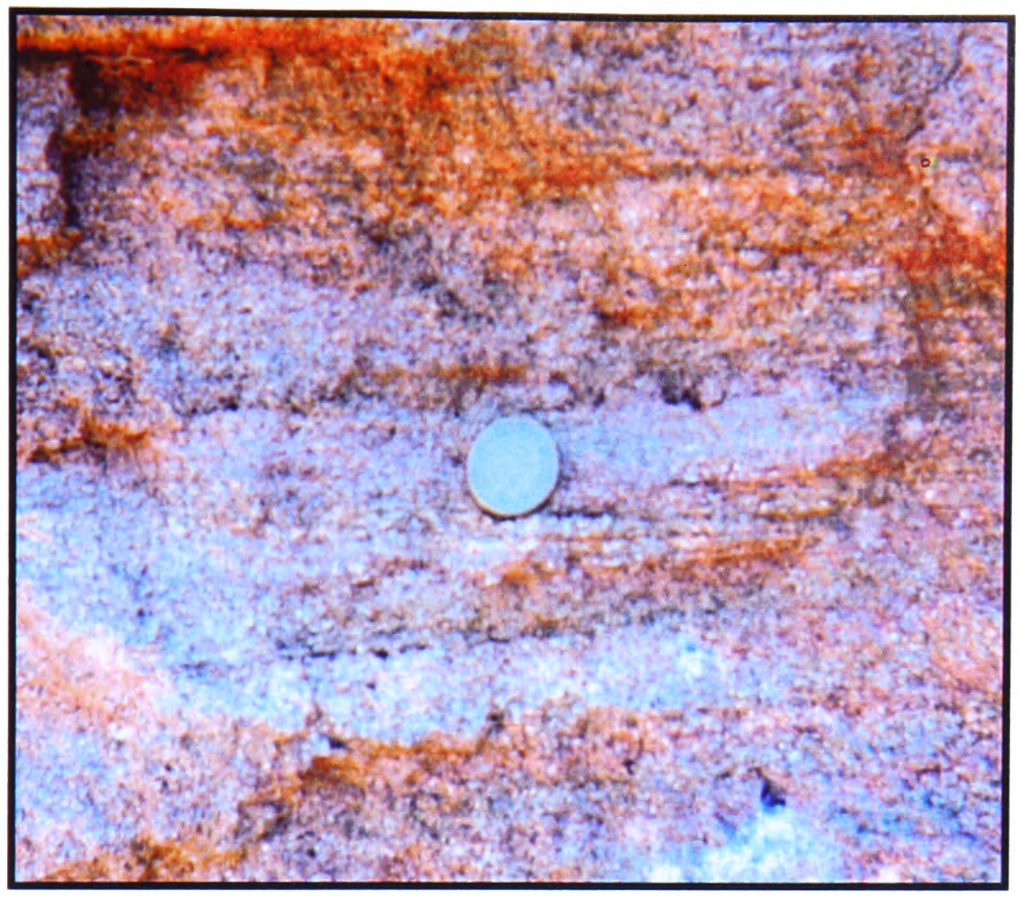

Figure 3.20: Low angle cross-laminated grainstone from upper shoreface- foreshore deposits of early Pleistocene age (Unit 2.4). Coin diameter ca. 4 cm.

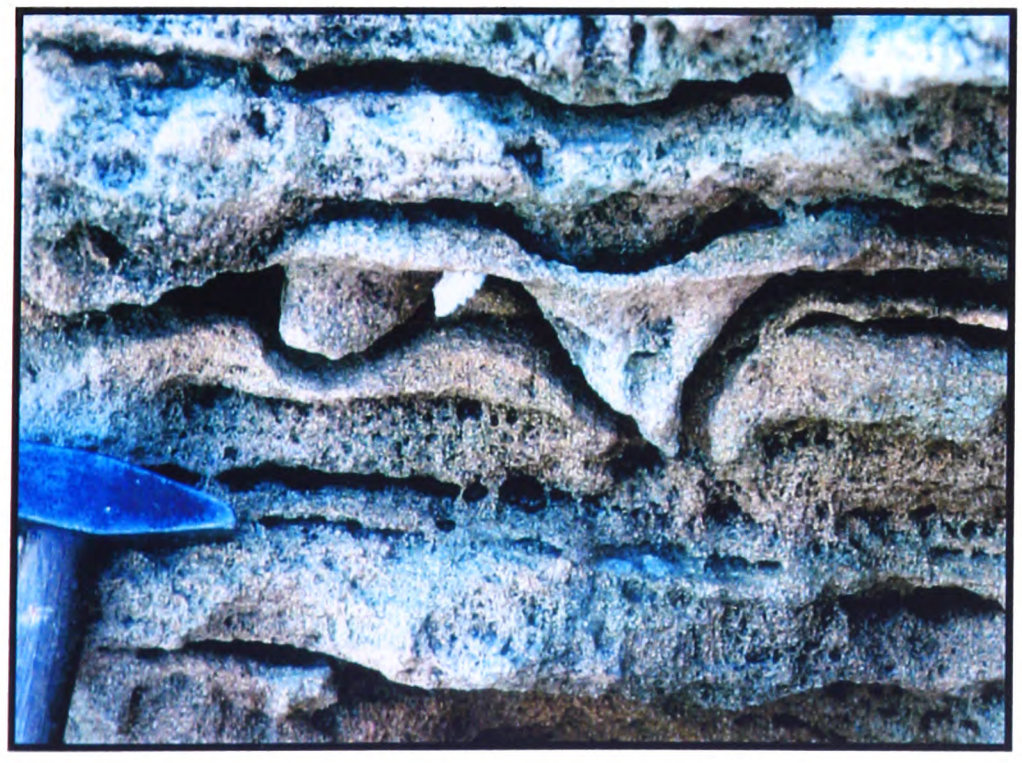

Figure 3.21: Coarse-grained, low angle cross-laminated grainstone with bivalve escape structures (centre of the photograph). Upper shoreface facies of Neotyrrhenian Unit 3.2. Marathopolis.

Figure 3.22: Reworked terra rossa with mammalian bone fragments. This late, or middle, Pleistocene soil was deposited in chasms within the early Pleistocene deltaic sediment of Unit 2.2. Gargaliani Quarry.

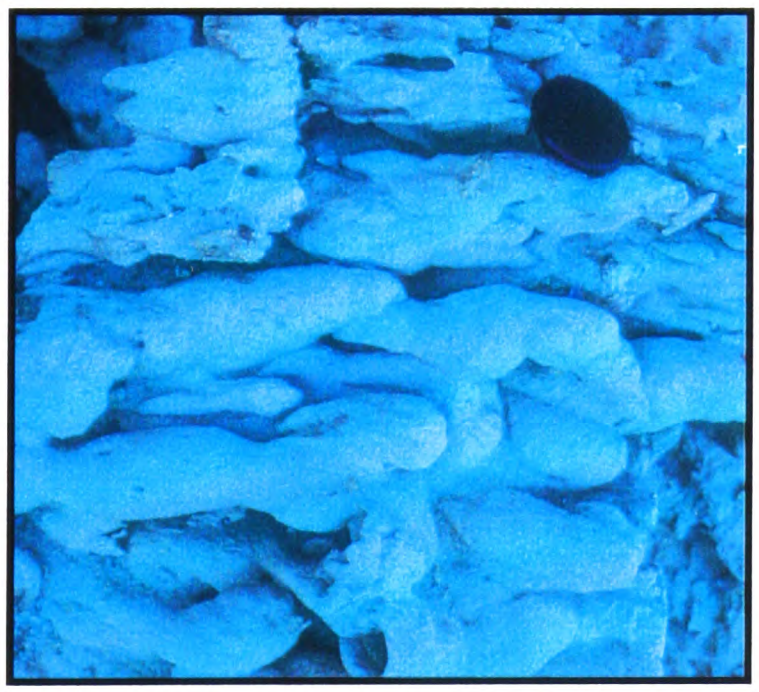

Figure 3.23: Liquifaction structures on the base of Eutyrrhenian (Unit 3.1) shoreface sandstone from Mati Beach.

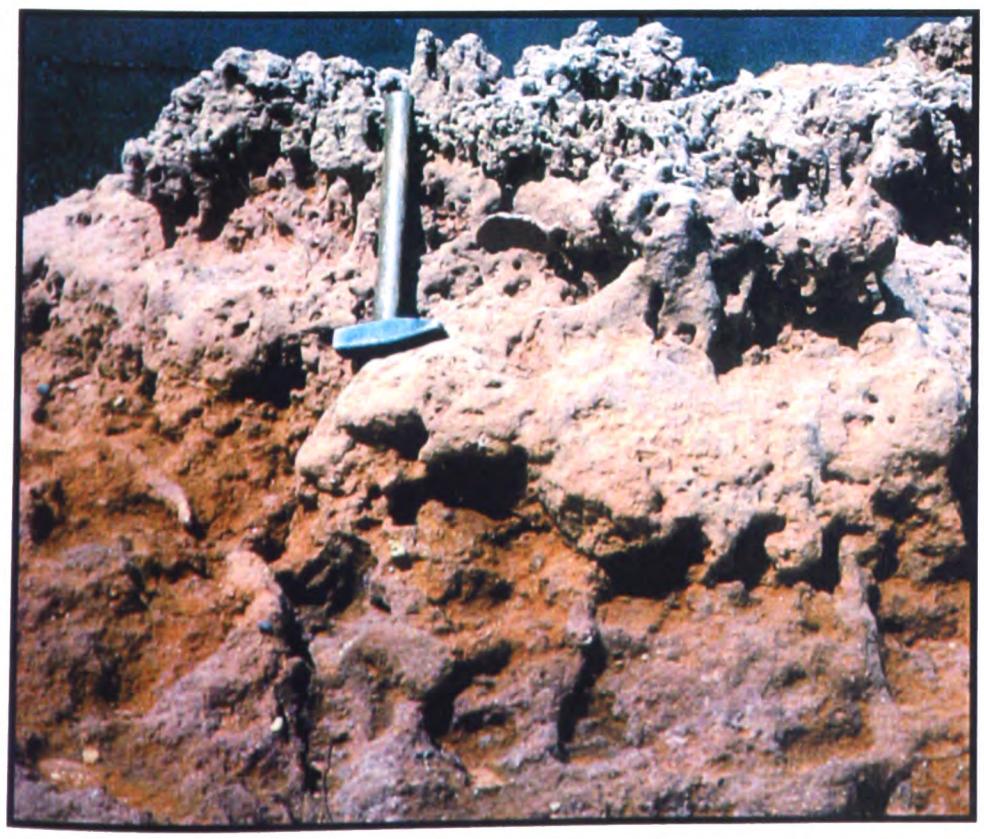

Figure 3.24 (left): Latest Pleistocene red palaeosol (Unit 3.6) followed by root-bioturbated aeolianite up-section (Unit 3.7). Note large calichified roots (*Rhizocretion*) within the palaeosol unit. These sediments, that cover the Neotyrrhenian terrace, were deposited during a latest Pleistocene sea level lowstand. Marathopolis.

CHAPTER 4: GEOMORPHOLOGY OF THE EASTERN LAKONIA PENINSULA: SURFACES AND DRAINAGE

4.1 INTRODUCTION

This chapter focuses on the geomorphology of the Eastern Lakonia Peninsula. The fault pattern of the area, that partly controlled morphological evolution, is discussed and fault-bounded morphologic units are introduced. The principal surfaces of subaerial erosion and marine terraces are then described, for the Eastern Lakonia Peninsula as a whole and for each morphologic unit separately. The last section of this chapter is a description of the drainage network of the peninsula, with emphasis on the tectonic and lithologic controls on its development. Streams that exemplify these controls, are discussed separately, within each morphologic unit.

4.1.1 Plate tectonic setting: The Eastern Lakonia Peninsula lies ca. 100 km east of the Ionian Trench (Figs. 1.1, 1.2). This is the easternmost terrestrial part of the SW Aegean Fore-arc; the back-arc basin of the Aegean sea is located a few km offshore (see Chapter 1).

4.1.2 Geological structure: The Eastern Lakonia Peninsula comprises the Tythean basement, including marble, phyllites, and neritic carbonates, and Late Pliocene-Holocene shallow-marine and suaberial sediments, unconformable above the latter (I.G.E.Y., 1970; Jakobschagen et al., 1978; I.G.M.E., 1981).

The Tethyan basement of the Eastern Lakonia Peninsula comprises three main units (see Fig. 4.1):

1) Marbles, with lenses or beds of chert in the lower parts of the succession, are attributed to the "*Plattenkalk Series*", generally believed to be the 'autochthton' basement (Thedoropoulos, 1973; Dufaure, 1977; Jacobschagen et al., 1978). The exact position of the "*Plattenkalk Series*" in relation to the surrounding unmetamorphosed units is debated. Kuss and Thorbecke (1974) interpreted it as the weakly metamorphosed eastern part of the Ionian Zone, whereas Jacobschagen et al.(1978 a,b) inferred a position intermediate between the Pre-Apulian and Ionian Zones.

2) The "*Phyllite Series*" comes above, thrusted over the "*Plattenkalk Series*". This comprises various HT/LP lithologies (phyllite, chlorite schist, quartzite, glaucophane schist and metavolcanics). The series is dated as Carboniferous-Permian, on the basis of locally

preserved foraminifera (I.G.M.E., 1984). In most places of the Eastern Lakonia Peninsula, the "*Phyllite Series*" is overthrusted by the "Tripolis Series" nappe; however, a gradational ransition from the "*Phyllite Series*" to the "Tripolis Series" is inferred from other parts of the Peloponnese. The "*Phyllite Series*" is considered as composite, including parts affected by pre-Tethyan (pre-Mesozoic) and Tethyan metamorphic events (Jacobschagen et al., 1978a). Dufaure (1977) viewed this unit as the metamorphosed lower part of the Tripolis nappe. Jacobschagen et al.(1978a) accepted this interpretation for only part of the unit. The latter authors considered the "*Phyllite Series*" as the lower part of the "Western Hellenic Nappes", thrusted over the autochthon basement ("*Plattenkalk Series*").

3) The "Tripolis Series" ("Tripolis Zone" for some authors) comprises thick, neritic limestone of Middle Triassic-Upper Eocene age, locally recrystallised in its lower parts, followed by turbidite facies ("flysch") of Upper Eocene-Aquitanian age. The main thrusting of the unit took place in Early Miocene (Kowalczyk et al., 1977). This unit was interpreted as the "upper Western Hellenic Nappe" by Jacobschagen et al. (1978a).

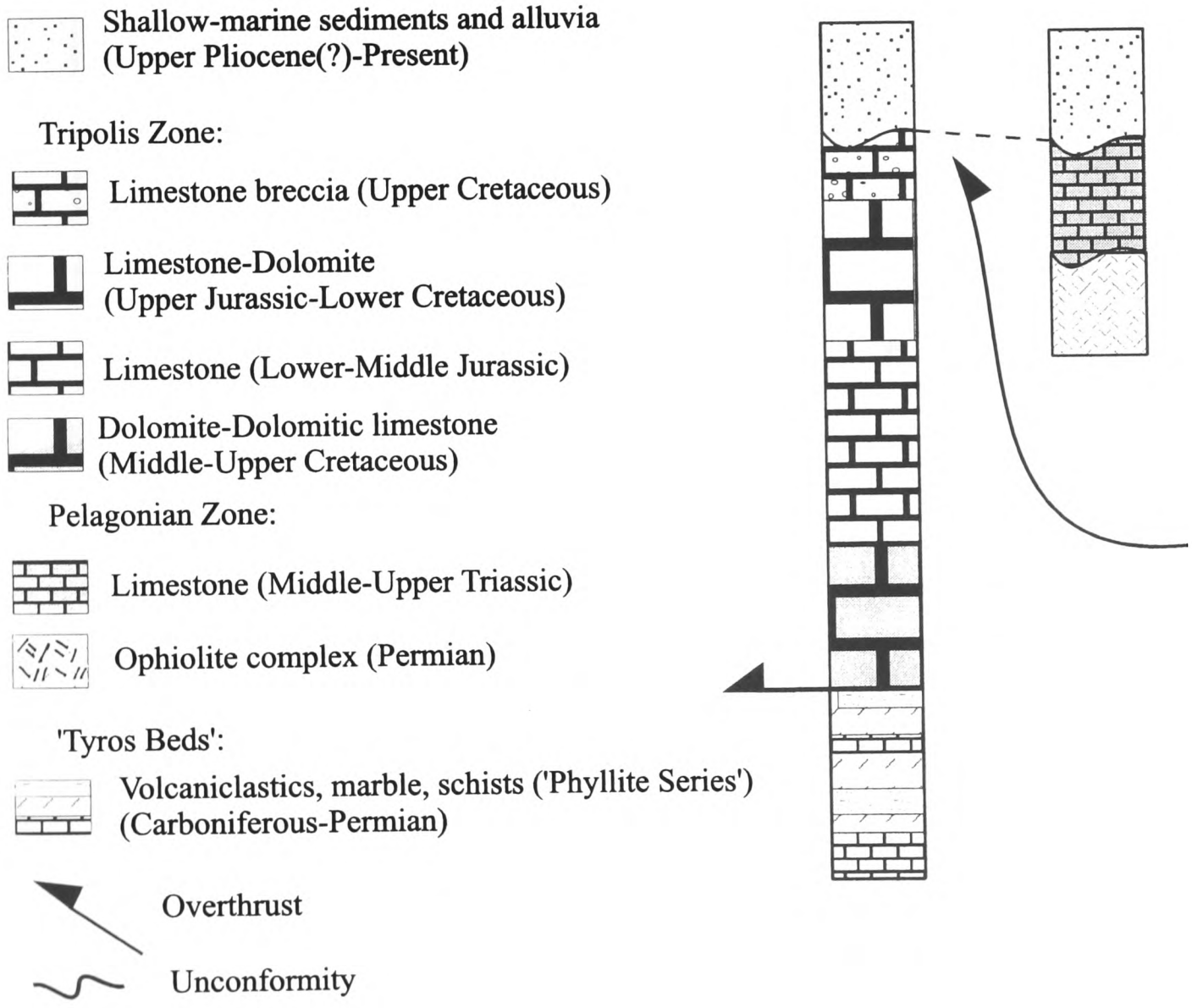

Figure 4.1: Tethyan stratigraphy of the Eastern Lakonia Peninsula. Pre-Neogene rocks comprise the autocthon "Plattenkalk Series", the "Phyllite Series" and the Tripolis Zone. These units are separated with tectonic contacts (thrusts) (see text). Sources: I.G.E.Y. (1970), Theodoropoulos (1973), Jacobschagen et al. (1978), I.G.M.E. (1984).

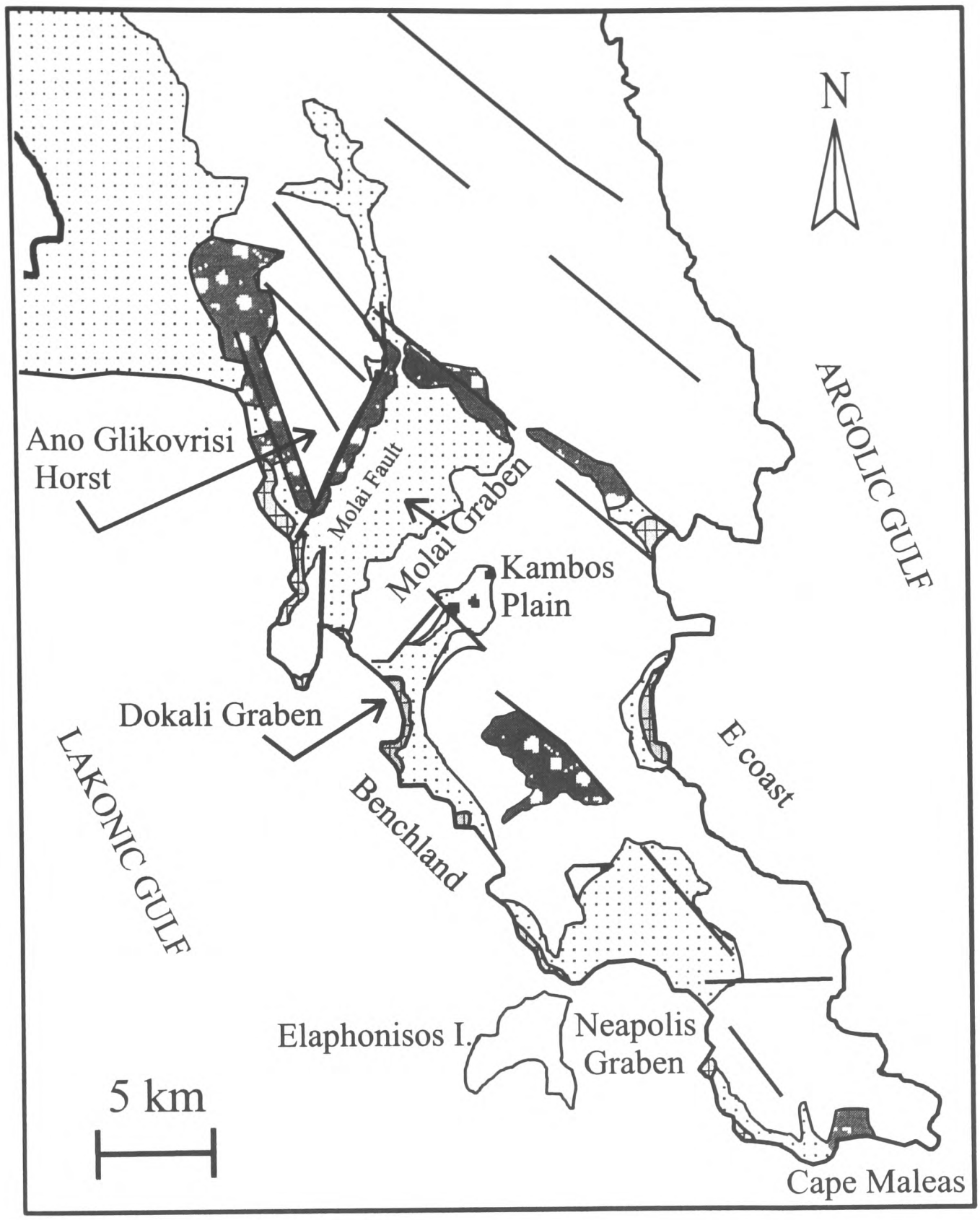

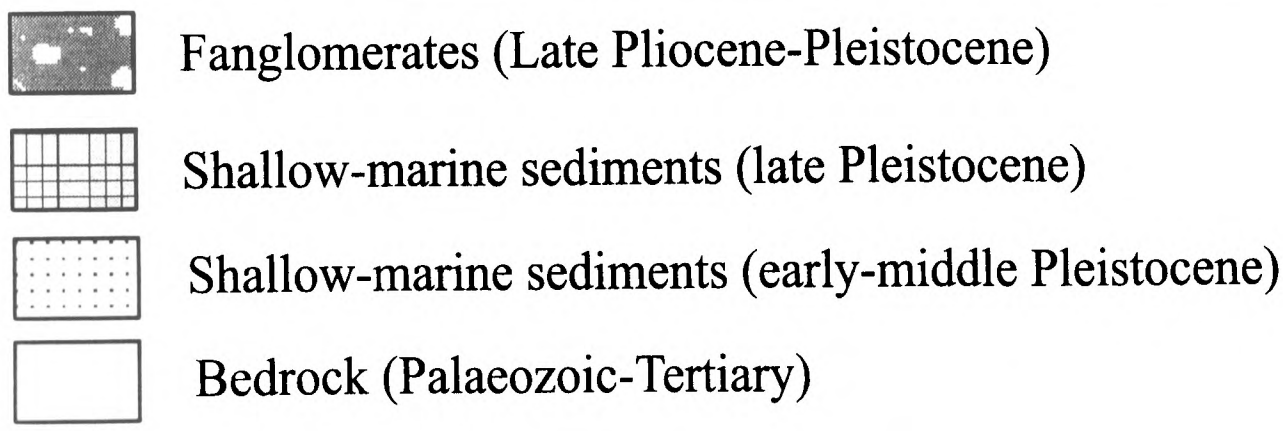

Figure 4.2: Outline geological map of the Eastern Lakonia Peninsula. Note the presence of the km-scale Molai Graben, bounded by NW-SE and later N-S faults.

4.2 FAULT AND JOINT PATTERN

Post-Tethyan sediments in the Eastern Lakonia Peninsula are cut by exclusively normal faults. Faults in this area are grouped in the following sets (Figs. 4.2, 4.3):

4.2.1 NNW-SSE faults: The strike of these faults coincides with the dominant direction of Tethyan folding in the region. Faults that cut through the Tethyan basement probably have a multiphase history of activity, dating back at least to the Midde-Late Miocene, when back-arc extension in the Hellenic Arc was initiated (Jacobschangen et al., 1978; Meulenkamp et al., 1988). Faults of this set accommodated the outward expansion of the Hellenic fore-arc since the Middle Miocene. Reactivation of even older, Tethyan structures can be hypothesised on the basis of similarities in strike between the Tethyan structural grain and that of this set.

At a megascopic scale (1:50,000 map, I.G.E.Y., 1970; I.G.M.E., 1981; see Figs. 4.2, M.2), NNW-SSE faults gave rise to narrow horsts and grabens (width: 0.4-1.8 km). The width of these grabens decreases systematically from the north (maximum width: 1.8 km) to the south of the peninsula (maximum width: 0.9 km) (Fig. M.2). Large NNW-SSE faults, in left-stepping, *en-echelon* sets, form the NE boundary of the Molai Graben (Figs. 4.2, 4.6, M.2; see below). The maximum length of a continuous mapped fault along that boundary is ca. 12 km (I.G.M.E., 1981). Large-scale karstification (poljie, ouvallas), associated with axial parts of NNW-SSE grabens, was also controlled by faults of this set (e.g. Vathia Lakka poljie, east of Molai; Velies; see Figs. 4.6, M.2). NNW-SSE faults of km-scale are commonly cut by N-S trending faults (Figs. 4.2, M.2). Faults of this set were active during the Pleistocene, after the emergence of early Pleistocene marine terraces, which are locally faulted, with throws of ca. 50-60 m (e.g., south of Ano Glikovrisi; Figs. 4.15, M.2). Numerous small-throw faults of NNW-SSE strike cut all Pleistocene units, up to the "Eutyrrhenian" (e.g. Limnakia; Figs. 4.12, M.2). Faults of the same set also downthrow Pleistocene sediments below present sea level along the SE flank of the Lakonic Gulf (Figs. 4.1, M.2). Small faults and joints of NNW-SSE strike in latest Pleistocene ("Neotyrrhenian") sediments and post-"Neotyrrhenian" red alluvia indicate sub-Recent activity of this fault-set.

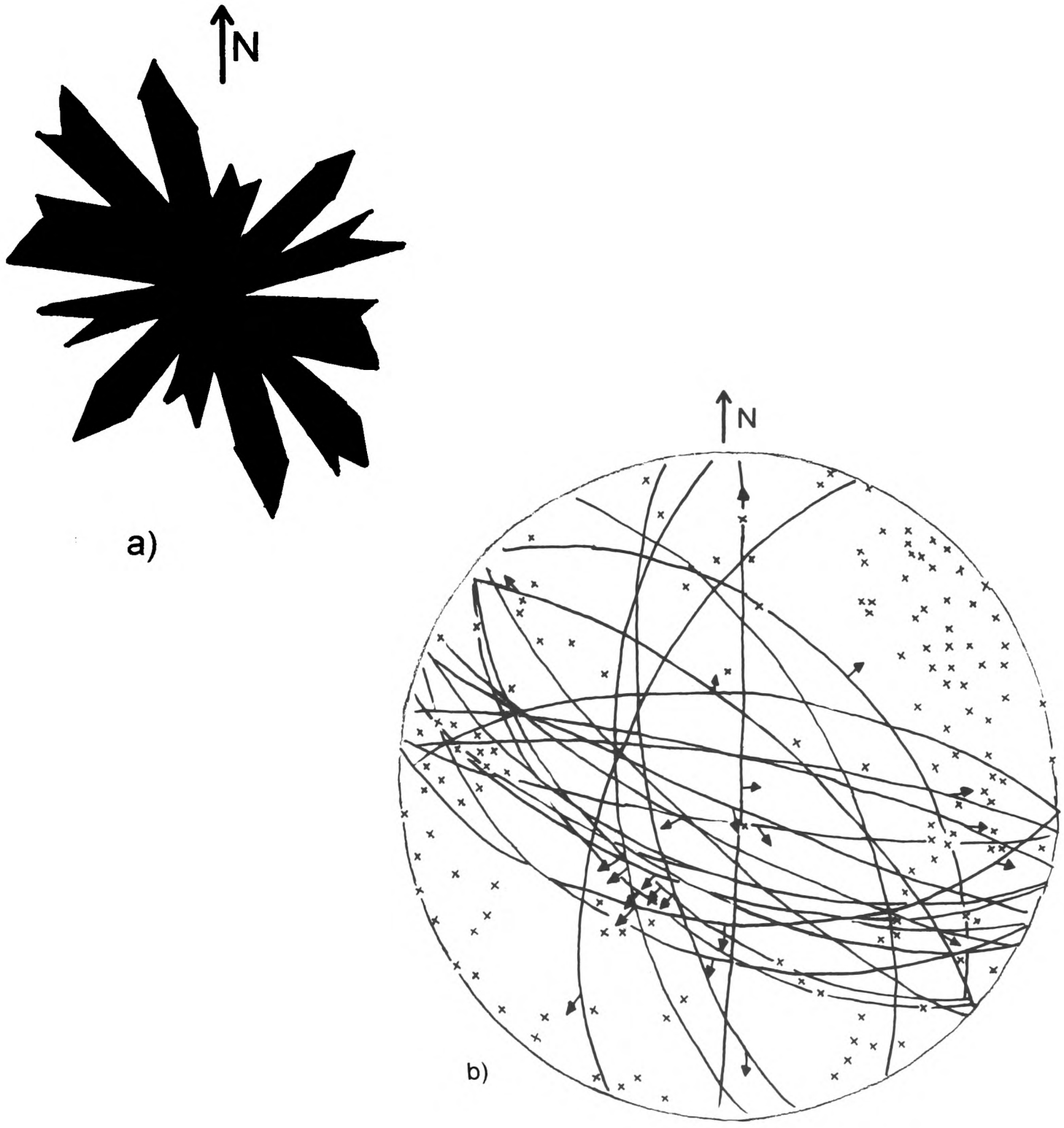

Figure 4.3: Stereoplots of joints **(a)** and normal faults **(b)** measured in the Eastern Lakonia Peninsula. **a)** Rose diagram of joints measured in Pleistocene shallow-marine sediments and alluvia. **b)** Normal faults (mainly in Tethyan bedrock.. Great circles and arrows represent planes and trend and plunge of slickensides, respectively. Crosses represent poles.

4.2.2 N-S faults: Faults of this set bound blocks at a scale of 20-30 km (e.g. Molai Fault, that forms the NW boundary of the Molai Graben against the Glikovrisi Horst; see Figs. 4.1, 4.3, M.2). The Molai Fault is a prominent structure, of 22 km total length and >700-900 m minimum total apparent throw (Figs. 4.1, 4.4, M.2). In the north, it begins as a N-S fault zone through bedrock and follows a NNE-SSW strike in the Molai Graben, where it juxtaposes bedrock (footwall) with Pleistocene marine and subaerial sediments

(hangingwall) (Figs. 4.1, 4.4, 4.5). The relative age relation between N-S and NNW-SSE faults is not revealed by cross-cutting relations, since faults of both sets cut each other. Large N-S faults (e.g. Molai Fault) date back to at least the Late Pliocene, as indicated by the inferred age of the oldest basin fill (Dufaure, 1977). Asymmetrical, westward tilting of the deeper, pre-Pleistocene (?), graben-filling sediments is suggested by borehole data (Doutsos, pers. com., 1998). By contrast, basinward tilting and large-scale offlap is inferred from the early Pleistocene regressive Subunit 3.2 (see Chapter 5), that drapes the uplifted footwall of the Molai Fault near Pakia (NW boundary of the Molai Graben; Figs. 4.4, 4.5). N-S faults cut even younger (middle-late Pleistocene ?) sediments around the Bozas Rema and Viglaphia areas (Figs. 4.1, M.2). Historical (Roman) coastline subsidence between Kokkinia and Plitra (Figs. 4.5, M.2) could be attributed to activity of N-S faults. The latter suggestion, although difficult to confirm based on the existing evidence, is consistent with Armijio's et al. (1991) hypothesis that the N-S striking Taighetos Fault was responsible for the 467 BC Sparta Earthquake, and also with the well documented E-W maximum extension in the region during the Quaternary (Hatzfeld et al., 1989,1990; Armijio et al., 1992).

4.2.3 E-W faults: These faults segment the peninsula across its morphological strike, and are perpendicular to the prominent N-S and NNW-SSE faults. E-W faults (e.g. Fig. 4.16) are, thus, interpreted as transfer faults. At the southern tip of the Eastern Lakonia Peninsula (Prophitis Ilias; Figs. 4.1, 4.6, M.2), E-W faults offset Pleistocene marine terraces of probably "Eutyrrhenian" age (ca. 120 ka). E-W faults also create fault-controlled depocentres in the footwalls of large peninsula-parallel faults (Figs. 4.1, M.2). Numerous small faults of E-W strike (cm-scale throws) cut "Neotyrrhenian" or later sediments, thus indicating latest Pleistocene-Recent activity of this fault set.

The initiation time of each fault set is uncertain and many peninsula-parallel faults might be reactivated Tethyan structures. However, all three fault sets were active during Pleistocene. This pattern of coeval activity is consistent with observations concerning active faulting in northern and central Greece, where complex patterns of fault-rupture are interpreted to reflect structural heterogeneity of the seismogenic zone (Pavlides, 1993). In Eastern Lakonia, maximum activity, evidenced by tilting of Pleistocene deposits and control on topography, is associated with N-S faults, in consistency with the regional stress field (e.g. Molai Fault; Figs. 4.1, 4.3, 4.4, 4.5, M.2). Smaller-scale faults are commonly associated with internal deformation of blocks bounded by the N-S faults (Fig. M.2). These faults also exercise control upon the topography (at a smaller scale), drainage pattern and evolution and alluvium distribution over the Eastern Lakonia Peninsula (see below).

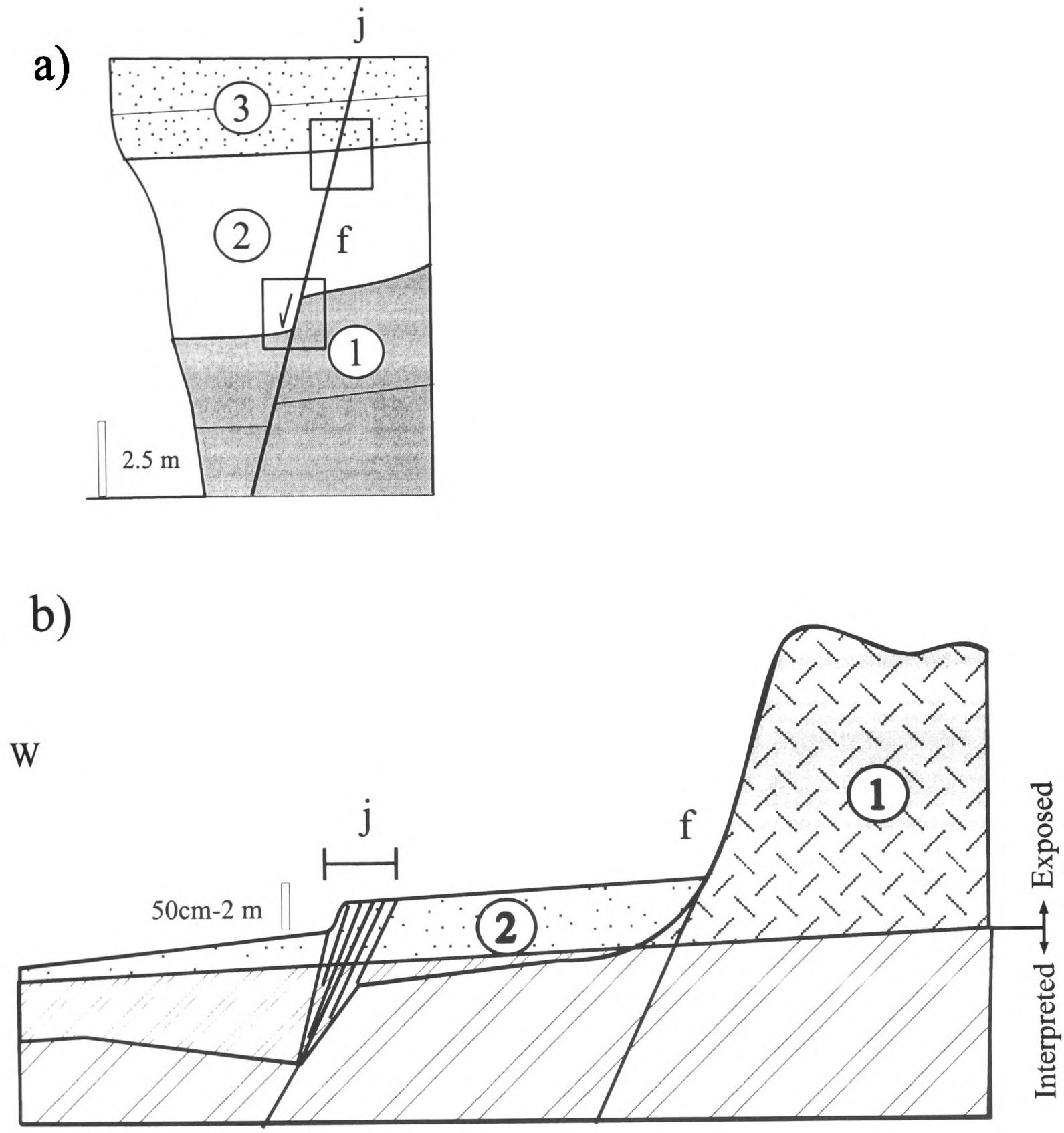

Figure 4.4: Field-relations between normal faults and extensional joints in the Eastern Lakonia Peninsula. **a)** A normal fault **(f)** cuts inferred early Pleistocene alluvia **(1)** and middle Pleistocene shallow-marine sediments **(2)**. The fault plain continues up-section as an extensional joint (without throw) that cuts late Pleistocene ("Eutyrrhenian") sediments **(3)**. Transition from faulting to jointing was accomplished within ca. 100-200 ka.
b) Densely-spaced joints **(j)** cut Pleistocene sediments **(2)**; the joints are parallel to normal faults **(f)** in bedrock **(1)** and commonly associated with 50-150 cm-high morphological scarps. Such sets of joints are interpreted as results of reactivation of faults buried under the Pleistocene sediments. The preservation of scarps in friable sediments (mainly sandstone/grainstone) suggests that the timing of faulting was relatively recent (middle-late Pleistocene?).

4.2.4 Joints: The joint pattern over the Eastern Lakonia Peninsula follows the principal directions of faulting, but strike variation is higher. NNW-SSE, N-S, NE-SW and approximately E-W sets of extentional joints are distinguished (Fig. 4.3). Joints cut all Pleistocene formations of the area, up to the latest Pleistocene (post-"Neotyrrhenian") aeolianite (see Figs 4.12, 4.18 and Chapter 5). The only deposits not affected by unambiguous jointing are Holocene beachrocks and Historical soils. Joint planes are generally sinuous, encrusted by calcite spar or red hardpan caliche, very similar to joints encountered in the Messenia Peninsula (see Chapter 2). Joints in Pleistocene sediments of the Eastern Lakonia Penisnula are very similar to those caused by Recent (Jackson et al., 1982a; Mariolakos et al., 1987, 1991) and Pleistocene (Mariolakos et al., 1997) earthquakes in other areas of the Peloponnese, including the Kalamata Graben (see Fig. 1.1). Locally, these joints exhibit a consistent alignment parallel to major, graben-bounding faults (e.g. Viglaphia; Fig. 4.12).

Progress of deformation from faulting to jointing through progressively younger units was observed locally. In the Bozas Rema mouth, early-middle Pleistocene(?) red alluvia are covered by middle Pleistocene (?) shallow-marine sand, in turn overlain by "Eutyrrhenian" shoreline facies. A NNE-SSW (6°) fault (dip 60° to the WNW) cuts the pre-Tyrrhenian alluvia and marine sediments. Its throw attains a maximum value of ca. 1.6 m near the base of the cliff (early-middle Pleistocene alluvia) but it gradually diminishes up-section, to ca. 1 m in middle Pleistocene shallow-marine sediments. The trace of the fault-plane through the "Eutyrrhenian" sediment is an open extensional joint (width: ca. 2-3 cm). This shows that a fracture activated as a fault in pre-Tyrrhenian time, functioned as a joint in post-"Eutyrrhenian" time (since ca. 120 ka).

Closely-spaced populations of numerous parallel striking, less sinuous joints are commonly concentrated in 2-8m wide zones, associated with <1-2 m high, almost vertical cliffs (e.g. inferred "Eutyrrhenian" sandstone in Limnakia, middle Pleistocene sandstone in Ayia Marina, Ayios Nikolaos, Pakia; Figs. 4.12, 4.18, M.2). These closely-spaced joints probably accommodated a certain amount of slip, distributed along many parallel planes. Their alignment parallel to major faults through bedrock suggests that they probably resulted from reactivation of faults buried beneath Pleistocene sediments. These could probably represent a more advanced stage of fault-reactivation than the example from Bozas Rema, discussed previously (Fig. 4.4).

4.3 SURFACES OF SUBAERIAL EROSION AND MARINE TERRACES

The Eastern Lakonia Peninsula exemplifies a piedmont benchland (*sensu* Ahnert, 1998), comprising morphological surfaces of three main age-classes, from higher to lower altitudes (Figs. 4.5, 4.6, 4.8, 4.9, 4.12, 4.12, 4.14, 4.19):

1) Uplifted surfaces of subaerial erosion (pediplains, pediments), of Late Miocene-Pliocene age.

2) Intramontane plains and poljie, of Late Pliocene-Quaternary age.

3) Pediments and marine terraces of Late Pliocene-Quaternary age.

Widespread normal faulting (see above) resulted in preservation of these morphological surfaces at various elevations in different parts of the peninsula (Figs. 4.3, 4.4, 4.4.5, 4.6). Scarps that connect older, uplifted pediments/peneplains with younger relief segments are largely fault-controlled. From the older (higher) to the younger (lower), six to seven distinct levels are distinguished:

4.3.1 Uplifted surfaces of subaerial erosion (Late Miocene-Pliocene): The number of "old" surfaces of subaerial erosion differs locally within the Eastern Lakonia Peninsula, in relation to relative intensity of uplift, denudation and fluvial erosion after their formation. These surfaces are preferentially preserved on Tripolis Zone limestone or "*Plattenkalk Series*" marble (see Figs. 4.2, 4.5, 4.6, 4.12, 4.19). The highest surface is uplifted to ca. 910 m in the Glikovrisi Horst (NW part of the peninsula; see Figs. 4.5, 4.5); its elevation decreases to ca. 490-520 m south of the Molai Graben (Figs. 4.5, 4.6, 4.7). This surface is commonly preserved as a narrow ridge (minimum width: ca. 100-200 m), parallel to the NNW-SSE morphological strike of the peninsula, and constitutes a remnant divide between pediments developed on both sides (Figs. 4.5, 4.6).

Up to four uplifted pediments occur at successively lower altitudes, separated from each other by ca. 10-50 m height cliffs (Fig. 4.4). Pediment surfaces were affected by advanced karstification, with numerous dolines and small poljie (Figs. 4.4, M.2). The largest dolines, that strike NNW-SSE, are situated in the axial zones of narrow grabens, controlled by NNW-SSE faults. Previous workers dated these surfaces as Miocene-Pliocene (Dufaure, 1976). Similar surfaces in central Peloponnese (Riedl, 1977), northern Greece (Vavliakis, 1981, Psilovikos and Vavliakis, 1981), Thasos Island (Weingartner and Hejl, 1994) and the Cyclades Islands (Riedl et al., 1982) were also dated as Late Miocene-Pliocene.

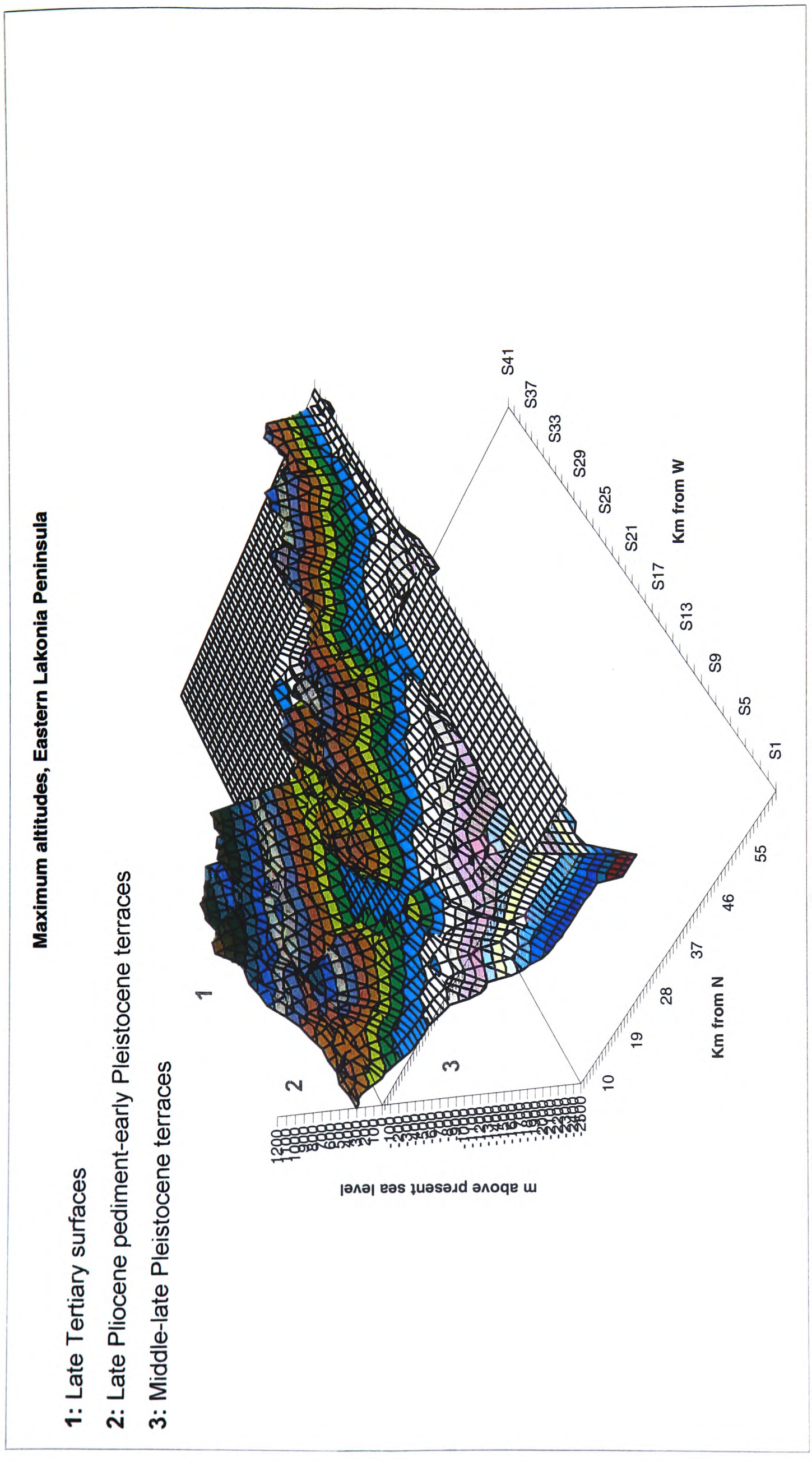

Figure 4.5: Relief model of the Eastern Lakonia Peninsula: 3D model of maximum altitudes (contour interval 100 m; grid dimension: 1×1 km). Note the different generations of relief and the segmentation of the peninsula into fault-bounded blocks.

Steep piedmont scarps (dip: 0.30-0.60%) separate these relatively closely-spaced surfaces above, from the Late Pliocene-early Pleistocene pediment below. In the area of Ano Glikovrisi (Figs. 4.5, 4.6, 4.15), these cliffs coincide with NNW-SSE fault scarps. In areas where fault-control over the piedmont is less evident (e.g. Fig. 4.6.ii), piedmont slopes are characteristically concave, probably controlled by wash denudation processes (Ahnert, 1998). Inselbergs occur in the latter areas, resulting from retreat of piedmont scarps (e.g. Katsikoros inselberg, Figs. 4.6.iii, M.2). These inselbergs correlate with lower members of the pediment flight further inland. Piedmont scarps are less conspicuous and less steeply inclined wherever they are formed on more easily eroded schists or volcaniclastics. In such terrains (e.g. near Dhaemonia; Fig. M.2), the outer margins of the uplifted Late Tertiary pediments merge with the Late Pliocene-early Pleistocene pediment/terrace (see below) via a series of conical hills (inselbergs), intercepted by wide, dry valleys. Based on their position on the margins of the Late Pliocene-early Pleistocene surface, the latter inselbergs are correlated with a similar inselberg on the Handrinos area in the Messenia Peninsula, further west (see Chapter 2, Fig. 2.4). The Handrinos surface, as the Late Pliocene-early Pleistocene pediments in the Eastern Lakonia Peninsula, is a pediment covered by early Pleistocene shallow-marine sediments. Similar inselberg relief in northern Greece and the Cyclades Islands was attributed to humid climate during Pliocene (Vavliakis, 1981; Psilovikos and Vavliakis, 1982/83; Riedl et al., 1982).

In more inland parts of the Eastern Lakonia Peninsula, uplifted Tertiary pediments are incised by polygenetic valleys. Valley incision started from the level of the Late Pliocene-early Pleistocene pediment (Figs. 4,5, 4,6.iii, 4.8, 4.9, M.2). Steep valley slopes are interrupted by segments of more gentle relief, which correlate with pediments on the seaward side of the piedmont benchland. These comparatively gentle surfaces are interpreted as valley side pediments (*sensu* Ahnert, 1998), formed contemporaneously with correlative pediments on the seaward side (e.g. Fig. 4.6. ii, iii, v).

4.3.2 Kampos Intramontane Plain (Late Pliocene-early Pleistocene ?): The Kampos depression is an intramontane polje, drained by internal, centripetal drainage. This drainage network was captured by the east-flowing Komata Rema (Fig. M.2). The long axis of the poljie strikes E-W, roughly parallel to ENE-WSW faults in bedrock (Tripolis Zone limestone) that control the northern flanks of the Kampos basin (Figs. 4.2, M.2). The Kampos plain surface, at altitude of ca. 140 m, is developed mainly on late Pleistocene-Holocene alluvia and soils. Its periphery merges with a concave surface, developed on carbonate bedrock (southern flanks of the basin) and at least two generations of

fanglomerates, tentatively correlated with the middle and late Pleistocene, respectively (northern flanks of the basin) (Figs. 4.6.iv, 4.10). Higher up, along the northern flanks of the Kampos basin, two uplifted surfaces, at 280-300 m and 320-340 m, respectively, probably correlate with some of the Tertiary pediments (see above). The altitude of the Kampos basin correlates the Late Pliocene-early Pleistocene pediment-terrace and its oldest exposed fill correlate with fanglomerates on the latter surface (Unit 4; see Chapter 5). On this basis, a Late Pliocene-early Pleistocene origin of the Kampos basin is proposed. Further incision of the basin and alluvial aggradation up to the present-day level took place in Pleistocene-Holocene times.

2.3) Pediment-terrace (Late Pliocene-early Pleistocene): This is the most extensive surface group of Pleistocene age in the Eastern Lakonia Peninsula, stretching for ca. 22 km along the western coast of the peninsula, south of the Molai Graben (Figs. 4.3, 4.12, 4.13, 4.14, 4.19, M.2). This surface is commonly narrow, generally <0.7-1 km wide. South of the Molai Graben, from Plitra to Viglaphia (Figs. 4.6, 4.8, M.2), this surface is found at altitudes of ca. 80-120 m (Fig. 4.6). North of the Molai Graben, in the Ano Glikovrisi Mountains (Figs. 4.6, 4.8), the same surface is cut by NNW-SSE faults and uplifted differentially up to ca. 280 m. In areas of its optimum development, south of the Molai Graben, this surface slopes down to the level of late Pleistocene terraces via a zone of steeper relief. The steep topographical dip of the latter is interrupted by a series of 3-4 narrow marine terraces (<70 m wide), separated by low cliffs (10-25 m high) (Fig. 4.6). This surface is not identified along the east coast of the Eastern Lakonia Peninsula, where the higher, Late Tertiary, pediments meet the late Pleistocene-Holocene coastal zone via steep, precipitous cliffs (Figs. 4.5, 4.6, 4.9, 4.13, M.2).

Figure 4.6 (following pages): Representative cross-sections of the Eastern Lakonia Peninsula, with the emphasis on the Quaternary geology. The Tethyan structure is indicated schematically (**Lim:** limestone, **Dol:** dolomite, **Mrb:** marble, **Phl:** phylite). Five main generations of alluvia are distinguished: **al 1:** Late Pliocene, **al 2:** early Pleistocene, **al 3:** middle Pleistocene, **al 4:** late Pleistocene, **al 5:** latest Pleistocene-Holocene. Pleistocene terraces were formed on shallow-marine sediments, at progressively lower altitude with decreasing age, and covered by prograding alluvial fans. Normal faults cut the terraces and segment the peninsula into narrow horsts and grabens (see text for details).

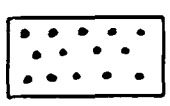 Alluvia 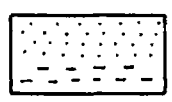 Pleistocene shallow-marine sediments

The positions of the sections are shown in Fig. M2 (back-pocket).

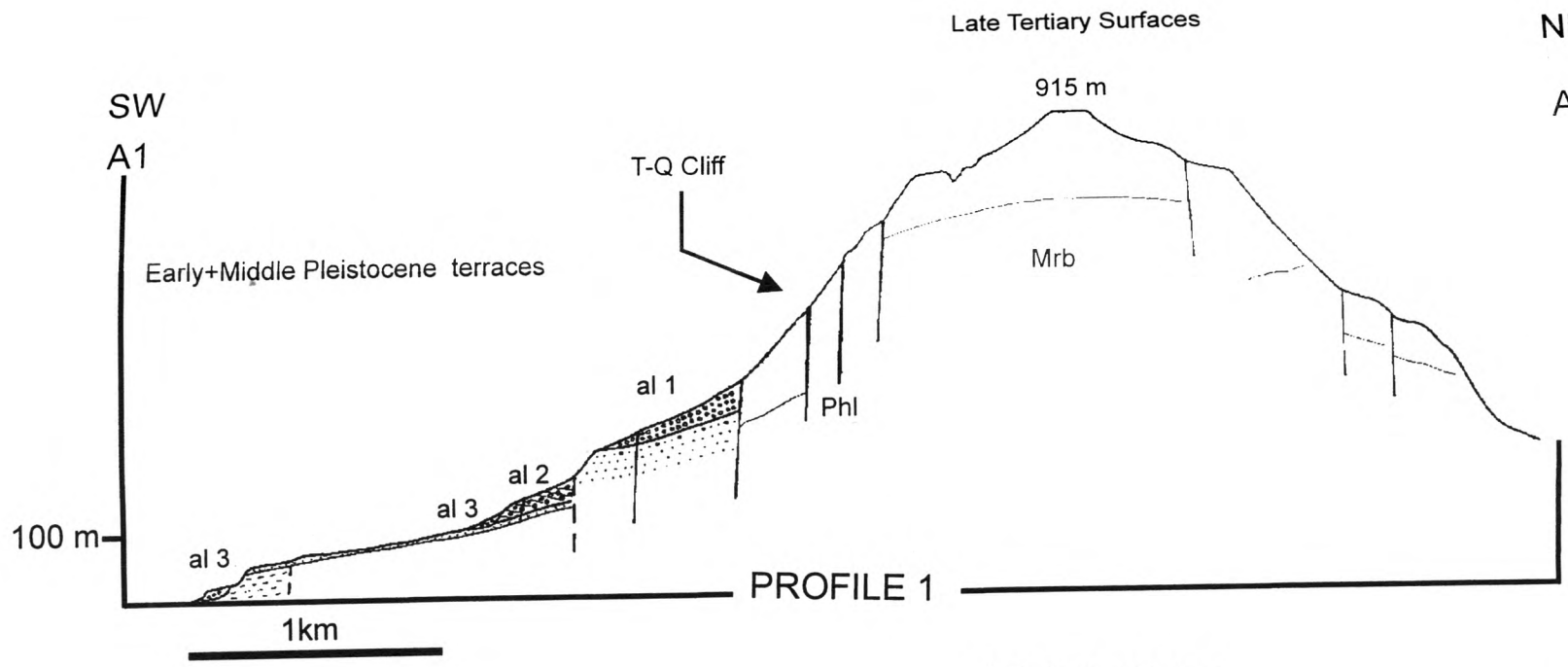
Late Tertiary Surfaces
NE
A
915 m
SW
A1
T-Q Cliff
Early+Middle Pleistocene terraces
Mrb
al 1
Phl
al 2
al 3
100 m
al 3
PROFILE 1
1km

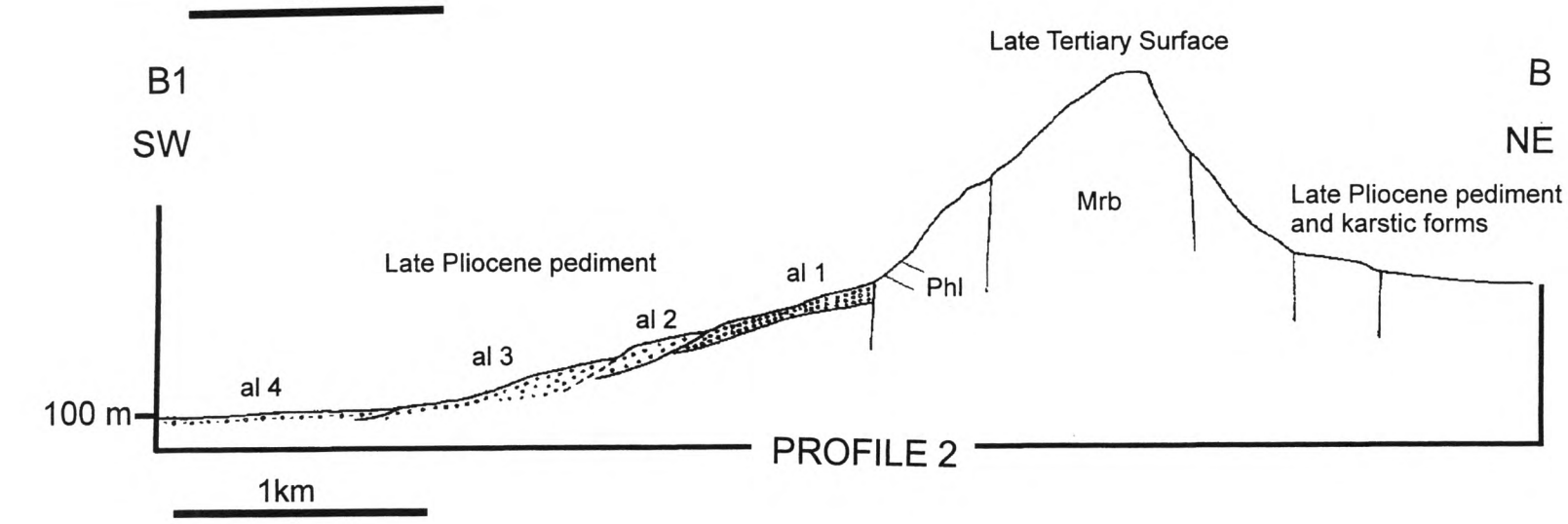
Late Tertiary Surface
B1
B
SW
NE
Mrb
Late Pliocene pediment
and karstic forms
Late Pliocene pediment
al 1
Phl
al 2
al 3
al 4
100 m
PROFILE 2
1km

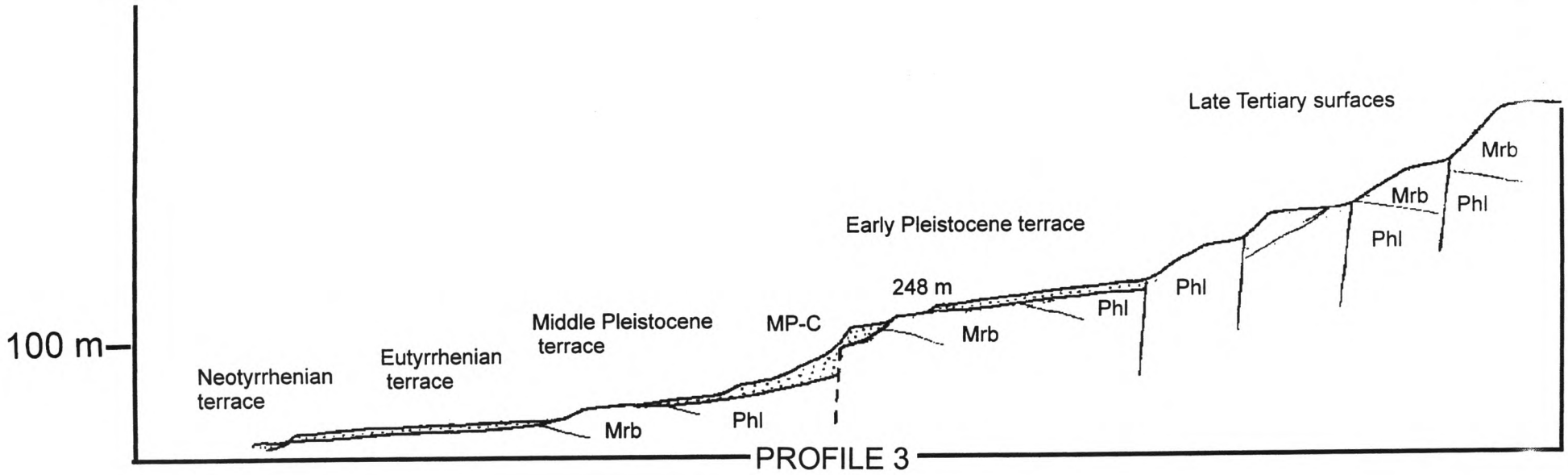
C1
WSW
C
ENE
Late Tertiary surfaces
Mrb
Mrb
Phl
Early Pleistocene terrace
Phl
248 m
Phl
Phl
Mrb
Middle Pleistocene
terrace
MP-C
Eutyrrhenian
terrace
Neotyrrhenian
terrace
Mrb
Phl
100 m
PROFILE 3

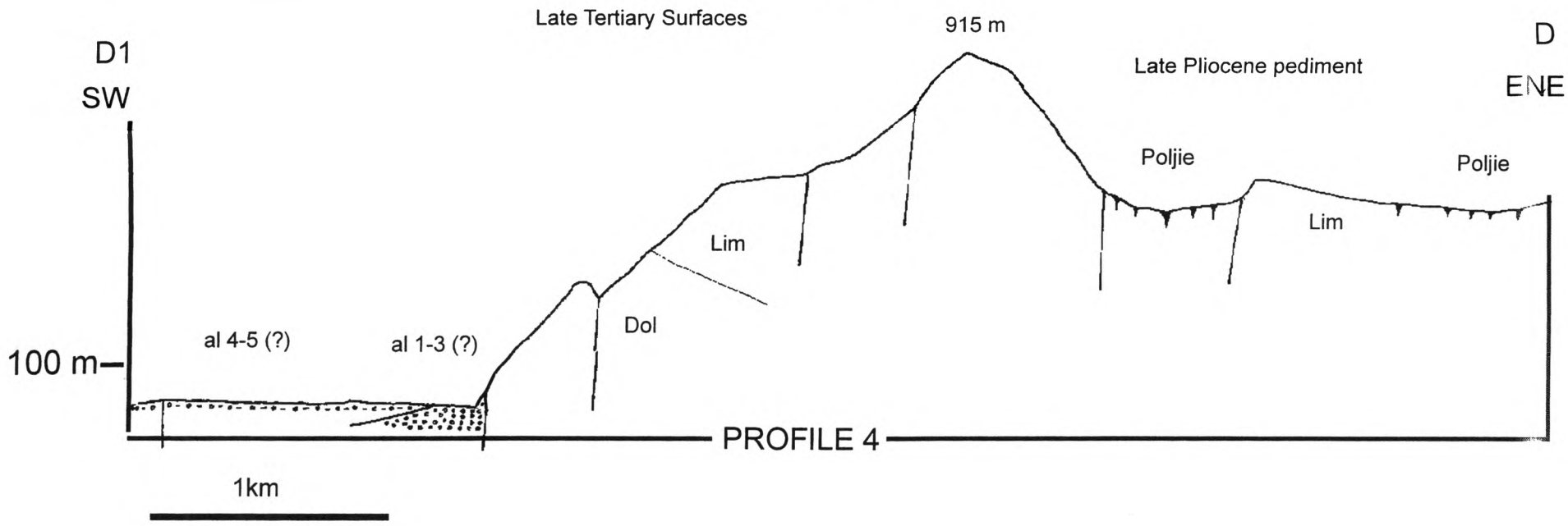
Late Tertiary Surfaces
915 m
D1
D
SW
ENE
Late Pliocene pediment
Poljie
Poljie
Lim
Lim
Dol
al 4-5 (?)
al 1-3 (?)
100 m
PROFILE 4
1km

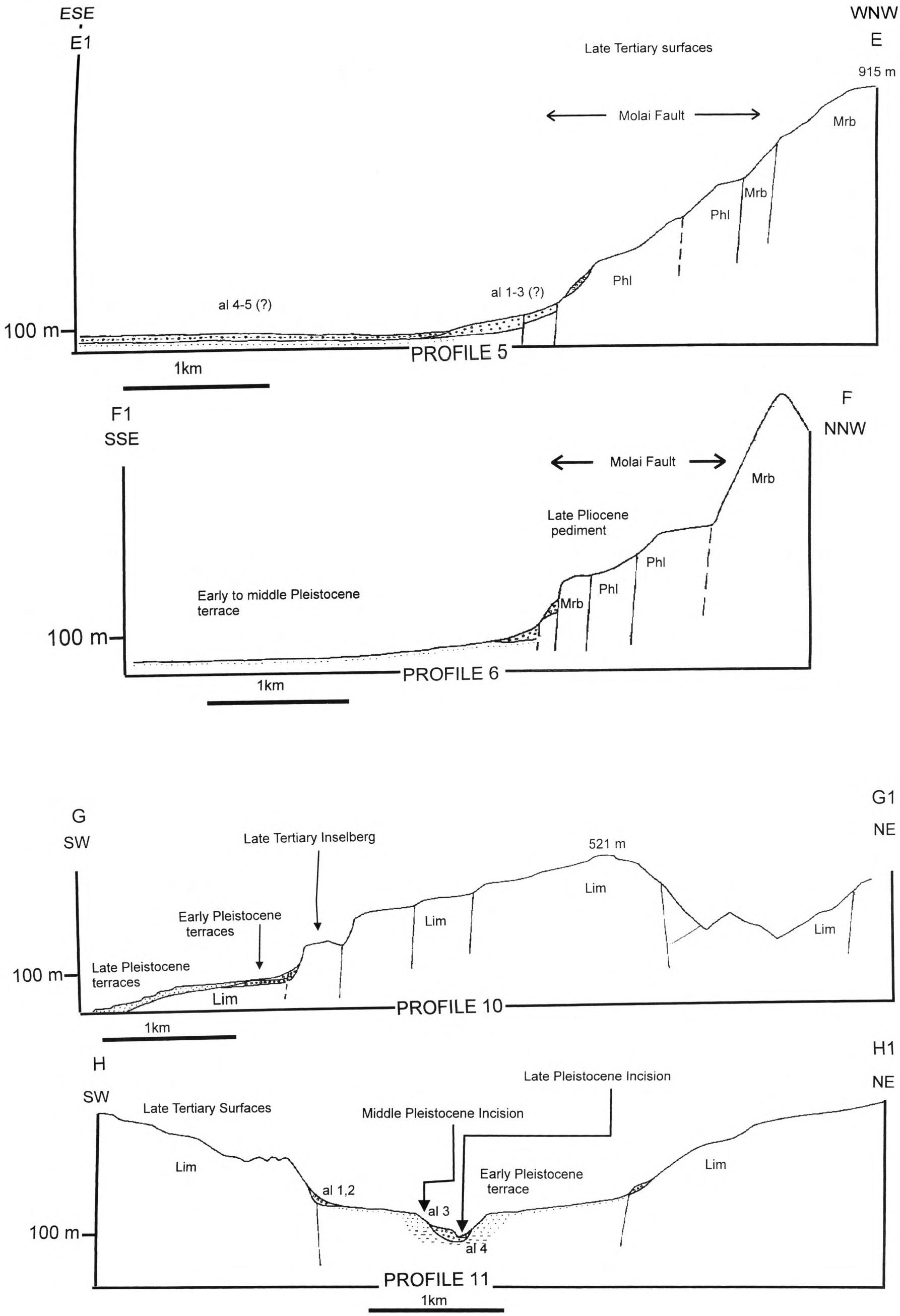
ESE
E1
WNW
E
Late Tertiary surfaces
915 m
Molai Fault
Mrb
Mrb
Phl
Phl
al 1-3 (?)
al 4-5 (?)
100 m
PROFILE 5
1km
F1
SSE
F
NNW
Molai Fault
Mrb
Late Pliocene
pediment
Phl
Phl
Mrb
Early to middle Pleistocene
terrace
100 m
PROFILE 6
1km
G
SW
G1
NE
Late Tertiary Inselberg
521 m
Lim
Lim
Lim
Early Pleistocene
terraces
Late Pleistocene
terraces
100 m
Lim
PROFILE 10
1km
H
SW
H1
NE
Late Pleistocene Incision
Late Tertiary Surfaces
Middle Pleistocene Incision
Lim
Lim
Early Pleistocene
terrace
al 1,2
al 3
al 4
100 m
PROFILE 11
1km

The Late Pliocene-early Pleistocene surface was formed on various bedrock lithologies and covered by various types of shallow-marine and subaerial sediments. On the Tzavari Hill, on the western flanks of Molai Graben (Fig. 4.5), this surface developed on bedrock and pisolithic flowstone of pre-Pleistocene age (Unit 2; see Chapter 5), and was partly covered by shoreline facies of inferred early Pleistocene age (Subunit 3.2; Chapter 5). This suggests that, locally, this surface existed before the Pleistocene, as a subaerial pediment, and was subsequently reworked during the early Pleistocene marine transgression. Dufaure (1976) interpreted similar surfaces all over the Peloponnese as polycyclic landforms, originally formed as Pontian (Late Miocene) pediments, faulted during the Late Pliocene-early Pleistocene ("*Plio-Villafranchian*") and reworked during the latest Pliocene-Pleistocene.

In most areas of the Eastern Lakonia Peninsula, however, the early Pleistocene terrace was formed on topsets of the early Pleistocene regressive sequence (Subunit 3.2; Chapter 5), that comprise shoreline to subaerial deposits (e.g. Ano Glikovrisi; Dokali Rema, Figs. 4.4, 4.5, 4.6, M.2). The inland fringes of this early Pleistocene surface are covered by early to middle Pleistocene red alluvia, traced to fan delta facies more distally (e.g. Dokali Rema, Fig. 4.10). These alluvia are incised by channels hosting even younger, late Pleistocene alluvia (Unit 12 in Chapter 5; Fig. 4.10). This shows that this surface functioned as a pediment since its emergence in early-middle Pleistocene times. Active talus cones are still prograding over the same surface at the southern tip of the peninsula (Ayia Marina; Figs. 4.6, M.2). In the area of Dokali Rema, the outer segment of the early Pleistocene surface was formed exclusively on sediments of the early Pleistocene regressive sequence, as an early-middle Pleistocene valley side pediment (*sensu* Ahnert, 1998), sloping gently from the fault-controlled mountain fronts (on bedrock) on both sides of the valley (Fig. 4.10). This surface was affected by subsequent, middle-late Pleistocene fluvial incision, that resulted in broad, U-shaped valleys in the area of Daemonia (e.g. Dokali Rema; Figs. 4.10, M.2), or V-shaped valleys in many other areas of the Eastern Lakonia Peninsula (e.g. Mourtitsa Rema; see Fig. 4.5). Wherever these valleys can be correlated with a neighbouring terrace flight (e.g. Viglaphia, SW coast of the peninsula; Fig. M.2), the V-shaped valleys are younger, resulting from headward erosion from the level of late Pleistocene terraces. V-shaped valleys locally rejuvenated older, U-shaped dry valleys, associated with higher base levels. This Late Pliocene-early Pleistocene pediment/terrace is cut by numerous joints and some N-S and NNW-SSE faults of considerable throw (up to 80-100 m in the Ano Glikovrisi area; see Fig. 4.8). In the coastal plains of the Molai and Neapolis Basins, the same surface developed on early Pleistocene shallow-marine sediments (Figs. 4.6, 4.9). Its altitude in these areas is ≤60-

80 m. Such altitudinal differences indicate that differential uplift of the flanks of the grabens has taken place since the early-middle Pleistocene.

As stated above, the Late Pliocene-early Pleistocene surface functioned as the base level of erosion for all the higher, Late Tertiary surfaces. In inland areas of the Eastern Lakonia Peninsula, large valley systems were incised down to the landward continuation of the Late Pliocene-early Pleistocene surface (Figs. 4.6, 4.8, 4.9, M.2). This incision probably took place in pre-Quaternary times, prior to the Late Pliocene(?)-early Pleistocene transgression of the pediment. In some areas (e.g. Dokali Rema, Ayia Marina; Figs. 4.2, 4.6, M.2), the distribution of early Pleistocene shallow-marine sediments maps out a rias palaeotopography, that resulted from early Pleistocene marine flooding of the outer reaches of these pre-existing, Pliocene (?) valley systems.

4.3.4 Middle Terraces (Middle Pleistocene): In general, marine terraces of middle Pleistocene age are eroded in sediments correlated with the early Pleistocene regressive sequence (Subunits 3.1, 3.2 and Unit 5; see Chapter 5), or in bedrock (Figs. 4.6, 4.7, 4.12, 4.13, 4.14, 4.19). These terraces commonly occur within a narrow zone, between altitudes of 80-30 m. Absence of sediment cover distinct from the early Pleistocene clinoforms makes regional correlation difficult.

An "accumulation" terrace, distinct from the early Pleistocene terrace higher up, is preserved at ca. 120-160 m in the area between Glikovrisi-Elea (Fig. 4.8). This terrace was formed on shallow-marine (lower shoreface) clastic sediments of inferred early middle Pleistocene Age (Unit 5; see Chapter 5). The latter sediments comprise offlapping clinoforms, indicating shoreline progradation prior to emergence and terrace formation.

4.3.5 "Eutyrrhenian" Terrace (ca. 120 ka): The regionally widespread terrace at altitude of ca. 17-25 m was correlated with the "Eutyrrhenian" sea level cycle (isotopic stage 5e; ca. 120 ka, *sensu* Imbrie et al., 1984; Martinson et al., 1984) by many previous workers (Theodoropoulos, 1978; Kelletat et al., 1976; Kowalczyk et al., 1992). Locally, this terrace was eroded on limestone bedrock (e.g. between Elea and Bozas Rema; Figs. 4.6, 4.7, 4.8), Late Tertiary (?) breccia (e.g. Cape Xili; Fig. M.2), or cemented shoreline carbonates of earlier Pleistocene age (e.g. Viglaphia; Fig. M.2). However, in many areas, this terrace is formed on silisiclastic or carbonate shoreline deposits, that commonly contain the

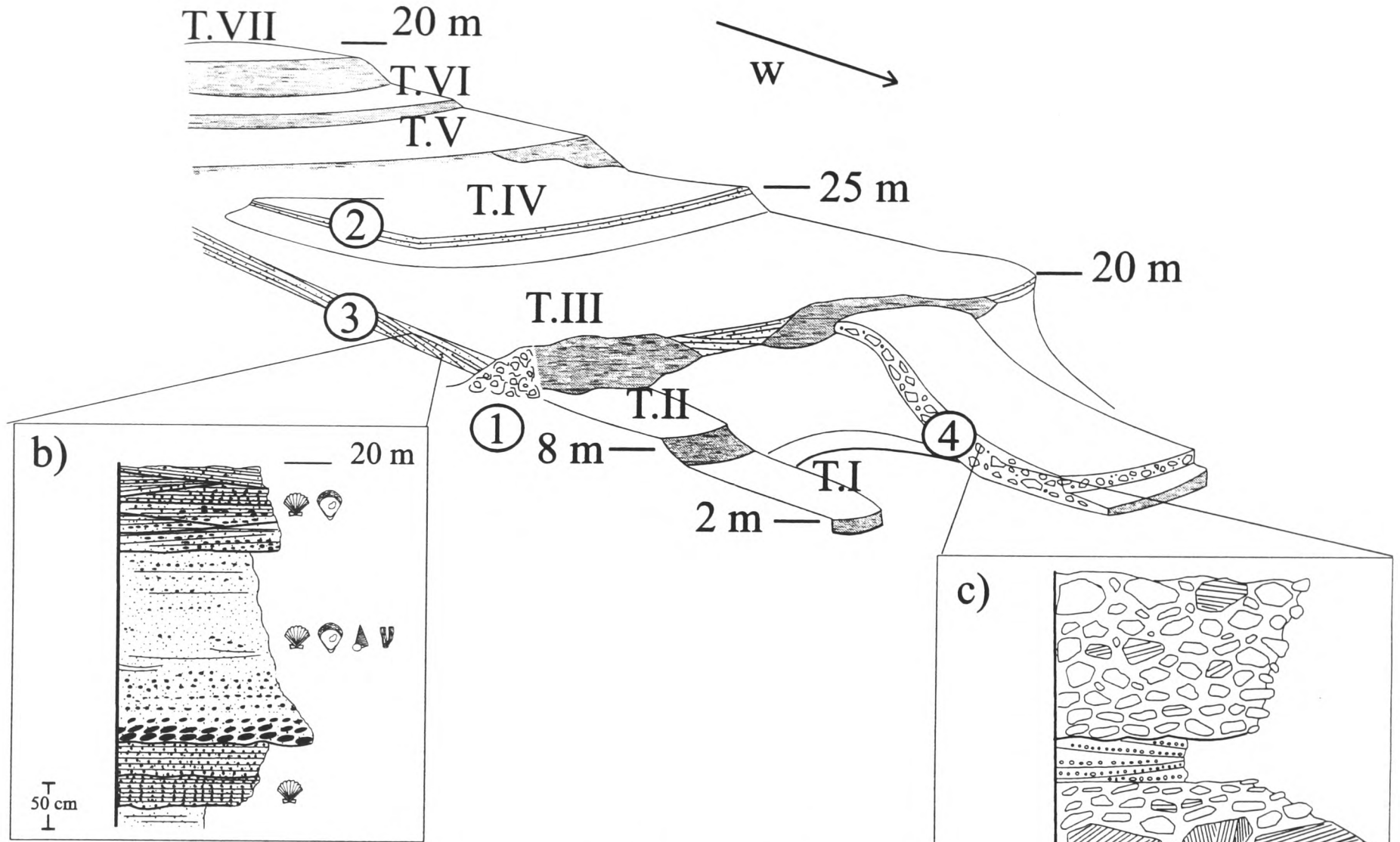

Figure 4.7: Field sketch of terrace flight in the southern part of the Bozas Rema coast (see Fig. M.2 for location). Seven terraces are distinguished; only two covered with marine sediment. The inferred ages of the terraces are: **I:** Holocene, **II:** "Neotyrrhenian", **III:** "Eutyrrheniam", **IV-VI:** Middle to early Pleistocene(?). The "Eutyrrhenian" terrace is the best preserved, formed on coral bufflestone and conglomerate with the characteristic gastropod, *Strombus bubonius*. Note the small, proximal alluvial cone with reworked boulders of the "Eutyrrhenian" terrace, deposited during a latest Pleistocene lowstand.

age-specific gastropod, *Strombus bubonius* (e.g. Bozas Rema coast; Kelletat et al., 1976; Kowalczyk et al., 1992; Subunit 8.2 in Chapter 5). Locally, these "Eutyrrhenian" deposits unconformably cover channel fill alluvia of a middle Pleistocene lowstand stage (see below), indicating that the "Eutyrrhenian" sea level rise was preceded by valley incision and alluviation. After its emergence, the "Eutyrrhenian" terrace was affected by fluvial incision that resulted in formation of V-shaped valleys. This terrace is cut by faults and joints of strikes correlated with all principal fault-sets (see above, Figs. 4.3, 4.7).

4.3.6 "Neotyrrhenian" Terrace (ca. 80-100 ka): The discontinuous, but widespread, terrace at elevations of ca. 1-4 m was attributed to the "Neotyrhrenian" sea level cycle by previous workers (Kelletat et al., 1976; Kowalczyk et al., 1992). This terrace is preserved either as a marine abrasion platform on bedrock and older Pleistocene marine deposits (e.g. around Monemvasia; Fig. M.2), or as an "accumulation" terrace on coarse shoreline facies (conglomerates, coarse-grained sandstones; Unit 11 in Chapter 5), with *Strombus bubonius* (e.g. Marathia; Kelletat et al., 1976; Kowalczyk et al., 1992; see Figs. 4.20, M.2). Aeolianite deposits (Unit 13 in Chapter 5), locally with still-preserved dune morphology (Fig. 4.20) constitute the upper parts of the sedimentary cover of the "Neotyrrhenian' terrace. Locally, the "Neotyrrhenian" terrace is covered by red alluvia of latest Pleistocene age. Same as the "Eutyrrhenian", this terrace is also cut by faults and joints of strikes correlated with all principal fault-sets (see Fig. 4.3).

4.3.7 Holocene Terrace ("Versilian" or Historic, <7 ka): The lowest terrace level, at ca. <1.5 m was interpreted as Holocene by Keraudren (1970, 1971) and Kowalczyk et al. (1992). In most coastal areas of the Eastern Lakonia Peninsula, this terrace is preserved as a marine abrasion platform, eroded either into bedrock (numerous sites), or Pleistocene sediments (e.g. Prophitis Ilias; Fig. 4.9). In some sites, this terrace is associated with pebbly beach deposits (e.g. Elea; Kowalczyk et al., 1992; Figs. 4.8) and Vermetid bioconstructions (e.g. Marathia; Fig. M.2). Keraudren (1970, 1971) correlated similar deposits from coastal sites in Greece and Turkey with the "Versilian" stage in the Holocene (ca. 6 ka). On the other hand, it is possible that these deposits are even younger, correlative with foreshore landforms and sediments uplifted all along the Aegean Arc during the "*Early Byzantine tectonic paroxysm*" (*sensu* Pirazzoli, 1986).

4.4 FAULT-BOUNDED MORPHOLOGIC UNITS

The morphologic grain of the Eastern Lakonia Peninsula strikes NNW-SSE, parallel to the dominant tectonic grain (Figs. 4.2, 4.3, M.2). As a whole, the Eastern Lakonia Peninsula can be viewed as an uplifted horst, between the Laconic Gulf to the west and the Argolic Gulf to the east (Figs. 1.1, 4.2). As inferred from the distribution of Pleistocene marine sediments, maximum elevation and Tertiary-Quaternary morphological surfaces, the western and the northern parts of the peninsula are more uplifted than the eastern and the southern ones (Fig. 4.5). Hence Kelletat et al. (1976) suggested that, on a 10's of km-scale, the peninsula can be interpreted as a block tilted to the south and also rotated to the east, around a NNW-SSE trending axis (see Fig. 1.5.c). This differential uplift was accommodated by a dense network of normal faults, broadly parallel and transverse to the NNW-SSE morphological grain of the peninsula (see above; Figs. 4.2, 4.3, 4.8, 4.9, M.2).

On a smaller scale (ca. 10x20 km), the Eastern Lakonia Peninsula is segmented into a series of horsts and grabens, with long axes orthogonal, or parallel to the elongation of the peninsula (Fig. M.2). Grabens of the latter category are bounded on all sides by two sets of faults, of N-S to NNE-SSW and NW-SE strikes, oblique to each other (e.g. Molai Graben; Figs. 4.5, 4.8). Pleistocene sediments, depositional architecture and relief differ considerably along these tectonic boundaries, manifesting the semi-independent evolution of fault-bounded blocks during the last 1.6 Ma. Each of these fault-bounded morphologic units is described in detail, as follows:

4.4.1 Ano Glikovrisi Horst:

4.4.1.1 Bounding Faults: The Ano Glikovrisi block is a relatively narrow horst (maximum width across strike ≈ maximum length along strike: ca. 8 km), controlled by NNW-SSE faults (Figs. 4.5, 4.8, 4.15, M.2). Its northern boundary, ca. 500 m NW of Ano Glikovrisi, is a NNE-SSW striking, WNW dipping fault, oblique to the graben-controlling faults (Figs. 4.2, 4.8). To the south, Ano Glikovrisi Horst is bounded by the NNE-SSW to N-S Molai Fault, that dips to the ESE/E. The WSW boundary of the horst coincides with NNW-SSE faults that downthrow Pleistocene terraces to the WSW and control the present coastline (Figs. 4.6, 4.8). The NE boundary coincides with NNW-SSE, NE-dipping faults, that cut and uplift Pleistocene alluvia. A dense set of large (up to 5.5 km long), NNW-SSE faults, spaced every 250-750 m, segment the Ano Glikovrisi Horst internally (Figs. 4.6, 4.8). Late Tertiary (Late Miocene ?) surfaces are uplifted to a maximum altitude of 915 m across the latter faults (Figs. 4.5, 4.6, 4.8). Other fault groups include shorter ENE-WSW "transfers" to the latter fault-set (maximum mapped length: 2 Km) and, at a lower frequency, an orthogonal

set of NNE-SSW faults (parallel to the Molai Fault) and ESE-WNW transfers (e.g. Molai-Pakia area; Figs. 4.2, 4.8). Faults of the latter orthogonal set truncate NNW-SSE ones (I.G.M.E., 1980; see Fig. 4.8); a younger origin of this orthogonal system is, thus, indicated.

The maximum number of morphological surfaces within the Eastern Lakonia Peninsula (10-12 surfaces) occurs within the Ano Glikovrisi Horst (Figs. 4.6, 4.8). Of these, the four or five higher ones are pre-Quaternary surfaces of subaerial erosion, formed on bedrock, whereas five or six surfaces at lower elevations are marine terraces of Quaternary (Pleistocene-Holocene) age.

4.4.1.2 Segmentation along-strike: Segmentation of the Ano Glikovrisi Horst along-strike is revealed by three parallel profiles (Figs. 4.6), from north to south. Along **pr (2)**, across the N part of the horst, the Late Pliocene-early Pleistocene pediment/terrace is uplifted to ca. 180 m. Faulting of the Quaternary terrace flight is not intense and minimum throw of individual faults does not exceed ca. 20-30 m. Along **pr (1)**, across the middle part of the horst, the Late Pliocene-early Pleistocene pediment/terrace is faulted and uplifted to ca. 240 m (marine sediments)-340 m (early-middle (?) Pleistocene alluvial fans). Faulting of the Quaternary terrace flight is intense, with throws of individual faults in the order of 40-50 m. The accumulated throws of the three main mapped faults that affect the Quaternary terrace flight is ca. 100-120 m. The morphologic dip of Quaternary surfaces in this area is high, probably as a result of intense faulting. Along **pr (3)**, across the southern part of the Ano Glikovrisi Horst, the Late Pliocene-early Pleistocene pediment/terrace is uplifted to ca. 260 m. Faulting of the Quaternary terrace flight is not intense; also the topography of the zone of Quaternary relief is smooth, in comparison with the middle parts of the horst (see Fig. 4.4 pr 1). These three profiles show that the intensity of Quaternary faulting differs along-strike of the NNW-SSE faults that control the Ano Glikovrisi Horst. Density of faulting, throws of individual faults and accumulated throws over the entire NNW-SSE fault system since the early Pleistocene, are maximum in the middle sector of the Ano Glikovrisi Horst.

4.4.1.3.1 Western Side of the horst: West of the Ano Glikovrisi Mountains (Figs. 4.6, 4.8), the Late Tertiary erosional surfaces are separated from the Quaternary terrace flight by steep cliffs, controlled by NNW-SSE faults. The minimum throw accumulated on these faults varies from ca. 450 m to ca. 150 m in the northern and southern part of the horst, respectively. In the north, these fault-controlled cliffs are of uniform morphological dip all along their surfaces, but in the south, they are interrupted by a series of four to five uplifted pediments (Fig. 4.6). Valley incision across the latter cliffs propagated from the base level

of the Late Pliocene-early Pleistocene pediment/terrace and resulted in formation of triangular facets. The longitudinal profiles of the latter valleys are very steep, with many knick-points, probably formed in response to the activity of NNW-SSE faults, that control the mountain front (see below; Fig. 4.11). Coalescent alluvial fans (Units 4 and 9; see Chapter 5) were deposited in front of incised valleys in the more inland parts of the Late Pliocene-early Pleistocene pediment/terrace (Fig. M.2).

4.4.1.3.2 Eastern side of the horst: By contrast with the western side, on the eastern side of the Ano Glikovrisi Horst, Late Tertiary surfaces are separated from the Molai Graben by highly precipitous slopes. The most inland parts of the latter correlate with the Late Pliocene-early Pleistocene pediment/terrace (Figs. 4.6, 4.8). Rapid uplift along NNW-SSE faults that bound the Molai Graben is suggested by steep morphological gradients, high minimum accumulated throws (ca. 450-650 m) and the narrow width of uplifted pediments, by contrast with the western side. Late Tertiary surfaces on the uplifted Ano Glikovrisi Horst are tilted to the west; the degree of tilting decreases with altitude (thence age) from 6-8° (highest surface) to 5-6° (lowest surface). This tilting probably resulted from activity of the Molai Fault (Figs, 4.2, 4.8) during the Late Tertiary-Quaternary.

4.4.2 Molai Graben:

4.4.2.1 Bounding Faults: The Molai Graben is a narrow structure, with ca. 7-8 km maximum width and ca. 16 km maximum length along its subaerial part (Figs. 4.1, 4.5, M.2). This graben is bounded to the west by the N-S to NNE-SSW Molai Fault (mapped length: ca. 22 km; I.G.M.E., 1984). Asymmetrical tilting of the basin fill to the W/NNW, against the Molai Fault, is suggested by borehole data (Doutsos, pers. com. 1998). The NE boundary of the graben is formed by a series of NW-SE faults, with maximum length ca. 16 km (counted along the most basinward fault; Figs. 4.5, M.2). Its SE boundary is less sharp, comprising a few, smaller faults (maximum length: ca. 4 km; see Figs. 4.5, M.2) in Pleistocene basin-fill. To the SW, the Molai Graben is open to the sea.

Figure 4.8 (following page): Geomorphological sketch-map of the Ano Glikovrisi Horst and the Molai Graben (NW part of the Eastern Lakonia Peninsula). Three main relief segments are distinguished, namely 1) Late Tertiary surfaces of subaerial erosion (on bedrock), 2) Late Pliocene pediment and early Pleistocene terrace(s) (on Pleistocene shallow-marine sediments and bedrock), 3) middle-late Pleistocene terraces (on Pleistocene shallow-marine sediments). Note that the Ano Glikovrisi mountain front is controlled by NNW-SSE trending faults, whereas the Molai Graben is controlled by older NNW-SSE and younger N-S to NNE-SSW trending faults (Molai Fault). Valleys that transverse the terraced morphology were filled with middle Pleistocene alluvia and later rejuvenated in late Pleistocene-Holocene time.

22° 45'

22° 29'

36° 48'

Late Tertiary surfaces (on bedrock)

Quaternary terraces (on sediment)

Quaternary terraces (on bedrock)

Mountain front

Steep cliffs

Incised valleys

Normal faults

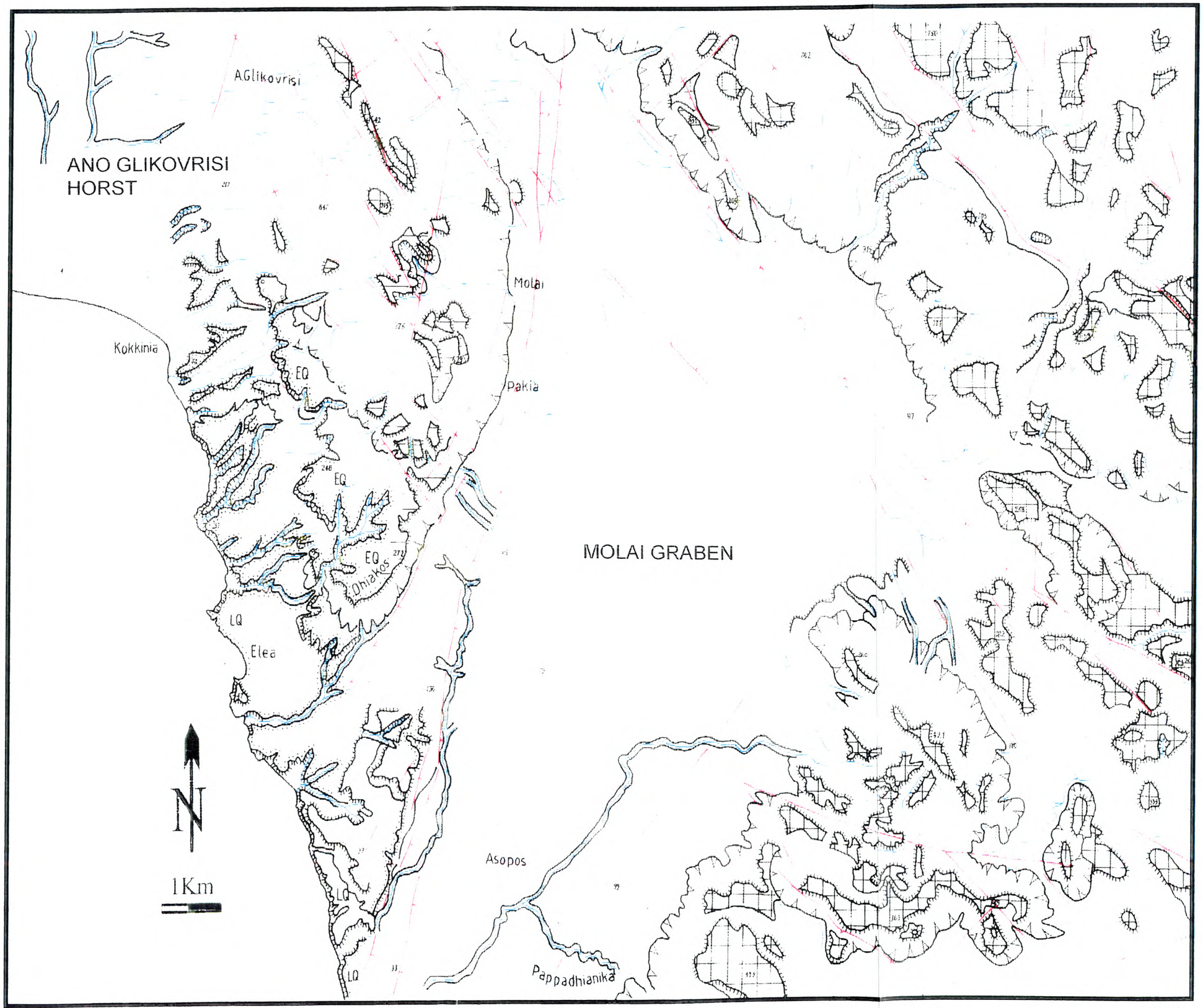

22° 45'

22° 29'

36° 45'

4.4.2.2 Morphological surfaces and segmentation along-strike of the Molai Fault: The steep slope that bounds the Molai Graben to W/WNW is controlled by the N-S (northern part) to NNE-SSW (southern part) branches of the Molai Fault (Figs. 4.2, 4.6: **pr 5, 6**, 4.8, M.2). The different numbers and altitudes of uplifted surfaces along the Molai Fault suggest along-strike segmentation (Fig. 4.6: **prs 5 and 6**).

4.4.2.2.1 Northern part of the Molai Graben: Along **pr 5** (Fig. 4.6), five uplifted surfaces are distinguished on the footwall of the Molai Fault. The highest, at 910 m, is correlated with the Late Miocene-Early Pliocene peneplain, whereas the lowest and widest one, at ca. 300-360 m, is correlated with the Late Pliocene-early Pleistocene pediment. On the footwall of the Molai Fault, a surface correlated with the early Pleistocene terrace is preserved at an altitude of ca. 80-120 m. The terraced slope that connects the flanks with the axis of the basin is ca. 2.5 km across (Fig. 4.6: pr 5). This relief is interpreted as a multiphase pediment, developed in several stages during the Late Tertiary-Quaternary. The minimum accumulated throw of the Molai Fault since the Late Miocene (estimated as the altimetric difference between the present-day surface on the hangingwall and the uplifted Late Miocene peneplain on the footwall) is ca. 800 m. Assuming that the age of this surface is between 10.2-5.2 Ma, the minimum rate of uplift along the Molai Fault since the Late Miocene ranges between 0.078-0.154 m/ka. The minimum accumulated throw since the early Pleistocene, estimated as the altimetric difference between the present day surface on the hangingwall (Molai Graben) and the inferred Late Pliocene-early Pleistocene surface on the footwall, is ca. 220 m. Assuming that the age of the latter surface is between 2-0.9 Ma, the minimum rate of uplift along the Molai Fault since the latest Pliocene-early Pleistocene ranges between 0.11-0.244 m/ka.

4.4.2.2.2 Southern part of the Molai Graben: Three uplifted surfaces are distinguished on the footwall of the Molai Fault along **pr 6** (Fig. 4.6). The highest one, at ca. 780-800 m, is a narrow ridge, interpreted as an erosional remnant of the Late Miocene-Early Pliocene peneplain. The lowest, and best-developed one, at ca. 300-380 m, is nearly planar on Triassic limestone but concave on "*Phyllite Series*" substratum. This surface is correlated with the Late Pliocene-early Pleistocene pediment/terrace. On the hangingwall of the Molai Graben, the altitude of the present-day graben surface is ca. 80-90 m. The width of the benchland slope along Fig. 4.6 (**pr 6**) is ca. 2 km across. The minimum accumulated throw on the southern sector of the Molai Fault is, thus, ca. 700 m since the Late Miocene and ca. 220 m since the early Pleistocene. Therefore, although there is no perceptible difference in throw along the Molai Fault since the early Pleistocene (last 2-0.9 Ma), along-strike

differences of ca. 100 m since the Late Miocene-Early Pliocene (last 10.2-5.2 Ma) are detected. These values provide a constraint for the timing and rate of along-strike segmentation of the Molai Fault.

4.4.2.2.3 NE part of the graben: The NE boundary of the Molai Graben (Fig. 4.6: **pr 4**) is controlled by NW-SE faults, spaced every 0.5-1 km (I.G.M.E., 1984). Three uplifted surfaces are distinguished across this fault system. The highest one, on the footwall of the latter faults, is uplifted to ca. 750-800 m. This surface is correlated with the Late Miocene-Early Pliocene peneplain. The second higher surface is narrow on the footwall of the graben bounding faults, but can be traced to an extensive pediplain at altitude of ca. 500 m, further NE (Fig. 4.6). The latter surface is correlated with the Late Pliocene pediplain. Karstification of this surface is extensive and dolines are controlled by NW-SE faults. These karstic forms were probably formed in latest Pliocene or early Quaternary times, after original formation of the surface, which could be of even older age ("Pontian" according to Dufaure, 1977). On the hangingwall of the graben-bounding faults, the present-day surface of the Molai Graben reaches an altitude of ca. 100 m. The minimum accumulated throw along the NW-SE faults is, thus, ca. 650-700 m since the Late Miocene-Early Pliocene and ca. 400 m since the Late Pliocene. Assuming an age between 10.2-5.2 Ma for the Late Miocene surface and an age of 3.5-1.65 Ma for the Late Pliocene surface, the uplift rate since the Miocene is 0.068-0.135 m/ka, whereas the uplift rate since the late Pliocene ranges between 0.114-0.242 m/ka.

4.4.2.2.4 Axial parts of the graben: In the axial parts of the Molai Graben (Fig. 4.6. **pr 7**), a gently inclined morphological surface on Pleistocene marine sediments (from "Eutyrrhenian" to early Pleistocene) is continuous from 20 to 80-100 m. The absence of knick-points does not allow identification of distinct terraces. Correlation with Pleistocene sea level cycles can only be based on the evidence of offlapping 4th order sedimentary sequences (see Chapter 5). This lack of distinct terrace morphology can be attributed to

Figure 4.9 (following page): Geomorphological sketch-map of the eastern flank of the Neapolis Graben and the Cape Maleas (southern part of the Eastern Lakonia Peninsula). The main relief segments are as in Fig. 4.7. The uplifted Late Tertiary surfaces are separated by the Late Pliocene-Pleistocene surfaces by means of steep cliffs. In the southern tip of the peninsula (Cape Maleas) Late Tertiary surfaces dip to the sea, suggesting that southward tilting took place during the Plio-Quaternary. Note the presence of broad, incised valleys of inferred Late Tertiary age, as well as common E-W trending faults that segment the Eastern Lakonia Peninsula across its axis.

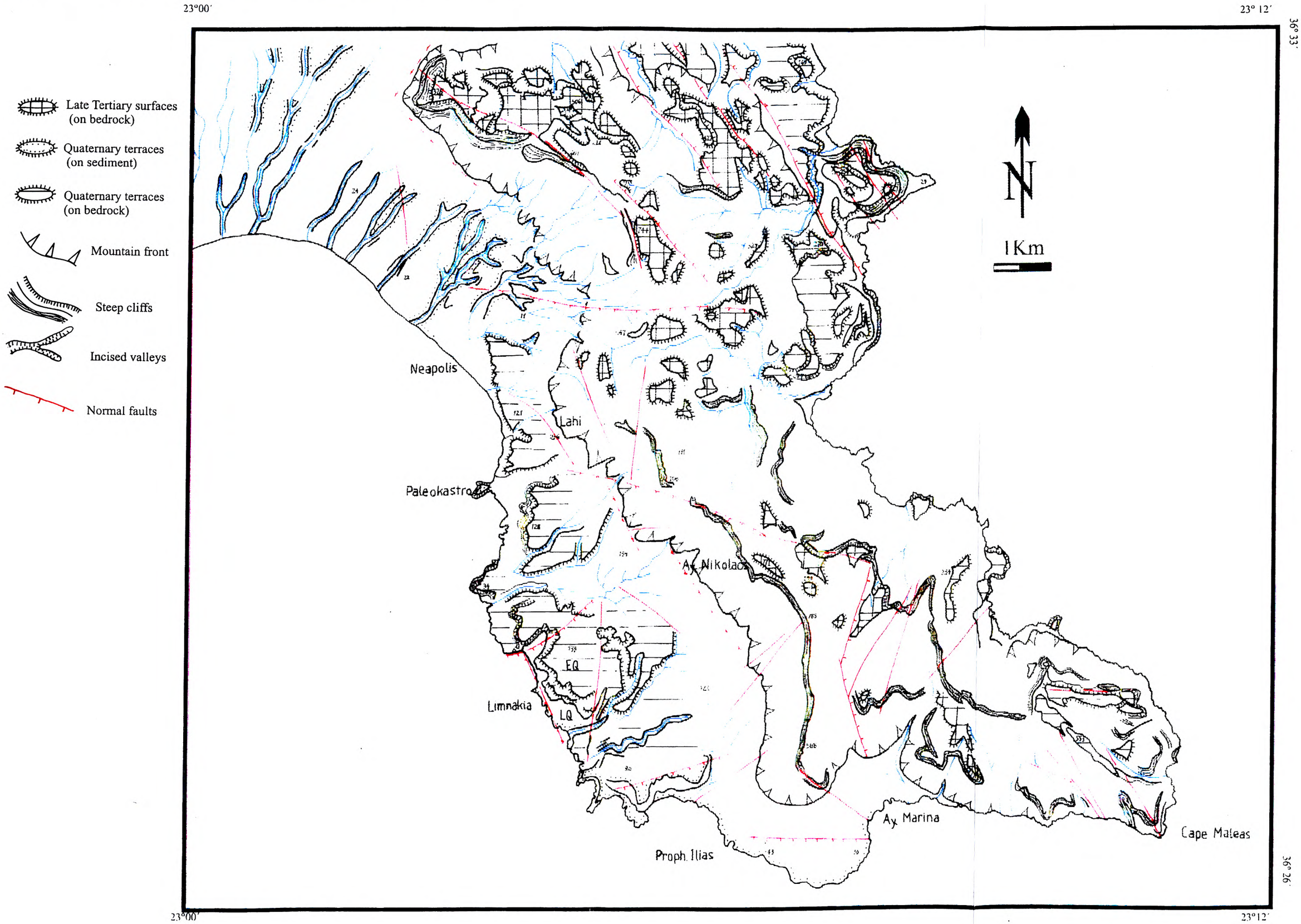
23°00′
23° 12′
36° 33′
36° 26′
Late Tertiary surfaces (on bedrock)
Quaternary terraces (on sediment)
Quaternary terraces (on bedrock)
Mountain front
Steep cliffs
Incised valleys
Normal faults
N
1 Km
Neapolis
Lahi
Paleokastro
Ay. Nikolaos
EQ
Limnakia
LQ
Ay Marina
Cape Maleas
Proph. Ilias

lower uplift rates of the axial part of the Molai Graben, as compared with the more rapidly uplifting flanks of the graben. Similar non-terraced morphologies resulted from computer modeling of relative sea level change in Sumba Islands, Indonesia, if low uplift rate is assumed (Bard et al., 1996).

4.4.3 SW coast benchland and Dokali Graben:

4.4.3.1 Faults and morphological surfaces: This is an uplifted area between the Molai Graben to the north and the Neapolis Graben to east-southeast (Figs. 4.2, 4.5, M.2). Its topography is mainly controlled by NNW-SSE faults, but ENE-WSW transfer faults and ESE-WNW oblique faults are also important (Figs. 4.2, M.2). Transfer and oblique faults are more widespread here, than within the Ano Glikovrisi Horst further north (I.G.E.Y., 1970; see Fig. M.2). The west-facing, seaward parts of this area comprise a step-like succession of surfaces, from the Late Miocene-Early Pliocene peneplain to the late Pleistocene marine terraces (Fig. 4.6). These surfaces strike NNW-SSE, parallel to the principal fault trend of the area. The **pr 10** (Fig. 4.6) exemplifies this morphological pattern. A series of five Pleistocene terraces ascend stepwise from the present sea level to the Late Pliocene-early Pleistocene pediment/terrace, at ca. 80-100 m. The mountain front, east of the latter surface, is controlled by NNW-SSE faults. Four to five closely-spaced Late Tertiary pediments occur along this profile. Uplifted pediments in the outer zone of the mountain range are isolated, in the form of zonal inselbergs (*sensu* Ahnert, 1998; see Fig. 4.6, photo). The highest surface, correlated with the Late Miocene peneplain, is uplifted to ca. 490-520 m. The minimum accumulated throw since the Late Miocene is ca. 420 m. Remnants of this surface are preserved on Tripolis Zone limestone substratum, isolated by broad (width: up to 1 km), fault-controlled zones of multiphase valley incision, that reaches the level of the Late Pliocene-early Pleistocene pediment-terrace (Fig. 4.6). Late Tertiary pediments are separated by relatively low cliffs (≤ 50-60 m) that commonly coincide with NNW-SSE faults.

Figure 4.10 (following page): Schematic cross section of the sedimentary fill of the Dokali Rema valley (see Fig. M.2 for location). A broad, U-shaped valley was incised into early Pleistocene shallow-marine sediments. Three main units of alluvial fill are distinguished, separated by erosional surfaces corresponding with periods of fluvial erosion. The red fanglomerates **(1)** are correlated with the middle Pleistocene Unit 4 or 7 (Chapter 5). Brown conglomerates and sands are correlated with a Eutyrrhenian marine terrace further towards the shore. Brown conglomerates with pottery fragments are of Holocene (Historical) age.

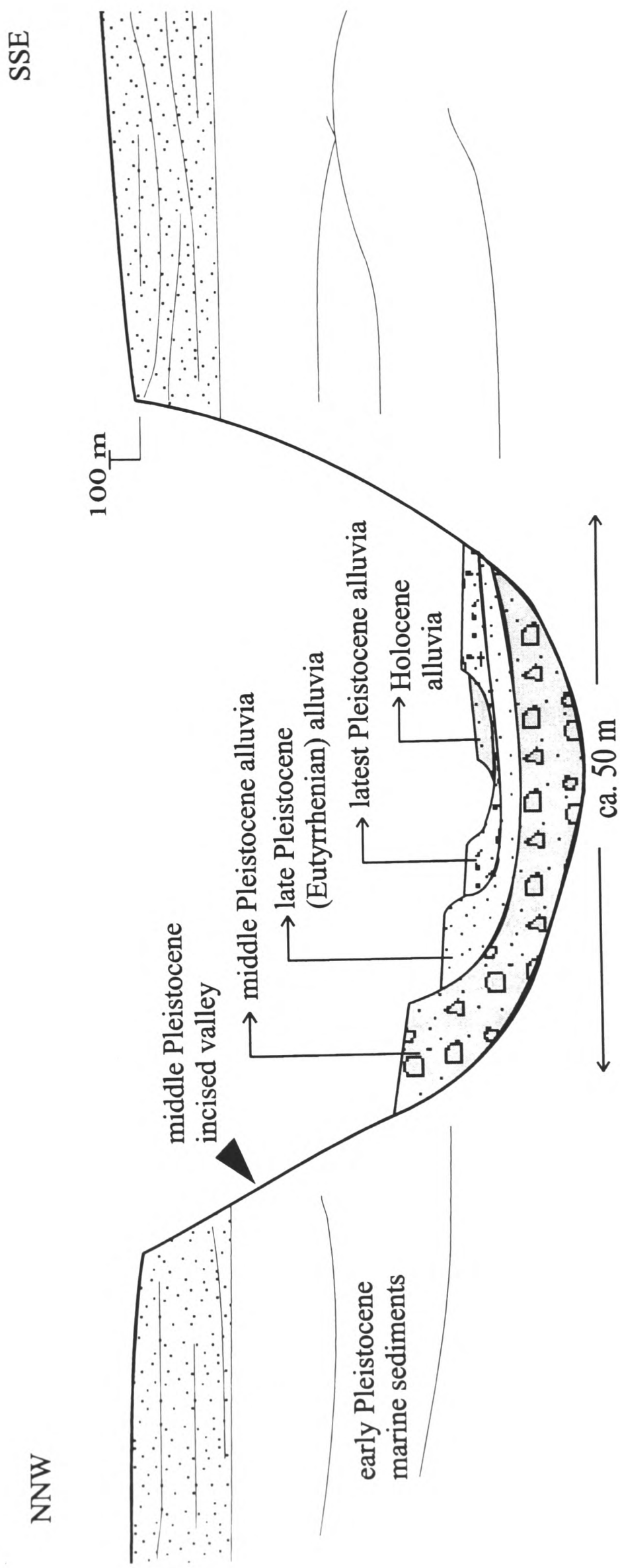
SSE
100 m
middle Pleistocene
incised valley
→ middle Pleistocene alluvia
→ late Pleistocene
(Eutyrrhenian) alluvia
→ latest Pleistocene alluvia
→ Holocene
alluvia
ca. 50 m
early Pleistocene
marine sediments
NNW

4.4.3.2 Dokali Graben: The continuity of this benchland morphology, as described above, is interrupted in the area of Dokali Rema by an ENE-WSW striking, uplifted, asymmetrical graben (see Figs. 4.2, M.2). The NNW side of this graben is bounded by ENE-WSW and NNE-SSW faults (maximum length: ca. 2.7 km; Fig. M.2), whereas its SSE side is less intensely faulted. The *Dokali Graben* is a narrow structure, ca. 5-6.5 km long (exposed part) and ca. 2.5-3 km wide. The **pr 11** (Fig. 4.6), across the long axis of the graben, reveals its asymmetry: on the NNW side of the graben the early Pleistocene terrace is faulted, with throws of ca. 20-40 m. The sedimentary fill of the Dokali Rema is distinguished in four main alluvial units, that span the time from middle Pleistocene to Holocene, suggesting a that successive episodes of incision and alluviation took place during the late Quaternary (see Fig. 4.10 and Chapter 5).

4.4.3.3 South of the Dokali Graben: The **pr 13** (Fig. 4.6), south of the Dokali Graben, reveals a morphology different from areas further north. Here, Quaternary surfaces comprise a terrace system from ca. 80-100 m (Late Pliocene-early Pleistocene pediment/terrace) to 0-10 m (latest Pleistocene). The highest and the lowest Pleistocene terraces are connected by a terraced cliff, extending from ca. 70 to 20 m (Figs. 4.6, photo). This cliff comprises many knick points, suggesting the presence of closely spaced terraces of probable middle Pleistocene age (see above). Faulting of Pleistocene terraces is implied by sedimentological evidence (see Chapter 5). The Late Pliocene-early Pleistocene pediment/terrace is separated by the Late Tertiary surfaces by steep cliffs, locally controlled by NW-SE faults. The height of these cliffs locally exceeds 300 m. East of the Aetopholia Hill (Figs. 4.6, M.2), three Late Tertiary surfaces are incised to the level of the Late Pliocene-early Pleistocene pediment. Low-angle slopes within the second Late Tertiary pediment are interpreted as degraded NW-SE fault scarps (Fig. 4.6). Erosional remnants of the Late Miocene-Early Pliocene peneplain are preserved at ca. 500-510 m, bounded by steep, fault-controlled scarps (maximum scarp height: ca. 80 m).

4.4.3.4 Viglaphia area: Further south, in the area of Viglaphia (see Figs. 4.2, 4.6: **pr 17, 18**, M.2), erosional remnants of the inferred Late Miocene-early Pleistocene peneplain are preserved at ca. 660-520 m, separated from lower Late Tertiary surfaces by fault-controlled cliffs (Fig. 4.6). The Late Tertiary pediments are also connected with the Late Pliocene pediment, at lower elevations, by fault controlled cliffs (maximum cliff height: 320 m). In this area, the Late Pliocene pediment is separated from the early Pleistocene terrace by ca.

50-70 m high cliffs. The early Pleistocene terrace, of concave longitudinal profile, truncates the Late Pliocene pediment at ca. 140-160 m. This partition of the two surfaces indicates that differential faulting took place prior to the early Pleistocene transgression, which, in this area, did not reach the uplifted Late Pliocene pediment. The Quaternary terrace flight comprises up to five closely spaced surfaces (including the early Pleistocene one; see Fig. 4.6).

In the southernmost part of the western coast of the peninsula (e.g. Ayii Apostoli; Fig. M.2), late Pleistocene sediments are covered by extensive dune fields and marshlands. This shows that relative uplift of that area since the late Pleistocene was weak, as compared with stretches of the coastline further north. Subsidence of the land bridge between the Viglaphia coast and the Elaphonisos island (Figs. 4.2, M.2) took place in Roman times (1st century BC), as a result of an earthquake (Symeonides, 1969).

4.4.4 Neapolis Graben:

4.4.4.1 Graben-bounding faults: The Neapolis Graben is a composite, NNW-SSE striking basin, with its greater part below present sea level. On the west, it is bounded by NNW-SSE faults, mapped in the area of Megali Spilia and their continuation in the Elaphonisos Island, further south (Figs. 4.2, 4.9, M.2). No large faults are mapped along its eastern boundary (I.G.E.Y., 1970), so the Neapolis Graben is probably an asymmetrical half-graben. The NE boundary of the graben coincides with degraded NW-SE fault scarps, incised by broad, multiphase valleys. These NW-SE faults are interrupted by ca. 2 km wide ramps (Fig, 4.9). The latter ramps are cut by NW-SE faults, up to 4.5 km long and spaced every 500-750 m. The S/SSW side of the graben is open to the sea, forming the Neapolis Bay (Fig. 4.6). The subaerial part of the Neapolis Graben is ca. 8 km wide (Fig. M.2). Evidence from the Elaphonisos Island (I.G.E.Y., 1970) suggests that the length of its axis exceeds ca. 10-12 km.

3.4.2) Morphological surfaces: The axial part of the Neapolis Graben, was uplifted since early Pleistocene, but at a rate slower than other areas of the Eastern Lakonia Peninsula. Quaternary relief stretches from present sea level to ca. 80 m (Fig. 4.9). No individual terraces are distinguished at the scale of the section (based on 1:50,000 maps) and distinction between early and later Pleistocene shallow-marine sediments in the field is difficult. The more inland portion of this gently inclined surface probably corresponds to the Late Pliocene-early Pleistocene pediment/terrace. This is separated from the uplifted

Tertiary pediments, further inland, by steep cliffs, controlled by discontinuous NW-SE faults. The height of the latter cliffs ranges from ca. 90-100 m in the central part of the fault system (**pr 19**), to >400 m in densely faulted areas near the edge of the graben (**pr 20**). Further inland, the Late Miocene-Early Pliocene peneplain was uplifted up to ca. 500 m (**pr 20**).

4.4.5 Cape Maleas:

4.4.5.1 Faults: Additional to NW-SE, NNW-SSE and NNE-SSW faults, common all over the Eastern Lakonia Peninsula (Figs. 4.2, 4.3, 4.9, M.2), the Cape Maleas area was also cut by relatively long, E-W trending, mainly south-dipping faults (maximum length: 2 km; see Fig. 4.6). These faults cut both bedrock and Pleistocene sediments and segment the peninsula across-strike (Figs. 4.2, 4.9). In the Cape Maleas area, Pleistocene sediments are generally rare, preserved above present sea level only in the SW tip of the peninsula (Fig. 4.2. M.2).

4.4.5.2 Morphological surfaces: As shown on **pr 23** (see Figs. 4.6, 4.9), on the western side of the Cape Maleas block, the Quaternary terrace flight is cut by NNW-SSE faults that downthrow late Pleistocene terraces below present sea level. A relatively steep terraced cliff separates the late Pleistocene terrace(s) (ca. 5-20 m) from the Late Pliocene pediment (ca. 140-220 m). Steep, locally fault-controlled cliffs (maximum height: ca. 650 m) connect the Late Pliocene pediment with Late Tertiary surfaces higher up. The highest Late Tertiary surfaces were uplifted to maximum altitude of 790 m, within the central mountain range of the Cape Maleas block.

In the SE part of the Cape Maleas block, Late Tertiary pediplains are bordered by precipitous cliffs down to present sea level (Figs. 4.5, 4.9). This topographical difference between the western and eastern coast possibly suggests that differential faulting took place during Pliocene time, after the development of the post-Late Miocene pediments and before the development of the Late Pliocene pediment. The absence of the Late Pliocene pediment from the SE part of the Cape Maleas area suggests that no uplift (or possible subsidence) of that area has taken place since early Pleistocene.

4.4.6 Eastern coast:

The eastern coast of the Eastern Lakonia Peninsula is in many respects different from the western one. Its main morphologic characteristics (Figs. 4.2, 4.5, M.2) are: 1) A narrow zone of precipitous slopes from the morphological spine of the peninsula to the present coastline and, 2) the relative scarcity of uplifted Pleistocene marine sediments.

South of Monemvasia the Late Miocene peneplain is preserved at a maximum altitude of ca. 600-790 m, bordered by steep cliffs (maximum height 550-500 m) that drop to present sea level (Figs. 4.5, 4.6, M.2). These cliffs are locally fault-controlled (NNW-SSE faults); generally, however, they cannot be correlated with mapped faults. Quaternary surfaces commonly comprise erosive terraces, devoid of sediment cover; these are correlated with middle and late Pleistocene sea levels. These terraces are restricted within a narrow zone, parallel to the present-day coastline (Figs. 4.5, 4.6). Their altitude is ≤ ca. 40 m.

In Epidhavros Limira-Ayios Ioannis, Pleistocene sediments are preserved in an uplifted basin, controlled by ESE-WNW and NW-SE faults (Figs. 4.2, 4.6, M.2). A terrace surface is present above these sediments, dipping gently to the sea from ca. 100 to <20 m. Although individual knick points are not identified, sedimentological evidence confirms amalgamation of at least three 4th-order depositional 'sequences' (see Chapter 5). Uplifted pediments were formed on fault-controlled blocks of bedrock that rise above that Pleistocene surface, at altitudes ≤ca. 180 m.

4.5 DRAINAGE OF THE EASTERN LAKONIA PENINSULA

The drainage of Eastern Lakonia Peninsula is controlled by bedrock lithology, morphology and age of the drained relief, neotectonic faulting and crustal uplift. These controls are illustrated and discussed in the following section. This discussion is based on evidence from 1:50,000 topographical maps with 20 m contour interval (H.A.G.S., 1970, 1978). Terminology of drainage types follows Howard (1967) and ordering of the drainage branches follows the method of Strahler (1954).

4.5.1 Drainage pattern in the Eastern Lakonia Peninsula

On a peninsula scale, drainage systems in Eastern Lakonia branch around a NNW-SSE trending divide, that parallels the elongation of the peninsula (Fig. M.2). This peninsular divide coincides with the watershed of uplifted and dissected Late Tertiary surfaces (see

above). It is more sharply expressed in the southern parts of the peninsula, where Tripolis Zone neritic carbonates are widespread (Fig. M.2). In the central and northern parts, by contrast, widespread outcrops of metamorphic bedrock ("*Phyllite Series*") are affected by a dense dendritic drainage. Advanced headward erosion of 1st-order valleys resulted in a rugged configuration of the divide in the latter areas.

4.5.2 Drainage pattern within each morphologic unit

The pattern described above, relatively simple at a peninsular scale, is further complicated by the different style and intensity of normal faulting locally, that led to the development of distinct morphologic units (see above), each with a characteristic drainage (Fig. M.2). The drainage within each morphologic unit is described, as follows:

4.5.2.1 Ano Glikovrisi Horst: The area of the Ano Glikovrisi Horst is bounded by NNW-SSE faults that cut through an anticlinal structure of Tethyan age (see above). There, a series of faulted terraces (early-middle to late Pleistocene), the Late Pliocene-early Pleistocene pediment/terrace and the Late Tertiary pediments are drained by a dense drainage of parallel-dendritic type (average spacing: every 250 m). This drainage is transverse to the grain of faults and morphological surfaces (*sensu* Ahnert, 1998) (see Fig. 4.8).

4.5.2.1.1 Western flanks of the Ano Glikovrisi Horst: The largest streams of this area are of 3rd order. These streams drain both Quaternary and Late Tertiary surfaces, and have incised their valleys through the fault-controlled Ano Glikovrisi mountain front (Fig. 4.5). Valley incision across the mountain front reaches ca. 300 m. Longitudinal profiles of 3rd order streams (e.g. Mourtitsa Rema; see Fig. 4.11) are generally convex and steep. Well-expressed convex knick points (440, 340, 240, 140 and 60 m) define multiple hanging valleys. All these knick points are located in the vicinity of normal faults (Figs. 4.8, M.2). All but the highest one are formed on readily eroded Pleistocene marine sediments. Gradients of these streams are the highest within the Eastern Lakonia Peninsula, reaching 13.3-20% in their middle reaches and 40% immediately downstream of knick points. Given the friable lithology of the drained terrain (Pleistocene sediments), the presence of hanging valleys on footwall blocks of NNW-SSE faults probably indicates late Pleistocene-Recent activity of the latter faults, that control the eastern flank of Lakonic Gulf (Keller and Pinter, 1996; Migón, 1998).

Most streams in this area, however, are of 2nd order and drain only Quaternary relief (Fig. 4.8). These 2nd order streams are probably younger than the larger, 3rd order ones. Incised valleys (width: 10's of m) also occur at the lower reaches of Quaternary, 1st and 2nd order streams. Incision of the latter probably took place in latest Pleistocene-Holocene times, since it affected alluvial channel fill of late Pleistocene age (Unit 12; Chapter 5).

4.5.2.1.2 Eastern flanks of the Ano Glikovrisi Horst: Streams that drain the fault controlled eastern flanks of the Ano Glikovrisi horst are short (length <1 km), with steep longitudinal profiles (Fig. 4.11), and incised throughout their course (Fig. 4.5). Fluvial incision affected Pleistocene alluvia and shallow-marine sediments (as young as late Pleistocene). Incision was probably enhanced by Pleistocene activity along segments of the N-S Molai Fault (Fig. 4.5); such activity is confirmed independently by offset of Pleistocene sediments (see above).

4.5.2.2 Molai Graben: The N-S to NNE-SSW *en echelon* faults that bound the Molai Graben to the west are tectonic lines of primary importance and probably still active, since their continuation cuts and uplifts an inferred "Eutyrrhenian" age (Bozas Rema -see above) (Figs. 4.8, M.2).

4.5.2.2.1 Seaward part of the Molai Graben: The outer, seaward part of the Molai Graben is drained by a low-density, parallel-dendritic network of 4th order streams that flow from the NNE to the SSW, parallel to the graben-bounding faults (Fig. 4.8). The Potamia Rema stream, parallel to the Molai Fault, exhibits an asymmetrical pattern. Its western tributaries are systematically shorter than the eastern ones, and, by contrast to the eastern tributaries, they are incised (Fig. 4.8). This asymmetry probably resulted from higher morphological gradient in the western side of the stream. The latter could be a possible consequence of unmapped faults within Pleistocene sediments, on the hangingwall of the Molai Fault. The longitudinal profile of the Potamia Rema stream is smooth, with gradients ranging between 0.8-1.6% (Fig. 4.11). A convex knick point, at ca. 20 m, probably marks the retreating cliff of the "Eutyrrhenian" terrace.

The upper reaches of the Bozas Rema stream (Figs. 4.8, M.2) are of rectangular pattern, with branches flowing to the SW and SE. The same pattern also prevails along one of its tributaries. This pattern coincides with the orthogonal NE-SW and NW-SE bedrock fault pattern in the SE, less conspicuously faulted, flanks of the Molai Graben (see Fig, M.2). This stream also exhibits a smooth longitudinal profile, with a stream gradient ca. 0.7% (4th

order trunk stream), to 1.6% (3rd order tributaries) (Fig. 4.11). The lower reaches of Bozas Rema follow broad valleys, incised trough alluvial and shallow-marine sediments of Pleistocene age (as young as the "Eutyrrhenian" terrace; see Fig. 4.8).

4.5.2.2.2 Inland part of the Molai Graben: The NE, inland part of the Molai Graben exhibits a rectangular drainage pattern (Fig. 4.8). NW-SE trunk streams are parallel to NW-SE graben-bounding faults. NE-SW tributaries are transverse to the fault-controlled pediments and parallel to NE-SW "transfer" faults (e.g. Hilorrema trunk stream: 4th order; Tsakona Rema transverse tributary: 3rd order; see Figs. 4.8, M.2).

The longitudinal Hilorrema stream (*sensu* Ahnert, 1998) exhibits a relatively smooth, concave longitudinal profile, with river bed gradient ranging from 0.7% (lower reaches)-4.4% (upper reaches) (Fig. 4.11). A concave knick point, at ca. 100 m, is probably associated with transition from cemented (late?) Pleistocene alluvia upstream, to more friable Pleistocene marine sediments downstream (Fig. M.2). A convex knick point, at ca. 220 m, coincides with the mapped trace of the N-S Molai Fault in cemented alluvia of inferred middle Pleistocene age (Unit 4; Chapter 5). Late Pleistocene-Holocene reactivation of this particular fault segment is, thus, inferred.

4.5.2.2.3 NE part of the Molai Graben: The transverse Tsakona Rema (Fig. 4.8) has a steep longitudinal profile, with well expressed convex knick points (140 m, 360 m; see Fig. 4.11) These knick points correlate with traces of NW-SE faults that control the NE boundary of the Molai Graben (Fig. 4.8). A broad, incised, hanging valley (average length: 3-4 km, average width: 200-300 m) occurs along the Tsakona Rema, on the footwalls of NW-SE graben-bounding faults (Figs. 4.8, 4.11). Away from convex knick points, the valley bed gradient ranges from 0.8% (lower reaches)-13.3% (upper reaches) (Fig. 4.11). Downstream of knick points the valley was rejuvenated, with dips reaching 40% (e.g. downstream of the 360 m knick point). This hanging valley is tentatively correlated with similar broad valleys of Late Tertiary age in other areas of the Eastern Lakonia Peninsula (e.g. Ano Glikovrisi, Ayia Marina; Figs. 4.8, 4.9). Therefore, fault offset of the valley bed (that caused the knick points), probably took place in Pleistocene time. The same is also inferred for Monoporo Rema, a transverse stream that crosses the uplifted footwall of the NW-SE Molai Graben-bounding fault and follows a Late Tertiary hanging valley in its middle-upper reaches (Figs. 4.8, 4.11).

The drainage in the northernmost part of the Molai Graben, developed on Pleistocene sediment substratum, is internal and its streams do not reach the sea (Fig. 4.8). This

probably results from the high permeability of the substratum and/or anthropogenic causes (use of water for irrigation purposes).

4.5.2.3 SW coast and Dokali Graben: South of the Molai Graben, the SW coast of the Eastern Lakonia Peninsula is chiefly drained by short, 2^{nd}-3^{rd} order, dendritic-parallel streams, restricted to the Plio-Pleistocene pediment and terrace system (Fig. M.2). These streams have relatively steep longitudinal profiles, with gradients ranging from 6.6-10 % along their middle-upper reaches (Fig. 4.11). Concave knick points occur at ca. 20 m, associated with the transition from the gently inclined late Pleistocene terrace downstream, to the middle, then early Pleistocene terraced benchland upstream (see Fig. 4.6). Convex knick points occur at ca. 40 and 80-100 m, associated with the cliffs of the main middle Pleistocene and the early Pleistocene terrace, respectively. Larger streams include Dokali Rema (5^{th} order), Stravolagadho Rema and Platanistos Rema (both 4^{th} order), that cut the pre-Quaternary mountain front and drain the domain of the fault-uplifted Late Tertiary surfaces further east (Fig. M.2).

4.5.2.3.1 Dokali Graben: The drainage of this graben comprises the axial Dokali Rema stream and its transverse tributaries (Fig. M.2). Dokali Rema (5^{th} order), of mixed dendritic-rectangular pattern, captures streams that flow to the NW and SE, parallel to the morphologic grain of the peninsula. Its lower and middle reaches follow a deep, broad valley. Incremental incision of this valley has resulted in formation and preservation of a series of "accumulation" terraces (Fig. 4.6). The lowest (and youngest) alluvial terraces are of Holocene age, whereas another terrace further upstream can be correlated with the "Eutyrrhenian" stage (Unit 9; Chapter 5). The longitudinal profile of the Dokali Rema trunk stream is smooth and concave, with a stream gradient ranging from 0.8% (lower reaches)-4.4% (upper reaches) (Fig. 4.11). No convex knick points are distinguished on the base-map scale.

Tributaries that drain the area south of the trunk stream exhibit considerably steeper and more irregular longitudinal profiles (Fig. 4.11). The tributary 12.1 has a stream bed gradient from 3.8% (lower reaches: 4^{th} order)-5.1% (upper reaches: 3^{rd} order). Convex knick points occur at 80 m (lithological boundary between Tripolis Zone limestone upstream and early Pleistocene carbonates downstream), 140 m (NE-SW normal fault), 220 m (NW-SE normal fault) and 260 m (lithological boundary between schists/phyllites downstream and marble upstream; I.G.E.Y., 1970) (see Fig. 4.11). The tributary 12.3 drains exclusively bedrock terrain, and its valley is incised through Tertiary relief for most of its length. Its longitudinal

profile is steeper and more irregular than the stream 12.1. Its stream gradient ranges from 3% (lower reaches)-7.6% (upper reaches), with even higher values (10-13.3%) directly downstream of convex knick points (Fig. 4.11). The following convex knick points were recognised: at 100 m (both the lithological boundary between "*Phyllite Series*" downstream and Tripolis Zone limestone upstream (I.G.E.Y., 1970) and also incision into the backslope of the Late Pliocene-early Pleistocene pediment, here on limestone), at 160 m (trace of a NW-SE fault) and at 280 m (NW-SE fault in marble bedrock). The maximum gradient of the stream (13.3%) occurs downstream of the latter knick point.

Tributaries that drain the area north of the Dokali Rema trunk stream transverse a relief steeper than that of the southern side (Figs. 4.5, 4.6, A.1). These streams cross the fault-controlled mountain front that separates the Late Pliocene-early Pleistocene pediment/terrace from the uplifted Tertiary surfaces. Morphological and sedimentological evidence (triangular facets, late Pleistocene-Holocene alluvial fans) indicate recent faulting along the mountain front. In contrast with the area south of the Dokali Rema trunk stream, the SE-flowing streams north of the Dokali Rema are significantly shorter, of 2^{nd}-3^{rd} order, and of simpler, less ramified pattern (Fig. M.2). These differences are recognised even between streams developed over the same substratum ("*Phyllite Series*" metamorphic terrain). Longitudinal profiles of the latter streams are convex, with knick points at ca. 80 and 100 m. These knick points could be associated either with unmapped NE-SW faults near the NW side of the Dokali Basin, or with lithological control by contrasting rock types in the inhomogeneous "*Phyllite Series*" substratum. Shorter streams, of simpler configuration and convex longitudinal profiles, in the NW side of the Dokali basin, probably indicate tilting of the drained terrain towards the NW flank of the basin. This suggests that the NW flank of the basin is more active than the SE one. The ENE-WSW striking Dokali Rema basin, thus, appears to be a half-graben, transverse to the principal, NNW-SSE fault-grain of the Eastern Lakonia Peninsula. Although smaller, the Dokali Graben is, thus, similar with the Molai Graben, in both the direction of graben-controlling faults and the principal direction of tilting.

4.5.2.3.2 SW Lakonia benchland: South of the Dokali Graben, near Elika, the 4^{th} order, dendritic Stravolagado Rema, with an entrenched meandering course, is the most sinuous stream in the SW coast of the Eastern Lakonia Peninsula (Fig. M.2). This drains exclusively metamorphic terrain, of schist and phyllite ("*Phyllite Series*"). Its valley is incised into the backslope of the Late Pliocene pediment and drains areas of Tertiary relief. Its longitudinal profile exhibits a low stream gradient, ranging from 1.5-5.7% (rejuvenated lower reaches),

to 1% (middle reaches, across the Late Pliocene pediment), then to 8-10% (3rd order upper reaches, across the Late Tertiary mountain front) (Fig. 4.11). Convex knick points occur at the following elevations: At ca. 60 m (cliff that separates middle to early Pleistocene terraces upstream from late Pleistocene terraces downstream), at ca. 100 m (transition from the Late Pliocene pediment upstream, to the terraced middle(?) Pleistocene cliff downstream). The gently dipping middle reaches of the Stravolagadho Rema are incised through fanglomerates correlative with early to middle Pleistocene alluvia (top of Unit 5; Chapter 5) in other sites of the Eastern Lakonia Peninsula (e.g. Ano Glikovrisi, Dokali Rema; Figs. 4.2 4.6, 4.8, M.2). Further upstream, the ca. 160, 240 and 280 m knick points correspond to NW-SE normal faults. A similar sequence of convex knick points occurs along the Platanistos Rema (Fig. M.2). This stream is parallel to the Stravolagadho Rema and drains the same metamorphic terrain.

4.5.2.4 Viglaphia: In the area of Viglaphia (Fig. M.2), the drainage density is very low, probably as a result of the permeable, faulted carbonate lithology of both the Tripolis Zone bedrock and the Pleistocene sediment cover. Dry, V-shaped valleys, incised through early Pleistocene carbonates and bedrock occur from ca. 20 m (the level of the "Eutyrrhenian" terrace) to ca. 90-100 m (the level of the early Pleistocene terrace). These V-shaped valleys, that propagated from base level corresponding to the "Eutyrrhenian" shoreline, cross a series of erosive terraces of inferred middle Pleistocene age. Headward erosion at the valley-heads of these streams rejuvenated the lower reaches of older, broad, U-shaped hanging valleys higher up. The latter are incised into bedrock and the topsets of the early Pleistocene terrace, from ca. 110 to 160 m. Their incision probably took place during middle Pleistocene, after the emergence of the early Pleistocene terrace and before the "Eutyrrhenian". Incision of the lowest, late Pleistocene terraces is minimal.

***4.5.2.5* Neapolis Graben:** The drainage of the Neapolis Graben is distinguished into two groups (Figs. 4.9. M.2):

1) Older, parallel-dendritic streams (4th order) drain both Quaternary and Tertiary relief and follow valleys incised into the fault-controlled flanks of the graben. The longer streams of this group drain the western and central parts of the Neapolis Graben (Fig. M.2). Three out of four of these streams follow a SE direction of flow along their upper reaches.

2) Younger, parallel, 'consequent' streams (1st and 2nd order) drain Pleistocene sediment terrain. The concave, crescent-shaped configuration of the present coastline enforces a centripetal convergence of these streams (Figs. 4.6, M.2).

4.5.2.5.1 Western part of the Neapolis Graben: The Valmandhrea Rema (4th order) drains the western end of the Neapolis Graben (Fig. M.2). Its longitudinal profile is markedly convex (Fig. 4.11). A convex knick point, at ca. 100 m, separates gently inclined segments downstream and upstream. This knick point is associated both with the lithological boundary between friable early Pleistocene sediments downstream, and Tripolis Zone limestone and cemented late Pleistocene or early Pleistocene(?) alluvia upstream and, also, with the lower reaches of a broad, NNW-SSE trending hanging valley (Fig. M.2). The latter is is a valley side pediment (*sensu* Ahnert, 1998) correlated with the Late Pliocene pediment. Upstream of the 100 m knick point, the hanging valley gradient is very low (0.6%). Downstream of the latter knick point, the longitudinal profile of the Valmandhrea Rema can be divided into two segments: The segment of the stream that drains early (to middle ?) Pleistocene marine sediments dips at 2.4%. A concave knick point at ca. 20 m separates this from a more gently graded segment (gradient: 1.2%), further downstream. The latter segment of the stream drains late Pleistocene (marine to aeolian) and Holocene (marshland to aeolian) sediments. This suggests that headward incision took place in late Quaternary time, propagating from the late Pleistocene-Holocene base level into the early Pleistocene marine sediments. The two parallel tributaries of the Valmandhreika Rema join only ca. 400 m inland of the present-day coastline (Fig. M.2). The same pattern of tributary joining near the shore, uncommon in other grabens of the Eastern Lakonia Peninsula, occurs also at the Haraka and Karasas Rema, ca. 1200 m to the east of the Valmandhreika stream (Fig. M.2). It is known that in Roman times (1st century BC; Simeonides, 1969) an earthquake resulted in subsidence of a land bridge that formerly connected the Elaphonisos Island with the mainland. It is possible that coastal subsidence, that accompanied that earthquake, resulted to landward retreat of the coastline and submergence of the most distal portion of the alluvial plain.

4.5.2.5.2 NE boundary of the Neapolis Graben: The streams Haraka and Karasas Rema (both 4th order) are incised into the NW-SE, fault-controlled mountain front that borders the Neapolis Graben to the NE (Fig. 4.9). Low-order tributaries of this drainage system transverse the trace of the normal fault that controls the mountain front. However, longer, 3rd order tributaries bypass the edges of the mapped fault trace (I.G.E.Y., 1970; see Fig. 4.9). Both streams exhibit very similar, convex longitudinal profiles (Fig. 4.11). Distinct

segments of these profiles can be related to contrasting lithology and different relief generations of the drained substratum. Both profiles have convex knick points on substratum of early Pleistocene marine sediments, at ca. 100 and 120 m, respectively. These knick points mark the retreating margin of the early Pleistocene terrace. Downstream of these knick points, the stream gradient increases gradually, from 1% (lowest reaches, on late Pleistocene-Holocene marine sediments), to 2.2-2.7% (further upstream, on Pleistocene marine sediment substratum). Directly downstream of the two knick points, the stream gradient ranges between 6.6% (Karasas Rema)-13.3 % (Haraka Rema). The stream gradient increases to 8.8-13% upstream of these knick points (Tripolis Zone limestone). These parts of the streams correspond to broad, hanging valleys of inferred Late Tertiary age, that become convex in their upstream parts (Fig. 4.9). Convex knick points at ca. 180 and 260 m are interpreted as resulting from multiphase rejuvenation of the latter valleys in Quaternary times. It is uncertain whether this rejuvenation was influenced by activity of the NW-SE faults that border the Neapolis Graben (Fig. 4.9), or from incremental relative sea level fall, controlled by regional uplift of the peninsula.

4.5.2.5.3 SE boundary of the Neapolis Graben: The stream **18** (4th order), at the SE end of the Neapolis Graben, is of dendritic type (Fig. 4.9). The trunk stream flows to the SW, perpendicular to the present coastline. The tributaries flow to the W/WNW and drain the uplifted highlands E/ESE of the Neapolis Graben. The trunk stream exhibits a strongly concave longitudinal profile (Fig. 4.11), with gentle lower reaches on Pleistocene marine and alluvial sediments (dip: 2.5%), and very steep upper reaches, on "*Phyllite Series*" metamorphics (dip: 8-20%). A concave knick point at ca. 60 m is correlated with the boundary between the latter lithological types and also with the boundary between areas of Late Pliocene-Pleistocene and Tertiary relief (Fig. 4.9). The upper reaches of the stream are punctuated by convex knick points, at elevations of ca. 160, 200 and 240 m. The two higher knick points possibly resulted from lithological heterogeneity within the "*Phyllite Series*" substratum. The ca. 160 m knick point probably indicates Pleistocene rejuvenation of a Late Tertiary incised valley, as elsewhere in the Eastern Lakonia Peninsula. The west flowing tributary (**18.2**) drains "*Phyllite Series*" terrain in the uplifted area SE of the Neapolis Graben (Figs. 4.9, M.2). This stream incised into coalescent alluvial fans of inferred late Pleistocene age (Unit 12; Chapter 5). Its longitudinal profile is strongly concave, with dips ranging from 2.5% (lower reaches) to 13% (upper reaches) (Fig. 4.11). Convex knick points occur at ca. 160 and 220 m. The first one probably resulted from rejuvenation of a Late Tertiary valley by Pleistocene incision, as elsewhere along the margins of Neapolis Graben. The second knick point is correlated with the trace of a large (ca. 5.5 km long), south-

Mo: Mourtitsa

Sl: Stravolagadho

Do: Dokali

Po: Potamia

Bo: Bozas

Ta: Tasou

He: Heilorema

Ts: Tsakonas

Figure 4.11: Longitudinal profiles of streams in the Eastern Lakonia Peninsula. Three types of streams are distinguished: **1)** Streams of very steep profile are more widespread along the western coast of the peninsula, especially within the Ano Glikovrisi Horst (see Figure M.2). These streams are commonly transverse to NNW-SSE faults that cut bedrock and Pleistocene sediments. **2)** Streams of step-like profile combine smooth, concave, low-gradient segments, correlative with the Late Pliocene-early Pleistocene and middle-late Pleistocene-Holocene surfaces, with steep segments bounded by knick points, correlative with cliffs, commonly fault-controlled. The most prominent steep sectors in the latter correlate with the middle Pleistocene cliff. Such streams are also more widespread along the western coast of the Eastern Lakonia Peninsula. **3)** Streams of smooth, concave, low-gradient profile. These streams form the axial drainage of grabens, probably uplifted at a slower rate than their flanks, or occur in areas of superimposed terraces, also suggestive of a lower uplift rate (e.g. Tasou Rema in the eastern coast of the peninsula; see Figure M.2). An overall eastward tilting of the Eastern Lakonia Peninsula is indicated by the higher altitude of valley heads and the overall steeper profiles of streams flowing towards the west.

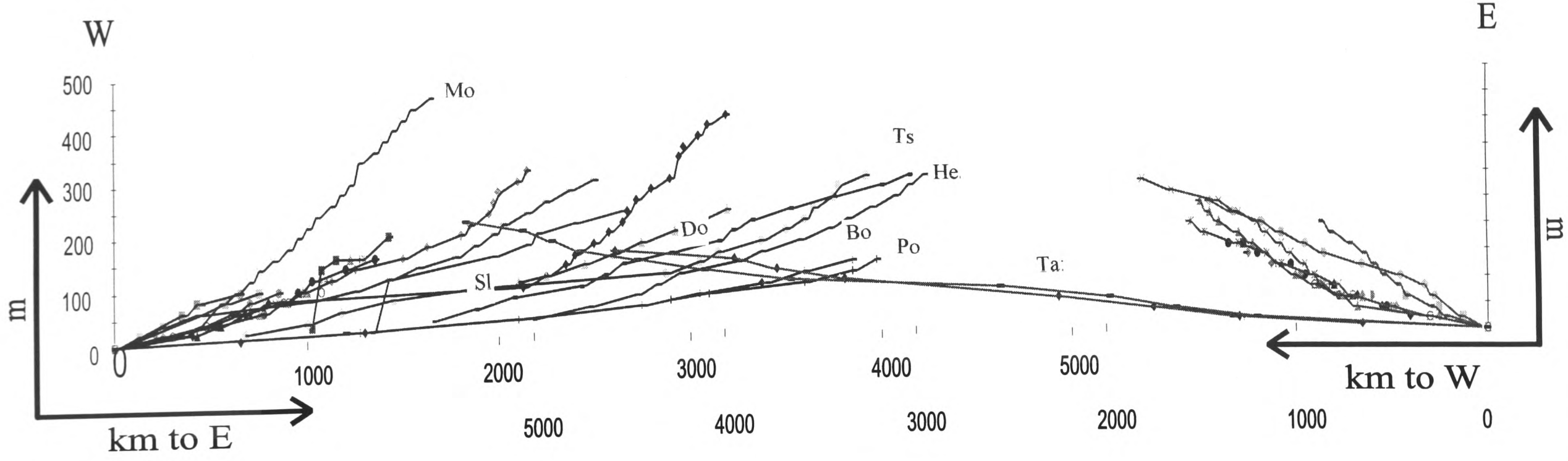

dipping, E-W fault. The stream gradient is exceptionally high (40 %) along a short segment (ca. 60 m) directly downstream of the latter knick point (on "*Phyllite Series*" substratum), The high gradient and the short length of the latter zone possibly resulted from Pleistocene activity of the E-W fault.

4.5.2.6 Cape Maleas: South of the Neapolis Graben, Quaternary and Late Tertiary relief is drained by 4th order streams of dendritic type (Fig. 4.9). These streams developed chiefly on a "*Phyllite Series*" substratum (I.G.E.Y., 1970). By contrast, Tripolis Zone limestone substratum is drained by a low-density network, of immature, 1st and 2nd order streams. Convex knick points, at ca. 70-80 m, are associated with the retreating margins of the Late Pliocene-early Pleistocene pediment (Fig. 4.11).

In the southernmost part of the peninsula (Cape Maleas), Late Tertiary relief on Tripolis Zone limestone is drained by 2nd order streams that occupy broad incised valleys (Fig. 4.9). The latter probably date back to the Late Pliocene, as in other parts of Eastern Lakonia Peninsula. In the area of Ayia Marina, the lower reaches of these valleys were partly buried by inferred early Pleistocene marine sediments (Subunits 3.1, 3.2; Chapter 5), thus delineating an early Pleistocene rias-type coastline (Theodoropoulos, 1973). V-shaped rejuvenation of the latter valley systems took place in later Pleistocene times. The lower reaches of these late Tertiary incised valleys are almost at present sea level locally. This indicates lower rates of uplift (or possibly local subsidence) in the southern part of the peninsula, as compared with other areas further north (e.g. Ano Glikovrisi area, see above).

4.5.2.7 Eastern coast: The peninsular drainage divide is closer to the eastern than to the western coast of the Eastern Lakonia Peninsula (Fig. M.2). The drained substratum is different as well, with more widespread Tripolis Zone carbonate lithologies, and less widespread Pleistocene marine sediments (Figs. 4.1, M.2). The drainage of the eastern coast, as a result, is more immature than that of the western coast, with shorter, less ramified streams, mainly of 1st to 3rd order, and nowhere higher than 4th order (Fig. M.2). The majority of these streams exhibit very steep longitudinal profiles (Fig. 4.11).

The Tasou Rema (Fig. M.2), is the longest, best developed and most ramified stream in the eastern coast of the Eastern Lakonia Peninsula. This stream drains a broad valley, incised into Pleistocene marine and alluvial sediments (as young as post-"Eutyrrhenian" alluvia) and

Tripolis Zone limestone. The Tasou Rema stream follows an eastward course, on the hangingwall side of a large E-W striking, north-dipping fault in bedrock (Fig. M.2). Although smooth, its longitudinal profile is overall convex, with gradients ranging from 0.8% (lower reaches) to 2.7-3.3% (middle-upper reaches) (Fig. 4.11). A convex knick point, at ca. 40 m, is probably associated with a retreating cliff between late Pleistocene relief downstream and early Pleistocene relief upstream. A second knick point, at ca. 80 m, is correlated with the boundary between early Pleistocene relief downstream and Tertiary relief upstream; the latter also coincides with the fault-controlled boundary between bedrock and Pleistocene marine sediments. A further convex knick point, at ca. 200 m, correlates with the trace of a NNE-SSW fault, transversed by the stream.

4.5.3 Controls and evolution of drainage in the Eastern Lakonia Peninsula

From the above is concluded that the drainage of the Eastern Lakonia Peninsula reflects the controls of: 1) lithology, 2) relative sea level change, 3) climate and 4) normal faulting.

Lithology largely controlled drainage density, with dense stream networks in "*Phyllite Series*" terrain and fewer streams per unit area in permeable, Tripolis Zone limestone terrain. The drainage of the Eastern Lakonia Peninsula probably originated in Middle to Late Miocene, after the end of thrusting in the 'external Hellenides' and the initiation of extension (Jacobschangen et al., 1978). The area underwent successive periods of pediment/peneplain formation and uplift during Late Miocene-Pliocene; incision of broad, U-shaped valleys in areas of Late Tertiary relief are correlated with periods of uplift before Late Pliocene. The Late Pliocene pediment functioned as the ultimate base level for such valleys. Normal faulting was an important control on the formation of these valleys, that generally tend to be transverse to faults that separate Late Tertiary from Late Pliocene-Pleistocene surfaces. During the Pleistocene, sea level (base level) cyclicity probably generated a cyclic response of the drainage, with alluviation during highstands (e.g. alluvial terraces correlated with the "Eutyrrhenian" terrace; see above), and incision and advance of streams over emergent marine sediments during sea level fall and lowstands. Regional uplift of the drained areas throughout the Quaternary resulted in gradual advance of a pre-existing drainage system over the emergent benchland topography. New streams were also formed during the Pleistocene; these are confined within the Pleistocene terrace flight. Quaternary normal faulting partly controlled the gradient of the relief and hence the gradient of corresponding streams; knick points along the courses of many streams correlate with traces of normal faults, thus indicating their recent activity.

4.6 SUMMARY-CONCLUSIONS

- Faulting in the Eastern Lakonia Peninsula during Late Tertiary-Quaternary was exclusively normal. NW-SE, NE-SW, N-S (to NNE-SSW) and E-W normal faults are distinguished. Cross-cutting relations do not allow relative dating of the above fault sets, since faults of any set are cut by each other locally. However, over a 10's of km-scale, faults of the first two sets (NW-SE and NE-SW trends) controlled grabens (e.g. Molai Graben), later modified by faults of the latter two sets (N-S faults and, locally, E-W transfers).
- Faults of all the above sets were active throughout the Quaternary.
- N-S faults are the longest mapped faults in the Eastern Lakonia Peninsula (e.g. Molai Fault). Pleistocene relief is largely contoled by N-S faults, suggesting that these are potentially active.
- Extentional joints in Pleistocene sediments are distinguished in the same sets as normal faults, but with a broader variation in strike. These joints are very similar to joints that resulted from Historical and Pleistocene earthquakes, as described from other areas of the Peloponnese.
- A progression of deformation, from normal faulting to jointing, through time is evidenced locally. This progression corresponds to the time span of the last 300-100 ka.
- Closelly spaced joints in Pleistocene sediments, that strike parallel to major faults in bedrock, are interpreted as reflecting the reactivation of faults buried underneath the Pleistocene sediments.
- The following generations of surfaces are recognised within the Eastern Lakonia Peninsula: 1) Late Miocene-Pliocene pediments-pediplains, 2) Late Pliocene pediment, 3) Early Pleistocene terrace(s), 4) Middle Pleistocene terraces, 5) Late Pleistocene terraces ("Eutyrrhenian" and "Neotyrrhenian"), 6) Holocene terrace ("Versilian" or Historical).
- In the Eastern Lakonia Peninsula, the relative altitude and distribution of surfaces of subaerial erosion, marine terraces and Pleistocene shallow-marine sediments allow the distinction of several fault-bounded morphological units, at the scale of 10×20 km, namely: 1) Ano Glikovrisi Horst, 2) Molai Graben, 3) SW Lakonia Benchland and Dokali Rema Graben, 4) Neapolis Graben, 5) SE Lakonia Horst, 6) E Coast.
- The maximum number of uplifted surfaces (10-12) and the highest alitudes (ca. 1200 m ASL) are present within the Ano Glikovrisi Horst. Of these, the 4-5 highest are Late Miocene-Pliocene surfaces of subaerial erosion, whereas the 5-6 lowest surfaces are Quaternary marine terraces.

- The main drainage types present within the Eastern Lakonia Peninsula are parallel and mixed parallel-dendritic.
- The drainage of the Eastern Lakonia Peninsula was controlled by lithology, relative sea level change (i.e. uplift and eustatic sea level change), normal faulting and climate.
- Each fault-bounded morphological unit within the Eastern Lakonia Peninsula is characterised by distinct drainage, reflecting lithology, faulting and relative uplift (or subsidence) of each unit during Quaternary.
- The oldest valleys within the Eastern Lakonia Peninsula are broad, commonly U-shaped and incised into uplifted Late Tertiary surfaces. These valleys were incised throughout Pliocene time; their ultimate base level corresponded to the Late Pliocene pediment. During the Quaternary, drainage advanced over marine terraces that emerged as a result of sea level cyclicity and regional uplift.
- Orientation of the Late Tertiary-Quaternary valley systems transversely to major faults suggests that normal faulting exercised and important control over relief and drainage development in the Eastern Lakonia Peninsula during the last 6-5 Ma.
- Many knick points present along the longitudinal profiles of valleys within the Eastern Lakonia Peninsula are correlated with traces of normal faults. This suggests that these faults were probably active in Pleistocene-Holocene time.

Figure 4. 12: At the foreground, a NNW-SSE trending normal fault cuts late Pleistocene sediments, of inferred Eutyrrhenian age. A fault zone, ca. 3 m wide, is defined by the presence of very closely spaced (1-2 cm) extensional fractures. This fault is parallel to faults through brecciated bedrock (limestone). At the background, the main morphological surfaces present in the Eastern Lakonia Peninsula are: **1)** Late Tertiary surfaces of subaerial erosion, **2)** Late Pliocene pediment-early Pleistocene terrace, **3)** middle and late Pleistocene terraces. From Limnakia Coast, looking N.

Figure 4.13: A cliff (right part of the photograph) separates Late Tertiary relief **(1, 2)** from late Pleistocene terraces **(3)**. The Late Tertiary relief is distinguished into uplifted surfaces of subaerial erosion **(1)** and a mature, graded slope **(2)**, interrupted with incised valleys. At least two erosive marine terraces are distinguished in the background **(3)**, correlated with the Eutyrrhenian and the Neotyrrhenian, respectively. From Epidhavros Limira, looking S (towards Monemvasia).

Figure 4.14 (left): Relief of the SE coast of the Eastern Lakonia Peninsula. The Late Tertiary surfaces **(1)** and the Late Pliocene pediment **(2)** are visible in the skyline. The late Pliocene pediment is bounded by a graded slope landwards and by the early Pleistocene terrace along its seaward side. Middle and late Pleistocene terraces **(3)** follow at progressively lower altitudes. From the road to Dhaemonia, looking S.

Figure 4.15 (left): Fault scarp (fault trend: 120°) in marble; one of the faults that control the Ano Glikovrsisi Mountain Front. Note the presence fault steps and striation, suggesting normal movement of the fault. Panayia, Ano Glikovrisi.

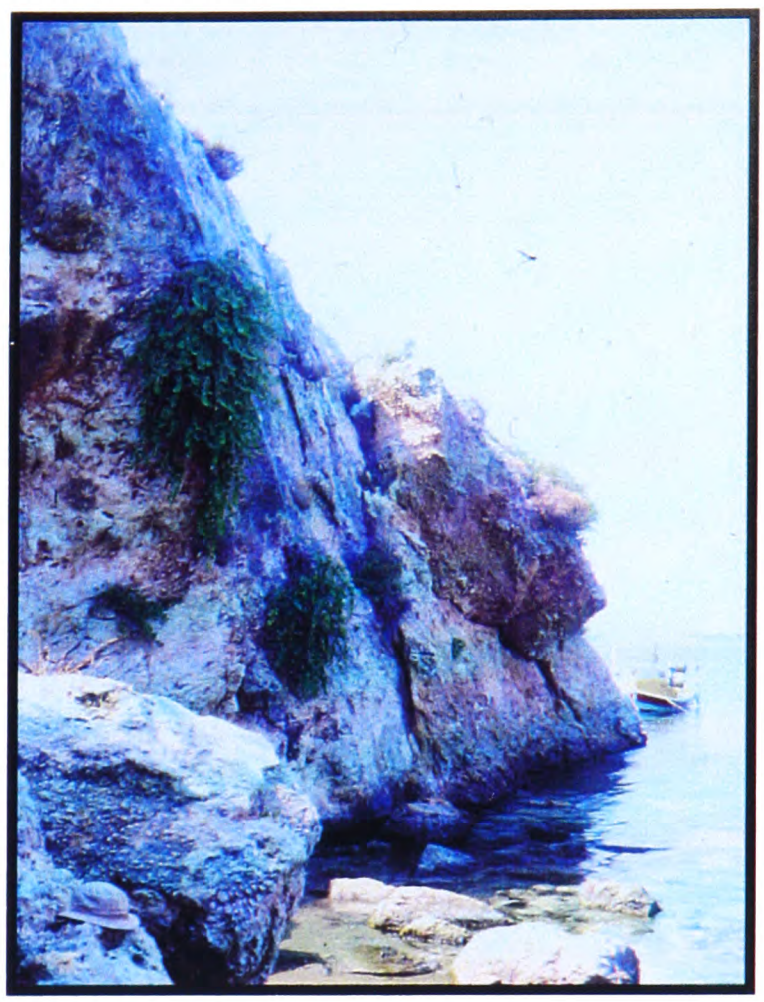

Figure 4.16 (right): ENE-WSW to E-W striking fault in brecciated limestone. The remnant of a late (?) Pleistocene colluvial wedge, deposited during a time of lower sea level, is preserved on the hangingwall side. Most of the colluvial material was probably removed during and after the Holocene transgression. Ca. 600m S of Plytra.

Figure 4.17: A V-shaped valley that crosses the fault-controlled slope that bounds the Molai Graben to the east. The valley incised its course into bedrock (background) and faulted and cemented alluvia (behind the church). This valley has a steep gradient, probably as a result of Pleistocene-Holocene faulting. Asopos.

Figure 4.18 (left): A roughly E-W trending, S-dipping normal fault cuts middle or late Pleistocene marine sediments. Note that the fault zone is defined as a set of closely spaced fractures. Prophitis Ilias.

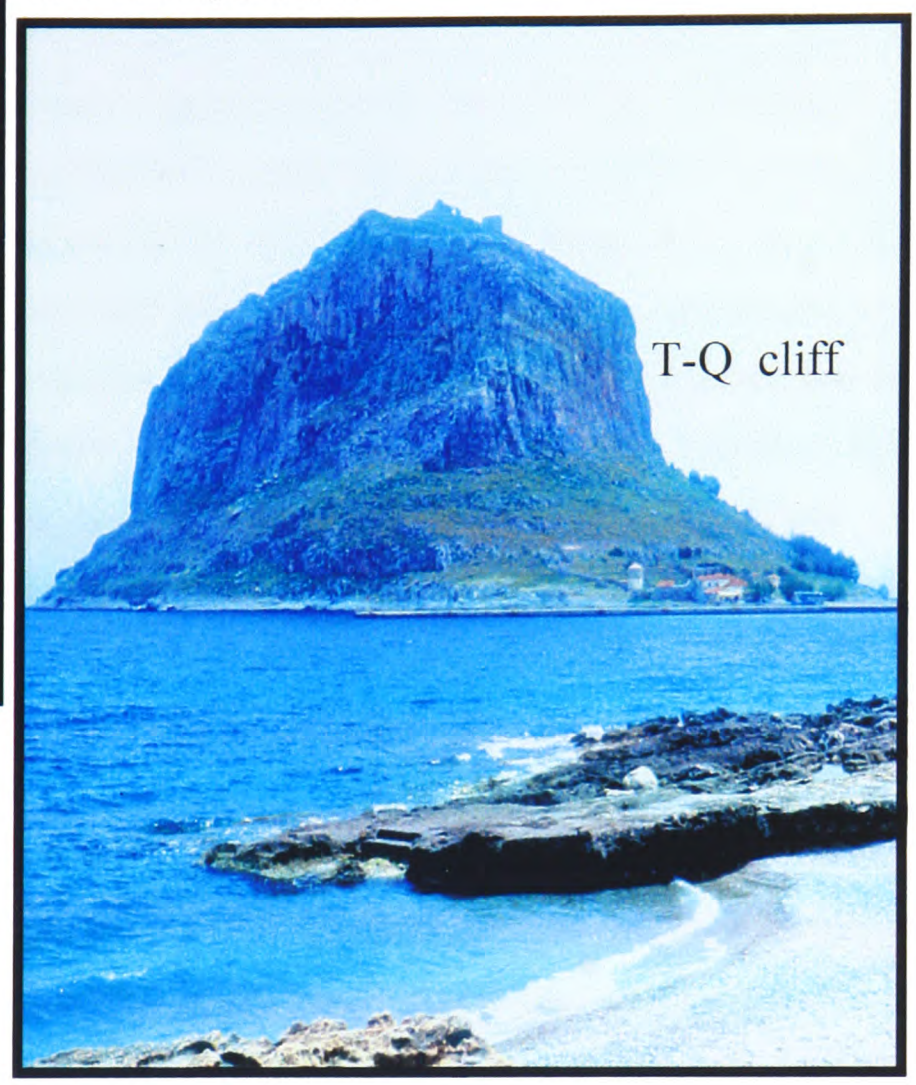

Figure 4.19 (right): A steep cliff **(T-Q)** separates Late Tertiary relief uphill from erosive marine terraces of Pleistocene age downhill. The sediment at the foreground is correlated with the Neotyrrhenian sea level cycle (late Pleistocene). Monemvasia.

Figure 4.20 (below): Late Pleistocene (Neotyrrhenian) terrace, ca. 700 m N of Elea. The terrace comprises upper shoreface to foreshore calcareous sandstone, followed by aeolianite and latest Pleistocene red soil.

CHAPTER 5: PLIO-QUATERNARY SEDIMENTATION IN THE EASTERN LAKONIA PENINSULA

5.1 INTRODUCTION

In this chapter, Pliocene to Holocene, shallow-marine and terrestrial sediments in the Eastern Lakonia Peninsula are described and interpreted in terms of sea level, tectonic and climatic controls. A relative stratigraphy of Plio-Quaternary sediments in this area is erected, based on integrated biostratigraphic, sedimentological, and geomorphological evidence (Chapter 4) and the correlation of sedimentary units with published sea level curves (Imbrie et al., 1984; Martinson et al., 1984; Haq et al., 1988). Finally, evidence concerning sedimentation, normal faulting and landscape development (Chapter 4) is synthesised into a model of geological evolution of the Eastern Lakonia Peninsula during the Late Pliocene-Quaternary.

5.2 CHRONOSTRATIGRAPHIC FRAMEWORK

5.2.1 Tertiary: The presence of Late Tertiary sediments in the Eastern Lakonia Peninsula, although reported by many authors, is not certain, mainly due to gaps in chronostratigraphic information. Onland, outcrops of Upper Miocene marine sediments are generally believed to be absent, as for the Peloponnese in general (Mariolakos, 1975). Dufaure (1977) mentions "Pikermian" (Upper Miocene) red beds in Taighetos pediments, further west (see Fig. 1.1; Chapter 1), but such sediments are not known from the Eastern Lakonia Peninsula. Marine Pliocene ("*Astian*") sediments are reported from many areas of the Eastern Lakonia; dating is based on molluscs (Symeonidis, 1969) and echinoids (Marcopoulou-Diakantoni, 1975). However, later stratigraphic studies, based on nannoplankton (Frydas, 1993; pers. comm., 1998) and foraminifera (Tsaila-Monopolis, pers. comm., 1998), proved that many of the latter sediments were of early Pleistocene, or younger, age. In this work, these deposits are grouped within Unit 3 (Subunits 3.1, 3.2), of early Pleistocene age (see Figs. 5.5, 5.6). However the deposition of Unit 3 may have started in the latest Pliocene. Kowalczyk et al. (1992) attribute these deposits to the Late Pliocene-early Pleistocene.

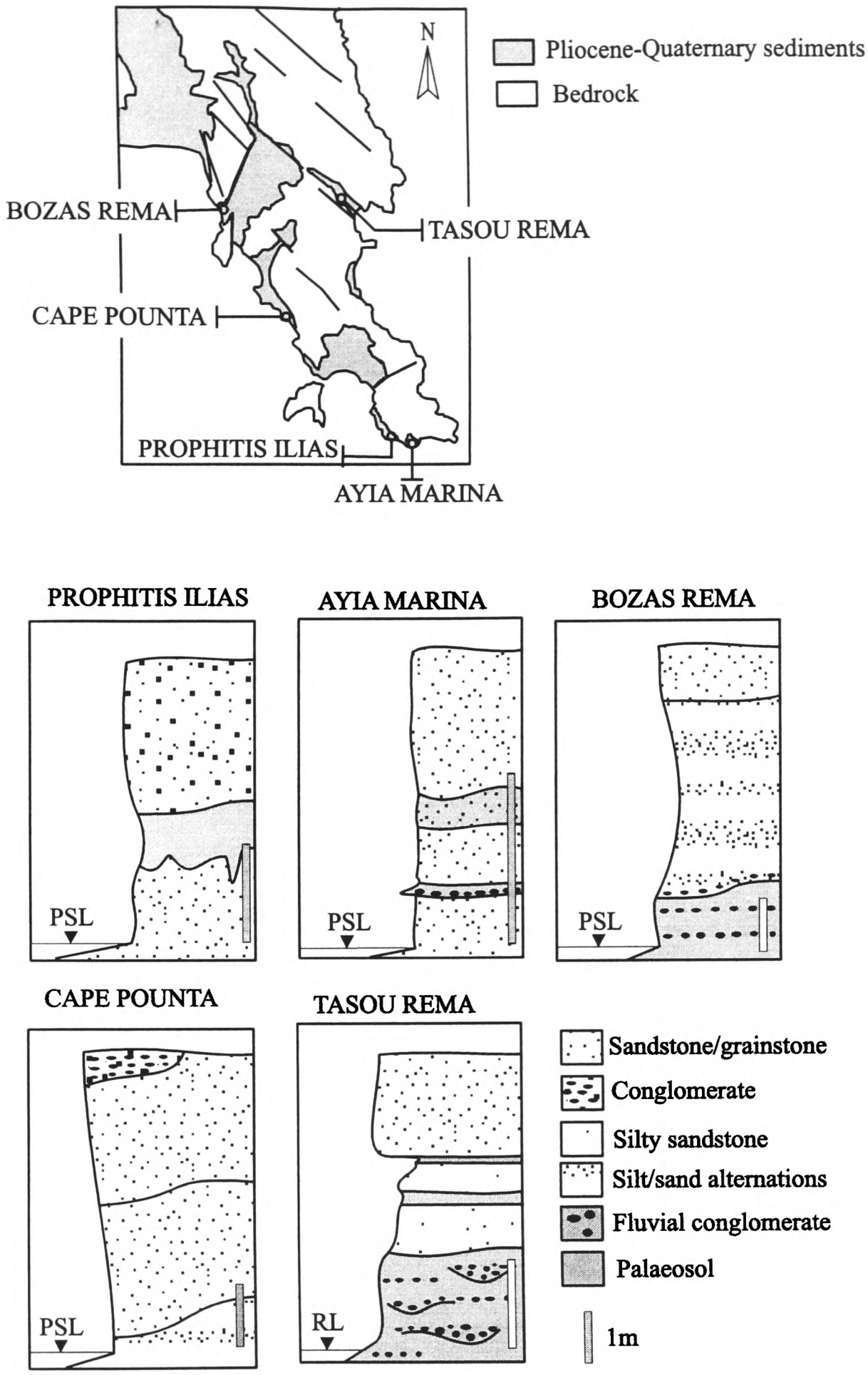

Figure 5.1: Field evidence for the stratigraphic subdivision of Quaternary sediments in the Eastern Lakonia Peninsula adopted in this work. Schematic logs of representative Pleistocene sections show disconformable shallow-marine units, separated by marine ravinement surfaces or subaerial horizons. White: Marine facies; Grey: Subaerial facies.

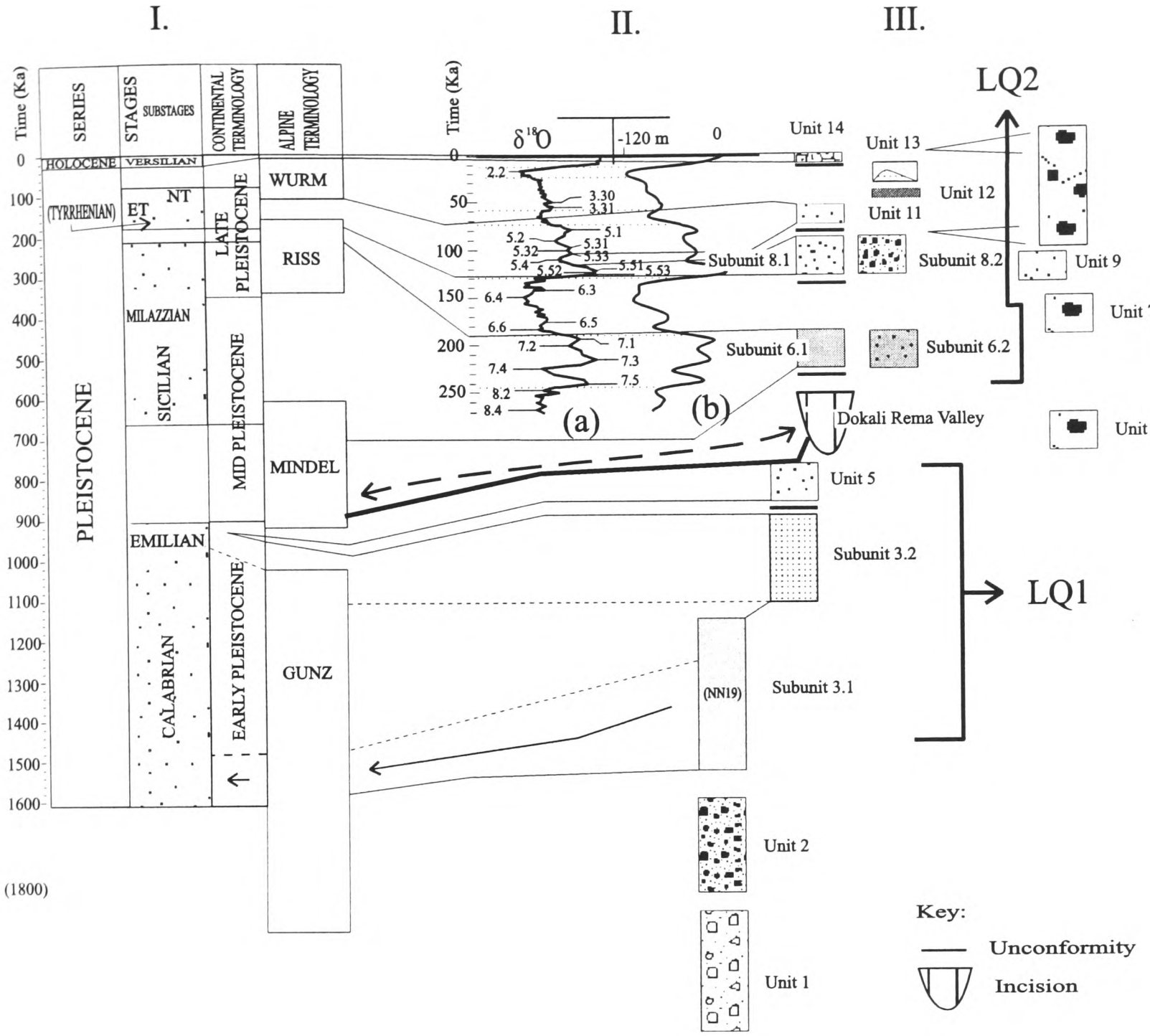

Figure 5.2: Age model for the Quaternary sediments of the Eastern Lakonia Peninsula: Pleistocene-Holocene time scale (the last 1.6 Ma). A Pleistocene stratigraphic scheme (modified from Bonifay, 1975) is shown on the left **(I)**. The beginning of the Pleistocene is set at 1.6 Ma. The easily identifiable "Versilian", "Euthyrrhenian"/"Neotyrrhenian" terraces in **(III)** (Units 14, 11 and 8, respectively) are correlated with the high-resolution oxygen-isotope curve (**II a**; Martinson et al., 1987) and the corresponding eustatic sea level curve (**II b**; Imbrie et al., 1984). In addition, the terraces between the dated early Pleistocene (Subunits 3.1, 3.2) and correlated "Euthyrrhenian"/"Neotyrrhenian" terraces (i.e. early and middle Pleistocene: Units 5, 6; see **III**) are assumed to relate to intervening eustatic highs (column **I**), although with major uncertainties owing to the presence of unresolved, multiple eustatic sea level highs.

5.2.2 Quaternary: Early Pleistocene marine sediments in the Eastern Lakonia Peninsula were first reported by Keraudren (1970, 1971), identified by the presence of the age-specific bivalve *Arctica islandica*. As mentioned above, Frydas (1993) demonstrated an early Pleistocene age for marine sediments previously considered as older ("*Astian*"). Likewise, upper Pleistocene shoreline deposits of "Tyrrhenian" (Last Intergalcial) age were identified by the common presence of the age-specific gastropod, *Strombus bubonius* (Dufaure, 1967, 1977; Theodoropoulos, 1973; Kelletat et al., 1976, 1978; Kowalczyk et al., 1992). Kelletat et al. (1976) and Kowalczyk et al. (1992) identified two distinct terraces with *S. bubonius*, attributed to the "Eutyrrhenian" and the "Neotyrrhenian" substages, respectively. Holocene ("Versilian") shorelines were reported by Kowalczyk et al. (1992). Subaerial conglomerates in the area were correlated with the "Villafrancian" (Pliocene-Pleistocene) boundary by Dufaure (1977), on the basis of palynological evidence (i.e. "*pre-Tiglian/Tiglian floras*"; Sauvage, 1978, 1979). Late Pleistocene red beds were dated indirectly, as they interfinger with "Tyrrhenian" terraces and, directly, by the presence of lithic tools (Kowalczyk et al., 1992). Two distinct lithic technologies are distinguished: a "Mousterian" (Middle Palaeolithic) one, associated with post-"Eutyrrhenian", but pre-"Neotyrrhenian" conglomerates, and a Late Palaeolithic one, associated with post-"Neotyrrhenian conglomerates.

5.2.3 Field evidence for stratigraphic subdivision: A series of five representative sections summarise the basis for the stratigraphic subdivision proposed in this chapter (Figs. 5.1, 5.2. 5.3, M.2). The Quaternary sediments of the Eastern Lakonia Peninsula are subdivided by the presence of intercalated unonformities/disconformities, locally marked by soil or alluvial horizons (Figs. 5.1, 5.25). The maximum number of subaerial unconformities present in any of the examined sections is three (Ayia Marina; see Figs. 5.1, 5.5, M.2). The lowest marine horizon is too proximal to yield any identifiable nannoflora (sand with intralittoral-upper circumlittoral foraminifera fauna); however, it is correlated with dated upper Pleistocene sections elsewhere in the Eastern Lakonia Peninsula (Frydas, 1993, pers. comm., 1998; see below). This correlation is consisted with its stratigraphic position, as the first exposed post-Tethyan unit above bedrock. The second marine horizon, between the two subaerial beds, is dated as middle Pleistocene. This proximal facies (sand with intralittoral-upper circumlittoral foraminifera fauna) probably corresponds to one of the several middle Pleistocene marine units predicted to occur in the Eastern Lakonia Peninsula as a result of sea level cyclicity (see Fig. 5.2, 5.3). The third marine horizon, a shoreface facies similar to the ones below, is correlated with deposits of the "Eutyrrhenian" sea level highstand (ca. 120 ka) elsewhere in the Eastern Lakonia Peninsula, on the basis of altitude and facies

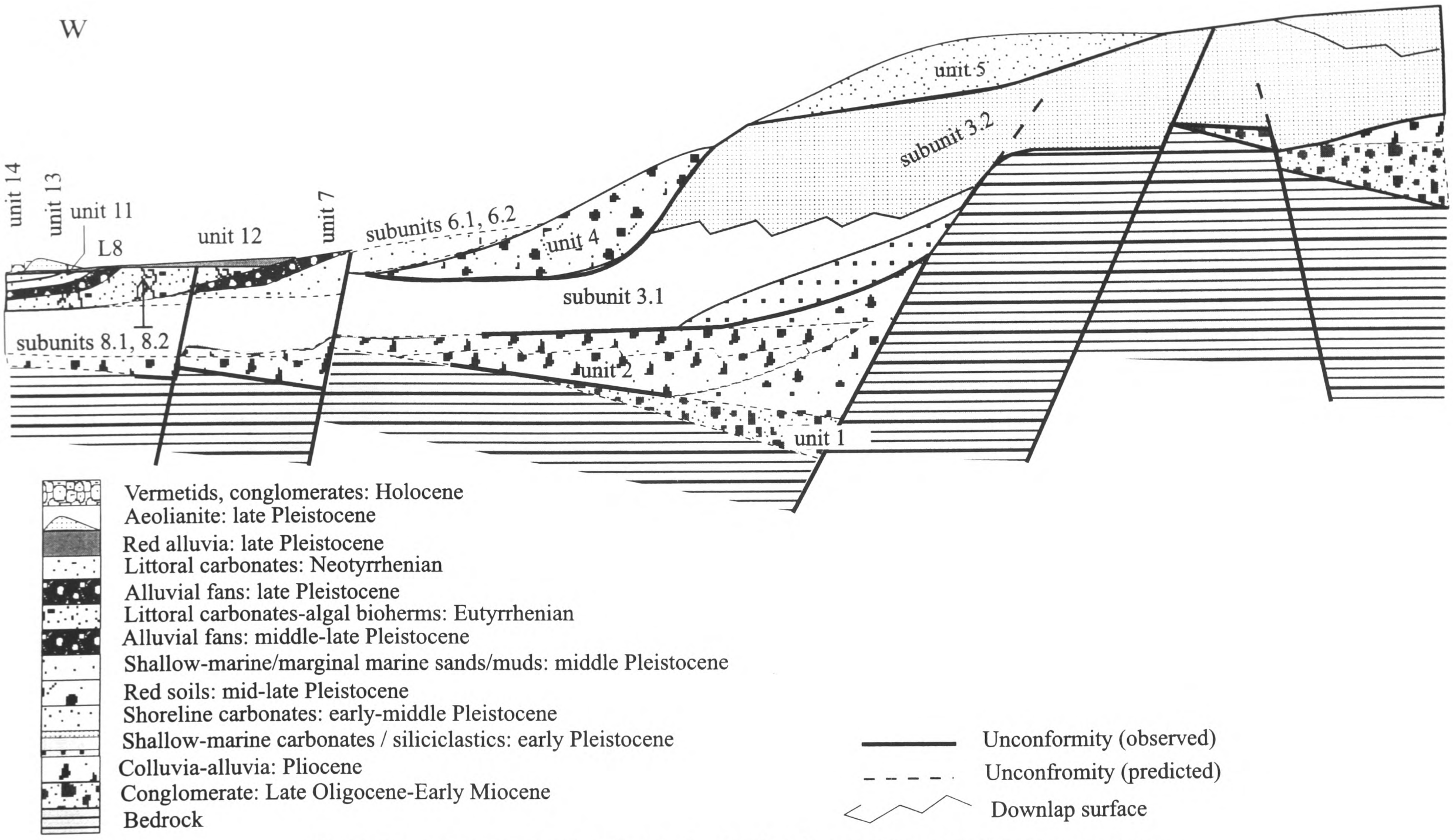

Figure 5.3: Tectonic-stratigraphic diagram showing the relative positions of the Plio-Pleistocene units discussed in the text. The figure illustrates the relationships of each of the units described and is *not* intended as an accurate cross-section, as the logs are projected onto a simplified E-W traverse (approximate horizontal scale: ca. 4 km across). The figure is mainly applicable to the Ano Glikovrisi Horst, where the stratigraphy is more complete.

similarities. Sections from the parts of the Eastern Lakonia Peninsula are also correlated with Pleistocene stages, following the same rationale (Fig. 5.2).

5.3 PLIO-QUATERNARY SEDIMENTS OF THE EASTERN LAKONIA PENISULA

In this work, Late Tertiary-Quaternary sediments of the Eastern Lakonia Peninsula are divided into informal stratigraphic units (see Figs. 5.2, 5.3). This division follows a sequence-stratigraphic approach, similar to that utilised for Late Tertiary-Quaternary sediments in the Messenia Peninsula. The chronological framework includes previously published biostratigraphic and archaeological information (Keraudren, 1970, 1971; Kelletat et al., 1976; Kowalczyk et al., 1992; Frydas, 1993), as well as new biostratigraphic data (nannoplankton; Frydas, pers. comm., 1998; foraminifera; Tsaila-Monopolis, pers. comm., 1998), obtained during the course of this study. Additional evidence includes the presence of at least three alluvial/soil units, locally intercalated with marine sediments in the same section (e.g. Ayia Marina, Fig. 5.1), and also disconformable contacts between shallow-marine sediments. Relative elevation of sediment bodies, depositional architecture and facies are taken into account to infer vertical and lateral relationships between depositional units. The following subdivision of the Plio-Pleistocene sediments in Lakonia into informal units, is proposed:

5.3.1 LATE TERTIARY UNITS:

5.3.1.1 Unit 1: Indurated Palaeosol and breccia: This is the oldest post-Tethyan sediment exposed in the Eastern Lakonia Peninsula: A well indurated, mature, orange brown pisolithic palaeosol crops out in the Dhiakos Hill area, in direct contact with bedrock marble (Figs. 5.3). Concentric flowstone pisoliths (diameter: 10-12 cm) consist of clear, or brown spar. Angular bedrock boulders, correlated with volcaniclastic and marble lithologies, occur in its lower parts (maximum clast size: 65 cm -volcaniclastic). This pissolithic flowstone crust is extensively karstified, with deep (≤3.5 m) solution cavities infilled with younger terra-rossa. The maximum preserved thickness of the unit is <4 m. A series of multiple terraces, with preserved remnants of shelly calcarenite with *Lithophaga*-bored boulders, were eroded on bedrock and lateral equivalents Unit 1 (altitude: 80-120 m). These terraces are correlated with early Pleistocene terraces elsewhere in the Peninsula (see Chapter 4).

Outcrops of indurated orange yellow breccia, in direct contact with carbonate bedrock at many areas in the Eastern Lakonia Peninsula (e.g. Bozas Rema, Plitra; see Fig. M.2) are correlated with Unit 1. These indurated breccia, that commonly form a m-thick carapace over normal faults, were affected by later faulting.

Interpretation: The age of Unit 1 is pre-Pleistocene, but field evidence does not allow any more specific dating. Nevertheless, its advanced diagenesis and its direct contact with the bedrock suggest a possible Late Miocene-Pliocene age.

5.3.1.2 Unit 2: Red Alluvium (Figs. 5.5, 5.6, 5.7, 5.28): This unit encompasses alluvial sediments older than the earliest dated Plio-Pleistocene sediments in the area. A typical section is situated on Dhiakos Hill, ca. 140-150 m, on the footwall of the NNE-SSW Molai Fault (Figs. 5.3, 5.7). There, alternations of matrix and clast supported, crudely bedded conglomerate and pebbly red silt beds cover "*Phyllite Series*" bedrock. Conglomerate beds (bed thickness: 20-60 cm) with erosive bed boundaries, dip at ca. 20° to the SSW (basinward). The clasts are angular, evenly shaped boulders (maximum clast size: 40 cm), correlated with marble and volcaniclastic lithologies. Individual beds are poorly sorted and structureless. Both fining- and coarsening-up trends are present. Intercalated red silt beds are rich in bedrock pebbles that form lenticular accumulations, ca, 1-2 m long locally. The uppermost silty bed consists of pebble-poor terra rossa. These subaerial facies are unconformably overlain by early Pleistocene shoreline facies of the Unit 3.

Interpretation: The coarsening-up nature of many beds, matrix supported texture and poor sorting indicate deposition by mass flow processes. Erosive lower and upper bed boundaries suggest a channel fill origin, probably within a braid stream environment, as suggested by the laterally extended, tabular bed geometry (Miall, 1992). Intercalated beds of pebbly red silt probably represent interfluve deposits. Conglomerate lenses within the latter are interpreted as the fill of small channels, or bars. High depositional dip and proximity to major fault-controlled escarpments suggest that these sediments were deposited as parts of a prograding alluvial fan, probably corresponding to the middle fan area.. Similar middle fan facies are described from the Quaternary of Cyprus (Poole, 1992; Poole and Robertson, 1998). The uppermost, pebble-poor terra rossa facies was deposited in a lower energy environment. It is interpreted as a palaeosol, possibly reflecting autocyclic changes within the middlefan zone, although it could also reflect from a pause in fan progradation accompanied with vegetation growth (Miall, 1992).

Figure 5.4 (following page): Geological map of the Ano Glikovrisi-Elea area (Ano Glikovrisi Horst and Molai Graben). Pleistocene sediments are cut by the N-S Molai Fault and NNW-SSE faults (Ano Glikovrisi mountain front). Valleys incised into Pleistocene marine sediments were partly infilled with middle and late Pleistocene alluvia. A geomorphological sketch-map of the same area is shown in Fig. 4.8.

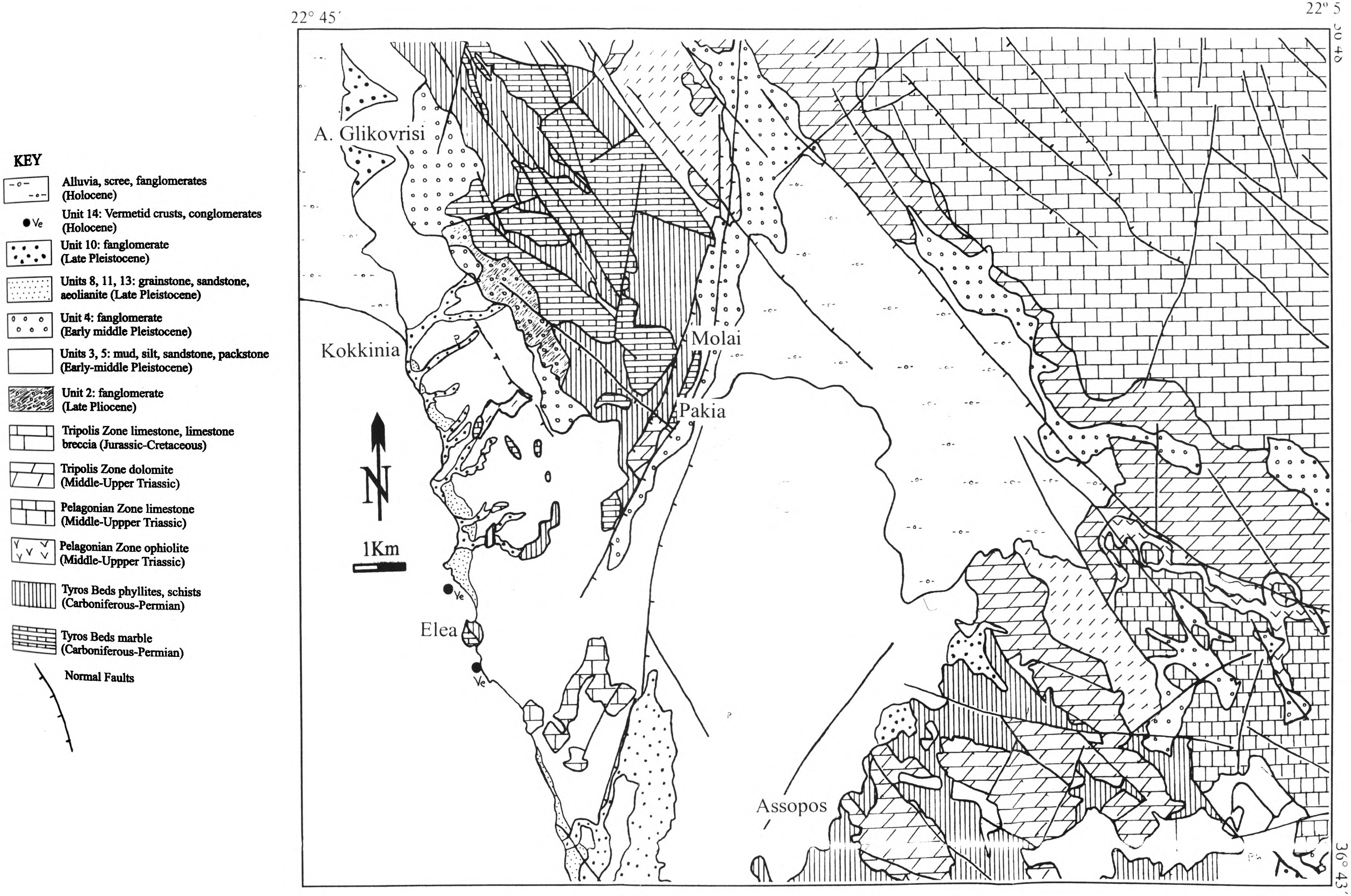
22° 45′
22° 5
36° 43′
22°45′
22° 59
KEY
Alluvia, scree, fanglomerates (Holocene)
Unit 14: Vermetid crusts, conglomerates (Holocene)
Unit 10: fanglomerate (Late Pleistocene)
Units 8, 11, 13: grainstone, sandstone, aeolianite (Late Pleistocene)
Unit 4: fanglomerate (Early middle Pleistocene)
Units 3, 5: mud, silt, sandstone, packstone (Early-middle Pleistocene)
Unit 2: fanglomerate (Late Pliocene)
Tripolis Zone limestone, limestone breccia (Jurassic-Cretaceous)
Tripolis Zone dolomite (Middle-Upper Triassic)
Pelagonian Zone limestone (Middle-Uppper Triassic)
Pelagonian Zone ophiolite (Middle-Uppper Triassic)
Tyros Beds phyllites, schists (Carboniferous-Permian)
Tyros Beds marble (Carboniferous-Permian)
Normal Faults
A. Glikovrisi
Kokkinia
Molai
Pakia
N
1Km
Ve
Elea
Ve
Assopos

The Unit 2 fanglomerate predates the early Pleistocene marine transgression of the 180-220 m pediment (see Chapter 2). Despite lack of direct stratigraphic evidence, the absence of cementation and karstification suggests that this unit is probably younger than the Unit 1 (pissolithic palaeosol) that covers more proximal sectors on the same pediment. A Pliocene to early Pleistocene (but pre-"Calabrian") age can, thus, be proposed for Unit 2.

5.3.2.1 Unit 3: Early Pleistocene shallow marine mud-sand/sandstone: This is the most widespread unit within the Eastern Lakonia Peninsula, extending all along the western and southern coasts and parts of the eastern coast (Figs. 4.1, 5.3, 5.4, M.2). The extensive early Pleistocene terrace is formed above sediments of this unit (Chapter 4). Unit 3 exhibits a shallowing-up trend, with a wide variation in facies from open marine, lower shelf mud, fine-grained sand (in the NE part), to coarse grained, upper shelf to shoreface calcareous sandstone (in the S) (Figs. 5.8, 5.9). Because of the considerable facies variation, outcrops of this unit from different areas are described separately:

5.3.2.1.1 Ano Glikovrisi Horst (Subunit 3.1)

Distal outcrops: In the NW part of the peninsula (Kokkinia-Elea; Figs. 5.3, 5.6. 5.8, 5.21) the lowest horizons of Unit 3 crop out at Kokkinia-Mourtitsa Rema. The lowest exposed beds comprise olive green calcareous mud with small thin-shelled bivalves and bryozoa. The microfauna are very rich, including benthic and planktic foraminifera, ostracods, bryozoa and fish-scales (Table 5.1). These beds are succeeded by laminated grey marl (laminae thickness: 1-2 cm) with 5-10 cm long oxidised burrows and cylindrical or irregular nodules. The sediment is parallel-bedded (bed thickness: 0.5-1.5 m); bedding is defined by 1-3 cm thick bioturbated layers, with oxidised *Planolites* burrows (diameter: 2 cm / length: 5-10 cm). Elongate biserial forms of the *Bulimina-Brizalina* group are predominant. Alternating grey and green mud with thin-shelled bivalves follows up-section, coarsening up into brown-grey, micaceous, sandy mud with cemented nodules and burrows. The mollusc fauna include mud-dwelling gastropods bivalve moulds. A high-density, but not very diverse, microfaunal assemblage is present, with mainly benthic foraminifera (Table 5.1) and marine ostracods.

Figure 5.5 (following page): Geological map of the Neapolis-Ayia Marina area (eastern side of the Neapolis Graben and Cape Maleas). Pleistocene sediments are cut by NNW-SSE, N-S and E-W faults. Note the widespread presence of alluvial fans, associated with normal faults. Pleistocene shallow-marine facies around Ayia Marina define a ria-type palaeoshoreline. A geomorphological sketch map of the same area is shown in Fig. 4.9.

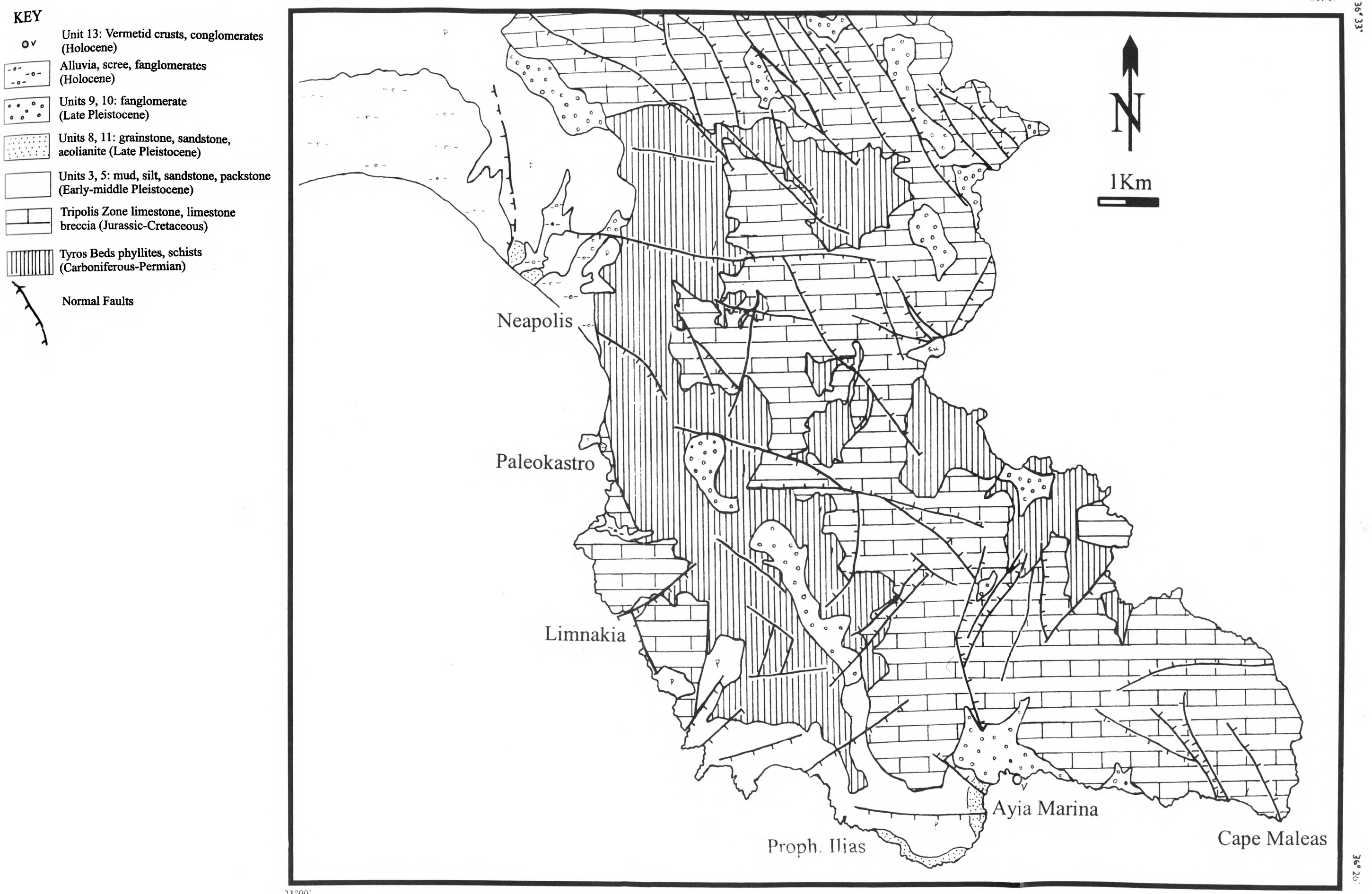
KEY
Unit 13: Vermetid crusts, conglomerates (Holocene)
Alluvia, scree, fanglomerates (Holocene)
Units 9, 10: fanglomerate (Late Pleistocene)
Units 8, 11: grainstone, sandstone, aeolianite (Late Pleistocene)
Units 3, 5: mud, silt, sandstone, packstone (Early-middle Pleistocene)
Tripolis Zone limestone, limestone breccia (Jurassic-Cretaceous)
Tyros Beds phyllites, schists (Carboniferous-Permian)
Normal Faults
23°00'
23° 12'
36°33'
N
1Km
Neapolis
Paleokastro
Limnakia
Ayia Marina
Proph. Ilias
Cape Maleas
36° 20'
23°00'
23°12'

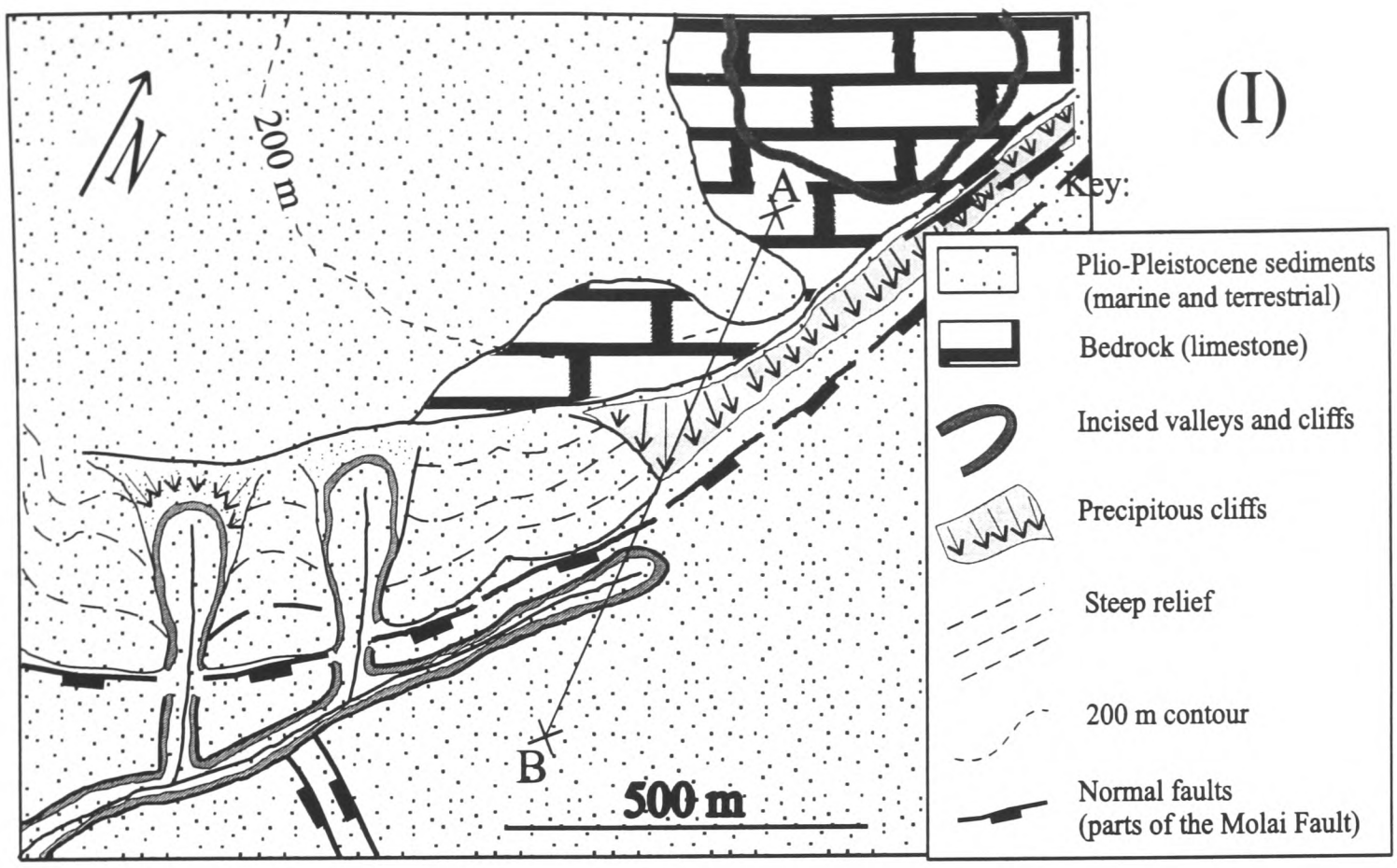

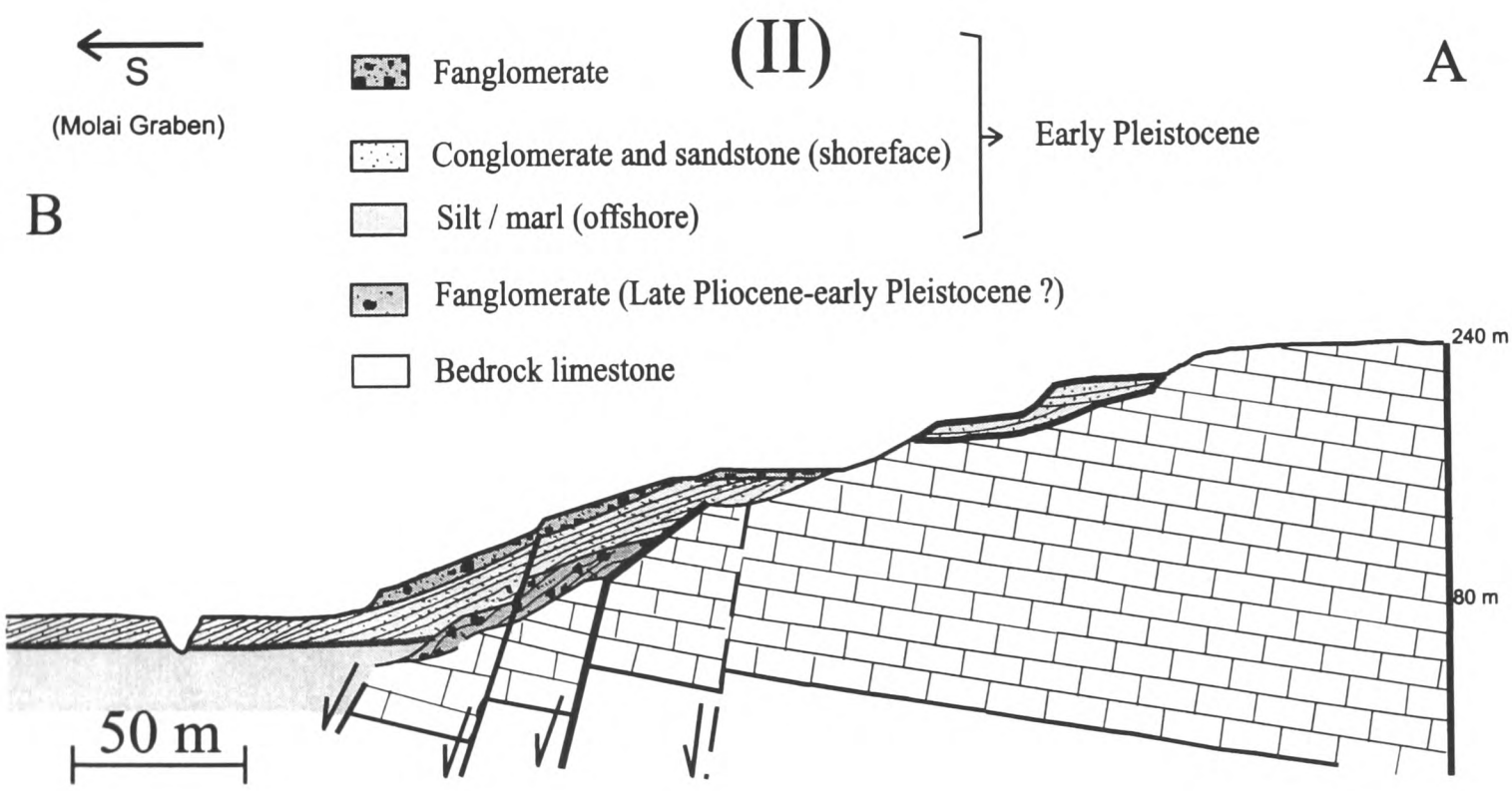

Figure 5.6: Field sketch **(I)** and cross-section **(II)** of the western flank of Molai Graben near Dhiakos Hill (see Fig. 5.3 for location). NNE-SSW faults cut early Pleistocene clinoforms that dip basinwards. Four erosional surfaces are distinguished on the footwall of the Molai Fault; three are uplifted marine terraces formed on early Pleistocene shallow-marine sediments. On the hangingwall side, coarse-grained clinoforms prograded over finer-grained offshore facies; their contact is a maximum flooding surface (MF). Cemented fanglomerates of inferred early to middle (and locally later) Pleistocene age prograded over the emergent marine sediments. Late Pleistocene valley incision post-dated the deposition of the cemented fanglomerates.

The maximum visible thickness of these lower, finer-grained facies is ca. 60 m. These are succeeded by granular conglomerate to coarse calcareous sandstone. Their contact with the underlying fine-grained sediments is either sharp or transitional, depending on the particular section. A gradual transition is accomplished via zones of tabular, matrix-rich beds of granular conglomerate that alternate with heavily bioturbated, silty fine sand (zone thickness: ca. 2-2.5 m). The latter pass up to low-angle cross-bedded tabular conglomerate, succeeded by horizontally bedded, SW- dipping (12° to 240°) granular conglomerate with oxidised bands, and coarse sandstone with current scours. Conglomerate beds are relatively well sorted, clast-supported, with angular bedrock clasts. Open-work structure is locally present, with interparticle porosity occluded by milky-white spar cement. Low angle cross-laminated sandstone with normally graded laminae forms the highest preserved parts of the sequence. The fauna in these upper parts consist of a few, poorly preserved, thick-shelled bivalves (*Ostrea sp.*, *Pecten sp.*). Pervasive *Rhizocretion* calichification and subhorizontal or locally bifurcating caliche crusts (mm to cm-thick) occur in these upper parts. The total thickness of the coarse topsets is ca. 8-10 m.

The ca. 40-80 m terrace is formed above these sediments, covered with brown soils with pottery fragments (Historical age). This terrace is not an uninterrupted surface. Low-relief cliffs (maximum height: c. 1.5-3.m) occur, associated with dense sets of closely-spaced fractures, are interpreted as low-throw normal faults.

Interpretation: The lower, grey mud outcrops are interpreted as offshore deposits. On the basis of the presence of *Cassidulina laevicata* var. *carinata,* together with diverse *Buliminidae* (including *Bulimina marginata*), the benthic microfauna exemplify the *"C. levicata carinata - Bm. marginata assemblage" sensu* Amorosi et al. (1998), characteristic of an outer shelf environment. Both the above species are found at depths >80 m in the present-day Adriatic Sea (Jorissen, 1988- from Amorosi et al., 1998). The presence of the genus *Gyroidina* spp., the high proportion of planktic foraminifera in the fauna and *Thalassinoides* bioturbation, confirm a bathyal palaeoenvironment of these sediments (Blanc-Vernet, 1969, Pemberton et al., 1992). The presence of typically intralittoral/circumlittoral benthic foraminifera assemblages (*Ammonia* spp.+*Elphidium* spp. and *Valvulineria bradyana*+*Bulimina elongata*+*Cassidulina laevicata* var. *carinata*, respectively, *sensu* Amorosi et al., 1998) among bathyal taxa suggests that the former were transported from shallower depths, possibly by storm-induced offshore currents. Nevertheless, no macroscopic evidence of storm activity (e.g. hummocky cross-stratification) was observed. Oxygen deficiency of the sea bottom is suggested by the

relative abundance of *Brizalina spathulata, Br. alata,* several *Buliminidae* and *Valvulineria bradyana* (Amorosi et al., 1998). These hypoxic conditions (that also allowed preservation of fish scales) were probably brought about by high fluvial runoff, as indicated by the presence of characteristically hyposaline foraminifera taxa (*Brizalina spp., Bulimmina marginata*). Coexistence of the latter with the normal marine to slightly hyposaline species *Cassidulina laevicata* var. *carinata* (Amorosi et al., 1998) possibly indicates temporal changes in intensity of fluvial runoff. All the above suggest that deposition of the dark grey mud took place in the offshore zone, at a depth probably >80 m, in the vicinity of a river mouth. These sediments are, thus, interpreted as prodeltaic facies. The planktic foraminifera fauna are not age-diagnostic. Although quantitative faunal analysis was not performed, all the taxa identified comprise warm and temperate water forms (Blanc-Vernet, 1969). Therefore, deposition of this unit probably took place during a "warm" interglacial stage. Nannoplankton content (Frydas, 1993, pers. comm., 1998) suggested an earliest Pleistocene age (NN 19a biochronozone *sensu* Martini, 1971). These sediments are, thus, correlated with the sea level cycle 3.9 of the early Pleistocene, *sensu* Haq et al. (1988) (Fig. 5.2).

The brown silty sand higher up was probably deposited at shallower depth, around the upper offshore-shoreface transition, within the same deltaic system. Shallowing-up is suggested by coarser grain-size, high terrigenous content (e.g. mica), the predominance of intralittoral foraminifera assemblages (mainly *Ammonia* spp. and *Elphidium* spp.) and the absence of characteristic deeper water taxa (Blanc-Vernet, 1969; Amorosi et al., 1998). Mixing of fresh and normal marine water is indicated by the presence of both hyposaline (e.g. *Elphidium granosum, Fursenkoina schreibergsiana*) and normal marine (e.g. *Elphidium crispum*) taxa (Amorosi et al., 1998).

Sandstone/conglomerate beds further up-section are interpreted as upper shoreface-foreshore deposits on the basis of grain size, sedimentary structures, and terrigenous character (Walker and Plint, 1992). Alternations of coarse sandstone with fine silty sand beds are interpreted as storm-dominated lower shoreface deposits, with coarse sandstone beds representing storm deposits and fine sand beds representing fair-weather deposition (Reading and Collinson, 1996; Reynolds, 1996). The uppermost, amalgamated sandstone/conglomerate, with low-angle planar cross-lamination, are interpreted as foreshore deposits. In some sections, sharp contact of the latter facies with underlying upper offshore-lower shoreface silty sand probably resulted from erosional removal of the upper shoreface deposits during relative sea level fall (a possible effect of storm wave activity) (Milton and Myers, 1996).

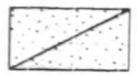
Sandstone / grainstone-packstone


Conglomerate

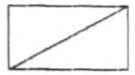
Mud / marl


Algal boundstone


Caliche (chalky / duricrust)


Red soil


Nodular caliche


Lenticular caliche

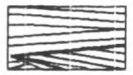
Low angle planar cross-lamination (-bedding)


Trough cross-lamination (-bedding)


Hummocky cross-stratification

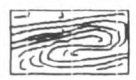
Slumps, disrupted bedding

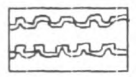
Convolute lamination


Current scours


Pectenidae


Ostrea


Glycimeris


Gastropods


Vermetidae

Scaphopods


Brachiopods


Echinoids


Thyssanopods (Balanus sp.)


Scleractenian corals (Cladocora caespitosa)


Branching bryozoa


Encrusting bryozoa


Serpulid worms


Rhodoliths

Figure 5.7: Key to logs in this chapter.

Proximal outcrops (Fig. 5.22): Higher up, in more inland parts of the same terrace surface, more proximal facies of Subunit 3.1 are exposed (Fig. 5.8). They start with well-sorted, medium grained yellow sand and conglomerate, with *Pecten* sp. and *Ostrea* sp., and pass upwards and eastwards into low-angle cross-laminated fine sand. This coarsens up into tangential cross-beds of coarse sand, followed by alternations of very coarse, well-sorted sand and granular conglomerate (maximum clast size: 0.5 cm; bed thickness: ca. 2-6 cm), with occasional beds of fine, well sorted, laminated sand (bed thickness: ca. 5-6 cm). The sediments gradually coarsen upwards into parallel bedded, clast-supported conglomerate (maximum clast size: 3-5 cm), with well sorted and rounded, predominately rod- and disc-shaped marble pebbles. This conglomerate is trough cross-bedded at metre-scale; individual bedsets can be followed for ca. 3 m laterally. The sediments dip to the SE-S (160-190°) at 20-23° and are cut by numerous small normal faults (maximum throw: 25 cm) of predominantly ENE-WSW strike (70-77°). No fossils were found in this facies. That conglomerate is succeeded by coarse pebbly sand, parallel bedded and steeply dipping to the SSW (50° to 200°). This high angle of dip, exceeding the angle of repose, probably results from fault-induced tilting. Conglomerate and pebbly sand are followed by a 12 cm-thick calichified layer and then by 1.5 m of brown mud with a dense / non-diverse fauna of gastropods and articulated freshwater ostracods. The mud bed is affected by pervasive calichification (caliche nodules); also a 20-30 cm thick chalky caliche layer has developed in its upper parts. This layer contains numerous spar-infilled moulds of gastropods and ostracods and its upper few cm are thinly laminated (see also Chapter 6). Above a sharp surface, alternations of calichified mud follow, similar to the ones described. They dip to the SW (220°) at 9-12°. The minimum thickness of these upper muddy facies is ca. 6 m. These sediments are covered by younger red alluvia of two distinct generations (probably of middle and late Pleistocene age; see below).

Interpretation: These sediments are interpreted as prograding shoreface to backshore facies, probably resulting from progradation of a fan delta system. The amalgamated bivalve-rich sand and conglomerate beds are interpreted as upper shoreface deposit, on the basis of faunal content (abraded thick-shelled taxa), coarse grain size and sedimentary structures (Reading and Collinson, 1996; Reynolds, 1996). Erosional bases and truncation of beds probably resulted from storm-wave activity. Low-angle cross-laminated sand, higher up, is interpreted as a foreshore deposit. Non-fossiliferous conglomerate, upwards and more proximal, is interpreted as fluvial channel-fill, as indicated by the absence of marine fauna and by metre-scale trough-cross bedding. The width of cross beds suggests deposition in wide, shallow channels. These channels probably represent distal braid streams, as

suggested by grain size (coarse sand-fine pebbles), good sorting and lateral amalgamation of channel-fill beds. The mud with freshwater ostracods and gastropods that comes above was probably deposited in interchannel ponds. The high density / low diversity character of this fauna suggests ecologically stressed conditions. Alternations of caliche-topped muddy beds probably result from periodic desiccation, reflecting an ephemeral, intermittent character of the ponds. Sedimentation within the latter probably terminated with their desiccation, possibly caused by their "silting up". Development of such ponds probably took place in conditions of low relief and elevated water table, as conditions that commonly prevail in the lower reaches of a braid plain system (Postma, 1996). The topsets of Subunit 3.1, therefore, were deposited in a braid plain-braid delta, prograding over shallow to deeper marine facies to the west.

Interpretation of subunit 3.1 as a whole: The above topsets, together with the earliest Pleistocene prodeltaic sediments further west (offshore) and down-sequence, constitute a prograding deltaic system. In sequence-stratigraphic terms, this progradational architecture probably developed during the highstand stage ('highstand systems tract") of the sea level cycle 3.10, *sensu* Haq et al. (1988). As evidenced by the grain-size and good sorting of channel fill deposits, as well as by the depositional environment of interchannel deposits, the drained area was of low relief. Since the Subunit 3.1 terrace sediments cover a pre-Pleistocene pediment (Kelletat et al., 1976; also Chapter 4), it is reasonable to argue that the low-relief morphology was largely inherited from the pre-Pleistocene surface.

5.3.2.1.2 **Dokali Graben and SE coast (Subunit 3.2: Figs. 5.8, 5.9, 5.10, 5.20):** South of the Molai Graben (Fig. M.2), the early Pleistocene Subunit 3.2 is represented by the following succession: In a proximal section, the lowest exposed horizons, situated on the road from Plitra to Dhaemonia (Fig. M.2), constitute a wedge-shaped body of disorganised, coarse, oligomict breccia-conglomerate (Fig. 5.10). This conglomerate is bouldery, very poorly sorted, matrix- to locally clast-supported, with matrix of orange-yellow sandy silt. The sediment is generally chaotic and structureless, with the exception of a few imbricated clasts. The clasts are poorly rounded; many are slab- or disc-shaped. Most clasts were derived from Pleistocene terrace sandstone or conglomerate (ca. 43%), but bedrock limestone and volcaniclastic lithologies are also present (23% and 30%, respectively). Reworked red conglomerate pebbles also occur (5%); these are correlated with pre-Pleistocene subaerial deposits. Bedrock slabs are much better-rounded than Pleistocene terrace clasts.

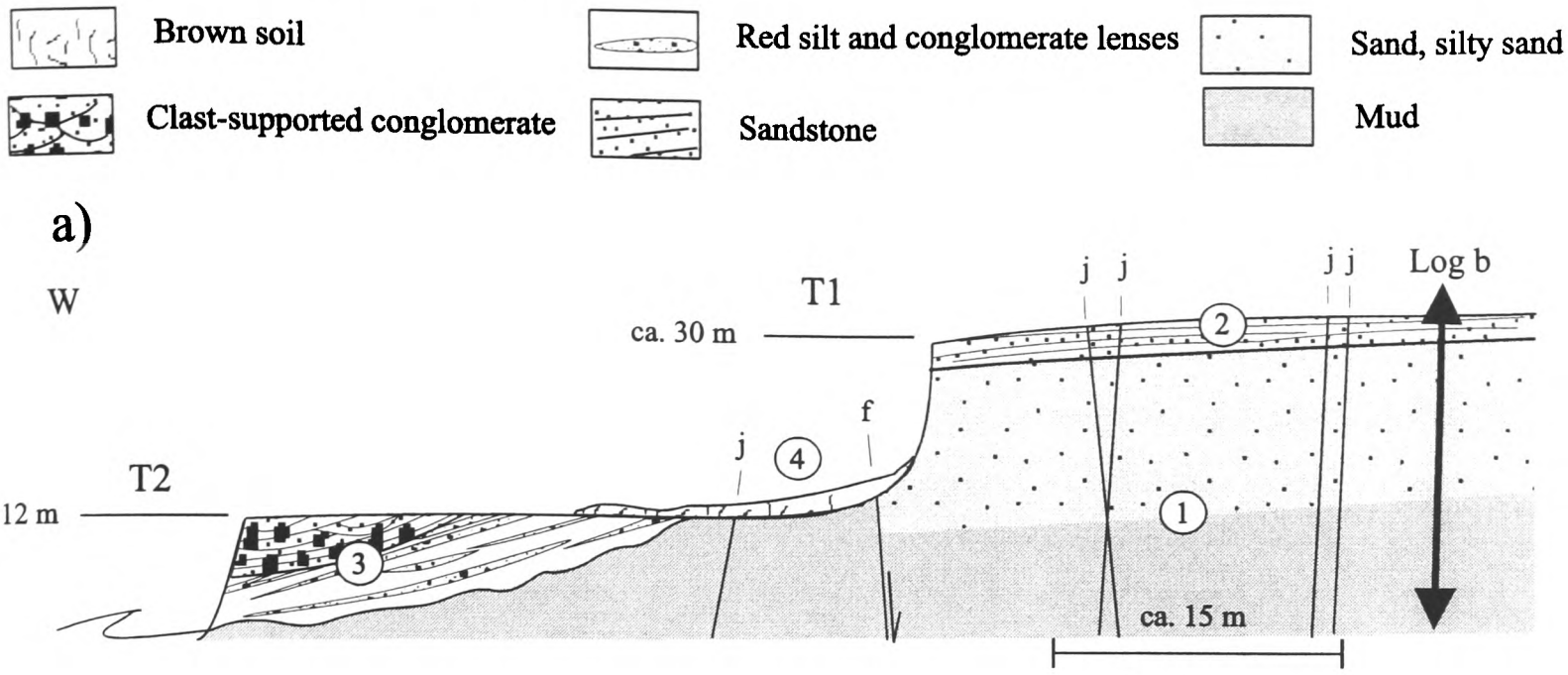

Figure 5.8: Logs of early Pleistocene shallow-marine sediments from the Eastern Lakonia Peninsula. For location of logs see Fig. M.2 (back-pocket). **a)** Section at the Kokkinia Coast (for location see Fig. 5.4). Early Pleistocene (NN 19a) offshore mud, to fine sand **(1)**, is overlain by sandstone/conglomerate of a prograding shoreface **(2)**; the latter probably corresponds to a middle Pleistocene sea level cycle. Channels incised in both **(1)** and **(2)** were infilled by coarsening-up red alluvia **(3)**, deposited by prograding alluvial fans. These are correlated with middle Pleistocene, pre-Tyrrhenian alluvia elsewhere. The ca.12m terrace eroded on the latter is correlated with the "Eutyrrrenian" base lavel; this is covered by brown alluvia and soils with pottery fragments **(4)**. Joints and faults affected the early and middle Pleistocene marine sediments but not the late middle Pleistocene alluvia. **b)** Logs of coarsening-up, offshore to shoreface/foreshore sediments of early Pleistocene age (Subunit 3.1). Site same as Fig. 5.9.a. **c)** Log of the progradational, coarsening-up top parts of the early Pleistocene Subunit 3.2 in Dhaemonia.

This sediment exhibits proximal to distal relationships from the eastern (inland) to the western (seaward) parts of the section (maximum exposed thickness along section: ca. 20-30 m; Fig. 5.9.a). In the most proximal, eastern part of the section (Fig. 5.9.b.1), there is a marked coarsening -then fining up trend (maximum clast size: 36 cm; reworked terrace clast -in the middle of the section). The macrofauna include unabraded, to slightly abraded *Ostrea* sp. and *Pectenidae* (*Pecten* sp., *Chlamys* sp.). The microfauna is relatively poor, including the mainly benthic and few planktic taxa (Table 5.1). This facies passes gradually into clast-supported angular conglomerate, with smaller clasts (maximum clast size: 15 cm) of similar provenance and characteristics.

In a more distal setting (Fig. 5.9.b.2: ca. 30 m W of the previous), the first 1.70 m comprise pale-coloured pebbly silt with *Balanus* sp. fragments. The sediment coarsens up into massive, chaotic, matrix-supported conglomerate (maximum clast size: 17 cm), with matrix of creamy-pale (or secondarily orange-yellow stained) mud. The conglomerate deposit fines upwards.

About 15 m further west (Fig. 5.9.b.3), the section comprises two distinct fining-up conglomerate units. The lower unit is matrix-supported, with matrix of yellow bioclastic silt. Clast provenance and shape are similar to those of more proximal sections. The maximum clast size is ca. 1.2 m at the lowest visible parts of the deposit. The maximum exposed thickness is ca. 2.5 m. This bed is succeeded by sharp-based bouldery conglomerate (maximum clast size: ca. 40 cm), fining up into crudely laminated silt (thickness: ca. 4-5 m). The macrofauna include thin-shelled bivalve fragments and scaphopods (*Dentalium* sp.).

Figure 5.9 (following page): Pleistocene terrace fight in the coast of Dokali Rema (for location see Fig. M.2). **a:** Cross-section, showing early to late Pleistocene terraces. The terraces were formed on progradational shoreline facies, unconformable above early Pleistocene clinoforms. **b:** A series of logs, from proximal to distal, across the hangingwall of a NNW-SSE fault, active during early Pleistocene. Matrix-supported, monomict breccia was deposited on the footwall of the scarp as a scree talus. Angular blocks of grainstone/packstone (shoreface facies) are mixed with mud with bathyal benthic foraminifera (offshore facies). A shoreface was reworked down a fault-controlled submarine slope during a relative sea level fall, probably triggered by eustatic sea level fall and/or activity of the fault. Absence of calichification from the packstone boulders suggests that any emergence of the corresponding shoreface was relatively short-lived. Absence of red pigmentation possibly indicates that deposition of the scree talus took place below sea level, although the evidence is not conclusive. Distally (W), the talus is draped by offshore muds with bathyal foraminifera and early Pleistocene nannoflora (Subunit 3.2; NN 19b biochronozone), probably deposited during resumed sea level rise.

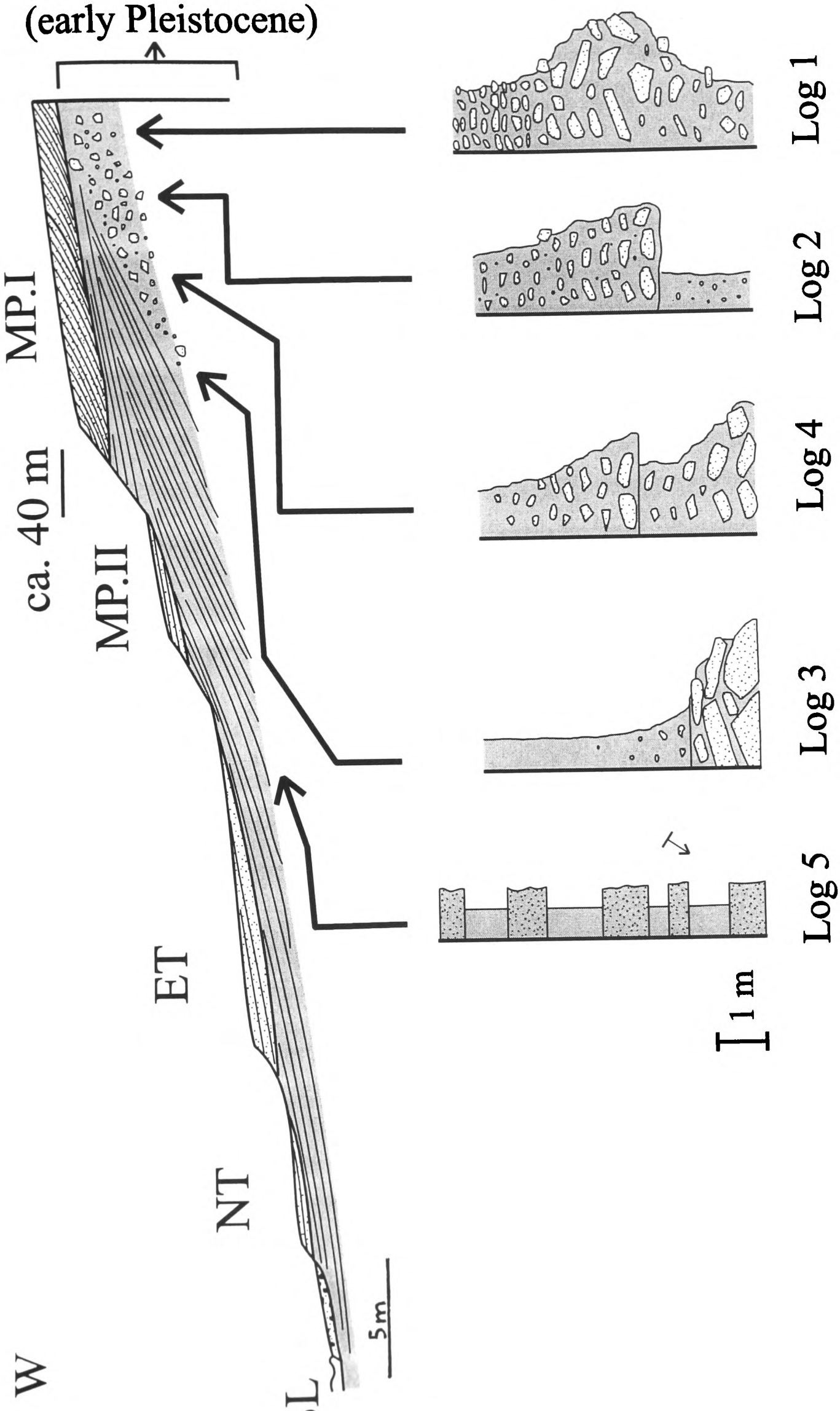
Subunit 3.1
(early Pleistocene)
MP.I
ca. 40 m
MP.II
ET
NT
PSL
W
5m
Log 1
Log 2
Log 4
Log 3
Log 5
1 m

More distally (ca. 20 m to the W; Fig. 5.9.b.4), the lower 2 m of the succession comprise a chaotic sedimentary mixture of large, angular blocks of terrace sandstone in yellow silt matrix (maximum clast size: 2 m). Above a sharp boundary comes pebbly silt, fining to yellow-green mud up section. This grades into alternations of mud with bioturbated silt up section and further W (seawards). The microfauna of the latter sediments are very rich in benthic and planktic foraminifera (Table 5.1).

Further west (seawards), these coarse-grained sediments are draped by a sigmoidal body of finer grade facies (Figs. 5.9.b.5, 5.20). The lowest exposed horizons of the latter crop out beneath "Eutyrrhenian" grainstone (Unit 8; see below), at Ayia Marina church (Figs. 5.9.a, M.2). These sediments comprise beds of brown carbonaceous mud, separated by zones of dense *Thalassinoides* burrow network infilled with coarser, irregularly cemented sediment (fine sand). The mud beds (bed thickens: ca. 10-14 cm) are sharp based, commonly with dense and diverse macrofauna accumulations near their base (e.g. irregular echinoids, *Pecten* spp., *Chlamys* sp., *Ostrea* sp., *Dentalium* sp., bryozoa). Monospecific clusters of densely packed scaphopods (*Dentalium* sp.) also occur. The fossils are commonly imbricated, constituting matrix-supported lags. Individual beds fine up to shell-poor mud, locally with discernible mm-scale lamination. Stacked beds, as described above, succeed each other for up to ca. 1.6-2 m. Successions are interrupted by *Thalassinoides*-bioturbated sandy mud, or silt beds (bed thickness: < 70 cm). Boundaries between alternating beds are sharp. Bedsets of this facies (10's of m thick) truncate each other. The length of untruncated bedsets reaches ca. 15-20 m. The microfauna of this facies are rich in benthic and planktic foraminifera (Table 5.1).

Interpretation: The conglomerate facies in the proximal and basal parts of the section is interpreted as a submarine fan deposit. This interpretation is supported by the position of the sediment body on the hangingwall of a mapped NNW-SSE fault (Fig. M.2), its wedge-shaped architecture (Fig. 5.9.a) and the textural/structural characters of the sediment. Structureless, coarsening upward, matrix-supported conglomerate in the most proximal parts of this facies suggest deposition by mass flow processes (probably debris flow) (Reineck and Singh, 1980; McCallum and Robertson, 1995; Postma, 1996). The majority of clasts were derived from cemented shoreline facies; this probably suggests catastrophic disintegration of a pre-existing shoreline, probably situated on the hangingwall of the fault. Rapid reworking and redeposition are suggested by poor rounding of the clasts and poor sorting of the sediment. Similar very coarse conglomerate facies in the Pliocene of the Mesaoria Basin, Cyprus were interpreted as fan deltas triggered by normal faulting

(McCallum, 1989; McCallum and Robertson, 1995). Foraminiferal fauna probably indicate mixing of biota from different environments. An intralittoral faunal association, including the *Ammonia* spp.+*Elphidium* spp. assemblage (*sensu* Amorosi et al., 1998) and many epiphytic forms (Blank-Vernet, 1969; Murray, 1973; Fernandez-Gonzales et al., 1994) is present together with a lower circumlittoral-upper bathyal faunal association, including the *Cassidulina laevicata* var. *carinata*+*Bulimina marginata* assemblage (*sensu* Amorosi et al., 1998), and *Uvigerina* sp. (see Table 5.1). The latter genus is found at depths >90 m in the present-day Adriatic Sea (Jorissen, 1988 -from Amorosi et al., 1998). These data suggest that deposition of the sediment took place in the upper bathyal-lower circumlittoral zone (outer shelf, below the storm wave base), but depositional processes involved transport of material from more proximal, intralittoral (shoreline-upper offshore) depths. This inference is supported by the broken and/or abraded state of many intralittoral index taxa. The presence of *Elphidium granosum* -an indicator of hyposaline conditions (Amorosi et al., 1998), if not derived from a distant depocentre, suggests the influence of freshwater runoff on the depositional environment.

The muddy sediments that drape the subaqueous fan are interpreted as outer shelf deposits. This is supported by the fine grain size, ichnofacies (*Thalassinoides;* Pemberton et al., 1992) and benthic foraminifera fauna. Allocthonous and autocthonous faunal assemblages can be distinguished, as in the subaqueous fan facies (see above). The *Ammonia* spp.+*Elphidium* spp. faunal assemblage, together with many epiphytic forms were probably reworked from a shoreline habitat. The *Cassidulina laevicata* var. *carinata*+*Bulimina marginata* assemblage (*sensu* Amorosi et al., 1998), together with bathyal index taxa (*Uvigerina peregrina, Lagena* spp., *Siphonodosaria monilis, Gyroidina umbonata*), suggest offshore deposition, probably at a depth >90-110 m, as indicated by the last two species (Blanc-Vernet, 1969; Jorissen, 1988 -from Amorosi et al., 1998). From the above it is evident that this fossiliferous mud was deposited well below the storm-wave base. Therefore, the presence of intralittoral foraminifera and high-energy sedimentary structures (sharp-based beds, shell imbrication) cannot be explained as a result of storm-wave activity. The latter features are interpreted as the result of storm-induced density currents. The presence of *Hyalinea balthica* dates the sediment as early Pleistocene (or younger). The planktic foraminiferal fauna are not age-specific. However, all the identified species are considered as warm to temperate water representatives (Blanc-Vernet, 1969). Nannoplankton identification (Frydas, pers. comm. 1998) allows correlation of these sediments with the biochronozone NN 19b (*sensu* Martini, 1971). These sediments are, thus, correlated with sea level cycle 3.9 (*sensu* Haq et al., 1988), of early Pleistocene (Calabrian) age, as found by Frydas (1993) for similar facies in

the Eastern Lakonia Peninsula, whose deposition post-date the first appearance of the benthic foraminiferum *Hyalinea balthica*.

Up section and further east (inland) (Figs. 5.8, 5.9.a, M.2), the fine-grained sediments described above are followed by a succession of relatively steeply dipping (>15°) clinoforms. A section of this facies is exposed at altitude ca. 80-90 m, along a ravine ca. 1.5 km NE of Dhaemonia (Figs. 4.1, M.2). This section shows discontinuous beds amalgamated at 10's of m-scale. 15-20 m long bedsets are bordered by undulating surfaces. The succession begins with medium-grained, incompletely cemented, yellow calcareous sandstone (maximum exposed thickness: ca. 1 m), with abundant *Thalassinoides* and *Skolithos* burrows. This is followed by fine-, then medium-grained, peloidal packstone with moldic porosity (total thickness: ca. 80 cm). The packstone is hummocky cross-stratified, with sharp-based beds that dip to the W-WNW (267-290°) at 20-24°. The sediment becomes gradually coarser-grained and more terrigenous up-section. The fauna include a variety of molluscs and foraminifera, with a predominance of *Milioliidae* and red algae (Table 5.1). Laminated calcareous sandstone to granular conglomerate comes above (total thickness: ca. 1 m). Bedsets are hummocky cross-stratified near the base and low-angle, wedge cross-stratified toward the top. A sharp surface on the previous facies is covered by calichified silt (thickness: 28-30 cm). Downlapping upon the latter come ca. 2 m of cyclic alternations of thin silty beds (average thickness: 7 cm) with fining upward, coarse to medium grained packstone/grainstone (average thickness: 15-20 cm). The packstone/grainstone beds are sharp-based, but their upper boundaries are gradational. The sediment is cross-stratified, with wide, shallow cross beds (width: ca. 2-3 m). Bedsets of this facies dip to the W (260-290°) at 15-22° in a distinct progradational architecture. Bivalve escape burrows are common in coarser-grained, grainstone beds. The latter sediment is succeeded by ca. 30 cm of coarsening-up, incompletely cemented calcareous sandstone, with *Skolithos* and *Thalassinoides* burrows. The latter terminates in a sharp, steep upper surface (dip: 32° to 275°), followed by fining-up granular conglomerate to sandstone. The next ca. 3-4 m up the sequence consist of cross stratified grainstone. Beds are sharp-based, ca. 15-20 cm thick. Orientation of current scours indicates a southwest current direction (200-240°). This sediment passes gradually into wedge-shaped bedsets of low-angle cross-laminated, coarse-grained calcareous sandstone and granular conglomerate. Laminae are 1-2 cm thick and normally graded. This facies can be traced laterally into *Ostrea sp.* banks, with the bivalves in life-position (articulated valves). The microfauna include mainly benthic and planktic foraminifera, ostracods, bryozoa, scaphopods, encrusting and articulating red algae (Table 5.1).

The 80-110 m terrace is formed above these sediments (Fig. 5.9.a). A distinct slope break divides it to two surfaces: 80-90 and 95-110 m, respectively. Each of these surfaces is formed on a distinct clinoform set, comprising facies similar to the ones described above. The clinoform set that underlies the 80-90 m terrace offlaps the one underlying the 95-110 m terrace. The contact surface between the two clinoforms is not exposed.

Interpretation: The lowest exposed beds (bioturbated sandstone) are interpreted as shoreface deposits, as suggested by their intralittoral foraminiferal fauna (Blanc-Vernet, 1969; Murray, 1973, Amorosi et al., 1998), bioturbation pattern ("*Skolithos* ichnofacies" *sensu* Pemberton et al., 1992) and cross-stratification. Amalgamated peloidal packstone beds higher up-sequence were probably deposited in the middle-upper shoreface zone (Reading and Collinson, 1996). Shallowing-up is indicated by a gradual increase in the abundance of the epiphytic foraminifera *Milioliidae* and increasing grain-size. Trough cross-stratified beds are interpreted as corresponding to 'ridge and runnel' structures in the upper shoreface, breaker zone, probably resulting from wave activity (Walker and Plint, 1992). Low-angle cross-laminated beds over the latter are interpreted as foreshore deposits, on the basis of grain-size and sedimentary structure (Walker and Plint, 1992). Alternating coarse- and medium-grained sandstone beds higher-up, suggest a shoreface depositional environment, as indicated by bioturbation ('*Skolithos* ichnofacies'), sharp-based beds and fauna. Water escape structures and bivalve escape traces indicate high rates of deposition (Reineck and Singh, 1980). Low-angle cross-laminated sandstone/conglomerate that follows was probably deposited in the foreshore zone (Reading and Collinson, 1996). This overall shallowing-up succession, can, thus, be divided into two shallowing-up cycles, each comprising shoreface to foreshore facies. In sequence-stratigraphic terms this section can be described as consisting of two stacked prograding parasequences. This evidence can be interpreted as a record of higher-order sea level oscillation within an overall shallowing-up cycle; the latter probably coinciding with a sea level highstand or the early stages of a sea level fall. Higher-order relative sea level fluctuation caused emergence (middlesection foreshore facies), but sea level rise subsequently resumed and a new shoreline cycle prograded. However, autocyclic controls on sedimentation (e.g. variations in sediment supply, abandonment and drawing of shoreline sandbanks) cannot be ruled out.

Similar successions of offlapping sedimentary bodies at progressively lower elevations can also be observed in the southern part of the Eastern Lakonia Peninsula, near Ayia Marina-Prophitis Ilias (Figs. 5.4, 5.9), where they typically comprise coarsening-up sequences of shallow marine sands at the bottom to shoreline sand-conglomerate at the top.

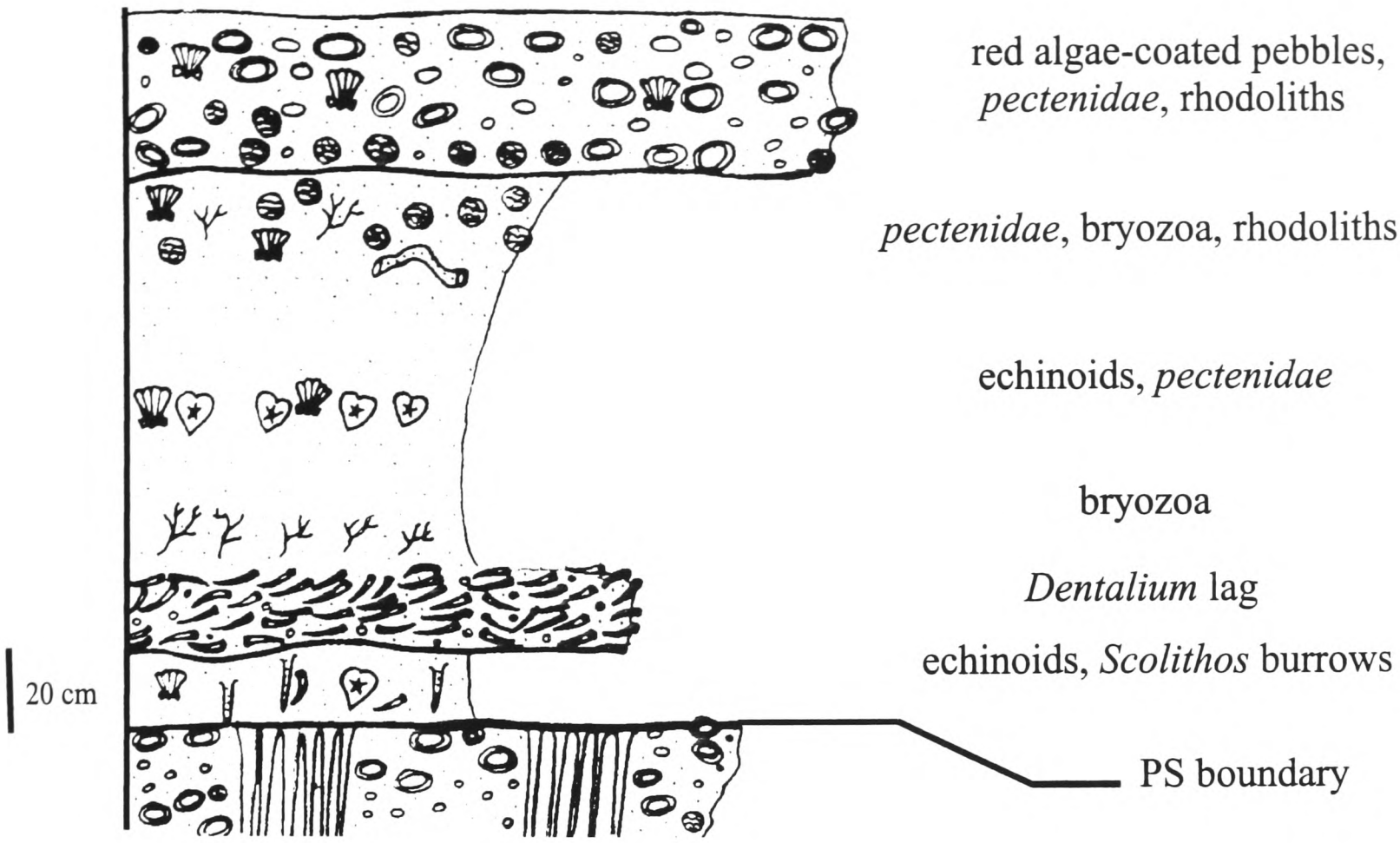

Figure 5.10: Prograding parasequences in inferred early Pleistocene sediments, Prophitis Ilias (for location see Fig. M. 2). Parasequences range in thickness form 20-70 cm. The finest-grained sediment occurs near the base of each parasequence, just above the maximum flooding surface. Sharp based beds/lenses of scaphopods (*Dentalium* sp.) probably resulted from reworking of the sea floor during storms. Bivalves and irregular echinoids represent the *in situ* fauna. The sediment coarsens upwards within each parasequence and sharp-based accumulations of reworked rhodoliths become increasingly abundant up section. Shallowing up is, thus indicated by increasing presence of material derived from more proximal shoreline zones. Evidently, storm processes played a crucial role in the progradation of such parasequences.

5.3.2.1.3 Interpretation of Unit 3 as a whole: Unit 3 represents an early Pleistocene transgressive-regressive sequence, with earlier offshore muds/silts (Subunit 3.1; NN 19a biochronozone) deposited over subaerial relief and sediments of Late Pliocene age, followed by progradational clinoforms of offshore-shoreface to foreshore carbonates or mixed carbonates-siliciclastics (Subunit 3.2; NN 19b biochronozone). Subunit 3.1 thus reflects conditions of maximum flooding, whereas Subunit 3.2 reflects conditions of shoreline progradation during relative sea level fall. This succession is remarkably similar with early Pleistocene sequences in other Eastern Mediterranean areas that experienced Pleistocene uplift, e.g. Rhodes (Bromley et al., 1991; Hansen, 1999) and Cyprus (Poole, 1992, Poole and Robertson, 1991, 2000).

5.3.2.2 Unit 4: Fanglomerate(s) (early-middle Pleistocene): This unit comprises subaerial to deltaic conglomerates that overlie early Pleistocene shallow-marine sediments (Unit 3, above). Sediments of Unit 4 crop out extensively on proximal parts of the Late Pliocene pediment (Chapter 4), on the Ano Glikovrisi Horst, the NNW boundary of the Molai Graben and the Dhaemonia Graben (Figs. 4.2, 4.6, 5.4, 5.6, 5.26, M.2).

Sediments of this unit are widespread on the western side of the Ano Glikovrisi Horst, where they rim the Late Pliocene pediment and the early Pleistocene terrace (Fig. 5.4). Unit 4 sediments form a series of coalescent fan lobes that prograded over fluvial-deltaic topsets of the early Pleistocene terrace (Subunit 3.2; see above). The Unit 4 alluvia were uplifted to about 520-600 m (e.g. Panaghia, E of Ano Glikovrisi; Fig. 5.4) as a result of NW-SE, NE-SW and N-S faulting. NE-SW faulting, in particular, resulted to preservation of these alluvia at various altitudes across strike.

At Mourtitsa Rema (Fig. 5.4; see also Figs. 4.6), three generations of Unit 4 fanglomerate are distinguished:

1) The oldest fan was deposited against the fault-controlled mountain front and was back tilted to the NE (30°) at low angles (5-7°). It consists of perfectly indurated, clast-supported, polymict conglomerate, with the majority of clasts correlated with marble bedrock lithologies. Various types of schist, phyllite ("*Phyllite Series*") and volcaniclastic are also present. Pebble imbrication is common, indicating mainly westward palaeocurrents (from WSW to WNW, but with considerable local variation). The matrix comprises well indurated red silt. The sediment is crudely bedded (bed thickness: ≤1.2 m). Its surface is extensively karstified and covered by thick caliche hardpan (thickness: 10′s of cm).

2) The above sediment is covered by conglomerate foresets (bed thickness: ca. 0.7-1 m) that dip at low angles (≤12°) to the SW/basinward (220°). These foresets comprise oligomict, clast-supported conglomerates, dominated by large, moderately rounded marble clasts (maximum clast size: 40-50 cm). These fanglomerates built coalescent fan lobes with heads located in the lower reaches of broad, V-shaped valleys incised through the fault-controlled mountain front (Figs. 4.7, 5.3). The ca. 320 m surface is formed above of this subunit.

3) The third fan lobe drapes erosional relief over the two later fanglomerate bodies. This third, younger fan, at an average altitude of ca. 290 m, still preserves a convex longitudinal profile. No differences in clast provenance or size were noticed by comparison with the previous subunits. Imbrication and matrix of the latter two fanglomerates are identical to those of the first one.

Further west, at ca. 200-220 m (Figs. 5.4), correlative conglomerates transitionally overlie the uplifted early Pleistocene marine terrace. Shoreline facies of the latter terrace pass upwards into subaerial conglomerate, via a ca. 6-7 m thick zone of clast-supported conglomerate with well-rounded, disc-shaped pebbles and sandstone/lithic grainstone matrix. The matrix is rich in peloids and highly abraded, evenly shaped bivalve fragments (see also Chapter 6). The benthic microfauna include foraminifera (mainly epiphytic taxa), echinoids and articulating red algae (Tables 5.1). This fossiliferous conglomerate passes up-section to "typical" red conglomerate of Unit 4 through a gradual increase in clast-size and sphericity and a gradual disappearance of fossiliferous sandstone matrix. No sharp contact between the shallow-marine and subaerial facies was observed.

Interpretation: The conglomerates with marine fauna are interpreted as foreshore deposits, on the basis of fauna, grain size and high proportion in discoidal pebbles (Kumar and Sanders, 1976). The foraminiferal fauna (*A. becarii+E. crispum* assemblage, *sensu* Amorosi et al., 1998) also support this interpretation. The depositional setting was probably a pebbly beach, associated with a prograding fan to fan-delta system. This facies can thus be considered as the upper part of the early Pleistocene regressive sequence, prograded over more distal facies, probably during the early Pleistocene highstand, or the early stages of subsequent sea level fall. This is covered by progradational fanglomerates, representing proximal fan facies (Postma and Nemec, 1991).

South of the Molai Graben (e.g. Dhaemonia, Elika; Fig. M.2), alluvia correlated with the Unit 4 fringe the fault-controlled interior of the Late Pliocene pediment (see Chapter 4); These prograded over shoreline facies of the early Pleistocene marine terrace (altitudes: 90-120 m). About 2 km NW of Dhaemonia, on the road to Talanta (Figs. M.2), these alluvia comprise indurated conglomerate beds, alternating with pebbly sandstone. Both conglomerate and sandstone beds are tabular and sharp-based, but without noticeable relief. They are <50 cm thick and dip to the NW (towards the axis of the Dhaemonia Graben), at ca. 7-10°. The conglomerate beds are clast-supported, with angular, mainly even-shaped clasts, correlated with bedrock (mainly "*Phyllite Series*", but also marble and Tripolis Zone limestone) and pre-Pleistocene breccia lithologies (e.g. Unit 1; see above). Individual beds commonly fine-up (maximum clast size ≤ca. 70 cm at their base, to ca. 10 cm at their top). Similar sediments fringe the inland margins of the Dhaemonia graben from all sides. Along the NNW side of the graben they are cut and uplifted by ENE-WSW faults (Fig. M.2).

Distally, near the Dhaemonia Basin axis (Fig. M.2), these deposits can be traced into alternating conglomerate and sandstone with occasional marine shells, directly above early Pleistocene marine sediments (Subunit 3.2; see above). Clast-supported conglomerate beds, with well to moderately rounded, imbricated bedrock pebbles (mainly "*Phyllite Series*" and carbonates; maximum clast size: 30 cm) and *Ostrea* sp. shells alternate with poorly sorted coarse sandstone and granular conglomerate. *Ostrea* shells and lithic grains are abraded and imbricated.

Interpretation: These Unit 4 sediments are interpreted as more distal counterparts of the previous fanglomerates, probably deposited in an upper shoreface to foreshore environment, as indicated by their circumlittoral mollusc fauna. Similar with their correlative sediments further N (e.g. Ano Glikovrisi; see above), they probably resulted from alluvial progradation or immediately after the early Pleistocene highstand, thus representing the early stages of a relative sea level fall.

Indurated alluvia fringe the margins of the Late Pliocene-early Pleistocene pediment/terrace at many other sites within the Eastern Lakonia Peninsula (Fig. M.2), but their relationship with the early Pleistocene marine sediments can not be directly established. They are tentatively correlated with the Unit 4 fanglomerate on the basis of their advanced diagenesis, association with the highest (and oldest) Pleistocene surface (see Chapter 4) and their unconformable succession by younger, uncemented alluvia.

Similar cemented alluvia in internal sectors of pediment surfaces elsewhere in the Peloponnese were dated as 'Pre-Tiglian' on the basis of palynological evidence (Sauvage, 1979; Dufaure, 1977). Sauvage (1978, 1979) correlated the continental "Pre-Tiglian" stage with a cold period before the start of the 'Pleistocene ss.', characterised by faunas of *Elephas* and *Archidiscodon meridionalis* in the basin of Megalopolis (South Peloponnese). The same author, based on palynological evidence from shallow-marine sediments (Greece, Italy), correlated the continental "Pretiglian" floras with the marine *Arctica islandica* + *Hyalinea balthica* faunal association. However, recent biostratigraphic data from the south Peloponnese (Frydas, 1990, 1993; Frydas and Bellas, 1994) suggest that the presence of *Hyalinea balthica* characterises sediments of the biochronozone NN 19b (*sensu* Martini, 1971), of early Pleistocene age, correlative with the sea level cycle 3.9 *sensu* Haq et al. (1988) (Fig. 5.2). An early Pleistocene probable age can, thus, be suggested for Unit 4.

5.3.2.3 Unit 5: Shoreline carbonates (early to middle Pleistocene): In the area of Dhaemonia (Fig. M.2), shoreface to offshore facies of the early Pleistocene Subunit 3.2 (see above) are overlain by three wedge-shaped, detrital carbonate bodies, progressively offlapping each other to the WSW (Fig. 5.9.a). The preserved length across strike of each offlapping carbonate body is ca. 20-30 m. The sediment is yellow, coarse-grained grainstone with mollusc-moldic porosity, essentially a debris of abraded shells of bottom-dwellers (see Chapter 6). The fauna include thick-shelled bivalves, scleractinean corals, scaphopods, gastropods and large rhodoliths (diameter: ca. 5 cm) (see Table 5.2). Most bivalves shells are convex side-up and parallel to each other. The microfauna include mainly epiphytic foraminifera (Table 5.1). The sediment is cross-stratified, with ca. 50-70 cm thick bedsets, bounded by undulating surfaces (average width: ca. 4-5m).

A gently stepping terrace is formed above the latter sediments (altitude: 60-25 m; average gradient: ca. 2-5°). Although relief-breaks were observed on this surface, they do not seem to relate with particular offlapping surfaces. By contrast, offlapping surfaces are truncated by the 60-20 m ASL terrace surface on a small hill east of Ayia Marina church (Fig. 5.9.a) showing that the formation of the terrace post-dated the deposition of the offlapping clinoforms.

Interpretation: This facies is interpreted as amalgamated upper shoreface to foreshore deposits. The large scale cross-stratified structure probably resulted from storm-wave influence (Walker and Plint, 1992). The molluscan and foraminiferal fauna indicate intralittoral depositional depth, probably in a high-energy shoreline, as suggested by abraded shells and the predominance of epiphytic foraminifera (Blanc-Vernet, 1969; Murray, 1973; Amorosi et al., 1998). The same depositional environment is also suggested by bioturbation (*Skolithos* ichnofacies; Pemberton et al., 1992). The uppermost, low-angle cross-stratified bedsets of matrix-free sandstone are interpreted as foreshore deposits (Walker and Plint, 1992). Unit 5 may reflect either 4^{th} or higher-order sea level cyclicity within the sea level cycle 3.9, or shoreline progradation during a later, probably early middle Pleistocene sea level cycle. The second interpretation is favoured, in view that Unit 5 was affected by deep fluvial incision (e.g. Dokali Rema; see Fig. 4.10) and cliff cutting of inferred middle Pleistocene age (Fig, 5.2).

5.3.3 MIDDLE PLEISTOCENE SEDIMENTS

5.3.3.1 Unit 6: Marginal-marine and normal marine sediments (middle Pleistocene):

This unit comprises marginal-marine sediments exposed on the banks of the Kambourani Rema (Figs. 5.2, 5.3, 5.4, 5.11, M.2) and along the retreating cliffs of the Elea coastline (Subunit 6.1), and also correlated shoreline sediments along the cliffs of the Bozas Rema coast (Subunit 6.2) (Fig. M.2).

5.3.3.1.1 Subunit 6.1: Lagoon to foreshore: Sediments of this subunit comprise a composite succession, with a characteristic tripartite pattern, from bottom to top and from proximal to distal settings (Fig. 5.11):

1) The lower exposed facies (thickness: ca. 1.6 m) (Fig. 5.11.a) consist of polymict, clast-supported conglomerate, with well rounded, commonly bored bedrock pebbles (maximum clast size: 40 cm). Pebble imbrication indicates bi-directional palaeocurrents, towards the ESE (100°-landwards) and towards the WSW (250°-seawards). The sediment is horizontally bedded (bed thickness: 20 cm); individual beds fine upwards. This is succeeded by cross-laminated, yellow-grey, coarse-grained sandstone, incompletely cemented locally. Sedimentary structures include mainly planar cross-bedding, with wedge-shaped bedsets (maximum thickness: ca. 25-30 cm), and trough cross-beds bounded by tangential surfaces. Reactivation surfaces of sigmoidal shape are abundant. Thin low-angle planar cross-beds also occur (thickness: ca. 5 cm). Beds are internally cross-laminated (laminae thickness: 0.7-1.5 cm) with high-angle tangential, trough, or low-angle planar laminae. Individual laminae are normally graded. Climbing current ripples are common (crest height: ca. 5 cm/wave length: ca. 30 cm). Palaeocurrent directions suggested from cross-bedding are bimodal (both shorewards and seawards), but the seaward trend predominates (Figs. 5.11, 5.23).

Figure 5.11 (following page): Middle Pleistocene sediments in the Kambourani Rema area (Subunit 6.1; For location see Figs. 5.2, M.2). **a:** Schematic section sediments cropping out along the walls of the Kambourani Rema incised valley. A tripartite subdivision is observed, from cross-bedded sandstone/conglomerate with progradational geometry (proximal part), to interbedded sand/mud with peat and caliche horizons (middle part) to sand, mud and landward dipping conglomerate foresets (distal part and up-section). This is interpreted as the fill of an estuary/ back barrier lagoon, deposited during transgression. Emergence and fluvial incision after middle Pleistocene and before the Eutyrrhenian (ca. 120 ka) led to the formation of V-shaped channels, later filled with alluvial sediments (Unit 7). Middle Pleistocene marginal marine sediments and middle-late Pleistocene alluvia are covered by Eutyrrhenian shoreline deposits (Unit 8). **b:**Log of middle Pleistocene alternations of mud with sandstone/conglomerate, interpreted as lagoonal facies (see text). **c:** Log of middle Pleistocene mud with peat and caliche alternations, interpreted as lagoon-shore/back-lagoon facies (see text).

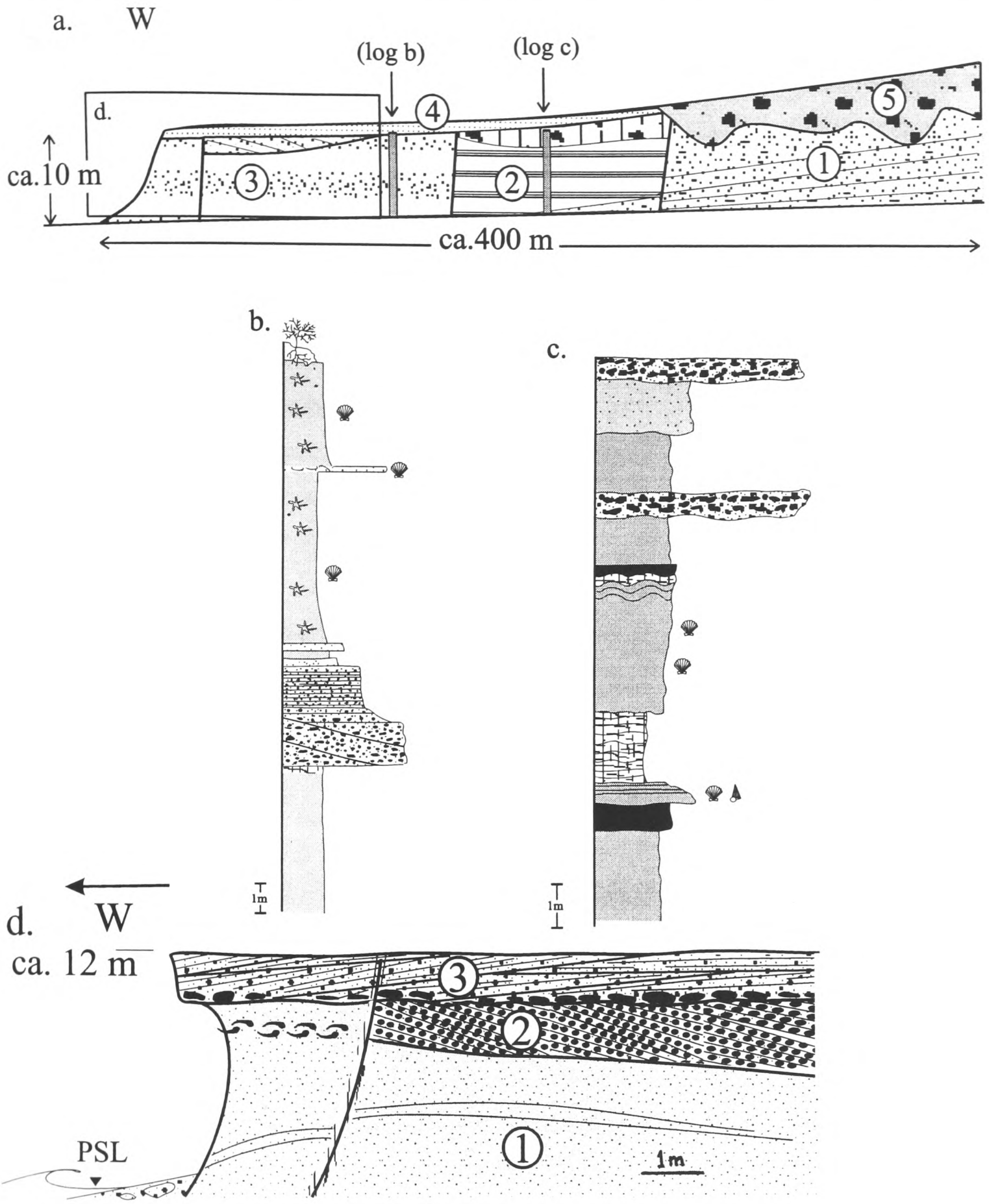

Figure 11 (continuing): d: Cliff section at the mouth of Kambourani Rema. **1)** Sands-silts interpreted as deposits within a back-barrier lagoon (middle part of Subunit 6.1; middle Pleistocene). **2)** Landward dipping conglomerate foresets, interpreted as deposits behind a wave-split barrier (top of Subunit 6.1; middle Pleistocene). **3)** Conglomerate (base), passing up to prograding sandstone/conglomerate foresets (Unit 8: "Eutyrrhenian"). The middle Pleistocene part of the section **(1, 2)** reflects retrogradation of a barrier-lagoon system, probably during rising sea level (see Fig. 5.12). The "Eutyrrhenian" part of the section **(3)** represents transgression (ravinement surface, followed by basal conglomerate) and subsequent foreshore progradation, during highstand or early stages of relative sea level fall. Note that the fault through the inferred middle Pleistocene deposits (1, 2) cuts the "Eutyrrhenian" deposit as a joint (without offset).

These densely laminated bedsets alternate with zones of dense bioturbation (mainly *Thalassinoides* burrows), commonly coinciding with finer-grained parts of the sequence. *Skolithos* burrows occur throughout the coarse-grained sandstone facies. A few horizontal burrows of the *Cruziana* ichnofacies also tend to be concentrated in coarser-grained parts of the sequence. The macrofauna include thick-shelled bivalves.

2) Up-sequence and to the west (more distally), the above facies is succeeded by carbonate mud and sand sediments, corresponding to a variety of shallow-marine/marginal-marine environments (Figs. 5.11.a, 5.11.b, 5.24). Sections start with ca. 5.2 m (maximum exposed thickness) of brown carbonate mud with low density and diversity benthic microfauna, including mud-dwelling and epiphytic foraminifera and echinoid spines (Table 5.1). This is followed by ca. 15-20 cm of sharp-based, medium-grained, quartz-rich, yellow sandstone, well sorted and incompletely cemented. The benthic microfauna are of low density and diversity, including foraminifera, fragments of bryozoa and ostracods (Table 5.1). After a sharp, even surface comes clast-supported, but matrix-rich, monomict conglomerate (thickness; ca. 1.6 m), with pebbles correlated with Tripolis Zone limestone bedrock. The clasts are well rounded and discoidal, spherical, or rod-shaped. The sediment is mainly parallel-bedded, although crudely defined tangential bedsets are also present. The conglomerate fines upwards, with maximum clast size ca. 7 cm (base) to ca. 2.5 cm (top). This conglomerate is succeeded by finning-up, pebbly or coarse-grained sand (thickness: ca. 50 cm), then by well sorted, medium-grained grey sand with cemented nodules (thickness: ca. 1.5-1.6 m). The following 60 cm of the section comprise very well sorted, fine-grained sandstone, alternating with carbonate silt/mud (average bed thickness: ca. 20 cm). The latter facies is succeeded by fining-up, silty carbonate mud. Bioturbated includes mainly horizontal, cm-scale, irregular burrows. Dense accumulations of bivalve shells come above, over a sharp boundary with the underlying beds. Most of the bivalve shells are preserved as mainly unfilled moulds; a few recrystallised shells also occur. These are succeeded by irregularly cemented brown silt (to siltstone). The sediment is heavily bioturbated (*Thalassinoides* burrows). Selective cementation took place within the burrow network or moulds of articulated bivalves. Thick-shelled molluscs dominate the fauna. The foraminiferal microfauna are very diverse, including both epiphytic and mud-dwelling benthic taxa, as well as planktic taxa. Ostracods are also present (Table 5.1).

More distally, these sediments pass into ca. 4 m thick alternations of brown, sandy carbonate mud with tabular beds of well sorted, coarse-grained, yellow-brown, incompletely cemented sandstone (Fig. 5.11.a, 5.11.c). The sandstone beds are bounded by sharp upper and lower

surfaces. The bed thickness decreases up section, from ca. 0.4-1 m (lower parts), to ca. 7-10 cm (top). Sandstone beds are replaced by trough-based lenses up-section. Current scours, infilled by sandstone and directed normal to the present-day coastline, are abundant in the mud beds. The bottom surfaces of the sandstone beds are extensively bioturbated, with *Cruziana* (length: ca. 10-30 cm / width: ca. 1-2 cm) and fewer *Skolithos* and possible *Diplocraterion* burrows (diameter: ca. 0.7-1 cm). The visible thickness of the whole unit is about 4m.

3) Sandwiched between the lower, coarse-grained sandstone and the upper, mud/conglomerate facies, there are outcrops of dark grey mud with dense accumulations of the bivalve, *Cardium edule*. The thickest exposures (ca. 10 m) occur in the seaward parts of the Kambourani Rema incised valley (ca. 500 m E of the present-day river mouth; Figs. 5.4, 5.11.a, 5.11.d). The lowest exposed parts comprise grey mud (thickness: ca. 1 m), followed by a sharp-based, discontinuous peat bed (maximum thickness: ca. 30 cm), with a dense fauna of the pulmonate gastropod, *Planorbis* sp. This is succeeded by sharp-based, dark grey mud with a dense fauna of *Cardium edule*, commonly articulated, and *Cerithid* gastropods, followed by laminated mud (mm-scale laminae). *Cerithid* gastropods predominate in the lower parts of beds, but are outnumbered by *Cardium edule* (bivalves) higher up. A thin-bedded layer of chalky caliche follows (thickness: ca. 80 cm). This is unconformably overlain by grey mud, locally with dense accumulations of articulated *Cardium edule*, that passes to undulating alternations of mud, chalky caliche and peat with *Planorbis* sp. Green-grey mud comes above, in sharp contact with the underlying sediment. This passes upwards to alternation of green-grey mud with lenses of clast-supported red conglomerate, sandy mud, and fine-grained, poorly sorted sand. The conglomerate lenses are trough-based, ca. 0.7-1 m thick and 1-2 m wide. The section as a whole, thus, coarsens upwards. These facies, as all sediments previously described, are unconformably covered by shoreline facies of late Pleistocene (Eutyrrhenian and Neotyrrhenian) age (Kowalczyk et al., 1992; Units 8, 11 below; see Fig. 5.11.a, 5.11.d).

Interpretation: The various facies of Subunit 6.1 are interpreted as deposits of a wave-dominated estuarine-lagoonal environment (Fig. 5.12). Lateral facies variations are interpreted to reflect local variations in depositional setting, whereas vertical facies changes probably reflect response of this environment to allocyclic controls (Reinson, 1992). Cross-bedded/laminated, coarse-grained sandstone at the base of the succession was probably deposited in a high-energy shoreline, as indicated by the benthic microfauna, sedimentary structures and grain-size. The foraminiferal fauna (*Ammonia becarii+Elphidium crispum*

assemblage, *sensu* Amorosi et al., 1998) are typical of the circumlittoral-upper intralittoral zone (Blanc-Vernet, 1969; Murray, 1973; Amorosi et al., 1998). Deposition took place above the fair-weather wave base, as indicated by wave-generated sedimentary structures (reactivation surfaces, wave ripples) and bi-directional, both landward and seaward, palaeocurrent directions. Predominance of seaward palaeocurrents and seaward progradation of medium-scale foresets allows interpretation of this facies as a shoreline sand wave, deposited in a wave-dominated environment. Superposition of low-angle 'master bedding planes' (*sensu* Allen, 1980) with smaller-scale bi-directional cross-stratification suggests that the sediment was deposited as a compound dune, shaped by currents of varying direction and intensity (Allen, 1980; Dalrymple, 1992). Although these forms are more common in tide-dominated environments, they also occur as bay-head deltas in wave-influenced/dominated settings (e.g. Gironde estuary, France; Dalrymple, 1992). The presence of various scales of dune and ripple cross-stratification, commonly separated by sigmoidal reactivation surfaces, makes this facies similar to the bedform classes V-VII *sensu* Allen (1980). The latter author suggested that these forms were deposited by 'expanded but unseparated flow', but the exact hydrodynamic conditions are still debated (Dalrymple, 1984, 1992). Deposition of this prograding sediment body took place after marine transgression of an already incised relief (flooded palaeovalley). The terrigenous origin of clasts, predominantly seaward palaeocurrents and position of the sediment body in the proximal zone of the flooded palaeovalley, allow interpretation of this facies as a bay-head delta deposited at the proximal zone of an estuary, near the river mouth (see Reinson, 1992; Reynolds, 1996).

Mud-sandstone-conglomerate alternations that follow, are interpreted as estuary fill sediments (Fig. 5.12). Muddy sediments with predominantly circumlittoral foraminifera were probably deposited below the fair-weather, but above the storm wave base, as indicated by presence of wave scours. The low density and diversity of the fauna suggest ecological stress, possibly resulting from reduced salinity due to freshwater input. Well sorted, fining-up sandstone and conglomerate intercalations are interpreted as storm beds (tempestites), deposited by winnowing currents (Reading and Collinson, 1996; Reynolds, 1996). The presence of such facies amidst relatively "distal", probably axial, estuarine facies, possibly records progradation of the bayhead delta into more basinal areas. This could be attributed to high-order relative sea level cyclicity. Alternatively, the same effect could result from purely autocyclic processes (avulsion of distributary channels). Bioturbated mud without sandstone intercalations up section was probably deposited in a more calm, possibly "internal lagoon", setting. Dark grey mud with oligospecific benthic microfauna indicate

ecological stress on the fauna. *Cardium edule* and *Cerithdidae* death assemblages reflect brackish conditions that probably prevailed in a restricted, to isolated, lagoonal environment, in view of evidence for development of a barrier further seaward (see below). These environments alternated with vegetated swamps (peat layers), followed by arid soils (caliche), developed after silting up, or desiccation. Alternations of subaquaeous and subaerial facies along the section indicate successive emergence events. It is uncertain whether this reflected high-order climate change (alternating wet with dry conditions), normal avulsion processes, or sea level change. Red conglomerate lenses higher up are interpreted as fluvial channel deposits. Their occurrence at the top of the section is interpreted as indicative of river rejuvenation further upstream. This could have resulted from climate change, or relative sea level fall (the latter potentially attributable to either uplift, or glacio-eustatic sea level change).

4) A section at the Kambourani Rema mouth comprises the most distal exposed outcrop of Subunit 6.1 (Fig 5.11.a, 5.11.d, photo). A N-S trending fault of apparent listric geometry (0-5°/72° W) juxtaposes finely-laminated, fine-grained silty sand and carbonate mud in the footwall (minimum thickness: ca. 6-8 m), with yellow silty sand with articulated *Ostrea* sp., few *Pectenidae*, and *Terebratula* sp. in the hangingwall. The silty sand in the hangingwall contains a poor, low diversity benthic foraminifera microfauna (Table 5.1). The fine sand/mud in the footwall side is bioturbated and contains *Cerithid* gastropods. Limonitic concretions rim the walls of bioturbation burrows. The microfauna encompass mainly benthic foraminifera (Table 5.1). This sediment is overlain by a clast-supported monomict conglomerate, that drapes an uneven erosional surface with a relief of up to ca. 7 cm (Tripolis Zone limestone clasts; maximum clast size: 2-7 cm). The conglomerate is constituted of steep, landward dipping, planar foresets (average dip: 10-20° to 54°). Pebbles are well rounded, spherical and rod-shaped, set within fine- to medium-grained sand matrix. These, as with all deposits of Subunit 6.1 in the area of Kambourani Rema (Fig. 5.11.a, 5.11.d), are unconformably overlain by "Eutyrrhenian" foreshore to shoreface facies (Kelletat et al., 1976; Kowalczyk et al., 1992). The N-S normal fault that cuts through Subunit 6.1 does not offset the overlying "Eutyrrhenian" terrace (Fig. 5.11.d).

Interpretation: The fine-grained sediments in the footwall of the faulted section are interpreted as lagoonal deposits, correlated with similar deposits in more proximal locations (see above; Fig. 5.12). Fine grain size, absence of evidence for wave activity and dominance mud-dwelling foraminifera over epiphytic forms (Murray, 1973; Amorosi et al., 1998) suggest a relatively central lagoonal setting. Of the foraminiferal species present, one is

considered to be an indicator of hyposaline conditions (*Ammonia tepida*), whereas two others (*Ammonia becarii, Fursenkoina schreibergsiana*) are tolerant of slightly hyposaline conditions (Berloti et alii, 1994, from Amorosi et al., 1998). Coexistence of these with normal marine species suggests mixing of marine and freshwater, possibly as a result of fluvial runoff. Given that the evidence from adjacent points to an estuarine-lagoonal system (see above), this facies probably represents the deeper part of a lagoon, connected with the open sea and receiving fluvial discharge, similar with the 'partially open lagoons' in Reinson's classification (1992). The downfaulted silt/sandstone of the hangingwall fault-block is interpreted as a shallower lagoonal deposit, on the basis of molluscan and foraminiferal fauna. The sharp-based sandstone body present is interpreted as lagoon-shoreface sediment, probably deposited after storm-wave breaching of a barrier. A shallowing-up of the lagoon through time is, thus, indicated. The sharp-based, landward-dipping conglomerate foresets are interpreted as washover deposits, probably formed from breaching of a pebbly barrier by storm waves. This is supported by sedimentary structure, primary landward dip of foresets (Reinson, 1992), and pebble shape / roundness (Kumar and Sanders, 1976). Landward progradation of washover facies over lagoonal facies probably took place during the course of shoreface retreat during rising sea level, as the effect of storms was amplified and the beach barrier was reworked (Reinson, 1992).

Interpretation of Subunit 6.1 as a whole: Subunit 6.1 can, thus, be interpreted as corresponding to an estuarine-lagoonal system (Fig. 5.12), deposited after marine transgression of an incised valley. The classic tripartite subdivision (bayhead delta-central basin-marine dominated coast), from proximal to distal environments, is recognised (Bird, 1967; Kulm and Byrne, 1967). This facies subdivision best develops along microtidal coasts, in estuaries of the lagoonal to partially closed type (following Reinson's (1992) classification scheme). The following environments can be recognised within Subunit 6.1: Prograding bayhead delta, deep lagoon, shallow lagoon alternating with marshland, prograding fluvial channels, retreating barrier (see above). Although high-order relative sea level cyclicity is probably recorded in sections of Subunit 6.1 (e.g. lagoon to marshland environments), the overall stratigraphy indicates coastal retreat, accomplished by reworking of the barrier by washover processes. This suggests that this unit was deposited during a relative sea level rise. The disconformity surface that separates lagoonal mud below, from landward prograding sand-conglomerate above, is, thus, interpreted as a marine ravinement surface. These estuarine deposits are placed in the lower part of the transgressive systems tract of their corresponding sea level cycle, in agreement with Darlymple's (1992) modification of Exxon's interpretation (Van Wagoner et al., 1990).

I. Middle Pleistocene Lowstand

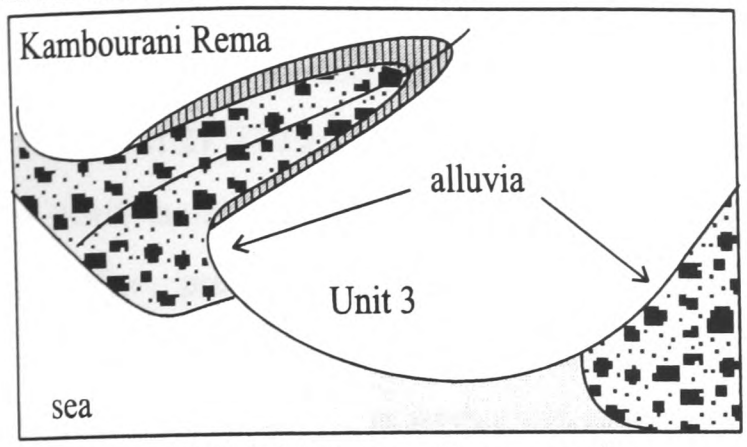

II. Late middle Pleistocene Transgression

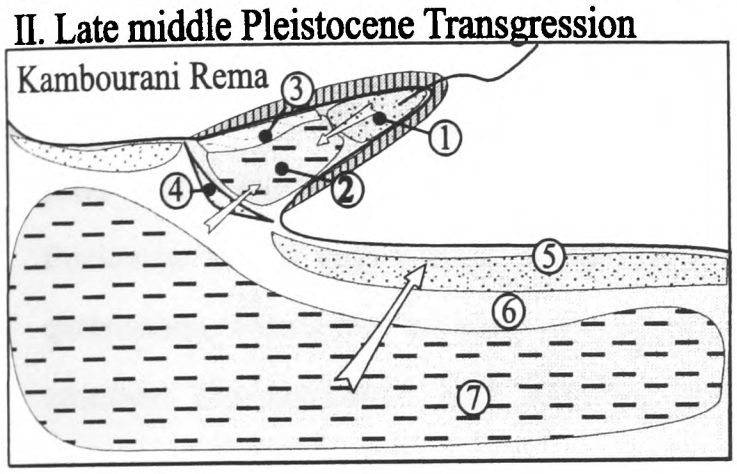

III. Middle-late Pleistocene Lowstand

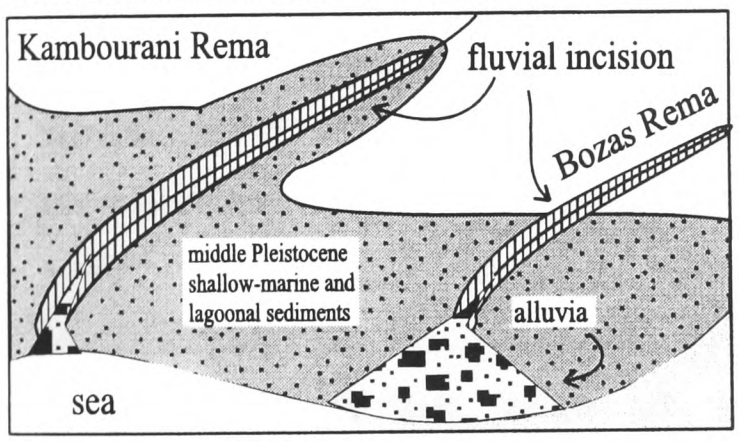

IV. Eutyrrhenian Transgression+Highstand

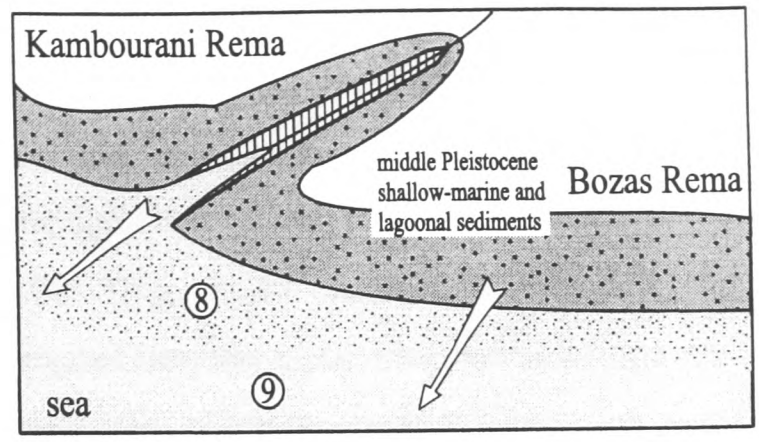

V. Late Pleistocene Lowstand

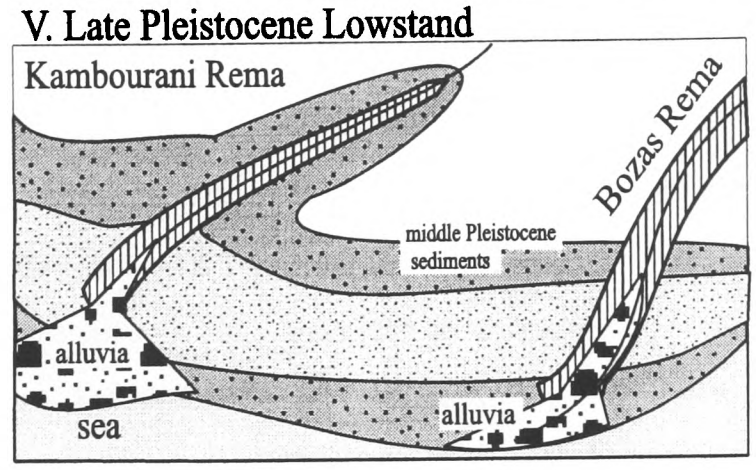

VI. Present

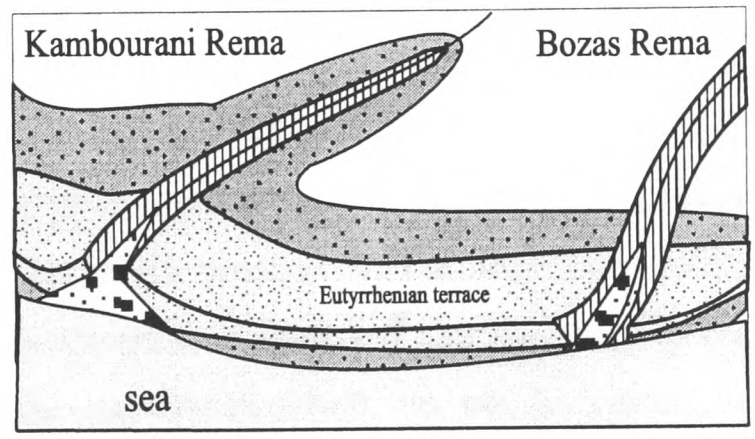

Eutyrrhenian:

⑧ Foreshore (sandstone, conglomerate)

⑨ Shoreface (sandstone, silt)

Seaward progradation

Middle Pleistocene:

① Bay-head delta (sandstone, conglomerate)

② Inner lagoon (silt, mud)

③ Lagoon shore (mud, peat, caliche)

④ Barrier (sandstone, conglomerate)

Progradation at the bay-head delta

Washover deposition in back-barrier setting

⑤ Open-marine shoreline (sandstone, conglomerate)

⑥ Shoreface (sand, silt)

⑦ Offshore (silt, mud)

Landward shift of shoreline facies

Figure 5.12: Interpretation of the middle Pleistocene facies in the NW coast of the Eastern Lakonia Peninsula (Subunit 6.1: Kambourani Rema/Subunit 6.2: Bozas Rema) **a:** Inferred topography during the middle Pleistocene lowstand. **b:** The middle Pleistocene transgression resulted to deposition of estuarine-lagoonal facies in drawn incised valleys (Subunit 6.1). Open-marine shoreline facies were deposited in non-incised areas. **c, d:** Sea level cyclicity in late Pleistocene-Holocene resulted to deposition of the Tyrrhenian terraces and valley incision.

5.3.3.1.2 Subunit 6.2: Shallow marine siliciclastics-carbonates: Shallow-marine sediments, beneath the '"Eutyrrhenian"' terrace, crop out at the Bozas Rema and Tassou Rema ravine mouths and also in the southern tip of the Peninsula (Figs. 5.13, 5.24, 5.34, 5.35, M.2). These sediments overlie alternations of red silt and conglomerate, interpreted as distal facies of inferred early-middle Pleistocene age (Unit 4; see above), although an even earlier, pre-Pleistocene age cannot be excluded (Fig. 5.26). Shallow-marine facies of Subunit 6.2 rest on a low-angle disconformity eroded into the underlying subaerial deposits. These sediments start with clast-supported, imbricated, polymict conglomerate, with well-rounded, predominantly discoidal and spherical pebbles (maximum clast size: 25 cm). After ca. 1 m of alternating conglomerate with silt, they then pass into alternations of yellow silty sand with lithic grainstone/packstone. The fine-grained, silty sand beds (maximum thickness: ca. 80 cm) contain a rich and diverse fauna of bivalves (some still articulated), gastropods, barnacles, bryozoa and scleractinean corals. The sediment is bioturbated, with common *Thalassinoides* and *Skolithos* burrows. Individual beds commonly fine upwards. Grainstone/packstone beds (grain size: coarse sand to granules) are bounded by sharp, uneven surfaces (bed thickness: ca. 40-65 cm). Cementation is selective, commonly following the *Thalassinoides* burrow network. The macrofauna are similar to that of the surrounding silt beds. However, most molluscs were dissolved to moldic pores. Dense shell accumulations form irregular clusters of both fragmented and intact shells (Fig. 5.34). Many bivalve valves and moulds are positioned vertically (life position ?). The upper parts of the section are relatively more silty, with a gradual decrease in thickness and frequency of the grainstone/packstone beds. Yellow silt in the uppermost 50-60 cm of the section is intensively calichified (nodular caliche).

Interpretation: The gently dipping disconformity at the base of the section, separating subaerial sediments below, from submarine sediments above, is interpreted as a ravinement surface, formed during marine transgression (Myers and Milton, 1996; Reynolds, 1996). The clast-supported conglomerate above that surface is, correspondingly, interpreted as a transgressive lag, deposited in the foreshore. This interpretation is supported by stratigraphic position, pebble shape and imbrication (Kumar and Sanders, 1976; Postma and Nemec, 1990). Similarity of clast-provenance in the transgressive lag above and the alluvial conglomerate below, suggests that the former clasts were derived from reworking of the latter deposit during transgression. The alternations of silt with grainstone/packstone higher-up is suggestive of deposition in the lower shoreface to upper offshore transition. Mollusc fauna, common occurrence of articulate (i.e. in life position) bivalves and ichnofacies, together with absence of wave-induced structures, probably indicates deposition of the

yellow silt beds below the fair-weather wave base (Reineck and Singh, 1980; Pemberton and Frey, 1992). The coarser-grained grainstone/packstone beds, with denser mollusc accumulations, probably resulted from storm-reworking of material from the upper shoreface/foreshore (i.e. storm beds; Walker and Plint, 1992). The presence of irregular lower surfaces, coincident with networks of non-truncated burrows in the underlying silt, suggest that the grainstone/packstone beds were deposited by relatively winnowed currents. Decreasing thickness and frequency of grainstone/packstone beds up section probably suggests increasing water depth; the upper parts of the section probably correspond to an offshore depositional environment. Thus, this succession corresponds to a fining-upwards, transgressive sequence, deposited during relative sea level rise. In sequence stratigraphic terms this succession can be assigned to the transgressive systems tract of a wave- and storm-dominated shallow-marine sequence (Walker and Plint, 1992; Reynolds, 1996).

5.4.2.1.3 Stratigraphic position of Unit 6: These sediments were in the past correlated with the early Pleistocene (Kowalczyk et al., 1992). In contrast, here they are correlated with the middle Pleistocene Unit 6, on the basis of the following evidence: The shallow-marine sediments overlie braidstream deposits that probably formed part of the fill of an incised valley. Channel incision and subsequent alluviation in areas west (seaward) of the (inferred) early Pleistocene shoreline took place after regression, probably in middle Pleistocene times. The possibility that the alluvial sediments under Subunit 6.2 predate the early Pleistocene (i.e. stratigraphic equivalents to Unit 2 alluvia; see above) can not be ruled out on the basis of available field evidence. If true, then the shallow-marine sediments of the Bozas Rema section, above the red alluvia, would constitute the lower, transgressive systems tract of the early Pleistocene marine sequence (base of Unit 3; see above). However, all the outcrops of early Pleistocene marine sediments in the western coast of the Eastern Lakonia Peninsula comprise aggrading to prograding, offshore to shoreline facies, probably attributable to maximum flooding and the highstand systems tract of the early Pleistocene sequence (see above). Exposure of the basal parts of the stratigraphy (pre-early Pleistocene alluvia and only transgressive early Pleistocene facies) in the Bozas Rema area would probably require local uplift rates higher than those prevailing in surrounding areas. However, no morphological evidence for higher uplift rates was found in this area. The Bozas Rema area, as part of the Molai Graben (Fig. M.2), was possibly affected by fault-induced subsidence, that counteracted regional uplift. Kelletat et al. (1976) considered this area as one of minor uplift, as compared with the surrounding western coast of the Eastern Lakonia Peninsula (see Fig. 1.5). By contrast, there is strong evidence for amalgamation of marine terraces, a

phenomenon characteristic of areas with moderate, to low, uplift rates (Kowalczyk et al., 1992) (see Fig. 4.5).

5.3.3.1.3 Interpretation of Unit 6 as a whole: As discussed above, sediments of inferred transgressive character are grouped into Unit 6, despite considerable facies heterogeneity. The variability of depositional environments is interpreted as reflecting the palaeogeography of the coastline (Figs. 5.12). Subunit 6.1 is interpreted as a transgressive lagoonal estuary that, after marine flooding, occupied the outer reaches of an incised river valley (see above). Subunit 6.2 is interpreted as a more distal, transgressive shoreface to offshore depocentre. Evidence for a lagoon situated further proximally was not found. This differentiation of environments could reflect the proximity of the Kambourani Rema sections (Subunit 6.1) to a river mouth. The same evidence could also suggest that the Bozas Rema valley (Subunit 6.2), presently incised through the above (and younger) sediments, was not preceded by an ancestral valley, prior to the deposition of the middle Pleistocene transgressive shallow-marine sequence. Taking the different tectonic position of these outcrops into account (Fig. M.2), these inferred differences in geomorphic and sedimentary history may reflect local differences in uplift rates. The Kambourani Rema section (Subunit 6.1) is situated in the southern part of the Ano Glikovrisi Horst, whereas the Bozas Rema section (Subunit 6.2) is situated in the seaward continuation of the Molai Graben. It is possible that fluvial incision in the Kambourani Rema prior to middle Pleistocene marine transgression resulted from higher uplift rates of the Ano Glikovrisi Horst, whereas minor (or negligible) incision of the Bozas Rema reflected lower uplift rates (or even subsidence) of the Molai Graben (Fig. 5.12).

5.3.3.2 Unit 7: Alluvia (Middle Pleistocene): This unit includes alluvial sediments that post-date early Pleistocene sediments (Unit 3; shallow-marine sediments and Unit 4; fanglomerate; see above), but predate the "Eutyrrhenian" marine terrace (Unit 8; see below) (Figs. 5.5, 5.6). This unit is well developed in the Ano Glikovrisi Horst but is also present in the eastern coast of the Peninsula (Figs. 5.2, 5.3, 5.4, 5.13), where field evidence allows clarification of its relations with other depositional units and geomorphic events (Fig. 5.29). In other parts of the Eastern Lakonia Peninsula, correlation of alluvia with Unit 7 can only be tentative.

5.3.3.2.1 In the area of Ano Glikovrisi (Fig. 5.4), proximal parts of this unit bury cliffs (degraded fault scarps ?) cut into early Pleistocene marine sediment. These parts are lobe-

shaped in plan view, with slightly convex longitudinal profile. Distally, they can be traced to alluvial fill of U-shaped channels cut into early (to early middle?) Pleistocene shallow-marine sediments (Units 3, 5; see Fig. 5.3). The latter channel-fill facies are more widespread, as compared with the proximal lobes. To the west, their more distal parts are locally covered by a thin veneer of foreshore sediment correlated with the "Eutyrrhenian" terrace (Unit 8; see below). These alluvia, together with the overlying "Eutyrrhenian" sediments, were cut by latest Pleistocene fluvial incision, so at present they are preserved as fluvial terraces (see Fig. 4.10).

An example of proximal facies of Unit 7 alluvia crops out at ca. 120-130 m, near the valley head of Mourtitsa Rema (Figs. 4.16, 5.4). This lobe-shaped sediment body drapes a ca. 30 m-high cliff (degraded fault scarp ?), cut into topsets of the early Pleistocene Unit 3. The section begins with incompletely indurated, calichified, deep-red to purple bouldery silt. Clasts are correlated with bedrock (mainly marble) and older subaerial deposits. The following subaerial facies were identified as reworked clasts within Unit 7: 1) Matrix-supported, indurated, monomict conglomerate with angular marble clasts in red siltstone, interpreted as reworked regolith, probably derived from fault-uplifted marble terrain. 2) Clast-supported, indurated, polymict conglomerate with well rounded pebbles of various bedrock types, interpreted as derived from early Pleistocene fanglomerate, higher up (Unit 4; see above). The relative abundance of clasts increases upwards. Caliche nodules and calichified *Rhizocretion* are abundant. A sharp surface, with ca. 20-30 cm of erosional relief, separates the latter facies below, from matrix- to locally clast-supported conglomerate beds above (matrix: moderately indurated pebbly silt). Individual beds have a tabular to tangential geometry (bed thickness: ca. 20-60 cm). Most beds are bounded by sharp, even surfaces; also uneven, concave surfaces with erosional relief of 50-60 cm are present locally. Clasts are moderately to poorly rounded, evenly shaped to flat and derived from various bedrock lithologies (mainly marble and volcaniclastics). Individual beds are generally structureless; they are either coarsening up, fining up, or massive. Overall, the sediment coarsens up, with maximum clast size from ca. 20 cm (base), to ca. 40-60 cm (top). The latter facies terminates against an uneven erosional surface; this is followed by ca. 10-25 cm of terra rossa with a low clast content. A concave erosional surface, with maximum relief of 3.5-4 m, truncates the latter sediment. This is overlain by a series of 4 to 5 lens-shaped conglomerate bodies (maximum length: ca. 6-8 m; maximum thickness: ca. 1.4-1.7 m), stacked upon each other and separated by trough-shaped erosional surfaces. Each lenticular sediment body starts as clast-supported, open-work conglomerate, with angular to moderately rounded, evenly or slab-shaped pebbles. Slab-shaped clasts are imbricated, commonly at a high angle of dip (up

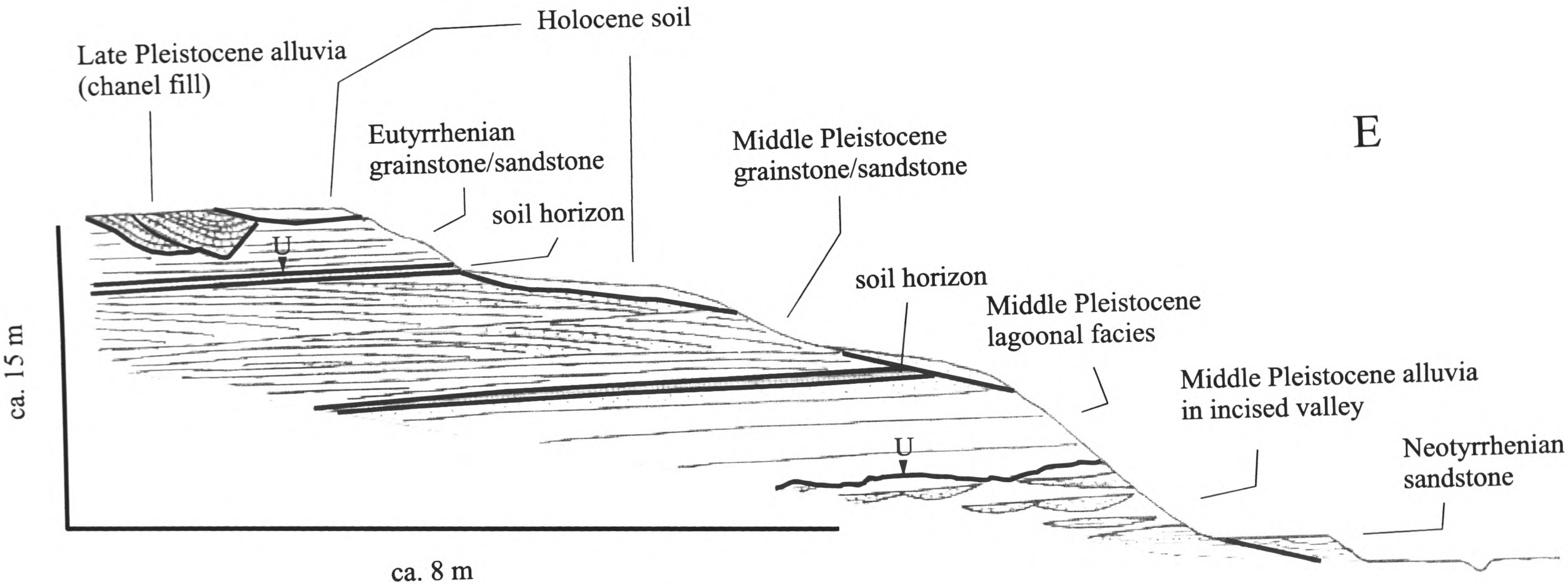

Figure 5.13.a: Field sketch of a middle to late Pleistocene outcrop in Tasou Rema. Middle Pleistocene alluvia were followed by two middle Pleistocene parasequences, each terminating with a soil horizon. It is possible that this outcrop evidences high-frequency sea level cyclicity in middle Pleistocene time, although autocyclic controls cannot be ruled out. These are followed by Eutyrrhenian shallow-marine sediments. Late Pleistocene alluvia filled channels cut into the latter sediment. The Neotyrrhenian terrace is also present, at lower elevations. A detailed log of this section is given in Fig. 5.13.b.

to 40°). These are succeeded by clast-supported, imbricated conglomerate beds, alternating with brown pebbly silt. Further up-sequence the sediment passes into sharp-based, tabular to slightly trough-shaped, clast-supported and imbricated conglomerate beds (bed thickness: 10-15 cm), alternating with pebbly silt beds. Individual conglomerate beds fine upwards. Clast roundness tends to decrease toward the top of each lenticular conglomerate body. Most clasts are correlated with marble, but volcaniclastic and "*Tyros Beds*" lithologies also occur; commonly represented by slab-shaped clasts.

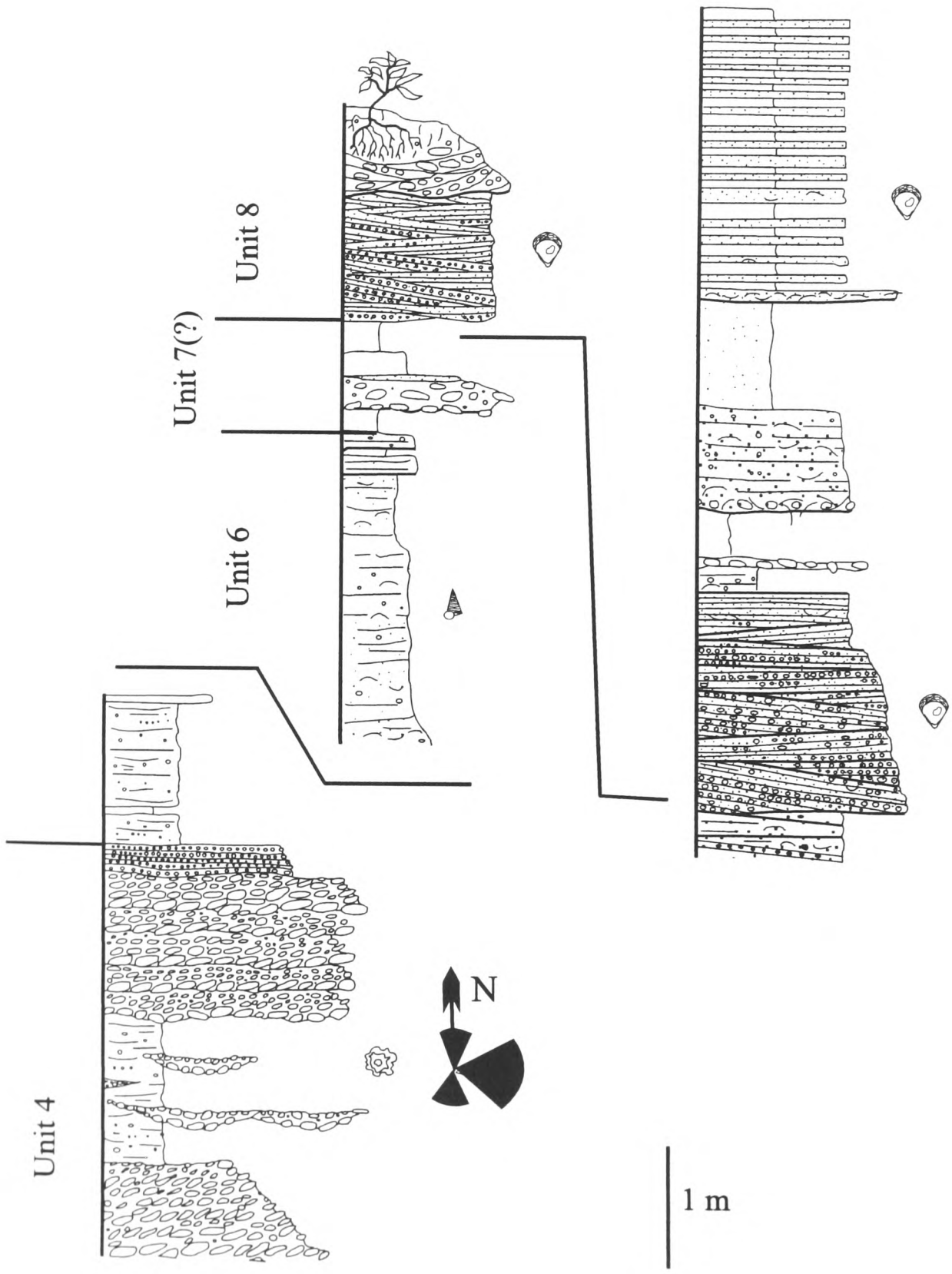

Figure 5.13: Logs of middle Pleistocene alluvia (Unit 4), followed by middle Pleistocene (Unit 6) and Eutyrrhenian shallow-marine sediments (Unit 8). Tasou Rema; for location see Fig. M.2.

Interpretation: The lower part of the section (pebbly silt to conglomerate) corresponds to the facies Gms ('massive sand-gravel') to Gm ('massive gravel'), *sensu* Miall (1978). This part is interpreted as proximal fan deposits, as evidenced by its lobe shaped geometry, deposition against a morphological scarp and sedimentary facies, suggesting deposition from a debris flow, or as lag in longitudinal bars (Miall, 1978, 1992). The calichified pebbly silt near the base corresponds to the facies P (fines) *sensu* Miall (1978). This is interpreted as a palaeosol, developed on overbank deposits, in interdistributary channel areas of the fan. This is supported by the relatively lower clast content and intense *Rhizocretion* calichification, resulting from vegetation cover. The conglomerate beds higher up-section are interpreted as gravel-bed braid stream deposits (Miall, 1992). Trough-based conglomerates (facies Gt *sensu* Miall, 1978) probably correspond to channel-fill deposits. Even based, coarsening-up conglomerates (facies Gm *sensu* Miall, 1978) probably represent longitudinal bar deposits. The overall coarsening-up trend suggests alluvial fan progradation. Purple terra rossa over the previous sediments is interpreted as an interchannel palaeosol. The upper part of the section, with stacked lenticular sediment bodies is interpreted as the fill of stacked shallow channels (Miall, 1992). Each of the channel-fill cycles suggests gradually decreasing energy of environment, from imbricated, channel bed lags (facies Gm, Gt *sensu* Miall, 1978) at the bottom, to interchannel, overbank pebbly silt at the top. Channel geometry, stacking pattern and sedimentary facies correspond to the gravel-bed braid-stream environment (Miall, 1992). Alluvial fan aggradation is suggested at scale of the section (<5 m).

5.3.3.2.2 Examples of more distal, channel-fill deposits of Unit 7 can be seen along many second and third order streams of the Ano Glikovrisi Horst (e.g. Mourtitsa and Kambourani Rema), as well as along coastal cliffs in the Kokkinia-Elea area (see Fig. 5.4). These deposits infill deep (ca. 10-12 m) channels cut through marine sediments of early and middle (?) Pleistocene age (Units 3, 5; see above). They begin with matrix- to clast-supported, fining-up conglomerate, that infills erosional relief in the underlying marine deposits. This is followed by orange yellow to red silt with clast-supported conglomerate lenses (thickness: 30-40 cm), or tabular conglomerate beds (thickness: up to 0.7-1 m), bounded by even, sharp surfaces. Both conglomerate beds and lenses commonly fine-up, although coarsening-up trends are locally present. The clasts are generally well rounded. In majority, they are correlated with local sources, e.g. marble (ca. 63%), "*Phyllite Series*" (ca. 11%) and early Pleistocene terrace lithologies (ca. 11%). A few pebbles of reworked early Pleistocene alluvia (Unit 4) also occur. The surrounding silty sediment is crudely bedded (bed thickness: 20-60 cm) and intensively calichified (***Rhizocretion*, nodular caliche**). An erosive surface

with a relief of <2 m truncates structures in the above sediments. This is followed by ca. 3-8 m of stacked, trough-shaped conglomerate bodies. Each of the latter (thickness: 0.5-1.5 m) starts as clast-supported, massive bouldery conglomerate (maximum clast size: 40 cm), locally with open-work fabric, and fines-up into trough cross-bedded conglomerate (maximum clast size: 10-15 cm), with alternations of pebbly red silt. Mainly tabular alternations of conglomerate with red silt beds (bed thickness: 7-20 cm; maximum clast size: 5-10 cm) occur towards the top. Individual conglomerate beds generally fine up, but coarsening-up trends are also observed locally. An overall coarsening-up trend is evident all through the section. The 12-40 m surface(s) were formed above these facies. These sediments were affected by valley incision (rejuvenation), that proceeded from, or below, present sea level. These sediments are, thus, presently preserved as fluvial terraces.

Interpretation: The lower, silt-dominated part of the succession is interpreted as corresponding to a braid-stream environment. Calichified and root-bioturbated silty beds (facies Fl, Fm, P, *sensu* Miall, 1978) are interpreted as overbank deposits, probably deposited within a vegetated interchannel setting. Mainly tabular, massive to trough cross-stratified conglomerate beds (facies Gm, Gt, *sensu* Miall, 1978) are interpreted as shallow channel fill and longitudinal bar deposits. This succession of facies reflects alternations of extreme conditions, from high discharge events, resulting to deposition of Gp facies, to very low-energy conditions, resulting to deposition of interbedded fines. The depositional architecture fits into the '*gravel bar and bed form*' class (GB, *sensu* Miall, 1992). Massive, matrix-supported conglomerate interbeds (facies Gms *sensu* Miall, 1978) are interpreted as debris flow deposits. Stacked beds of this facies are interpreted as 'sediment gravity flows' (SG, *sensu* Miall, 1992). GB and SG architectural elements are characteristic of alluvial fan systems; the presence of the latter element possibly results from catastrophic runoff from unvegetated areas (Miall, 1992). An increase in the ratio of gravel to fine-grained sediment up-section suggests alluvial fan progradation. The depositional environment probably corresponds to the intermediate to proximal zones of a prograding alluvial fan system. Similar facies in early to middle Pleistocene fanglomerates in Cyprus were interpreted as intermediate fan zones (Poole, 1992; Poole and Roberston, 1998). The upper, coarser-grained part of the succession (facies Gm, Gt, *sensu* Miall, 1978) is interpreted as channel-fill cycles, deposited in broad, shallow, high-energy channels. As in the more proximal settings described above, stacking pattern, channel geometry and sedimentary facies suggest that deposition took place in a pebble-bed braid channel environment, probably during alluvial fan progradation.

5.3.3.2.3 Stratigraphic Position of Unit 7: The age of the Unit 7 fanglomerate can only be inferred tentatively, on the basis of its relation with marine sediments. In Kambourani Rema (Figs. 5.4, 5.11.a), Unit 7 overlies estuarine-lagoonal facies of inferred middle Pleistocene age (Subunit 6.1; see above). On cliffs exposed along the present-day coastline, sediments correlative with Unit 7 are locally covered by shoreline facies of Eutyrrhenian age (see also Kowalczyk et al., 1992). Unit 7 is, thus, assigned a late middle Pleistocene age (Figs. 5.5, 5.6). This unit was deposited after a period of fluvial incision, responsible for the downcutting of broad valleys into the underlying marine sediments. This period probably coincided with a major relative sea level fall, correlative with the "Riss" interglacial in classic chronostratigraphic schemes (e.g. Bonifay, 1975) (Fig. 5.2). In sequence-stratigraphic terms, this unit represents a lowstand deposit, probably formed during maximum sea level fall and/or the early stages of (slow) relative sea level rise (Richards, 1996). The stratigraphy of Unit 7 implies that alluvial fan progradation was possibly incremental, interrupted by periods of aggradation, stabilisation, or erosion. The highest-energy facies, associated with development of stacked braid channels, occurs systematically in the upper parts of the unit. This could be explained, either as result of climate change (transition to more wet climate, with increased transport potential of the feeding drainage), or as result of relative sea level change, leading to increasingly steeper longitudinal stream profiles. The latter cause could have resulted from resumed high-order glacio-eustatic sea level fall, or tectonic triggering (land uplift), or from a combination of both the above.

5.3.4 LATE PLEISTOCENE-HOLOCENE SEDIMENTS

5.3.4.1 Unit 8: Eutyrrhenian: shallow-marine carbonates and siliciclastics: Sediments of the "Eutyrrhenian" terrace crop out widely along the western coast of the Eastern Lakonia Peninsula (Keraudren, 1970, 1971; Theodoropoulos, 1973; Kelletat et al., 1976, 1978; Kowalczyk et al., 1992) (Figs. 4.2, 4.8, 5.4, 5.5, 5.13, 5.14, 5.15, 5.16, 5.25, 5.26, 5.38, 5.39, M.2). The Eutyrrhenian Unit 8 is distinguished in Subunit 8.1 (NW part of Eastern Lakonia), comprising siliciclastics and bioconstructed carbonate facies, and Subunit 8.2, comprising sandstone/conglomerates (S part of Eastern Lakonia) (Fig. 5.2).

5.3.4.1.1 Subunit 8.1 (Siliciclastics): In the Kambourani Rema ravine mouth (Figs. 5.4, 5.11.a,d), "Eutyrrhenian" sediments unconformably overlie inferred middle Pleistocene deposits (distal facies of Subunit 6.1), over a sharp erosive surface with undulating relief (10s of cm). This surface truncates a fault of apparent listric geometry (0°/72°W), that offsets the underlying sediments, but not the "Eutyrrhenian" sediments above (Fig. 5.11.a).

The "Eutyrrhenian" sequence starts as polymict conglomerate with moderately rounded, slab-shaped clasts, correlated with various bedrock lithologies (marble, bedrock limestone, schist, volcaniclastics) and Pleistocene algal limestone (maximum clast size: 30-40 cm). Most pebbles are coated with crustose coralline algae. The sediment fines upwards into planar cross-stratified, coarse-grained sandstone/conglomerate, with wedge-shaped bedsets that dip seawards (to 190-200°) at 15° (average dip). The upper parts of the "Eutyrrhenian" sandstone are root-bioturbated, with abundant *Rhizocretion*. The total thickness of the unit is ca. 1.8 m. A terrace, at ca. 15-17 m, was formed above these sediments.

About 500m further inland, within the Kambourani Rema valley (Fig. 5.4), lagoonal sediments of inferred middle Pleistocene age (sand, silt, conglomerate) are unconformably overlain by a basal lag, passing up into *Cladocora caespistosa* bafflestone, with calcareous sandstone to lithic grainstone baffled by coral colonies in life position. The coral colonies are encrusted by cm-thick red algal crusts. Moldic dissolution of *Cladocora caespistosa* colonies resulted into coral-moldic pores through the calcareous sandstone (see Chapter 6).

A well preserved "Eutyrrhenian" deposit occurs around the mouth of the Bozas Rema ravine (Kowalczyk et al., 1992) (Figs. 4.2, 5.14, 5.26, 5.39, M.2). The "Eutyrrhenian" sediment (total thickness: ca. 2 m) covers a sharp erosional surface in calichified sands/silts of inferred middle Pleistocene age (Subunit 6.2; see above). It comprises wedge-shaped bedsets of low-angle planar cross-laminated lithic grainstone or conglomerate. The pebbles (maximum clast size: 4-6 cm) are well rounded, spherical or discoidal, and correlated with various bedrock types (marble, Tripolis Zone limestone, "*Phyllite Series*" metamorphics, volcaniclastics). Many pebbles are bored and encrusted by crustose coralline algae. Individual laminae (thickness: 1-3 cm) either fine, or coarsen upwards. Palaeocurrent data (pebble imbrication) display a bipolar pattern, with both landward and seaward trends (Fig. 5.14). The fauna include bivalves, rhodoliths, scleractinean corals, and, in coarser-grained facies (i.e. granular conglomerate), dense accumulations of the gastropod *Strombus bubonius* (Table 5.2, photos). As around Elea (see above), *Cladocora caespitosa* bafflestone facies are also encountered here, but moldic dissolution has removed coral colonies (Fig. 5.33).

The 15-20 m terrace was formed above these sediments 4.7 (Fig. 5.26). It is characterised by very low relief, a thick, purple terra rossa soil-cover and rock-pool morphology in its exposed parts (maximum diameter of rock-pools: ca. 30 cm; maximum depth ca. 12 cm); see Fig. 5.39). Relatively high elevation of the "Eutyrrhenian" in Bozas Rema is attributed to

very recent activity of generally N-S extensional faults, a seaward continuation of faults that bound the NW side of the Molai Graben (Figs. 4.2, M.2; see also Chapter 4).

Interpretation: All the "Eutyrrhenian" sections described above overlie a sharp erosional surface and exhibit a common fining-, then coarsening-up trend. The disconformity surface at the base of "Eutyrrhenian" successions is interpreted as a marine ravinement surface (Myers and Milton, 1996). Polymict conglomerate, that commonly succeeds the ravinement surface, was probably deposited in the foreshore zone, as a basal lag, as indicated by rounding of pebbles and their boring and encrustation by coralline algae (Kumar and Sanders, 1976; Reading and Collinson, 1996). Irregular depressions in the ravinement surface accommodate the coarsest clasts; these are interpreted as plunge steps, corresponding to the boundary between the shoreface and the foreshore zones (Kumar and Sanders, 1976). Pebbly sand, planar cross-stratified sandstone and silty sand higher up-section, were probably deposited in middle-upper shoreface environments, as suggested by sedimentary structures and fauna (Walker and Plint, 1992; Reading and Collinson, 1996). Low-angle laminated sandstone and conglomerate that form the top beds of these successions are interpreted as foreshore deposits, whereas sandstone with *Rhizocretion* was probably deposited in the backshore (Myers and Milton, 1996; Reading and Collinson, 1996). In proximal sites, *Cladocora caespitosa* bafflestone within a surrounding coarse-grained sandstone was probably deposited in a lower energy, protected environment, possibly in a flat, or back-barrier lagoon. Low wave energy and high sedimentation rates within these environments would allow for the delicate branching style and the *in situ* preservation of *C. caespitosa* colonies (see also Wilson, 1974; James, 1983; Tucker and Wright, 1990). All the above sections, thus, exhibit a deepening, then shallowing-up trend, beginning with marine ravinement, followed by foreshore deposits (bottom), shoreface (middle), and foreshore-coral flat, then backshore (top). In sequence-stratigraphic terms, the above sections are interpreted as a transgressive-regressive sequence, deposited during the fourth-order "Eutyrrhenian" sea level cycle (isotopic stage 5e, ca. 120 ka; Fig. 5.2). The transgressive systems tract, deposited during rising sea level, coincides with the lower part of the section, from the basal lag to the shoreface deposits (interpreted as a maximum flooding zone, *sensu* Myers and Milton, 1996). The highstand systems tract coincides with the regressive upper part of the sequence and includes the upper part of the shoreface deposits and the overlying foreshore/backshore deposits. Very similar transgressive-regressive shoreline deposits of "Eutyrrhenian" age are reported from the Quaternary of Cyprus (Poole, 1992, Poole and Robertson, 1992, 2000).

Dhaemonia: South of the Molai Graben, along the SE coast of the Lakonic Gulf, the "Eutyrrhenian" shoreline is preserved at many sites, at elevations generally ≤7-12 m (Kelletat et al., 1976; Kowalczyk et al., 1992). At Harahia (Dhaemonia coast; see Fig. M.2), the second distinct shoreline deposit (from present sea level upwards) is correlated with the "Eutyrrhenian" stage (Fig. 5.9). The ca. 7-10 m terrace was formed above this deposit. The "Eutyrrhenian" sediment body is relatively small (preserved length across strike ca. 12-15 m; maximum thickness: ca. 2.3-2.5 m) and of sigmoidal geometry. It covers a sharp sigmoidal surface cut in upper offshore facies of early Pleistocene age (Unit 3) (Fig. 5.9). This deposit begins with a shell lag, with imbricated bivalve shells, diverse gastropods (including *Astrea rugosa*), bryozoa and large rhodoliths (diameter: <6 cm), with coarse-grained moldic grainstone matrix. Most faunal elements are preserved as moulds. The presence of *Spondylous gaederopous* shells, however, together with possible *Astrea rugosa* moulds, favours attribution of this sediment to a "Tyrrhenian" sea level cycle (Papapetrou-Zamanis, 1971; Poole, 1992; Poole and Robertson, 2000). Poorly rounded slabs of bioturbated packstone/grainstone also occur near the base of the unit, correlated with cemented hardgrounds in the underlying early Pleistocene sediment. Up-section, the sediment passes into massive, coarse-grained moldic grainstone, with no discernible structures. However, lateral equivalents comprise sharp-based alternations of medium- to coarse-grained, hummocky cross-stratified grainstone with bioturbated carbonate siltstone. The upper parts of the section are calichified, with red bioclastic hardpan and irregular karstic relief. *Rhizocretion* bioturbation is locally abundant.

Interpretation: The sigmoidal unconformity at the base of the deposit is interpreted as a marine ravinement surface, eroded in the early to middle Pleistocene substratum during transgression (Myers and Milton, 1996). The accumulation of shells and grainstone slabs that follows is interpreted as a basal lag, partly reworked from the underlying sediment. Above this, alternations of sharp-based, hummocky cross-stratified, moldic grainstone with carbonate silt is interpreted as a lower shoreface deposit, below the fair-weather wave base, but above storm wave base, in a storm-influenced setting (Reading and Collison, 1996; Walker and Plint, 1996). The macrofauna indicate a circumlittoral depth and normal marine salinity (Georgiades-Dikeoulia, 1984). Seaward transport of shells is attributed to storm-generated rip currents (Kumar and Sanders, 1976; Walker and Plint, 1996). Calichification and karstic dissolution obliterated structures in the uppermost parts of the section. The presence of local *Rhizocretion* bioturbation, however, suggests that these topsets also include backshore deposits. The section is, thus, interpreted as a transgressive-regressive

sequence, deposited during the "Eutyrrhenian" sea level cycle (isotopic stage 5e, ca. 120 ka; see Fig. 5.2).

5.3.4.1.2 Subunit 8.2: conglomerate: At Elika coast (Figs. 4.2, M.2), the "Eutyrrhenian" terrace is mainly erosive, either into bedrock (e.g. Pirgos tou Phonia), or in cemented sediments of early and middle(?) Pleistocene age. At Cape Pounta (Figs. 5.16, A.12), however, at an elevation of ca. 17 m, small (maximum length across strike: ca. 2 m) conglomerate bodies of sigmoidal geometry come unconformable above earlier Pleistocene sandstone (Unit 3; see above). This conglomerate (maximum thickness: ca. 1.5-2 m) is clast-supported, with well rounded, even or discoidal, imbricated pebbles of Tripolis Zone limestone, and matrix of coarse-grained sandstone. The fauna include thick-shelled bivalves, scaphopods and rhodoliths. Most shells are fragmented and moderately abraded. The dominant palaeocurrent direction indicated by both shells and pebbles is towards the WSW (Fig. 5.14).

Interpretation: This conglomerate is interpreted as a "Eutyrrhenian" basal lag, corresponding to the transgressive systems tract of the "Eutyrrhenian" sea level cycle (Fig. 5.2).

South Lakonia: In the southernmost part of the Eastern Lakonia Peninsula, uniformity of the Pleistocene facies (mainly coarse-grained shallow-marine sediments) and less distinct terrace relief, complicate the recognition of 4^{th}-order Pleistocene shorelines. Nevertheless, such cycles can be distinguished in a few sections (see Figs. 5.2, 5.14).

At Ayia Marina (Fig. 5.4), a coastal cliff section includes two subaerial horizons intercalated between shallow-marine sediments (Figs. 5.16, 5.25). The lowest one, a red fluvial conglomerate, is taken to separate early Pleistocene marine sediments below, from middle Pleistocene marine sediments above. The second subaerial horizon (well-sorted, red, cross-laminated sandstone, probably of aeolian origin) is inferred to separate middle Pleistocene marine sediments (Subunit 6.2) below, from "Eutyrrhenian" marine sediments above. The latter comprise medium- to coarse-grained, incompletely cemented, olive-grey sand, with a rich fauna of thick-shelled bivalves, gastropods, various echinoids (Marcopoulou-Diakantoni, 1975), scaphopods and cyclostomata bryozoa. The sediment is extensively bioturbated, with *Skolithos* and *Thalassinoides* burrows. *Rhizocretion* structures abound, mainly in the upper part of the section. Depositional structures include swalley cross-

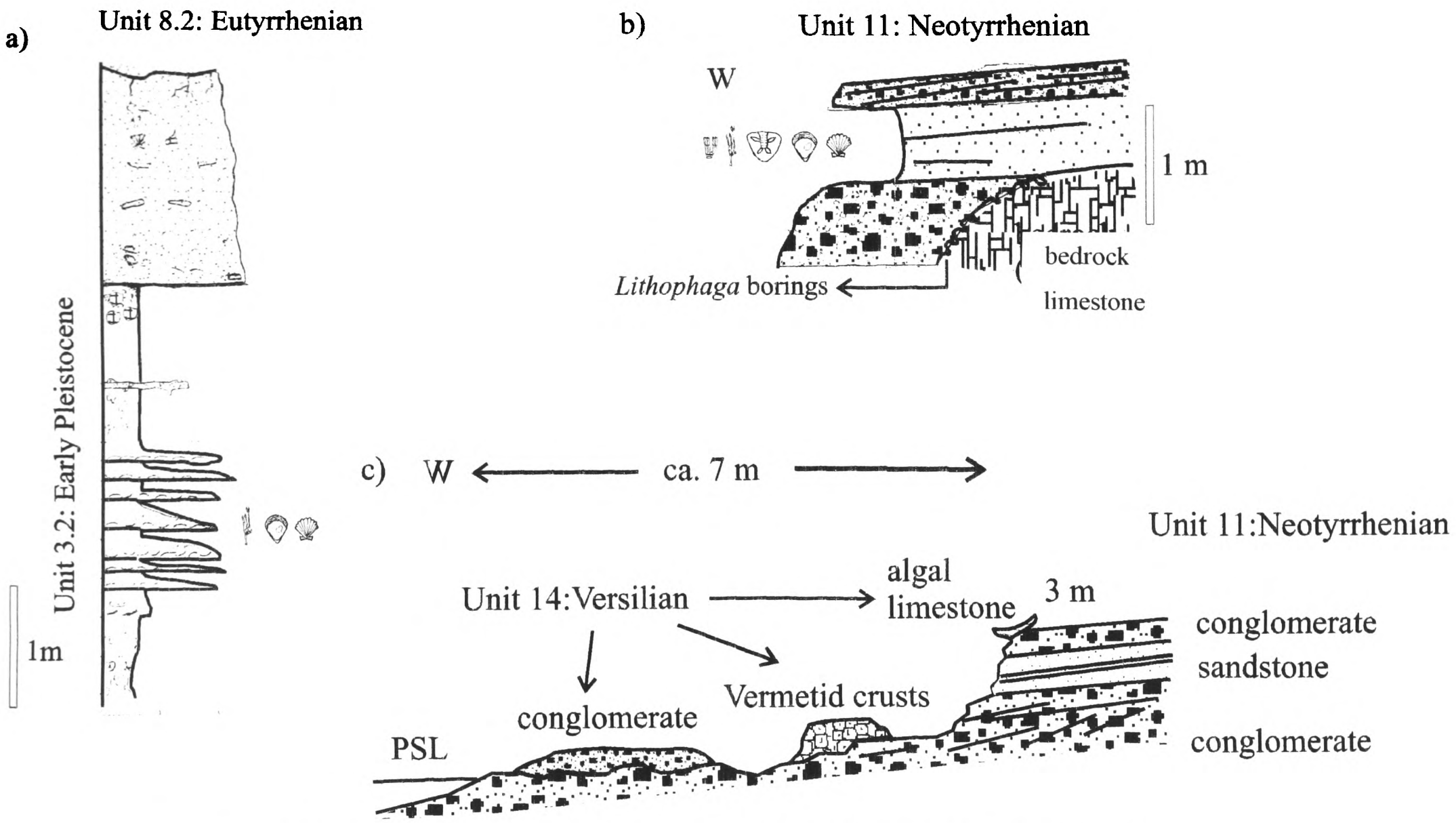

Figure 5.14: Logs of late Pleistocene shallow-marine sediments (Subunits 8.1, 8.2: Eutyrrhenian/ Unit 11: Neotyrrhenian). For locations see Fig. M.2.

stratification (lower part) and low-angle lamination (upper part). Thin (thickness: 0.5-1 cm), normally graded laminae of micaceous sandstone occur towards the top (dip: ca. 5° seawards). Above this, offlapping conglomerate bedsets cover the olive-green sand after a sharp surface. These conglomerate besets (thickness: 20-35 cm) are sigmoidal in shape, successively offlapping one another and prograding seawards (to the ESE). Pebbles are mainly even-shaped, poorly rounded to angular, correlated with Tripolis Zone limestone. Individual bedsets coarsen upwards. Low-angle cross-laminated, coarse-grained sandstone/granular conglomerate beds occur in the upper part of these conglomerate deposits. These sediments are cut by a series of E-W faults and uplifted up to 20 m ASL. Similar facies, cut by NNW-SSE faults, crop out in the area of Limnakia, south of Neapolis (Theodoropoulos, 1973) (Fig. 5.15).

Interpretation: As with other "Eutyrrhenian" successions, this also starts with a marine ravinement surface (Walker and Plint, 1996), eroded in underlying aeolianite (purple grainstone). In contrast with other "Eutyrrhenian" sections further north, no basal lag is observed in this section between the ravinement surface and the overlying sediments. The latter are interpreted as amalgamated shoreface deposits, on the basis of lithofacies, fauna and bioturbation (*Skolithos* ichnofacies, *sensu* Pemberton and Frey, 1996). Swalley cross-stratification is characteristic of storm-dominated, middle to upper shoreface environments (Walker and Plint, 1996). Low-angle laminated sand higher-up was probably deposited in the upper shoreface-foreshore zone (Reading and Collinson, 1996; Walker and Plint, 1996). The conglomerate that tops the succession is interpreted as an upper shoreface-foreshore deposit, fed by a fan delta system. This interpretation is supported by its altimetric correlation with coarse-grained, subaerial conglomerates further inland. The section, thus, comprises a progradational 'sequence', from shoreface to foreshore to fan delta. In sequence-stratigraphic terms, the whole section can be correlated with the prograding, highstand systems tract of the "Eutyrrhenian sea level cycle, deposited during the late stages of sea level rise (slow-rate of sea level rise) and/or the early stages of sea level fall. The sharp contact of the conglomerate topsets with the underlying sandstone possibly resulted from high-order intra-"Eutyrrhenian" sea level cyclicity. In this interpretation, the conglomerate would correspond to a second "Eutyrrhenian" highstand, after a short-lived relative sea level fall. Such high-order sea level cyclicity during isotopic stage 5e (correlative with the "Eutyrrhenian") is radiometricaly documented in the Red Sea (Plaziat et al., 1995), and also inferred from the "Eutyrrhenian" of Corinth (Keraudren, 1971) and Messenia (Kourampas and Robertson, 2000; Chapter 3). Alternatively, coarsening of the section from sand to conglomerate upwards could result from increased supply of

terrigenous material from the adjacent drainage. This effect might have resulted from either climatic or tectonic causes (i.e. relative sea level fault due to land uplift during a single "Eutyrrhenian" sea level cycle).

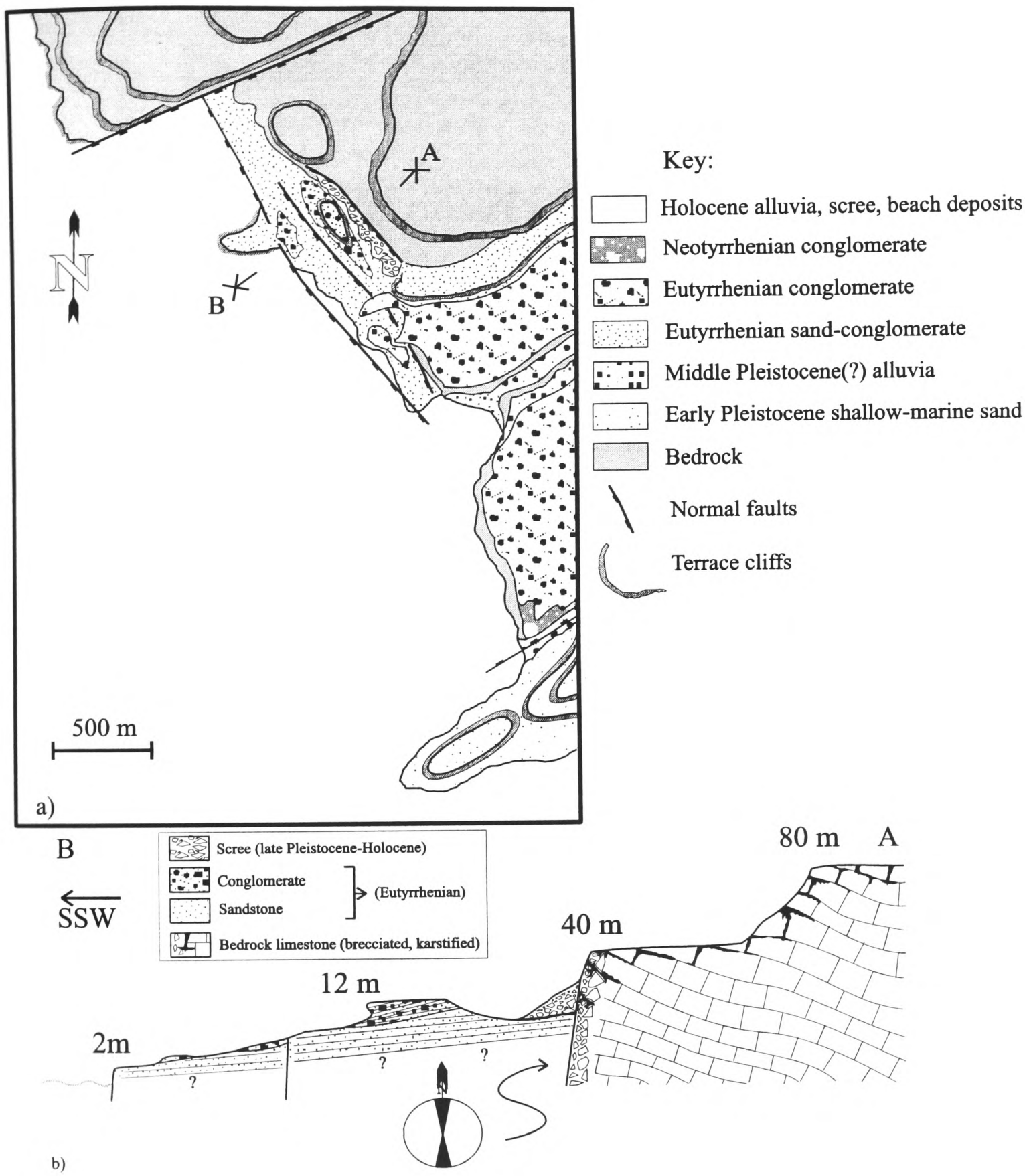

Figure 5.15: Field-sketch and cross-section of Limnakia coast (for location see Figs. 5.5, M.2). **a:** Late Pleistocene shallow-marine and alluvial sediments were deposited on a relief controlled by ENE-WSW and N-S faults, that cut bedrock and early Pleistocene shallow-marine sediments. "Eutyrrhenian" sediments were cut by NNW-SSE faults. Four erosional marine terraces are distinguished on bedrock. The two lower terraces are correlated with the "Eutyrrhenian" and "Neotyrrhenian" stages. **b:** Section across the Limnakia terraces. "Eutyrrhenian" clinoforms (packstone, coarsening up to conglomerate) were deposited on the hangingwall of a N-S fault in bedrock limestone. The "Eutyrrhenian" sediment is a coarsening upward, regressive sequence. The "Eutyrrhenian" terrace is offset by NNW-SSE to N-S faults. The 2m terrace is correlated with the "Neotyrrhenian" sea level cycle.

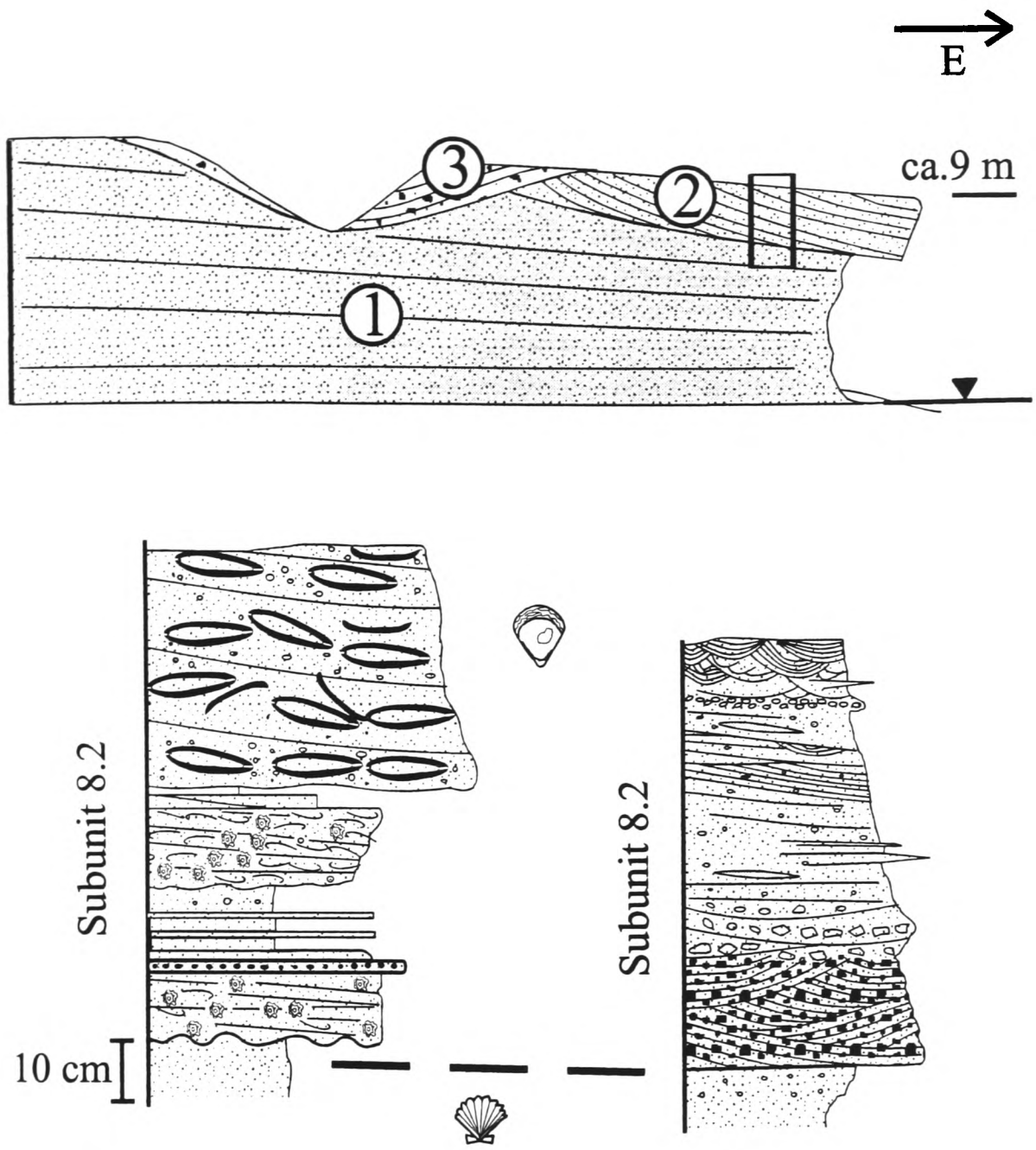

Figure 5.16: Middle and late Pleistocene sediments from the eastern coast of the Eastern Lakonia Peninsula. Middle Pleistocene sand (**1:** Subunit 6.2) is covered by Eutyrrhenian sediments (**2:** Subunit 8.2). Late Pleistocene alluvia (**3:** Unit 12) come unconformably above). Psiphia Coast.

Eastern Coast: In the eastern coast of the Eastern Lakonia Peninsula, sediments correlated with the "Eutyrrhenian" sea level cycle crop out at Psiphia (Fig. M.2), in association with the 10-20 m terrace. The Psiphia section (Fig. 5.16) begins with well sorted, olive-green (dip: 8° to ESE). The fauna include well preserved bivalves (*pectenidae*), scaphopods, echinoids and bryozoa. This sediment probably corresponds to the seaward continuation of the 40 m terrace sediment, of inferred middle Pleistocene age (Subunit 6.2). After a sharp, east-dipping, gently inclined (5-6° to 80-90°) erosional surface, with undulating relief of ca. 3-5 cm, follows grey lithic grainstone (thickness: ca. 30-40 cm), with a rich fauna of bivalves, barnacles, scaphopods, scleractinean corals and rhodoliths. Bioclasts are closely packed, and the bed locally transits to a matrix-supported shell-rhodolith lag. A sharp surface on top of the latter is followed by ca. 20-25 cm of alternating granular bioclastic

conglomerate with grey sand to sandstone. The conglomerate beds are well cemented, ca. 3-5 cm thick, and contain well-rounded clasts (maximum clast size: 3 cm) derived from bedrock. Individual beds fine upwards. The faunal content are as in the underlying bed. After a sharp surface, rhodolith-mollusc-coral sandstone follows. The sediment becomes coarser-grained, more bioclastic and closely packed up-section. The following ca. 10 cm comprise low-angle laminated sandstone, with normally graded laminae. The uppermost ca. 30 cm-1 m comprise dense accumulations of closely packed, articulated shells or moulds *Ostrea* sp. set in coarse-grained sandstone matrix (Fig. 5.36). These mollusc-rhodolith-coral beds exhibit a low-angle sigmoidal geometry, offlapping the underlying olive-green sand and progressively each other (Fig. 5.16). The ca. 10-20 m terrace was formed above these sediments.

Interpretation: The gently inclined erosional surface at the base of the section is interpreted as a marine ravinement surface (Walker and Plint, 1996). The overlying sediments are interpreted as upper shoreface foreshore deposits, as suggested by grain size, sediment structures and fauna. Bedsets are bounded by sharp surfaces followed by bioclastic lags. These surfaces probably resulted from wave activity, as indicated by their sigmoidal geometry (Collela, 1991). The progradational architecture of the deposit suggests that the latter was deposited during the highstand or early stages of sea level fall of the "Eutyrrhenian" sea level cycle (Fig. 5.2).

5.4.3.2 Unit 9: Alluvial terraces ("Eutyrrhenian"): The ca. 15 m fluvial terrace in Dokali Rema (Figs. 4.10, 5.17, M.2) is correlated with the 7-10 m "Eutyrrhenian" marine terrace on the coast (Subunit 8.1; Fig. 5.9). The basal 0.9-1m of the succession comprise clast-supported, imbricated conglomerates (bed thickness: 7-15 cm). The sediment is very well sorted, with most clasts falling within the 1-2 cm size-range (maximum clast size: 7 cm). Clasts are very well-rounded, derived from various bedrock lithologies. Oxidised bands of black or red colour occur occasionally (thickness: ca. 10-20 cm). Structures include planar and trough cross-stratification (trough width: ca. 0.7-1 m) and convolute lamination. Pebbles are rotated and aligned parallel to the fault plains of mesoscopic normal faults (throw <10 cm) (Fig. 5.17). Interbeds of very well sorted, medium-grained sand (average thickness: 4 cm), with normally graded, mm-scale laminae, also occur. Laminated sand beds (thickness: 10-20 cm) are present in the upper parts, intercalated with conglomerate (bed thickness: 20 cm). Structures include trough cross-bedding and small-scale trough cross-lamination (trough width: ca. 3 cm). The upper 2.5-3m of the section comprise matrix-supported conglomerate beds, with occasional intercalations of clast-supported conglomerate and fine-

grained sand. The lower bounding surfaces of bedsets are sharp, with 2-3 cm of erosive relief locally. Both bed thickness (bottom: 30 cm / top: 70 cm) and maximum clast size (bottom: 12 cm / top: 25 cm) increase up-section. Most individual beds fine-up; some coarsening-, then fining-up beds occur near the base of the section. The pebbles are generally imbricated. The matrix comprise yellow or grey, coarse-grained sandstone. The upper parts of the section are conspicuously more cemented, as compared with the lower parts.

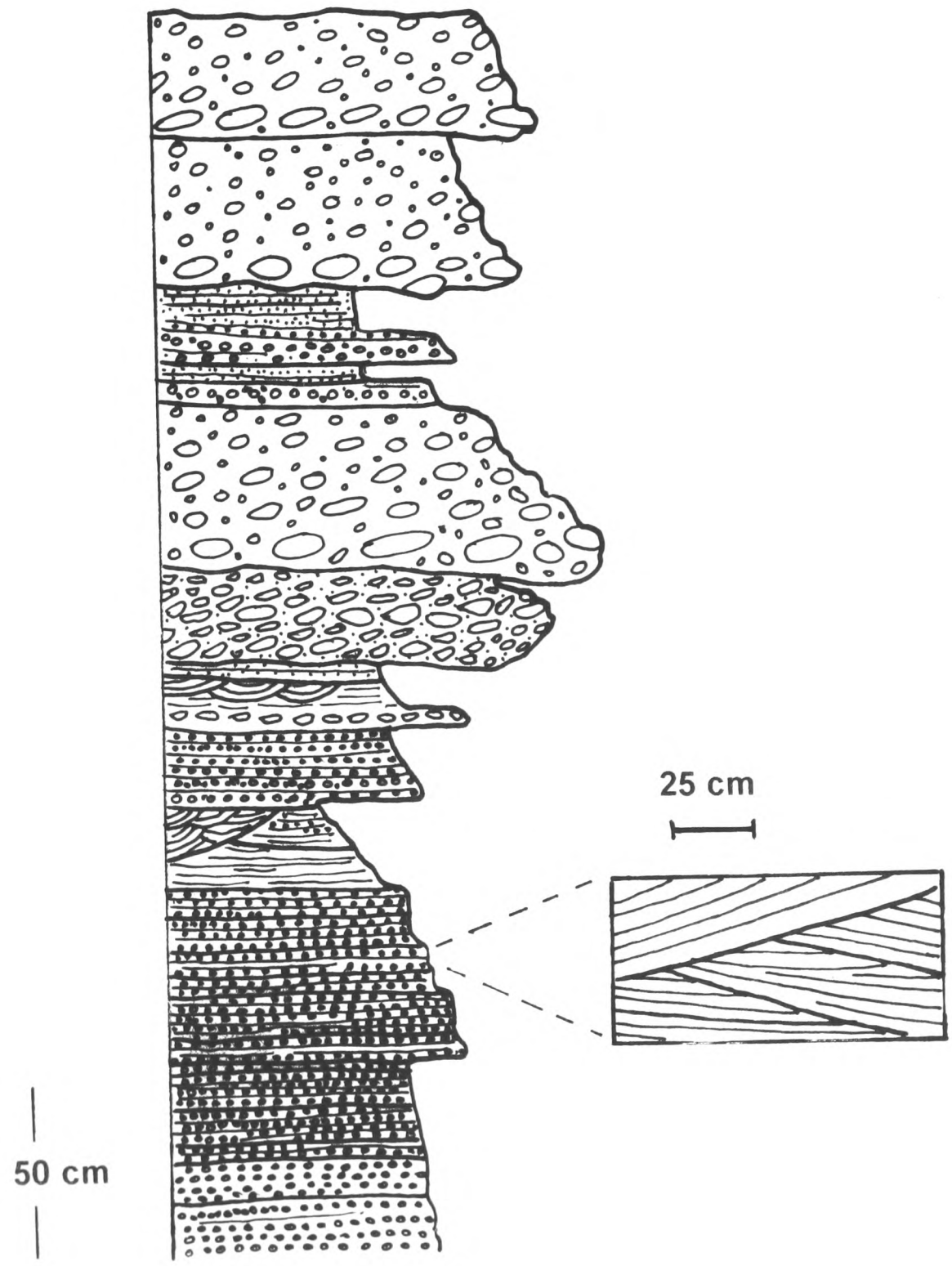

Figure 5.17: Fluvial sediments correlated with the Eutyrrhenian stage, Dokali Rema.

Interpretation: The absence of marine fossils suggests that Unit 9 was deposited in a fluvial environment. The lower, coarser-grained parts of the section include the facies Gm ('massive gravel'), Gp ('planar cross-stratified gravel') and Gt ('trough cross-stratified gravel'), *sensu* Miall (1978). These facies probably reflect deposition in small channels and bars (Miall, 1992), developed within a braided river environment. Good sorting indicates sediment transport for long distances, probably by a mature fluvial system. Convolute lamination resulted from dewaternig, possibly associated with syndepositional faulting. Sandy interbeds facies are correlated with the facies St ('trough cross-stratified sand'), Sp ('planar cross-stratified sand') and Sr ('ripple cross-laminated sand'), *sensu* Miall (1978), probably reflecting deposition in small dunes and ripples (Miall, 1992). Increasing presence of sandy beds upwards suggests decreasing energy of the environment, possibly reflecting the filling-up of a braid-channel system. Massive, clast-supported conglomerate in the upper parts of the section (facies Gm *sensu* Miall, 1978) is attributed to debris flow processes (Miall, 1978, 1992). The lower part of the section, thus, reflects decreasing energy conditions, with fluvial aggradation and filling-up of a braid channel system, whereas the upper part of the section reflects higher-energy conditions, with progradation of debris-flow deposits over the underlying channel fill.

As noted above, the altitude of this deposit correlates with a transgressive-regressive "Eutyrrhenian" terrace on the coast, interpreted as highstand deposit (Subunit 8.1; see above). However, field evidence does not allow unequivocal correlation of the fluvial terrace with a particular stage in the "Eutyrrhenian" sea level cycle, since no intercalated marine and fluvial are present. Depositional architecture of fluvial sediments could provide clues for an interpretation at systems-tracts level (Richards, 1996), but this cannot be based on extrapolation of information from one examined section. However, a tentative correlation can be made between the aggradational, followed by progradational trend of the fluvial terrace, and the transgressive-regressive sequences characteristic of the "Eutyrrhenian" marine terrace in the Eastern Lakonia Peninsula (Unit 8; see above), Messenia Peninsula (Unit 3.1; Kourampas and Robertson, 2000; Chapter 3) and Cyprus (Poole, 1992; Poole and Robertson, 1991, 2000). Following this correlation, the aggrading, lower part of the fluvial terrace corresponds to deposition due to base level rise (controlled by relative sea level rise); consequently it correlates with retrograding to aggrading shoreline facies further distally (transgressive systems tract and maximum flooding zone). The prograding, upper part of the fluvial terrace corresponds to stable, or slowly falling, base level (controlled by sea level highstand); consequently it correlates with prograding shoreline facies further distally (highstand systems tract).

5.3.4.3 Unit 10: Alluvia (Late Pleistocene lowstand I): These sediments constitute alluvial terraces at low elevation, in valleys incised into the "Eutyrrhenian" terrace (Figs. 4.8, 5.4, 5.13, 5.16, 5.18, 5.27, 5.31). These replicate the same coarsening-up trend characteristic of Unit 7 alluvia (see above). The Unit 10 deposits begin with red mud or silt, with occasional pebbles, and pass upwards into alternations of sharp-based, tabular beds of polymict conglomerate (Fig. 5.27). Up section, the latter are succeeded by massive, or trough cross-stratified, coarsening-up, polymict conglomerate. Middle and late Palaeolithic stone tools were found in alluvia of this unit, near Elea (Fig. 5.4) (Kowalczyk et al., 1992).

Interpretation: Like Unit 7 (see above), these sediments are also interpreted as deposits of prograding alluvial fans. The lower red silt / pebbly silt (facies F *sensu* Miall, 1978) is interpreted as interchannel deposit. Tabular conglomerate beds (facies Gm *sensu* Miall, 1978), higher-up, are interpreted as channel and bar deposits, whereas the uppermost massive and trough cross-stratified conglomerates (facies Gm, Gt *sensu* Miall, 1978) are interpreted as channel fill deposits. Sediment architecture and stacking pattern indicate that these sediments were deposited in an aggrading to prograding, bed-load braid stream system (Miall, 1992). This system probably developed within an intermediate, then proximal, alluvial fan environment (Miall, 1978, 1992; Reynolds, 1996). Similar intermediate to proximal alluvial fan facies were described from the Pleistocene of Cyprus (McCallum and Robertson, 1990, 1995; Poole, 1992; Poole and Robertson, 1991, 1998) and SW Turkey (Glover and Robertson, 1998a).

These sediments postdate the "Eutyrrhenian", since they are deposited in valleys incised into the latter terrace. Their relation with the "Neotyrrhenian" is less clear, but Kowalczyk et al. (1992) suggested that these sediments are sandwiched between the "Eutyrrhenian" and the "Neotyrrhhenian" terraces (as inferred from Elea; Fig. 5.4). Unit 10 deposits can also be distinguished from earlier and later alluvia by artefacts of Middle Palaeolithic industry. On the above evidence, these alluvia are attributed to the first late Pleistocene lowstand ("Würm I" *sensu* Kelletat et al., 1976; Kowalczyk et al., 1992), correlated with the sea level fall between the "Eutyrrhenian" and the "Neotyrrhenian" in Bonifay's chronostratigraphic scheme (1975) (see Fig. 5.2).

5.3.4.4 Unit 11: Shoreline conglomerates, carbonates ("Neotyrrhenian"): The discontinuous "Neotyrrhenian" terrace (locally with *Strombus bubonius*) is preserved at many sites, particularly along the western coast of the Eastern Lakonia Peninsula (Kelletat et al., 1976; Kowalczyk et al., 1992) (Figs. 4.2, 4.20, 5.4, 5.37). It usually comprises one or two fining, then shallowing-up cycles (from basal conglomerate, to coarse-grained mollusc-rhodolithic sandstone or grainstone, to conglomerate and/or aeolianite). "Neotyrrhenian" shallow-marine sediments are commonly red or orange-red, as in many other parts of the Peloponnese (Keraudren, 1970, 1971; Kowalczyk et al., 1992; Chapter 3, this work). Discrete red terrigenous silt intercalations commonly occur within the latter facies.

At Marathia (Elika's coast; Figs. 5.37, M.2), a very coarse-grained sediment body, at maximum altitude of ca. 3 m, was in the past correlated with the "Neotyrrhenian" sea level cycle (Kowalczyk et al., 1992). This sediment is plastered against terraced cliffs, eroded in the limestone bedrock in earlier Pleistocene time. The lowest exposed parts consist of poorly sorted, clast-supported, polymict conglomerates, with angular clasts (maximum clast size: 3 cm) of various bedrock lithologies (i.e. metamorphic, volcaniclastic, carbonate). The fauna include large thick-shelled bivalves and gastropods (including *Strombus bubonius*). This sediment is followed by silty-pebbly sandstone with bivalves and *Skolithos* burrows. Wave scours in the latter (depth: ca. 3-6 cm) are infilled with fining-up pebbly lags. The above sediment is offlapped by steep conglomerate bedsets (ca. 12-15° to the SSW/seawards). These begin with bouldery, massive, polymict conglomerate (maximum clast size: ca. 30 cm) with moderately rounded, even-shaped bedrock clasts and red, coarse-grained sandstone matrix. Boulders bored by *Lithophaga* sp. are common. The fauna comprise thick-shelled bivalves, including *Spondylous gaederopous*. Above come beds of clast-supported, matrix-poor, angular conglomerate (bed thickness: 20-50 cm), with occasional trough-shaped sandstone intercalations (thickness: 10-25 cm). Individual beds fine upwards. The fauna, besides taxa occurring in lower beds, also include the coral *Cladocora caespitosa*. Almost identical successions of coarse-grained facies were also described from many other sites of the Eastern Lakonia Peninsula and attributed to the "Neotyrrhenian" sea level cycle (Kowalczyk et al., 1992).

Interpretation: In agreement with Kowalczyk et al. (1992), Unit 11 is interpreted as deposits of a high-energy shoreline. The lower conglomerate is interpreted as a submarine scree talus, deposited in front of a wave-eroded cliff. This is supported by the preserved palaeotopography, poor sorting of the sediment and predominance of locally derived, angular clasts with borings of the rock-dwelling bivalve *Lithophaga* sp. Given its

circumlittoral mollusc fauna, this sediment was deposited nearshore, possibly in the upper shoreface-foreshore zone (Georgiades-Dikeoulia, 1984). Silty-pebbly carbonate sand that comes above is interpreted as a shoreface deposit, as suggested by mollusc fauna (Georgiades-Dikeoulia, 1984), bioturbation (*Skolithos* ichnofacies; Pemberton and Frey, 1996), and presence of wave scour structures (Koumar and Sanders, 1976, Reynolds, 1996). Offlapping conglomerates that follow probably represent a prograding submarine scree talus, as indicated by angular clasts and poor sorting. Clast-supported, matrix-poor conglomerate and sandstone higher up probably correspond to a prograding pebbly beach (Postma and Nemec, 1990). Trough-shaped interbeds of coarse-grained sandstone are attributed to wave scouring (Reading and Collinson, 1996). Their presence indicates that deposition took place in the upper shoreface (to foreshore?). Therefore, this deposit was deposited in deepening-, then shallowing-up conditions. In sequence-stratigraphic terms, the lower conglomerate, with part of the intermediate sandstone correspond to the transgressive systems tract of the "Neotyrrhenian" sea level cycle, terminating at the maximum flooding zone (Reynolds, 1996). The prograding, scree talus to beach facies further up probably correspond to the highstand systems tract of the "Neotyrrhenian" sea level cycle. The presence of the age-specific gastropod, *Strombus bubonius* within the sediment indicates its "Tyrrhenian" (Last Interglacial) age (Papapetrou-Zamanis, 1968; Keraudren, 1970, 1971), as already noted by Kowalczyk et al. (1992).

In Ayia Marina (Figs. 5.5), a terrace at ca. 1,5-2.5 m is correlated with the "Neotyrrhenian". The sediment is deposited over a sharp, almost horizontal surface, cut into fossiliferous sand of inferred early Pleistocene age (Unit 3). The latter surface, at altitude of ca. 0.7-1 m, is covered by ca. 40 cm of root-bioturbated calcareous sandstone, probably reworked from the underlying sediment. Above come ca. 50-60 cm of low-angle tabular beds of angular, oligomict conglomerate, with pebbles derived from local bedrock lithologies (e.g. limestone, marble). Each conglomerate bed is ca. 20-30 cm thick and fines upwards. The fauna include moderately abraded, thick-shelled bivalves. This is followed by ca. 50 cm of coarse-grained grainstone, with low-angle cross-lamination and fenestral porosity (pore diameter: ca. 0.5-1 cm). Bedsets in the latter are defined by low-angle tabular surfaces that dip seawards (SSE) at 8-10° (bedset thickness: ca. 17-25 cm). Pervasive *Rhizocretion* bioturbation affected this and the underlying sediment (diameter: ≤2-4 cm).

Interpretation: The upper, reworked and root-bioturbated zone of the underlying early Pleistocene sediment probably corresponds to an immature palaeosol, formed before the "Neotyrrhenian" transgression. The nearly horizontal erosional surface above the latter is

interpreted as a marine ravinement surface (Myers and Milton, 1996). Low-angle cross-laminated grainstone that comes above is interpreted as a foreshore deposit, based on sedimentary structure and fenestral porosity (Coudray and Montaggioni, 1986; Tucker and Wright, 1990).

5.3.4.5 Unit 12: Alluvia (late Pleistocene lowstand II): These latest Pleistocene alluvia were previously described by Kowalczyk et al. (1992). At the Ano Glikovrisi Horst (Fig. 5.4, M.2), they fill V-shaped valleys incised through "Eutyrrhenian" and older marine and subaerial deposits. Their lower exposed parts comprise thick terra rossa (thickness: 0.8-1 m), with discontinuous lenses of polymict conglomerate (thickness: 10-15 cm; maximum clast size: 2-5 cm). This is succeeded by ca. 5-10 cm of coarsening-up, clast-supported, imbricated conglomerate, followed by poorly structured to massive, matrix- to clast-supported, polymict conglomerate, with a red silt matrix (reworked terra rossa ?). Clasts are generally angular and irregular in shape. Tabular, fining-up beds of clast-supported, imbricated conglomerate follow up section. These beds are more oligomict than the lower ones, and well-rounded, elongate clasts, correlated with local bedrock limestone, predominate. Clasts of Pleistocene grainstone/packstone also occur. The total thickness of the conglomerate beds reaches ca. 6-7 m. These red beds are incised by the Assopos ravine (Figs. 5.4, M.2) and the 10-15 m ASL fluvial terrace is formed on their surface.

Alluvia of late Pleistocene age are widespread along the Molai Fault system, on its hangingwall side (Figs. 5.4, M.2). These were deposited in coalescent alluvial fans around the mouths of V-shaped valleys incised into the hangingwall of the Molai Fault system (Fig. 5.20). They comprise coarse, crudely bedded, clast- and matrix-supported conglomerates with angular clasts, deposited from debris flows. These alluvia are interpreted as very proximal, fan-head facies (Poole, 1992; Miall, 1996; Poole and Robertson, 1998).

A locally derived, proximal alluvial fan is situated in the Bozas Rema area (Figs. 4.7). This fan drapes the cliff of the ca. 20 m "Eutyrrhenian" terrace (see Chapter 4). The base of the fan rests on yellow cemented breccia of inferred Late Tertiary age (Unit 1). The succession begins with ca. 65 cm of clast-supported, fining-up beds of polymict conglomerate (bed thickness: 12-18 cm). Pebbles (maximum clast size: 20 cm) are well rounded, derived mainly from bedrock limestone (Tripolis Zone) and also from "Eutyrrhenian" grainstone. The sediment is well sorted and clast imbrication is absent. Many clasts bear *Lithophaga* borings. The basal parts of the beds are characterised by open-work fabric. A few mollusc

shells (e.g. *Ostrea* sp., *Murex* sp.), are also present in this lower part, probably reworked from the "Eutyrrhenian" terrace. These beds are succeeded by ca. 30 cm of matrix-supported conglomerate with angular clasts in red silt matrix. In sharp contact with the latter come 2-2.5 m of bouldery oligomict conglomerate. The sediment is matrix-supported, with large (maximum clast size: 2 m), angular boulders of "Eutyrrhenian" grainstone/bafflestone and bedrock limestone in red silt matrix. Bedrock clasts are commonly perforated by large *Lithophaga* borings, infilled with "Eutyrrhenian" grainstone. *Lithophaga* shells are locally preserved in borings. "Eutyrrhenian" terrace boulders contain *Cladocora caespitosa* colonies in life position. This conglomerate bed is massive, with a coarsening-, then finning-up trend. Many boulders lie with their long axis inclined steeply. This facies is succeeded by ca. 50 cm of matrix-supported, angular conglomerate, similar to the underlying bed (see above). The succession terminates with ca. 1.7-2 m of coarsening-up, clast-supported, matrix-rich, oligomict conglomerate, with angular clasts (maximum clast size: 25-30 cm, near the top). The origin of the clasts is similar to that of the underlying sediment (predominantly "Eutyrrhenian" shoreline facies).

Interpretation: This deposit is interpreted as a proximal alluvial cone, fed by reworking of a "Eutyrrhenian" terrace at a topographically higher level. The lowest beds, correlated with the facies Gm (massive gravel) *sensu* Miall (1978), are interpreted as sieve gravel lobes, as indicated by their open-work fabric, good sorting and absence of imbrication (Hooke, 1967). The massive, disorganised breccia which follow are correlated with the facies Gms *sensu* Miall (1978) and interpreted as debris flows. Very large clast size (m-scale boulders), angular clast shape and almost exclusive presence of "Eutyrrhenian" terrace facies, indicate that this is a very proximal deposit, probably deposited episodically. This deposit post-dates the "Eutyrrhenian". This alluvium possibly post-dates the "Neotyrrhenian", as well, for the following reasons: 1) Although the "Neotyrrhenian" strandline is preserved a few metres above present sea level in most parts of the western coast of the Eastern Lakonia Peninsula (Kelletat et al., 1977; Kowalczyk et al., 1992; Chapter 4, this work), and this deposit can be followed down to present sea level (Fig. 4.6), it does not display any indication of marine reworking. 2) A marine abrasion platform, at ca. 1.5 m, tentatively correlated with the "Neotyrrhenian" is draped by the Unit 12 fan. If the latter inference is valid, the Unit 12 alluvium probably corresponds with the latest Pleistocene lowstand, recognised also in Messenia (Kourampas and Robertson, 2000; Chapter 3), and elsewhere, and correlated with the Würm II in classical chronostratigraphic schemes (e.g. Bonifay, 1975, Kelletat et al., 1976).

Unit 10
(Bozas Rema)

Unit 10
(Molai)

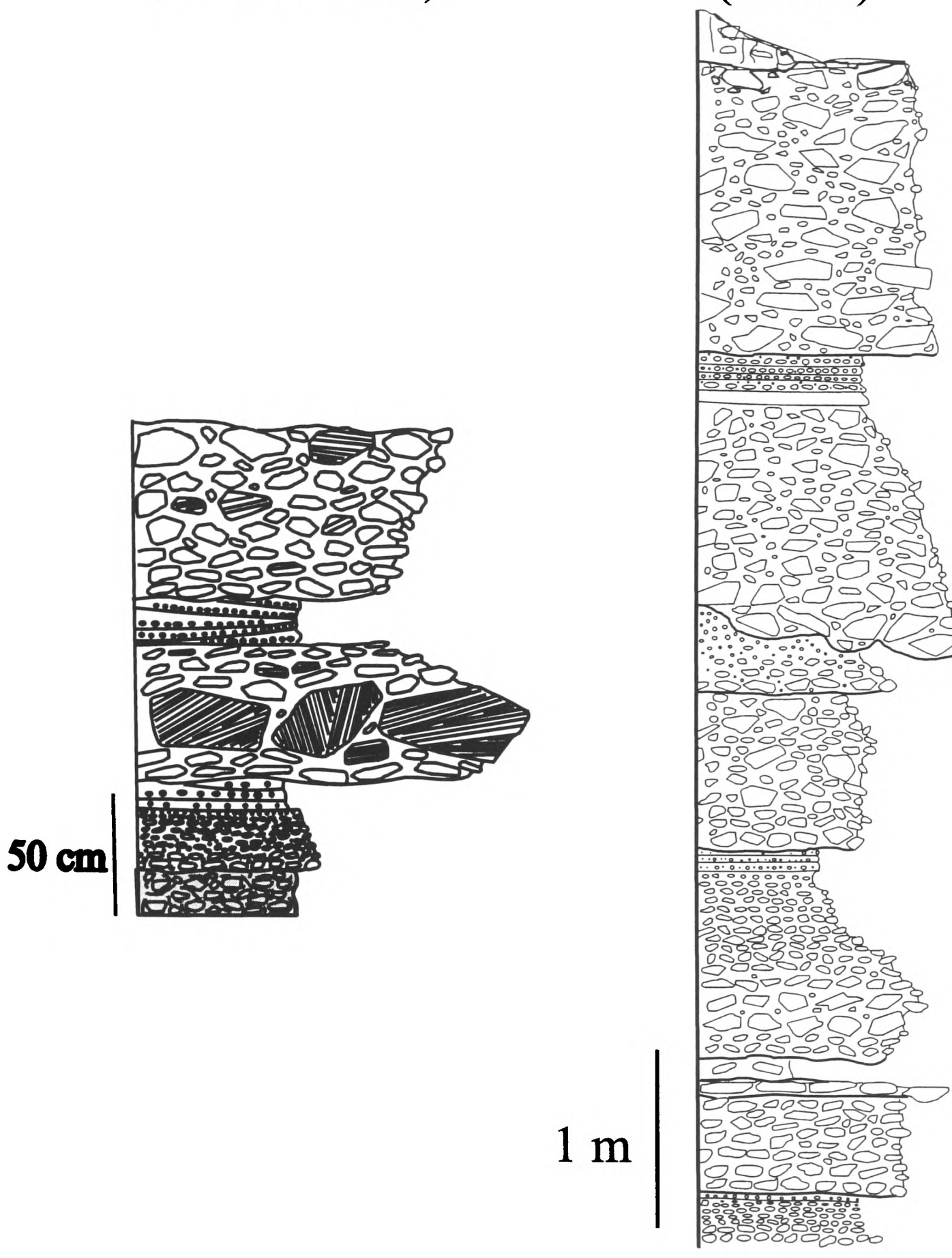

Figure 5.18: Late Pleistocene fanglomerates (Unit 10) interpreted as proximal fan facies.
a: Bozas Rema, **b:** Molai.

5.3.4.6 Unit 13: Aeolianite (latest Pleistocene): Cemented aeolianites, with a well preserved dune morphology and abundant *Rhizocretion*, are present at a few sites along the western coast of the Eastern Lakonia Peninsula (e.g. Elea, Plytra, Marathias; see Figs. 4.20, 5.38, M.2). These despots cover shoreline deposits or marine abrasion platforms correlated with the Neotyrrhenian sea level cycle. They comprise well sorted, trough cross-laminated medium- to fine-grained grainstone, affected by karstification. Its stratigraphic position above the Neotyrrhenian terrace (Figs. 5.2. 5.3) allows its correlation with the widespread latest Pleistocene aeolianite in NW Messenia (Chapter 3; Kourampas and Robertson, 2000).

5.3.4.7 Unit 14: Vermetid trottoires, conglomerates and micritic laminae ("Versilian", or younger)

5.3.4.7.1 NW Coast: Kowalczyk et al. (1992) described a Holocene terrace from the area of Elea (Figs. 5.4). In the proximal zones of this terrace, at ca. 30-50 cm, the sediment comprises conglomerate. This is deposited against a cliff cut in red alluvia of probable "post-Tyrrhenian" age (correlated with Unit 12). The lower part of the deposit consists of alternations of clast-supported conglomerate with sandstone/grainstone, with preserved low-angle planar cross-lamination locally (bed thickness: 10's of cm). The clasts are mainly discoidal and aligned with their long axes parallel to the shore. Clasts were derived from reworking of polymict alluvia, similar to those previously described (e.g. Unit 12). The fauna comprise thick-shelled bivalves. The latter conglomerate is draped by ca. 20 cm of well sorted grainstone/sandstone, with pervasive *Rhizocretion* bioturbation. The total thickness of this deposit is ca. 1.2 m.

5.3.4.7.2 SW Coast: At the Dhaemonia and Elika coasts (Figs. 5.14, M.2), bioeroded relief in "Neotyrrhenian" (or older) sediments is covered by a massive, structureless conglomerate (seaward part of the deposit), or *Lithophaga*-bored vermetid bioconstructions (landward part of the deposit). This deposit, partly within the present day foreshore-upper shoreface zone, is traced to a maximum altitude of ca. 0.7-1 m. This is a bouldery conglomerate, with poorly to moderately rounded, slab-shaped clasts derived mainly from terrace grainstone (maximum clast size: 80 cm). The fauna include thick-shelled bivalves and large blue-green algal oncoids ('algal biscuits'). On the Elika coast, vermetid bioconstructions are preserved in a bioeroded relief into Neotyrrhenian shoreline sediments (Unit 12) and post-Neotyrrhenian aeolianite and alluvia (Units 12, 13; see Fig. 5.41).

Interpretation: These sediments are correlated with the "Versilian" sea level highstand, ca. 6000 a (Labeyrie et al., 1987; Kambouroglou, 1989) Fig. 5.5). The disorganised conglomerate is taken to represent the transgressive systems tract (Myers and Milton, 1996), fed from rapid disintegration of pre-existing deposits, whereas the vermetid bioconstructions probably represent conditions of stabilisation of the coastline during maximum flooding. A younger, historical age of this deposit, correlative with uplifted shorelines of the '*Early Byzantine tectonic paroxysm*' (Pirazzoli, 1986) is also possible.

5.3.4.7.3 S Coast: At Ayia Marina (Figs. 5.5, 5.40), ca. 5 m landwards of the "Neotyrrhenian" terrace (see above), and on a wave-cut platform at ca. 1.5-3 m, there are thick (thickness: ca. 4-10 cm), upright, hollow, laminar carapaces, up to 1.7 m tall and 40-60 cm wide. These crusts consist of blue-green algal bindstone, comprising alternating laminae of dark micrite and well sorted, grain-supported, fine sand/silt, with grains derived from various bedrock lithologies (see Chapter 6). Their internal surfaces preserve a dense *Rhizocretion* network

Interpretation: These laminated carbonate carapaces probably represent biogenic deposits. Dark micrite laminae are interpreted as resulting from microbial/blue-green algal biofilms, whereas the detrital laminae probably resulted from trapping of aeolian sand on the microbial mat surface. The preserved cylindrical shape of these formations, together with local preservation of a dense network of calcified roots in their inner surface, indicate that they originated as microbial-blue-green algal crusts around trees, possibly in a seasonally flooded, mangrove environment. It is uncertain whether the inferred mangrove resulted from elevation of the groundwater table during the short-lived Versilian highstand, about 6000 a. before present (Labeyrie et al., 1987), or from wet climatic conditions in the Holocene. Mangrove vegetation in unsustainable in the present-day conditions of the area: Maquis vegetation, by contrast, develops in the relatively arid Eastern Lakonia Peninsula, with low annual rainfall.

5.3.4.8 Beachrocks (Holocene), Neolithic to Historical alluvia and soils: Beachrocks comprise lithic grainstone, calcareous sandstone and conglomerate, situated within the present day foreshore and probably still 'active'. Detailed descriptions are given in Chapter 6.

Holocene to historical terrestrial sediments abound in the Eastern Lakonia Peninsula, with a wide variety of facies. Some examples include low-elevation alluvial terraces in the Dokali Rema (Fig. 4.10), brown soils with obsidian chips around Ayia Marina, brown conglomerates with pottery fragments in Kokkinia and brown soils with Mycaenean pottery in Bozas Rema (see Fig. M.2). The present-day sedimentation in the Eastern Lakonia Peninsula is represented by modern beaches, dunes (e.g. Viglaphia-Ayii Apostoli), alluvia, scree cones (e.g. Ayia Marina) and soils.

5.4 DISCUSSION-CONCLUSIONS: LATE TERTIARY-QUATERNARY EVOLUTION OF THE EASTERN LAKONIA PENINSULA

The following main stages are distinguished in the evolution of the Eastern Lakonia Peninsula during the Late Tertiary-Quaternary (Fig. 5.19):

5.4.1 Late Tertiary (Fig. 5.19.1): In the Southern Peloponnese, the 'Neotectonic' period began in the Middle Miocene, after the completion of thrust movements that led to the formation of the external Hellenic Nappes (Mariolakos, 1975; Jacobschagen et al., 1978; see Chapter 1). Prolonged subaerial erosion followed during Late Miocene-Early Pliocene, under tropical-humid climatic conditions (Riedl, 1977; Riedl et al., 1982; Verginis and Nagl, 1982). This led to the formation of peneplain-pediplain surfaces that now are uplifted to elevations >800 m locally. At least three periods of uplift took place between Late Miocene and Late Pliocene, alternating with periods of planation and pediment formation (Chapter 1). Three uplifted pediments that fringe the Late Miocene (?) peneplain correlate with similar landforms, of inferred Late Miocene-Pliocene age in other areas of the Peloponnese (Riedl, 1977), central Greece (Sweeting, 1967, after Mariolakos, 1975), the Cyclades (Riedl et al., 1982) and northern Greece (Vavliakis, 1981; Psilovikos and Vavliakis, 1982). Normal faults were active during that period, as evidenced by the offset of geomorphic surfaces (Dufaure, 1977). Cemented calcareous breccia, plastered on bedrock scarps (Unit 1), that constitute the oldest post-Alpidic sediments in the peninsula, probably resulted from this Late Miocene-Pliocene faulting. Movement along faults parallel and oblique to the strike of the Eastern Lakonia Peninsula led to the formation of large asymmetrical grabens, oblique to the main, NW-SE tectonic grain of the peninsula (e.g. Molai Graben, Dokali Graben; Figs. 5.4; M.2). The presence of graben filling sediments of inferred Pliocene age (Dufaure, 1977) suggests that some of these grabens were already formed in Pliocene time. A broad pediment surface, of peninsula-wide extent, formed in Late Pliocene time (Kelletat et al.,

1975; Dufaure, 1977; Theodoropoulos, 1978), associated with deposition of alluvial fans and palaeosols (Unit 2; see above).

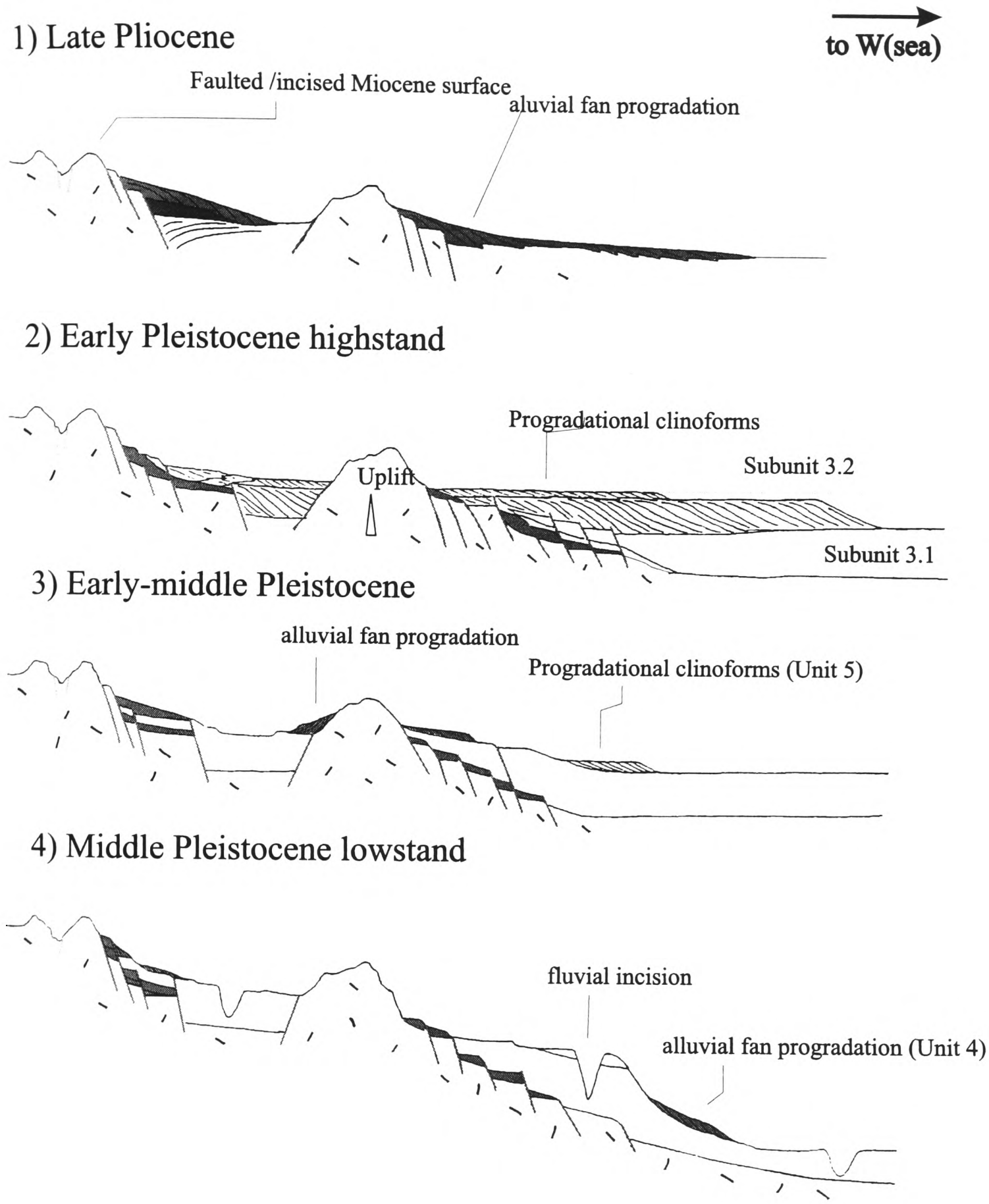

Figure 5.19 a,b: Interpretative cross-sections showing the recognisable stages in the Late Pliocene-Holocene development of the Eastern Lakonia Peninsula. The dominant control on sedimentation was regional tectonic uplift, with marine terraces and associated shallow-marine sediments being related to marine transgressions and eustatic sea level highs. Additional accommodation space was mainly provided by localised subsidence along the hanging walls of extensional faults that are inferred to have remained mainly collectively active. See text for details.

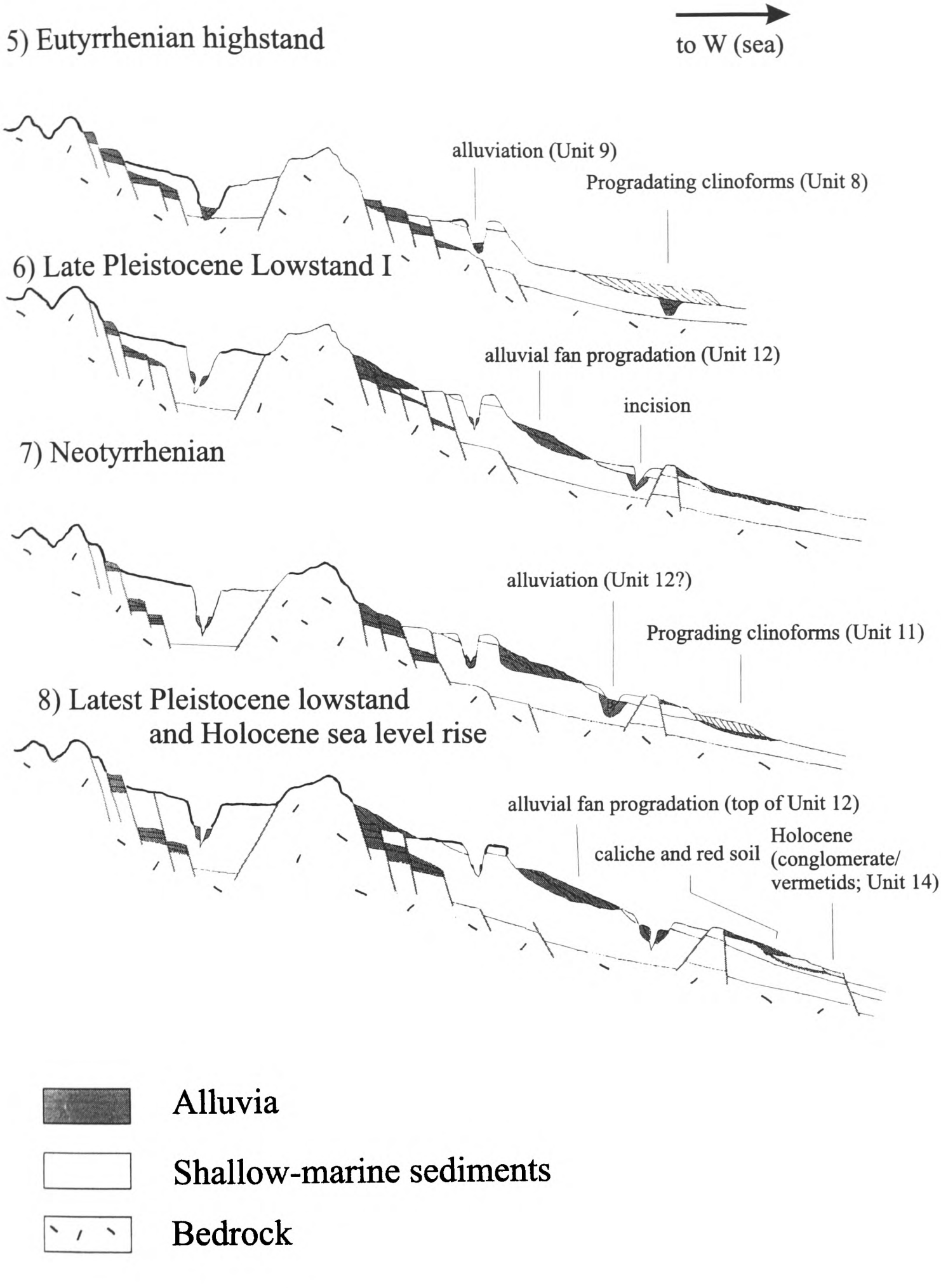
5) Eutyrrhenian highstand
to W (sea)
alluviation (Unit 9)
Progradating clinoforms (Unit 8)
6) Late Pleistocene Lowstand I
alluvial fan progradation (Unit 12)
incision
7) Neotyrrhenian
alluviation (Unit 12?)
Prograding clinoforms (Unit 11)
8) Latest Pleistocene lowstand
and Holocene sea level rise
alluvial fan progradation (top of Unit 12)
caliche and red soil
Holocene
(conglomerate/
vermetids; Unit 14)
Alluvia
Shallow-marine sediments
Bedrock

by the height of middle Pleistocene cliffs. Alluvial fans prograded through incised valleys during the middle Pleistocene lowstand. The bulk of the transported material was probably deposited in areas currently below sea level and only fan-head to middlefan facies are presently preserved onland (Unit 4). Normal faults were active during this period, locally offsetting the early Pleistocene terrace for ca. 70 m (e.g. Ano Glikovrisi Horst; Fig. 5.3). Faulting and alluvial fan progradation were broadly contemporaneous, as shown by alluvial fans burying fault scarps through Early Pleistocene sediment, and also by abundant evidence of syndepositional faulting in alluvial fan facies.

5.4.4 Middle Pleistocene transgression: Sea level rose later in the middle Pleistocene, and valleys incised during the middle Pleistocene sea level fall were flooded by the sea. Lagoonal-estuarine systems developed, to accommodate various marginal-marine to foreshore facies (Subunit 8.1). In shelf areas away from incised valleys (inter-estuarine areas), deposition was mainly controlled by wave and storm processes and fully marine facies were deposited over alluvia of the previous lowstand systems tract (Subunit 8.2). Syndepositional faulting took place during this period as well.

5.4.5 Middle to late Pleistocene lowstand (Fig. 5.19.4): Sea level fell after the "Sicilian", and valleys were incised through marine deposits exposed on the emerging shelf. During the lowstand that followed, alluvial fans prograded through incised valleys and bypassed the coastal zone now emergent, to be deposited further seawards. As a consequence, only proximal, fan-head to middlefan facies of this generation are presently preserved onland (Unit 7). Other deposits associated with this lowstand also include thick terra rossa soils stabilised by vegetation and patchy remnants of aeolianite (Fig. 5.16). These sediments occur in the southern tip of the Eastern Lakonia Peninsula, that, as today, was probably characterised by low-density, ephemeral drainage, possibly as a result of lithologic control (both bedrock and Pleistocene sediments are permeable carbonate rocks).

5.4.6 Eutyrrhenian (Fig. 5.19.5): Sea level rise during "Eutyrrhenian" highstand led to deposition of shoreline deposits over earlier marine and subaerial sediments and bedrock. "Eutyrrhenian" deposits commonly comprise a transgressive-regressive sequence, with basal lags, passing up to shoreface facies (transgressive systems tract and maximum flooding zone), succeeded by prograding foreshore, fan deltas, or aeolianite (highstand systems tract) (Unit 8). The "Eutyrrhenian" marine terrace, well developed along the west coast of the Eastern Lakonia Peninsula, is identified by presence of the characteristic gastropod *Strombus bubonius* (Keraudren, 1970, 1971; Kelletat et al., 1976; Kowalczyk et al., 1992).

Base level rise during the "Eutyrrhenian" also deposition of alluvia, inside valleys incised during the previous lowstand (e.g. Unit 9). The "Eutyrrhenian" stage is correlated with the isotopic stage 5.5, *sensu* Imbrie et al. (1984). Tectonic activity during and after "Eutyrrhenian" involved normal faulting (e.g. Limnakia section; Fig. 5.15) and reactivation of buried faults as extensional joints (e.g. Bozas Rema section; Fig. 5.13).

5.4.7 Late Pleistocene lowstand I (Fig. 5.19.6): Sea level fell after the "Eutyrrhenian" and minor valley incision, cliff cutting and alluvial progradation took place, as a result. Alluvial sediments attributed to this stage are preserved in the Ano Glikovrisi Horst (Fig, 5.4). Their distinction from older and younger alluvia is made on the basis of Middle Palaeolithic (Mousterian) lithic industry present within Unit 10 (Kowalczyk et al., 1992).

5.4.8 Neotyrrhenian (Fig. 5.19. 7): Resumed sea level rise during "Neotyrrhenian" led to the deposition of a generally coarse-grained terrace with *Strombus bubonius* (Keraudren, 1970, 1971; Kelletat et al., 1976; Kowalczyk et al., 1992) (Unit 11). Higher-order, "intra-Neotyrrhenian" sea level cyclicity is indicated by the superposition of at least two fining-, then coarsening-upwards cycles; each tentatively correlated with the isotopic substages 5.3 and 5.1, respectively (*sensu* Imbrie et al., 1984). In areas away from terrigenous influence (e.g. Ayia Marina; Fig. 5.5), the "Neotyrrhenian" terrace comprises a carbonate shoreline. Tectonic activity during this period (or later) was locally intense, as indicated by extensive jointing, or low-throw faulting, of "Neotyrrhenian" deposits.

5.4.9 Late Pleistocene lowstand II (Fig. 5.19.8): Sea level fall after "Neotyrrhenian" (and during Last Glacial Maximum), resulted to incision of all previous marine and subaerial deposits, manifested by steep, V-shaped valleys. Alluvial fan progradation took place all over the Eastern Lakonia Peninsula. Alluvia of this stage (Unit 13) are distinguished from those of Late Pleistocene lowstand I (Unit 10; see above) by the Latest Palaeolithic industry present (Kowalczyk et al., 1992). Dunes were deposited locally (e.g. Marathia, Viglaphia; Unit 14), fed by reworking of self exposed during the lowstand. The late Pleistocene lowstand II correlates with the Würm II lowstand in classical chronostratigraphic schemes (e.g. Bonifay, 1975; Kelletat et al., 1976).

5.4.10 Holocene (Fig. 5.19.8): Sea level rose after Last Glacial Maximum and during the "Versilian" (ca. 5.5-6 ka BP), leading to deposition of vermetid trottoires and pebbly beach deposits (Unit 15). Flooding of the backshore during the short living "Versilian" highstand led to local development of a mangrove environment. Hollow carapaces of laminated micrite

(bindstone), probably deposited on microbial-algal mats, are preserved in erect position, marking the place of former trees in presently unvegetated areas (e.g. Ayia Marina; Figs. 5.5). Alternatively, emergent foreshore and mangrove deposits could be of even younger, historical age, uplifted during the 'Early Byzantine Tectonic Paroxysm' (*sensu* Pirazzoli, 1986). At least two episodes of alluviation and incision can be identified in valleys of the Eastern Lakonia Peninsula, probably reflecting a response of fluvial systems to climatic and anthropogenic controls. Historical sea level change in the area is well documented (Flemming, 1969, 1978) and thought to result from post-glacial isostatic readjustment of the crust and, locally, from movement along normal faults (Flemming, 1969, 1978; Lambeck, 1995). An example of crustal movement in historical times is the separation of the Elaphonisos Island from the Eastern Lakonia mainland after an earthquake in the 1st century BC (Symeonides, 1969).

Table 5.1: Foraminiferal fauna of Pleistocene sediments from the Eastern Lakonia Peninsula

	UNITS					
FORAMINIFERA	SU 3.1	SU 3.2 (lower part)	SU 3.2 (upper part)	SU 6.1	SU 6.2	Unit 8
1) BENTHIC						
Ammonia becarii	+	+	+	+	+	+
A. convexa			+			
A. inflata		+	+	+		+
A. papillosa						
A. perlucida				+	+	+
A. tepida	+	+		+	+	+
Am. sp.		+	+		+	
Angulogerina angulosa	+	+				
Anomalina sp.	+	+				
Asterigerina planorbis	+	+	+	+	+	+
Asterigerinata mamilla			+		+	
Bigenerina nodosaria	+	+				
Brizalina alata	+	+				
Br. Dilatata		+				
Br. Sistina		+				
Br. Spinescens	+					
Br. Spathulata	+	+			+	
Br. Striata					+	
Br. spp.		+			+	
Bulimina aculeata	+	+				
Bl. Aculeata var. basispinosa	+					
Bl. Afinis					+	
Bl. Elegans	+					
Bl. Elegans var. marginata	+	+				
Bl. Elnea	+	+				
Bl. Elongata					+	
Bl. Elongata var. lappa						
Bl. Fussiformis	+					
Bl. marginata	+	+				
Bl. ovata	+					
Bl. ovula	+	+				
Bl. pupoides						

FORAMINIFERA	SU 3.1	SU 3.2 (lower part)	SU 3.2 (upper part)	SU 6.1	SU 6.2	Unit 8
Bl. pyrgula	+					
Bl. spp.	+	+			+	
Cancris auricolus	+	+	+	+	+	+
Cn. oblongus		+				
Cassidulina laevicata	+	+				
Cs. laevicata var. carinata	+	+				
Cs. oblonga	+					
Cs. subglobosa	+					
Cibicides boueanus	+					
C. bourdigalensis	+	+				
C. dutemplei	+		+			
C. floridanus						
C. lobatulus	+	+	+	+	+	
C. refulgens		+	+	+	+	
C. gr. ungerianus-pseudungerianus	+	+			+	
C. sp.	+	+		+	+	
Coryphostomum sp.		+				
Dentalina leguminiformis		+				
Discorbis spp.	+	+	+		+	
Dorothia gibbosa	+		+	+	+	
Elphidium aculeatum		+				
E. advenum		+	+		+	
E. complanatum		+		+		
E. crispum	+	+	+	+	+	+
E. excavatum						
E. fichtelianum			+			
E. granosum		+	+	+		
E. jenseni			+			
E. macellum		+	+			+
E. margaritaceum						
E. minutum				+		
E. pulvereum		+				
E. semistriatum	+					
E. transluscens	+					
E. spp.		+	+	+	+	+
Eponides umbonatus		+				

FORAMINIFERA	SU 3.1	SU 3.2 (lower part)	SU 3.2 (upper part)	SU 6.1	SU 6.2	Unit 8
Eponides sp.	+					
Fursenkoina schreibergsiana	+	+	+	+	+	+
Glandulina glans	+				+	
Gl. laevicata	+					
Globocassidulina oblonga		+				
Gs. subglobosa		+				
Globulina gibba		+				
Gb. gibba var. tuberculata		+				
Guttulina sp.						
Gyroidina orbicularis						
Gr. soldanii	+	+				
Gr. umbonata	+					
Gr. sp.		+				
Hanzawaia sp.	+	+			+	
Homotrema rubrum					+	
Hopkinsinella glabra	+					
Hyalinea balthica	+	+				
Laevidentalina inflexa						
Lagena acuticosta						
L. aperta						
L. hexagona	+	+				
L. marginata		+				
L. quadricostulata		+				
L. semistriata						
L. squamosa		+				
L. striata var. strumosa		+				
L. sp.		+				
Lagenodosaria sublineata		+				
Lenticulina calcar						
Ln. sp.	+	+				
Loxostomum perforatum		+				
Lx. pseudodigitate			+			
Lx. sp.		+				
Mertinoitiella communis	+					
Nonion boueanum	+				+	+
N. commune	+					

FORAMINIFERA	SU 3.1	SU 3.2 (lower part)	SU 3.2 (upper part)	SU 6.1	SU 6.2	Unit 8
N. crassatulum						
N. depressulum			+	+		
N. granosum	+					
N. gratelupii			+			
N. incrassatum		+				+
N. padanum		+				
N. pompillioides	+	+				
N. spp.	+	+	+	+		
Nonionella turgida	+	+		+	+	
Ozawaia sp.		+	+		+	
Peneroplis sp.						
Paliolatella (Lagena) orbignyana		+				
Planorbulina mediterranensis	+	+			+	
Planulina arriminensis	+	+				
Pl. wüllerstorfi	+	+			+	
Pl. sp.		+				
Pleurostomella sp.	+					
Pullenia bulloides	+	+				
P. quinqueloba	+	+				
Pyrgo depressa	+					
Pg. oblonga	+					
Pg. sp.						
Quinqueloculina aspera		+				
Q. agglutinata	+					
Q. oblonga			+			
Q. padana	+					
Q. spp.			+		+	
Rectuvigerina sp.						
Reussella spinulosa	+	+	+	+	+	+
Rs. sp.		+				
Rossalina globularis	+	+		+		
R. orientalis						
Sagrinella lobata						
Sigmoilina tenuis						
Sigmomorphina semitecta						
Sipholagena benevistina			+			

FORAMINIFERA	SU 3.1	SU 3.2	SU 3.2	SU 6.1	SU 6.2	Unit 8
Siphonodosaria monilis		+				
Sphaeroidina bulloides	+	+				
Spiroloculina depressa		+				
Textularia agglutinans	+					
Tx. conica	+					
Tx. sagitula	+					
Tx. sagitula var. soldanii	+					
Tx. truncata						
Tx. spp.		+	+		+	+
Trifarina sp.	+	+				
Triloculina sp.	+		+		+	
Valvulineria bradyii	+	+				
V. complanata	+	+				
Uvigerina mediterranea		+				
U. peregrina	+	+				
U. proboscidea						
U. sp.		+				
2) PLANKTIC						
Globigerina apertura (?)	+			+	+	
G. bulloides	+	+				
G. falconensis	+	+				
G. quinqueloba	+	+				
G. spp.	+	+	+			
Globigerinella aequilateralis	+	+		+		
Gl. quinqueloba		+				
Globigerinoides conglobatus	+	+				
Gs. obliquus extremus	+		+		+	
Gs. suculifer	+	+				
Gs. ruber	+	+	+	+	+	
Gs. trilobus	+	+			+	
Globorotalia crassaformis	+			+		
Gr. inflata	+	+			+	
Gr. truncatulinoides	+					
Neogloboquadrina acostaensis		+				
Nq. humerosa	+	+				
Orbulina bilobata, O. UNiversa	+					

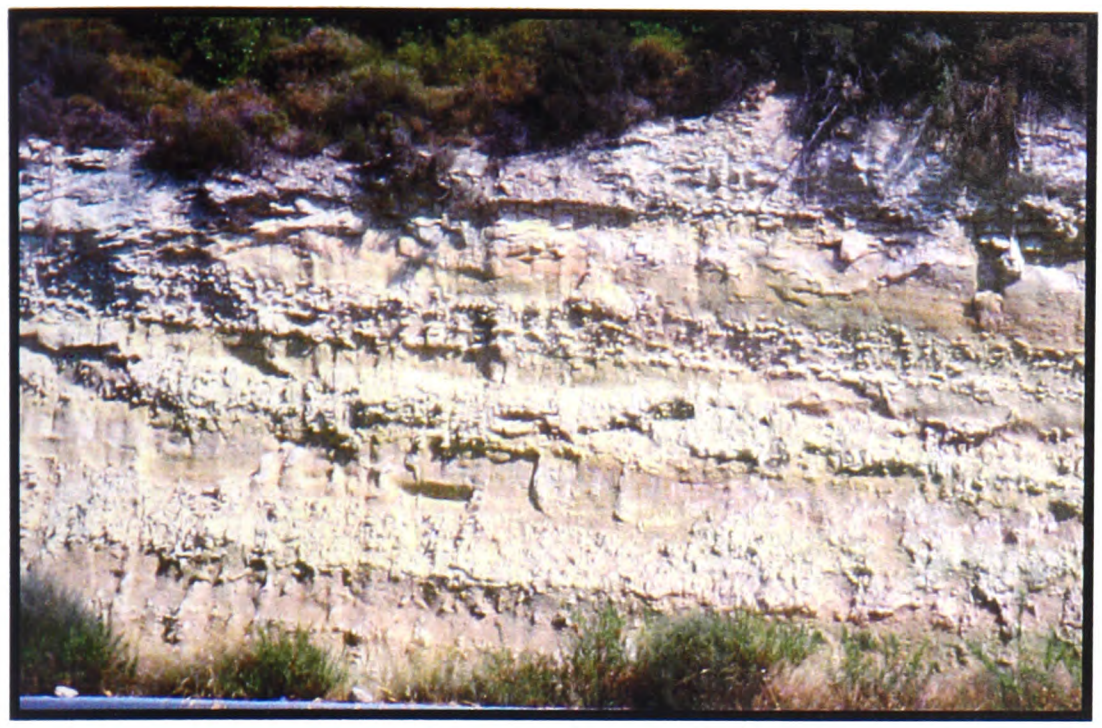

Figure 5.20: Early Pleistocene (NN 19b) offshore sediments (Subunit 3.1). Note the alternation of burrowed and homogeneous beds. The top ca. 1-1.5 m of the section are calichified, with platy to hardpan caliche. Height of cliff: ca 6 m. Dhaemonia.

Figure 5.21: Early Pleistocene (NN19a) offshore silt and mud (Subunit 3.1). The terrace formed above them is of a later, probably late Pleistocene age. Elea.

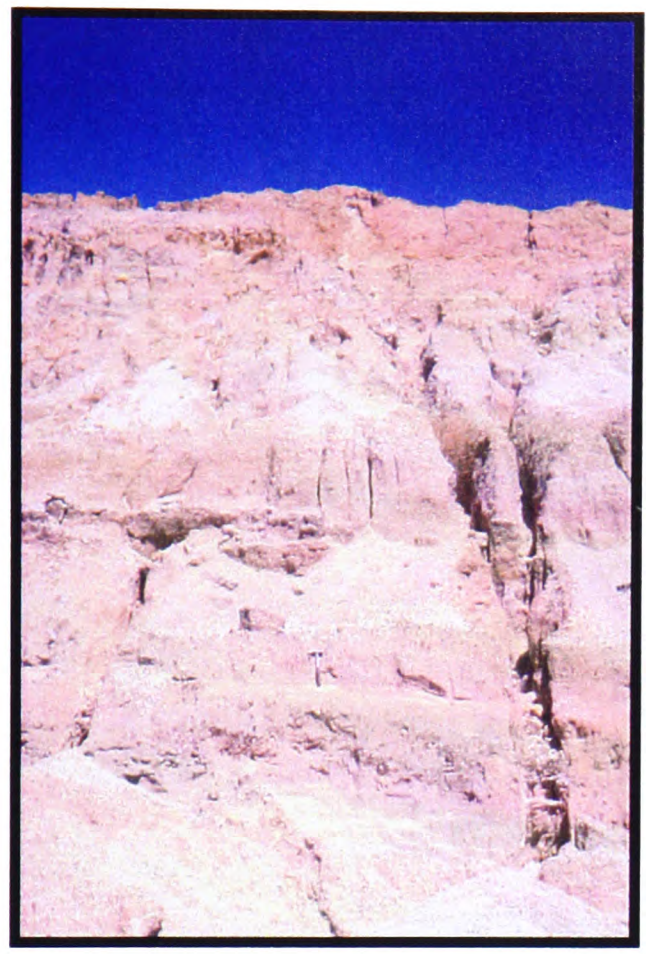

Figure 5.22: Early Pleistocene sands/conglomerates near the top of the regressive Subunit 3.2. These sediments are interpreted as topsets of a prograding deltaic system. They lack marine fauna and were probably deposited in a distal braid stream environment, in the subaerial part of the delta. Note hammer fore scale. Mourtitsa Rema.

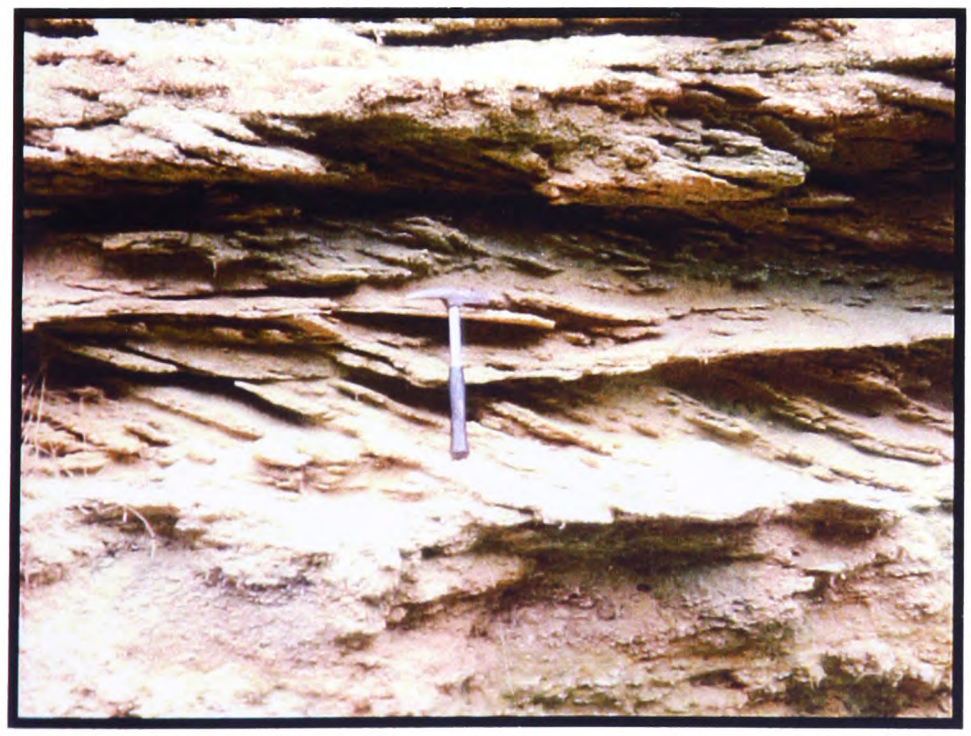

Figure 5.23: Sedimentary structures in coarse-grained sandstone of the middle Pleistocene Subunit 6.1. Bedsets bounded by gently dipping surfaces comprise sigmoidal beds/laminae and climbing ripples. These structures resulted from progradation of medium scale ripples in a high-energy shoreface environment. Cross-bedding suggests offhsore-directed current (to the right). Also note that the sediment comprises alternating bioturbated (below base of hammer) and cross-bedded zones, resulting form fluctuating energy of the depositional environment. Kambourani Rema.

Figure 5.24: Mud, pebble and sandstone, interpreted as lagoonal deposits of middle Pleistocene age (Subunit 6. 1). Middle to late Pleistocene faulting of the sediment (N-S fault) resulted in alignment of pebbles with their long axis parallel with the fault scarp.The throw of this fault is >2.5 m. Note pencil for scale. Kambourani Rema.

Figure 5.25: Middle-late Pleistocene unconformity: A red soil with *Rhizocretion* separates inferred middle Pleistocene (Subunit 6.2) shallow-marine sandstone below from inferred Eutyrrhenian (Subunit 8.2) shallow-marine sandstone above. Preservation of the soil under a marine ravinement possibly suggests that the transgression took place quite rapidly. Prophitis Ilias.

Figure 5.26: Middle Pleistocene conglomerates and silts (Unit 4; mid-fan facies) are overlain unconformably by middle Pleistocene (Subunit 6.2), then Eutyrrhenian (Unit 8), marine conglomerates and sands (see arrows). The ca. 17-20 m terrace was formed above the Eutyrrhenian deposits. A N-S striking fault that cuts the underlying alluvia dies not affect the Eutyrrhenian sediments. Bozas Rema coast.

Figure 5.27: Late Pleistocene alluvia (Unit 10). Note the coarsening-up the section, from mud and silt at the bottom to conglomerate at the top and also the predominance of tabular versus channel-filling conglomerate bodies, probably suggesting a braid-stream environment. Kokkinia; cliff height:.

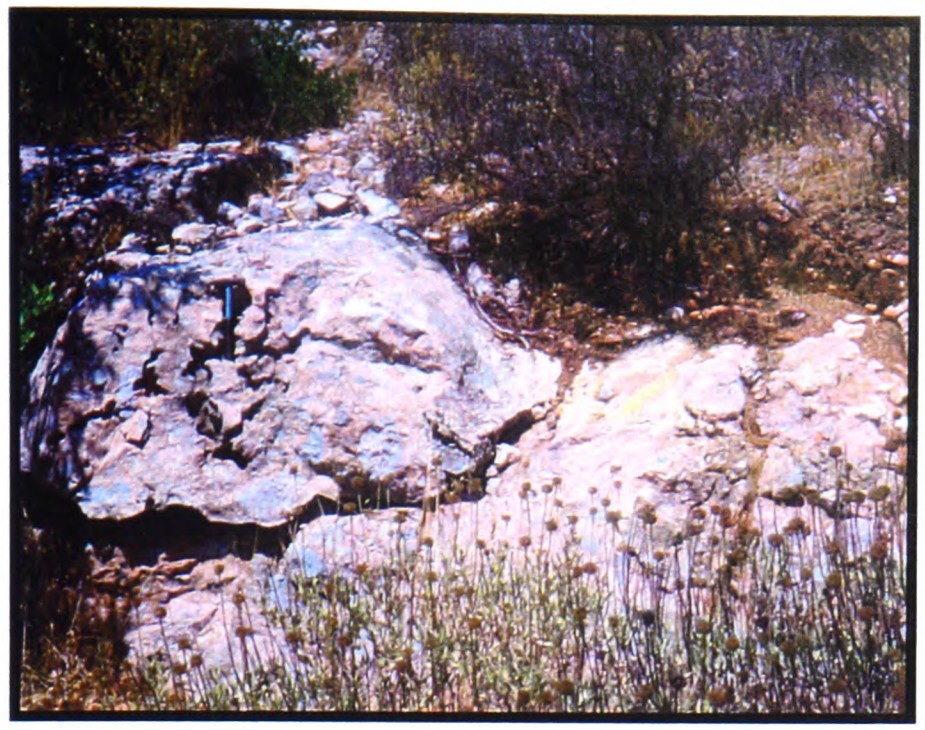

Figure 5.28: Well-cemented red breccia of inferred Late Pliocene age (Unit 2.2). These breccia and correlative conglomerates rim the Late Pliocene pediment. Note hammer for scale. Elika.

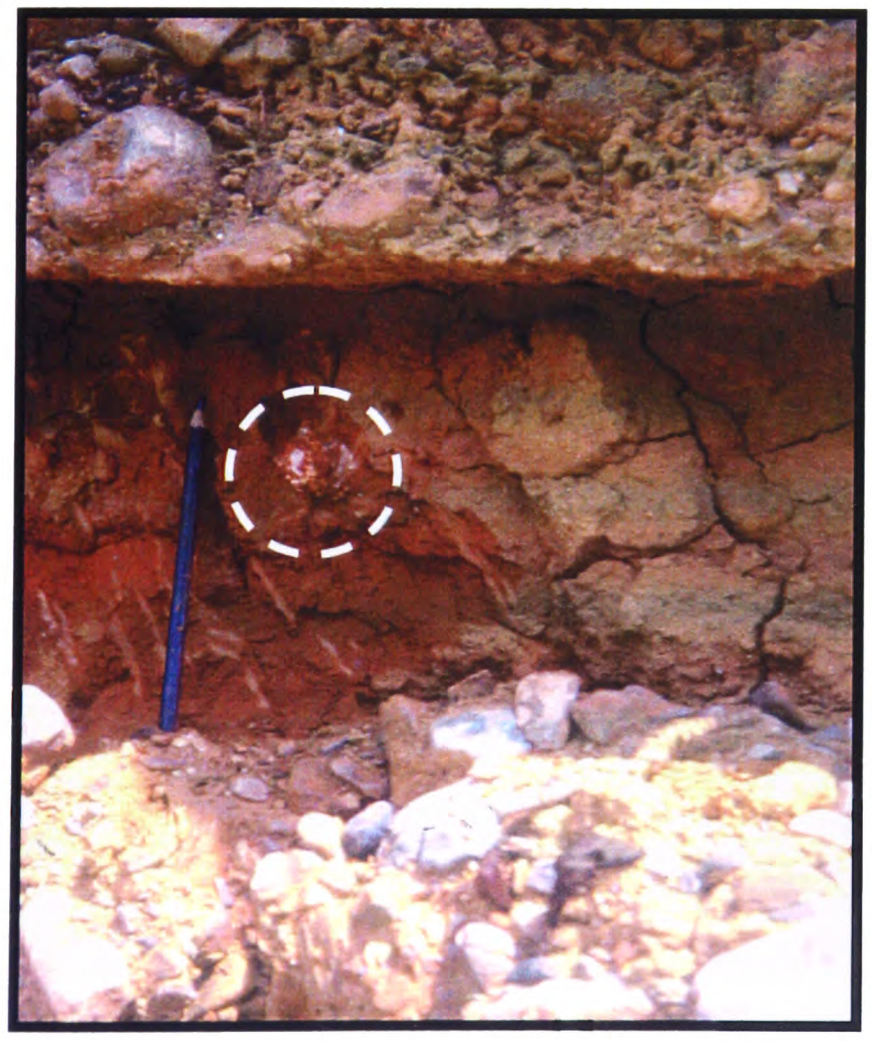

Fig. 5.29: Close-up of the unconformity between middle Pleistocene alluvia (Unit 4) below and middle(?) Pleistocene shallow-marine and lagoonal sediments (Subunit 6.1) above. The unconformity is a sharp, gently dipping marine ravinement surface, formed during marine transgression. The marine succession starts with a fining-up, clast-supported conglomerate with calcareous sandstone matrix, interpreted as basal conglomerate. Pebbles were probably derived from the reworking of conglomerate beds within the alluvial unit below. A middle Pleistocene age for the alluvial unit is inferred by the presence of rhodoliths (circle), probably reworked from an early Pleistocene marine deposit. Tasou Rema.

Figure 5.30: Late Pleistocene alluvia (Unit 9or 10). Note the coarsening-up trend, from red silt to clast-supported conglomerate above (hammer for scale). Elea.

Figure 5.31: Late Pleistocene fanglomerates (Unit 10). Note the poor sorting, the tabular geometry of beds and the coarsening of the sediment upwards. Such sediments are attributed to progradation of alluvial fans during late Pleistocene lowstands. Monemvasia.

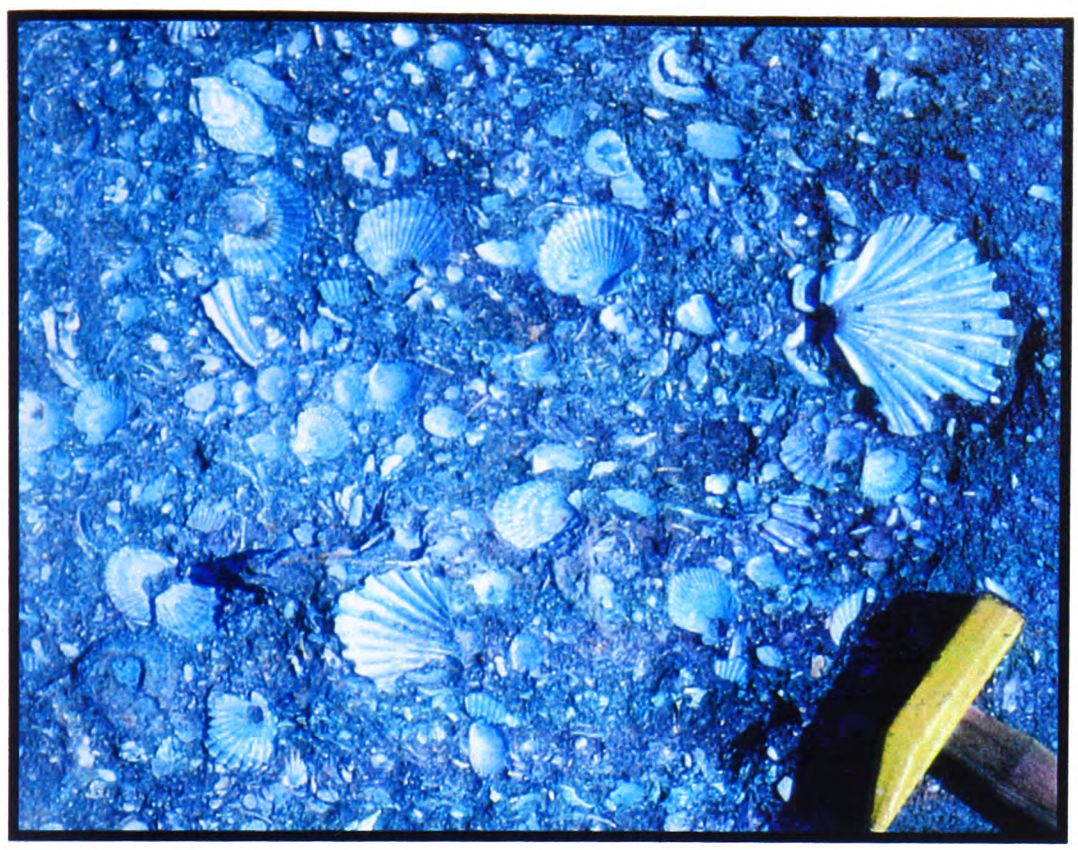

Figure 5.32: Early Pleistocene sandstone with pectenidae (*Pecten* spp., *Chlamys* sp.) and echinoids. Both unbroken shells and valves are present; many shells are imbricated. Ayia Marina coast.

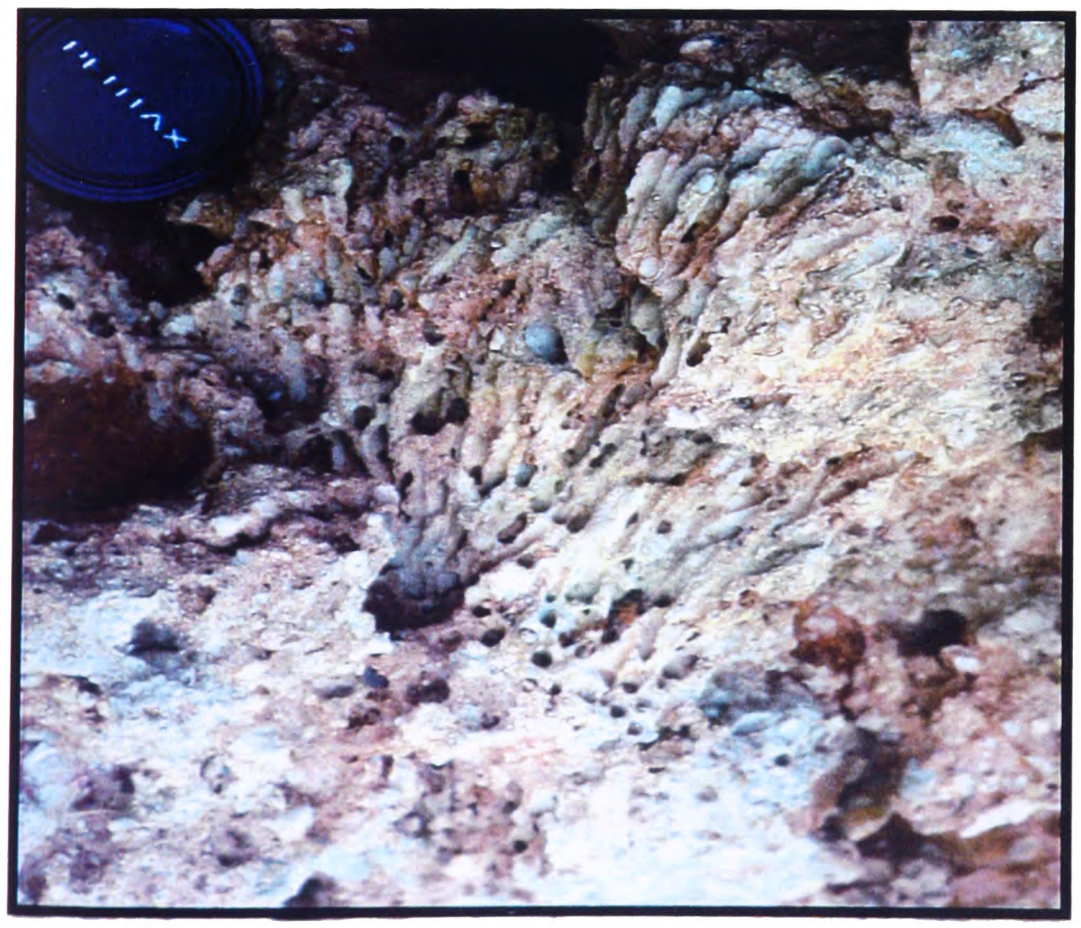

Figure 5.33: Late Pleistocene (Eutyrrhenian: Subunit 8.1) coral-algal bafflestone with *in situ* colony of the scleractinean coral *Cladocora caespitosa*. Plytra.

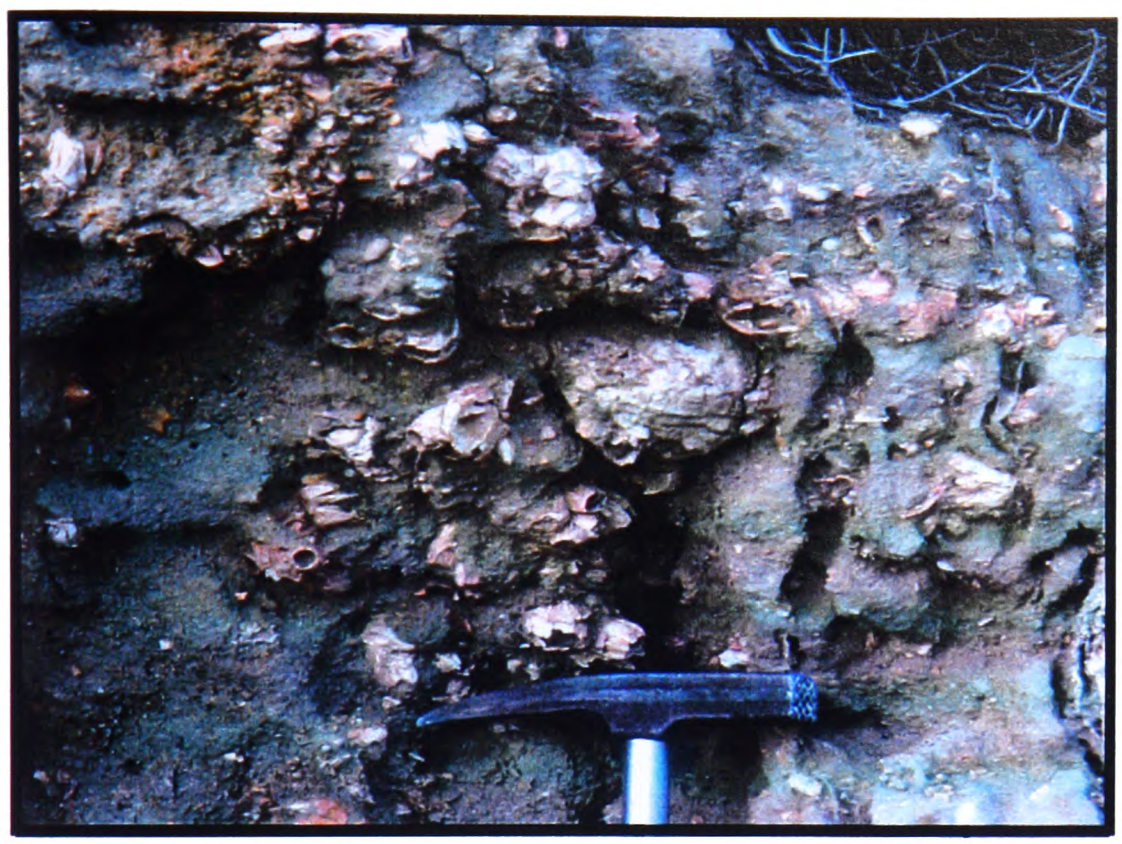

Figure 5.34: Dense accumulation of barnacles (*Balanus* sp.) and the bivalve, *Spondylus* sp. (centre) in middle Pleistocene shallow-marine sandstone (Subunit 6.2). Paleokastron, S of Neapolis.

Figure 5.35: *Ostrea* sp. and other bivalve shells in middle Pleistocene shallow-marine sand/silt (Subunit 6.2). Many shells are articulated. Bozas Rema.

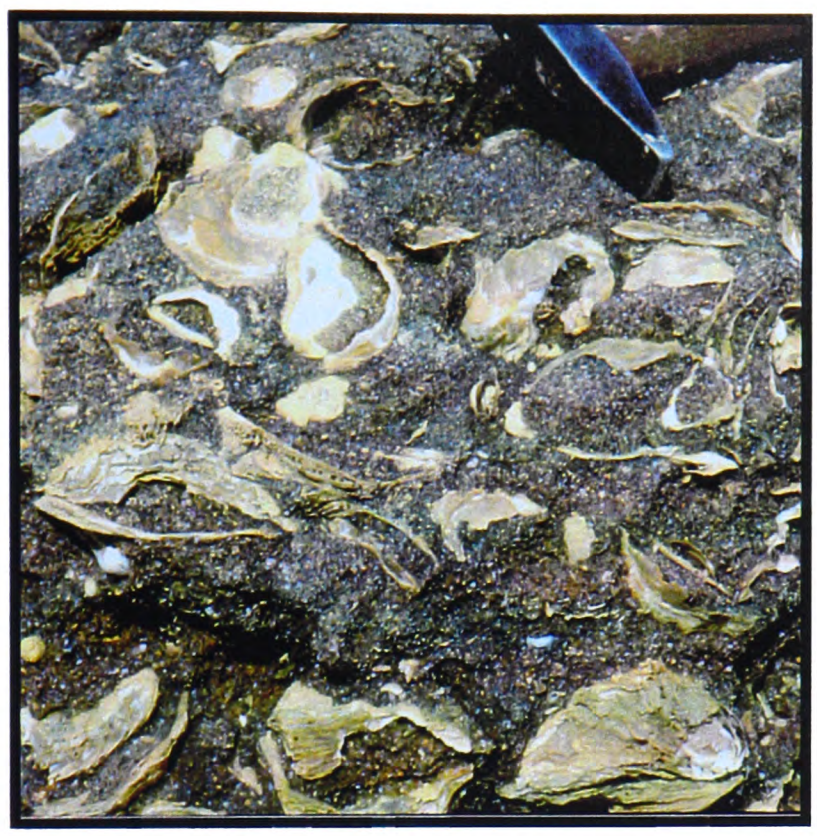

Figure 5.36: *Ostrea* sp. bank in coarse-grained sandstone with rhodoliths. Note that many shells are articulated. Eutyrrhenian (Subunit 8.2), upper shoreface facies, Psiphia Coast.

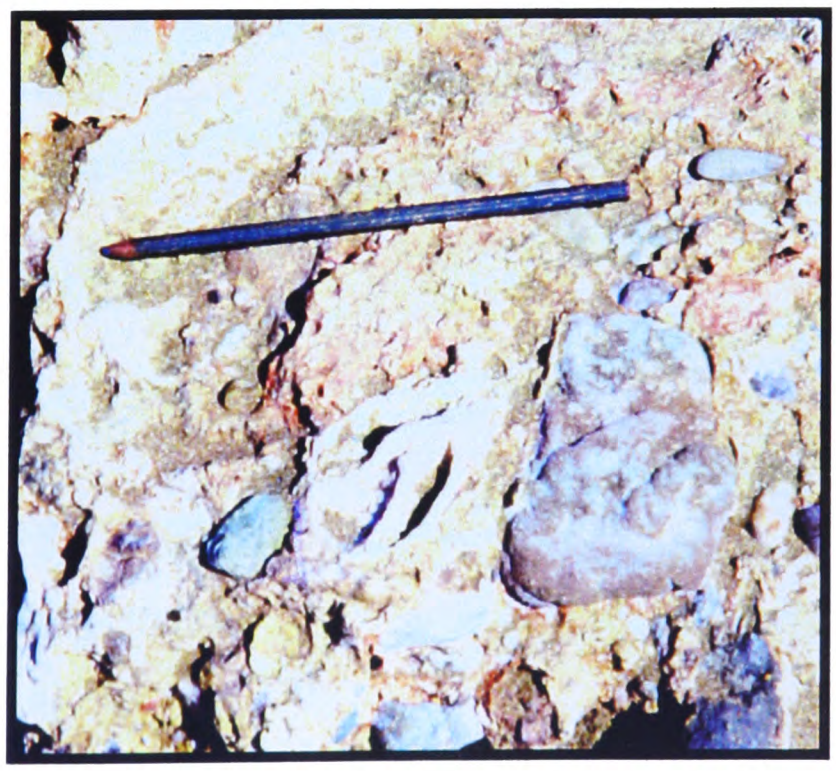

Figure 5.37: The gastropod, *Strombus bubonius* (centre), characteristic of the Tyrrhenian stages in the Mediterranean, and red algae-coated pebbles in Neotyrrhenian (Unit 11) conglomerate. Elika coast.

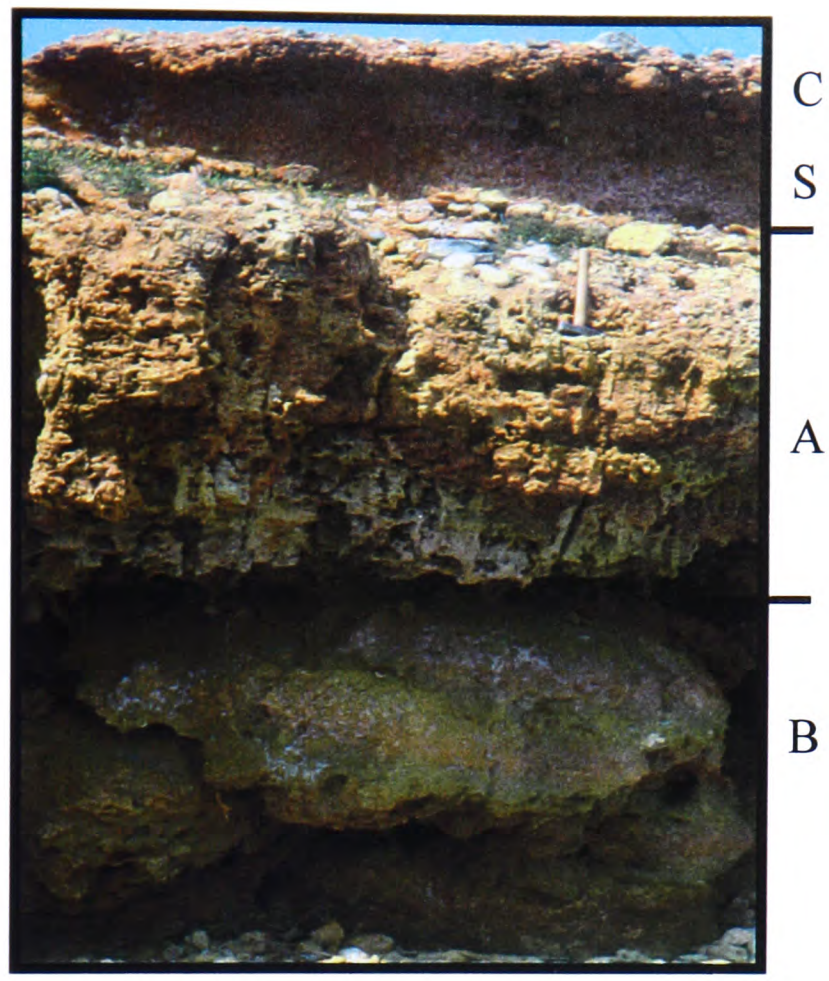

Figure 5.38: Late Pleistocene algal boundtone (**B**), correlated with Subunit 8.1 (Eutyrrhenian), is followed by latest Pleistocene aeolianite with *Rhizocretion* (**A:** Unit 13). This is in turn followed by latest Pleistocene alluvia, coarsening upwards from calichified silt **(S)** to clast-supported conglomerate **(C)**. Note hammer for scale. Plytra.

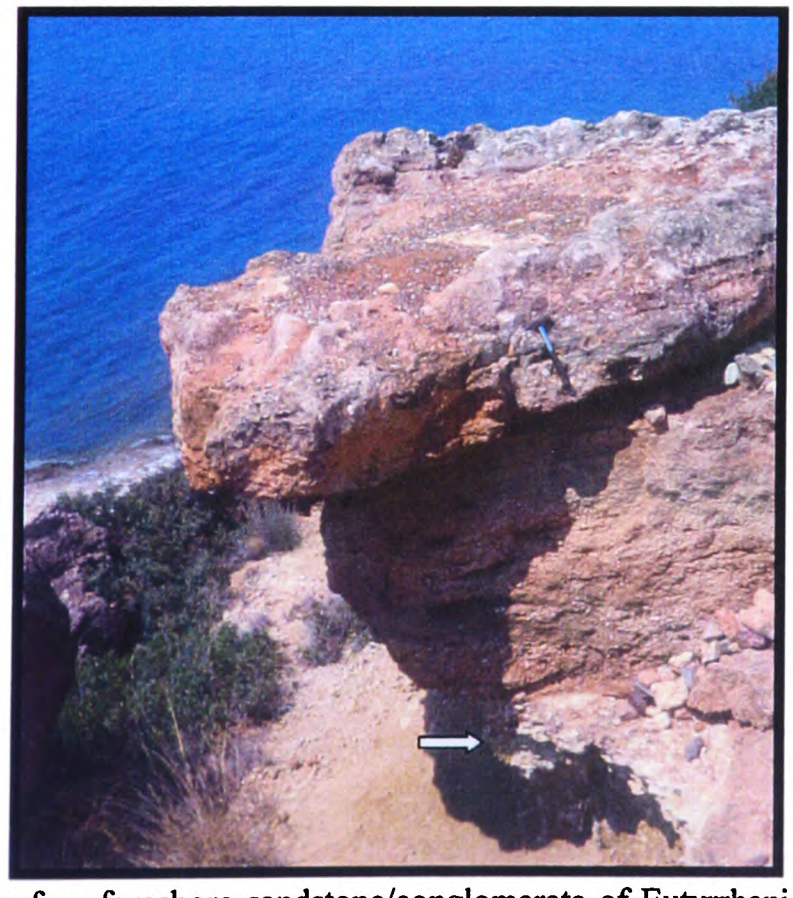

Figure 5.39: Upper shoreface-foreshore sandstone/conglomerate of Eutyrrhenian age (Subunit 8.2). A chalky caliche horizon (arrow) marks the unconfromity between the Eutyrrhenian deposit above and middle Pleistocene silt/ fine-grained sand below. Note hammer for scale. Bozas Rema.

Figure 5.40: Hollow carapaces of algal-microbial limestone (Unit 13 bindstone) on the 1-1.7 m erosive platform. These deposits (height up to 1.5 m) probably formed around roots and trunks of palm trees during a higher relative sea level in the Holocene. Ayia Marina. **Insert:** Close-up of the internal wall of an algal-microbial carapace, showing a dense network of calichified roots (*Rhizocretion*). Fine-grained detrital material (brown silt) of aeolian origin was trapped by the root network. Coin diameter: ca. 5 cm. Ayia Marina.

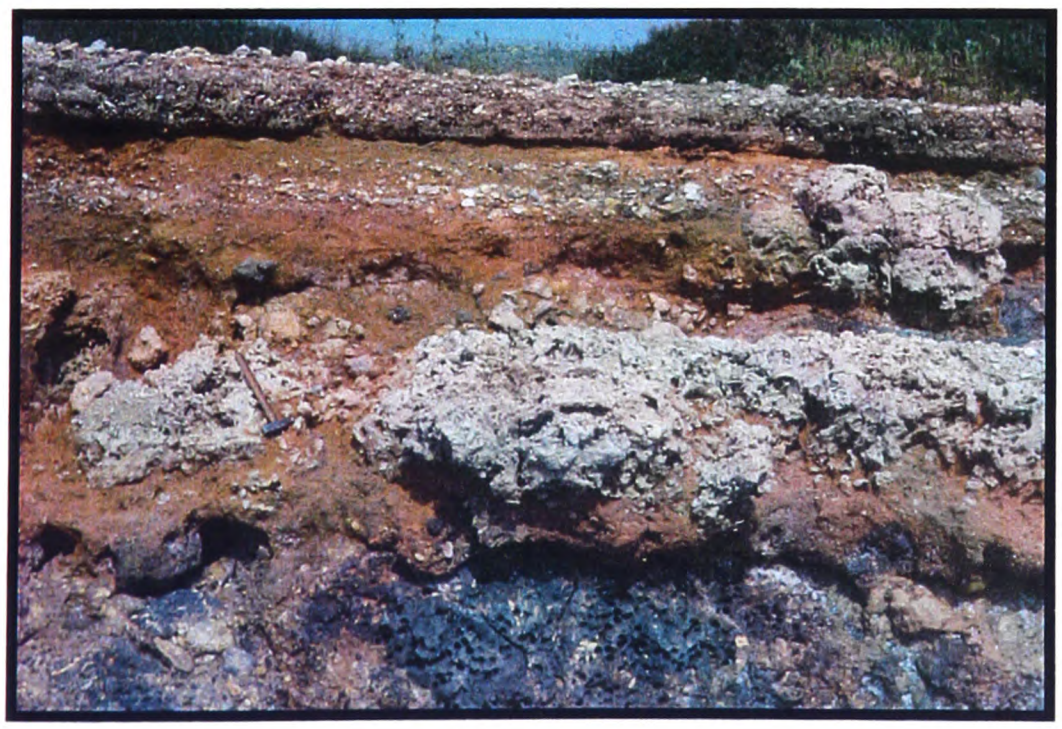

Figure 5.41: A Holocene strandline, at ca. 1.5 m, is defined by encrustations of red algae and vermetid gastropods (white). This Holocene deposit (Unit 13) was formed on late Pleistocene alluvia. Plytra.

CHAPTER 6: MICROFACIES AND DIAGENESIS OF QUATERNARY SEDIMENTS AND PALAEOSOLS FROM THE MESSENIA AND EASTERN LAKONIA PENINSULAE

6.1 INTRODUCTION

This chapter focuses on the petrography and diagenesis of Plio-Quaternary terrace deposits from the Messenia and Eastern Lakonia Peninsulae and supplements outcrop data presented in Chapters 3 and 5. The purposes of this chapter are **a)** to describe and interpret previously undocumented shallow-marine and terrestrial microfacies from an Eastern Mediterranean area and **b)** to demonstrate how petrographical evidence can be used to document Quaternary uplift and relative sea level change in the area of study.

6.1.1. Techniques: Observations were made with low-power optical microscope, supplemented by X-ray diffraction of bulk rock samples and fossils (Appendix C). Standard staining techniques (Dickson, 1966; Miller, 1989) were used for the identification of carbonate minerals in selected thin sections. Quantitative and semi-quantitative data were collected by standard point-counting techniques and estimation charts (see Folk, 1974; Flügel, 1982) (Appendix B). For practical reasons, the emphasis is placed on relatively well cemented sediments of sand to granule grain size, since thin sections could not be easily made of finer-grained and unconsolidated sediments.

6.1.2. Microfacies: As defined by Flügel (1982; pp.1), "*Microfacies is the total of all the paleontological and sedimentological criteria which can be classified in thin-sections, peels, and polished slabs*". Similar definitions were also given by Fairbrige (1954) and Wilson (1975).

6.1.3. Microfacies Types: The main lithologies present in Pliocene-Pleistocene terrace deposits in the Southern Peloponnese are distinguished into the following main microfacies types (Table 6.1): 1) Detrital carbonates and mixed carbonate-terrigenous microfacies, 2) Terrigenous microfacies, 3) Bioconstructed carbonate microfacies, 4) Calcareous palaeosols (caliche) microfacies. Place names mentioned in the text are shown in Figures M.1 and M.2 (back-pocket map). The locations of samples mentioned in the text (in italics) are given in Appendix A.

TABLE 6.1

A. DETRITAL CARBONATE MICROFACIES:

FACIES: A1: Lithic Grainstone

A2: Coated Grainstone

A3: Lithic Packstone

A4: Ostracod-Gastropod-Peloidal Wackestone/Packstone

B. CALCAREOUS SANDSTONE-GRANULAR CONGLOMERATE MICROFACIES:

FACIES: B1: Matrix-poor Calcareous Sandstone-Conglomerate

B2: Matrix-rich Calcareous Sandstone-Conglomerate

C. ALGAL-CORAL BOUNDSTONE MICROFACIES:

FACIES: C1: Red Algal Framestone and associated cavity fill

C2: Coral-red Algal Bafflestone

C3: Blue-green Algal Bindstone

D. CALICHE FACIES:

FACIES: D1: Hardpan Caliche

D2: Platy Caliche

D3: Chalky Caliche

D4: Nodular Caliche

D5: Rhizocretion Palaeosols

Table 6.1: Principal microfacies of Plio-Pleistocene shallow-marine sediments and palaeosols from the Messenia and Eastern Lakonia Peninsulae. Terminology for carbonate rocks is based on Dunham's classification (1962).

6.2 CARBONATE AND MIXED CARBONATE-TERRIGENOUS MICROFACIES

This group includes the following microfacies (Table 6.1): 1) Lithic grainstone, 2) Coated grainstone, 3) Lithic packstone, 4) Ostracod-gastropod-peloidal wackestone/packstone.

6.2.1 Lithic Grainstone (Figs. 6.1.1, 6.1.2, 6.1.6, 6.1.7, 6.1.8, 6.1.12, 6.7.2, 6.10.1):

6.2.1.1. Occurrence and stratigraphic distribution: This facies occurs in the upper parts of regressive sequences, in early Pleistocene (e.g. *Glf 14*; Pakia, E. Lakonia), early-middle(?) Pleistocene (e.g. *Dem 8*; Dhaemonia, E. Lakonia), Sicilian (*MSN 17*; Filiatra,

Messenia), Euthyrrhenian (*BoRe 7*; Bozas Rema, E. Lakonia) and Neotyrrhenian (*Mar*; Marathopolis; Messenia) terraces. Some Holocene beachorcks in the Messenia Peninsula also comprise grainstone sediments (see Chapters 3, 5; Kourampas and Robertson, 2000).

6.2.1.2. Description *(e.g. MSN 17; Dem 8, 19; Plyt 20*)*: This detrital carbonate microfacies is distinguished from matrix-poor calcareous sandstone (see below) by its more terrigenous composition (see Appendix A). Pleistocene grainstones are commonly well sorted, with well to moderately rounded grains, of coarse sand to granule size.

6.2.1.2.1. Terrigenous grains: These constitute ca. <10-50% of the sediment, defining the latter as lithic grainstone. Chert and bedrock limestone clasts predominate in samples from the Messenia Peninsula (e.g. *MSN 17*). In samples from the Eastern Lakonia Peninsula, quartz grains are common, in the form of composite grains with strongly undulose extinction and well rounded, single grains with microliths. Volcaniclastics occur as well rounded, elongate clasts, commonly of coarse sand size. They include andesite-type lithologies, with pyroxene phenocrystals, as well as welded lavas, tuffs and olivine-basalt. Rare olivine gabbro clasts are also present. Elongate grains of metamorphic lithologies are common, including phyllite, greenschist and mica schist. A few, very well rounded grains of bedrock packstone (correlated with Tripolis zone carbonates; see Chapters 3, 5) and recrystallised limestone also occur. Moderately, to well rounded, grains of xenotropic dolosparite are abundant. Rare, well rounded clasts of coarse-crystalline carbonate, with bladed to prismatic spar crystals, coated by red oxide films, are interpreted as flowstone fragments, probably derived from pre-Pleistocene pedogenic deposits (e.g. Unit 2; Chapter 5).

6.2.1.2.2 Carbonate grains: Their abundance ranges from 50 to 80% of the sediment. Foraminifera are present in variable quantities. A rich foraminiferal fauna comprise mainly epiphytic forms. *Milioliidae* and *Elphidium* spp. are the commonest benthic foraminifera, whereas *Rotaliidae* dominate locally (e.g. *Plyt 20**). Planktic taxa are relatively few, represented by *Globigeriniidae* or *Globorotaliidae*. Red algae are principally represented by encrusting forms (*Melobesioidaea*), locally as rhodolith encrustations (Fig. 6.1.7). Articulating red algae (e.g. *Amphiroa sp.* and *Corallina* sp.) are also common locally. The abundance of red algae defines the sediment as a Corallinacean grainstone (e.g. *MSN 17*; Filiatra, Messenia). Charophytes occur rarely (e.g. *Plyt 20**). Other allochems include cyclostomata bryozoa, serpulids (commonly associated with red algal crusts; see Fig. 6.1.7), bivalve fragments (commonly abraded), gastropods, scaphopods and echinoids. Gastropods, including both elongate and trochospiral forms, are the dominant molluscs, locally (e.g. *Plyt*

*20**). The abundance of coated grains varies locally, but large mollusc fragments, or whole shells, are commonly coated with micritic envelopes of variable thickness (Fig. 6.1.12). Some samples of inferred early-middle Pleistocene age (e.g. *Plyt 20**) are rich in articulated juvenile bivalves, also heavily micritised. Echinoderm spines are commonly micritised. Peloids are locally abundant, probably derived from heavily bored bioclasts. Pellets are common, forming part of the matrix and filling intraskeletal porosity. Blue-green algal lumps with incorporated quartz grains are common in Holocene beachrock samples (e.g. Mati; Messenia).

6.2.1.2.3 Cements: 1) Early cements of this microfacies include isopachous circumgranular rims and intraskeletal cements (Fig, 6.1). These comprise micrite (Fig. 6.1.12, 6.8.1), prismatic to equant circumgranular microspar (Figs. 6.1.1, 6.1.6), and, less commonly, circumgranular rims of accicular crystals (Figs. 6.1.2, 6.1.6, 6.1.9, 6.1.12). The latter two types of cement were precipitated around both allochems (commonly coated) and non-carbonate, terrigenous grains (e.g. quartz) (see Fig. 6.1.12). Prismatic microspar, by contrast, grew preferentially around carbonate grains (Fig. 6.1.1). In a few samples, where a succession of early cements can be observed (e.g. *Plyt 20**), prismatic to equant cements succeeded accicular rims (Fig. 6.1.6). Accicular cement rims exhibit an irregular periphery, depicting a sharp front of microboring (Figs. 6.1.5, 6.1.6).

2) Isopachous rims of equant to columnar, circumgranular spar are also present, locally surrounding non-carbonate terrigenous grains (Fig. 6.1.2).

3) Circumgranular cements were succeeded by syntaxial overgrowths of calcite, around non-micritised echinoid grains (Figs. 6.1.1, 6.1.2, 6.1.8). By contrast, coated echinoderm grains developed narrow overgrowths. Syntaxially overgrown crystals engulfed sediment grains in a poikilotropic fabric (Figs. 6.1.1, 6.1.2). The growth of these cements reduced primary intergranular pores, but moulds of coated bioclasts, engulfed by the poikilotropic crystals, remain open (Fig. 6.1.1).

4) Equant-equicrystalline microspar completely infilled intraskeletal cavities (e.g. bryozoa) in early-middle Pleistocene grainstones (e.g. *Dem 8*; E. Lakonia). Finely-crystalline spar also occluded bivalve-moldic and serpulid-moldic pores. In some samples, finely-crystalline spar precipitated as pendant cement, beneath carbonate grains, as observed in oriented samples (Fig. 6.1.5). Locally, such cements are in optical continuity with echinoderm grains (e.g. *Dem 19*). In these samples, "typical" syntaxial overgrowths of echinoderm grains were generally not developed.

5) Intraskeletal pores of large foraminifera (e.g. *Sphaeroidina bulloides*) were occluded by equant-drusy spar.

Figure 6.1 (following pages): Microfacies and diagenesis of Pleistocene sediments from the Messenia and Eastern Lakonia Peninsulae. For locations of samples see Figures M.1, M.2 (Back-pocket maps) and Appendix A. Horizontal bar: 0.1 mm.

1) Algal-mollusc grainstone of early Pleistocene age (Subunit 3.2; E Lakonia). Isopachous circumgranular rims of finely crystalline calcite **(1)** surround carbonate grains (red algae and bivalves). This cement precipitated within the active marine phreatic zone and was followed by syntaxial overgrowth of echinoderm grains **(E)**. The latter cement comprises euhedral crystals of calcite **(2)**, that enclose carbonate and non-carbonate grains **(Nc)** in a poikiltic fabric. The overgrowth cement **(2)** probably precipitated within the freshwater phreatic zone. Both primary and bivalve-moldic pores are present **(P)**. Sample *Dem 8*; Dhaemonia.

2) Algal-mollusc grainstone of early Pleistocene age (Subunit 3.2; E Lakonia). Isopachous rims of acicular fabric **(2)** surround skeletal grains **(A:** articulating red alga *Amphiroa* sp.). This cement, now consisting of low-Mg calcite, originally precipitated in marine phreatic conditions, as aragonite or high-Mg calcite. Isopachous rims of blocky spar **(1)**, of high width/length ratio, surround both skeletal and non-skeletal grains (e.g. **Mst**: mudstone clast). This cement probably precipitated in the freshwater phreatic conditions. Syntaxial overgrowth of echinoderm grains **(E)** post-dated the precipitation of the previous cements. Syntaxial overgrowths tended to develop euhedral crystals **(3)**. Syntaxial overgrowth probably took place within the freshwater phreatic zone. Sample *Dem 8*; Dhaemonia.

3) Poorly sorted, matrix-supported, coarse-grained calcareous sandstone of early or early-middle Pleistocene age (Subunit 3.2 or Unit 5; E Lakonia). Note the bimodal distribution of grain size (**Nc**: terrigenous grains). Intergranular cavities were reduced by normally graded geopetal infill **(Gp)**, deposited within the freshwater vadose zone. Umbrela porosity, under large bivalve fragments **(B)** was reduced by calcite spar of microstalactitic fabric **(C)**. This cement precipitated within the freshwater vadose zone. Primary porosity is preserved locally **(P)**. Sample *Kok 17*; Mourtitsa Rema.

4) Granular conglomerate of early or early-middle Pleistocene age (Subunit 3.2 or Unit 5; E Lakonia). Terrigenous grains **(Tg)**, from various bedrock lithologies, were cemented with an equant-drusy mosaic of low-Mg calcite spar **(C)**. This pervasive cementation reflects freshwater phreatic conditions that probably developed locally within the vadose zone (perched acquifer). Intercrystalline porosity **(P1)** probably represents remaining primary voids, although secondary enlargement by local dissolution of cement crystals cannot be excluded. Intracrystalline porosity **(P2)** is secondary. Sample *Kok 17.2*; Mourtitsa Rema.

5) Poorly sorted lithic grainstone of middle Pleistocene age (Subunit 6.2; E Lakonia). The sediment comprises non-carbonate terrigenous grains **(Nc)**, benthic foraminifera (**F**: the epiphytic species, *Cibicides lobatulus*), abraded bivalve fragments surrounded with micritic envelopes **(B)** and detrital matrix **(M)**. Intraskeletal cavities (e.g. within the foraminiferum **F**) were infilled with finely crystalline micite **(1)**, followed by isopachous rims of acicular crystals **(2)**. Precipitation of both cements **(1)** and **(2)**, and also microboring and formation of micritic envelopes, took place in marine phreatic conditions. Micritised zones within the acicular rim **(arrows)** probably resulted from boring activity of microrganisms, followed by resumed cement precipitation. Circumgranular cements comprise rims of microspar **(3)**. These show a microstalactitic fabric on the lower side of grains **(arrows)**, suggesting precipitation within the marine or freshwater vadose zone.

Figure 6.1 (continued)

Equant spar mosaics developed locally **(4)**, reflecting freshwater cementation. Both intergranular and intraskeletal pores **(P)** remain open. Sample *AyMar 18*; Ayia Marina.

6) Lithic grainstone-calcareous sandstone of middle Pleistocene age (base of Subunit 6.2; E Lakonia). The sediment comprises red algae **(A)** and well-rounded clasts of gabro **(G)** and greenschists **(S)**. Micritised zones **(arrow)**, resulted from microboring activity, follow the outline of, and growth boundaries inside algal grains. Isopachous rims of acicular cement **(1)** were deposited around algal grains. Their sharp, indented outline was probably modified from microboring activity. Isopachous rims of cryptocrystalline micrite **(2)** were deposited from biofilms around non-carbonate grains ('constructive micritic envelopes'). Intergranular spaces were infilled with fine-grained detrital matrix **(M)** as the sediment passed to lower energy conditions as a result of sea level rise. Porosity **(P)** is secondary, a result matrix dissolution after emergence. Bladed calcite cement, of pendant fabric **(4)**, formed within tthe freshwater vadose zone. Note microstalagmites of microcrystalline spar that also reduce secondary porosity **(arrows)**. Sample *Plyt20*; Plitra.

7) Algal framestone of middle Pleistocene age (base of Subunit 6.2; E Lakonia). Algal crusts developed around pebbles within the basal lag of the middle Pleistocene succession. Encrusting organisms included red algae **(A)**, serpulids and encrusting foraminifera **(E)**. The algal crusts were draped with fine-grained sediment with planktic foraminifera **(M)**, as sea level rose and the energy of the environment decreased (transgressive part of the sequence). Three classes of borings are distinguished: Micritised zones **(mb)** outline algal crusts. Large borings **(B1)** were infilled with pelletal matrix (pelletal wackestone). Even larger borings, of irregular outline **(B2)** were infilled with mudstone with planktic foraminifera, identical with the matrix **(M)**. Sample *Plyt 10*; Plitra.

8) Matrix-rich calcareous sandstone of middle Pleistocene age (base of Subunit 6.2; E Lakonia). The sediment originated as a matrix-poor calcareous sandstone; fine-grained matrix with foraminifera **(M)** was introduced later, as sea level rose and the energy of the environment decreased. Grains include clasts of recrystallised bedrock limestone **(L)**, gabro **(G)** and greenschist **(S)**.

9) Calcareous sandstone of early Pleistocene age (Subunit 3.2; E Lakonia). The sediment comprises terrigenous grains **(Tg)**, echinoids **(E)**, red algae **(A)** and peloids **(P)**. Isopachous fringes of acicular **(1)** and microcrystalline cement **(3)** were deposited within the marine phreatic zone. Equant sapr mosaics **(4)** precipitated within the freshwater phreatic zone. Blocky spar rims **(2)** around peloids **(P)** probably formed within the freshwater phreatic zone, as indicated by growth relations between these and equant spar mosaic **(arrow)**. Sample *Kok 36*; Kokkinia.

10) Ostracod-pelletal wackestone of early Pleistocene age (top of Subunit 3.2; E Lakonia). this facies was probably deposited in ephemeral freshwater ponds. It comprises ostracods **(O)**,commonly articulated, and fine quartz grains **(Q)** in a matrix of homogenous **(M)** or pelletal micrite (**Plt**: faecal pellets). Pellet-rich areas were cemented by microspar, giving rise to a pelletal grainstone texture locally **(arrow)**. Intraskeletal pores **(P)** in ostracods were reduced by low-Mg calcite cement of pendant fabric. Two generations of cement are distinguished. The first comprises bladed spar that grew in optical continuity with the fibrous ostracod wall **(1)**. The second comprises finely crystalline spar of pendant fabric **(2)**. The two generations of cement are separated by a sharp boundary. Diagenesis of the sediment took place within the saturated freshwater vadose zone. Sample *Kok 22*; Mourtitsa Rema.

Figure 6.1 (continued)

11) Algal framestone (lower part) and grainstone (upper part) of middle Pleistocene age (Unit 3.1; Messenia). The lower, bioconstructed part of the section comprises red algae (**L**: *Lithophyllum* sp., **Ms**: *Mesophyllum* sp.) and vermetid gastropods **(V)**. Fine-grained matrix **(M)** surrounds algal crusts and infills intraskeletal pores in vermetids. The matrix is a fine-grained, pelletal wackestone. The upper, detrital part of the section comprises benthic foraminifera (**F**: mainly *Milioliidae*), abraded bivalve fragments **(B)**, gastropods **(G)** and algal fragments. Bivalve fragments were surrounded with crusts, including *Tenarea* sp. (**T**: encrusting red alga), *Gypsina plana* (**Gy**: encrusting foraminiferum) and *Mesophyllum* sp (encrusting red alga). Diagenesis of the sediment included microboring and formation of micritic envelopes **(Me)** in the marine phreatic zone. Diagenesis in the freshwater phreatic zone resulted to moldic dissolution of gastropods and bivalves, and neomorphism of bivalve shells to low-Mg calcite, with preservation of the original skeletal fabric. Equant-drusy spar in interparticle pores and moulds was deposited in freshwater phreatic conditions. Transition to the freshwater vadose zone resulted in further moldic dissolution of bioclasts (**P:** moldic pore) and deposition of ferric oxides in pore spaces **(RO)**. Sample *Lim 13*; Limenari.

12) Lithic grainstone of late Pleistocene ("Neotyrrhenian") age (Unit 3.2; Messenia). The sediment comprises articulating red algae **(A)** and well rounded chert grains **(C)**, surrounded by micritic envelopes **(1)**. Micritic envelopes around chert grains are probably constructive, deposited from biofilms on the sea floor. Isopachous fringes of acicular cement **(2)**, that followed, were deposited in the active marine phreatic zone. Transition of the sediment to the freshwater vadose zone was marked by deposition of ferric oxides **(3)** in intergranular pores. Primary intergranular porosity remains high **(P)**. Sample *Mar 10*; Marathopolis.

13) Relatively well sorted lithic grainstone of latest Pleistocene age (Unit 3.7; Messenia). This aeolianite was deposited above Neotyrrhenian deposits. The sediment comprises calcite grains of detrital origin **(Cc)**, chert **(C)**, polycrystalline quartz **(Q)**, articulating red algae (**A:** *Amphiroa* sp.), echinoids **(E)**, and other bioclasts. Cements include finely-crystalline calcite of pendant and meniscus fabric **(1)** and bladed spar **(2)**, also of pendant fabric. Moldic dissolution of micritised bioclasts (**Me**: micritic envelopes) resulted in the formation of secondary pores **(P)**, Vadose silt **(3)** was deposited in primary interparticle pores. Diagenesis of the sediment took place within the freshwater vadose zone. Sample *Rom 3*; Romanos.

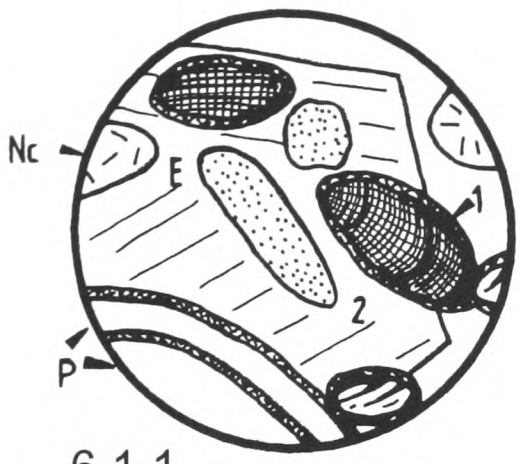

6.1.1

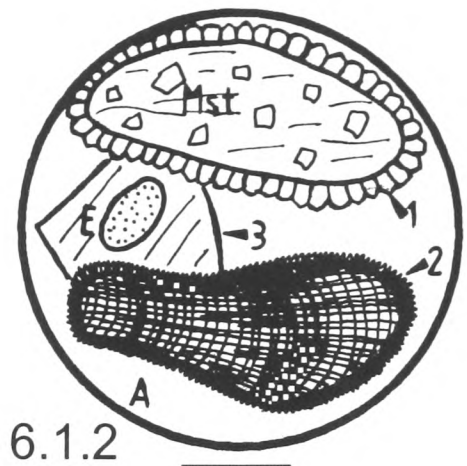

6.1.2

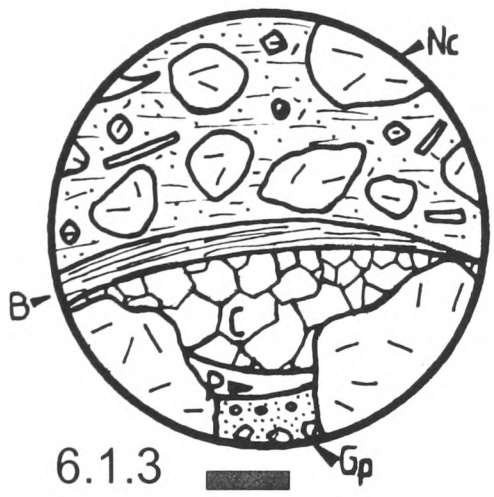

6.1.3

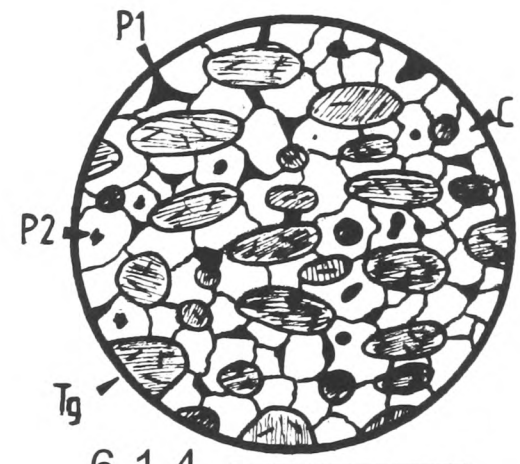

6.1.4

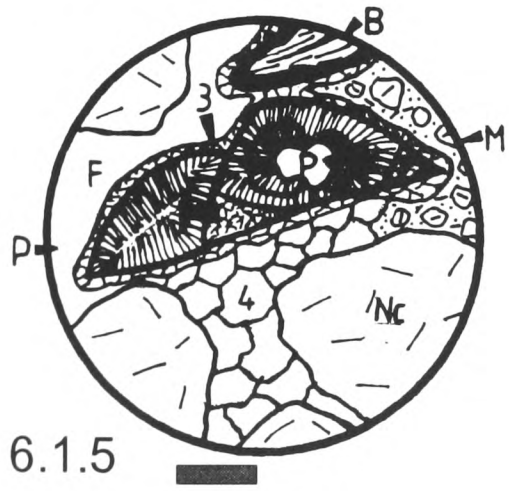

6.1.5

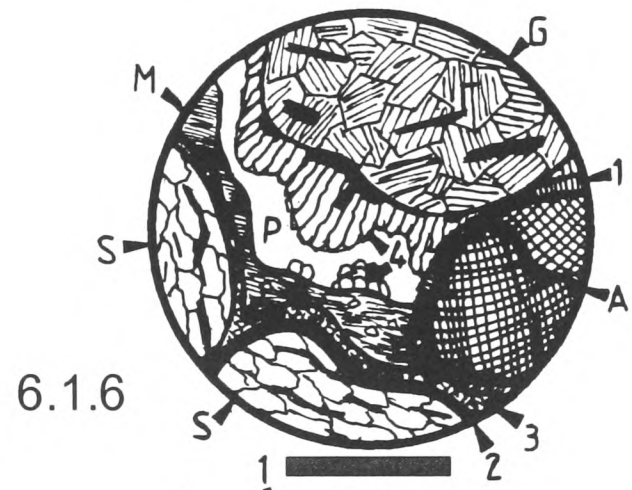

6.1.6

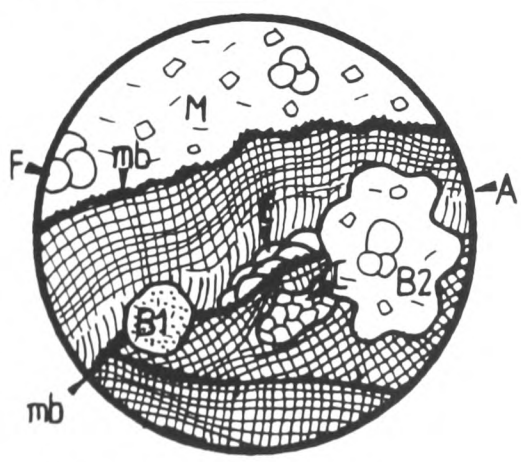

6.1.7

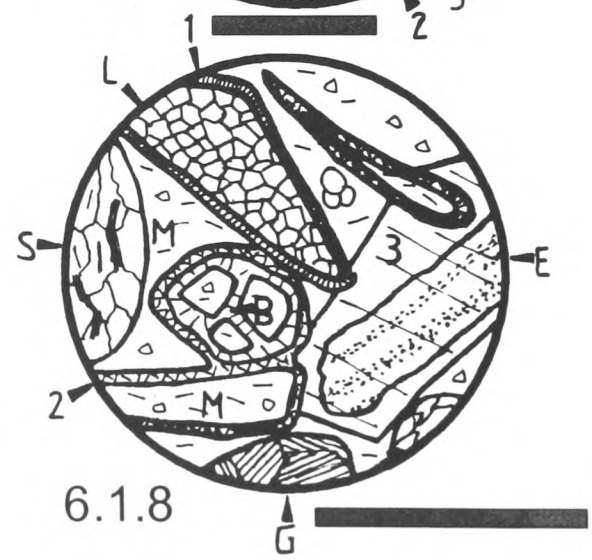

6.1.8

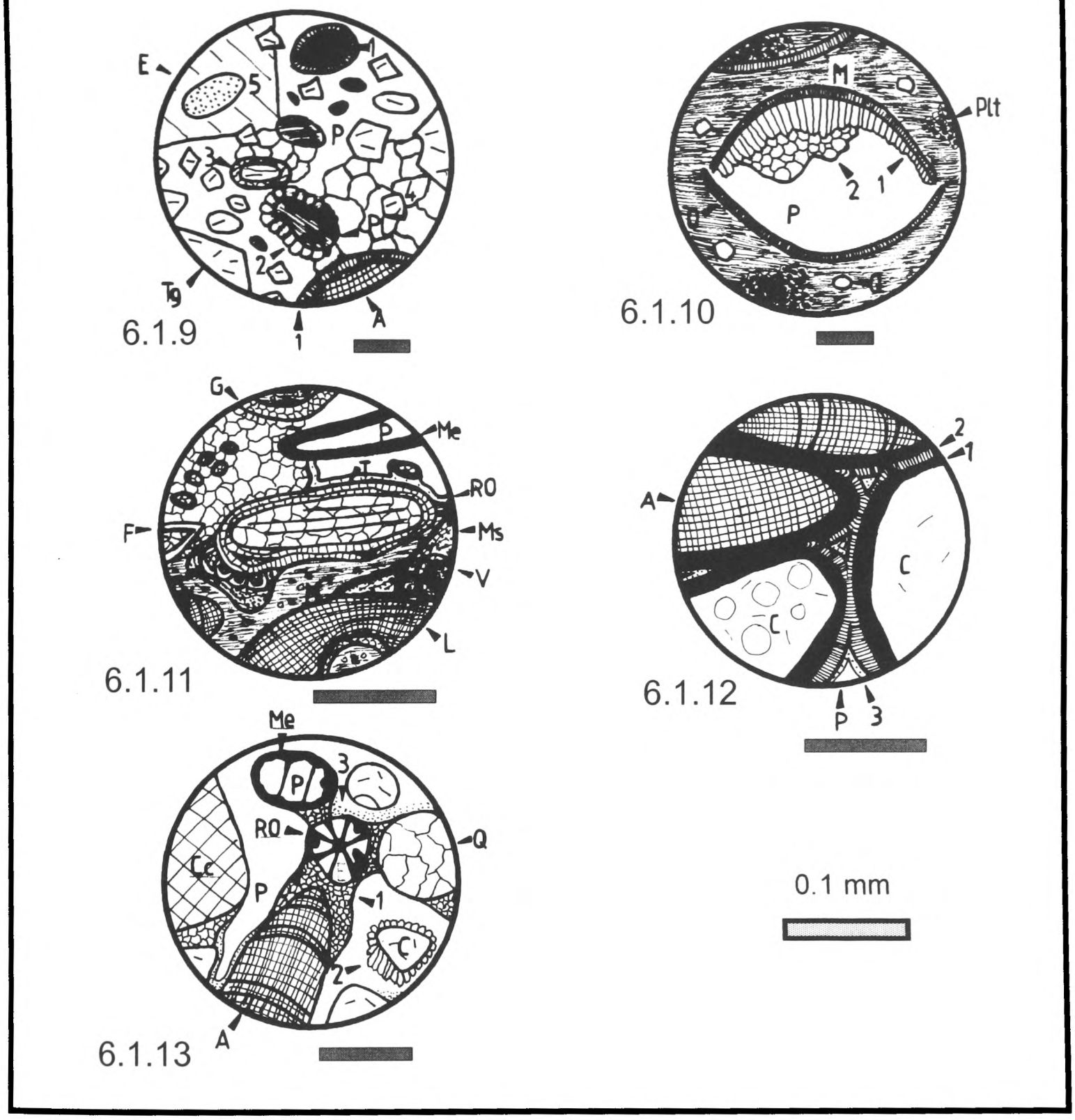

6) Prismatic spar grew in pendant form (Fig. 6.1.6), commonly on the internal sides of moldic pores (e.g. *MSN 17, Plyt 20**). Although prismatic spar exceptionally grew on the underside of non-carbonate grains (Fig. 6.1.6), this type of cement was preferentially precipitated around earlier accicular circumgranular cements, or micritic envelopes remaining after moldic dissolution. In some samples (e.g. *Plyt 20**), prismatic spar was followed by coarse crystalline, equant-drusy, clear spar, that occluded moldic and intergranular porosity.

6.2.1.2.4 Porosity: Porosity of grainstone microfacies varies from 8 to 25%, depending on the relative age of the outcrop and its position in relation to the active soil zone. High porosity values (>20%) are common. In this and the following descriptions, the porosity terminology of Choquette and Pray (1970) is followed.

1) Primary intergranular porosity is largely preserved, reduced by syntaxial overgrowth and equant spar cement only locally (Fig. 6.1.1).

2) Secondary porosity (mainly moldic, but also vuggy pores) is relativelly more abundant. This was locally reduced by syntaxial overgrowth, equant-drusy and microstalactitic cement (Figs. 6.1.6, 6.1.9, 6.1.11, 6.1.13). Local dissolution of these cements shows that some porosity was generated after pervasive cementation (e.g. *MSN 17*). Cement-moldic pores are nascent (Fig. 6.1.4, 6.1.13), and locally reduced by microspar cement (e.g. in bivalve fragments; *Dem 8*), or ferric oxide films (e.g. *MSN 17*; Messenia) (Fig. 6.1.13).

6.2.1.3 Deposition and diagenetic history: Pleistocene grainstone microfacies in the Southern Peloponnese were deposited in various sub-environments of high-energy, shoreline to backshore settings:

The majority of these sediments correspond to the Standard Microfacies 11 to 14 (coated grainstone, coquina, rodolithic grainstone, lag), of Facies Belt 6 ("*shoal environment in agitated water*"), with local participation of the Standard Microfacies 17 (grapestone grainstone) of Facies Belts 7 and 8 ("*restricted marine shoals*") (*sensu* Wilson, 1975; p. 65-67). All these microfacies were deposited in high-, to moderately high-energy environments, probably above the wave base (Wilson, 1975; Flügel, 1982). Reworking of such sediments into deeper marine settings (lower shoreface-offshore) by storm-induced currents is also inferred, by local outcrop evidence (see Chapters 3, 5). The high energy of the depositional environment is indicated by the ubiquitous abrasion of grains and the absence, or scarcity, of matrix. A predominance of the benthic foraminifera *Milioliidae* and *Elphidium* spp. indicates deposition in normal marine, high-energy intralittoral, to upper circumlittoral, environments (Blanc-Vernet, 1969; Murray, 1973), coincident with a foreshore, to upper shoreface, depth.

By contrast, corallinacean-mollusc grainstones, rich in the hyposalininty-tolerant red alga *Corallina* sp. (Johnson, 1954; Wray, 1977) were possibly deposited in fluvially influenced shorelines (e.g. *MSN 17*). Grainstones rich in peloids and coated grains (including constructive micritic envelopes) were probably deposited in, or near, a *Thalassia*-vegetated environment (Perry, 1998).

Grainstones with lower circumlittoral benthic foraminifera (e.g. *Textularia spp., Sphaeroidina bulloides;* see Blanc-Vernet, 1969; Murray, 1973) are interpreted as deposits

of a storm-dominated lower shoreface-offshore environment, with coarse sediment provided from reworking of more proximal facies (see Chapters 3, 5; Kourampas and Robertson, 2000). Based on published ecological data (Blank-Vernet, 1969; Murray, 1973; Tziavos and Chronis, 1994), depositional depth was probably ≤20-30 m.

Medium to fine-grained, well-sorted grainstones (Figs, 6.1.13, photo) that overlie "Neotyrrhenian", shoreface to foreshore, deposits in Messenia and Eastern Lakonia are interpreted as aeolinanites (Units 3.7, 13; see Figs. 3.5, 5.6, Chapters 3, 5). This interpretation is based on the very good sorting of the sediment, the exclusive presence of pendant microspar cement (meteoric vadose zone) and outcrop-scale structures (dune morphology and cross-bedding; Chapters 3, 5).

The diagenesis of grainstones (with the exception of aeolianites) began in the marine phreatic zone, with precipitation of isopachous rims of circumgranular, or intragranular cement. As suggested by crystal morphology, equant to prismatic microspar cements probably originated as high-Mg calcite, whereas the less common accicular cements probably formed from an aragonite precursor (Alexandersson, 1969, 1972; Land, 1970; Longman, 1980, Coudray and Montaggioni, 1986). Early cementation of this type probably took place in the active marine phreatic zone (Longman, 1980; Tucker and Wright, 1990); effective pore-water circulation was favoured by the high-energy conditions of the upper shoreface-foreshore environment.

In some samples (*Dem 8*), the earliest circumgranular cement is equant, low-Mg calcite spar (Fig. 6.1.2). This can be interpreted either as an effect of heteroaxial transformation of earlier marine cements (Coudray and Montaggioni, 1986), or as evidence for transition of the sediment from the stagnant marine phreatic zone, where little cementation took place, to the active saturated freshwater phreatic zone, where circumgranular low-Mg calcite was deposited (Longman, 1980). Such a diagenetic sequenece could also be the product of submarine discharge from a groundwater acquifer.

Well-developed syntaxial overgrowth of echinoderm grains probably took place in the active saturated freshwater phreatic zone, as with the pervasive cementation by clear, equant-equicrystalline or equant-drusy, low-Mg calcite spar (Land, 1970; Longman, 1980; Coudray and Montaggioni, 1986).

Many of the sediments examined underwent widespread, mainly moldic dissolution prior to their cementation by low-Mg cement. This dissolution could have taken place in the undersaturated freshwater phreatic zone (i.e. at, or just below the water table), or the undersaturated vadose zone (Longman, 1980). Porosity fabric alone does not allow distinction between vadose and phreatic conditions (Choquette and Pray, 1970; Longman,

1980; Coudray and Montaggioni, 1986); however, it is inferred that this dissolution took place within the undersaturated freshwater phreatic zone, since a stage of freswater phreatic conditions is expected to follow marine phreatic conditions during a relative sea level fall (Longman, 1980; Coudray and Montaggioni, 1986; see Figs. 6.3, 6.4). Prior existence of relatively shallower, undersaturated freshwater phreatic conditions before relatively deeper, active saturated freshwater phreatic conditions, could be controlled by relative position of the groundwater table, in turn influenced by sea level and climate (Longman, 1980; Coudray and Montaggioni, 1986; Tucker and Wright, 1990).

Neomorphism (homoaxial transformation) of unstable, early high-Mg calcite and aragonite cements and bioclasts to stable, low-Mg calcite probably took place in the active freshwater phreatic zone (Land, 1970; Longman, 1980; Coudray and Montaggioni, 1986). Lithic grainstones, deposited as foreshore sediment in the upper parts of regressive sequences (see Chapters 3, 5), commonly do not show evidence of diagenesis in the freshwater phreatic zone (e.g. MSN 17). Early marine cements and primary and secondary porosity were, instead, followed by microcrystalline or prismatic spar of pendant, and locally meniscus, character, deposited in the lower, saturated part of the freshwater vadose zone (Bathurst, 1974; Longman, 1980; Coudray and Montaggioni, 1986). Pendant spar in optical continuity with echinoderm grains was probably deposited in the same environment, as indicated by cement fabric and mineralogy (i.e. low-Mg calcite). Deposition of ferric oxides in moldic and vuggy pores probably took place in the upper part of the freshwater vadose zone (i.e. soil zone).

6.2.2 Coated-grainstone (Fig. 6.15.1)

6.2.2.1 Occurrence and stratigraphic distribution: This facies covers inferred "Neotyrrhenian" shallow-marine sediment in the area of Marathopolis (NW Messenia; see Figs. 3.6, M.1). Its age is probably latest Pleistocene (see Chapter 3).

6.2.2.2 Description (*Mar 7*): The sediment comprises well sorted, well rounded grains of medium sand size, in a mosaic of spar to microspar cement.

6.2.2.2.1 Terrigenous grains: These include quartz, feldspar, chert and bedrock limestone, correlated with the Tripolis zone. The majority of grains are coated with thick, almost isopachous, cryptocrystalline crusts, of inferred blue-green algal-microbial origin.

6.2.2.2.2 Allochems: These comprise benthic foraminifera (including many epiphytic forms), mollusc shell-fragments (abraded and reduced to average grain size), bryozoa, serpulids and peloids, probably derived from extensive micritisation of abraded bioclasts. Almost all carbonate grains are coated with blue-green algal-microbial crusts. Ferric oxide penetration in carbonate grains is common.

6.2.2.2.3 Matrix: Intergranular matrix (brown finely crystalline micrite) is rare within this microfacies.

6.2.2.2.4 Cement: The sediment is well cemented, with a mosaic of clear, equant-drusy microspar, precipitated in intergranular spaces. The latter cement locally exhibits a pendant character. Locally, bivalve grains were recrystallised to microspar, with preservation of the original skeletal fabric.

6.2.2.2.5 Porosity: Primary porosity is preserved in the form of remnant intergranular pores, reduced by spar cement.
Secondary porosity comprises incomplete moldic dissolution of coated grains and, possibly, local dissolution of cement. However, distinction of secondary, from residual primary, porosity is not straightforward in this microfacies.

6.2.2.3 Deposition and diagenetic history: On the basis of field relations (i.e. position on the top of a regressive, shoreface to backshore sequence), this sediment is interpreted as a backshore facies, deposited in an agitated lagoon, behind a barrier (Chapter 3; Kourampas and Robertson, 2000). Moldic dissolution and cementation of the sediment took place in the freshwater vadose zone, as indicated by a microstalactitic cement fabric (Longman, 1978; Tucker and Wright, 1999).

6.2.3 Foraminiferal-echinoid-peloidal lithic packstone (foraminiferal micrite) (Figs. 6.10.2, 6.11.2, 6.16.2):

6.2.3.1 Occurrence and stratigraphic distribution: This microfacies is common in coarsening-up, regressive parts of shallow-marine sequences, commonly above mud/mudstones, but below grainstone facies. This microfacies is distinguished from matrix-rich calcareous sandstone (ltihic wacke; see below) by higher presence of carbonate grains. Fossiliferous packstone is more widespread in the Messenia Peninsula, were sediments are systematically less terrigenous, as compared with those of the Eastern Lakonia Peninsula

(see Chapters 3, 5, 8). Lithic packstone occurs within prograding clinoforms of the early Pleistocene terrace and in early-mid Pleistocene and Eutyrrhenian terrace sediments, in both peninsulae (Units 2.2, 2.4, 2.3, 3.1 in Messenia; Units 3.2, 5, 8 in Eastern Lakonia; see Chapters 3, 5).

6.2.3.2 Description (*Kok 30, Kok 32; Dem 1; Vigl 3, AyMar 33; TaRe 19*): Grain-size ranges from medium to coarse sand. The grain population is commonly well sorted (e.g. *Vigl 3*). Most samples of this microfacies exhibit grain-supported fabric.

6.2.3.2.1 Terrigenous grains: These constitute ca. 30-50% of the sediment, and they are more abundant in samples from the Eastern Lakonia Peninsula. In Messenia Peninsula, chert and several types of limestone are the commonest terrigenous grains, correlated outcrops of Pindos and Tripolis zones. In the Eastern Lakonia Peninsula, quartz (both single and composite) and metamorphic grains (commonly elongate) dominate, followed by various types of recrystallised limestone, dolomite, and marble. Overall, the terrigenous grains present in this microfacies are as those present in the grainstone microfacies (see above).

6.2.3.2.2 Carbonate Grains: These constitute ca. 50-70% of the sediment grains. Benthic foraminifera comprise ca. 4 to >10%, mostly represented by epiphytic forms (including *Milioliidae*, that locally dominate the fauna; e.g. *Dem 1*). Agglutinated foraminifera (*Textulariidae, Valvulinidae*) are common in relatively finer grained microfacies (e.g. *Vigl 3*). Planktic foraminifera are sparse in coarse-grained microfacies, but their presence increases with decreasing grain-size (e.g. ca. 15% in *Vigl 3, Plyt*12*). Red algae are very common, in the form of rhodoliths, algal crusts, and branching taxa. Molluscs are common, either as large shell fragments, or as abraded grains, reduced to the average grain-size. Other allochems include rare ostracods, scaphopods, cyclostomata bryozoa (including many encrusting forms), echinoids, scleractinean corals, serpulids, blue-green algal crusts and lumps, pellets and peloids derived from micritised mollusc grains. Aggregates are common, comprising peloids, less micritised allochems and, rarely, terrigenous grains. Many mollusc grains are coated with relatively thick micritic envelopes. Green algae are rarely present in a few samples from Messenia. Different relative abundance of allochems gave rise to a variety of lithic packstone types. Foraminiferal-molluscan-bryozan lithic packstone and algal-molluscan-bryozoan lithic packstone are the commonest.

6.2.3.2.3 Boring: Boring of allochems is locally extensive (e.g. *Vigl 3*). Thick micritic envelopes commonly developed around bioclasts. Serpulid and bivalve fragments are also affected by larger borings, infilled with matrix or glauconite.

6.2.3.2.4 Matrix: Matrix comprises ca. 12-18% of the sediment. It consists of cryptocrystalline micrite, or, less commonly, dense accumulations of pellets, probably of a fecal origin. Various degrees of pellet homogenisation were observed in the same sample, with pelletal packstone with clearly discernible pellets grading to a mass of lime mudstone to floatstone fabric (wherever other small-sized allochems are also present within the matrix). Microcrystalline micrite matrix is less common. It resembles the unsorted "geopetal bioclastic micrite" of Aissaoui and Purser (1983), deposited within the subtidal-lower intertidal zone.

6.2.3.2.5 Cement: **1)** Early carbonate cements include rims of accicular crystals in intraskelletal (e.g. foraminifera tests; see Fig. 6.1.5) and, less commonly, circumgranular location. Circumgranular micritic cement forms isopachous rims, mainly in fine-grained microfacies.

2) Circumgranular cements are commonly buried by equant-drusy spar, that also infills moldic porosity (e.g. moulds of molluscs, corals), as well as intraskeletal pores in foraminifera, bryozoa, serpulids and red algae (Fig. 6.1.11). Sparry cement is less developed in finer grained microfacies (e.g. *Vigl 3*); in the latter microfacies spar mosaics tend to be equicrystalline instead of drusy.

3) Syntaxial overgrowths of echinoderm grains are common in both coarse- and fine-grained microfacies (Figs. 6.1.2, 6.1.8, 6.1.9).

4) In samples of inferred early Pleistocene age, irregular shaped microspar clusters occur within micritic matrix (Fig. photos).

5) Coarse- or finely-crystalline spar, locally of pendant or meniscus type, commonly reduces (or completely infills) vaggy and moldic pores. Locally, pendant cement comprises prismatic calcite crystals (e.g. *Kok 32*) (Figs. 6.1.6, 6.1.13). The relative abundance of pendant cement varies widely from sample to sample. In some (e.g. *Kok 32*), pendant cements co-exist with isopachous rims of blocky spar that reduce incipient peloid-moldic pores.

6) Porosity in densely jointed samples was reduced by euhedral prismatic crystals of calcite, growing perpendicular to the extentional joint walls (e.g. *Vigl 3*).

Authigenic cryptocrystalline glauconite is common in fine-grained packstones. It fills intraskeletal pores (e.g. foraminifera tests), borings in larger skeletal elements (e.g. *Vigl 3, Plyt*12*), or, rarely, intergranular spaces (e.g. *Dem 1*). Glauconite locally buries earlier microcrystalline spar cement. Most glauconite-infilled foraminifera are intensely fractured; cracks that run through the glauconite are infilled by later microspar to spar cement.

6.2.3.2.6 Porosity: Samples of this microfacies are generally porous (porosity ca. 5-30%).

1) Primary porosity (ca. 4-7%) is mainly preserved in intraskelletal pores (e.g. foraminiferal tests), partly reduced by cements (Fig. 6.1.6).

2) Most porosity is secondary (>25%). This comprises moldic porosity (after molluscs, corals and other allochems) and vuggy dissolution that locally enlarged primary and secondary (moldic) pores. In some samples (e.g. *Vigl 3*), dissolution affected matrix and echinoid grains. Secondary porosity is locally reduced by equant-drusy and pendant spar cement. Vuggy and moldic pores near the present-day surface are commonly rimed, or completely filled, by ferric oxides (Fig. 6.1.13).

6.2.3.2.7 Pedogenic features: Locally, clusters of accicular clay minerals developed in primary and secondary pore spaces of packstones exposed near the soil zone (e.g. *TaRe 19*). These clay minerals are closely associated with ferric oxides.

Calichification features are present in many samples, with development of aureolar strucures, intense micritisation of carbonate grains and corrosion of quartz and chert grains (e.g. *Dem 1*).

6.2.3.3 Deposition and diagenetic history: Lithic packstone deposits correspond to a variety of shoreface, to offshore, environments, as inferred from outcrop relations (Chapters 3, 5), circumlittoral foraminifera fauna and other allochems. Highly peloidal varieties, with presence of constructive micritic envelopes and aggregates, were probably deposited within sea-grass vegetated shoreface environments (Perry, 1998). Microfacies with high mollusc, bryozoa and rhodolith contents, alternating with mudstones, are interpreted as lower shoreface-offshore storm deposits (see Chapters 3, 5).

Diagenetic sequences of lithic packstones are similar to those of shallow-marine grainstones and sandstones occuring in a similar regressive setting. Most of the samples examined were cemented within stagnant marine phreatic conditions, as evidenced by the relative scarcity of well developed circumgranular rims and the prevalence of local intragranular cements (Longman, 1980).

Moldic dissolution of mollusc, coral, and other aragonitic skeletons took place within a freshwater environment (Choquette and Pray, 1970; Longman, 1980), followed by equant-drusy cementation, probably within the active saturated freshwater phreatic zone (Land, 1970; Longman, 1980). Production of low-Mg calcite microspar within the micritic matrix of the sediment is interpreted as the result of aggrading neomorphism (*sensu* Bathurst, 1975). The latter recrystallisation, accompanied by neomorphism of mollusc shells to equant spar, probably took place within the freshwater phreatic zone, as well.

These stages were followed by vuggy dissolution and precipitation of pendant cement within the freshwater vadose zone (Longman, 1980, Tucker and Wright, 1990). Introduction of ferric oxide into the pore system (mainly vuggy, but also moldic) was probably accomplished within the upper parts of the freshwater vadose zone, near the active soil zone. Calichification, evidenced by aureolar structures, dissolution of stable carbonates (e.g. low-Mg calcite of echinoderms) and extensive micritisation of carbonate grains (Esteban and Klappa, 1983; Pye, 1983), took place in the upper part of the freshwater vadose zone.

6.2.4 Ostracod-gastropod-peloidal wackestone (pelmicrite) (Figs. 6.1.10, 6.7.1):

6.2.4.1 Occurrence and stratigraphic distribution: This sediment covers fluvial/deltaic sands-granular conglomerates on the 120 m terrace in the area of Kokkinia-Mourtitsa Rema (Lakonia; see Figs. 5.2, 5.3, M.2). This sediment belongs to the uppermost parts of an early Pleistocene regressive sequence (Subunit 3.2, Chapter 5).

6.2.4.2 Description (e.g. *Kok 22*): This microfacies comprises a very dense accumulation (i.e. taphocoenosis) of ostracods and gastropod shells in micritic matrix. Fossils are aligned parallel to bedding planes.

6.2.4.2.1 Terrigenous grains: Their presence is restricted to a few single and composite quartz grains and mica-schist clasts.

6.2.4.2.2 Carbonate grains: These include a high-density fauna of ostracods and gastropods, as well as abundant pellets, probably of a faecal origin. The ostracod valves are not ornamented and probably belong to a single species (i.e. low-diversity fauna). Many ostracod valves are articulated. Most gastropod shells are dissolved. Moulds and shells are surrounded by thick micritic envelopes.

6.2.4.2.3 Matrix: This consists of fine-grained, pelletal packstone ('clotted micrite'), locally homogenised to brown micrite.

6.2.4.2.4 Cements: Crystalline cements are present only locally, reducing primary (intraskeletal) and secondary porosity.

1) Equant-drusy spar has occluded moldic porosity in gastropods. The same type of cement was also deposited in fenestral pores within the matrix, thus creating a 'bird's eye' fabric.

2) Crystals of prismatic euhedral spar grew in a pendant form, at the lower side of intraskeletal cavities of articulated ostracods, in optical continuity with the fibrous walls of ostracod valves (Fig. 6.1.10).

3) The latter cement was succeeded by equant microcrystalline spar of pendant character. These two generations of cement are separated by a sharp boundary (Fig. 6.1.10).

4) Euhedral calcite crystals commonly rim pores that probably resulted from root penetration into the sediment. The c-axes of the latter crystals are perpendicular to the tube walls.

6.2.4.2.5 Porosity: 1) Fenestral porosity is present at various scales (10's of μ-mm). Primary intraskeletal porosity within articulated ostracods is also preserved, commonly reduced by two generations of spar cements (Fig. 6.1.10).

2) Moldic dissolution of gastropods was complete, but was later reduced by equant spar (see above). By contrast, ostracods were less affected by moldic dissolution. Vuggy pores, probably resulting from root-tube bioturbation, are abundant.

6.2.4.3 Deposition and diagenetic history: As suggested by the high-density, but low-diversity, fauna of ostracods and gastropods and the absence of marine organisms, this sediment was deposited in freshwater conditions. Micritisation, abundant pellets and scarcity of siliciclastic material point towards the existence of a short-lived pond in the low reaches of a fluvial system (as indicated by fluvial sand and gravel above and below this facies; see Chapter 5). This microfacies, thus, corresponds to the Standard Microfacies 19 ("*pelletal mudstone-wackestone*") *sensu* Wilson (1975), deposited in very restricted bays and ponds.

Moldic dissolution and cementation took place within the freshwater vadose zone, as shown by the pendant cement fabric. The transition of the sediment to the upper parts of the vadose zone (soil zone) resulted in root bioturbation and calichification.

6.3 CALCAREOUS SANDSTONE-GRANULAR CONGLOMERATE MICROFACIES

This microfacies occurs locally in early, middle, late Pleistocene terraces and Holocene beachrocks in both Peninsulae (Units 2.1, 2.2, top of Unit 2.5, Units 3.1, 3.2, 3.8 in Messenia; Units 3.2, 3.5, 6, 8, 11, 14 in Eastern Lakonia; see Chapters 3, 5). Two end-members of this group are distinguished:

6.3.1) Matrix-poor calcareous sandstone-conglomerate.

6.3.2) Matrix-rich calcareous sandstone/conglomerate.

Both facies occur in the upper parts of coarsening-up, shallowing-up successions.

6.3.1 Matrix-poor calcareous sandstone-conglomerate (litharenite and related facies)

6.3.1.1 Occurrence and stratigraphic distribution: Sediments of this microfacies occur in coarse-grained, upper shoreface-foreshore successions of Pleistocene age and in Holocene beachrocks, in both peninsulae. Typical outcrops are located at Gargaliani (early Pleistocene; Messenia), the Ano Glikovrisi Mountains (early Pleistocene; Lakonia), the Laghouvardhos area (middle Pleistocene; Messenia), the Filiatra area (Sicilian; Messenia), Bozas Rema (Eutyrrhenian; Lakonia), Romanos (Neotyrrhenian; Messenia), Mati (Holocene; Messenia) and Limnakia (Holocene; Lakonia) (see Chapters 3, 5; Kourampas and Robertson, 2000; Figs. M.1, M.2).

6.3.1.2 Description (Figs. 6.1.4, 6.1.13, 6.12.2): Most sediments of this facies comprise moderately to well-sorted calcareous litharenite, transitional to lithic grainstone with an increase in carbonate grains (e.g. *Kok 29, Vigl 4*). Few samples are poorly sorted conglomerates with bimodal grain size distribution (e.g. *Kok 17*). Grain-size commonly falls within the medium sand-granule range. Grains are generally moderately to well rounded.

6.3.1.2.1 Terrigenous Grains: Their abundance ranges from ca. 41-45% to ca. 30-35% in microfacies close to the "litharenite" and "lithic grainstone" ends of the spectrum, respectively. Terrigenous grains were derived from various bedrock lithologies. Radiolarian chert, from Pindos Zone outcrops, is commonly the principal terrigenous component in the Messenia Peninsula (up to 32%), followed by various types of bedrock limestone (5-7%), from outcrops of Tripolis and Pindos Zones. In the Eastern Lakonia Peninsula, most grains consist of composite quartz of undulose extinction, presumably derived from metamorphic lithologies of the "*Phyllite Series*". Phyllite and greenschist grains are also common in the

latter peninsula, together with various types of bedrock limestone and marble. Chert and minerals of metamorphic origin (e.g. kyanite in *Vigl 4*; Viglaphia), are rare (<1%).

6.3.1.2.2 Carbonate grains: These constitute ca. 18-25% of the sediment, comprising mainly non-encrusting organisms (15-20%) and a few encrusters (ca. 2-3 %). The majority of the skeletal grains were derived either from red algae (e.g. *Rom 3*), or benthic foraminifera (e.g. *Vigl 4*). The ratio between articulating and encrusting red algae varies from 6:1 (e.g. *Rom 3*), to a clear predominance of encrusting forms (e.g. *Vigl 4*). Encrusting red algae, comprising several genera, are present in the form of crust fragments or rhodoliths. Rhodoliths are commonly bored, and borings are infilled by glauconite (e.g. *Vigl 4*), or matrix. Benthic foraminiferal assemblages are dominated by epiphytic forms (*Milioliidae*, *Elphidium* spp.). The abundance of planktic foraminifera varies from a total absence (e.g. *Rom 3*), to rare presence of *Globigerinidae* and *Globorotaliidae* (e.g. *Vigl 4*). Other carbonate grains include bivalve shell fragments (commonly abraded and bored by *Clionid* sponges), echinoid spines, various bryozoa, peloids, very rare ooids (in samples from Messenia), pellets and a few micritic, probably algal/microbial, lumps, with incorporated terrigenous grains (e.g. quartz). Grains coated with micritic envelopes are abundant in most samples.

6.3.1.2.3 Matrix: This microfacies is matrix-poor (<2%). Where present, the matrix is micritic and locally pelletal. In some samples the matrix is largely recrystallised to microspar (e.g. *Kok 17*).

6.3.1.2.4 Cement: The abundance of crystalline cement appears to decrease systematically with relative age of the sediment. Thus, cement constitutes ca. 25% of some early Pleistocene samples (e.g. *Kok 29*), 17-20% of Neotyrrhenian samples and 13-18% of Holocene beachrock samples. However, exceptions to this trend are common, since the abundance of cement also depends on the diagenetic history of each outcrop (see below). The following types of cement are present:

1) A few early Pleistocene calcareous sandstones from the Eastern Lakonia Peninsula are cemented with constructive micritic envelopes, probably precipitated by grain-coating biofilms (Perry, 1997).

2) Circumgranular microspar forms isopachous rims (e.g. *Rom 5*).

3) Intergranular microspar is also common (e.g. *Rom 5*).

4) Syntaxial overgrowths of echinoderm fragments buried earlier circumgranular cements in many Pleistocene samples, from both peninsulae. In rare cases, syntaxial overgrowths developed around caclite crystals of probable detrital origin (e.g. *Kok 36*).

5) Circumgranular blocky calcite crystals form isopachous rims around carbonate grains (e.g. *Kok 29*; early Pleistocene, *Kok 36*; middle Pleistocene).

6) Coarsely crystalline, equant spar mosaics of poikilotropic fabric, surrounding terrigenous grains, are very well developed in inferred middle Pleistocene sandstones (e.g. *Kok 17*) (Fig. 6.1.4). Locally, the same grain is embedded in poikilotropic spar on one side and blocky spar on the other side (e.g. *Kok 36*). Primary porosity is still preserved between interfaces of poikilotropic spar crystals. The latter crystals were affected by incipient crystal-moldic dissolution (Fig. 6.1.4).

7) Clear crystals of drusy calcite spar also bury earlier circumgranular cements. Clear spar cement locally exhibits pendant or meniscus fabrics (Fig. 6.1.3). Samples from the inferred Eutyrrhenian terrace in Bozas Rema, Eastern Lakonia Peninsula (see Chapter 5), include prismatic spar and echinoderm overgrowths, that both exhibit a pendant development, preferentially precipitated at the undersides of granules (e.g. *BoRe 15, Vigl 4*). In such samples, neomorphism of mollusc grains to an equant spar mosaic took place without obliteration of the original skeletal fabric of the grains (Fig. 6.1.11).

6.3.1.2.5 Porosity: The porosity of the calcareous sandstone microfacies is generally high (up to ca. 22%). In early Pleistocene outcrops, the ratio of primary *versus* secondary porosity varies, depending on the proximity of the outcrop to the soil zone. In Neotyrrhenian outcrops (e.g. *Rom 5*), primary pores (ca. 20%) outnumber secondary ones (ca. 0.5-1%). Many primary pores, however, where enlarged secondarily.

1) Primary porosity is intergranular, intraskeletal and shelter porosity, located at the undersides of large bioclatsts (Fig. 6.1.3).

2) Secondary porosity is mainly moldic; this was locally reduced, or completely filled, by spar cement. An incipient cement-moldic porosity was developed within poikilotropic spar mosaics (Fig. 6.1.4). Vuggy porosity, that locally enlarged previous moldic pores, is high in outcrops near the active soil zone. In such settings, walls of vuggy and moldic pores are rimmed by ferric oxide films.

6.3.1.2.6 Pedogenic features: Accicular rims of clay mineral, of pendant growth-fabric are closely associated with earlier pendant prismatic spar (e.g. *Vigl 4*). Corrosion of quartz and chert grains locally suggests early stages of calichification (Goudie, 1983; Tucker and Wright, 1990).

6.3.1.3 Deposition and diagenetic history: Sediments of this microfacies were deposited in the upper shoreface, to foreshore zone, as shown by outcrop evidence (i.e. sedimentary structures, macrofauna, etc.; see Chapters 3, 5; Kourampas and Robertson, 2000), lithology and circumlittoral microfauna (Blanc-Vernet, 1969; Murray, 1973). Depositional environments range from exposed, wave-dominated clastic shorelines, to bayhead deltas in the landward part of estuarine-lagoonal systems (Chapters 3, 5). Microfacies rich in micritised and coated grains, cemented by constructive micritic envelopes, were probably deposited in lower energy conditions, within *Thalassia*-vegetated shorelines (Perry, 1997).

Some early cementation took place within the active marine phreatic zone, with precipitation of isopachous microspar cement (Longman, 1980; Coudray and Montaggioni, 1986). Precipitation of glauconite within intraskeletal pores of foraminifera reflects the development of a reducing environment, within stagnant marine phreatic conditions, locally. This probably took place below the sediment-water interface (Bathurst, 1971; Berner, 1981). Most samples of this microfacies reflect further diagenesis in the saturated freshwater phreatic zone, involving syntaxial overgrowths of echinoderm grains, pervasive cementation with equant spar (low-Mg calcite) and neomorphism of aragonitic, or high-Mg calcite grains, to low-Mg calcite (Land, 1970; Longman, 1980; Coudray and Monataggioni, 1986; Tucker and Wright, 1990). Neomorphism commonly involved homoaxial transformation of metastable minerals to calcite, as evidenced by preservation of original skeletal fabrics (Coudray and Montaggioni, 1986). Also, circumgranular cementation by blocky spar probably took place within the saturated freshwater phreatic zone (Land, 1970; Longman, 1980). The development of poikilotropic mosaics of coarse-crystalline, equant spar were coeval with blocky spar precipitation, as evidenced by cement growth relations (see above). This stage of pervasive cementation is, thus, attributed a saturated freshwater phreatic environment, known to leave the most distinct diagenetic signature in uplifted Pleistocene shorelines elsewhere (e.g. Bermuda; Land, 1970).
This was followed by diagenesis in the freshwater vadose zone, involving moldic dissolution of mollusc grains, cementation by meniscus and pendant spar cements and local development of clay minerals with pendant growth fabric.

Elsewhere, (e.g. inferred Eutyrrhenian terrace in Bozas Rema, Eastern Lakonia) upper shoreface-foreshore calcareous sandstone went through a different diagenetic sequence, involving extensive, mainly moldic, dissolution, followed by precipitation of prismatic spar and syntaxial overgrowths around echinoderm grains. The latter cements were probably precipitated in the saturated freshwater vadose zone, as suggested by their pendant

development. Echinoderm overgrowths, in particular, are generally considered to be characteristic of the active freshwater phreatic zone (Longman, 1980; Coudray and Montaggioni, 1986), although the same authors acknowledge that overgrowths can also form in vadose environment with pore fluids saturated with respect to CaCO3. Echinoderm overgrowths in samples from Bozas Rema do not exhibit poikilotropic development. This distinguishes them from well developed poikilotropic overgrowths, interpreted as resulted from rapid and extensive cementation within the freshwater phreatic zone (see above).

6.3.2 Matrix-rich calcareous sandstone-conglomerate (lithic wacke and related facies) (Figs. 6.1.3, 6.13.1)

6.3.2.1 Occurrence and stratigraphic distribution: This terrigenous microfacies participated in the topsets of early Pleistocene deposits (Unit 2.2) in Messenia (e.g. Eleophyton area; Chapter 3) and Eastern Lakonia (Subunit 3.2; e.g. Mourtitsa Rema; Chapter 5). Terrigenous facies within Unit 2.2/Subunit 3.2 reflect enhanced fluvial input (Chapters 3, 5). This microfacies is widespread in the Eastern Lakonia Peninsula, within terraces of any Pleistocene stage, locally alternating with beds of matrix-poor sandstone (e.g. *Kok 17*; Mourtitsa Rema). "Tyrrhenian" terraces in the Eastern Lakonia Peninsula almost invariably comprise matrix-rich conglomerate within their prograding topsets (e.g. *AyMar 35*; Limnakia) (see Chapter 5; Theodoropoulos, 1973; Kowalczyk et al., 1992).

6.3.2.2 Description: In general, sediments of this microfacies are poorly sorted, and grain size ranges from fine to coarse sand-pebbles (e.g. *AyMar 18*). Grain populations are locally bimodal, encompassing coarse-grained sand/granules and fine-grained sand. Most samples comprise well rounded grains, but angular grain populations are also common (e.g. *Kok 17, Elik 4*). Normal grading is present in samples from middle to late Pleistocene terraces (e.g. Laghouvardhos area; Messenia). In coarsening-up successions, a matrix-supported fabric tends to be succeeded by a grain-supported fabric up-section (e.g. Mourtitsa Rema; Lakonia). Grain-supported fabrics prevail in prograding clinoforms of inferred early Pleistocene age that drape the Molai Fault in the Eastern Lakonia Peninsula (e.g. *Kok 32*; see Chapter 5).

6.3.2.2.1 Terrigenous grains: These constitute ca. 47-49% of the sediment. In samples from Messenia Peninsula, most terrigenous grains were derived form radiolarian chert (18-24%), followed by quartz (commonly spherical grains) and bedrock limestone, in almost equal proportions (ca. 9-14% and ca. 10-13%, respectively) and rare feldspars and mica (<3%).

Abundance of chert grains appears to increase with increasing grain size. Grains are generally well rounded in coarser facies; in finer facies chert and quartz grains are commonly angular. In samples from Eastern Lakonia, terrigenous grains reflect bedrock lithologies in the source area (see Figs. 5.3, 5.4). Quartz, feldspars (including microcline), volcaniclastics, metamorphics, correlated with "Phyllite Series" source rocks, and various types of bedrock limestone occur in sediments from the north and the west of the peninsula (e.g. *Kok 17*; Mourtitsa Rema), whereas sediments from the south and the east coasts are rich in various types of bedrock limestone, correlated with the Tripolis zone carbonate platform (e.g. oolithic grainstone, algal bindstone, dolosparite), marble and quartz (e.g. *AyMar 18*). Radiolarian chert grains are common locally in samples from the NW part of Eastern Lakonia (e.g. *Kok17*; Mourtitsa Rema).

6.3.2.2.2 Carbonate grains: These range from 5-20% of the sediment. Benthic foraminifera commonly dominate the fauna, represented mainly by epiphytic taxa within coarse-grained microfacies and longispiral mud-dwellers, *Textulariidae* and non-identified small forms within fine-grained microfacies. Planktic foraminifera are rare in coarse-grained facies, but locally common in fine-grained facies, where they outnumber the benthic taxa (planktic:benthic ratio≈3:1; e.g. *Kok 35*). Other allochems include echinoids, mollusc fragments (commonly abraded and reduced to average grain size), red algae, cyclostomata and other bryozoa, scaphopods, serpulids (bioeroded tubes), and, less commonly, scleractinean corals and ostracods. Charophytes are rarely present (e.g. Laghouvardhos area; Messenia). Aggregates are also present, mainly in fine-grained facies (<3-7%). Aggregates locally consist of agglomerated pellets (e.g. *Kok 32*) and are arranged in clusters of elliptical outline, possibly as a result of bioturbation. Peloids are locally abundant, especially in samples from Eastern Lakonia (e.g. *Kok 18*, *Kok 32*), probably produced from micritisation of bioclasts. Many grains of peloid-rich microfacies are coated with micritic envelopes. Constructive micritic envelopes also coat non-carbonate lithic grains in the latter microfacies. By contrast, in samples from Messenia, coated grains and peloids are almost absent from fine-grained facies, and rare in coarse-grained facies (<2%).

6.3.2.2.3 Matrix and internal sediment: Matrix ranges from ca. 30% in fine-grained facies, to ca. 12% in coarse-grained facies. This consists of brown mud with mica flakes (e.g. *Elf 5*, Messenia; *Kok 17*, Eastern Lakonia), or micrite (numerous sites in both peninsulae). Pelletal matrix (probably fecal pellets) is also present, mainly in matrix-poor facies (e.g. *Kok 18*, Lakonia). In coarsening-upward successions (e.g. Mourtitsa Rema, Lakonia Peninsula), the

abundance of matrix tend to decrease upwards, in keeping with the inferred shallowing-upward trend (see Chapter 5).

Geopetal pore fill, distinct from matrix, was deposited within shelter porosity, prior to its occlusion by cement (Fig. 6.1.3).

6.3.2.2.4 Bioturbation: Burrows in inferred Eutyrrhenian sediment from Limnakia (e.g. *AyMar 35*; Eastern Lakonia) were infilled with fine-grained arenaceous sandstone, with a cement-supported fabric (equant spar cement). Areas of matrix-supported siltstone, within surrounding sandstone, are characterised by circular arrangement of quartz grains or pelletal aggregates (see above). These are also attributed to burrowing (e.g. *Elik 4*). Root-bioturbation is evidenced by development of aureolar fabric, circular to elliptical vuggy pores, locally occluded by microspar and, also, aureolar micorspar accumulations (*Rhizocretion*; e.g. *Kok 17*).

6.3.2.2.5 Cement: Crystalline cement is rare in fine-grained, but common in coarse-grained facies (≤ca. 24%).

1) Early cements include accicular crystals (Fig. 6.1.5) and isopachous rims of blocky spar, that reduce intraskeletal porosity (e.g. foraminiferal tests), mainly in early Pleistocene coarse-grained facies (e.g. *Elf 5*, *AyMar 18*). Accicular cement fabric was preserved despite later recrystallisation to equant spar mosaic.

2) Circumgranular cements are rare; a noteworthy example comprises broad, equant crystals of a low length/width ratio, precipitated around carbonate grains (e.g. *AyMar 18*) (Fig. 6.1.2).

3) Early cements of the above types were followed by clear poikilotropic spar, that locally occluded intergranular porosity. Poikilotropic crystals commonly enclose euhedral calcite crystals (e.g. *Elf 5*).

4) Early and middle-late Pleistocene facies from both peninsulae were cemented by equant-drusy spar, deposited in intergranular spaces, moulds of molluscs and corals and shelter porosity (Fig. 6.1.3). Equant cement of pendant and meniscus fabric, with fine impurities within its crystals, is also present locally, occluding intergranular and moldic porosity (e.g. *Kok 18; Elf 5*). Abundance of equant spar cement can vary greatly within the same section, with areas of completely occluded primary porosity alternating with areas of little cementation. In some samples (e.g. *Elf 5*), pendant and meniscus cements were buried by later matrix. All cement types now consist of low-Mg calcite.

Locally, intraskeletal pores in foraminiferal tests were infilled by glauconite. This is particularly common in fine-grained facies, relatively rich in planktic foraminifera (e.g. *Kok 35*), but it also occurs in coarser-grained, more proximal facies (e.g. *Kok 48*).

6.3.2.2.6 Porosity: The porosity of this facies is generally low (7-20%), but locally it reaches higher values, especially in samples from the vicinity of the active soil zone.

1) In sediments of early Pleistocene age, primary porosity (ca. 2.5%) is preserved in coarse-grained facies, in the form of intergranular and intraskeletal voids. Secondary porosity is higher (4-10%), comprising bivalve-moulds and, less commonly, irregular vuggy voids.

2) Middle-late Pleistocene sediments do not preserve much of their primary porosity. Secondary dissolution was commonly moldic. In many late Pleistocene samples (e.g. *AyMar 35*; Eastern Lakonia), bivalve-moldic porosity is high, whereas fabric selective dissolution of red algae is incipient, with small (<0.1 mm), circular, apparently unconnected pores. Primary and secondary pores, in sediments of any age, commonly host ferric oxides and, locally, clay minerals.

6.3.2.3 Deposition and diagenetic history: As discussed above (Chapters 3, 5), sediments of this facies occur in coarsening-up, regressive shoreline sequences that terminate in early Pleistocene (in the Messenia Peninsula), or younger (in the Eastern Lakonia Peninsula) terraces. Finer-grained calcareous sandstone was deposited within a lower shoreface-offshore environment, whereas coarser-grained sandstone was deposited within an upper shoreface-foreshore environment. A high terrigenous content in this facies is interpreted as reflecting proximity of fluvial-deltaic systems (see Chapters 3, 5; Kourampas and Robertson, 2000). The benthic foraminifera fauna reflect deposition in shallow, circumlittoral zone (Blanc-Vernet, 1969; Murray, 1973). The abundance of epiphytic forms, constructive micritic envelopes and intense micritisation of bioclasts suggest that peloid-rich facies were deposited in the proximity of *Thalassia*-vegetated areas (Tucker and Wright, 1990; Perry, 1998). The relative abundance of planktic foraminifera in fine-grained facies reflects an open-marine character of the latter. The presence of intralittoral foraminiferal taxa within inferred lower shoreface-offshore facies probably resulted from reworking of the shoreline during storms (see Chapters 3, 5; Kourampas and Robertson, 2000).

Diagenesis of the sediment started at the sea bottom. Most sediments of this microfacies reflect diagenesis in stagnant marine phreatic conditions (Longman, 1980, Tucker and Wright, 1990), with precipitation of glauconite, probably within slightly reducing conditions, beneath the sediment-water interface (Berner, 1991), or accicular cement within

intraskeletal pores, probably in relatively active conditions, near the sediment-water interface (Longman, 1980; Tucker and Wright, 1990). Accicular cements are now preserved low-Mg calcite that still retains the original accicular fabric.

Diagenesis of coarser-grained microfacies involved cementation within the saturated freshwater phreatic zone. This comprised circumgranular blocky or equant spar, syntaxially overgrown poikilotropic spar and homoaxial transformation of accicular cements and aragonite shells to low-Mg calcite (Land, 1970; Longman, 1980; Coudray and Montaggioni, 1986, Tucker and Wright, 1990).

Moldic and vuggy dissolution, associated with ferric oxide penetration, resulted from transition of the sediment to the freshwater vadose zone and then to the pedogenic zone. In some middle-late Pleistocene sediments, matrix infiltrated the remaining porosity after cementation in the freshwater vadose zone. This type of internal sediment, with meniscus and aureolar fabric, is similar to the "centrifugal micrite", described by Aissaui and Purser (1983). The deposition of the latter was controlled by percolation of vadose water and surface tension at grain contacts.

6.4 ALGAL-CORAL BOUNDSTONE FACIES

This facies includes bioconstructed limestones ("boundstones" *sensu* Dunham, 1962), with encrusting red algae (*Melobesioidea*), scleractinian corals (*Cladocora caespitosa*) and blue-green algal/bacterial laminae as the main constituents. Pleistocene boundstones in the Messenia and Eastern Lakonia Peninsulae fall into one of the following three categories (Table 6.1):

6.4.1 Red algal (±scleractinean coral) framestone.

6.4.2 Scleractinean coral-red algal bafflestone.

6.4.3 Blue-green algal bindstone.

6.4.1 Red Algal framestone and associated cavity-filling sediment (Figs. 6.1.7, 6.1.11, 6.17.1, 6.17.2, 6.18.1)

6.4.1.1 Occurrence and stratigraphic distribution: Algal framestone facies are widespread in the Northern Messenia Block; they also occur, less commonly, in the Southern Messenia Block and the Eastern Lakonia Peninsula (see Chapters 3, 5). Deposits of this facies constitute algal or coral-algal reefs, of dimensions ranging from <1m to 10's of metres across, commonly concentrated in the middle and upper parts of transgressive-

regressive sequences. These deposits probably correspond to periods of decreased fluvial runoff, inferred to reflect conditions of maximum flooding (Chapters 3, 5; Kourampas and Robertson, 2000; Poole and Robertson, 2000). Small (<7m across) patch-reefs of algal boundstone are present within early and early-middle Pleistocene successions in both peninsulae. The inferred "Sicilian" terrace in the Northern Messenia Block is largely composed of this facies group; small individual or amalgamated algal patch reefs also occur within the "Eutyrrhenian" terrace in NW Messenia (Chapter 3; Kourampas and Robertson, 2000) and Eastern Lakonia (Chapter 5). No certain post-Eutyrrhenian sediments of this facies were identified so far.

6.4.1.2 Description: This facies comprises hard, massive, grey limestone ('biolithite'), commonly karstified. Three principal microfacies are distinguished within the algal boundstone facies:

a) Algal framestone constitutes the bioconstructed framework,

b) Pelletal-foraminiferal-mollusc wackestone, to packstone, constitute the fill of reef-growth cavities,

c) Terrigenous siltstone, to pebbly siltstone, is bound by red algal crusts in one locality (Filiatrino Rema, Messenia; Fig. M.1).

The relative abundance of bioconstructed framework and cavity fill and/or bound detrital sediment vary. Most samples are relatively closely bound; the facies comprising algae-bound siltstone are, however, loosely bound (e.g. *MSN 8*).

6.4.1.2.1 Terrigenous grains: Their presence in the sediment is commonly low; from <5% in framestone microfacies, as grains entrapped within the algal framework, to <15% in wackestone-packstone microfacies. However, boundstones with siltstone as bound sediment are rich in terrigenous grains (≤26%). In sediments from the Messenia Peninsula, terrigenous grains of fine sand to silt size were derived from chert (equant quartz, radiolarian chert and rare reworked radiolaria) and quartz. In samples from the Eastern Lakonia Peninsula, terrigenous grains were derived from various sources (volcaniclastics, metamorphic, limestones).

6.4.1.2.2 Algal framestone: This microfacies constitutes a closely, or loosely, bound bioconstructed framework, mainly formed by various encrusting coralline algae (Fig. 6.1.7). Other encrusting organisms (foraminifera, bryozoa, serpulids, vermetid grastropods) are also present, but in lower abundance (Figs 6.1.7, 6.1.11). Encrusting successions are very complex. Characteristic associations of the red algae, *Tenarea* sp. and *Mesophyllum* sp. with

serpulid worms and the encrusting foraminiferum, *Carpenteria utricularis* are prevalent on the undersides of bioconstructed knobs, or as the lining of frame-growth cavities, in direct contact with geopetal sediments. Algal crusts were penetrated by borings, later infilled by geopetal sediment. *Mesophyllum* sp. crusts were micritised preferentially (Martindale, 1974). Rhodoliths, mainly composed of *Mesophyllum* sp. and *Tenarea* sp. with encrusting foraminifera and bryozoa, formed around the nuclei of bioclasts (including, *Vermetid* gastropods), or non-carbonate, terrigenous clasts (e.g. chert pebbles; *MSN 8*).

Non-encrusting organisms, incorporated within the framework, include benthic foraminifera, ostracods, cyclostomata bryozoa, echinoids, bivalves, gastropods and numerous fragments of red algal crusts. Epiphytic forms are prevalent amongst the foraminifera; diverse genera of *Milioliidae* constitute the commonest group. Agglutinated foraminifera are also common. Various types of borings are present in this bioconstructed framework, ranging from dense networks of μ-sized tubes, to mm-sized cavities, infilled with cryptocrystalline micrite with a high concentration of terrigenous grains (Fig. 6.1.7). The latter borings probably resulted from boring by sponges.

6.4.1.2.3 Wackestone-Packstone: This microfacies, up to ca. 20% of the sediment, is commonly present as geopetal fill of primary, frame-growth cavities, or early (submarine) borings in the algal framestone (Fig. 6.1.7). As mentioned above, the relative density of the algal framework varies, and, locally, the sediment mainly comprises wackestone-packstone microfacies. Carbonate grains include fragments of encrusting and articulating red algae, benthic (and rare planktic) foraminifera, bryozoa, bivalves, gastropods, corals and peloids. Coated grains and blue-green algal lumps are common. The relative abundance of peloids, probably derived from micritisation of bioclasts, is higher near framestone composed of sciaphilic fauna (i.e. serpulids and encrusting formanifera; Martindale, 1974; Hayward et al., 1996).

6.4.1.2.4 Matrix: Three types of matrix are present: I) Homogenous brown micrite, II) Dark-brown, pelletal micrite, with pellets of probable faecal origin, and III) Dark-brown isotropic carbonate mud, with a high presence of terrigenous grains (quartz, calcite crystals). The latter facies is common as fill of large borings, similar to the ones produced by the boring activity of *Clionid* sponges.

6.4.1.2.5 Cement: The abundance of crystalline cement varies, depending on the fabric and relative age of the sediment and the position of samples in relation to the active soil zone. Older sediments and algal framestone-dominated microfacies are richer in crystalline

cement, as compared to younger sediments and wackestone/packstone-dominated microfacies. The maximum abundance of crystalline cement is ca. 20%. A wide variety of cement types are present in the algal boundstone facies group:

1) Microspar is present in intraskeletal pores of red algae, foraminfera and other allochems. Larger pores (e.g. red algal conceptacles) are infilled by clear equant-drusy spar (Fig. 6.1.7).

2) Blocky spar forms isopachous circumgranular rims, or surrounds, loosely packed crusts of red algae.

3) Radiaxial spar forms circumgranular fringes.

4) Clear microspar forms interpelletal cement in pelletal packstone-wackestone microfacies.

5) Isopachous fringes of accicular crystals, probably aragonite, were deposited in intraskeletal pores of gastropods, corals and foraminifera. These cements were buried by latter isopachous microspar and/or geopetal cavity fill.

6) Fan-shaped botryoids (originally aragonite) are present in frame-growth pores of the algal framework. These cements were also buried by microspar and/or geopetal cavity fill.

7) Syntaxial overgrowths of echinoderm grains are very common.

8) Prismatic to blocky spar cement locally infills frame-growth porosity. Calcite crystals of the latter type have a radial development, with the c-axis almost perpendicular to the cavity wall. The same type of cement also lines the walls of worm(?) burrows.

9) In early Pleistocene sediments (e.g. *MSN 8*), equant microspar infilled primary intraskeletal, or frame-growth, pores. The precipitation of microspar post-dated the incomplete filling of pores by internal sediment, but predated vuggy dissolution and equant-drusy spar precipitation (see below). Irregular clusters of microspar mosaic are also present within homogenous micritic matrix.

10) Equant-drusy mosaics of clear spar filled mollusc-moldic and coral-moldic porosity. This cement locally exhibits a pendant character. Very fine-grained detrital material is concentrated at crystal terminations within this cement facies; crystal faces directly below detrital layers are rounded. This type of cement is prevalent in older representatives of this microfacies group (e.g. "Sicilian" terrace in NW Messenia), locally forming intergranular mosaics in matrix-free areas.

11) Bivalve shells were commonly recrystallised to a calcite spar mosaic, with preservation of 'ghost' skeletal fabric (Fig. 6.1.11). Vermetid gastropod shells were also recrystallised to equant-equicrystalline spar, but without preservation of skeletal fabric (Fig. 6.1.11).

All the above types of crystalline cement now consist of low-Mg calcite.

6.4.1.2.6 Porosity: Porosity of algal boundstones varies greatly, depending on the fabric, relative age of the sediment, and proximity of the outcrop to the active soil zone. Porosity values range from >17% in "Eutyrrhenian" sediment (e.g. Mati; Messenia), to <5% in well cemented "Sicilian" sediment (e.g. Filiatra-Limenari area; Messenia). In general, primary porosity is lower than secondary porosity. The following types of porosity are present:

6.4.1.2.6.1 Primary Porosity: 1) Frame-growth porosity within the algal framework is present at various scales (10's of μ - <10 cm). Macroscopic frame-growth cavities, in inferred "Sicilian" and "Eutyrrhenian" outcrops, are still open, constituting an interlinked pore network.

2) Intraskeletal porosity is present, as cavities within the encrusting framework (e.g. red algae, serpulids, bryozoa), foraminifera, and gastropods (Fig. 6.1.7). Intraskeletal pores were locally enlarged by later dissolution.

3) *Polychaete* burrows in matrix-dominated fabric locally remained unfilled.

4) Shelter porosity is present beneath bivalve shells.

Primary porosity was reduced (or, in older sediments, occluded) by geopetal sediment and cement.

6.4.1.2.6.2 Secondary Porosity: 1) Moldic porosity after various carbonate grains occurs in all samples examined. Moldic dissolution reached variable stages within the same section: algal crusts in the first stages of dissolution coexist with open or cement-infilled moulds of bivalve shells. Moldic pores were generally reduced by equant-drusy spar mosaics, locally of pendant character. Crystal-moldic dissolution of equant spar crystals also took place, showing that pervasive cementation was followed by further dissolution.

2) Vuggy porosity is the commonest type of secondary porosity within the algal framestone microfacies. Vuggy pores commonly exhibit some degree of fabric-selectivity; locally, they resulted from enlargement of primary or previous moldic porosity. Reduction of vuggy pores by cement ranges from almost complete occlusion (e.g. *MSN 8*; early Pleistocene), to only minor cementation (e.g. *Lim* samples; "Sicilian"). In early Pleistocene sediments, vuggy dissolution affected algal crusts, geopetal sediment and microspar fill of frame-growth pores alike (e.g. *MSN 8*).

Most vuggy, and many moldic pore walls were later rimmed with ferric oxide films.

6.4.1.3 Deposition and diagenetic history: Sediments the algal framestone facies group were deposited in algal-coral reefs. Densely bound, framework-dominated facies were probably deposited in a high-energy, wave-agitated environment, by analogy with recent reefs in Bermuda and the Pacific Islands (Martindale, 1974; James, 1981) and Miocene reefs in Turkey (Hayward et al., 1996). The benthic foraminiferal fauna, dominated by epiphytic forms, mainly *Milioliidae*, suggest upper circumlittoral, to intralittoral, depositional depth, in conditions of normal salinity (Blanc-Vernet, 1969; Murray, 1973; Amorosi et al., 1999). A characteristic association of encrusting organisms (*Tenarea* sp.+encrusting foraminifera+serpulids) is systematically present around the walls of cm to mm-scale cavities. This faunal association bears similarities with '*skiaphilic*' ("shadow-loving") faunas, described from Recent and Quaternary reefs in Bermuda (Martindale, 1974) and Miocene reefs in Turkey (Hayward et al. 1996). Similar with the latter cases, the presence of skiaphilic fauna is interpreted as reflecting normal reef-growth processes, that involved gradual enclosure of bioconstructed cavities, resulting in their isolation from sunlight and subjection to low-energy hydrodynamic conditions. This isolated microenvironment allowed deposition of a fine-grained cavity fill (wackestone-packstone microfacies). A large amount of the cavity-fill was derived from faecal pellets.

Loosely bound varieties of algal framestone, by contrast, are surrounded by fine-grained detrital sediment with upper bathyal benthic fauna (e.g. Filiatrino Rema, Messenia; see Marcopoulou-Diakantoni et al., 1991 and Chapter 3). These facies were deposited in a more tranquil environment, probably below the fair-weather wave base.

Field evidence suggests that algal framestones normally overlie deepening-up detrital successions and are succeeded by shallowing-up, prograding detrital successions. This facies is interpreted as reflecting conditions of maximum flooding during relative sea level rise (see Chapters 3, 5; Kourampas and Robertson, 2000; Poole and Robertson, 2000).

The diagenesis of algal framestones was complicated, depending on fabric, proximity to the soil zone and age of each particular outcrop. Nevertheless, it can be summarised as the following general succession: Early cementation within the marine phreatic zone involved precipitation of accicular aragonite cements and various types of microspar (intraskeletal, circumgranular, intergranular). that probably consisted of aragonite, or high-Mg calcite (Longman, 1978; Coudray and Montaggioni, 1986; Tucker and Wright, 1990). This was followed by extensive moldic dissolution of carbonate grains and precipitation of equant-drusy spar; both processes took place under freshwater conditions. Moldic dissolution was probably a diachronous process, as suggested by presence in the same sample of moldic pores at different stages of development. Cementation proceeded in more than one stages;

the latest stage probably took place in the freshwater vadose zone, as indicated by the pendant character of the cement and presence of detrital impurities at the base of cement crystals (Coudray and Montaggioni, 1986). Local dissolution of this cement, under freshwater vadose conditions, is indicated by rare crystal-moldic porosity. Extensive vuggy dissolution, associated with ferric oxide penetration, was probably the latest diagenetic event, associated with the transition of the sediment to the upper freshwater vadose zone (i.e. soil zone). The diagenetic sequence, thus, reflects the transition of the sediment from marine to subaerial conditions.

6.4.2 Scleractinean coral (+red algal) bafflestone (Fig. 5.33)

6.4.2.1 Occurrence and Stratigraphic distribution: This facies occurs in the Eastern Lakonia Peninsula, in the areas of Kambourani Rema, Bozas Rema, and Tasou Rema (see Chapter 5; Figs. 5.3, M.2). The two first sites are of inferred "Eutyrrhenian" age (Kowalczyk et al., 1992); the third probably corresponds to a late middle Pleistocene, or the Eutyrrhenian sea level cycle (Chapter 5). Bafflestone sediments are associated with prograding, detrital carbonate or siliciclastic shorelines, commonly occurring at, or near, the top of regressive sequences. Two different paleoenvironmental settings are inferred from outcrop evidence:

1) A 'low-energy' setting, with baffled sediment of silt-fine silty sand grain size, probably corresponded to a protected environment, possibly that of a back-barrier lagoon with normal circulation (e.g. Tasou Rema; see Fig. 6.3.a).

2) A 'high-energy' setting, with baffled sediment of coarse sand grain size, probably corresponded to exposed, wave-dominated shorelines (e.g. Bozas Rema; see Fig. 6.3.b).

6.4.2.2 Description: Low-energy sediments of this group comprise a bioconstructed framework of *in situ* coral colonies and red algae, draped by peloidal wackestone, to packstone, sediment. High-energy sediments compise a similar bioconstructed framework, draped by well sorted, grain-supported, calcareous sandstone.

6.4.2.2.1 Bioconstructed framework: *In situ* colonies of the scleractinean coral, *Cladocora caespitosa* form a branching network. The coral skeletons were encrusted by crustose red algae (*Melobesioidea*) and a variety of other encrusting organisms (foraminifera, bryozoa, serpulids). Small serpulid colonies are also present within low-energy bafflestone facies, encrusted by thick, composite crusts of red algae. The following sequences of encrustation were noted (from the core to the periphery of the bioconstructed framework):

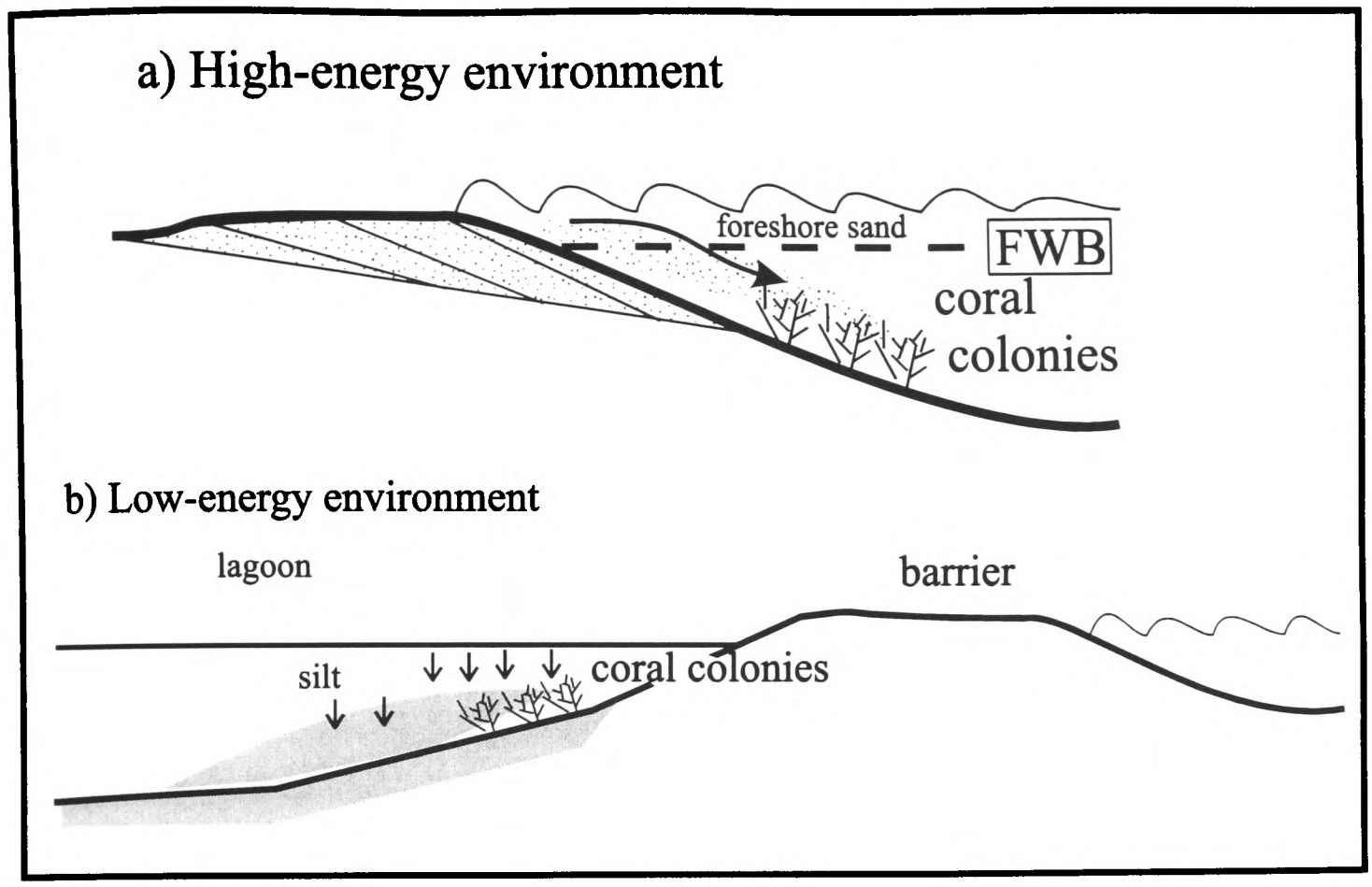

Figure 6.2: Depositional model of Pleistocene algal bafflestone in the Messenia and Eastern Lakonia Peninsulae (see text for explanation).

I) Serpulid tubes ⇒ *Tenarea* sp. (red alga), bored and coated with micritic envelope. *Planorbulina* (encrusting foraminifera) occur within the peripheral parts of the crust ⇒ *Gypsina plana* (encrusting foraminiferum) ⇒ *Lithophyllum* (?) sp. + *Mesophyllum* sp. (red algae) ⇒ *Mesophyllum* sp. (red alga), with bioeroded margins.

II) *Cladocora caespitosa* (coral), coated with micritic envelope ⇒ *Tenarea* sp. (red alga), with heavily micritised periphery. A sharp and idented micritisation front separates the unaffected from the micritised skeleton ⇒ *Archaeolithothamnium* sp. (red alga), with non-bioeroded margin.

III) *Cladocora caespitosa* ⇒ *Gypsina plana* ⇒*Tenarea* sp. ⇒ *Mesophyllum* sp.

Besides *in situ* colonies, fragmented colonies of corals and serpulids are present within lags, together with red algal rhodoliths and intraclasts. Encrusting successions in rhodoliths are complex, with intraclasts surrounded by *Tenarea* sp. crusts, whose periphery is intergrown with *Cladocora caespitosa*; both the latter organisms were encrusted by *Mesophyllum* sp.

6.4.2.2.2 Baffled sediment and cavity-fill: Detrital sediment comprises lithic-pelloidal wackestone/packstone in low-energy settings, and coarse-grained sandstone in high-energy settings.

6.4.2.2.2.1 Terrigenous grains: Terrigenous grains are abundant within the baffled sediment, comprising mainly quartz, feldspar, calcite crystals (probably from bedrock limestone) and rare heavy minerals (e.g. tourmaline). Quartz grains are of fine-medium sand size, angular to moderately rounded.

6.4.2.2.2.2 Carbonate grains: In low-energy settings, they comprise a rich benthic foraminiferal fauna (with abundance of *Elphidium* spp., *Ammonia* spp., and agglutinated taxa), a few planktic foraminifera (*Globigerinidae*), ostracods, molluscs, echinoids, red algae (commonly as rhodoliths), fragments of the baffling framework (*Cladocora caespitosa* and serpulids) and numerous pellets, probably of faecal origin. Molluscs are abundant, mainly represented by thin-shelled bivalves, heavily bored by *Clionid* sponges; gastropod shells are relatively rare. Mollusc shells and echinoid grains are coated with thick micritic envelopes. In high-energy settings, carbonate grains comprise benthic foraminifera of the *Ammonia+Elphidium* faunal association (*sensu* Amorosi et al., 1998), abraded fragments of thick-shelled bivalves and echinoids.

6.4.2.2.2.3 Matrix: In low-energy settings, the matrix consists of micrite with a high terrigenous content; locally it has a fine-grained pelletal packstone texture. The same material also infills intraskeletal pores as internal sediment. Aureolar structures are locally present within the matrix, especially in the vicinity of vuggy pores (root-tubes?). Sediments from high-energy settings are matrix-poor.

6.4.2.2.3 Cement: In low-energy settings, the presence of crystalline cement is restricted to intraskeletal pores (corals, serpulids), or incipient secondary pores (in serpulids). The cement comprises equant spar mosaics and prismatic spar, commonly of pendant fabric. Coral skeletons are invariably recrystallised to equant spar, without preservation of primary skeletal fabric. Finely-crystalline pendant spar is also present in moulds of bivalves and gastropods. In high-energy settings, cement comprises mainly microcrystalline spar of pendant or meniscus character, present in intergranular and intraskeletal areas and also in coral-moldic and bivalve-moldic pores.

6.4.2.2.4 Porosity: In low-energy settings, primary intraskeletal porosity was largely occluded by internal sediment and cement. Secondary porosity includes moulds of corals, bivalves and gastropods (reduced by prismatic and finely-crystalline spar cement) and vuggy dissolution that affected the baffling framework, rhodoliths and matrix. Fabric selective dissolution of serpulids is less advanced, with small, unconnected pores thet "trace" the

growth-laminae of the serpulid skeleton (Fig. photo). The latter pores were not reduced by cementation. In high-energy settings, primary porosity is generally preserved, only partly occluded by meniscus and pendant cement. Secondary porosity is similar to that of low-energy settings.

6.4.2.3 Deposition and diagenetic history: As mentioned above, two different depositional settings of coral-algal bafflestone and related sediments are distinguished (Fig. 6.3). This distinction is mainly based on the nature of the baffled sediment, that reflects the energy of the depositional environment. Coral-algal bafflestone, with wackestone/packstone, was deposited under low-energy conditions. Microfacies of this low-energy facies spectrum correspond to the Standard Microfacies 7 ("*boundstone*"), 8 ("*whole fossils wackestone*"), 9 ("*bioclastic wackestone*"), 10 ("*coated packstone / wackestone*"), and 22 ("*rhodolithic micrite*"), *sensu* Wilson (1975). Their presence suggests deposition within a back-barrier lagoon, probably during relative sea level rise (Fig. 6.3.1). The conditions that favoured original growth of bafflestone microfacies were probably changing, as evidenced by the gradual prevalence of more schiaphillic encrusters in the encrusting successions (e.g. *Mesophyllum* sp., *Arcaheolithothamnium* sp.; Martindale, 1974; Wray, 1977). Silting-up of the coral colonies probably resulted from reef-drawing due to relative sea level rise (Fig. 6.3.1). Coral-algal bafflestone, with coarse sandstone, by contrast, was deposited in an exposed clastic shoreline, probably draped by a prograding foreshore during regression (Fig. 6.3.2).

The absence of early marine cements and intense micritisation indicates that diagenesis of the low-energy bafflestones begun within the stagnant marine phreatic zone, that commonly occurs in lagoonal environments (Longman, 1980). Recrystallisation (heteroaxial transformation) of coral skeletons and syntaxial overgrowths of echinoderm grains possibly took place within the saturated freshwater phreatic zone (Land, 1970; Longman, 1980; Coudray and Montaggioni, 1986). Transition of the sediment to the freshwater vadose zone is evidenced by extensive moldic dissolution of coral and mollusc skeletons, whereas dissolution of serpulid skeletons was far less advanced. This was followed by minor cementation by pendant finely-crystalline and prismatic spar. Vuggy dissolution was commonly associated with development of aureolar structures, probably as a result of root penetration, within the soil zone (Esteban and Klappa, 1983; Goudie, 1983).

6.4.3 Blue-green algal bindstone (Fig. 6.19.1)

6.4.3.1 Occurrence and stratigraphic distribution: This facies occurs exclusively in the southern part of the Eastern Lakonia Peninsula (e.g. Ayia Marina; Figs. 5.5, 6.19.1, M.2), on a marine abrasion platfrom of inferred Holocene age (see Chapter 5).

6.4.3.2 Description: This facies forms high (up to 1.5 m), ca. 60 cm wide, hollow carapaces. The internal walls of the latter are rimed with dense *Rhizocretion* (Figs. 5.40). The structure of the carapaces is laminar, with <1-3cm thick alternating laminae of darker, clast-rich siltstone and pale-white algal bindstone (Chapter 5). The clast-rich areas comprise well sorted grains of quartz and feldspar (fine sand size). Carbonate grains include fragments of red algae and small benthic foraminifera.

6.4.3.3: Cements and porosity: This sediment is mainly cemented with microcrystalline and micritic cements, locally of microstalactitic fabric. Crystalline cements are rare, comprisisng finely cryatlline microstalactitc spar.

Primary porosity includes interlaminar pores (in loosely bound areas) and intergranular pores between detrital grains. Secondary porosity is fabric-selective, following the microlamination of the sediment.

6.4.3.4: Deposition and diagenetic history: Algal bindstone was deposited by algal-microbial mats around tree trunks, as shown by its preserved morphology (see Chapter 5). The environment was probably a mangrove, flooded during a Holocene se level rise. Detrital grains were wind-blown seidment trapped and incorporated within the algal-microbial laminae.

The diagenesis of this microfacies took place in freshwater vadose conditions.

6.5 DIAGENESIS OF CARBONATE AND MIXED CARBONATE-TERRIGENOUS SEDIMENTS IN THE SOUTHERN PELOPONNESE

Late Pliocene-Holocene shallow-marine carbonate and mixed carbonate-terrigenous sediments in the Messenia and Eastern Lakonia Peninsulae went through a limited number of diagenetic sequences (*sensu* Coudray and Montaggioni, 1986), representing a specific succession of postdepositional conditions within the near-surface diagenetic realm (the "*eogenetic*" and "*telogenetic*" zones of Choquette and Pray, 1970). Evidence for burial diagenesis (i.e. in the "*mesogenetic*" zone of Choquette and Pray, 1970) was not found in any of the examined samples. Given the relativelly recent age of the sediments and the long-term (Plio-Quaternary) uplift of both Peninsulae, burial diagenesis probably did not take place in any of the shallow-marine sequences currently exposed as marine terraces.

6.5.1 Diagenetic Zones: The diagnostic characteristics of each diagenetic zone identified in sediments of the Messenia and Eastern Lakonia Peninsulae are summarised below. The identification of diagenetic zones was based on Bathurst (1964), Alexandersson (1969, 1970), Taylor and Illing (1969), Land (1970), Folk (1974), Longman (1980), Coudray and Monntaggioni (1986), Tucker (1990), and Tucker and Wright (1990) (Figs. 6.3, 6.4):

6.5.1.1 Active marine phreatic zone (Fig. 6.4.1): Development of isopachous cement rims, in circumgranular and intragranular position took place within this zone. Cements comprise micrite, equant microspar, or acicular crystals. Fan-shaped botryoids of accicular crystals are also present within this zone. All these cements now consist of low-Mg calcite (as shown by XRD analysis; see Appendix C). The former two types of cement possibly can have resulted from recrystallisation of either original high-Mg calcite or aragonite (Given and Wilkinson, 1985; Tucker and Wright, 1990). Their diffrent morphology probably reflects different relation between rate of crystal growth and rate of nucleation. Accicular cements resulted from rapid growth as compared with nucleation, whereas micorcrystalline-micritic cements resulted form rapid nucleation as compared with the rate of growth (Given and Wilkinson, 1985). Botryoids of accicular crystals probably resulted from original aragonite cement (Logman, 1980; Coudray and Montaggioni, 1986; Tucker and Wright, 1990). Early cementation of red algal framework, presumably by high-Mg calcite, and its subsequent boring, also took place in the high-energy conditions of this zone (Alexandersson, 1970).

6.5.1.2 Stagnant marine phreatic zone (Fig. 6.4.2): Cementation was restricted in intraskeletal pores (e.g. foraminifera, red algal conceptacles). Cements are mainly represented by finelly-crystalline calcite (of aragonite or high-Mg calcite precursor) and, to

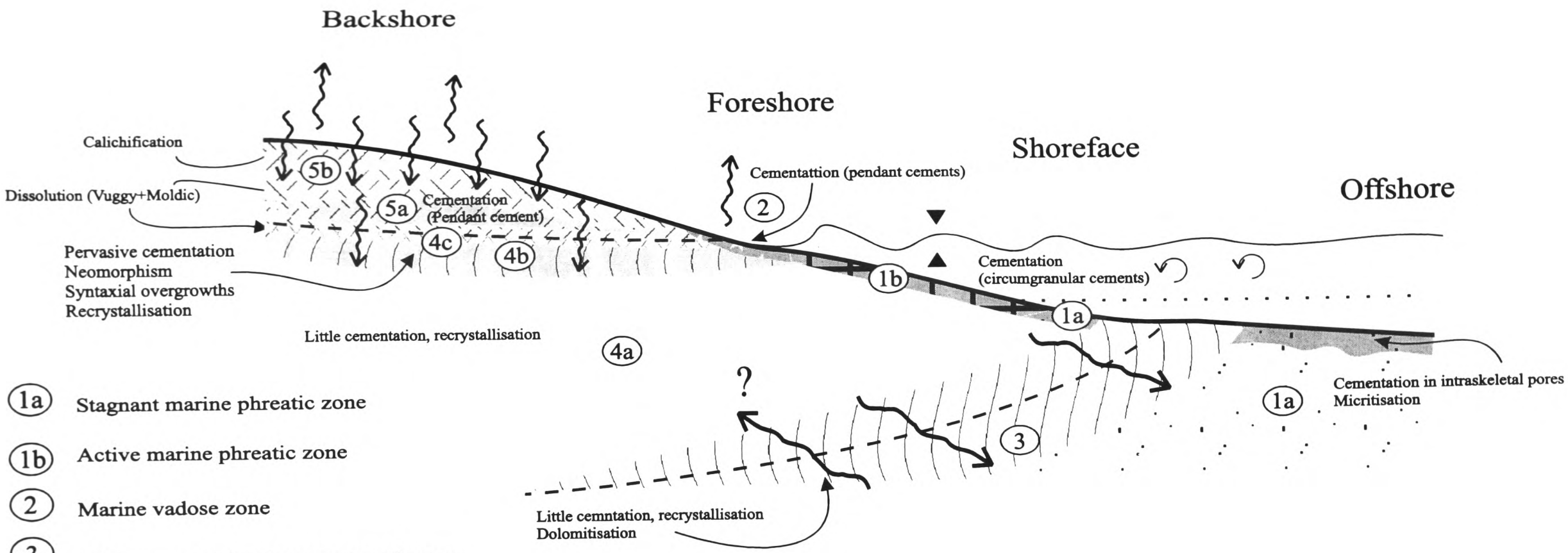

Figure 6.3: Near-surface diagenetic environments within the shoreline to backshore zores of deposition (see text for explanation). Sources: Longman, 1980; Coudray and Montaggioni, 1986; Tucker and Wright, 1990.

a lesser extent, botryoids of accicular crystals (of aragonite precursor). Both types of cement now comprise low-Mg calcite, as shown by XRD analysis (Appendix C). Extensive micritisation of carbonate grains and abundance of peloids (micritised bioclasts) are also characteristic of this environment. Glauconite precipitated within intraskeletal pores (mainly foraminifera), borings, and rarely intergranular pores.

6.5.1.3 Active marine vadose zone (Fig. 6.4.3): This environment is characterised by deposition of cements of 'vadose' (i.e. pendant and meniscus) fabric (see below) and a metastable mineralogy (i.e. high-Mg calcite and aragonite). Cements commonly comprise very finely-crystalline or micritic rims, with pendant development, on the undersides of grains. These cements probably consisted of high-Mg calcite, as other beachrock cements in the Mediterranean (Alexandersson, 1972). The original high-Mg calcite minaralogy was preserved only in Holocene beachrocks; similar foreshore facies of Pleistocene age now comprise low-Mg calcite (XRD evidence). Fan-shaped bortyoids of accicular crystals (aragonite precursor) are rare.

6.5.1.4 Saturated freshwater phreatic zone (Fig. 6.4.4): Pervasive cementation of the sediment took place within this zone (Land, 1970). Cements included roughly isopachous rims of equant, blocky, or prismatic spar and equant-equicrystalline or equant-drusy mosaics. Syntaxial overgrowths around echinoderms were well developed, locally attaining poikilotropic fabric. Poikiltotropic calcite crystals are also present in some samples, apparently not associated with syntaxial overgrowths around echinoderms. All these cement types comprise clear, inclusion-free, low-Mg calcite (XRD evidence). Pervasive neomorphism of aragonitic and high-Mg calcite to low-Mg calcite took place within this zone (Land, 1970; Longman, 1980). This latter included both homoaxial transformation of metastable carbonate minerals to low-Mg calcite, with preservation of primary skeletal and cement fabrics, and heteroaxial transformation, with complete obliteration of primary fabrics. Aggrading neomorphism of high-Mg caclite micrite (commonly matrix) is also took place under the conditions of the saturated freshwater phreatic zone (Lomgman, 1980; Coudray and Montaggioni, 1986).

6.5.1.5 Undersaturated freshwater phreatic, or vadose, zone: Pervasive, fabric-selective dissolution of metastable carbonate grains (aragonite and high-Mg clacite bioclasts) occured within this zone. The degree of dissolution differed according to the origin of carbonate grains. The following succession was observed, in order of decreasing solubillity:

Gastropods + scleractinian corals < bivalves < seprulids < red algae.

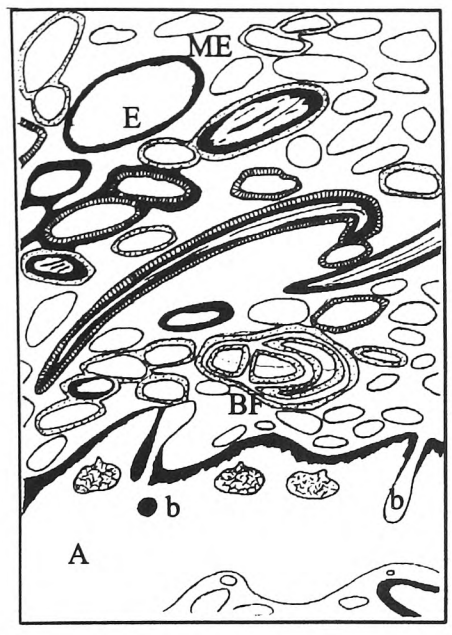

1: Active Marine Phreatic

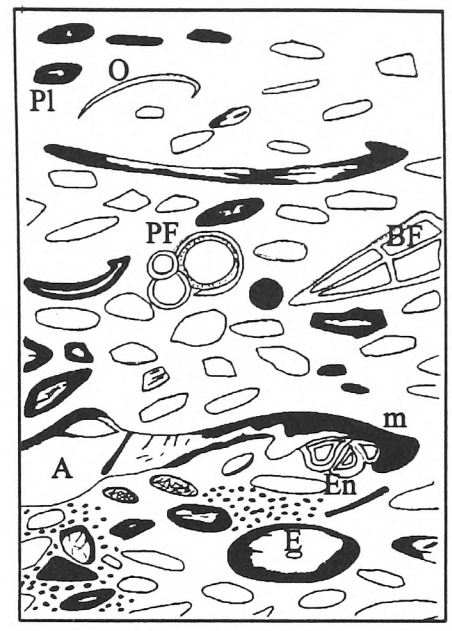

2: Stagnant Marine Phreatic

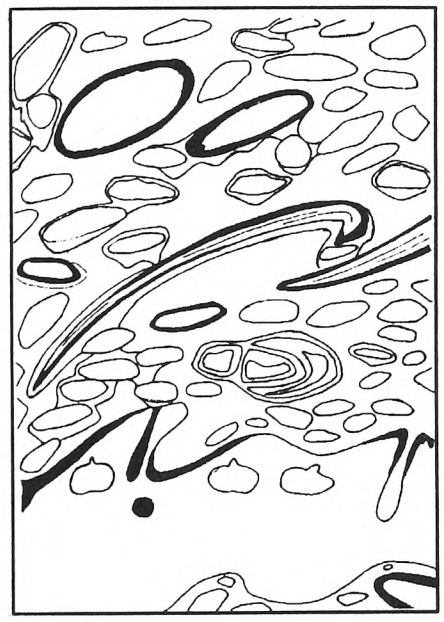

3: Marine Vadose

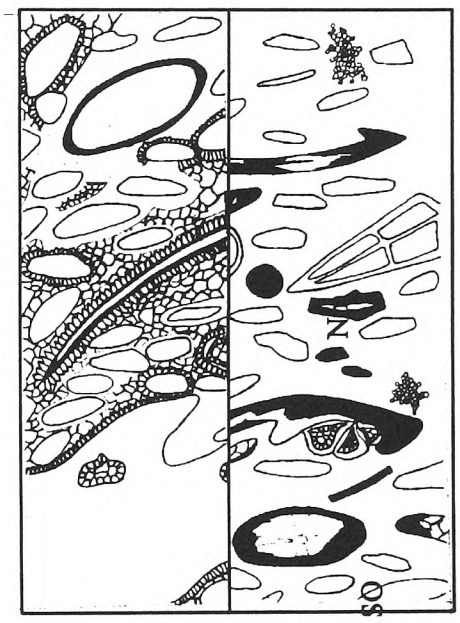

4: Saturated Freshwater Phreatic

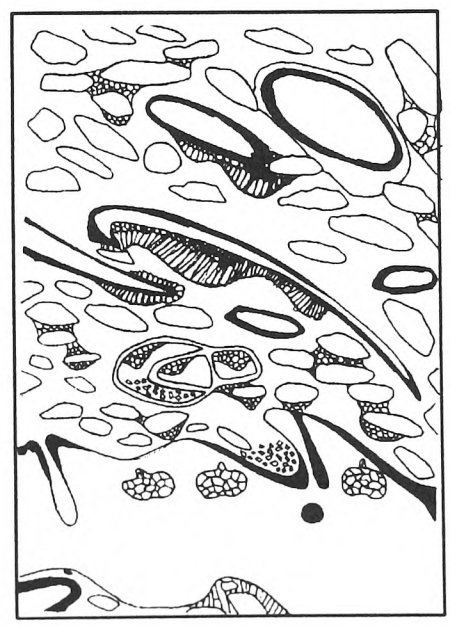

5: Freshwater Vadose

Figure 6.4: Characteristics of near-surface diagenetic zones; the emphasis is placed on environments of cementation and zones of undersaturation and dissolution are excluded (see text).

Vuggy porosity is also present at various scales. Distinction between undersaturated freshwater phreatic and vadose conditions is impossible on the grounds of dissolution fabrics alone (Choquette and Pray, 1970; Longman, 1980; Coudray and Montaggioni, 1986); vadose or phreatic conditions were, thus, inferred indirectly, from the fabric of the earliest pore-filling cement.

6.5.1.6 Saturated freshwater vadose zone (Fig. 6.4.5): Cementation by pendant and meniscus cements (on the undersides and contacts of grains, respectively) is characteristic of this zone. These cements include finely-crystalline equant spar, but this is not the typical vadose cement as in other areas (Land, 1970; Longman, 1980, Coudray and Montaggioni, 1986; Poole, 1991). In the southern Peloponnese, by contrast, pendant cements commonly comprise prismatic spar rims. Another unsusual vadose cement is syntaxial overgrowth around echinoderms, with pendant growth fabric. This fabric, together with the narrow size of the overgrown zone, distinguish these from overgrowths in the freshwater phreatic zone. Cements in this zone comprise low-Mg calcite crystals (XRD evidence), that commonly contain inclusions. Vadose silt (Coudray and Montaggioni, 1986) and normally graded geopetal pore-fill (Aissaoui and Purser, 1983) occur, but rarely.

6.5.1.7 Undersaturated freswater vadose zone: Vuggy and moldic dissolution were locally extensive within this zone. Red oxides, and, less commonly, authigenic clay minerals reduced pore spaces; the latter commonly grew in pendant fabric. Aureolar structures, *Rhizocretion* and *Microcodium* are common, as a result of biological activity within the soil zone (Esteban and Klappa, 1983; Wright et al., 1988). This is the zone of calichification, evidenced by micritisation and incipient corrosion of carbonate grains, and generation of caliche fabrics, as described below.

Among the near-surface diagenetic zones referred in the literature, only one is not identified in the Plio-Quaternary sediments from the Messenia and the Eastern Lakonia Peninsulae. This is the mixing marine-freshwater phreatic zone. The mixing marine-freshwater phreatic zone, with conditions of good pore-water circulation, is identified by presence of dolomite (Bathurst, 1976; Logman, 1980; Coudray and Montaggioni, 1986). Since all other characteristics of this zone are similar to those of the freshwater phreatic zone (Longman, 1980), this zone would not be expected to leave an easily recognisable diagenetic signature. Futhermore, conditions in this zone are commonly stagnant, and its position is impermanent, largely controlled by climatic factors, e.g. seasonal distribution of rainfall (Longman, 1980; Coudray and Montaggioni, 1986).

6.5.2 Diagenetic sequences: Using the terminology proposed by Longman (1980), diagenetic sequences identified during this study are as follows (Figs. 6.5, 6.6):

1) Stagnant marine phreatic zone ⇒ saturated freshwater phreatic zone ⇒ undersaturated freshwater phreatic and/or vadose zone ⇒ saturated freswater vadose zone ⇒ undersaturated freshwater vadose zone (soil zone).

2) Active marine phreatic zone ⇒ undersaturated freshwater vadose zone ⇒ saturated freshwater vadose zone ⇒ undersaturated freshwater vadose zone.

3) Undersaturated freshwater vadose zone ⇒ saturated freshwater vadose zone ⇒ undersaturated freshwater vadose zone.

4) Active marine phreatic zone ⇒ marine vadose zone ⇒ undersaturated freshwater vadose zone ⇒ saturated freshwater vadose zone ⇒ undersaturated freshwater vadose zone.

5) Active marine phreatic zone ⇒ stagnant marine phreatic zone ⇒ (saturated freshwater phreatic zone) ⇒ undersaturated freshwater phreatic (or vadose) zone ⇒ saturated freshwater vadose zone ⇒ undersaturated freshwater vadose zone.

All the above diagenetic sequences suggest transition to increasingly near-surface environments through time and, thus, reflect the history of relative sea level fall inferred through other lines of evidence (see Chapters 3, 5). The diagenetic record of the sediments indicates a history of emergence, where sediments deposited within a marine environment were finally subjected to subaerial conditions. Widespread calichification after the emergence of the sediments indicates that climatic conditions were semi-arid to arid for at least part of the Pleistocene (see below).

Figure 6.5 (following page): Diagenetic sequences identified in Quaternary shoreline sediments of the Messenia and Eastern Lakonia Peninsulae. Sediments originally deposited below sea level, within the marine phreatic zone (active or stagnant) migrated into freshwater phreatic, then vadose conditions through time. The effects of water table fluctuations notwithstanding, the general occurrence of such diagenetic sequences in the Messenia and Eastern Lakonia Peninsulae resulted from relative sea level fall, associated with Quaternary land uplift.

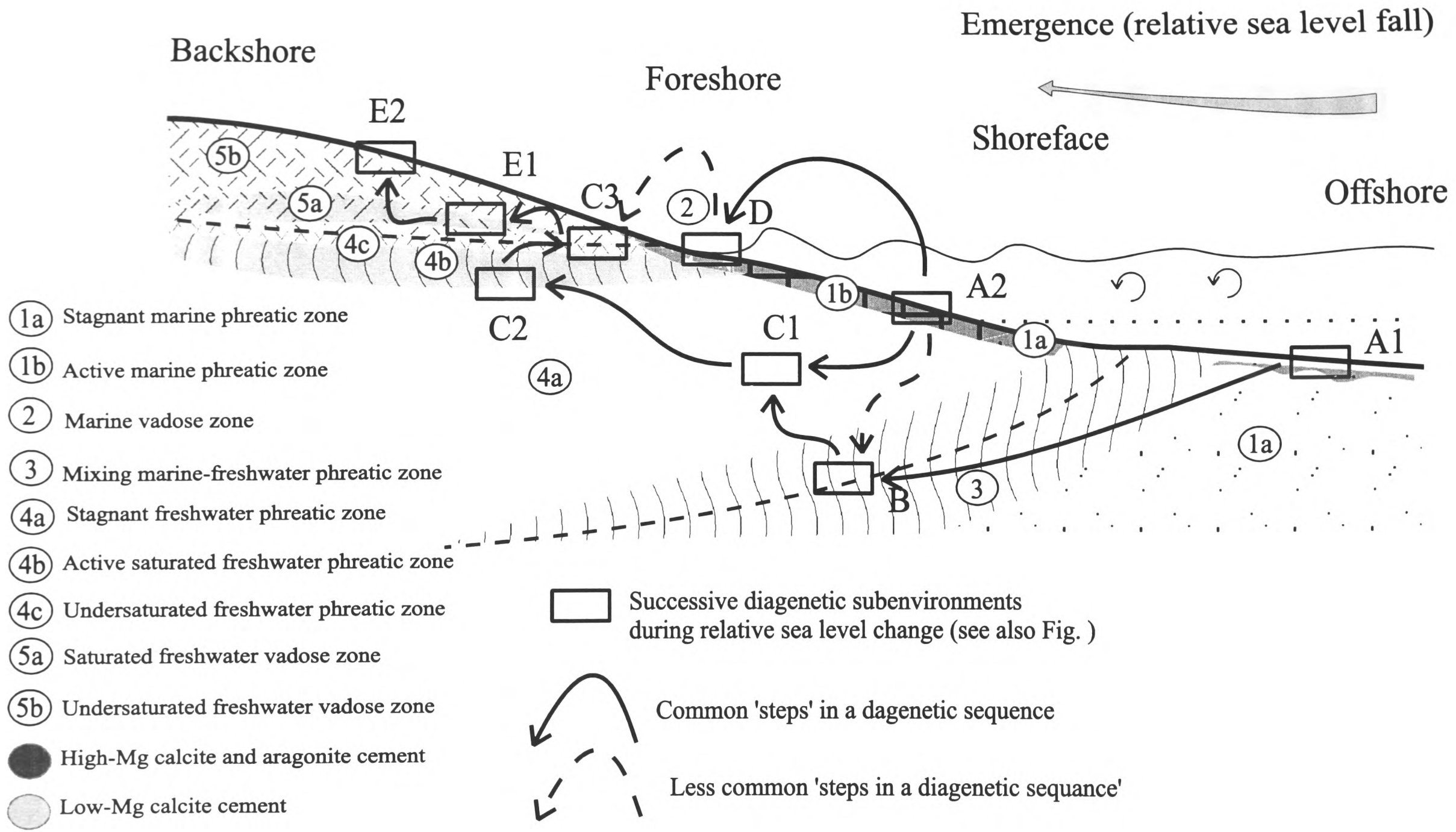
Emergence (relative sea level fall)
Backshore
Foreshore
Shoreface
Offshore
E2
E1
C3
2
D
5b
5a
4c
4b
C2
C1
4a
1b
A2
1a
A1
B
3
1a Stagnant marine phreatic zone
1b Active marine phreatic zone
2 Marine vadose zone
3 Mixing marine-freshwater phreatic zone
4a Stagnant freshwater phreatic zone
4b Active saturated freshwater phreatic zone
4c Undersaturated freshwater phreatic zone
5a Saturated freshwater vadose zone
5b Undersaturated freshwater vadose zone
High-Mg calcite and aragonite cement
Low-Mg calcite cement
Successive diagenetic subenvironments during relative sea level change (see also Fig.)
Common 'steps' in a dagenetic sequence
Less common 'steps in a diagenetic sequance'

6.6 CALCAREOUS PALAEOSOLS ("CALICHE") FACIES GROUP

This facies group comprises fine-grained calcareous palaeosols (Esteban and Klappa, 1983; Goudie, 1983; Wright et al., 1988), formed over, or within, marine terraces, aeolianites, or carbonate bedrock. Following the classification scheme proposed by Esteban and Klappa (1983), caliche deposits in Messenia and Eastern Lakonia Peninsulae comprise the following types: 1) Hardpan, 2) Platy, 3) Nodular, 4) Chalky caliche. To these a fifth type can be added, that of *Rhizocretion* palaeosols. Caliche types of the above categories are described, as follows:

6.6. Hardpan caliche

6.6.1.1 Occurrence and stratigraphic distribution: This occurs within both the Messenia and Eastern Lakonia Peninsulae, in the following settings:

1) On planated erosional surfaces on carbonate bedrock (Tripolis zone limestone), altimetrically above the early Pleistocene marine terrace (e.g. Methoni; Messenia). Hardpan caliche occurring in such settings could be of pre-Pleistocene or Pleistocene age.

2) On the extensive early Pleistocene terrace surface(s), developed on coarse-grained shallow-marine sediments of early Pleistocene age (see Chapters 2, 4). Hardpan caliche in this setting is very widespread in the Eastern Lakonia Peninsula (e.g. Ano Koroghonas surface; Fig. M.2); it is also well developed locally in the Messenia Peninsula. The age of these caliche deposits is early Pleistocene or younger. Similar hardpan caliche also developed on inferred middle Pleistocene calcareous sandstone in the Eastern Lakonia Peninsula (Ayia Marina; see M.2).

3) Lithified caliche occurs along the walls of extensional joints that cut through coarse-grained shallow-marine carbonates in both peninsulae. Sediments hosting this type of caliche span the time from early to latest Pleistocene (e.g. post-Neotyrrhenian aeolianite in both peninsulae; see Chapters 3, 5).

6.6.1.2 Description: By definition (Esteban and Klappa, 1983, Goudie, 1983), hardpan caliche comprises well indurated, fine-grained, non-porous calcareous palaeosol, mainly consisting of low-Mg calcite. In the idealised caliche profile proposed by Esteban and Klappa (1983), this type of caliche forms at the uppermost levels of calichification, directly below the active soil zone. In the southern Peloponnese, outcrop relations and macroscopic characteristics allow distinction between two types of caliche hardpan:

6.6.1.2.1 'Red' caliche hardpan commonly occurs as a 5-20 cm thick crust on carbonate bedrock, but also over the walls of joints in Pleistocene shallow-marine sediment (mainly grainstone/packstone). This caliche facies commonly contains a high content of angular, corroded carbonate clasts, as well as less common non-carbonate clasts of more distal provenance, forming a matrix-supported fabric. The matrix comprises a mass of red micrite, to microcrystalline spar, intercepted by a network of bifurcating, spar-infilled veins. Aureolar structures and *Microcodium* are present locally. Red caliche hardpan probably originated as a superficial soil mantle, indurated during later diagenesis, probably under dry climatic conditions (James, 1976; Esteban and Klappa, 1983).

6.6.1.2.2 'Pale' caliche hardpan commonly forms ca. 2-15 cm thick crusts over coarse-grained terrace deposits. This caliche facies comprises a mass of microcrystalline micrite, intercepted by blocky spar laminae (flowstone) and numerous spar-infilled vains. Ghost fabrics of the parent sediment are locally preserved within this facies, in the form of heavily micritised carbonate grains. Root bioturbation is locally important, as revealad by the presence of aureolar fabrics. *Microcodium* structures are also abundant locally. This, as with the red caliche hardpan, was affected by vuggy dissolution, followed by precipitattion of pendant spar, commonly of blocky morphology.

6.6.2 Platy Caliche

6.6.2.1 Occurrence and stratigraphic distribution: This caliche facies occurs exclusively on fine-grained shallow-marine sediments of early and early-middle Pleistocene age, commonly below pale-yellow hardpan caliche crusts. This transitional relation between platy caliche below and hardpan caliche above was noted by Esteban and Klappa (1983), who considered platy caliche as a relativelly less mature palaeosol horizon. Given the age of the parent sediments and its less advanced stage of development platy caliche probably formed in post-middle Pleistocene time in the Southern Peloponnese.

6.6.2.2 Description: Platy caliche commonly forms well to moderately indurated, discontinuous, cm-thick plates, of pale-white colour. Its microscopic characteristics are the same as those of hardpan caliche crusts, with aureolar structures, *Microcodium*, spar-infilled veins and micritised carbonate grains of the host sediment. Vuggy porosity and pendant cements are common.

6.6.3 Nodular Caliche

6.6.3.1 Occurrence and stratigraphic distribution: This caliche facies occurs within fine-grained host-lithologies (silt to mud grain-size), of both shallow-marine and subaerial deposits. Nodular caliche developed in shallow-marine mud of early Pleistocene age in the Messenia and Eastern Lakonia Peninsulae and also in alluvial fans of inferred middle Pleistocene age in the Eastern Lakonia Peninsula (e.g. Bozas Rema; Fig M.2). In a few sections where a caliche stratigraphy can be observed (e.g. Gargaliani Road Cut section, Messenia; Fig. M.1), nodular caliche occurs below platy and hardpan caliche. This may reflect its relative immaturity, as predicted by the idealised caliche of Esteban and Klappa (1983), or the lithological difference between fine-grained host of nodular caliche, within the lower-middle parts of coarsening-up successions and coarser-grained hosts of hardpan/platy caliche near the top of coarsening-up successions (see Fig. 3.11.a).

6.6.3.2 Description: This caliche facies comprises nodules of pale-white, friable to hard, micritic/microcrystalline low-Mg calcite. The nodules (long axis < 8 cm) are locally elongate along their vertical or subhorizontal axis. Vertically elongated nodules, probably related to root-penetration, are common within alluvial host-sediments. Aureolar structures, also attributed to root bioturbation, are common. Ghost fabrics of marine parent sediment are preserved rarely, in the form of micritised allochems.

6.6.4 Chalky caliche

6.6.4.1 Occurrence and stratigraphic distribution: This type of caliche was encountered in the Messenia Peninsula, above inferred "Eutyrrhenian" algal boundstone and sandstone, and below latest Pleistocene terra rossa (Mati section; Figs. 3.14.b; M.1). Chalky caliche is, thus, of late Pleistocene, post-Eutyrrhenian age (earlier than ca. 120 ka). Chalky caliche is thought to be relatively immature in comparison with the latter caliche types (Esteban and Klappa, 1983); this is in agreement with its late Pleistocene age in the Messenia Peninsula.

6.6.4.2 Description: This palaeosol comprises a tabular, ca. 12-18 cm thick bed of pale-white, friable, low-Mg micrite. The top 1-1.5 cm of the latter bed are locally hardened as a result of flowstone precipitation. This probably suggests transition to platy-hardpan caliche type. Aureolar structures are abundant, same as wedge-shaped *Rhizocretion* structures with indurated walls.

6.6.5 *Rhizocretion* palaeosols

6.6.5.1 Occurrence and stratigraphic distribution: Two types of *Rhizocretion* palaeosols are distinguished in the area of study:

6.6.5.1.1 'Red' *Rhizocretion* palaeosols separate inferred middle Pleistocene from inferred "Eutyrrhenian" shallow-marine sediments in the Eastern Lakonia Peninsula (Prophitis Ilias; see Figs. 5.16, M.2). Palaeosols of the same type also separate stacked shallow-marine sequences of inferred "Neotyrrhenian" age in the Messenia Peninsula (Marathopolis; Figs. 3.14.c; M.1). These palaeosols are, thus, younger than ca. 100-80 ka.

6.6.5.1.2 'Pale' *Rhizocretion* palaeosols, developed on aeolianite and related backshore grainstones of inferred latest Pleistocene (post-"Neotyrrhenian") age, in both peninsulae (see Chapters 3, 5). They reflect stabilisation of coastal dunes and aeolian sands by vegetation, thus being broadly contemporaneous with the deposition of their host sediment (younger than ca. 80 ka).

6.6.5.2 Description: This caliche facies comprises a dense network of cylindrical, commonly bifurcating *Rhizocretion* tubes, separated by weakly calichified host sediment. The thickness of individual tubes ranges between ca. <0.5 to >3 cm. Caliche tubes exhibit a concentric, aureolar structure, with white, friable or indurated micrite (±microspar) around a central channel that locally remains open. The *Rhizocretion* network tends to be very dense in the 'pale' palaeosol variety, whereas individual tubes are thicker in the 'red' palaeosol variety. These differences probably resulted from different types of vegetation developed on each particular substratum.

6.7 CALICHE STRATIGRAPHY

In the Southern Peloponnese, well developed vertical successions from one to the other type of caliche are rare. Exceptions include transitions from platy to hardpan caliche, commonly within < 1 m up-sequence. Nevertheless, the presence of different caliche types over surfaces and sediments of different ages allows a relative stratigraphy of caliche facies to be erected (Fig. 6.7):

1) 'Red' caliche hardpan, developed on Late Pliocene to early Pleistocene erosional surfaces, is pre-Pleistocene to early-middle Pleistocene in age.

2) 'Pale' caliche hardpan, developed on early to early-middle Pleistocene terraces, is early to middle Pleistocene in age. Platy caliche is a form transitional to the latter and represents less advanced calichification; therefore it is probably contemporaneous with, or slightly younger than hardpan caliche.

3) Nodular caliche occurs within fine-grained facies of the early Pleistocene regressive sequence and inferred middle Pleistocene alluvia. In continuous caliche profiles this facies is, thus, stratigraphically below the coarse-grained facies that host the latter two caliche types. Given that calichification proceeds from the surface to the interior of the ultimately unaltered rock, nodular caliche probably represents a relatively immature palaeosol of early to middle-late Pleistocene age.

3) Chalky caliche occurs above "Eutyrrhenian" shallow-marine sediments and below red alluvia correlated with the Last Glacial Maximum (Kourampas and Robertson, 2000). Its formation took place in the latest Pleistocene, between 120-12 ka.

4) Rhizocretion caliche, resulting from development of vegetation, occurs in middle Pleistocene alluvia and post-"Neotyrrhenian" aeolianites. Given that the maximum age of these marine sediments is at the order of ca. 80 ka, the development of this type of caliche was relatively rapid.

The above conclusions are in agreement with those of Esteban and Klappa (1983), who suggested that in an idealised caliche profile, the most mature caliche type is represented by caliche hardpan, followed by platy, then nodular, then chalky caliche as we move to the unaltered host rock.

Figure 6.6: Relative stratigraphy of caliche facies in the Messenia and Eastern Lakonia Peninsulae, showing the relationship between caliche types and Quaternary landforms (see text for explanation).

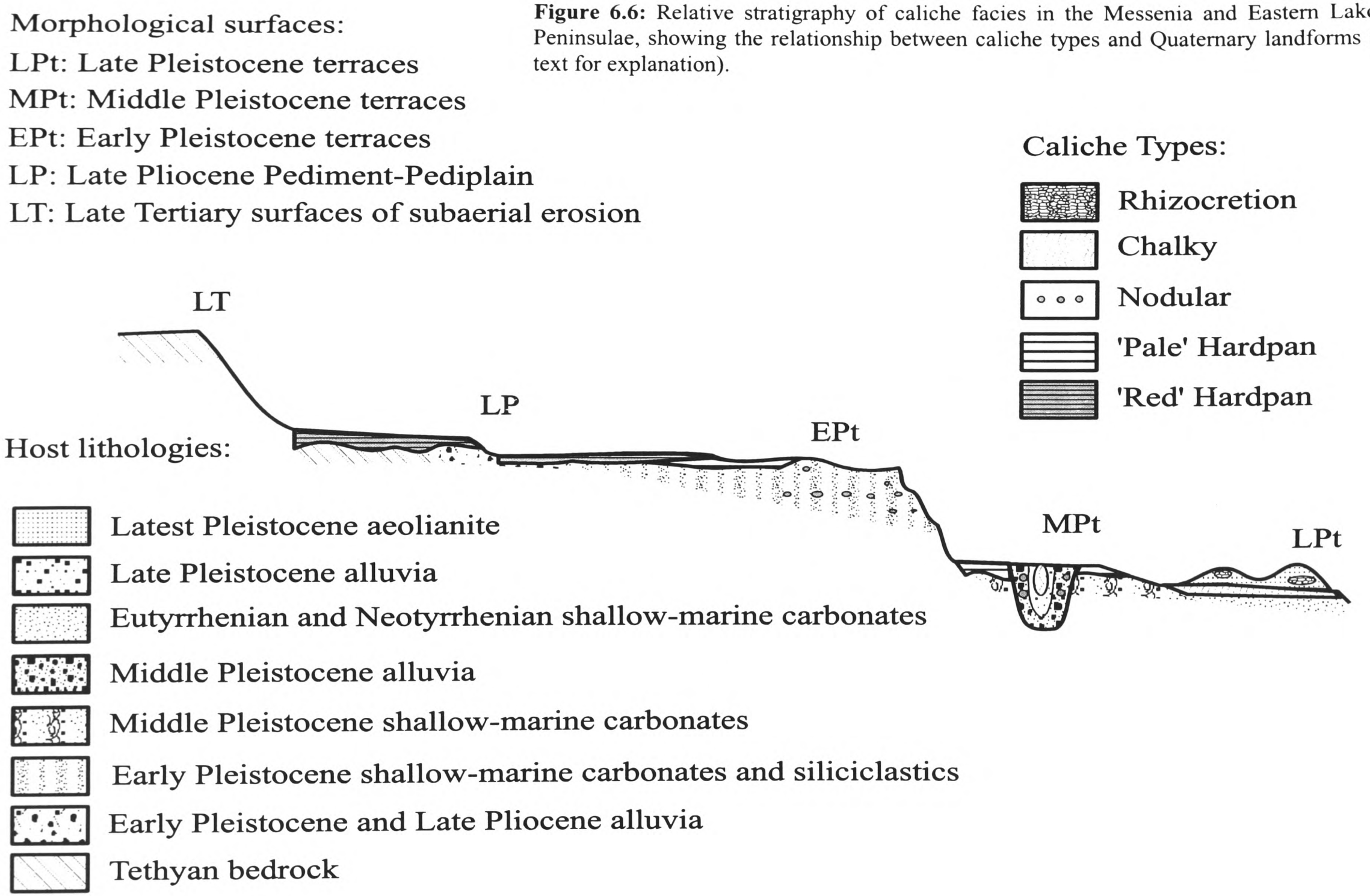

6.8 SUMMARY-CONLCUSIONS:

- The main microfacies present within Pleistocene-Holocene shallow-marine sediments in the Messenia and Eastern Lakonia Penisnulae comprise detrital carbonates, commonly with a high terrigenous content (i.e. lithic grainstone and packstone, peloidal packstone, foraminiferal wackestone), siliciclastics (i.e. calcareous sandstone, conglomerate) and bioconstructed carbonates (i.e. red algal framestone, coral-red algal bafflestone, blue-green algal bindstone).

- The terrigenous content of Pleistocene shallow-marine sediments is systematically higher in the Eastern Lakonia Peninsula as compared with the Messenia Peninsula, possibly reflecting bedrock lithology (widespread outcrops of "*Phyllite Series*") and more widespread alluviation, triggered by closely spaced normal faulting.

- The diagenetic evolution of shallow-marine sediments, in both Penisulae, is divided into the following sequences:

1) Active marine phreatic zone ⇒ (marine vadose zone) ⇒ (freshwater phreatic zone) ⇒ freshwater vadose zone.
2) Active marine phreatic zone ⇒ stagnant marine phreatic zone ⇒ freshwater phreatic zone ⇒ freshwater vadose zone.
3) Stagnant marine phreatic zone ⇒ freshwater phreatic zone ⇒ freshwater vadose zone.

- The diagenetic sequences (1) and (3) are the commonest. These are commonly present in the middle and upper parts of depositional sequences, whereas sequence (2) characterises lags near the base of depositional sequences. The diagenetic sequences (1) and (3) exemplify a transition of the sediment from a submarine depositional environment to a subaerial environment, during and after emergence (i.e. relative sea level fall). The diagenetic sequence (2) exemplifies a transition of the sediment from a high to a low energy submarine environment, during transgression (i.e. relative sea level rise).

- Palaeosols developed on shallow-marine sediments and alluvia are of the caliche type, suggesting that a semi-arid climate prevailed in the Southern Peloponnese during some periods of the Pleistocene. Many of these semi-arid periods coincided with sea level lowstands, as shown by intercalation of caliche with alluvial sediments. Caliche types present in the Messenia and Eastern Lakonia Peninsulae include hardpan, platy, chalky, nodular caliche and *Rhizocretion* palaeosols.

- Besides climate, the age and lithology of the host sediment also controlled the development of caliche: Mature caliche types (hardpan and platy caliche) are generally absent from late Pleistocene sediments, but widespread on early Pleistocene sediments. Nodular caliche is present in fine-grained facies of early to middle Pleistocene host rock. *Rhizocretion* palaeosols developed in shallow-marine sediments, aeolianites and alluvia of middle and late Pleistocene age.

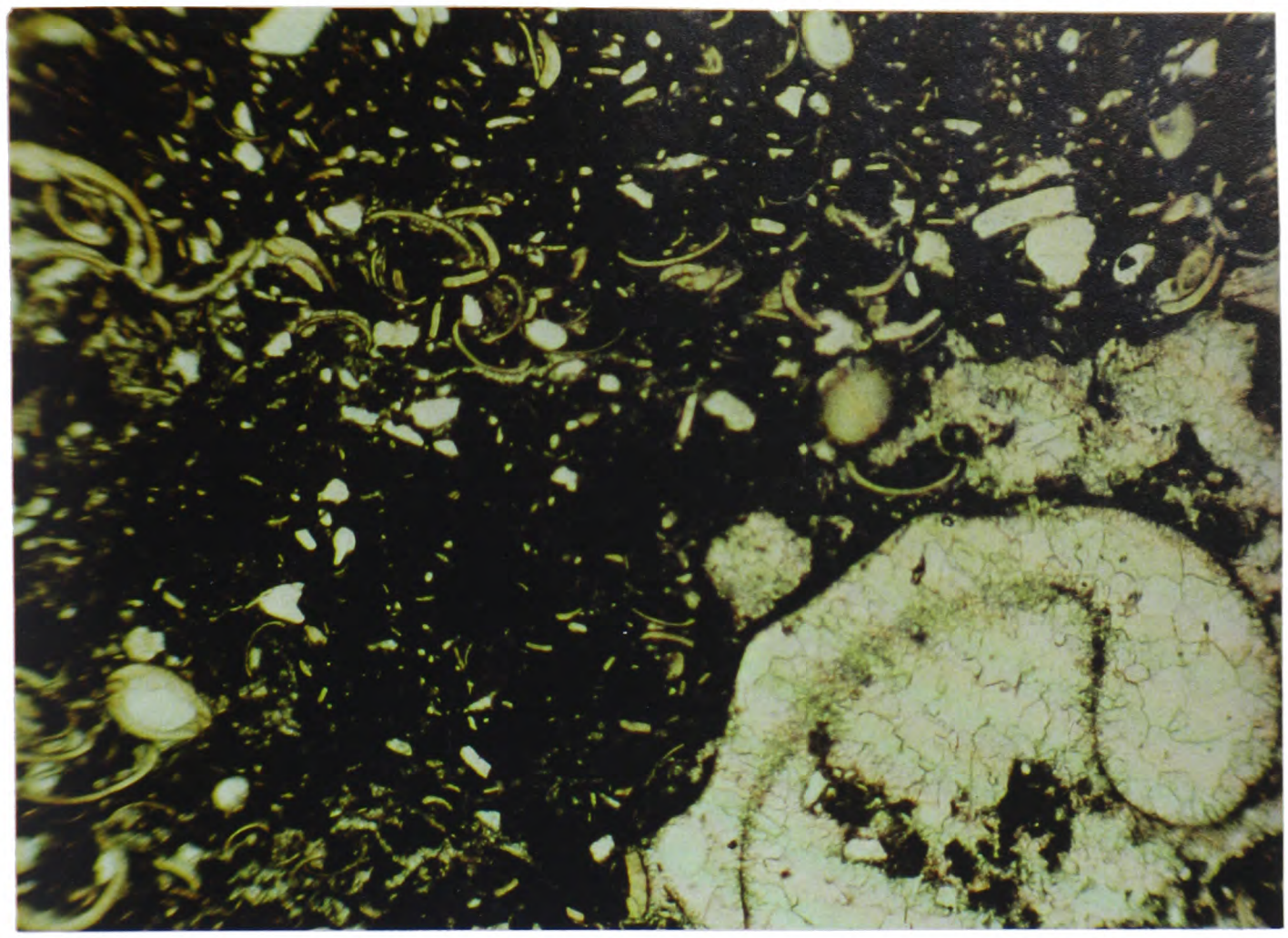

Figure 6.7.1 Ostracod-gastropod wackestone. Note the dense accumulation of ostracod valves (middle of the photograph). The gastropod shell (upper left) was recrystallised in an equant-drusy spar mosaic. The same type of spar also filled articulated ostracod valves (upper right) and vuggy porosity within matrix. Most of the matrix consists of faecal pellets. Early Pleistocene (Subunit 3.2), Eastern Lakonia (Sample *Kok 36*; Kokkinia). Scale: 1mm across.

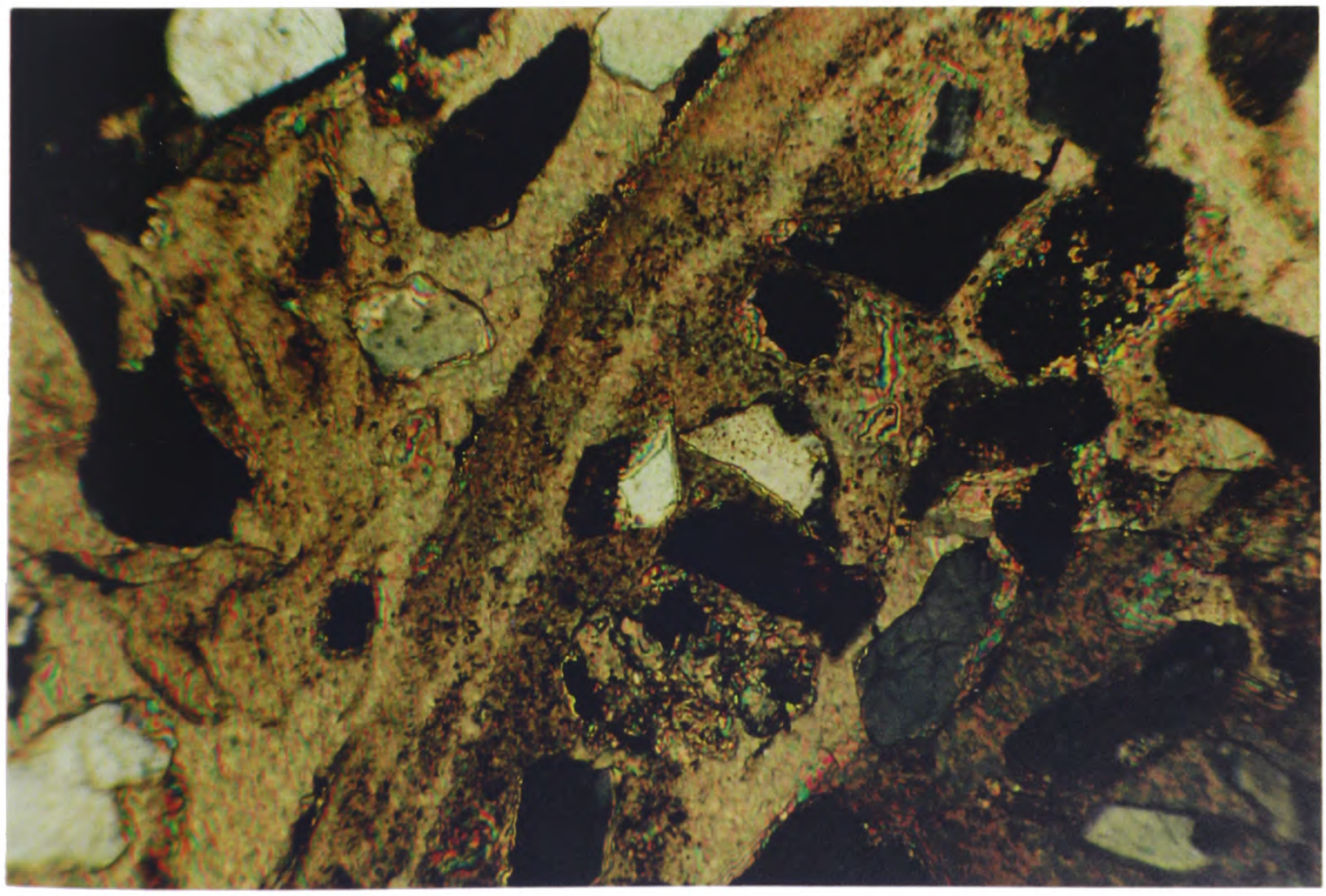

Figure 6.7.2: Poikiltic spar cement in lithic grainstone of early Pleistocene age. Note that cement crystals engulf quart grains. Early Pleistocene Subunit 3.2, Eastern Lakonia (Sample *Glyko 2a*: Ano Glikovrisi). Scale: 1 mm across.

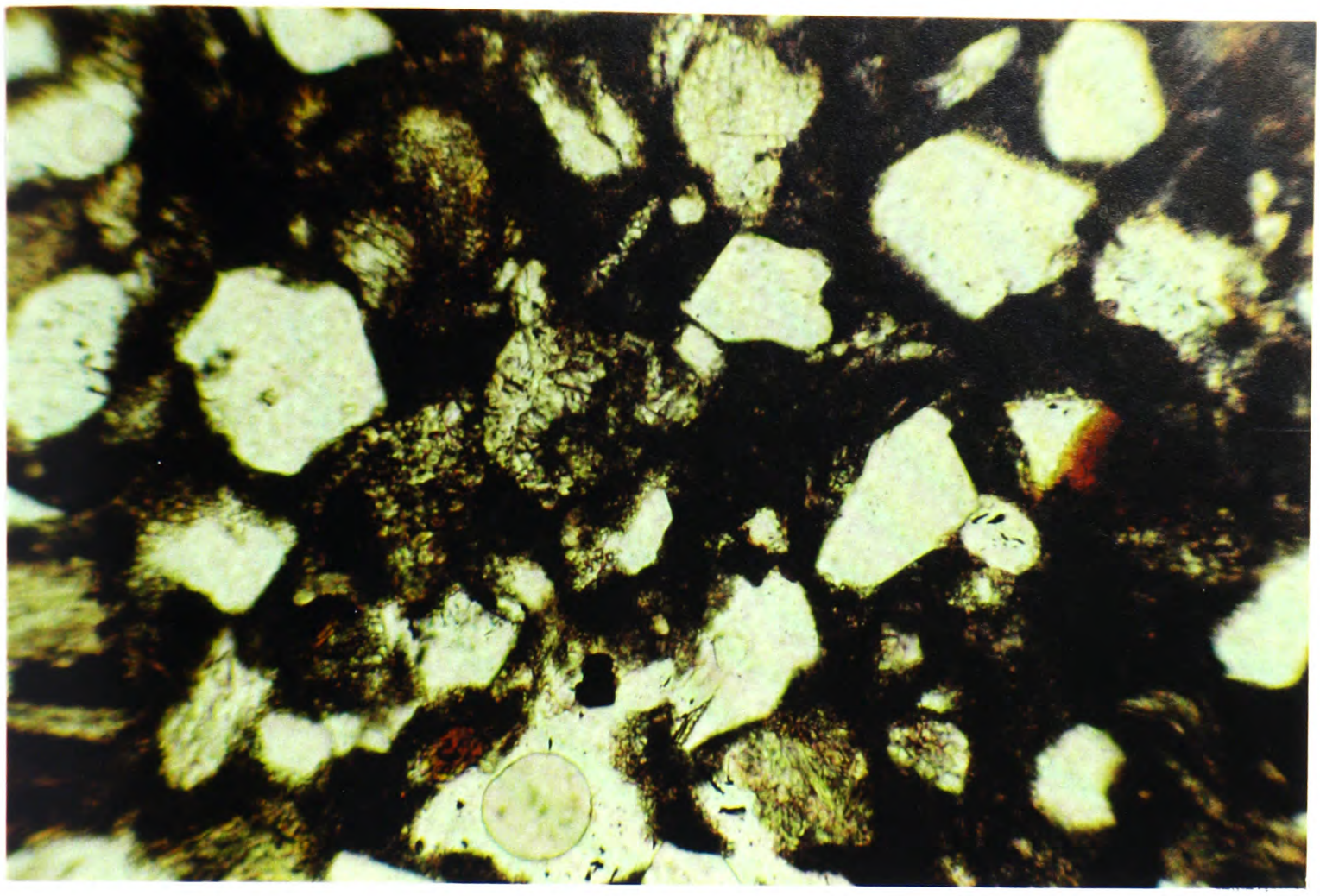

Figure 6.8.1: Constructive micritic envelopes in calcareous sandstone. Grains of quart and feldspar are cemented with micritic cement. Early, or middle Pleistocene, Eastern Lakonia (Sample *AyMar 4*; Ayia Marina). Scale: 1 mm across.

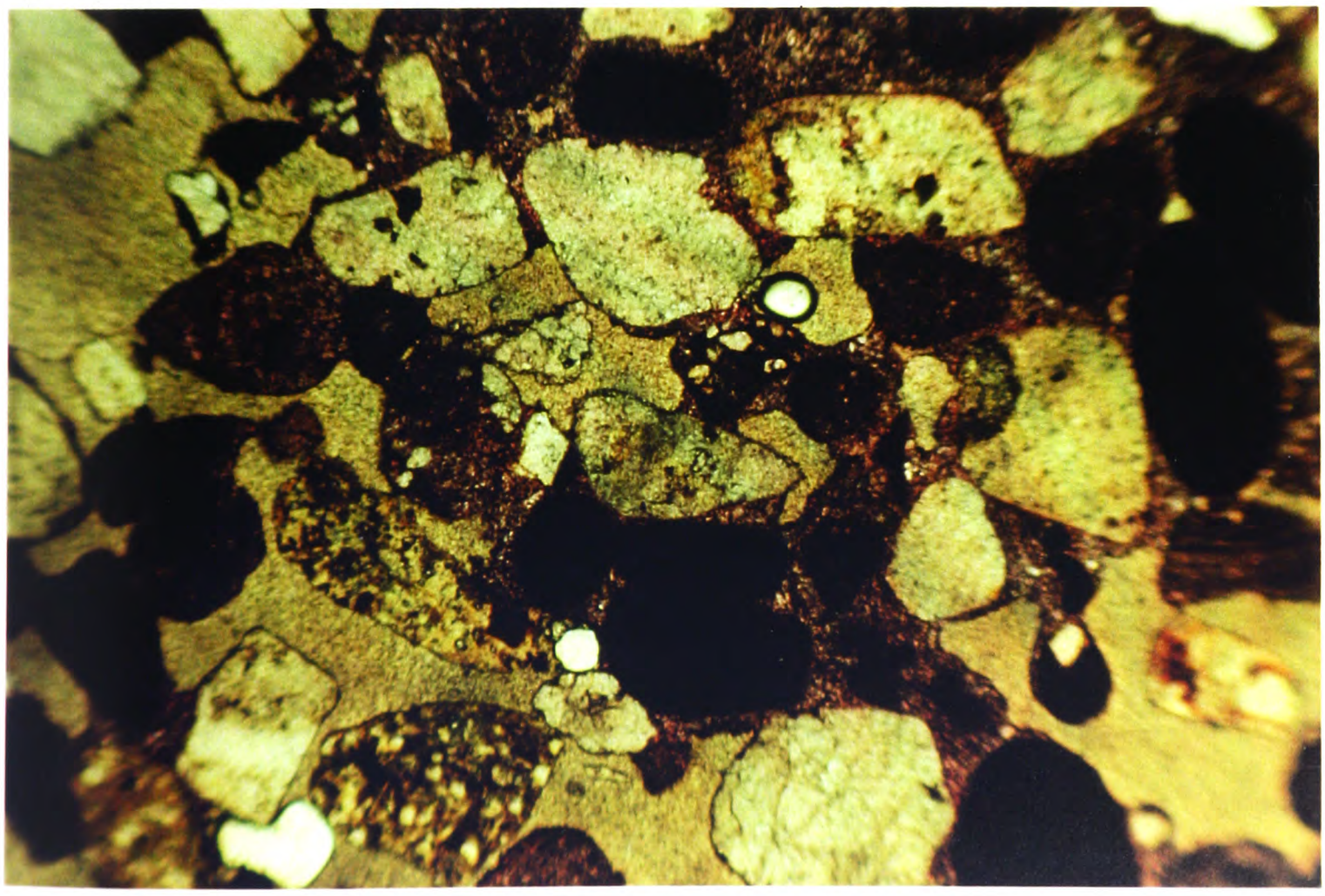

Figure 6.8.2: Late Pleistocene aeolianite: Moderately to well rounded, terrigenous (pale) and carbonate (dark) grains are cemented with microcrystalline spar cement (purple). Note the meniscus fabric of the cement and the high primary porosity of the sediment. Unit 3.7, Messenia (Stained sample *Rom 3*: Romanos). Scale: 1 mm across.

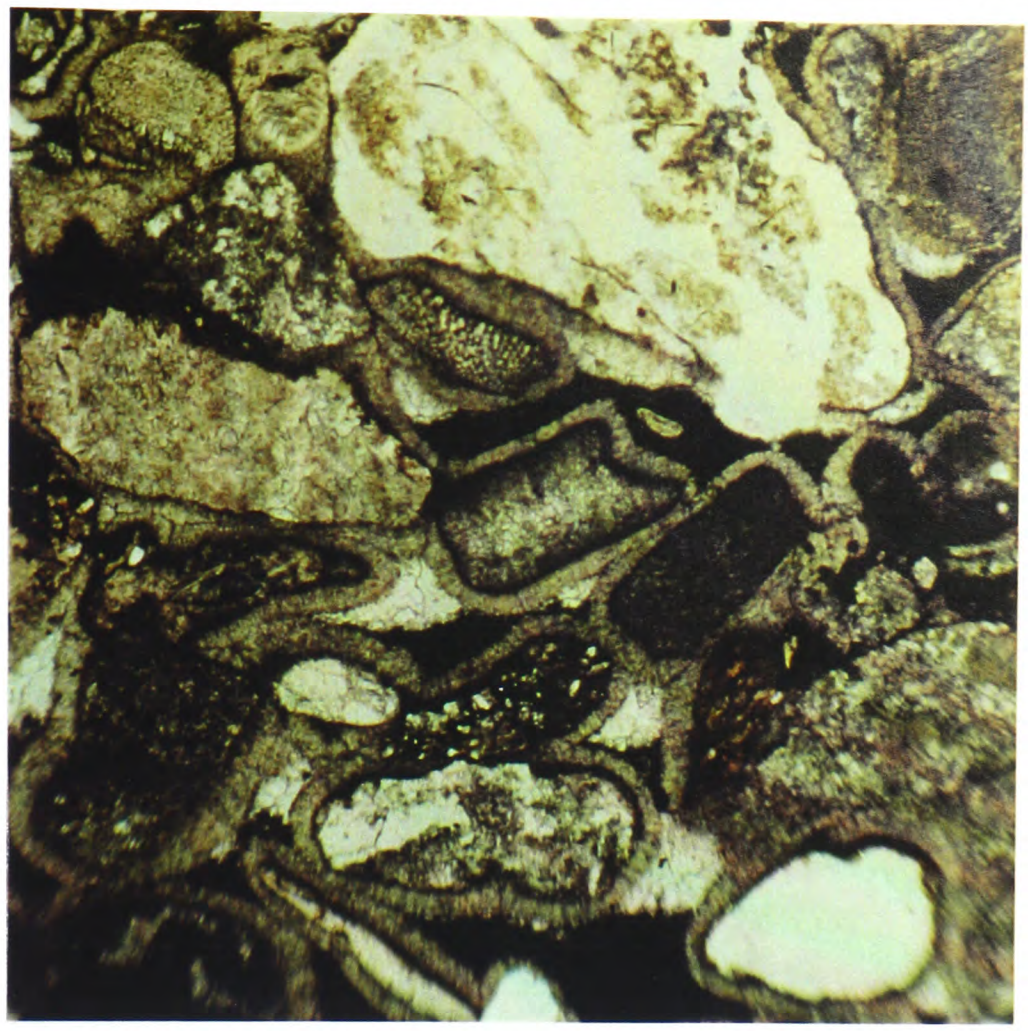

Figure 6.9.1: Mollusc-pelloidal packstone. Note the succession of cements, from isopachous circumgranular rims of acicular crystals (active marine phreatic zone), followed by micritic, or pelletal matrix (stagnant marine phreatic zone) of a geopetal fabric. Remaining intergranular pores were filled with equant drusy spar, probably deposited in the saturated freshwater phreatic zone. Eutyrrhenian Subunit 8.1; Eastern Lakonia (Oriented sample *Plyt 22*; Plytra). Scale: 0.66 mm across.

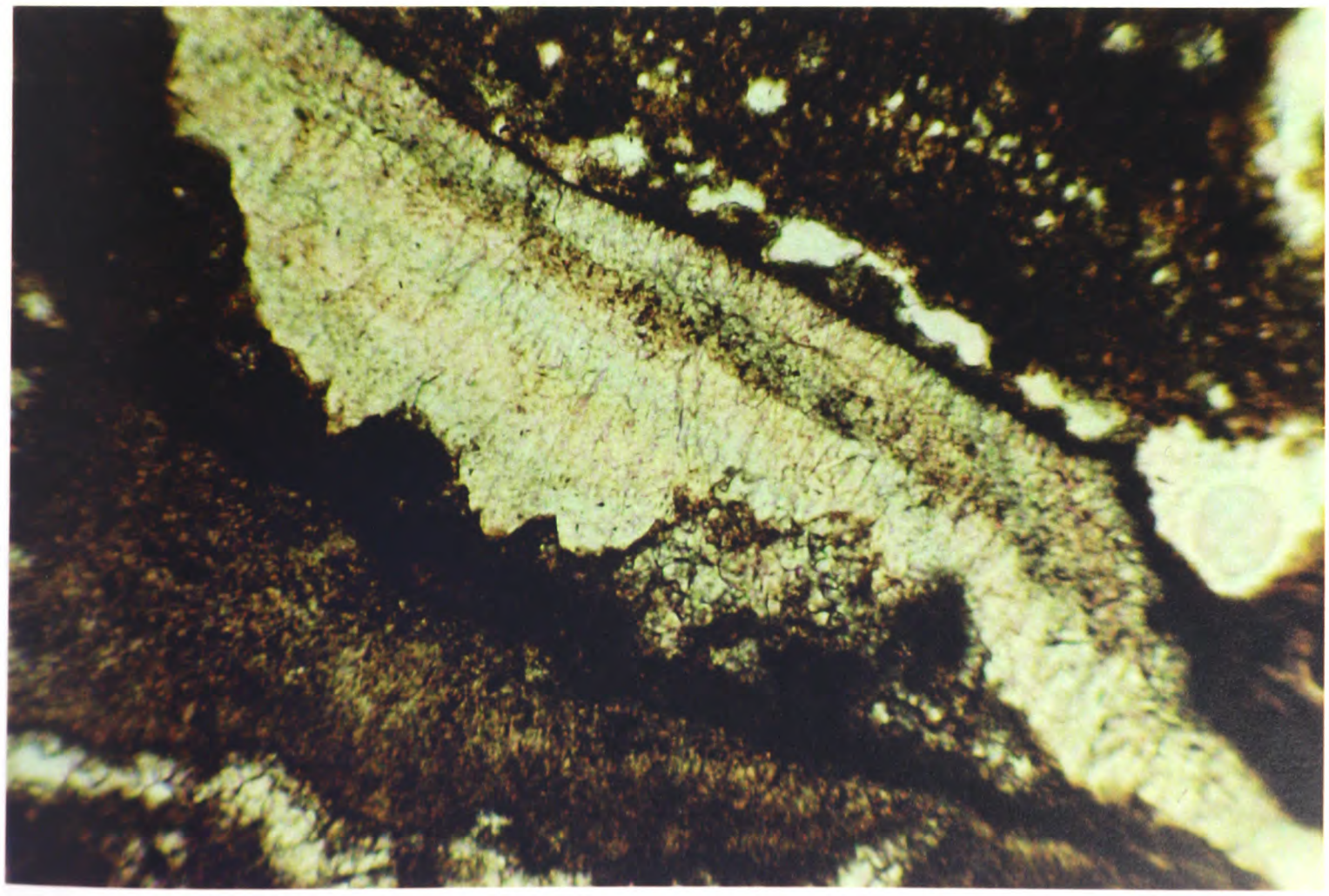

Figure 6.9.2: Bladed, low-Mg spar cement. Its microstalactitic fabric suggests deposition in the freshwater vadose zone. Detail of previous sample; scale: 1 mm across.

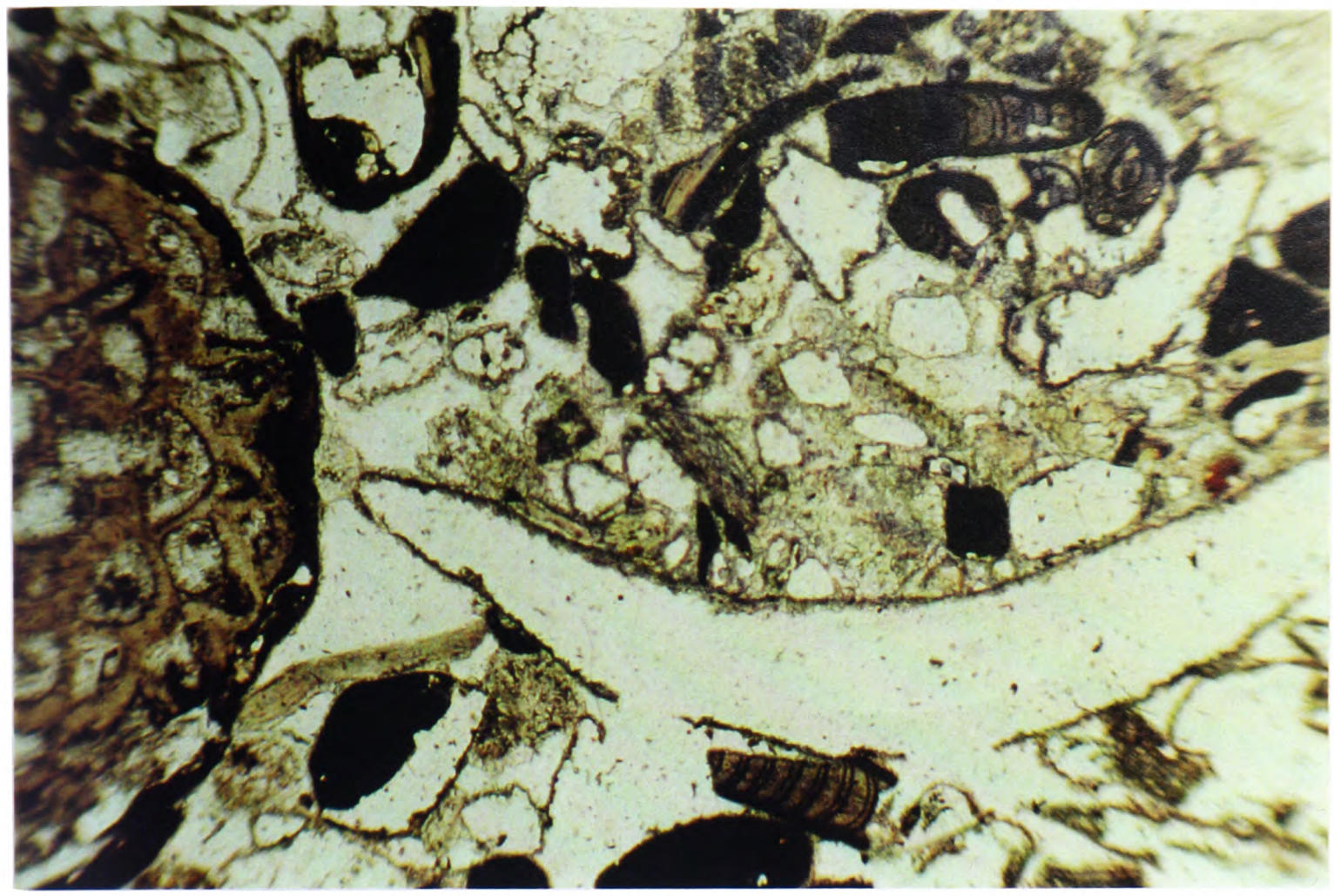

Figure 6.10.1 Grainstone with bivalves, red algae (*Amphiroa* sp.), bryozoa, peloids and terrigenous grains. Note moldic pore (middle of the photograph), defined by surviving micritic envelope. Early to early-middle Pleistocene (Unit 5), Eastern Lakonia (Sample *Dem 8*; Dhaemonia). Scale: 1 mm across.

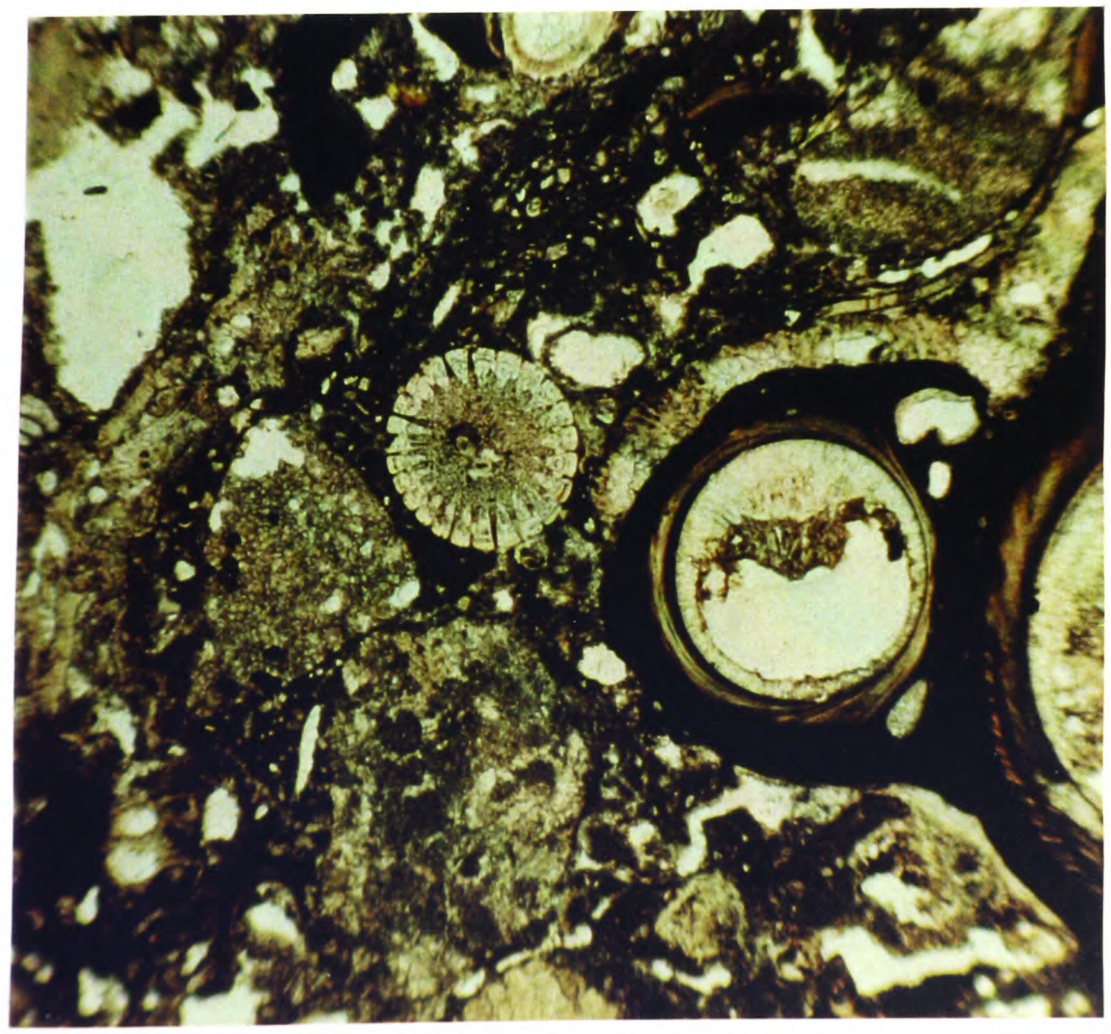

Figure 6.10.2: Lithic packstone with serpulids (right), echinoids (centre), foraminifera and terrigenous grains (volcaniclastics). Note the deposition of microstalactitic spar cement (clear) inside serpulid tubes, followed by clay minerals (brown). These cements precipitated in the freshwater vadose zone, after emergence of the sediment. Eutyrrhenian, Eastern Lakonia (Sample *Kok 36cg*: Kambourani Rema). Scale: 0.66 mm across

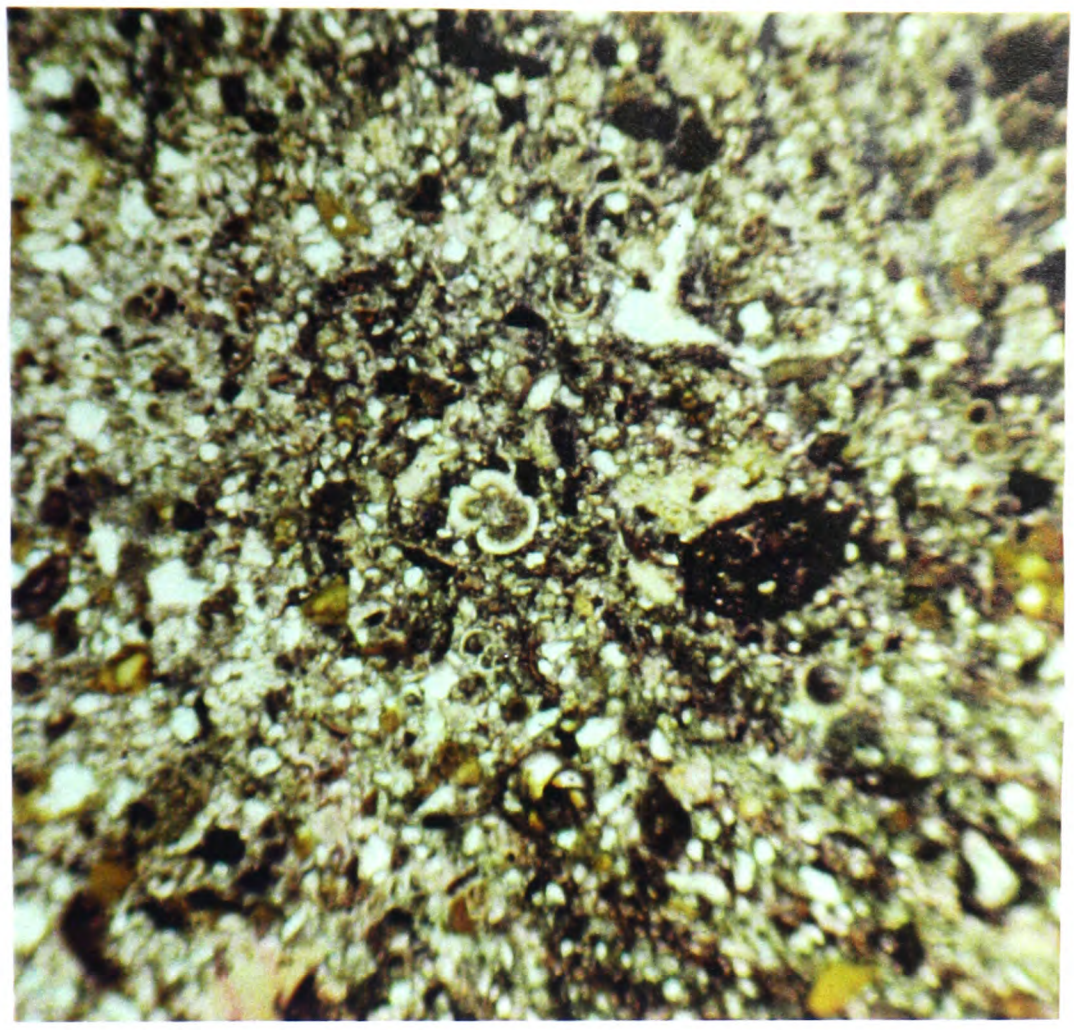

Figure 6.11.1: Siltstone with benthic and planktic foraminifera. A globigerinid foraminiferum (*Globigerinoides ruber*?) is shown at the centre of the photograph. Early Pleistocene, Eastern Lakonia (Sample: *Vigl 9*: Viglaphia). Scale: 0.55 mm across

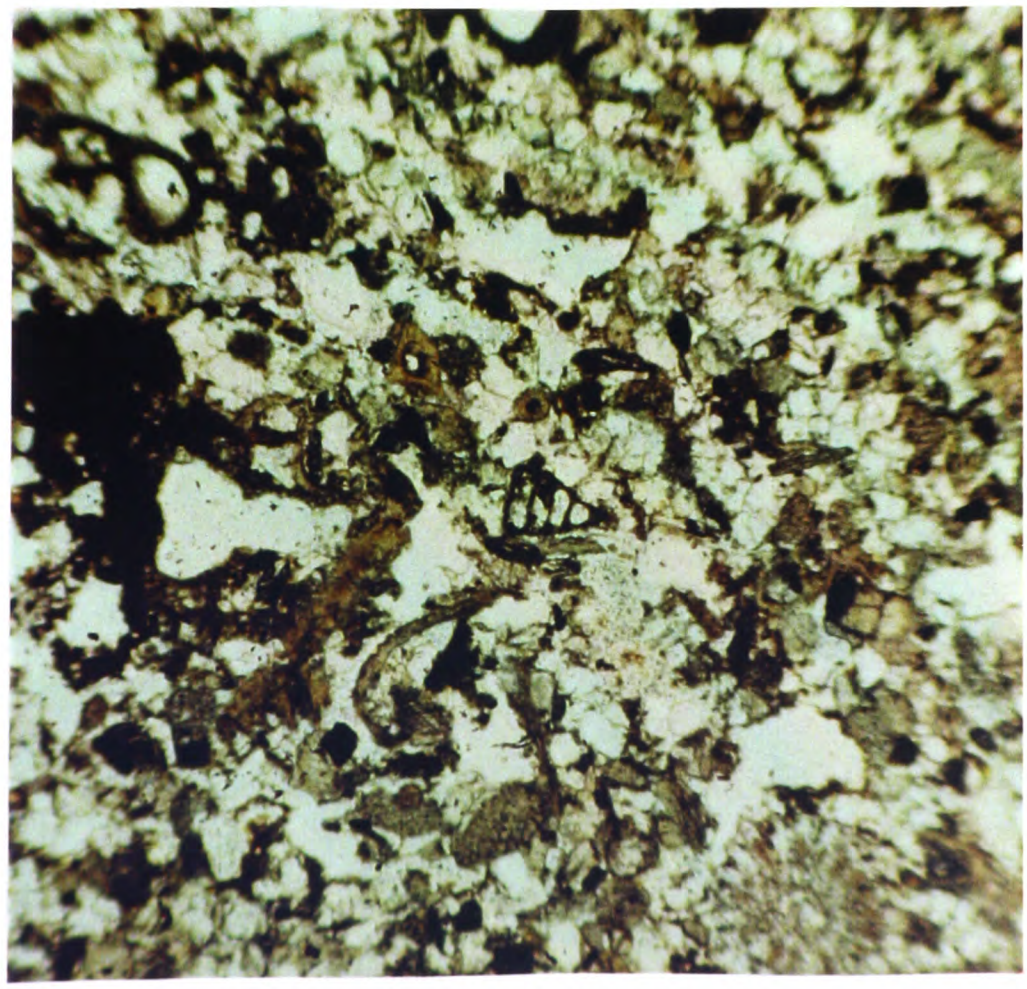

Figure 6.11.2: Lithic packstone with peloids, foraminifera and terrigenous grains. An arenaceous foraminiferum is shown in the centre of the photograph. Early Pleistocene (Subunit 3.1), Eastern Lakonia (Sample *Plyt 12*; Plytra). Scale: 0.55 mm across.

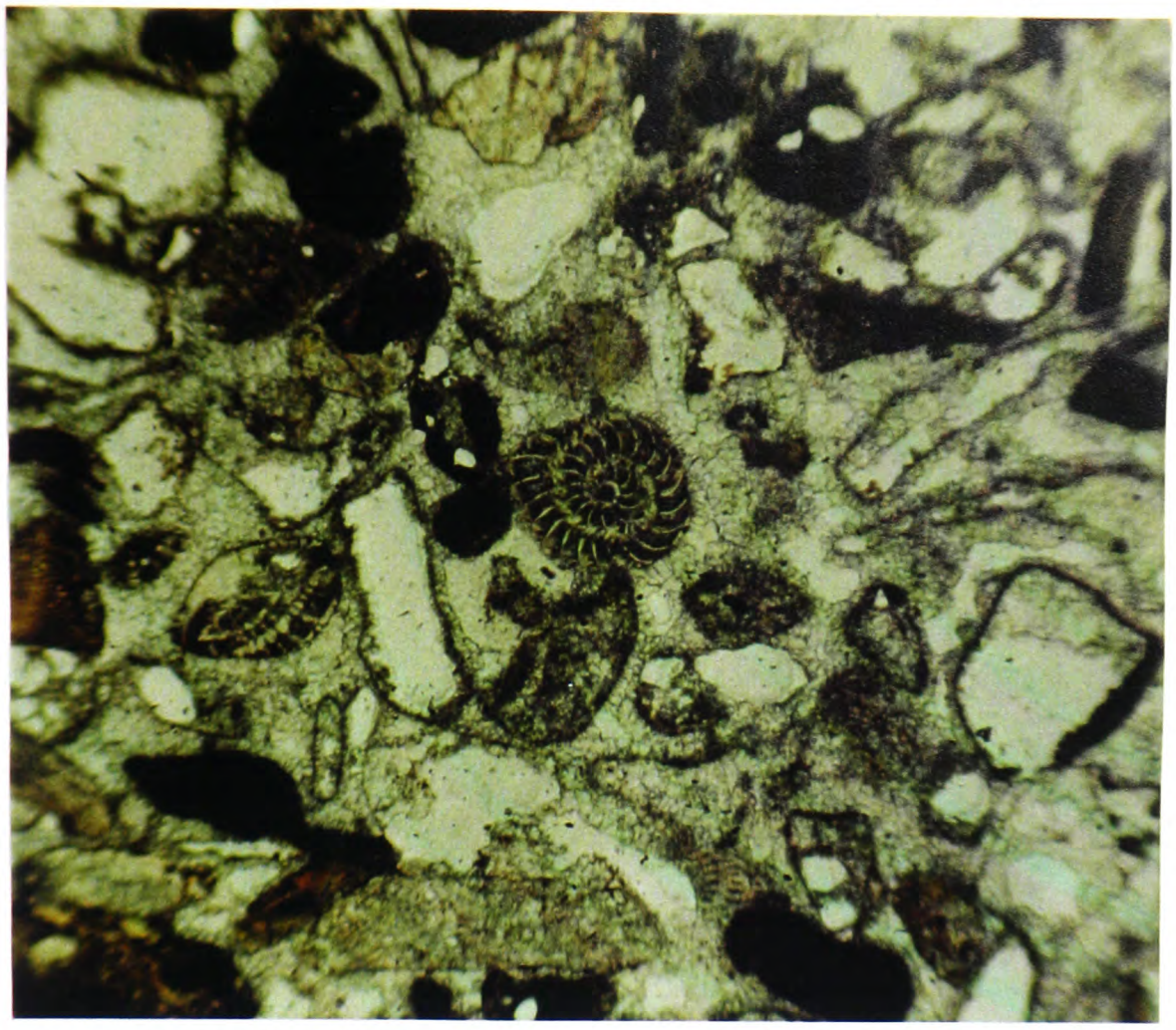

Figure 6.12.1: Grainstone with peloids, foraminifera, mollusc fragments and terrigenous grains. *Elphidium* sp. are shown at the centre and right. Note the extensive development of moldic porosity, probably after mollusc fragments, and the equant spar cement in intergranular areas. Early to early-middle Pleistocene, Eastern Lakonia (Sample *AyMar 22*; Ayia Marina). Scale: ca. 0.70 mm.

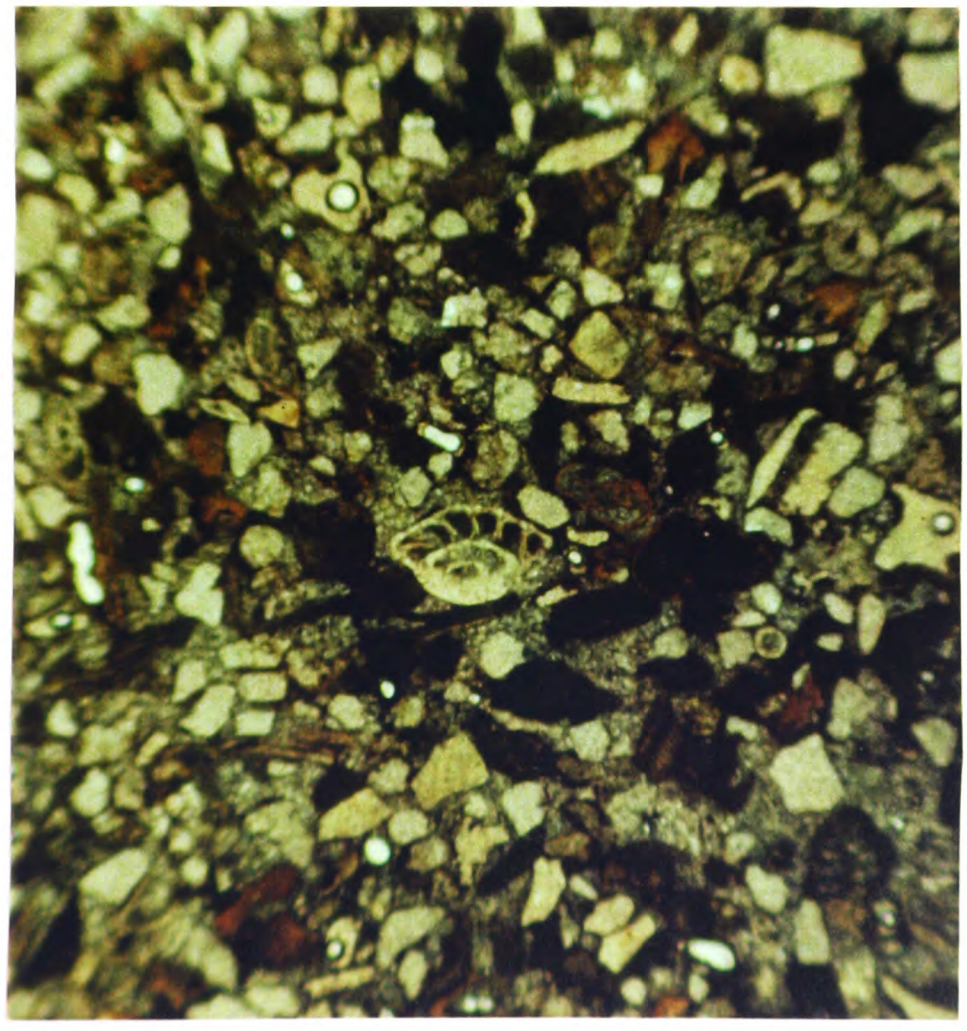

Figure 6.12.2: Calcareous sandstone with terrigenous grains, peloids, foraminifera and mollusc fragments. A rotaliid foraminiferum (*Ammonia* sp.) is shown at the centre. The sediment is cemented with finely-crystalline spar. Middle or late Pleistocene, Messenia (Sample *MSN 16*; Laghouvardhos Rema). Scale: ca. 0.50 mm across.

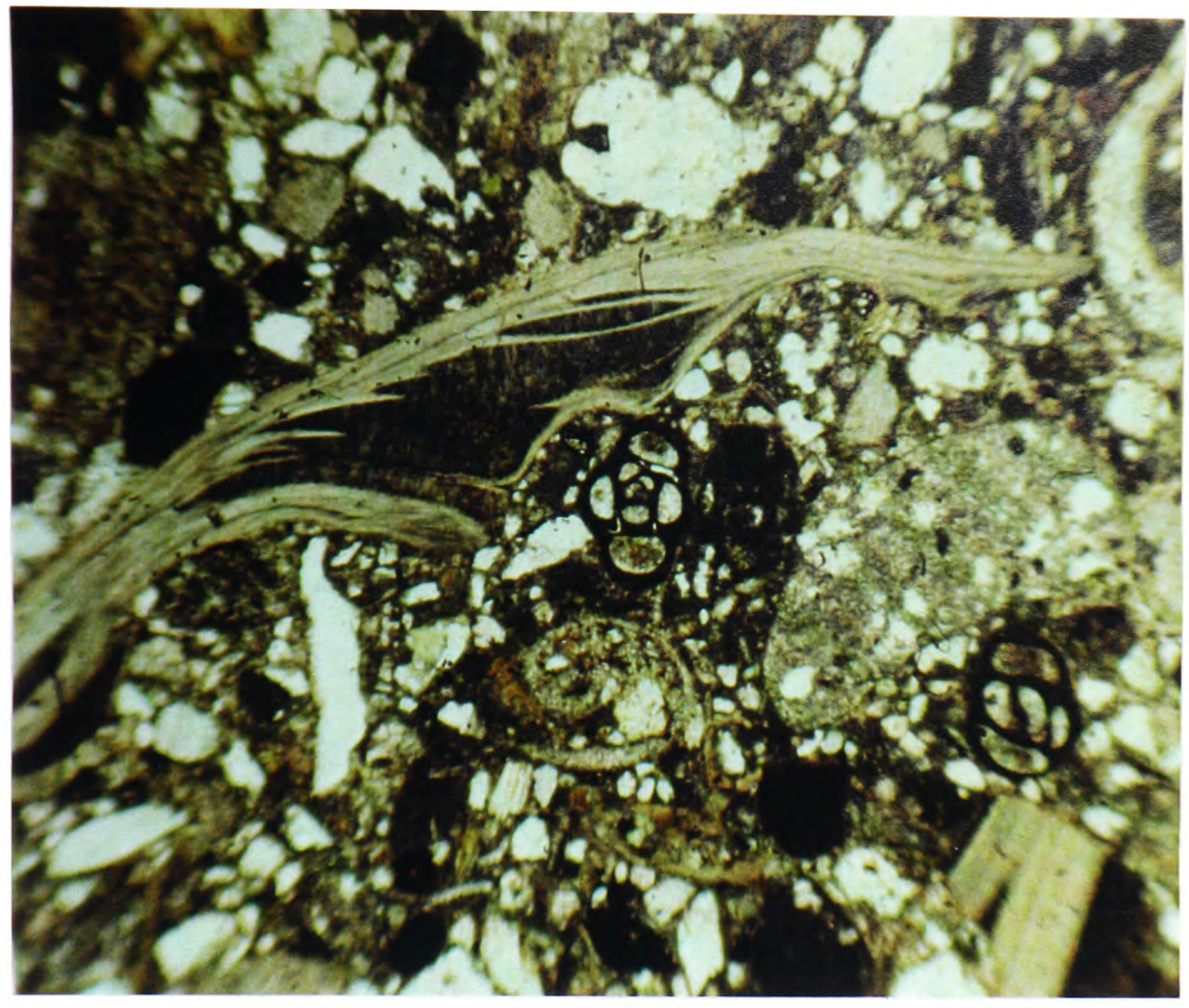

Figure 6.13.1: Matrix-rich calcareous sandstone, with bivalve fragments (centre), miliolid foraminifera (centre and right) and terrigenous grains. Note the poor sorting of the sediment. The foraminiferum at the centre is a *Quinqueloculina* sp. Early Pleistocene, Eastern Lakonia (Sample *Kok 39cg*: Dhiakos). Scale: 0.70 mm across.

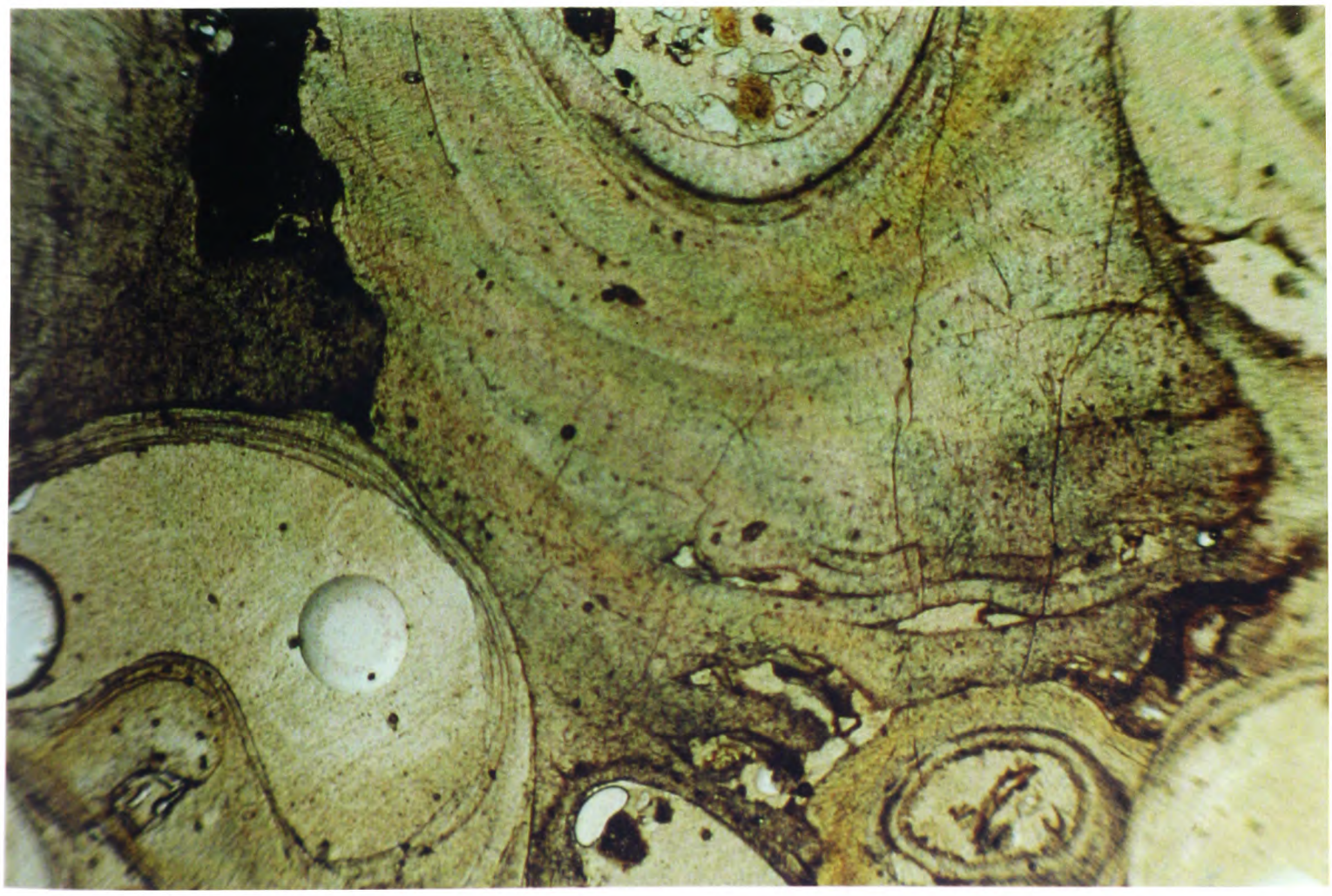

Figure 6.13.2: Detail of vermetid gastropod colony. Holocene Unit 3.8, Messenia (Sample *MSN 8*; Romanos). Scale: 1 mm across.

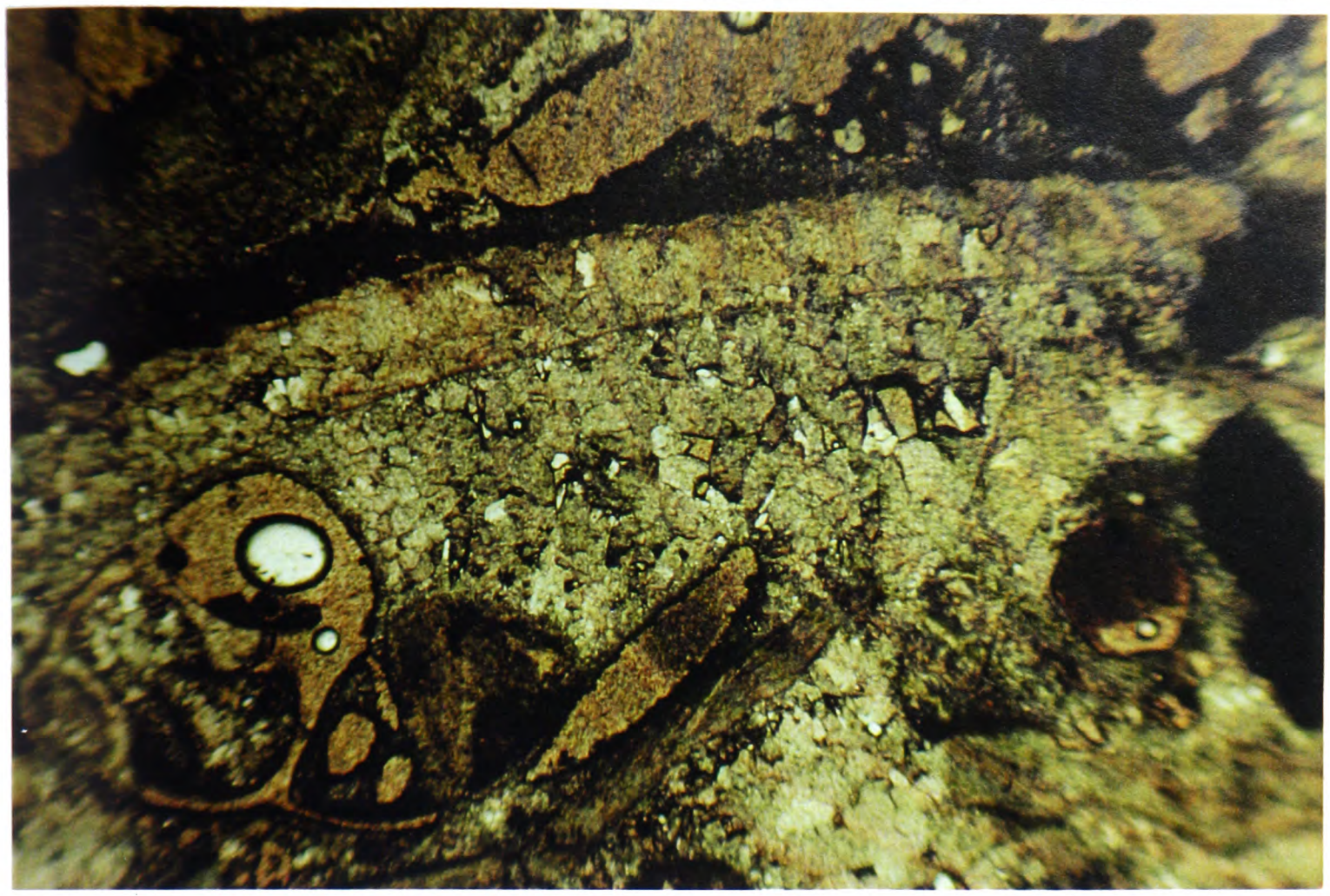

Figure 6.14.1: Grainstone with recrystallised and dissolved bivalves and gastropods. Note the recrystallisation of the bivalve fragment (centre) to low-Mg calcite. A mass of low-Mg calcite spar also filled umbrella porosity (underneath the bivalve fragment) and intraskelletal pores (lower left). The gastropod shell (lower left) was completely removed but geopetal infill of skeletal cavities (brown) remained intact. Eutyrrhenian (Unit 3.1), Messenia (sample *Ko 10*; Koroni). Scale: 1 mm across.

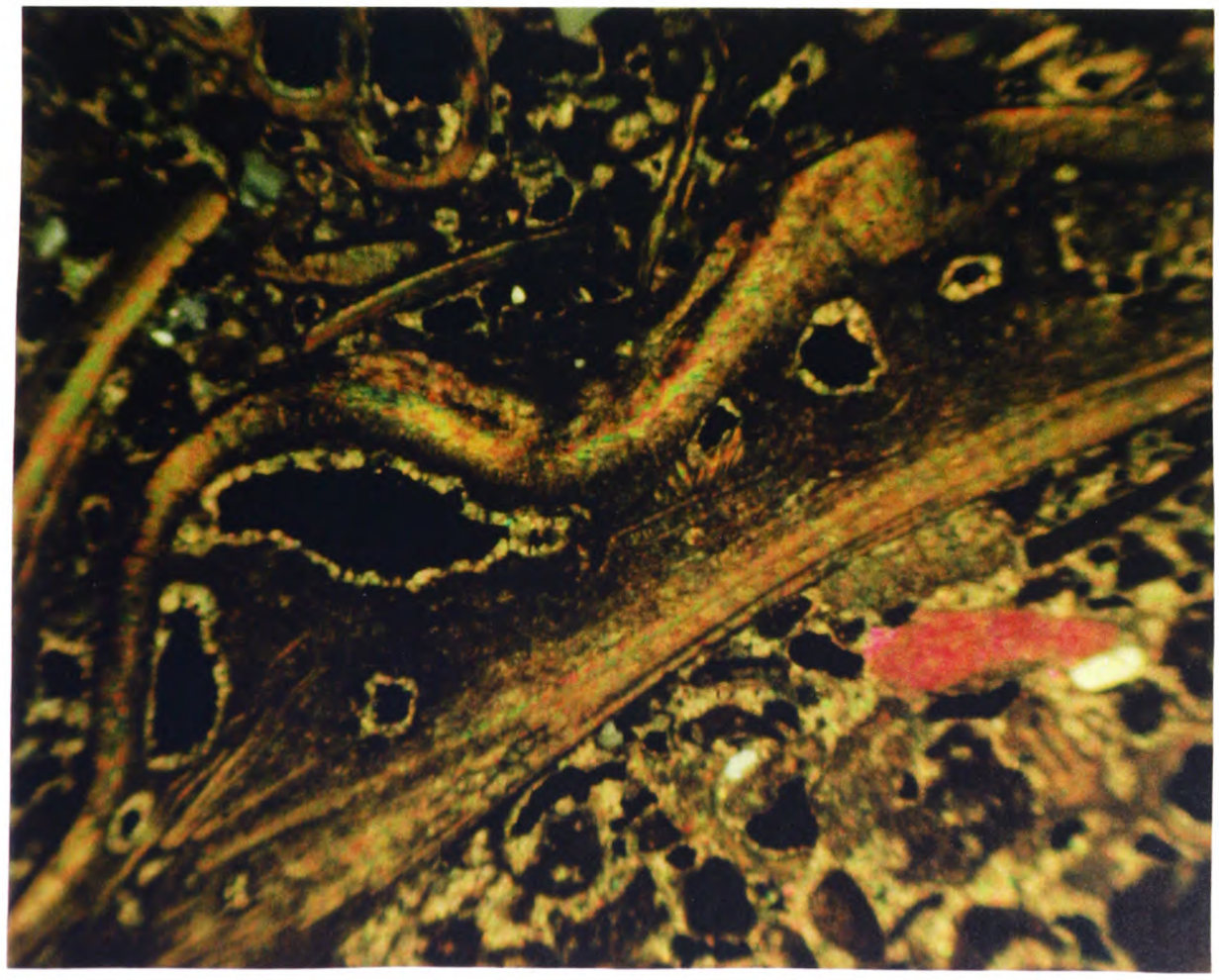

Figure 6.14.2: Incipient dissolution of a bivalve shell: Small, apparently non-connected pores were reduced with spar cement, showing that dissolution and cementation are broadly contemporaneous. Early Pleistocene packstone; Messenia (sample *GB4/5A*: Gargaliani). Scale: 0.70 mm across.

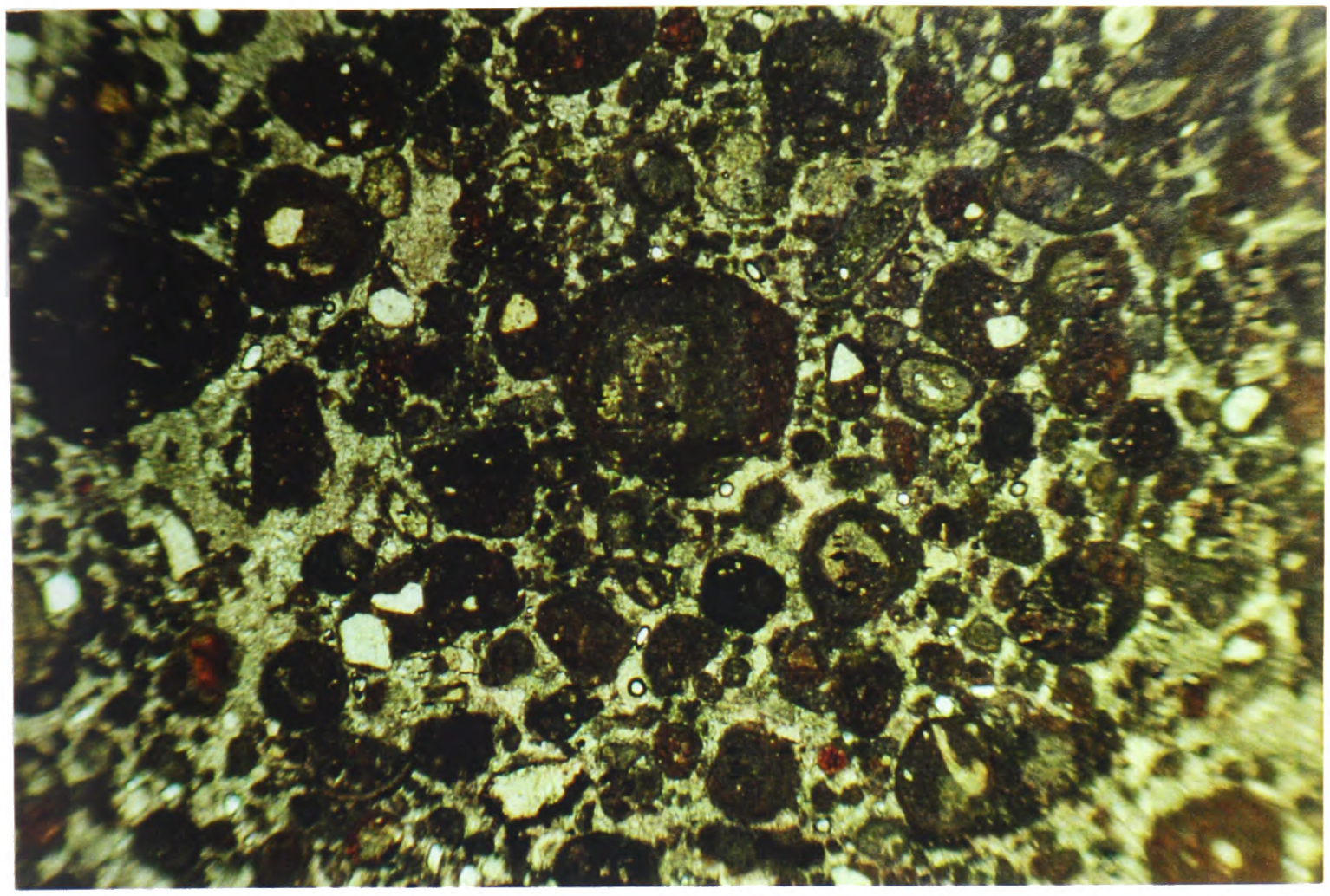

Figure 6.15.1: Coated grainstone: Rounded pissoids, aggregates and pellets, cemented with spar cement. Late Pleistocene, Messenia (Sample *Mar 7*: Marathopolis). Scale: 1 mm across.

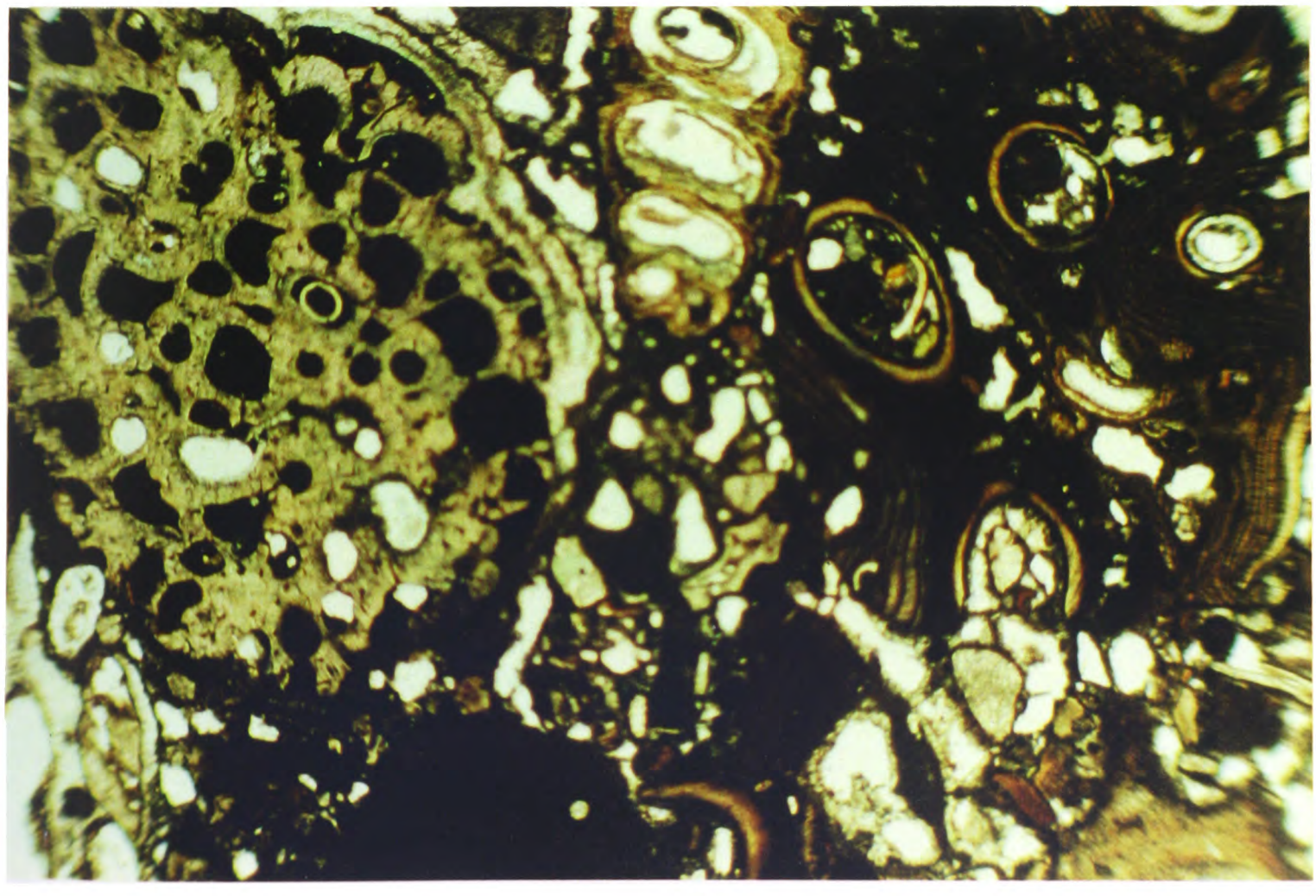

Figure 6.15.2: Algal-molluscan-bryozoan lithic packstone. Note the abundance of terrigenous grains in interskelletal areas. Late Pleistocene, Eastern Lakonia.

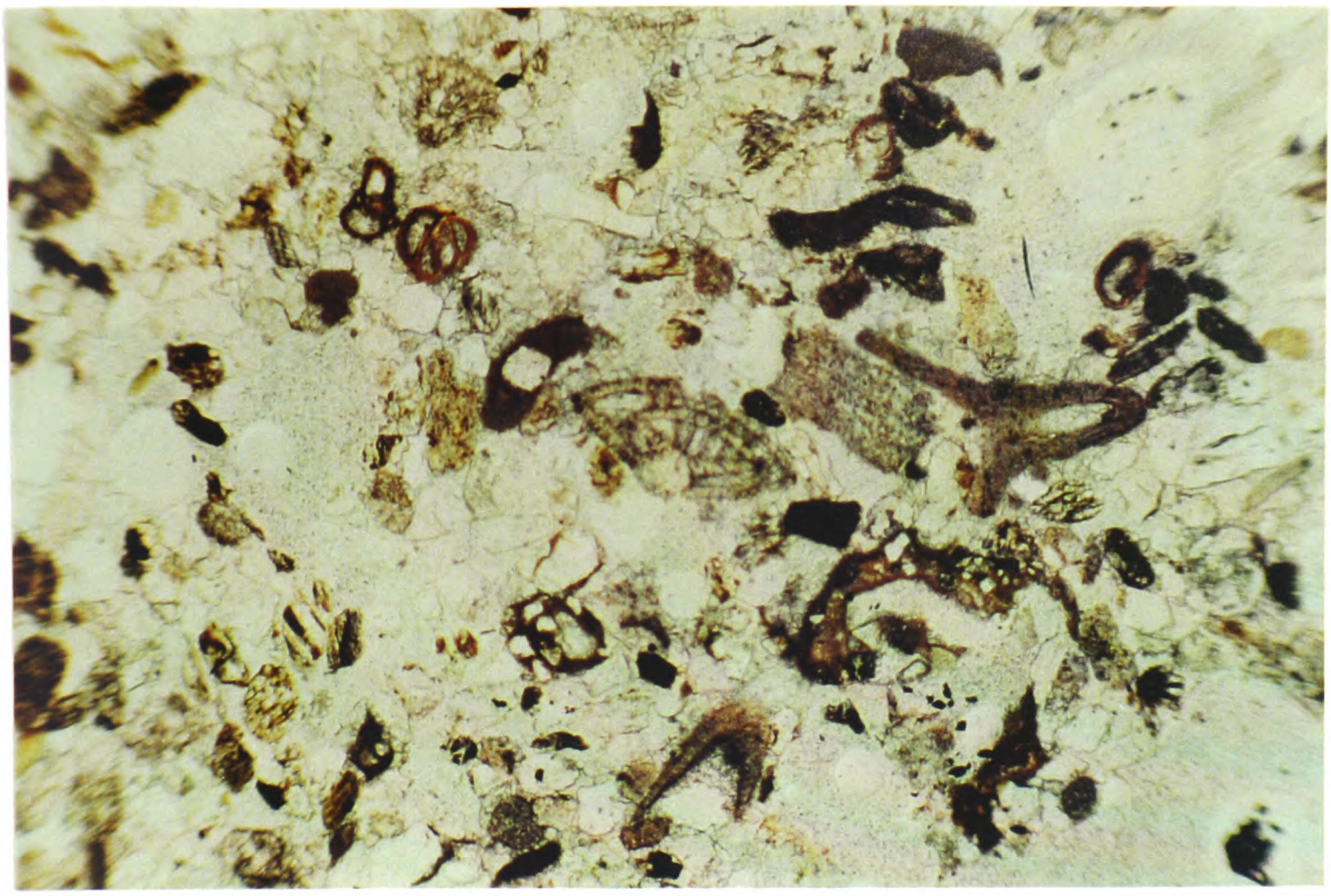

Figure 6.16.1: Lithic grainstone with foraminifera, mollusc fragments, echinoids and peloids, cemented with low-Mg calcite cement. Note the presence of the intralittoral *Elphidium* sp. (centre) and Milioliidae (upper left). Middle Pleistocene, Eastern Lakonia (sample *Kok 26crd*: Kambourani Rema). Scale: 1 mm across.

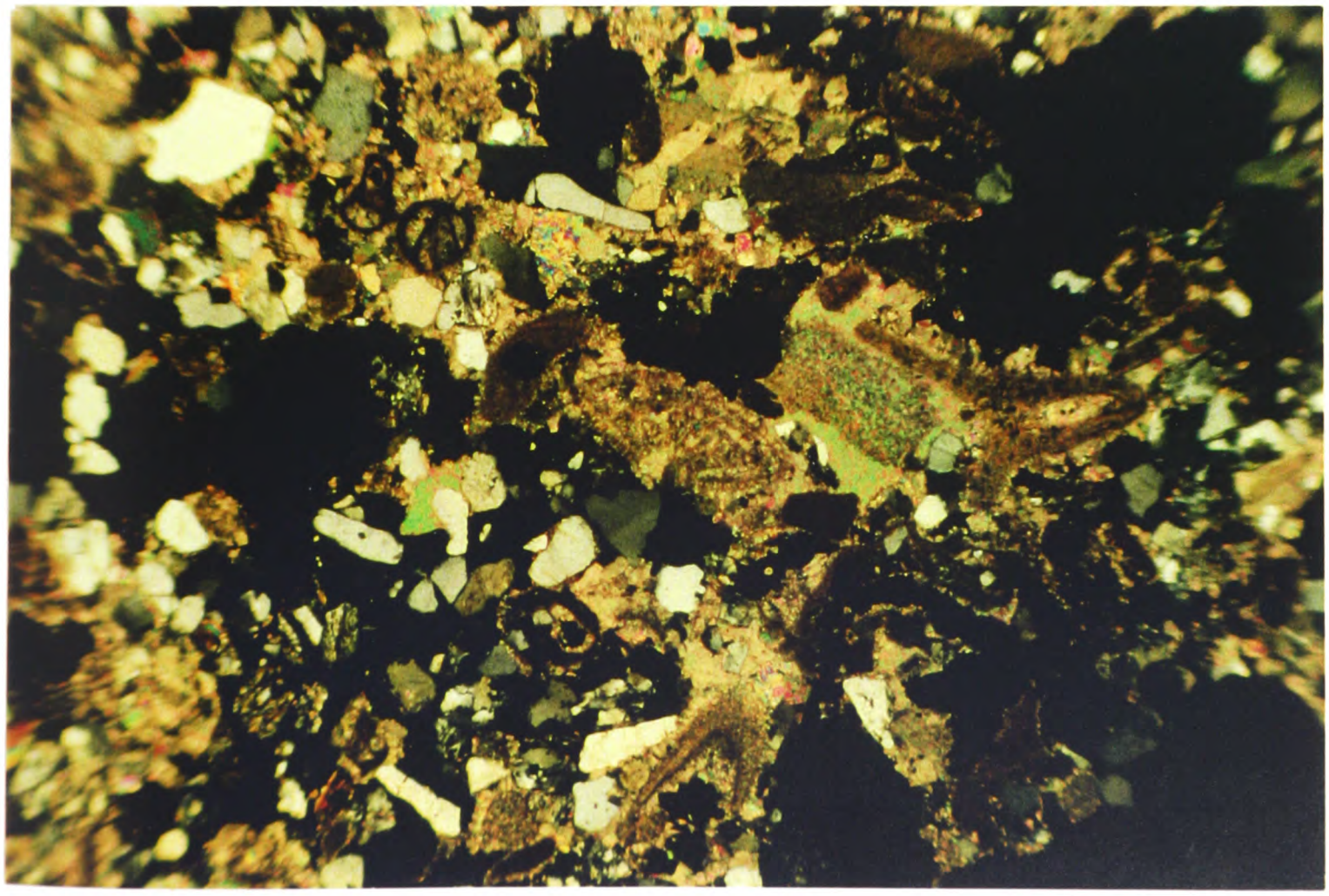

Figure 6.16.2: The same sample with N(+): Note the high percentage of the terrigenous grains (mainly quart), the high primary porosity (dark areas) and the development of syntaxial overgrowths around echinoderm grains (centre-right).

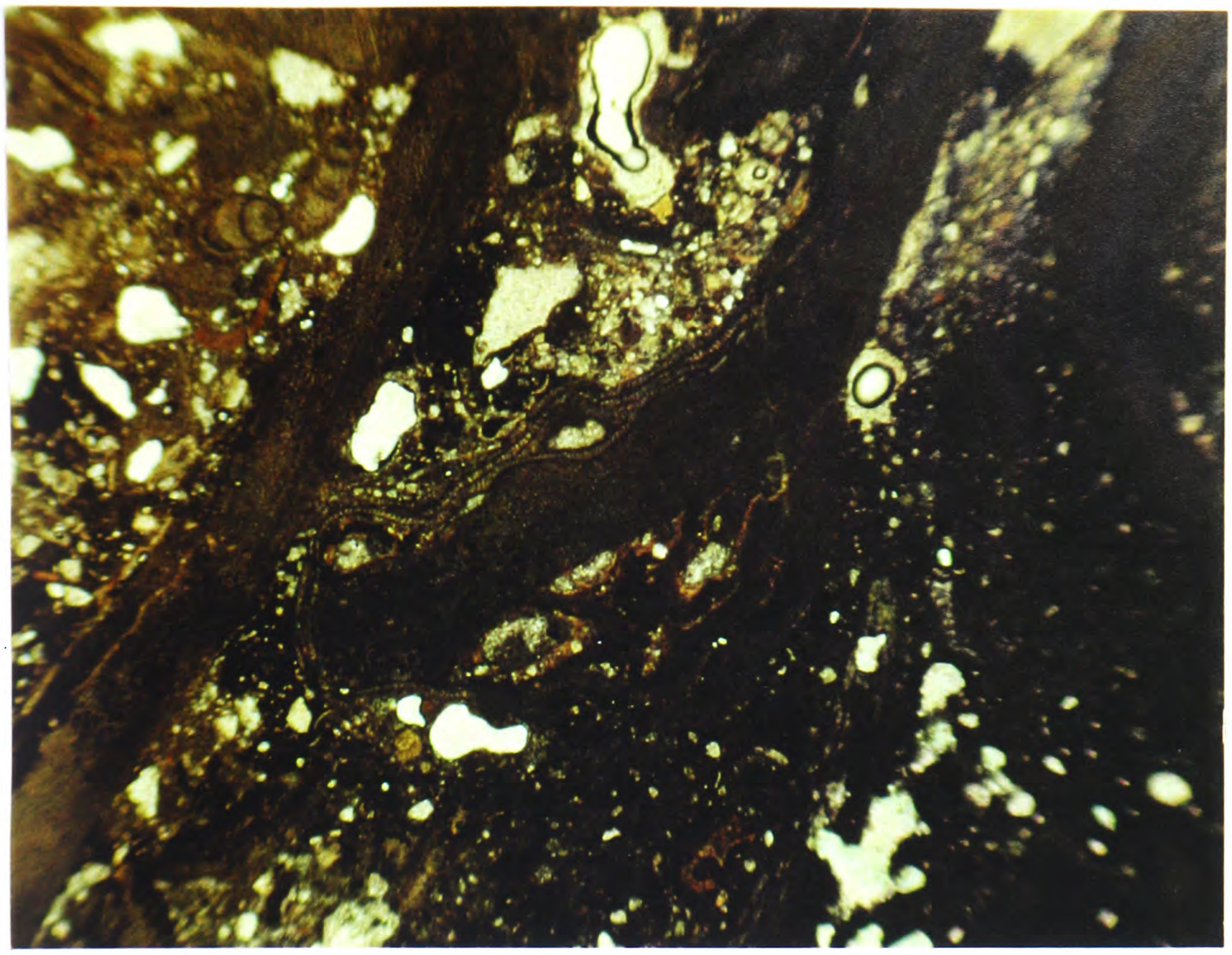

Figure 6.17.1: Algal boundstone: Encrusting red algae (*Lithophylum* sp., *Tenarea* sp.) and foraminifera (lower part of the crust) form a framework that trapped matrix, terrigenous and carbonate grains (faecal pellets, mollusc fragments, bryozoa, articulating red algae). Note the vuggy porosity of the sediment (white). Middle Pleistocene, Messenia (sample *Lim 3*: Filiatra). Scale: 0.8 mm.

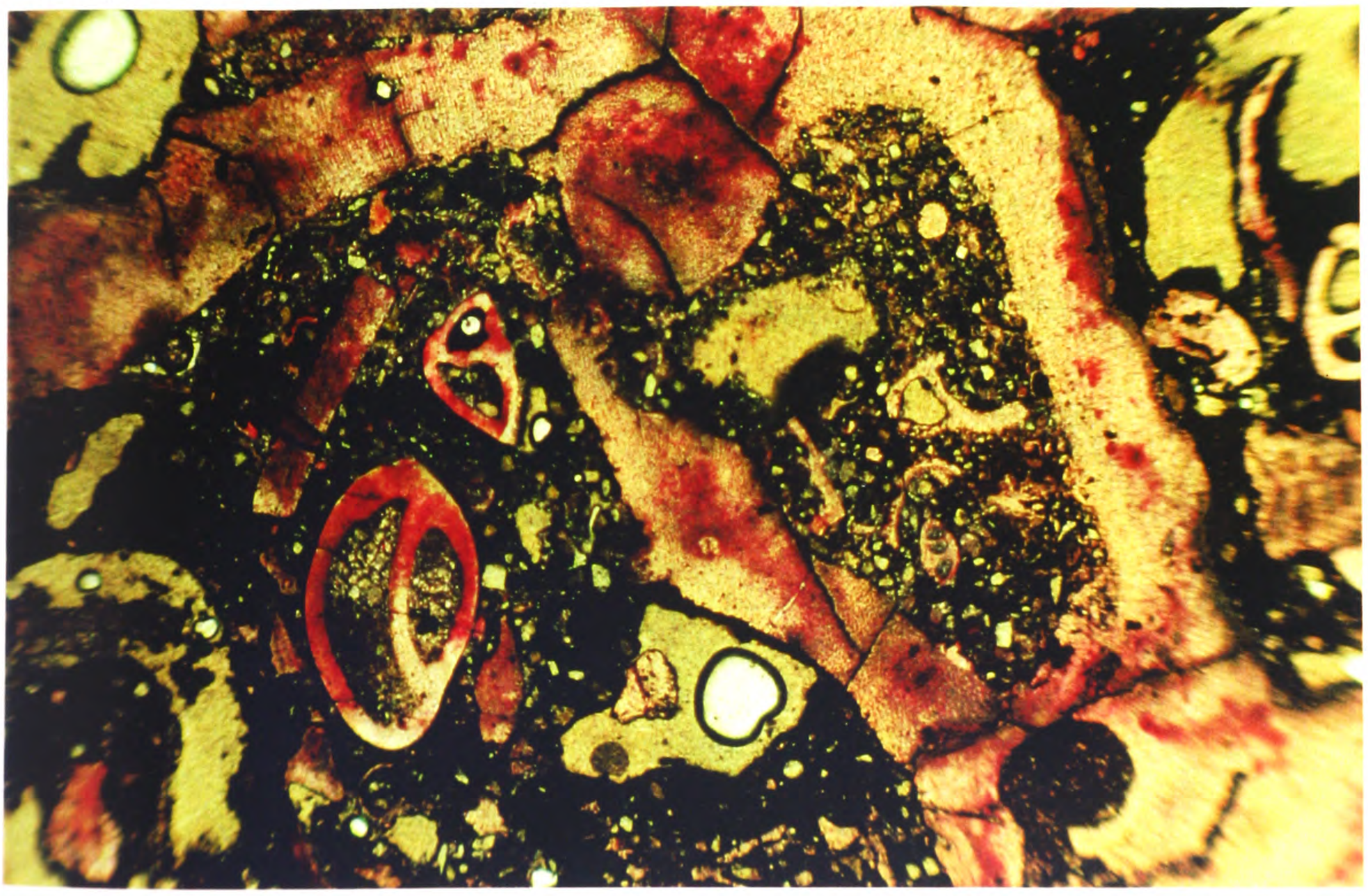

Figure 6.17.2: Algal boundstone: Note the boring of the algal framework (lower right) and the presence of miliolid foraminifera in the sediment. Intraskeletal cavities of the foraminiferum in the centre of the photograph were filled with geopetal matrix (lower part), followed by equant spar cement (upper part). Middle Pleistocene, Messenia (etched sample *Lim 2*: Limenari). Scale 1 mm across.

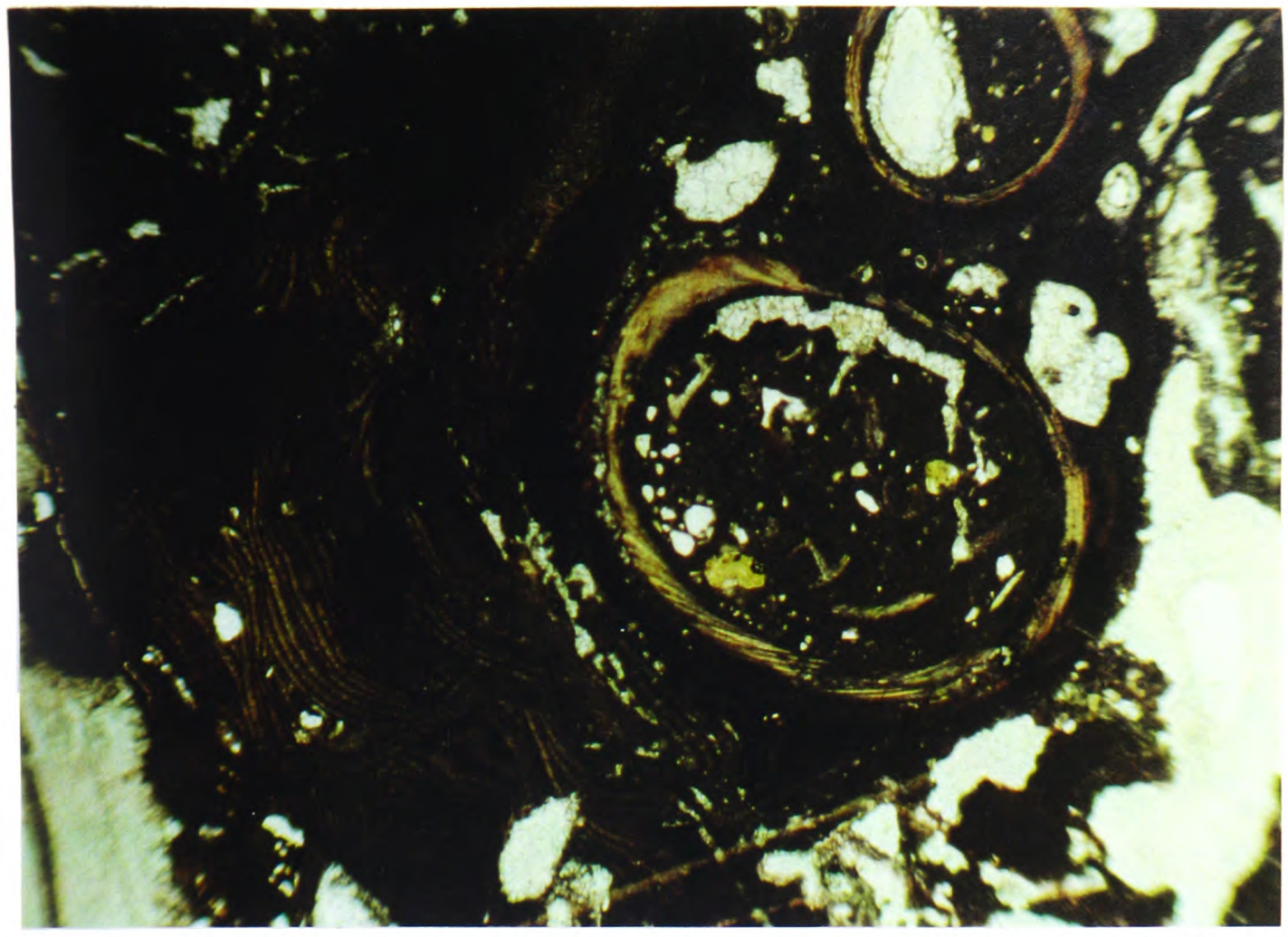

Figure. 6.18.1: Algal boundstone: An encrusting succession, from the outer (left) to the inner (right) part of the crust includes *Lithophyllum* sp., *Mesophyllum* sp. and serpulid tubes. Although pores in the encrusting framework were sealed with equant-dusy spar, a pore in matrix within a serpulid tube (upper right) was only reduced with cement. This might indicate a succession of dissolution/cementation events. Eutyrrhenian, Eastern Lakonia (sample *BoReT1*: Bozas Rema). Scale: 0.80 mm across.

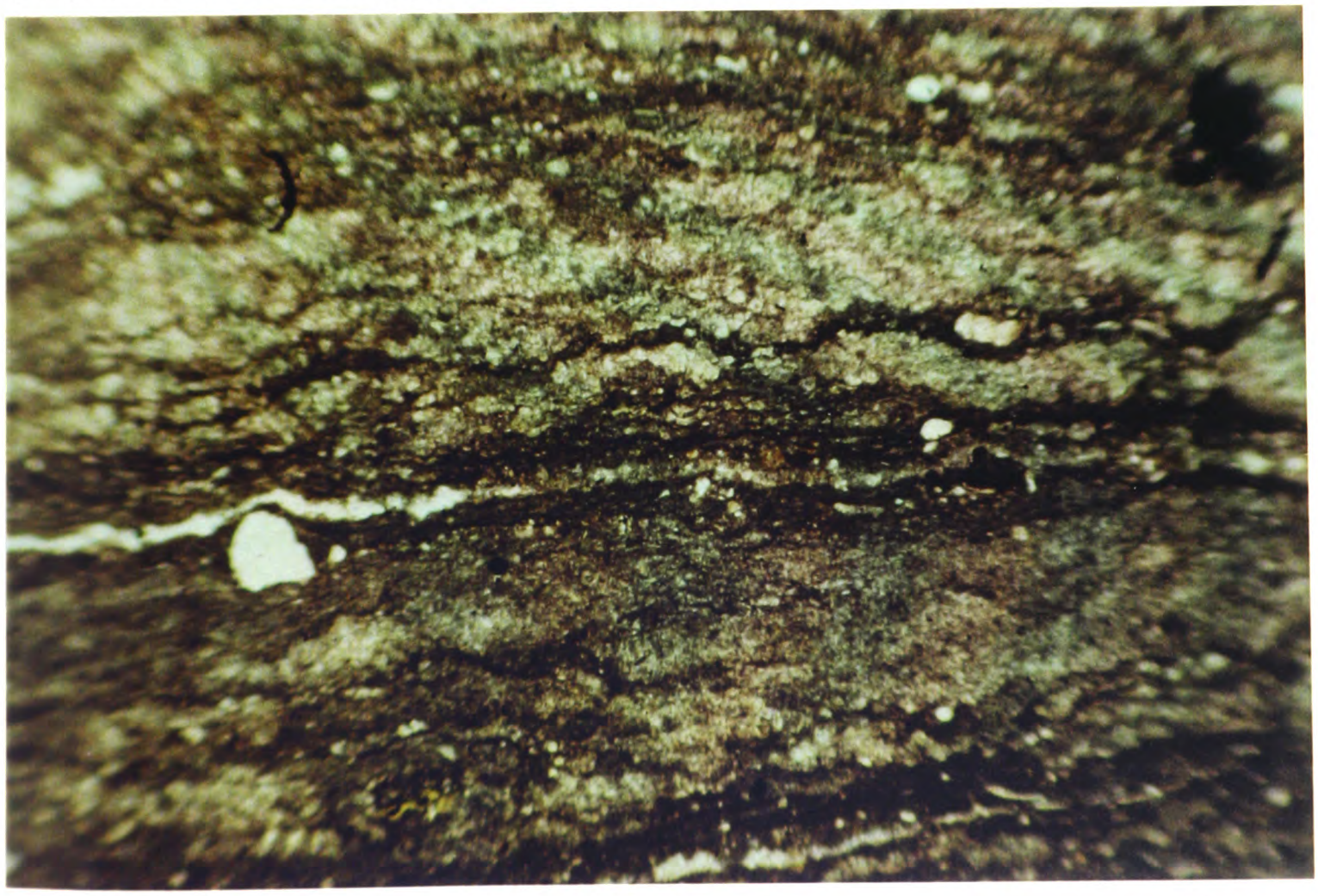

Figure 6.18.2: Caliche hardpan: Note the laminated microstructure, probably resulting from microbial activity. Early or middle Pleistocene, Eastern Lakonia (sample *Glf 17*: Glifada). Scale: 1mm across.

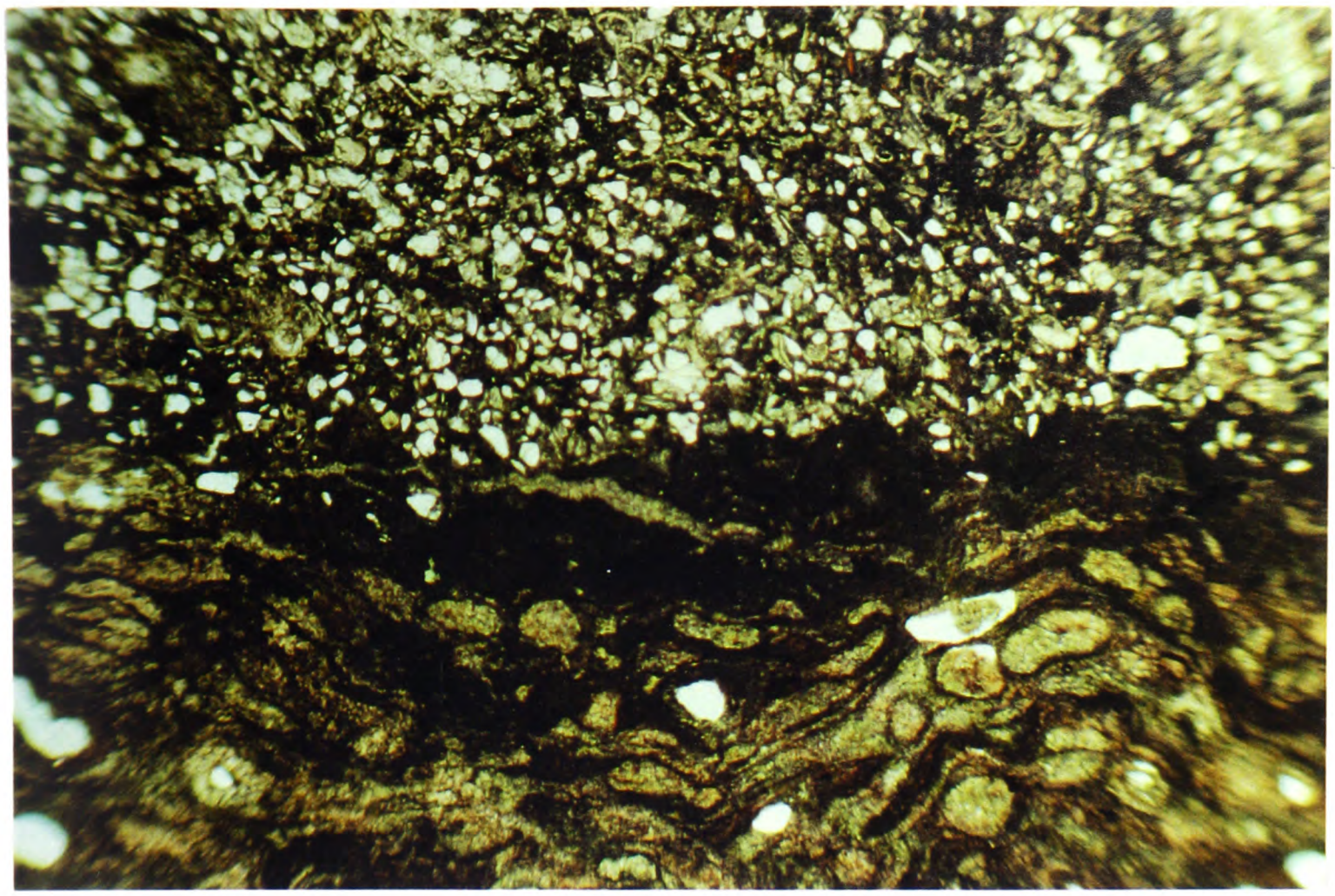

Figure 6.19.1: *Rhizocretion* caliche (lower part) and fine-grained, well-sorted aeolian sandstone (upper part). Wind-blown terrigenous grains were probably trapped on microbial mats View of the Holocene bindstone carapaces also shown in Fig, 5.40. Eastern Lakonia (sample *AyMar 3*: Ayia Marina). Scale: 1 mm across.

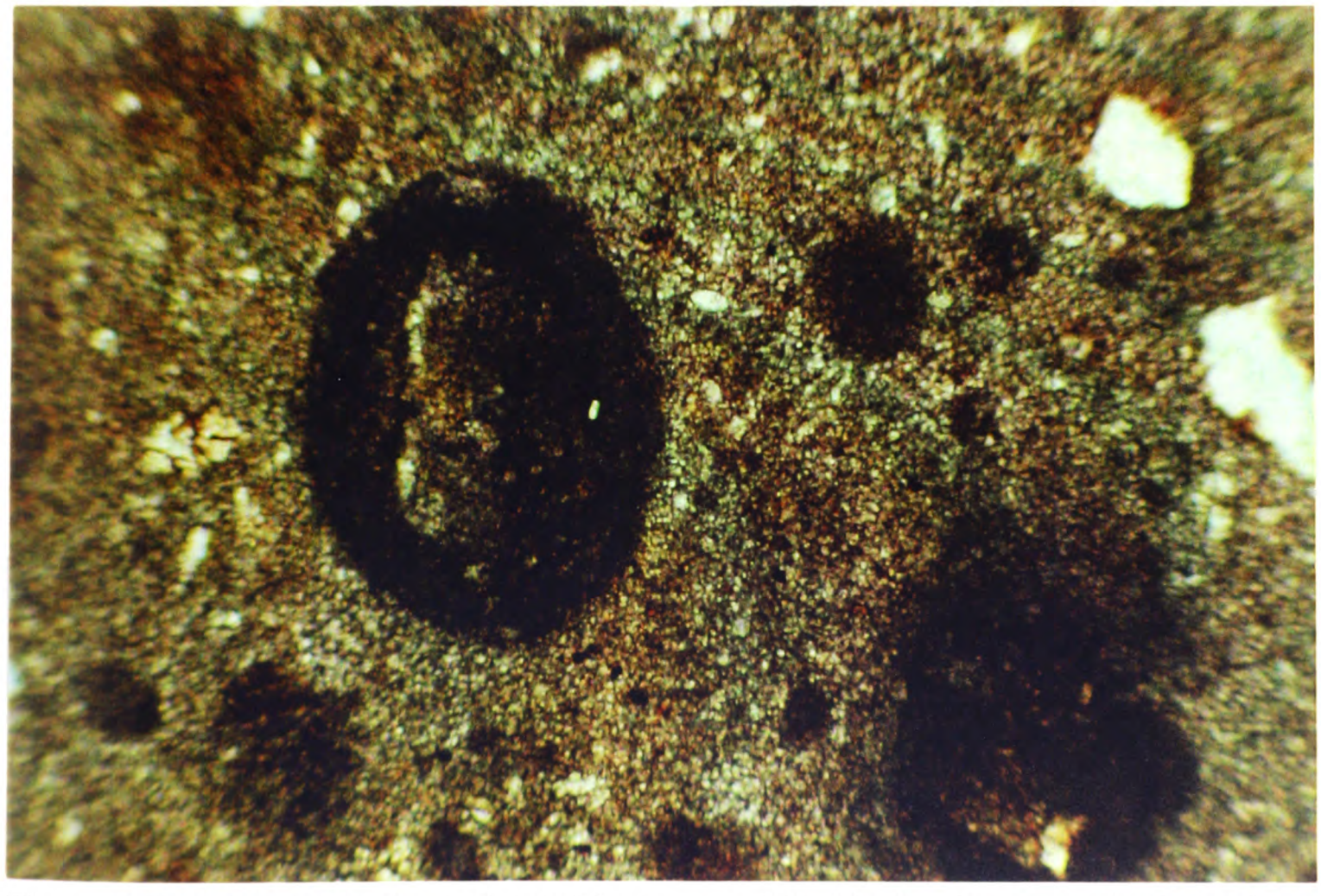

Figure. 6.19.2: Caliche hardpan of pissolithic texture: Micritised carbonate grains (centre) float in a mass of microcrystalline spar and micrite. Early or middle Pleistocene, Messenia (sample P.I.4: Prophitis Ilias). Scale: 1 mm across.

CHAPTER 7: PLIOCENE-QUATERNARY EVOLUTION OF THE MESSENIA AND EASTERN LAKONIA PENINSUALE, SOUTH PELOPONNESE: CORRELATION AND SYNTHESIS

7.1: INTRODUCTION

This chapter combines sedimentological, petrological, geomorphological and tectonic data, presented in previous chapters, in a correlation and synthesis of the evolution of the Messenia and Eastern Lakonia Peninsulae during the Pliocene-Quaternary. The pages that follow address the issue of the principal controls in the sedimentation and geomorphic development of the Messenia and Eastern Lakonia Peninsulae.

7.2: CORRELATION BETWEEN THE MESSENIA AND EASTERN LAKONIA PENINSULAE

As discussed in Chapters 3 and 5, Pliocene-Pleistocene stratigraphic units in the Messenia and Eastern Lakonia Peninsulae were established independently, based on various lines of evidence (published and new micropalaeontological data, outcrop relations, geomorphology), and their interpretation through a sequence-stratigraphic approach. The same sequence-stratigraphic approach, utilised for both Peninsulae, leads to the correlation shown in Figure 7.1. This correlation is based on the following considerations:

1) Sediments of unequivocal Early Pliocene (Zanclean) age were, so far, reported only from the Messenia Peninsula (Frydas, 1990; Frydas and Bellas, 1994; Unit 1.4; Fig. 7.1.A). In the Eastern Lakonia Peninsula, Early Pliocene sediments were possibly deposited in cross-peninsular grabens (e.g. Molai Graben, Figs. 5.4, M.2; see also Dufaure, 1976); nevertheless, these sediments were either missed during previous work on the stratigraphy of the area, or they are not exposed.

2) Sediments of Late Pliocene (Piacenezian) age were reported from the Messenia Peninsula (Frydas, 1990, Frydas and Bellas, 1994; Unit 1.5; Fig. 7.1.A). Sediments of the same age were not, so far, reported from the Eastern Lakonia Peninsula.

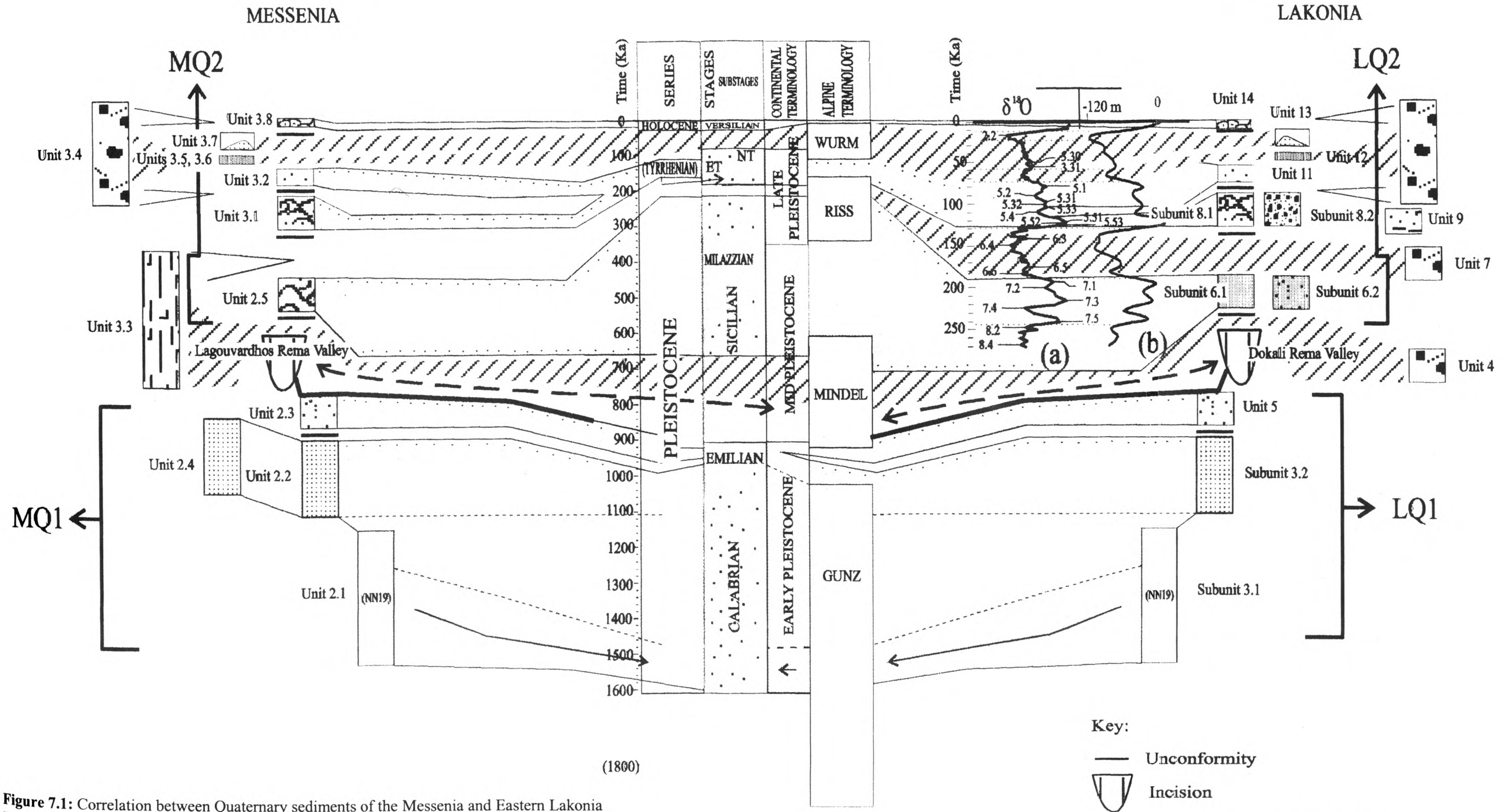

Figure 7.1: Correlation between Quaternary sediments of the Messenia and Eastern Lakonia Peninsulae. Pleistocene sediments are resolved into two 3rd-order sequences, corresponding to sea level cycles of early Pleistocene (MQ1, LQ1) and middle-late Pleistocene-Holocene (MQ2, LQ2) age. The post-middle Pleistocene sequence is further subdivided into three 4th order 'sequences' *s.l.* (formally parasequences), defined by disconformities (Messenia Peninsula) and/or subaerial horizons and soils (Eastern Lakonia Peninsula). Each of the latter sequences *s.l.* is correlated with peaks in the eustatic sea level curve during the last ca. 250 ka (curve b).

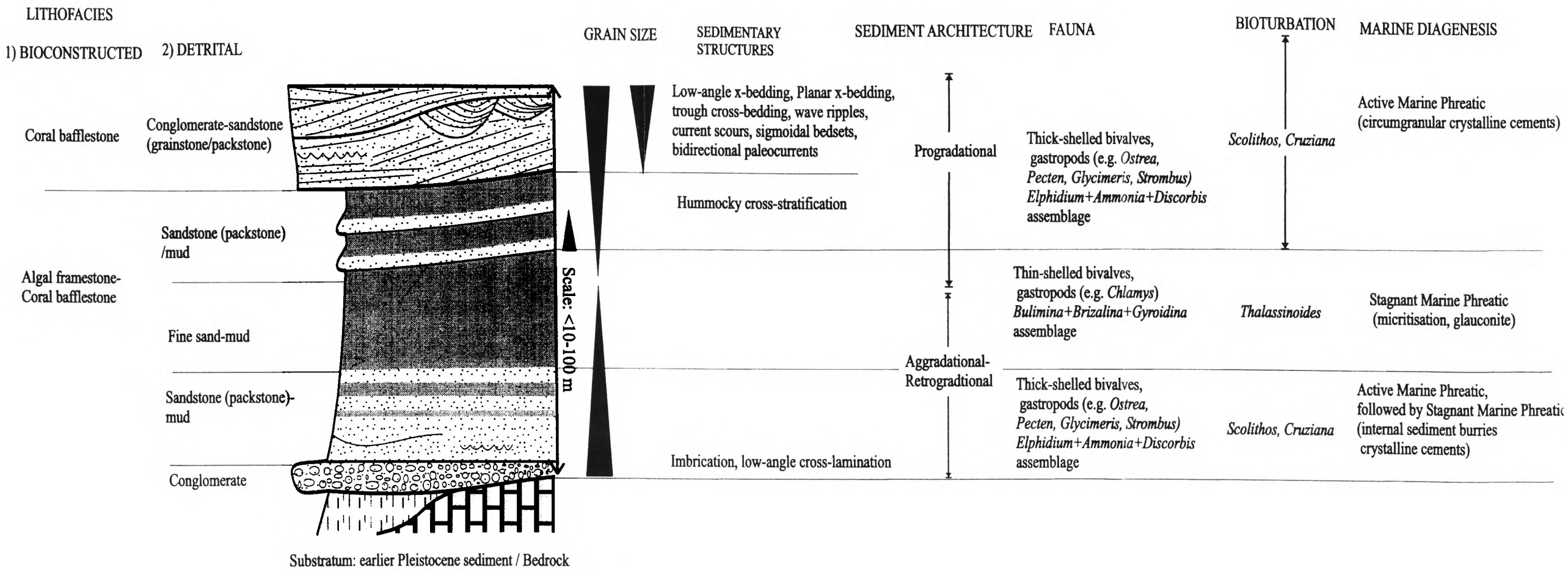

Figure 7.2: Summary of the sedimentology of Pleistocene terrace deposits in the Messenia and Eastern Lakonia Peninsulae. The emphasis is on detrital deposits, as these constitute the majority of terrace deposits in the two areas of study.

1) Terrace sediments overlie surfaces of erosion, on Tethyan bedrock, palaeosols, subaerial sediment, or, more commonly, older shallow-marine facies. On an outcrop-scale, these surfaces are commonly gently dipping. Where eroded on soft sediment substratum, the relief of these surfaces is even to slightly irregular (< 10 cm). However, these surfaces can be of very irregular, karstic relief, where eroded on bedrock limestone.

Interpretation: Gently-dipping, even surfaces of erosion, followed by marine sediment (see below) are interpreted as marine ravinement surfaces, eroded during transgression (Myers and Milton, 1996). Preservation of subaerial facies (e.g. palaeosols) under such surfaces probably suggests that the transgression was relatively rapid, so these subaerial facies did not remain within the foreshore zone long enough to be completely eroded. Highly irregular surfaces in carbonate substratum are interpreted as buried subaerial relief. Their preservation is also attributed to relatively rapid transgression.

2) Terrace sediment directly above basal erosion surfaces is commonly coarse-grained, including dense accumulations of well-rounded pebbles and abraded shells of thick-shelled, intralittoral molluscs. In these facies, early circumgranular cements of the active marine phreatic zone were followed by internal sediment (mud, micrite) of the stagnant marine phreatic zone.

Interpretation: These sediments are interpreted as basal lags, deposited in the foreshore during transgression. The succession of high-energy by low-energy diagenetic features is attributed to the subsequent removal of the sediment from the shoreline as sea level rose and the energy of the environment decreased.

3) Grain size decreases to fine-grained sand to mud up-sequence. This decrease is accompanied by decrease of high-energy sedimentary structures (e.g. wave scours), gradual predominance of circumlittoral to bathyal, commonly mud-dwelling macrofauna and microfauna, replacement of vertical burrows (*Skolithos* ichnofacies) by *Thalassinoides*, disappearance of marine phreatic cement, increasing micritisation of carbonate facies and presence of glauconite, especially within finest-grained facies.

Interpretation: All the above characteristics indicate that these facies were deposited under conditions of increasing water depth. Most were probably deposited within lower shoreface to offshore depth, below the fair-weather wave base, as suggested by benthic fauna, diagenesis in the stagnant marine phreatic zone and absence of wave-induced sedimentary

structures. Greyish sediment colours and the presence of glauconite suggest sub-oxic conditions at, or directly below, the sediment-water interface (Berner, 1981). The finest-grained beds, of the most distal facies characteristics, are interpreted as deposits of the maximum flooding zone (*sensu* Reynolds, 1996), deposited when the relative sea level attained its highest value (Reynolds, 1996; Myers and Milton, 1996). Following this interpretation, the part of the sequence from the marine ravinement surface to the maximum flooding zone represents the transgressive systems tract of the corresponding sea level cycle (Myers and Milton, 1996; Reynolds, 1996).

4) The finest-grained beds within the sequence are followed by coarse-grained facies up section. In some outcrops these two are bounded by sharp contacts, of even, or slightly undulating, relief. In other sections, these sharp contacts are preceded by alternations of bioturbated sand with mud, of an overall progradational architecture. Sandy beds are commonly rich in mollusc shells. Transitional contacts with the overlying coarse-grained facies (see below) are accomplished through gradual decrease in the thickness of mud beds and amalgamation of sand beds up section.

Interpretation: Sharp contacts between the deepest marine beds of the sequence, below, and progradational, shallower-marine facies, above, are interpreted as maximum flooding surfaces (*sensu* Myers and Milton, 1996). In sections that exhibit more transitional contacts, where fine-grained beds are followed by progradational clinoforms of alternating fine- with coarse-grained beds, the maximum flooding surface is located at the base of the first progradational bed. Field evidence, however, from the areas of study, rarely allows such precision. The progradational clinoforms that come above are interpreted as deposits of the upper offshore (offshore-shoreface transition; see Chapters 3, 5). These beds were probably deposited in a storm-influenced setting, below the fair weather wave base, but commonly above the storm wave base; increasingly so further up section, as indicated by hummocky cross-stratification and mixed intralittoral and circumlittoral faunal assemblages.

5) Terrace successions commonly terminate with coarse-grained (sand to pebble size) facies up section. The sediment architecture is progradational and high-energy, wave- and current-generated structures are abundant (e.g. wave ripples, reactivation surfaces, current scours, planar and trough cross-bedding, etc.). The fauna of these upper beds comprise thick-shelled molluscs, commonly abraded, and benthic foraminifera of the *Ammonia+Elphidium* faunal assemblage (*sensu* Amorosi et al., 1998). Bioturbation varies in intensity, comprising mainly *Thalassinoides* burrows in the lower parts and *Cruziana* and *Skolithos* burrows in the upper

parts, although successions of burrow types greatly depend on lithofacies. Early marine cements suggest deposition in the active marine phreatic zone, with precipitation of circumgranular rims of high-Mg calcite and aragonite and less micritisation, as compared with the underlying beds. A coarsening upward trend is evident in many sections. The uppermost beds are commonly low-angle planar cross-laminated sandstones-conglomerates, with evidence for bidirectional palaeocurrents. Alternatively, these uppermost beds comprise bioconstructed facies (e.g. coral-algal bafflestone, algal-coral framestone), draped by thin beds of progradational detrital facies (Chapters 3, 5, 6).

Interpretation: On the basis of their sediment structures, fauna and active marine phreatic diagenesis, these sediments are interpreted as shoreface, to foreshore, deposits. All the above characters suggest deposition under progressively shallower water conditions, which, given the progradational architecture of the deposits, were brought about by shoreline progradation. These sediments are, thus, interpreted as the highstand systems tract of the corresponding sea level cycle, deposited during highstand or early stages of sea level fall (Myers and Milton, 1996; Reynolds, 1996).

6) The above facies are followed by fluvial sediments, locally prograded over marginal marine (lagoonal) facies (e.g. Subunit 2.2.3 in the Messenia Peninsula; see Chapter 3).

Interpretation: The presence of fluvial sediments prograding over shallow-marine sediments below, without any marked unconformity suggest continuous progradation of an alluvial plain. These sediments are, thus, interpreted as parts of the highstand systems tract of the corresponding sea level cycle. On the grounds of grain size, sediment structures and depositional architecture, these sediments are interpreted as braid stream deposits (Mial 1978; 1992; see Chapters 3, 5).

7) Terraces are also covered by unconformable alluvial facies (red alluvia, red palaeosols) and, the two youngest ones ("Eutyrrhenian" and "Neotyrrhenian"), by aeolianite. Red alluvia commonly comprise alternations of tabular beds of clast-supported conglomerates with red silt, of an overall coarsening-up character. These sediments fill channels, or bury irregular relief, eroded in the underlying shallow-marine sediments of the terrace succession. Their depositional geometry is generally progradational in their upper parts; their lower-middle parts, however, commonly exhibit aggradational geometry. Palaeosols, developed over both shallow-marine and terrestrial sediments, are dominated by various caliche types,

according to the age of the host sediment, host lithology and proximity to the surface (Chapter 6).

Interpretation: Channels and associated irregular relief on marine terraces are interpreted as subaerial in origin, eroded after emergence of the terraces, during sea level fall. Fluvial sediments that fill these channels are braidstream deposits. Their markedly bipolar grain size (silt-mud vs. conglomerate) coarsening up trends suggest that these sediments were deposited episodically, in a prograding midfan to proximal fan environment (Miall, 1978, 1992; Poole and Robertson, 1995). These sediments are correlated with the lowstand systems tract of the successive sea level cycle (Myers and Milton, 1996); their deposition took place during lowstand, or the first stages of relative sea level rise.

From the above is, thus, evident that Pleistocene terrace successions in the Messenia and Eastern Lakonia Peninsulae can be interpreted in sequence-stratigraphic terms. The common presence of identifiable systems tracts in terraces of both Peninsulae, irrespective of facies and age, suggests that sea level cyclicity was the dominant control in terrace formation. Regional correlation of marine terraces suggests that relative sea level change that controlled the formation of marine terraces, had a dominant eustatic component. Wherever terrace flights are present, the principal four to five marine terraces shown in Figure 7.3 can be identified and correlated. Consequently, local relative sea level histories did not deviate much from the general pattern, established for both Peninsulae. Local deviations were, instead, reflected in different number of mainly, but not exclusively, erosive terraces; the latter differ in number from area to area and cannot be correlated regionally. It is assumed that different number of erosive terraces reflect different rates of vertical movement of fault-bounded blocks, in agreement with Zelilidis (1988). An alternative explanation could be that these terraces correspond to short-lived stillstands, correlated with unresolved, high-frequency sea level cycles. Following the latter interpretation, differences in their number reflect local differences in preservation/erosion of such terraces and not relative sea level histories of fault-bounded blocks. This cannot be resolved without radiometric dating and large-scale mapping of these terraces, both unavailable at present.

7.3.2: Terrace flight architecture: Focusing on the five principal, regionally correlated marine terraces, there is a pattern of terrace-flight architecture, common in both the Messenia and Eastern Lakonia Peninsulae (Fig. 7.3). The highest terrace, of inferred early Pleistocene age (see above), is formed above an aggradational, then progradational,

transgressive-regressive sequence (Units 2.1. 2.2, 2.4 and Unit 3, in the Messenia and Eastern Lakonia, respectively). The second terrace, of inferred late-early (Emilian), or early-middle Pleistocene age (Units 2.3, 5), is dominated by progradational bedsets. This terrace rests on sediments of the early Pleistocene terrace; commonly on the upper, progradational bedsets, but it is not separated from the early Pleistocene terrace by conspicuous cliffs. Wherever these cliffs were observed, their height is <10 m. All younger terraces, of inferred middle to late Pleistocene age (Units 2.5, 3.1, 3.2 and Units 6, 8, 11 in Messenia and Eastern Lakonia, respectively) are dominated by progradational bedsets; aggradational bedsets are present, but considerably thinner. These terraces are present at altitudes considerably lower than the early and late-early (or early-middle) Pleistocene terraces (cliff height: 60 to >120 m; Fig. 7.3). These three terraces are commonly separated from each other by conspicuous cliffs, with the exception of the youngest, "Neotyrrhenian" terrace, that appears to be stacked on the "Eutyrrhenian" terrace locally (Kowalczyk et al, 1992). Wherever middle and late Pleistocene terrace sediments are in contact with earlier Pleistocene terraces, they rest unconformably on offshore facies of the lower, aggradational part of the early Pleistocene marine terrace. Terrace flights in both Messenia and Eastern Lakonia, thus, comprise a thick, widespread aggradational-progradational sequence and three to four, mainly progradational sequences, in gradually decreasing altitude with decreasing age of deposition.

Figure 7.3 (following page): Quaternary forced regression in the Messenia and Eastern Lakonia Peninsulae. The early Pleistocene sea level cycle 3.9 (*sensu* Haq et al., 1988), resulted into the deposition of the 3rd-order sequence **Q1**. The middle Pleistocene-Present sea level cycle 3.10 resulted in the deposition of the 3rd-order sequence **Q2**. The sequences **Q1** and **Q2** are separated with erosional relief of up to 120 m; **Q2** shorelines were deposited above **Q1** offshore facies. This detachment of **Q1** and **Q2** shorelines suggests that much of the uplift of the two Peninsulae tool place in the earlier part of the middle Pleistocene, after emergence of the sequence **Q1** and before deposition of the sequence **Q2**. The sequence **Q2** is further divided into at least four 4th or higher order 'sequences' (parasequences *s.s.*), namely **3:** Sicilian (4th order), **4+5:** Tyrrhenian (4th order, subdivided into **4:** "Eutyrrhenian and **5:** "Neotyrrhenian") and Holocene (a raised beach). These are shown as sequences **(3)** to **(5** in the diagram. The 3rd order sequence **Q1** is subdivided into at least two higher order sequences: The oldest **(1)** is attributed to the early Pleistocene ("Calabrian"), the latest **(2)** is attributed either to the latest part of early Pleistocene, or to a 4th order sea level cycle at the beginning of the middle Pleistocene. Fourth and higher-order 'sequences' are attached to each other (i.e. successively younger deposits are of the same facies belt as their underlying deposits), showing that uplift between the formation of each terrace was moderate. These overall regressive sediments reflect the interplay between land uplift and eustatic sea level cyclicity.

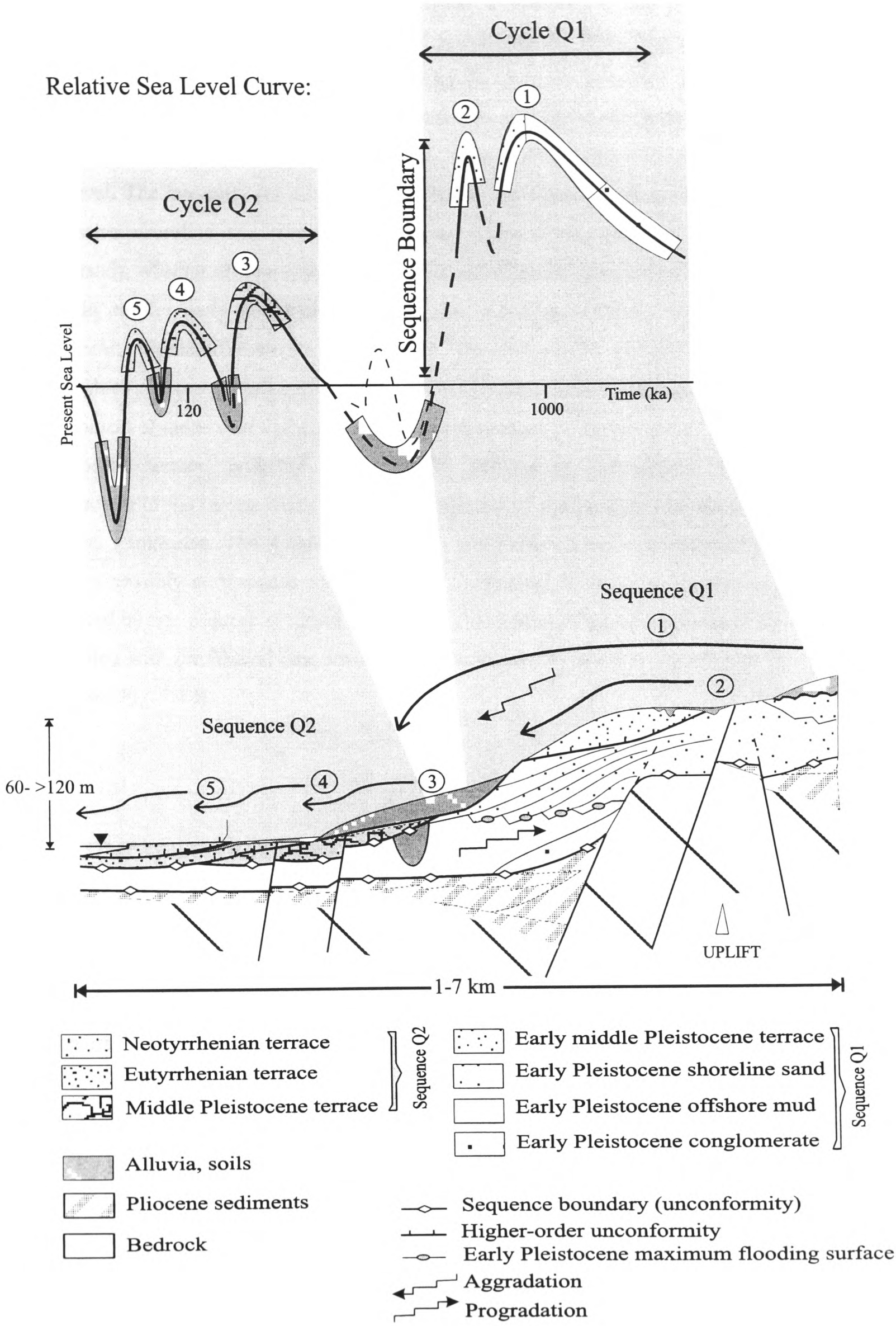
Relative Sea Level Curve:
Cycle Q1
Cycle Q2
Sequence Boundary
Present Sea Level
Time (ka)
120
1000
Sequence Q1
Sequence Q2
60- >120 m
UPLIFT
1-7 km
Neotyrrhenian terrace
Eutyrrhenian terrace
Middle Pleistocene terrace
Sequence Q2
Early middle Pleistocene terrace
Early Pleistocene shoreline sand
Early Pleistocene offshore mud
Early Pleistocene conglomerate
Sequence Q1
Alluvia, soils
Pliocene sediments
Bedrock
Sequence boundary (unconformity)
Higher-order unconformity
Early Pleistocene maximum flooding surface
Aggradation
Progradation

Interpretation: Terrace flights, of depositional architecture as described above, can be interpreted as a forced regressive sequence set (Reynolds, 1996; Hanke, 1999), resulting from superposition of glacio-eustatic cyclicity on longer-term crustal uplift. Any terrace younger than the early Pleistocene is regressive in relation to the latter, deposited further seawards and at progressively lower altitudes, in reference to the early Pleistocene relative sea level. The late-early (or early-middle) Pleistocene terrace is, thus, an attached forced-regressive shoreline (i.e. overlying shoreline facies of the previous early Pleistocene highstand), whereas all lower/younger terraces are detached forced-regressive shorelines in relation to the early Pleistocene terrace (i.e. overlying offshore facies of the early Pleistocene highstand; *sensu* Reynolds, 1996). The three middle to late Pleistocene terraces themselves also constitute a set of attached forced-regressive shorelines. It is evident that the detachment of the terrace flight took place after deposition of the late-early (or early-middle) Pleistocene terrace, probably during middle Pleistocene, but before "Sicilian". The architecture of the terrace flight was, thus, controlled by uplift of the Messenia and Eastern Lakonia Peninsulae. The middle Pleistocene, pre-Sicilian time of detachment of marine terraces possibly corresponds to a period of accelerated uplift, with its effects possibly enhanced by one or more sea level lowstands. This period of erosional downcutting can be correlated with the Mindel-Riss lowstand in traditional Pleistocene stratigraphy (Bonifay, 1975; see Fig. 7.1.I).

7.4: COMPARISON BETWEEN THE MESSENIA AND EASTERN LAKONIA PENINSULAE

First-order similarities in the sedimentary and geomorphological record of Messenia and Eastern Lakonia notwithstanding, cross-peninsular differences imply different local patterns of evolution during Pliocene-Pleistocene, possibly resulting from different tectonic conditions.

7.4.1: Fault spacing: Figures 7.4, 7.5 show the spacing between peninsula-parallel (NNW-SSE, N-S to NE-SW) and cross-peninsular (ENE-WSW, NE-SW) normal faults of mappable dimensions (longer than 500 m) in the Messenia (Fig. 7.4) and the Eastern Lakonia Peninsulae (Fig. 7.5). Despite the significant difference in sample size (62 faults in Messenia; 289 faults in Eastern Lakonia), both plots reveal essentially identical patterns, with mappable faults clustering in five distinct classes:

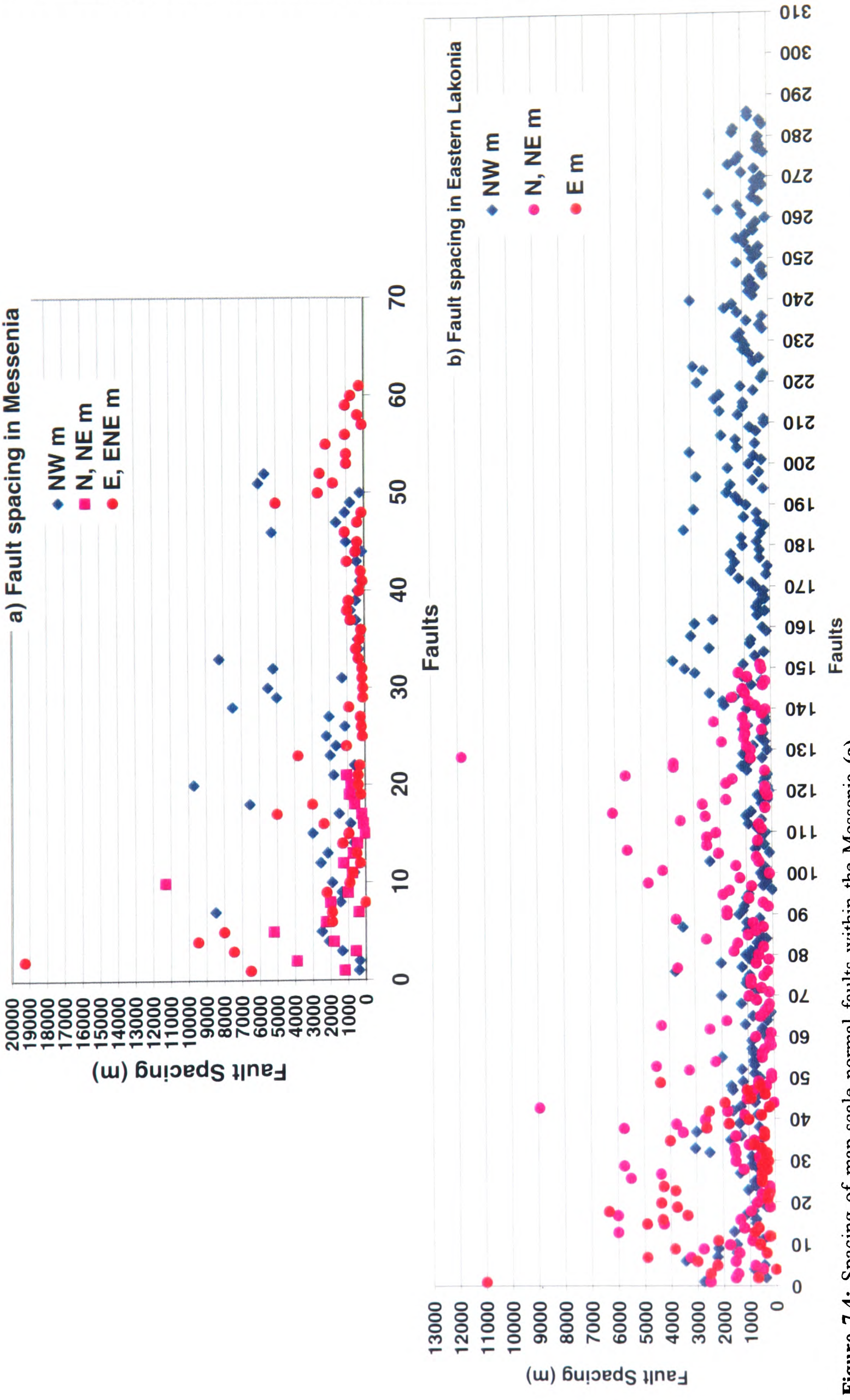

Figure 7.4: Spacing of map-scale normal faults within the Messenia (**a**) and the Eastern Lakonia Peninsulae (**b**).

1) Closely-spaced faults, <1000 m, are the commonest in both Peninsulae. This predominance of closely spaced faults is observed in faults of all direction-groups.

2) Faults spaced from 1000-3000 m are the second commonest in both Peninsulae, again irrespective of direction group.

3) Faults spaced from 3000-7000 m are relatively more abundant in the Messenia Peninsula than in the Eastern Lakonia Peninsula. In both Peninsulae, most faults of this class trend E-W. Peninsula-parallel faults of this group are more common in the Messenia Peninsula than in the Eastern Lakonia Peninsula. No NW-SE faults of spacing at every 3000-7000 m are mapped in the Eastern Lakonia Peninsula.

4) Faults spaced from 7000-12000 m are relatively rare in both Peninsulae, but remarkably more common in the Messenia than in the Eastern Lakonia Peninsula, despite the far larger sample size of the latter. In both Peninsulae, this group is dominated by peninsula-parallel faults (NNW-SSE, NW-SE and NNE-SSW).

5) Faults spaced every >12000 m are the rarest in both Peninsulae, more common, however, in Messenia than in Eastern Lakonia. The maximum determined fault spacing is also considerably higher in Messenia (ca. 19200 m) than in Eastern Lakonia (ca. 11900 m). Most widely spaced faults are of cross-peninsular (ENE-WSW) direction in the Messenia Peninsula and of peninsula-parallel (NW-SE and N-S) direction in the Eastern Lakonia Peninsula.

These observations suggest that the upper crust in the Eastern Lakonia Peninsula is more densely faulted as compared with the Messenia Peninsula. This is not unexpected, given the more "internal" location of Eastern Lakonia, distant from the plate boundary and proximal to the thinned crust of the Aegean Sea. Lacking chronostratigraphic data from offshore settings (i.e. Argolic, Lakonic and Messenian Gulfs; see Fig. 1.1), it cannot be concluded whether closer fault spacing in Eastern Lakonia reflects locally more intense extension, or earlier initiation of extension and graben formation. The latter interpretation, involving westward migration of extension through time (toward the plate boundary), would make the Late Neogene evolution of the SW Aegean Arc comparable to that of the Tyrrhenian Basin-Calabrian Arc system (Kastens and Mascle, 1990; Spadini and Podlachikov, 1996) as also to the Cyprus Arc (Payne and Robertson, 1995, 2000) (see Chapter 8).

7.4.2. Initiation of deposition: As noted above, no unambiguous pre-Pleistocene sediments were reported from the Eastern Lakonia Peninsula, although Early Pliocene (Zanclean) sediments are present in the Messenia Peninsula (Jacobschagen et al., 1978; Frydas, 1990, 1993; Frydas and Bellas, 1994; Zelilidis and Doutsos, 1992). The reported sediments are offshore facies, deposited in grabens controlled mainly by peninsula-parallel (NNW-SSE) faults, and fewer cross-peninsular (ENE-WSW and NE-SW) faults (I.G.E.Y., 1970; Jacobschagen et al., 1978; I.G.M.E., 1980a,b, 1984; Zelilidis, 1988; Zelilidis and Poulimenos, 1996; Zelilidis and Doutsos, 1992). The absence of dated Pliocene outcrops from the Eastern Lakonia Peninsula could be interpreted as indicating earlier initiation of graben formation in the Messenia Peninsula further west. However, such an interpretation would ignore the limited extent of the existing chronological evidence and the markedly more faulted state of the upper crust in the Eastern Lakonia Peninsula (Figs. 7.4, 7.5, M.1, M.2), that suggests a longer history of normal faulting in that area (see above). It is probable that pre-Quaternary sediments in the Eastern Lakonia Peninsula are currently below sea level, caused to subside by peninsula-parallel, NNW-SSE faults that control the eastern flank of the Lakonic Gulf (Mascle et al., 1982; Figs. 1.1, M.1). This interpretation entails that the bottom of the Lakonic Gulf underwent more extreme extension than that of the Messenian Gulf. Offshore evidence from the Argolic Gulf, east of the Eastern Lakonia Peninsula (see Fig. 1.1), suggest that the deposition of the >400 m thick basin fill probably started in latest Miocene-Early Pliocene (Papanikolaou et al., 1994). At a smaller, intrapeninsular scale, a similar westward progress of extensional deformation through Pliocene-Pleistocene is also inferred within the Messenia Peninsula, where grabens along the SE coast of the peninsula appear to predate those of the NW coast (Zelilidis and Doutsos, 1996; Kourampas and Robertson, 2000; Chapter 3).

7.4.3. Shallow-marine facies: Although shallow-marine facies of Pleistocene age are very similar across the two Peninsulae, sediments tend to be systematically more terrigenous in the Eastern Lakonia Peninsula. As demonstrated from point-counting results (Appendix B), sandstone and terrigenous rich, mixed carbonate-siliciclastic facies prevail in the Eastern Lakonia Peninsula. In the Messenia Peninsula, by contrast, the commonest facies are packstones and algal boundstones (Chapter 6). This compositional difference is noticeable in sediments of any Pleistocene stage and is particularly marked in sediments of the "Eutyrrhenian" and "Neotyrrhenian" stages. Thus, typical "Eutyrrhenian" sediments comprise sandstone and terrigenous-rich coral bafflestone facies in the Eastern Lakonia Peninsula (Unit 8, Fig. 7.1.B; see also Chapters 5, 6) and algal boundstone or grainstone facies in the Messenia Peninsula (Unit 3.1, Fig. 7.1.A; see also Chapters 3, 6). Typical

"Neotyrrhenian" sediments comprise sandstone and conglomerate in the Eastern Lakonia Peninsula (Unit 11, Fig. 7.1.B; Chapters 5, 6) and grainstone in the Messenia Peninsula (Unit 3.2, Fig. 7.1.A; Chapters 3, 6). This compositional difference may reflect different bedrock lithologies in the two Peninsulae (phyllite and greenschists in Eastern Lakonia versus 'flysch' and radiolarian chert in Messenia; see Figs. 2.1, 3.5, 3.6, 4.1, 5.4, 5.5). This may, however, reflect the denser fault pattern of the Eastern Lakonia Peninsula, which probably resulted in higher clastic input into marine depocentres.

7.4.4. Alluvial sediments: Alluvial sediments are present in both Peninsulae, mainly in the form of braid-stream facies, associated with alluvial fans (Chapters 3, 5). However, alluvial sediments are far more widespread in the Eastern Lakonia Peninsula than in the Messenia Peninsula (Figs. M.1, M.2). Alluvial fans are related to steep slopes, which, in both areas of study, are mainly fault-controlled (Chapters 2, 4). Their wider spread within the Eastern Lakonia Peninsula is attributed to the denser fault pattern in the area (Chapter 4), with more closely spaced faults (Figs. 7.4, 7.5, M.1, M.2). Smaller dimensions of fault blocks in the Eastern Lakonia Peninsula, in contrast with those of the Messenia Peninsula (see Chapters 2, 4), resulted in higher ratios of steep slopes per unit area, a condition expected to facilitate alluvial fan deposition. Similar normal faulting controls on alluvial fan deposition were proposed for the Plio-Quaternary of the Messaoria Basin, Cyprus (McCallum, 1989; McCallum and Robertson, 1995) and Vera Basin, SE Spain (Stokes and Muther, 2000).

7.5: RATE OF UPLIFT

Quantification of uplift rates cannot be precise without firm geochronological evidence. Such evidence from the areas of study is still lacking. Furthermore, in areas segmented by normal faults into blocks of semi-indepented evolution (see Chapters 2, 4), it is more meaningful to discuss uplift rates of individual blocks rather than uplift rates at a regional scale. The interpeninsular correlation presented above, however, provides potential age constrains for major depositional units in both Peninsulae. The present-day elevation of these depositional units was constrained in the field, with resolution of ±10 m. An estimation of the depositional depth for each of the latter units was reached through interpretation of their sedimentary facies and faunas (Chapters 3, 5, 6). Therefore, the three variables necessary for the deduction of uplift rates (Collier, 1990; Collier et al., 1992; Keller and Pinter, 1996), are constrained, albeit loosely. Provided that the above constrains are valid, a generalised uplift rate for each of the two studied Peninsulae can be proposed. This model must allow for uncertainties in the age of middle Pleistocene terraces, different

number of identified terraces in each area and segmentation of the Messenia and Eastern Lakonia Peninsulae into fault-bounded blocks.

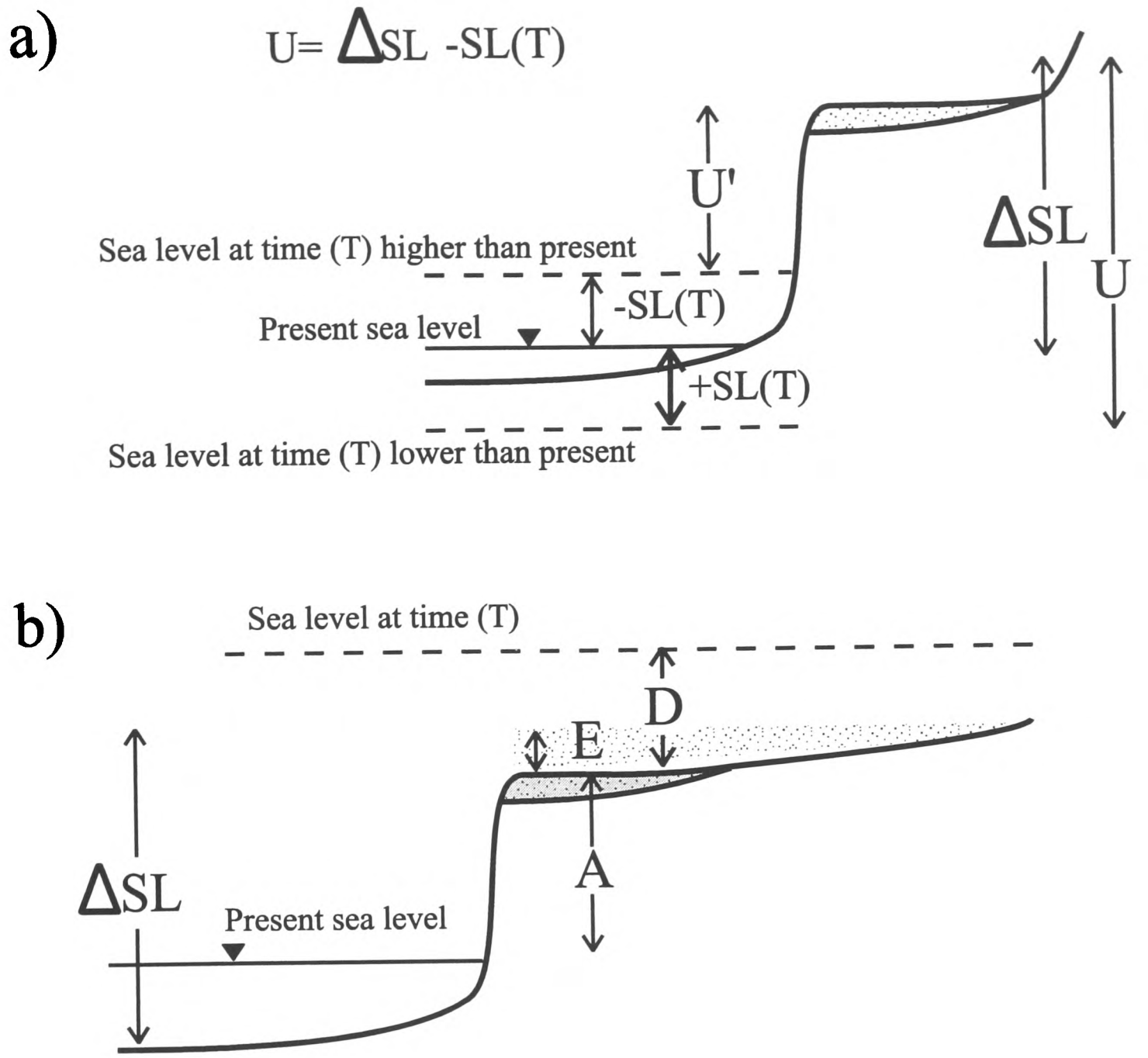

Figure 7.5: Variables taken into account for the calculation of uplift rate (see text for explanation).

Before introducing the method of deduction of uplift rate its actual meaning should be discussed. In the Peloponnese, as in other forearc areas (e.g. Crete, Cyprus, Taiwan, Japan), Quaternary vertical movements were the net result of land uplift, probably due to crustal underplating by the subducting slab, normal faulting, and isostatic readjustment of the crust in response to asthenospheric flow since the last glaciation (Flemming, 1969, 1978; LePichon and Angelier, 1979; Ota, 1984; Collier, 1990; Collier et al., 1992; Keller and Pinter, 1996; Lambeck, 1995; see also Chapter 1). Some of these components of net vertical movement may have been mutually opposing (e.g. en-block land uplift versus hangingwall

subsidence along normal faults). Quantification of the relative contribution of each of the above factors to the net uplift (or subsidence) can be very difficult. In studies where sea level indicators are used to constrain vertical movement (Van de Plassche, 1986) additional uncertainty is introduced by the -often insecure- estimate of the actual amount of relative sea level change. The net relative sea level change (ΔSL) since the formation of a given sea level indicator is related to the net uplift (U) of the same sea level indicator through the equation:

$$\Delta SL = U + SL(T) \Rightarrow$$

$$\Rightarrow U = \Delta SL - SL(T), \qquad (1)$$

where SL(T) is the eustatic sea level during time (T) of formation of the sea level indicator, by reference to present sea level (Fig. 7.5.a). The sign of the value SL(T) is positive or negative, according to whether the sea level at time (T) was lower or higher than the present one, respectively. The value SL(T) can be derived from published sea level curves (e.g. Fig. 1.3)

7.5.1. Constructive marine terraces: In this study, the amount of relative sea level change (ΔSL) is derived from the present altitude of marine terraces. In general, the amplitude of relative sea level change (ΔSL) since the deposition of the corresponding terrace sediment equals the depth of deposition of the sediment (D), plus the present altitude of the outcrop (A), minus the thickness of sediment removed due to erosion after emergence (E) (Fig. 7.5.b), i.e.:

$$\Delta SL = D + A - E. \qquad (2)$$

7.5.1.1. Depositional depth: An estimation of the depositional depth (D) of a particular sedimentary facies can be inferred from trace fossils (Pemberton and Frey, 1991), benthic foraminifera (Blanc-Vernet, 1969; Murray, 1973), molluscan fauna (Georgiades-Dikeoulia, 1984) and other lines of sedimentological and palaeontological evidence (see Table 1.3; Chapter 1). In the course of the present study, sedimentary structures, benthic foraminifera (identified by Tsaila-Monopolis, pers. com., 1998) and, to a lesser extent, trace fossils were used to constrain the palaeobathymetry of any given facies (see Chapters 3, 5, 6). In most cases such evidence allowed an estimation of the broader palaeoenvironmental-palaeoecological zone of deposition (e.g. foreshore, shoreface), but not any precise palaeodepth range. Wherever benthic foraminifera were utilised as paleobathymentric indicators, only a minimum depositional depth was inferred from the presence of the most bathyal taxa (see Tables 3.1, 5.1).

The meaningfulness of any palaeobathymetric estimate depends on the resolution of distinct facies. While it is, thus, meaningful to discuss the depositional depth of a m-thick sediment body with uniform sedimentological characteristics, it is not meaningful to infer a precise depositional depth of a 10's of m thick clinoform-set, deposited on a primary slope with relief of several 10's of metres. Furthermore, in both areas of study, marine sediments underlying terrace surfaces record a history of changing sea level, controlled by glacio-eustatic sea level cyclicity and tectonics (Kourampas and Robertson, 2000; Chapters 3, 5). Although progradational sets of foreshore-shoreface facies, deposited during the highstand, are the most widespread, most terraces overlie deeper water facies, correlated with the highest sea level, attained during peak of the corresponding transgression ('maximum flooding'; Myers and Milton, 1996). In this work, the maximum estimated depth of transgressive sediments underlying a terrace is taken to represent the maximum depositional depth of the corresponding terrace (Dmax).

7.5.1.2. Erosion: The thickness of sediment removed due to erosion since emergence of each terrace is difficult to estimate (Jardine, 1986). This thickness would be expected to increase with increasing time of exposure, i.e. increasing age of the marine terrace. Most shallow-marine sequences, in both the Messenia and Eastern Lakonia Peninsulae, preserve foreshore-backshore facies up section, interpreted as the 'highstand systems tract' of transgressive-regressive sequences (Chapters 3, 5). The thickness of Quaternary shoreline sediment bodies in other Eastern Mediterranean areas commonly does not exceed ca. 20 m (Keraudren, 1970, 1971; Pirazzoli, 1986; Poole, 1991). This allows the inference that the thickness of sediment removed due to subaerial erosion in the Messenia and Eastern Lakonia Peninsulae did not exceed the top 10-20 m of the original successions. This value is well below the range of altitude variation for the highest/oldest (hence most eroded) terraces. In the case of the lowest/youngest (hence least eroded) terraces, the thickness of sediment removed due to erosion is expected to be even lower. The preservation of aeolianite and related backshore facies over shallow-marine sediments of latest Pleistocene ("Neotyrrhenian") age, in both the Messenia and Eastern Lakonia Peninsulae, suggests that subaerial erosion since the latest Pleistocene was not intense enough to remove any considerable thickness of marine deposits underlying the aeolianite. For the reasons stated above, the factor (E) is not taken into consideration for the calculation of the amount of relative sea level change. Thus, formula (2) is modified to the form:

$$\Delta SLmin = Dmax + A. \qquad (3)$$

7.5.2. Erosive marine terraces: In the case of erosive marine terraces, a distinction should be made between primarily erosive landforms, without sediment cover ("marine abrasion platforms"), and "striped marine terraces", with their sediment cover removed after emergence (Ahnert, 1998). In marine abrasion platforms, the mean sea level during the time of their formation coincides with the knick-point that separates the basis of the back-terrace cliff from the terrace platform (Keller and Pinter, 1996). The amount of relative sea level change (ΔSL) is, thus, given by the formula:

$$\Delta SL = A(kp), \qquad (5)$$

where A(kp) is the elevation of that knick-point above present sea level. In practice, however, this knick-point is commonly difficult to identify, due to erosion, soil cover and accumulation of colluvial wedges over the base of the cliff (Keller and Pinter, 1996). Although this knick-point can be estimated by extrapolation of large-scale morphological sections, such sections were not studied during the course of this study. As for "striped marine terraces", only a minimum estimation of the amount of relative sea level change can be attempted, since the previous discussion about the estimation of the thickness of eroded sediment is relevant to these terraces, as well.

7.5.3. Rate of uplift: The rate of uplift (RU) of any particular terrace (in m/ka), averaged over the time (T) since the formation of the terrace, is given by the equation:

$$RU = [_{(T)} \quad dU / dt] / T, \qquad (6)$$

where dU / dt is the instantaneous rate of uplift at any distinct point in time since the formation of the terrace. The time (T) is taken to coincide with the deposition of the deepest marine sedimentary facies in the case of "constructive" marine terraces and with the occurrence of the correlative mean sea level in the case of "marine abrasion platforms". The deposition of any transgressive-regressive shallow-marine sequence was diachronous, lasting as long as its correlative 3rd, or higher-order sea level cycle that controlled it (see Chapter 3). Since no absolute geochronological evidence is available from the Messenia and Eastern Lakonia Peninsulae (Chapters 3, 5), the time (T) since the formation of a given terrace is estimated as follows:

1) All biostratigraphicaly dated early Pleistocene sediments are contemporaneous with the 3rd order sea level cycle 3.9 *sensu* Haq et al. (1988) (Units 2 in Messenia; Units 3 in Eastern Lakonia; see Fig. 7.1). Progradational clinoforms, deposited during the highstand/early stages of sea level fall constitute the most prominent architectural element of these units.

The age of this progradational part, broadly contemporaneous with the peak of the sea level cycle 3.9, is taken to represent the age of the early Pleistocene terrace.

2) Late-middle ("Sicilian") and late Pleistocene 'constructive' terraces are correlated with 4^{th} and higher-order sea level cycles (Imbrie et al., 1984; Martinson et al., 1984). The age of each of these terraces, dominated by progradational sediments, is correlated with the peak of the glacio-eustatic sea level curve, characteristic of the correlative sea level cycle.

3) Constructive marine terraces of inferred late-early or early-middle Pleistocene age in both the Messenia and Eastern Lakonia Peninsulae (Units 2.3 and 5, in Messenia and Eastern Lakonia, respectively; Fig. 7.1) can be correlated with either the 3^{rd} order sea level cycles 3.9, or with one of the early sea level cycles in high resolution curves of the middle and late Pleistocene (i.e. within the 3^{rd} order sea level cycle 3.10; see Imbrie et al., 1984; Martinson et al., 1984; Haq et al., 1988). Following the first alternative, and since the 3^{rd} order sea level cycle 3.9 is not resolved into higher-order cycles, these terraces are viewed as broadly contemporaneous with the early Pleistocene terraces and in practice omitted from the analysis.

4) Erosive marine terraces of inferred middle and late Pleistocene age in the Eastern Lakonia Peninsula are correlated with peaks in high-resolution Pleistocene sea level curves (Imbrie et al., 1984; Martinson et al., 1984), assuming that the time of terrace formation coincided with the time of highest sea level, i.e. with the peak of each correlative sea level cycle.

5) The uplifted "Versilian" strandline, in both the Messenia and Eastern Lakonia Peninsulae, can be correlated with either the short-lived 'Versilian' highstand, ca. 6 ka ago (Labeyrie et al., 1987; Kambouroglou, 1989), or with the 'Early Byzantine tectonic paroxysm', ca. 1.55 ka ago (Pirazzoli, 1986b; Kelletat, 1991).
It is evident that, lacking firm geochronological evidence, a multitude of correlation alternatives produce a multitude of alternative age models.

7.5.4. Assumptions: Equation (4) is a theoretical expression of uplift rate, without any implicit assumption about the temporal character of uplift. However, this equation is inapplicable, since the instantaneous uplift rate (dU / dt) is not known. Three alternative approaches can be followed for addressing this problem (Fig. 7.6):

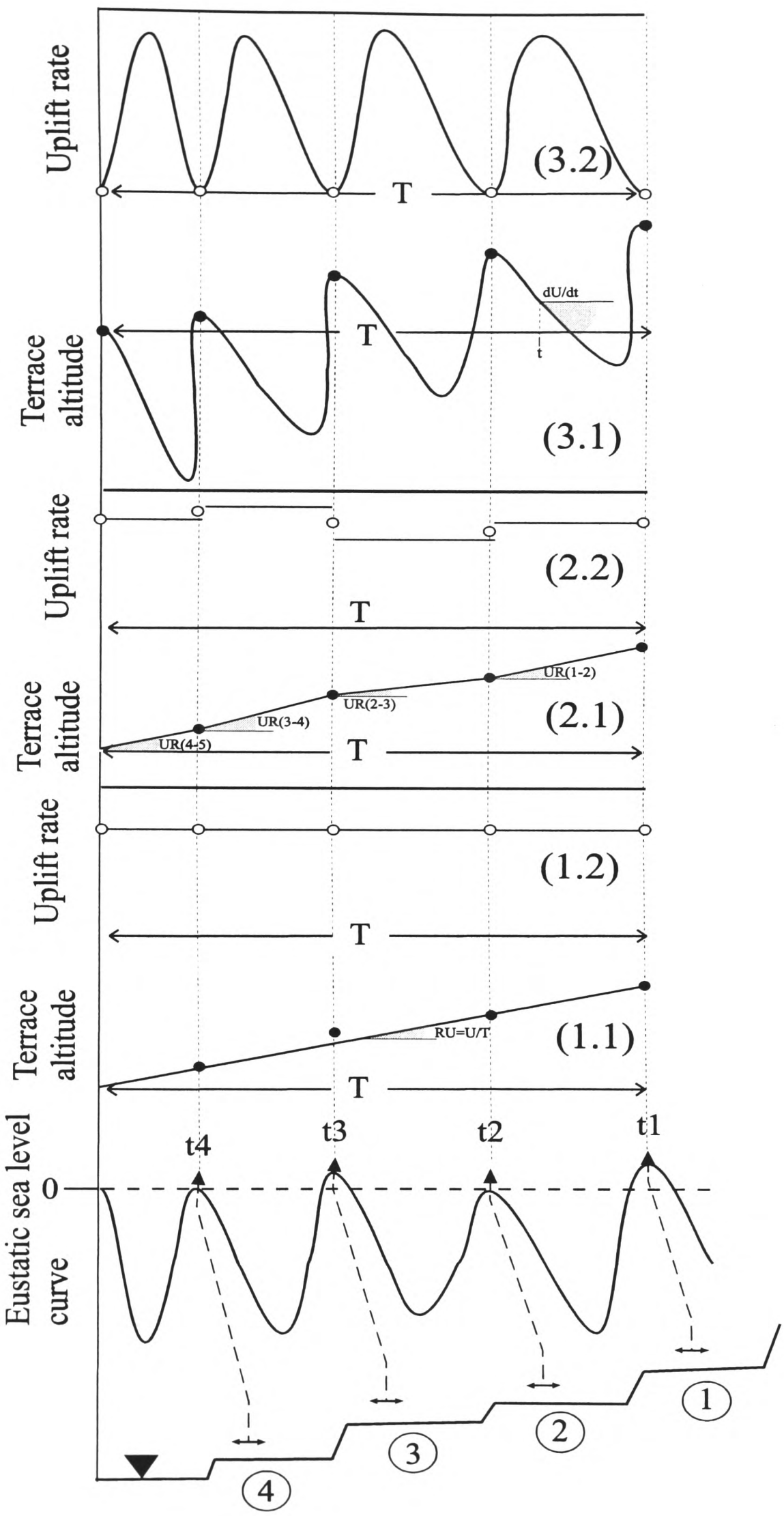

Figure 7.6: Assumptions for constant and changing uplift rate during the formation of a terrace flight (see text for explanation).

7.5.4.1. Assumption of constant rate of uplift (Fig. 7.6.1): If the rate of uplift is assumed to be constant since the time (T) of formation of the oldest/highest terrace, i.e. if dU / dt = C, then equation (6) takes the form:

$$RU = U / T = [(C \times T) - K] / T \qquad (7)$$

where U is the net uplift since the formation of the terrace, calculated from equation (1), and K a constant value, corresponding to the predicted relative elevation of the sea level during formation of the terrace (i.e. T=0), measured in reference to the present sea level. If the assumption of constant uplift rate is valid, the value K should coincide with the elevation of eustatic sea level during the time of terrace formation, as measured from published high-resolution sea level curves (e.g. Imbrie et al., 1984; Martinson et al., 1984). The sign of the value K is positive or negative, depending on whether the sea level at the time of terrace formation was lower or higher than present sea level, respectively.

The validity of the assumption of constant uplift rate largely depends on the time-scale over which this uplift rate is averaged. In general, a model of steady rate uplift would probably be more applicable in case studies involving long time spans. Accepting the suggestion that the background control of uplift in the Hellenic fore-arc is the underplating of the overriding crust by the subducting slab (LePichon and Angelier, 1981), the progress of this process is controlled by plate-boundary conditions. Since no radical change in the plate boundaries of the Hellenic Arc and Trench System during the last 2 Ma (Pliocene-Quaternary) has been inferred, it is reasonable to assume that the time span of the Pliocene-Quaternary is long enough for this process to be modelled as a steady-rate one. Superimposed on this background trend are other processes, which potentially can lead to acceleration, deceleration, or a switch in direction of the land movement. These include normal faulting and isostatic readjustment of the crust after Pleistocene glaciations and deglaciations and are generally thought to operate at time-scales of 1-100 ka. The assumption of constant uplift rate during Pleistocene, thus, necessitates the additional assumption that these shorter-term trends tended to cancel each other's effects over the time-span of the Pleistocene. The example of the '*Early Byzantine tectonic paroxysm*' illustrates the significance of the time scale over which uplift rates are inferred. Strandlines correlated with this tectonic event occur all around the Eastern Mediterranean, from Antikythira Island, south of Peloponnese, Greece, to the coasts of Israel and Lebanon (see Fig. 1.1), and were uplifted ca. 1550 years before present (Pirazzoli et al., 1982, 1989; Pirazzoli, 1986b; Kelletat, 1991). Their uplift, of maximum amplitude of 10 m in western Crete (Pirazzoli et al., 1982), is attributed to an inferred peak in earthquake activity in the area ca. 450 A.D., also manifested by historical records and archaeological evidence (Pirazzoli et al., 1982; Pirazzoli, 1986; Kelletat, 1991).

In this case of episodic uplift, the uplift rate averaged over the last 2 ka would be higher than that averaged over the last 3 ka, or 0.4 ka. Furthermore, local evidence (e.g. western Crete) suggests that the episodic uplift at ca. 450 AD was preceded by incremental subsidence (Pirrazoli et al., 1982). This shows that at time-scales of 1-2 ka not only the rate, but also the direction of vertical movements is liable to change. On the other hand, all published rates of uplift from the Peloponnese (Collier, 1990; Collier et al., 1992; Marcopoulou-Diakantoni, 1991; Bassiakos, 1993, Stamatopoulos et al., 1994) and other fore-arc areas of the Eastern Mediterranean (Poole, 1991; Poole and Robertson, 1991) are based on the assumption that uplift rate was constant during at least part of the Pleistocene (commonly late-middle and late Pleistocene). The assumption of constant uplift rate for the Messenia and Eastern Lakonia Peninsulae allows a comparison of the results with those from other areas, the poor chronological resolution in the areas of study notwithstanding (Fig. 7.8). An additional practical advantage is that this model does not require a good chronological resolution of all marine terraces. In fact, assuming constant uplift rate since early Pleistocene, correct correlation of just one uplifted marine terrace with the eustatic sea level curve is enough to infer the uplift rate of the entire terrace flight (Fig. 7.6.1).

7.5.4.2. Assumption of constant rate of uplift between formation of successive terraces (Fig. 7.6.2): In this case, it is assumed that the uplift rate was constant during the time necessary for the formation of each pair of terraces, but not during the time necessary for the formation of the whole terrace flight. Accordingly, the uplift of the terrace flight as a whole is viewed as a succession of distinct periods, each characterised by constant uplift rate, that can differ from the uplift rate during previous or succeeding periods of uplift (Fig. 7.6.2). Assuming a terrace flight of n terraces, its uplift is resolved into n periods of steady-rate uplift. The rate of uplift during each of these periods is given by the formula:

$$RUi = (U_{(i-1)-i} / T_{(i-1)-i} = [C_{(i-1)-1} \times T_{(i-1)-i} + k_{(i-1)-i}] / T_{(i-1)-i} \qquad (8)$$

where U(i-1-i) is the amount of uplift that took place between the formation of two successive terraces i-1 and i, $T_{(i-1)-1}$ the time between the formation of these successive terraces, $C_{(i-1)-i}$ the rate of uplift between the emergence of the terrace i-1 and the formation of the terrace i (assumed constant) and $k_{(i-1)-i}$ a constant, corresponding to the predicted elevation of sea level during formation of the terrace i-1.

This assumption is probably more realistic than the previous one, since it allows the long processes of uplift and relative sea level change to be resolved into shorter increments (Fig. 7.6.2). If each marine terrace is correlated with a distinct sea level cycle of the published high-resolution sea level curves (e.g. Imbrie et al., 1984; Martinson et al., 1984), then the

time span between formation of two successive terraces is of the order of ca. 50-70 ka. Such time is probably long enough to allow change in rate or direction of vertical land movements, as demonstrated by Holocene (last 10 ka) subsidence of shorelines that underwent previous Pleistocene uplift (Pirazzoli et al., 1982). This renders all the inadequacies of the previous model implicit in this one, as well. Furthermore, this model, by requiring higher chronological resolution than the previous model, is more sensitive to misdating of marine terraces. A further problem arises from the potential presence, at the same altitude, of more than one 4^{th}, or higher-order marine terraces, each one correlative with sea level cycles separated by 10's of ka (see Kowalczyk et al., 1992 and Stamatopoulos and et al., 1994, for examples from the SE and NW Peloponnese, respectively). Lacking firm geochronological evidence, or unusually good exposure, such superposition of terraces is difficult to recognise in the field. Erroneous correlation of this multiple terrace system with a single sea level cycle would lead to deduction of unrealistic rates of uplift. The above criticism notwithstanding, this model offers results comparable with published rates of uplift, deduced from radiometricaly dated late to late-middle Pleistocene terraces (commonly "Tyrrhenian" and younger), based on the assumption that uplift rate remained constant during part of the late Pleistocene-Holocene (Collier, 1990; Collier at al., 1992; Poole, 1991; Poole and Robertson, 1991).

7.5.4.3 Assumption of non-constant rate of uplift (Fig. 7.6.3): If the rate of uplift is assumed non-constant since the formation of the highest/oldest terrace in the terrace flight, then a curve can be fitted through the points of a plot of Terrace Altitude vs. Time. The resulting polynomial curve is a relative sea level curve, predicting the present elevation of any past sea level marker younger than the oldest/highest terrace in the terrace flight. Differentiation of the equation of the relative sea level curve results to the equation of uplift rate versus time, i.e.:

$$RU(t) = d[\Delta SL(t)]/dt \qquad (9)$$

In theory, this approach carries the least arbitrary assumptions; it is, thus, potentially the most realistic model of relative sea level change. The practical problem, however, is that fitting a non-linear curve would be meaningless unless there is an adequate number of points in the Terrace Altitude vs. Time plot to define a curve; a condition not satisfied by this work. Moreover, this approach requires very good chronological resolution of distinct terraces; increasingly so with increasing sensitivity of the curve (i.e. increasing degree of the best-fit polynomial equation). For all these reasons this approach was not followed during the present study.

7.5.5. Middle-Late Quaternary uplift of the Messenia and Eastern Lakonia Peninsulae:

In this study, A model of uplift was produced for each studied area (Messenia and Eastern Lakonia Peninsulae) (Figs. 7.7.a,b), based on the assumption that uplift rate was constant since the formation of the early Pleistocene terraces. The emergence of these terraces is assumed to have taken place ca. 1 Ma to 900 ka ago, during the culmination of the sea level cycle 3.9 (Haq et al., 1988). The palaeodepth of the uplifted terrace facies is assumed ≤ 20 m, since terraces were formed above shoreface to foreshore facies, with intralittoral-upper circumlittoral benthic microfauna, in both Peninsulae (Chapters 3, 5). On this basis, the maximum rate of uplift was ca. 0.33 m/ka for the NW part of the Messenia Peninsula (Northern Messenia Block: see Chapter 2; Fig. 7.7.a) and ca. 0.30 m/ka for the NW part of the Eastern Lakonia Peninsula (Ano Glikovrisi Horst: see Chapter 4; Fig. 7.7.b). Also, the minimum rate of uplift was ca. 0.09 m/ka for the SE part of the Messenia Peninsula (Southern Messenia Block: see Chapter 2; Fig. 7.7.a) and ca. 0.08 m/ka for the Southern part of the Eastern Lakonia Peninsula (Fig. 7.7.b). Pleistocene marine terraces, in both Peninsulae, were offset by normal faults (see Chapters 2, 4). As a result, local uplift rates are of values between the ones shown in Figure 7.7. Assuming that the relative dating of marine terraces proposed here is correct, altitudinal differences between terraces of the same age increase with increasing geological age of the terraces. Thus, whereas altitudinal differences between Eutyrrhenian terraces are ≤ 10 m, the altitudes of early Pleistocene terraces can differ up to ca. 200 m. This was probably the result of repeated normal faulting during the last ca. 1 Ma.

The similarity between both the maximum and minimum uplift rates of the Messenia and the Eastern Lakonia Peninsulae is noteworthy. Local differences are manifested by: 1) the fault-induced subsidence of grabens (e.g. Messenian and Lakonic Gulfs; see Fig. 1.1), and 2) by the presence of relatively subdued, fault-bounded areas within 10′s of km-scale megahorsts (e.g. Messenia and Eastern Lakonia Peninsulae). Quaternary terrace flights within areas of minor uplift are commonly incomplete (e.g. Southern Messenia Block; see Chapter 2, Molai and Neapolis Grabens; see Chapter 4). However, wherever complete Quaternary terrace flights are present the rate of uplift during the last ca. 1 Ma falls within the range of 0.08-0.33 m/ka. This suggests that, on the time scale of the last ca. 1 Ma, there was a common background control over an area extending ca. 100 km across the SW part of the Aegean fore-arc. Underplating of the Peloponnese crust by buoyant sediments was proposed as an explanation of the Plio-Quaternary uplift (Le Pichon and Angelier, 1979). Such a model, also in agreement with seismological data (Berckhemer and Kowalczyk, 1978; Hertzfeld et

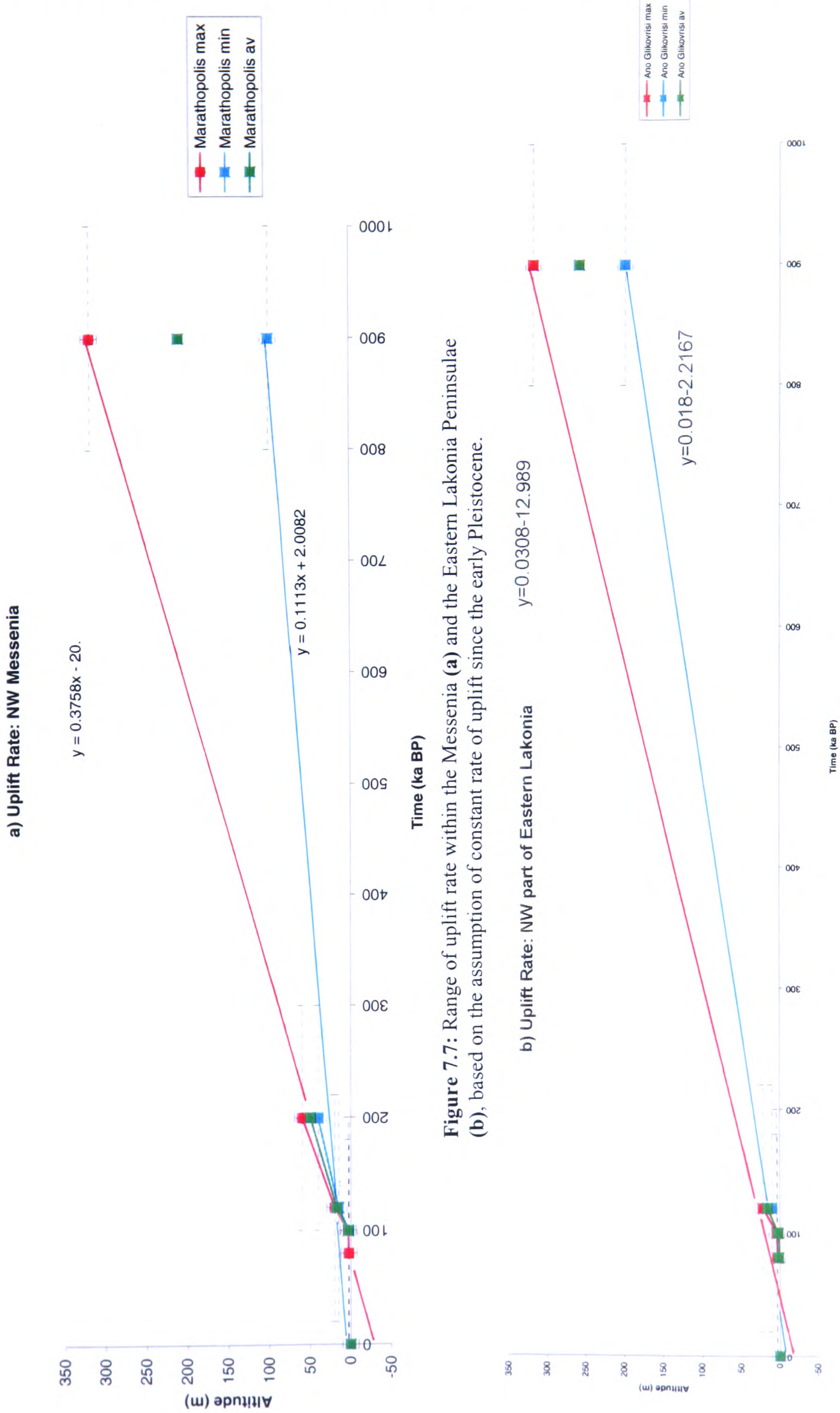

Figure 7.7: Range of uplift rate within the Messenia **(a)** and the Eastern Lakonia Peninsulae **(b)**, based on the assumption of constant rate of uplift since the early Pleistocene.

al., 1989), probably explains the similar uplift rates between the NW parts of the Messenia and the Eastern Lakonia Peninsulae.

7.6. A SYNTHESIS OF THE PLIO-QUATERNARY EVOLUTION OF THE MESSENIA AND EASTERN LAKONIA PENINSULAE

The evidence and interpretations presented above are summarised to the following model for the tectonic-sedimentary evolution of the Messenia and Eastern Lakonia Peninsulae during the Pliocene-Quaternary (i.e. last ca. 5 Ma):

7.6.1. Miocene: The late stages of the Alpine orogenesis took place in the Early-Middle Miocene, with the thrusting of the Tripolis and Pindos Zones over the Pre-Apulian platform, represented in the Eastern Lakonia Peninsula by the '*Plattenkalc*' and '*Phyllite Series*' (Jakobschangen et al., 1978, I.G.M.E., 1984). Deposition of coarse, 'molasse'-type conglomerates in the Messenia Peninsula ("Messenian Conglomerate") took place in the foreland of the advancing thrust sheets. Both areas were probably emergent during the Late Miocene. Subaerial denudation under humid-tropical climatic conditions led to the formation of 3-5 pediments/pediplains, separated with cliffs and incised valleys, correlative with periods of base level fall. It is possible that Late Miocene periods of base level fall correspond to periods of accelerated uplift of the Messenia and Eastern Lakonia Peninsulae, in analogy with similar surfaces in other parts of the Peloponnese (Riedl, 1977), the Cyclades Islands (Riedl et al., 1982) and Northern Greece (Vavliakis, 1981; Psilovikos and Vavliakis, 1981; Weingartner and Hejl, 1994). Late Miocene uplift of the Southern Peloponnese was probably triggered by the establishment of the Hellenic Arc and Trench system, as a consuming boundary between the African and the European plates (Le Pichon and Angelier, 1979). Normal faulting also took place during the same period, with creation of faults parallel and transverse to the Tethyan tectonic grain. These faults resulted in the segmentation of the Messenia and the Eastern Lakonia Peninsulae into fault-bounded blocks with dimensions of ca. 10×20 km, or smaller. These faults exercised control on the development of the landscape, as demonstrated by the present distribution of Late Miocene surfaces of erosion and incised valleys.

7.6.2. Pliocene: In the Messenia Peninsula, mainly NNW-SSE, peninsula-parallel faults were active during the Early Pliocene (Zanclean: ca. 5.2-3.5 Ma). In the eastern part of the peninsula, these faults controlled large, km-scale grabens that subsided below sea level, as parts of the ancestral Messenian Gulf. Shallow-marine sediments deposited in these basins

are correlated with the 3rd order sea level cycles 3.4 and 3.5 (*sensu* Haq et al., 1988). Deepening-, then shallowing-upward trend in these sediments reflects the eustatic control on their deposition (transgressive-regressive sequences). In the eastern part of the Messenia Peninsula, by contrast, marine sediments were not deposited during the same period, possibly as a result of lower rates of extension along the NNW-SSE graben-controlling faults. The activity of these faults is, however, indicated by the switch of the peninsular drainage from peninsula-parallel to cross-peninsular directions, cutting across the boundaries of NNW-SSE grabens. Subaerial erosion continued in emergent areas of the Messenia Peninsula, resulting in the formation of U-shaped valleys and possibly some of the lower/younger pediment surfaces. Periods of alluvial aggradation resulted in deposition of red conglomerate fill in these U-shaped valleys.

By contrast with the Messenia Peninsula, Early Pliocene marine sediments have not, so far, been reported. If such sediments were deposited, they are now below sea level, in the submerged areas of the Lakonic and Argolic Gulfs, on both sides of the Eastern Lakonia Peninsula. Normal faults in the Eastern Lakonia Peninsula exhibit a broader variation in direction and closer spacing as compared with those in the Messenia Peninsula, but a similar pattern of faults parallel and transverse to oblique to the Tethyan tectonic grain is discernible. It is possible that the more crumbled state of the upper crust in the Eastern Lakonia Peninsula reflects its proximity to the Aegean, where neotectonic extension is maximum as compared with the rest of the Aegean Arc and Trench System. Faults of all the above directions were active during the Early Pliocene, as shown by thick breccia and flowstone carapaces over the fault surfaces.

During the Late Pliocene (Piacenzian: ca. 3.5-1.65 Ma) activity of NNW-SSE, peninsula-parallel faults continued in the western part of the Messenia Peninsula, resulting in the deposition of transgressive-regressive shallow-marine sequences, correlated with the 3rd order sea level cycles 3.6, 3.7, 3.8 (*sensu* Haq et al., 1988). Continuing extension in the fault-bounded grabens in the eastern parts of the peninsula caused them to subside below sea level and to accommodate Late Pliocene marine sediments. In emergent parts of the peninsula, as well as in the Eastern Lakonia Peninsula, subaerial sediments were deposited, encompassing caliche palaeosols and various fanglomerate facies.

By the end of the Pliocene, after the culmination of the sea level cycle 3.8, sea level fell and both the Messenia and Eastern Lakonia Peninsulae were exposed to subaerial erosion. An extensive pediment developed in both areas, probably under the dry subtropical conditions of the Villafrancian (Bonifay, 1975; Koufos et al., 1989).

7.6.3. Early Pleistocene Sea Level Cycle: A marine transgression that began in Late Pliocene time culminated in early Pleistocene, when large areas of both the Messenia and Eastern Lakonia Peninsulae were below sea level. This led to the deposition of a very widespread, transgressive-regressive shallow-marine sequence Q1, correlated with the 3rd order sea level cycle 3.19 (*sensu* Haq et al., 1988). This sequence encompasses a wide variety of offshore-shoreline to marginal marine facies and associated fluvial-deltaic sediments, reflecting different paleogeographic settings (Fig. 7.3). Normal faulting influenced sedimentation by controlling the geometry of grabens that hosted the deeper marine facies and also the configuration of the early Pleistocene coastline. Correlative early Pleistocene sediments are more terrigenous in the Eastern Lakonia Peninsula than in the Messenia Peninsula, probably as a result of closer fault-spacing within the former, that resulted in larger alluvial input to marine depocentres. The upper parts of the early Pleistocene sequences, in both Peninsulae, comprise prograding clinoforms probably deposited during highstand and the early stages of slow relative sea level fall. Their depositional architecture is characteristically regressive, with spectacular development of offlapping clinoform sets (Fig. 7.3). This probably suggests that relative sea level fall resulted from forced regression, controlled from land uplift. Disconformable shallow-marine parasequences within the early Pleistocene sequence Q1 probably resulted form higher-order cyclicity within the 3rd order sea level cycle 3.9 (Fig.7.3).

7.6.4. Middle Pleistocene Lowstand: Sea level fall after the end of the early Pleistocene resulted in the erosion of cliffs and incised valleys into exposed early Pleistocene shallow-marine sediments and bedrock, in both the Messenia and the Eastern Lakonia Peninsulae. The height of these erosional features reaches 120 m in NW Messenia. This period of low sea level was probably contemporary with the Mindel glaciation in N Europe and the Alps (Bonifay, 1975). Alluvial fan deposition was extensive in the Eastern Lakonia Peninsula, probably enhanced by closely spaced normal faulting. In the Messenia Peninsula, by contrast, alluvial fan deposition was localised near major, mainly NNW-SSE trending normal faults, whereas siliceous soils developed above the emergent shallow-marine sediments of the extensive early Pleistocene terrace(s). This subaerial relief (and its associated sediments) formed a regionally correlative sequence boundary between the early Pleistocene sequence Q1 and the middle-late Pleistocene sequence Q2 (see below).

7.6.5. Middle-late Pleistocene Sea Level Cycle: Sea level rise during the middle Pleistocene caused the deposition of the transgressive-regressive sequence Q2 above the subaerial relief fashioned during the previous sea level lowstand. Deposits of this sequence

span the time from middle to late Pleistocene and they are correlated with the 3rd order sea level cycle 3.10 *sensu* Haq et al. (1988). Shallow-marine sediments were deposited above a ravinement surface that truncates the bedrock, Pliocene and early Pleistocene shallow-marine sediments and middle Pleistocene alluvia. Higher-order sea level cyclicity during the middle Pleistocene sea level cycle resulted in the deposition of at least two transgressive-regressive parasequences, separated by disconformities, as described below:

7.6.5.1 Middle-late Pleistocene Lowstand: Sea level fall resulted in emergence of middle Pleistocene shallow-marine sediments and erosion of cliffs and valleys in both Peninsulae. Alluvial fan progradation was widespread within the Eastern Lakonia Peninsula, but only local within the Messenia Peninsula, adjacent to major faults. This lowstand is tentatively correlated with the Riss glaciation in N Europe and the Alps (Bonifay, 1975). Caliche palaeosols formed during this highstand in both emergent shallow-marine and alluvial host rocks, suggesting that an arid/semiarid climate prevailed in the Southern Peloponnese during that time (Esteban and Klappa, 1983; Goudie, 1983).

7.6.5.2 Eutyrrhenian Sea Level Cycle: Sea level rise during the Eutyrrhenian stage resulted in deposition of extensive Eutyrrhenian terraces in both the Messenia and Eastern Lakonia Peninsulae. Warm climatic conditions during the Eutyrrhenian highstand allowed the migration of mollusc species from the Atlantic coast of Africa into the Mediterranean Sea ("*Senegalese fauna*"; Keraudren, 1970, 1971; Bonifay, 1975). The commonest representative of this 'warm' fauna in the Southern Peloponnese is the gastropod *Strombus bubonius* (Keraudren, 1970, 1971; Kelletat et al., 1976, 1978; Kowalczyk et al., 1992). The Eutyrrhenian highstand is correlated with the isotopic stage 5.5, ca. 120 ka (Martinson et al., 1984; Imbrie et al., 1984). The Eutyrrhenian sea level rise caused reduction of the stream gradient and deposition of alluvial fill at altitudes correlative with the Eutyrrhenian marine terrace further offshore (e.g. Dokali Rema; see Chapter 5). Normal faults were active during the Eutyrrhenian in both Peninsulae (Chapters 2, 4).

7.6.5.3 Late Pleistocene Lowstand I: Sea level fall after the Eutyrrhenian resulted in subaerial exposure and erosion of shallow-marine sediments, as during previous lowstands. Calichification, under arid/semiarid climatic conditions, resulted in formation of relatively immature, chalky and rhizocretion caliche. In the Eastern Lakonia Peninsula, alluvia were deposited in coarsening-up successions, resulting from prograding alluvial fans. Mousterian (Middle Palaeolithic) tools found in the latter alluvia facilitate their relative dating (Kowalczyk et al., 1992).

7.6.5.4 Neotyrrhenian Sea Level Cycle: The Neotyrrhenian sea level rise resulted in the formation of marine terraces, disconformably above Eutyrrhenian shallow-marine sediments and alluvia of the previous lowstand (Chapters 3, 5). Warm water molluscs are present in deposits of this stage, as in the Eutyrrhenian (e.g. the gastropod *Strombus bubonius*). The Neotyrrhenian substage, part of the isotopic stage 5.5, is tentatively correlated with the highstands 5.5.1+5.5.3 (ca. 100-80 ka; Martinadale et al., 1984; Imbrie et al., 1984), similar with correlative uplifted shorelines in the Mani Peninsula (Bassiakos, 1993; see Fig. 1.1). Superposition of at least two progradational shoreline deposits, separated by a disconformity, probably suggests that the Neotyrrhenian terrace comprises the amalgamated deposits of these two highstands, although autocyclic processes cannot be ruled out (e.g. Messenia Peninsula; Chapter 3).

7.6.5.5 Latest Pleistocene Lowstand II: Sea level fall after the Neotyrrhenian stage resulted in subaerial exposure of shelf deposits and their reworking in aeolianites, deposited mainly along the western coast of the Messenia Peninsula (Chapter 3). Subaerial exposure also resulted in calichification and karstification of all previous shallow marine deposits (Chapter 6). The culmination of sea level drop, during the latest Pleistocene, caused stream rejuvenation and fluvial incision into the uplifted Pleistocene terrace flight. Alluvial fan deposition was widespread in the Eastern Lakonia Peninsula (Chapter 5). Latest Pleistocene alluvia in the latter contain Late Palaeolithic tools (Kowalczyk et al., 1992). Latest Pleistocene (to Holocene) tectonic activity is evidenced by local faulting and jointing of such sediments. This latest Pleistocene sea level lowstand is correlated with the Würm glaciation in Northern Europe and the Alps (Bonifay, 1975), as well as in the mountains of Northern Greece (Vavliakis, 1981; Psilovikos and Vavliakis, 1981; Palmentola, 1994; Smith et al., 1994) and the Peloponnese (Dufaure, 1977; Riedl., 1977; Verginis and Nagl, 1982; Palmentola, 1994). This well documented sea level fall lowstand culminated ca. 12 ka ago, during the 'Last Glacial Maximum', when sea level was >100 m lower than the present one (Martinson et al., 1984; Imbrie et al., 1984; Chappell and Shackleton, 1986).

7.6.6 Holocene: The Holocene sea level rise resulted in the drowning of parts of the shelf that were emergent during the previous lowstand. The coastline topography in the Messenia and Eastern Lakonia Peninsulae reached its present shape, as a result. Shorelines with *vermetidae* encrustations, in both Peninsulae are correlated with the well documented Versilian highstand, ca. 6 ka ago, when sea level reached a level slightly higher than at present (Labeyrie et al., 1987; Kambouroglou, 1989). However, the same shorelines could also be of a younger, Historical age, uplifted during the 'Early Byzantine tectonic paroxysm'

that uplifted many areas in the Eastern Mediterranean during ca. 450 AD (Pirazzoli, 1986; Kelletat, 1991). Holocene beachrocks are present in both Peninsulae, locally uplifted <1 m above present sea level. Holocene valleys, in both Peninsulae, were incised into latest Pleistocene alluvia. Several successive episodes of incision and alluviation are present within the latter, reaching up to Historical times.

CHAPTER 8: REGIONAL COMPARISONS

8.1 INTRODUCTION

In this chapter the areas of study (the Messenia and Eastern Lakonia Peninsulae) are compared with other areas of similar (fore-arc), or contrasting (back-arc) tectonic setting.

8.2 COMPARISON OF MESSENIA AND EASTERN LAKONIA PENINSULAE (PELOPONNESE) WITH OTHER FORE-ARC AREAS

8.2.1 Crete Island (central part of the Aegean Fore-arc): The island of Crete is situated at the southernmost tip of the Aegean Fore-arc, north of a characteristic bend of the Hellenic Trench (Le Pichon and Angelier, 1979) (see Fig. 1.2). The western part of Crete, in particular, is directly comparable with the southern Peloponnese. Offshore geodynamic conditions are similar in both regions, comprising northwestward underthrusting of Ionian oceanic crust under the Aegean fore-arc (Le Pichon and Angelier, 1979; Mascle et al., 1982; Casten and Makris, 1998; Makris and Egloff, 1998; Nikolich, 1998; Robertson and Kopf, 1998). Offshore from the eastern part of Crete, by contrast, the Pliny and Strabo trenches (Fig. 1.2) accommodate left-lateral slip of the Aegean relative to African crust (Le Pichon and Angelier, 1979; Angelier et al., 1982; Ten Veen and Meijer, 1998).

Crete is dissected by a network of ENE-WSW to ESE-WSW and NNW-SSE to NNE-WSW trending normal and oblique, to strike slip, faults that controlled relief and sedimentation since the late Middle Miocene (Kronberg and Günther, 1978; Meulenkamp et al., 1988, 1994; Duermeijer et al., 1998; Ten Veen and Meijer, 1998). The scale of post-Tethyan vertical movements is documented by uplift and exhumation of HP-LT metamorphics in the footwalls of major normal faults (Fassoulas et al., 1994b), by stratigraphic data of Neogene-Quaternary sediments (Meulenkamp et al., 1988, 1994; Ten Veen, 1998), as well as by satellite imagery and digital elevation modelling (Ten Veen, 1998; Ten Veen and Meijer, 1998). These fault-sets, parallel and perpendicular to the arc and the long axis of the island, are comparable with the peninsula-parallel and cross-peninsular fault-sets within the Messenia and Eastern Lakonia Peninsulae (Chapters 2, 4). Both in Crete and in the Southern Peloponnese, these faults accommodated the outward expansion of the Aegean fore-arc, probably corresponding with periods of trench 'roll-back' (Meulenkamp et al., 1988). Some

authors (e.g. Fassoulas et al., 1994b; Fassoulas, 1998; Ten Veen and Meijer, 1998) conclude that E-W island-parallel faults in Crete are of Late Miocene age, earlier than the N-S, cross-island faults, of Late Pliocene to Present age. Oblique slip reactivation of pre-existing faults took place since the Late Miocene, as a result of rotation and left lateral transtension, possibly related to transform 'resistance' along the Pliny and Strabo strike-slip trenches (Ten Veen and Meijer, 1998). A similar difference between the timing of E-W and N-S faulting was also inferred from the Messenia Peninsula, mainly on the basis of geomorphological evidence (see Chapter 2).

An important difference between Crete and the Southern Peloponnese is that Crete underwent at least one period of compression after the Late Miocene (Fassoulas et al., 1994); other authors have inferred several Neogene to early Quaternary compressional periods (Meulenkamp et al., 1988), from compressional structures (e.g. folds, reverse and oblique-slip faults) present all over the island (Meulenkamp et al., 1988; Fassoulas et al., 1998). These structures indicate NE-SW directed $\sigma 1$ axis of maximum stress (Meulenkamp et al., 1988; Fassoulas et al., 1994b). Meulenkamp et al. (1988) attributed the compressional features to periods of inception of trench roll-back. During periods of trench roll-back, gravitational spreading of the Aegean crust over the colliding African margin probably resulted in compression, thickening, uplift, and northward tilting of the fore-arc and extension, thinning and foundering of back-ark regions (Crete and Cretan Sea, respectively). The Pliocene-Quaternary neotectonics of Crete comprised movement of individual fault-bounded blocks, that also involved faulting and tilting of Neogene-Quaternary sediments (Paraskevaidis, 1961a,b; Psarianos, 1961a,b; Symeonidis, 1967; Gradstein, 1972; Angelier et al., 1976, 1982; Butner and Kowalczyk, 1978; Kopp, 1978; Le Pichon and Angelier, 1979; Faugeres et al., 1987/88; Meulenkamp et al., 1988, 1994; Nemec and Postma, 1993; Ten Veen and Meijer, 1998). This is very similar with the neotectonic conditions in the Eastern Lakonia Peninsula (Chapters 4, 5). Post-Late Miocene rotations in Crete were anticlockwise, generally ranging from 10-20°, but locally reaching 40° (Duermeijer et al., 1998). Similar rotations in the Southern Peloponnese have yet to be tested.

Although marine sediments of Miocene age have not, so far, been reported from the Peloponnese, these are common in Crete. There, marine deposition in fault-controlled basins started locally in the Seravallian (Middle Miocene) and became widespread during the Tortonian, followed by evaporite deposition during the Messinian (Büttner and Kowalczyk, 1978; Meulenkamp et al., 1988, 1994; Bellas et al., 1998; Frydas, 1998).

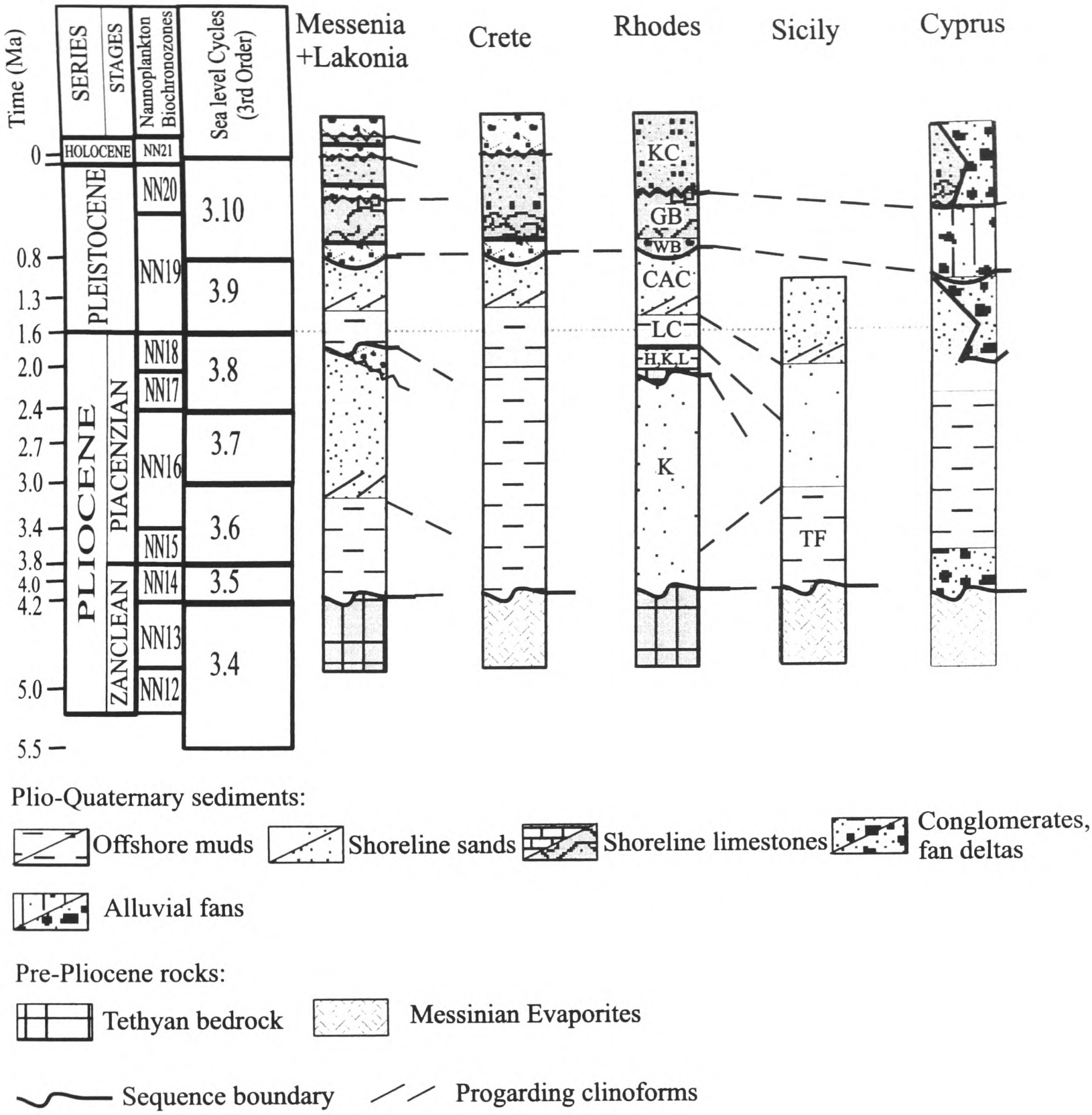

Figure 8.1: Correlation of Plio-Pleistocene sediments from the S Peloponnese (Messenia and Lakonia; this study) with other fore-arc areas in central and eastern Mediterranean. Crete: Meulenkamp et al. (1988, 1998); Rhodes: Hanken et al. (1996), Sicily: Buttler and Grasso, 1993; Cyprus: Poole and Robertson, 1991; McCallum and Robertson, 1989. Rhodes Log: **K:** Kritika Formation, **H,K,L:** Haraki and Kolymbia Limestones, Ladiko Sand, **LC:** Lindos Bay Clay Facies Group, **CAC:** Cape Arhangelos Calcarenite Facies Group, **WB:** Windmill Bay boulder bed, **GB:** Gialos algal biolithite, **KC:** Kleopoulou calcirudite. Sicily Log: **TF:** Trubi Formation.

Pliocene sedimentation in Crete began with a marine transgression, followed by deeper, then shallower environments up-section; the marine facies are then succeeded by lacustrine and fluvial facies (Fig. 8.1). This general pattern, most pronounced in the western part of Crete (Büttner and Kowalczyk, 1978), is similar with the Pliocene transgressive-regressive stratigraphy of the Messenia Peninsula (W part of the Southern Peloponnese; see Fig. 3.3).

Pleistocene sediments in Crete rest unconformably on earlier Neogene sediments and bedrock (Bellas et al., 1998). In the western part of Crete, widespread red conglomerates of post-early Pleistocene age are interpreted as resulting from renewed uplift of the island (Bellas et al., 1998). These sediments are correlative with the fanglomerate complexes of Units 3.4 and 12 in the Messenia and Eastern Lakonia Peninsulae, respectively (see Fig, 7.1); these are also thought to be partly controlled by uplift and normal faulting (Kourampas and Robertson, 2000; Chapters 3, 5, 7). Tyrrhenian sediments are widespread in Crete (Psarianos, 1961; Symeonidis, 1967; Keraudren, 1970, 1971; Papapetrou-Zamanis, 1971; Dermitzakis, 1972; Angelier et al., 1976). Commonly, they rest unconformably above faulted and tilted early Pleistocene marine sediments, or middle Pleistocene alluvia. Tyrrhenian outcrops in Crete are, thus, very similar with those of the Messenia and Eastern Lakonia Peninsulae (Chapters 3, 5, 7). The facies present in the Tyrrhenian terraces of Crete (Keraudren, 1970, 1971; Papapetrou-Zamanis, 1971; Angelier et al., 1976) are very similar with the carbonate facies present in the Southern Peloponnese (Kowalczyk et al., 1992; Kourampas and Robertson, 2000, Chapters 3, 5, 6).

In Crete, Holocene beachrock, marine notches, alluvia and archaeological sites of various ages were affected by faulting (Dermitzakis, 1972, 1974; Dermitzakis and Theodoropoulos, 1974; Pirazzoli et al., 1982; Postma and Nemec, 1990). The Holocene tectonics of Crete first attracted interest in the nineteenth century, both because of its spectacular effects (e.g. uplift and subsidence) on archaeological sites and the increased interest in the sites themselves. Dermitzakis (1972) presented a review of models proposed until that time. Pirazzoli et al. (1982), based on evidence of dated Holocene marine notches (radiocarbon dating), suggested that vertical movements of changing direction affected large-scale blocks (ca. 500 km) in western Crete-Antikythera and in eastern Crete. Incremental subsidence was followed by uplift (maximum throw: ca. 10 m), accompanied by northeastward tilting. This last uplift was interpreted as coseismic in origin. This sequence of vertical movements was correlated with the progress of subduction along the plate boundary SW of Crete (see Figs. 1.1, 1.2). Following this interpretation, incremental subsidence was associated with the 'locking' of a part of the subducting slab and accumulation of strain; subsequent release of

strain resulted in uplift and northeastward tilting of large crustal blocks. The latest uplift took place ca. 450 AD and affected areas all along the Eastern Mediterranean coast ('*Early Byzantine tectonic paroxysm*'; Pirazzoli, 1986; Kelletat, 1991). It is possible that uplifted strandlines of Holocene age in the Messenia and Eastern Lakonia Peninsulae can be correlated with the dated marine notches and deposits uplifted as a result of the 'Early Byzantine tectonic paroxysm' in Crete and other parts of the Aegean fore-arc.

8.2.2 Rhodes (eastern part of the Aegean fore-arc): Rhodes Island is situated in the eastern part of the Aegean fore-arc (see Figs. 1.1, 1.2). In Rhodes, as in the Messenia and Eastern Lakonia Peninsulae, normal faulting has resulted in the formation of fault-controlled basins that evolved semi-individually during the Pliocene-Pleistocene (Meulenkamp et al., 1972; Pirazzoli et al., 1989; Hanken et al., 1996). The earliest post-Tethyan sediments, unconformable above bedrock, are Late Pliocene shallow-marine carbonates (Meulenkamp et al., 1972; Hanken et al., 1996). The relative sea level history of Rhodes during the Late Pliocene-Pleistocene (Hanken et al., 1996; Hansen, 1999) is, as a first approximation, similar to that of the Messenia and Eastern Lakonia Peninsulae. Relative sea level rise, towards the end of the Pliocene, culminated in maximum transgression and deposition of offshore facies, interpreted as a highstand systems tract, during Late Pliocene-earliest Pleistocene ('*Lindos Bay Clay Facies Group*'; Hanken et al., 1996). This sediment is very similar to Unit 2.1 in the Messenia Peninsula and Subunit 3.1 in the Eastern Lakonia Peninsula (Fig. 8.1). This was followed by deposition of forced-regressive, detrital carbonate clinoforms during early Pleistocene time ('*Cape Archangelos Calcarenite Facies Group*'; Hanken et al., 1996; Hansen, 1999). This facies group is very similar to Units 2.2, 2.3, 2.4 in the Messenia Peninsula and Subunit 3.2 and Unit 5 in the Eastern Lakonia Peninsula (Fig. 8.1). Similarities between facies groups and units present in Rhodes and the Southern Peloponnese include facies, depositional architecture, stratigraphic position and sequence-stratigraphic interpretation (Fig. 9.1). The different extent and architecture of the regressive '*Cape Archangelos Calcarenite*' in local basins of Rhodes was attributed to local tectonic controls (Hanken et al., 1996; Hansen, 1999). However, the presence of correlative sedimentary units all along the Aegean fore-arc, from the Messenia Peninsula, to Crete, then to Rhodes, suggests that a common, probably glacio-eustatic control underlies Late Pliocene-early Pleistocene sedimentation.

After the early Pleistocene, sedimentation in Rhodes followed the same broad trend as in the Messenia and the Eastern Lakonia Peninsulae (Fig. 8.1). A marked unconformity, attributed

to sea level fall, separates progradational early Pleistocene clinoforms from the later Pleistocene '*Windmill Bay boulder bed*' and the '*Gialos algal biolithite*'. Unconformably above the latter come coastal carbonates of the '*Kleopolu calcirudite*' (Hanken et al., 1996). Stratigraphic position, facies and relative elevation allow tentative correlation of the '*Gialos algal biolithite*' facies group in Rhodes (Hanken et al., 1996) with Unit 2.5 in the Messenia Peninsula, of inferred middle Pleistocene age (Kourampas and Robertson, 2000). On similar grounds, the '*Kleopolu calcirudite*' facies group, undivided in Rhodes (Hanken et al., 1996), can be correlated with both the "Eutyrrhenian" and "Neotyrrhenian" Units 3.1, 3.2 of the Messenia Peninsula and Units 8, 11 of the Eastern Lakonia Peninsula, respectively (Fig. 8.1). These tentative correlations suggest that, despite probable local differences in tectonic activity, galcio-eustatic sea level change was a major control on middle-late Pleistocene marine sedimentation all along the Aegean fore-arc.

8.2.3 Cyprus: The island of Cyprus is situated in the Cyprus fore-arc, an eastward continuation of the Aegean fore-arc (Robertson and Grasso, 1995a,b; Payne and Roberston, 1998a,b; see Fig. 1.2). The island was uplifted for >2400 m since the Late Pliocene (McCallum, 1989; McCallum and Robertson, 1990). Pulsed uplift was focused in the core of the Troodos ophiolite and attributed to the collision of the continental Eratosthenes seamount from the south; this probably also triggered serpentinite diapirism ('*Troodos Massif*; Robertson et al., 1995; Robertson, 1998). As in the Messenia and Eastern Lakonia Peninsulae, four principal shallow-marine depositional units of Late Pliocene-Pleistocene age are distinguished in Cyprus (Fig. 8.1), each correlated with a major Pleistocene sea level highstand (Poole, 1992; Poole and Robertson, 1991, 2000). These units comprise detrital carbonate and siliciclastic facies similar to those present in the Southern Peloponnese. Sedimentary architecture, including progradational clinoforms of detrital carbonates, is also similar in Cyprus and the Southern Peloponnese (Poole, 1990; Poole and Robertson, 1991; Kourampas and Robertson, 2000). The lowest (and youngest) marine terraces of Cyprus were dated radiometricaly (U-series) as 115-134 and 185-219 ka old (Poole et al., 1990). These can, thus, be tentatively correlated with the inferred Eutyrrhenian and late middle Pleistocene (Sicilian) terraces in the Southern Peloponnese (Units 2.5 and 6 and 3.1, 3.2 and 8, 11 in the Messenia and Eastern Lakonia Peninsulae, respectively; see Fig. 8.1). Marine terraces in Cyprus are also associated with four main fanglomerate units, correlated with sea level lowstands and the early stages of sea level rise, as in the Southern Peloponnese (Poole, 1992; Poole and Robertson, 1991, 1998, 2000; Kourampas and Robertson, 2000). The principal difference between the two areas is in the remarkable continuity of landforms and

depositional units within Cyprus, as contrasted with their fragmentary, discontinuous development within the Southern Peloponnese. While marine terraces, shallow-marine sediments and fanglomerates in Cyprus extent around the centre of uplift in the Troodos Massif, in the Messenia and Eastern Lakonia Peninsulae continuous outcrops and terraces are rarely preserved for distances greater than ca. 10-20 km along strike (Chapters 2, 3, 4, 5). This reflects the extensive normal faulting during Pleistocene-Holocene times in the Southern Peloponnese (Zelilidis, 1988; Zelilidis and Doutsos, 1992; Kourampas and Robertson, 2000), in contrast to the focused, largely regional uplift of Cyprus (Poole and Robertson, 1991; Poole, 1992). This difference in the pattern of uplift could reflect both the different geodynamic conditions between the SW part of the Aegean fore-arc and the Cyprus fore-arc (see Fig. 1.2) and also the older, more mature stage of the former. The collision of the Eratosthenes Seamount with the Cyprus active margin is considered as the triggering mechanism of Plio-Quaternary uplift in Cyprus (Robertson et al., 1995; Robertson, 1998). On the other hand, Plio-Quaternary extensional faulting was active in the western part of Cyprus (Polis graben and Pegia half-graben) where marine sediments and terraces show some influence of faulting (Payne and Robertson, 1995, 2000). These two grabens in Cyprus, parallel to the plate boundary, are comparable with the peninsula-parallel horst and graben structure of the Southern Peloponnese (Messenian and Lakonic Gulfs; see Fig. 1.1).

In addition, well developed Quaternary terraces are known from the Kyrenia Range, Northern Cyprus (Dreghorn, 1978), but these have not been dated or studied in detail. Similar terraces further east (Latakia region, northern Syria) are currently under study by Matt Hardenburg (Ph.D. project, University of Edinburgh).

8.2.4 Sicily (Tyrrhenian fore-arc): The island of Sicily is situated in the foreland of the Tyrrhenian Arc (see Fig. 1.2). The opening of the Tyrrhenian Sea took place since the Late Torrtonian-Early Pliocene (Rehaul et al., 1987; Kastens and Mascle, 1990), as a succession of consecutive fault-controlled basins (Spadini and Podladchikov, 1996). The Sicilian foreland underwent compression during the Late Neogene-early Quaternary, as evidenced by open folds and thrusts that affected Plio-Pleistocene sediments (Butler and Grasso, 1993; Butler et al., 1995; Lentini et al., 1995). In this, Sicily contrasts with the fore-arc region of the Southern Peloponnese, where compression probably ended by Middle Miocene (Jacobschangen et al., 1978). However, a few kilometres west of the Peloponnese (e.g. Ionian Islands; see Fig. 1.2) thrusting was active until Early Quaternary times (Zelilidis et al., 1998). As in the Southern Peloponnese, the Late Neogene-Quaternary sedimentary

record of Sicily is thought to reflect the interplay between glacio-eustatic sea level cyclicity and local tectonic controls (Butler and Grasso, 1993). The latter included local uplift, as a result of thrusting, and regional flexural subsidence of the Tyrrhenian thrust belt. However, flexural subsidence ceased in Late Pliocene times, after the orogenic hinterland was unloaded (Butler and Grasso, 1993).

Thick Tortonian-Messenian deposits are present in Sicily, including well developed evaporite successions correlated with the "Messenian salinity crisis" (Grasso and Pedley, 1988; Pedley and Grasso, 1993; Pedley, 1996a,b). These sediments differentiate Sicily from the Peloponnese, where such deposits remain, so far, unknown (Mariolakos, 1975; Berkhemer et al., 1978), probably because the Peloponnese was emergent during the Late Miocene (Chapter 7). Plio-Pleistocene sedimentation in Sicily started ca. 5.35 Ma ago (Early Pliocene; Zanclian), with deposition of pelagic chalks ('*Trubi Formation*'), followed by blue clays, silts and muds, then by progradational clinoforms and coastal carbonates and siliciclastics (Di Grande et al., 1976; Grasso et al., 1997; see Fig. 8.1). This marine succession spans the Early Pliocene-early Pleistocene. Characteristic facies boundaries within the succession are diachronous across Sicily, with progressively younger ages southwards (i.e. away from the orogen; see Fig. 1.2). The Plio-Pleistocene succession was interpreted as a transgressive-forced regressive megasequence and regression was attributed to Late Pliocene-Pleistocene tectonic uplift (Grasso et al., 1997). The earliest Pleistocene sediments in Sicily (pelagic chalks of '*Trubi Formation*') are correlative with the offshore muds of Unit 1.4 in the Messenia Peninsula, also of Early Pliocene (Zanclian) age (Frydas, 1990; Frydas and Bellas, 1994; see Fig. 8.1). Unit 1.4 was also deposited above a maximum flooding surface (Kourampas and Robertson, 2000) that marks the early Pliocene inundation of the Mediterranean after the Messinian salinity crisis (Zelilidis, 1988; Zelilidis and Frydas, 1994). Plio-Pleistocene successions in both Sicily and the Southern Peloponnese (Messenia and Eastern Lakonia) exhibit a similar coarsening-up trend. The facies boundary between blue clays, silts and muds (below) and coastal carbonates and siliciclastics (above) in Sicily is comparable with transitions from offshore carbonate muds to transitional offhsore-lower shoreface muds-sands, then to shoreface-foreshore detrital carbonates-silicicalstics in the Messenia and Eastern Lakonia Peninsulae. In Sicily, Late Pliocene to early Pleistocene shallow-marine carbonates comprise spectacular offlapping parasequences, reminiscent of the progradational carbonates of Units 2.1, 2.2, 2.4 in the Messenia Peninsula and Unit 3 in the Eastern Lakonia Peninsula (Figs. 3.5, 5.6, 7.1, 8.1), but at a larger scale. Coarsening-up trend and offlapping depositional architecture are interpreted as the results of forced-regression, triggered by uplift of both Sicily and the Southern Peloponnese in latest

Pliocene-Pleistocene time. In Sicily, coastal facies become progressively younger towards the south, away form the orogenic interior and the areas of maximum uplift. This is similar to the progressive basinward decrease in age of Pleistocene shallow-marine sediments in the Messenia and Eastern Lakonia Peninsulae (Chapters 3, 5, 7). These similarities in facies, depositional architecture and up-sequence development of Plio-Pleistocene sediments, deposited in two areas of different tectonic setting, suggest that glacio-eustatic sea level change was the dominant control over sedimentation. Maximum net accumulated uplift since the Early Pliocene is estimated as ca. 2000 m in Sicily (Abate et al., 1982, after Grasso et al., 1997) and ca. 400-300 m in the Messenia and Eastern Lakonia Peninsulae (Kelletat et al., 1976; Mariolakos et al., 1994; Chapters 2, 4). Higher values of Plio-Pleistocene uplift in Sicily possibly reflect Plio-Pleistocene folding and thrusting, as opposed with crustal extension and normal faulting in the Southern Peloponnese.

8.3 COMPARISON WITH THE CORINTH-PATRAS GULF BACK-ARC

The Corinth-Patras Gulf is among the best researched areas in the Peloponnese and its Plio-Pleistocene stratigraphy is relatively well understood (see Chapter 1). The Corinth-Patras rift is a back-arc basin that comprises three distinct grabens (Corinth, Rio and Patras grabens; Doutsos and Poulimenos, 1992). These were formed as a result of listric faulting along strikes generally oblique to transverse to the strike of the Ionian trenches (Jackson et al., 1982a; Doutsos and Piper, 1990; Doutsos and Poulimenos, 1992) (Figs. 1.1, 1.2). Listric faulting was associated with uplift and extension that followed the westward migration of the orogen after Middle Miocene time (Doutsos et al., 1988). A diachronous migration of subsidence form east to west along the rift axis during the Late Pliocene-Pleistocene was inferred (Doutsos and Poulimenos, 1992). A similar westward progression of grabben formation further south, in the Messenia and Eastern Lakonia Peninsulae, was also inferred from the available biostratigraphic data (Zelilidis and Doutsos, 1992; Kourampas and Robertson, 2000).

As in the Messenia and Eastern Lakonia Peninsulae further south, Plio-Pleistocene sedimentation in the Corinth-Patras rift reflects the interplay between regional uplift, subsidence (due to normal faulting) and glacio-eustatic sea level change (Collier 1990; Collier et al., 1991, 1993; Doutsos and Piper, 1990; Poulimenos et al., 1993; Seger and Alexander, 1993; Stamatopoulos et al., 1994). Post-alpine deposition started in the Early Pliocene in the eastern parts of the Corinth-Patras Rift (Corinth area), with lacustrine marls and alluvial conglomerates (Freyberg, 1973; Collier and Dart, 1991), with evidence for

syndepositional faulting. Alluvia were succeeded by progradational conglomerates, interpreted as braid stream delta-top deposits (Collier and Dart, 1991). In the eastern parts of the basin, lacustrine to brackish marls, interpreted as a microtidal estuary, follow up-sequence, succeeded, in turn, by deltaic sands (Collier and Dart, 1991). Early Pliocene deposition terminated with fanglomerates to submarine fans, from the western to the eastern part of the basin (Collier and Dart, 1991). Deposition of these sediments was controlled by listric normal faulting. Lacustrine to brackish conditions, with marine incursions during sea level highstands, persisted until middle Pleistocene time (isotopic stage 7; Piper et al., 1990, or isotopic stage 9.3; Stamatopoulos et al., 1994). Early to middle Pleistocene marine transgressions progressed from the eastern (Corinth area) to the western (Patras area) part of the rift. The Pleistocene sedimentation comprised deposition of transgressive-regressive, lacustrine to marine sequences ('*Corinth Marl*'; Collier, 1990), followed by up to 500 m-thick fan deltas (Poulimenos et al., 1993), and up to five progradational shallow-marine '*sub-sequences*', each correlated with a major highstand of Pleistocene to Holocene age (Collier, 1990). Radiometric dating of these sub-sequences, correlative with the terrace-sequences in the Messenia and Eastern Lakonia Peninsulae, suggested minimum uplift rates ca. 0.2-0.3 m/ka, averaged across the last 312 or 205 ka, respectively (Collier, 1990; Collier and Dart, 1991; Collier et al., 1992). Other workers, however, inferred exceptionally high rates of uplift locally, e.g. 4 m/ka in Kastritsi, near Rion, in the western part of the Corinth-Patras rift (Stamatopoulos et al., 1994).

8.4 TERRACES IN THE SOUTHERN PELOPONNESE IN THE CONTEXT OF THE GLOBAL RECORD OF QUATERNARY TERRACES

8.4.1 Meditteranean and Red Sea terraces: Quaternary terraces (and associated erosional landforms: e.g. marine notches) are present in many Mediterranean coasts, wherever Pleistocene-Holocene uplift has taken place (Keraudren, 1970, 1971; Ahnert, 1998). Well known examples include SE Spain (Almeria region: Goy and Zazo, 1986), South France (Flemming, 1968b), Italy and Sicily, the coasts of Turkey, Syria (Al-Riyami, pers. comm. 1999), Cyprus (Poole, 1991; Poole and Robertson, 1991, 2000) and Israel (Neev et al., 1987). Quaternary terraces of the Mediterranean typically comprise mixed terrigenous-carbonate sediments and small coral-algal reefs. The latter are commonly correlated with highstands and reflect the warm climatic conditions of Pleistocene interglacials (Pirazzoli, 1986b; Taviani, 1998; Poole, 1992; Kourampas and Robertson, 2000; Poole and Robertson, 2000). This interplay between terrigenous and carbonate deposition is though to be influenced by the rate and direction of relative sea level change (Arvidson et al., 1994).

Tyrrhenian terraces are widespread along the Mediterranean coasts, commonly identified by the characteristic gastropod, *Strombus bubonious* (Keraudren, 1970, 1971; Papapetrou-Zamanis, 1971; Pirazzoli, 1986b). The terraces of the Southern Peloponnese are, thus, of a 'typical' Mediterranean type, in both their mixed terrigenous-carbonate lithologies and the prominent development of the Tyrrhenian outcrops locally.

Quaternary terraces also occur along the Red Sea coast, commonly consisting of patch coral-algal reefs and detrital carbonates, intercalated with terrigenous sediments (El-Asmar, 1997; Plaziat et al., 1998; Purser et al., 1998; Taviani, 1998). It was suggested that such alternations reflected sea level cyclicity at a high frequency, although autocyclic controls cannot be excluded (Arvidson et al., 1994). Late Pleistocene terraces in the Southern Peloponnese exhibit similar lithological alternations up section (see Chapters 3, 5, 7).

8.4.2 Terraces in the Oceanic Islands: Some of the best documented examples of Quaternary terraces occur in oceanic islands at tropical latitudes (e.g. Papua New Guinea: Chappell, 1974, Sumba Island, Indonesia: Bard et al., 1996, Barbados: Bard et al., 1990). In these areas, moderate to high uplift rates and proliferation of reef building organisms during the warm conditions of the Pleistocene interglacials led to the formation of flights of marine terraces on Pleistocene limestones. Isotopic dating of coral samples form these Pleistocene reefs have resulted in commonly quoted eustatic sea level curves (e.g. Imbrie et al., 1984; Martinson et al., 1984). Like isotopically dated terraces elsewhere, these of the Southern Peloponnese formed as a result of Quaternary tectonic uplift. Deposition took place incrementaly, giving rise to regionally correlative unconformities during sea level lowstands (see Chapter 7). Terraces in the Southern Peloponnese, therefore, as elsewhere along the Mediterranean coast, are potential indicators of eustatic sea level fluctuations and must be taken into account in any global assessment of glacio-eustatic sea level change.

CHAPTER 9: CONCLUSIONS AND SUGGESTIONS FOR FURTHER STUDY

9.1 CONCLUSIONS

The following conclusions are drawn from this study of the Plio-Quaternary evolution of the Messenia and Eastern Lakonia Peninsulae:

- The Plio-Pleistocene sedimentary and geomorphological record of the Messenia and Eastern Lakonia Peninsulae (Southern Peloponnese) is very well preserved, shedding light on the tectonic-sedimentary evolution of a fore-arc area in the western part of the Hellenic arc, between the Ionian subduction zone to the west and the Aegean back-arc to the east. The results of the present study supplement observations from an area between the better known Corinth-Patras and Cretan areas to the north and south, respectively.

Faults and joints

- **Faults:** The Messenia Peninsula is cut by two sets of faults, namely peninsula-parallel faults of NNW-SSE and N-S to NNE-SSW strikes and cross-peninsular faults of ENE-WSW to E-W strikes. ENE-WSW to E-W faults are interpreted as transfers to the NNW-SSE to N-S ones. Faults of both groups show evidence for oblique slip. Faults of both groups were active during the Quaternary.

- The Eastern Lakonia Peninsula is cut by NW-SE and NE-SW faults, oblique to the long axis of the peninsula, and also N-S to NNE-SSW and E-W faults. These fault sets are orthogonal to each other. Morphological evidence suggests that the set of N-S and E-W faults is probably the youngest. However, faults of all four groups were active during the Quaternary. N-S faults show evidence of the greatest activity during the Quaternary.

- Faults of all directions are more closely spaced in the Eastern Lakonia Peninsula than in the Messenia Peninsula. The maximum spacing is ca. 12 km in the Eastern Lakonia Peninsula (counted between NW-SE faults), as compared with ca. 20 km in the Messenia Peninsula (counted between ENE-WSW faults). The more fractured superficial crust in the Eastern Lakonia Peninsula reflects the more 'internal' position of the latter within the

SW Hellenic fore-arc, in close proximity to the actively extending Aegean back-arc to the east and the highly extended Kythera-Antikythera Ridge to the south.

- **Joints:** In both the Messenia and Eastern Lakonia Peninsulae, extensional joints follow the same directions as normal faults, but with a wider scattering of trends. Extensional joints often affect sediments of all ages, including latest Pleistocene sediments. These joints are very similar to joints that have resulted from earthquakes in Historical time (e.g. Gulf of Corinth), as well as well documented palaeoseismic joints near the areas of study (e.g. eastern parts of Kalamata graben). Local outcrop evidence shows that fractures that functioned as mesoscopic normal faults (throws < 1 m) in middle Pleistocene time were reactivated as joints in late Pleistocene ("Eutyrrhenian") time (e.g. western coast of the Eastern Lakonia Peninsula). These outcrops, thus, document the evolution of extensional fractures over time scale of ca. 300-100 ka. Closely spaced (every 2-10 cm) sets of linear joints in Pleistocene detrital sediment are concentrated in narrow zones (ca. 0.7-1.5 m), parallel to faults in bedrock and associated with morphological scarps. These joints are interpreted as the result of Quaternary reactivation of faults buried beneath Pleistocene sediments. In view of the easily eroded Pleistocene lithologies, the good preservation of such joints suggests late Pleistocene or younger age of faulting.

Block faulting

- Cross-peninsular faults divide the Messenia Peninsula into two blocks, of dimensions in the order of 10x20 km, namely the Northern Messenia Block and the Southern Messenia Block. These blocks evolved semi-independently during Pliocene-Pleistocene time. The Northern Messenia Block experienced incremental uplift and forced regression since the Late Pliocene, as evidenced by a well development flight of marine terraces and transgressive-regressive sedimentary sequences (see below). The Southern Messenia block probably experienced southward tilting and subsidence since early or middle Pleistocene time, as evidenced by the relative altitude of early Pleistocene terraces and the absence of unambiguous late Pleistocene terraces.

- Parallel and oblique faults divide the Eastern Lakonia Peninsula into composite horsts and grabens, at the scale of ca. 5x15 km. These blocks evolved semi-independently during the Pleistocene, as shown by the number and altimetric distribution of morphological surfaces and marine terraces, drainage patterns and facies of shallow-

marine sediments. The main fault-bounded morphological blocks distinguished in the Eastern Lakonia Peninsula are: 1) The Ano Glikovrisi Horst, 2) The Molai Graben, 3) The Dokali Graben, 4) The SW Lakonia Benchland, 5) The Neapolis Graben, 6) The Cape Maleas, and 7) the Eastern Coast. Faults of rhombic pattern (NW-SE and NE-SW strikes), in particular, control narrow grabens oblique to the strike of the peninsula (e.g. Molai Graben). These grabens were major depocentres of Pleistocene sediments, now exposed onland in the Eastern Lakonia Peninsula.

- The Molai Graben, bounded by ca. 20 km long faults of N-S to NNE-SSW trend and ca. 12-15 km long faults of NW-SE trend, is probably the most active neotectonic structure within the Eastern Lakonia Peninsula. The length of these graben-bounding fault systems is at the same scale as the thickness of the seismogenic layer of the crust (ca. 20 km), comparable with that of other major faults in central Greece and the Gulf of Corinth, and probably capable of generating earthquakes of magnitude up to 7.

Drainage

- In both the Messenia and the Eastern Lakonia Peninsulae, the drainage is controlled by bedrock lithology, morphology and age of the drained relief, normal faulting, crustal uplift and glacio-eustatic sea level change.

- The drainage network of the Messenia Peninsula is divided into peninsula-parallel, NNW-SSE and cross-peninsular, generally E-W flowing drainage. High ($>4^{th}$) order streams of the first group, that drain bedrock, were probably formed during the Pliocene, controlled by regional uplift, relative sea level fall and the activity of cross-peninsular, E-W striking normal faults. Streams of the second group were formed during the Pleistocene, controlled by regional uplift, relative sea level fall and the activity of peninsula-parallel NNW-SSE and N-S faults. Peninsula-parallel streams were captured by cross-peninsular streams during the Pleistocene.

- In the Eastern Lakonia Peninsula, drainage systems branch around a NNW-SSE trending divide, parallel to the long axis of the peninsula. Drainage density is higher in the northern and central parts of the peninsula, on metamorphic bedrock, and lower in the southern part of the peninsula, on Tripolis Zone limestone bedrock. Fault-bounded morphologic units developed distinct drainage networks.

- In both Peninsulae, the gradient of valleys reflects the lithology, uplift and activity of normal faults along their courses. Streams of steep longitudinal profile are typical of synthetic fault blocks active during the Quaternary (e.g. Ano Glikovrisi Horst). Streams of step-like longitudinal profile are typical of uplifted blocks with terraced morphology and only local (or absent) normal faulting (e.g. Gargaliani area, SW coast of the Eastern Lakonia). Streams of low-gradient, concave profile with few (or absent) knick points characterise the axial drainage of grabens with rates of uplift lower than the surrounding horsts (e.g. Molai Graben).

Surfaces, terraces and valleys

- The following main generations of surfaces of subaerial erosion and marine terraces (with sediment) are identified within, and correlated across, both the Messenia and the Eastern Lakonia Peninsulae: 1) Late Miocene-Pliocene(?) pediments/pediplains (varying number), 2) Latest Pliocene pediment, 3) Early Pleistocene terrace(s), 4) Late early to early-middle Pleistocene terrace(s), 5) Middle Pleistocene terrace(s), 6) Eutyrrhenian terrace, 7) Neotyrrhenian terrace, 8) Holocene raised beaches, vermetid bioconstuctions and marine notches. Intramontane plains and polje, of Late Pliocene-Quaternary age, are also present within the Eastern Lakonia Peninsula.

- Pleistocene terraces without sediment cover are present locally in both Peninsulae (in varying numbers). These can be assigned relative ages locally, on the basis of their relation with identifiable terraces with sediment. However, their lack of sediment cover prevents their correlation within each peninsula or between the two Peninsulae.

- In the Messenia Peninsula, six main Quaternary terraces with overlying shallow-marine sediments are present within the Northern Messenia Block, at altitudes of <200-340 m (early Pleistocene), ca. 240 m (late early (to middle) Pleistocene), 40-60 m (middle Pleistocene: "Sicilian"), 15-20 m ("Eutyrrhenian"), 2-4 m ("Neotyrrhenian") and 0.2-1.5 m (Holocene: "Versilian").

- In the Eastern Lakonia Peninsula, six main Quaternary terraces with overlying shallow-marine sediments are again present in the Ano Glikovrisi Horst, at altitudes of 100-240 m, 120m, 60-80 m, 15-20 m, 2-5 m and 0.2-1 m, the SW Lakonia Benchland and the Dokali Graben, at altitudes of 120 m. 80-100 m, 40 m, 15-20 m and 0.2-1 m, for the

early, early-middle Pleistocene, "Eutyrrhenian", "Neotyrrhenian" and "Versilian" terraces, respectively.

- In the Northern Messenia Block (see above), from the mountain front to the present-day coastline, the following succession of valley types is present: 1) Narrow, V-shaped wind gaps dissect the mountain front into degraded triangular facets. 2) Downstream, these are succeeded by broad, relatively mature valleys eroded through friable shallow-marine and alluvial sediments of the early and early-middle Pleistocene terraces. 3) Narrow, V-shaped gorges, up to >120 m deep, were eroded through shallow-marine sediments and bedrock across the cliff that separates the early and early-middle Pleistocene terraces upstream, from middle and late Pleistocene terraces downstream. d) Meanders of U-shaped valley profile were entrenched into bioconstructed carbonates of the middle Pleistocene ("Sicilian") terrace. e) Slightly V-shaped valleys were eroded through the shallow-marine carbonates of the "Eutyrrhenian" terrace. f) Shallow, immature ravines were eroded through shallow-marine carbonates of the "Neotyrrhenian" terrace, probably corresponding to a base level below the present sea level. The lower reaches of these streams received alluvial fill since the latest Pleistocene. Several episodes of latest Pleistocene-Holocene down-cutting and alluviation are present within the latter.

- A similar succession of valley forms from the mountain front to the present-day coastline is also present within the Eastern Lakonia Peninsula: 1) Broad, U-shaped dry valleys or valley side pediments, of probable Late Pliocene age, were eroded through uplifted Late Miocene-Early Pliocene (?) pediments, 2) Broad, shallow valleys were eroded through friable early Pleistocene sediments on the early Pleistocene terrace. 3) Steep, V-shaped valleys were eroded into friable sediments and bedrock across the middle Pleistocene cliff, 4) Shallow, immature valleys were eroded through late Pleistocene sediments. As in the Messenia Peninsula, several episodes of Holocene alluviation and incision are present.

- In both the Messenia and the Eastern Lakonia Peninsulae, the younger marine terraces occur at successively lower levels. This implies that both Peninsulae underwent relative marine regression since the beginning of the Pleistocene (ca. 1.6 Ma). On time scales of the order of 1-2 Ma (Late Pliocene to Holocene) regional tectonic uplift, punctuated by glacio-eustatic sea level change, exercised the dominant control over shallow-marine sedimentation. On the time scale of the last 1 Ma (middle Pleistocene-Holocene) the

uplift rate (assumed to be constant), ranges from 0.33-0.23 m/ka in the NW Messenia block, to 0.24-0.10 m/ka along the western coast of the Eastern Lakonia Peninsula. The uplift rate of the NW Messenia block is comparable with that that inferred for the Gulf of Corinth region further north (ca. 0.3 m /ka; Collier, 1990). The lower uplift rate of Eastern Lakonia Peninsula may reflect its more distal position in relation to the active plate boundary. Possible causes for this lower uplift rate could be 1) Less intense effect of crustal underplating, as compared with more external Messenia Peninsula, and/or 2) Higher rates and closer spacing of normal faulting, that would, locally, contest the effects of regional uplift. However, during the last ca. 120 ka (late Pleistocene-Holocene), the two Peninsulae were uplifted at a similar rate (ca. 0.16 m/ka).

Neogene-Quaternary sediments

- Plio-Quaternary marine sediments, from both Peninsulae, were dated using nannofossils for the Pliocene-early Pleistocene time interval. In addition, late Pleistocene sediments are correlated with the well known "Eutyrrhenian" (isotopic stage 5.5; ca. 120 ka) and «Neotyrrhenian» (isotopic stages 5.3+5.1; ca. 100-80 ka) deposits elsewhere in Greece and other Mediterranean areas (e.g. Cyprus). A sequence-stratigraphic approach, involving correlation of successive marine terraces with known, dated, global sea level highs was used to infer possible ages for the "Calabrian" and "Sicilian" stages (although with uncertainties resulting from unresolved multiple sea level highs).

1) Messenia Peninsula

- In the Messenia Peninsula, marine sedimentation began in the Early Pliocene (Zanclian; ca. 5 Ma) and continued until the Holocene, interrupted by periods of emergence, subaerial erosion, alluviation and pedogenesis. The Pliocene-Holocene sedimentary record of the Messenia Peninsula is resolved into 19 informal units. Marine sediments are resolved into 9 distinct depositional units, bounded by unconformities. Subaerial sediments (10 units) are distinguished on the basis of their relation to marine sediments, major landforms (e.g. river valleys, erosional surfaces) and facies. However, at least some of the suabaerial units may be contemporaneous, reflecting differences of depositional environment.

- The Pleistocene-Holocene sedimentary record of the Messenia Peninsula (last ca. 1,6 Ma), is grouped into two 3rd-order depositional sequences, namely: MQ1, of early Pleistocene age, correlated with the sea level cycle 3.9 *sensu* Haq et al. (1988) and MQ2,

of middle Pleistocene-Holocene age, correlated with the sea level cycle 3.10. Sequence MQ1 was deposited on Late Pliocene subaerial relief (pediment, palaeovalleys) and terminates upwards with soils. The early Pleistocene marine terrace(s) were formed above sediments of Sequence MQ1. Sequence MQ2 was deposited on middle Pleistocene subaerial relief (cliffs, pediments) that locally reach ca. 120 m. This sequence terminates upwards with soils and aeolianite. The middle and late Pleistocene terraces and the Holocene marine abrasion platform were formed above sediments of Sequence MQ2. The post-middle Pleistocene sequence MQ2 is resolved into at least three 4^{th}-order 'sequences' (formally parasequences), bounded by unconformities, namely: "Sicilian", "Tyrrhenian" and Holocene. These are correlated with 4^{th}-order sea level cycles that reflect glacio-eustatic sea level change. The "Tyrrhenian" is further subdivided into "Eutyrrhenian" and "Neotyrrhenian" units, reflecting higher frequency glacio-eustatic cyclicity within isotopic stage 5. The early Pleistocene Sequence MQ1 is resolved into at least two higher-order 'sequences', also bounded by unconformities. The earliest 'sequence' is correlated with the regressive "Calabrian" stage of the early Pleistocene. The latest 'sequence' can be correlated with either an intra-"Calabrian", 4^{th} or higher-order sea level cycle (by comparison with the 4^{th}-order 'sequences' present within Sequence MQ2), or with an early middle Pleistocene sea level cycle, predating emergence and cliff-cutting.

2) Eastern Lakonia Peninsula

- The earliest dated post-orogenic marine sediments in the Eastern Lakonia Peninsula are of early Pleistocene age (NN 19a biochronozone); these were predated by Late Tertiary subaerial deposition. Marine sedimentation continued until the Holocene, interrupted by periods of emergence, subaerial erosion, alluviation and pedogenesis. The Late Tertiary-Quaternary sedimentary record of the Eastern Lakonia Peninsula is resolved into 13 informal units. Marine sediments are divided into 7 distinct depositional units, bounded by unconformities. Subaerial facies are distinguished on the basis of their relation to marine units (e.g. interfingering), landforms, and facies.

- As in the Messenia Peninsula, the Pleistocene-Holocene sedimentary record of the Eastern Lakonia Peninsula (last ca. 1.6 Ma), is grouped into two 3^{rd}-order depositional sequences, namely: LQ1, of early Pleistocene age, correlated with the sea level cycle 3.9 *sensu* Haq et al. (1988) and LQ2, of middle Pleistocene-Holocene age, correlated with the sea level cycle 3.10. Sequence LQ1 was deposited on subaerial relief (pediment,

palaeovalleys) of Late Pliocene, or earlier age. This sequence terminates upwards with alluvial fans and soils. The early Pleistocene marine terrace(s) were formed above sediments of Sequence LQ1. Sequence LQ2 was deposited on middle Pleistocene subaerial relief (cliffs, pediments) that locally reaches ca. 80 m. This sequence terminates upwards with alluvial sediments, soils and aeolianite. The middle and late Pleistocene terraces and the Holocene marine abrasion platform were formed above sediments of Sequence LQ2. The post-middle Pleistocene sequence LQ2 is resolved into at least three 4^{th}-order 'sequences' (formally parasequences), bounded by unconformities, namely: "Sicilian", "Tyrrhenian" and Holocene. These are correlated with 4^{th}-order sea level cycles that reflect glacio-eustatic sea level change. The "Tyrrhenian" is further subdivided into "Eutyrrhenian" and "Neotyrrhenian" units, reflecting higher-frequency glacio-eustatic cyclicity within isotopic stage 5. The early Pleistocene Sequence LQ1 is resolved into at least two higher-order 'sequences', also bounded by unconformities. The earliest 'sequence' is correlated with the regressive "Calabrian" stage of the early Pleistocene. The latest 'sequence' can be correlated with either an intra-"Calabrian", 4^{th}- or higher-order sea level cycle (by comparison with the 4^{th}-order 'sequences' present within Sequence LQ2), or with an early middle Pleistocene sea level cycle, predating emergence and cliff-cutting.

Significance of the correlation across the two Peninsulae

- **Background controls:** The correlation of Quaternary marine deposits across the Messenia and Eastern Lakonia Peninsulae was achieved through correlation of their terminal surfaces (unconformities, surfaces of subaerial erosion). The same approach provided the means for correlation of many, but not all, of the subaerial units identified, as well as major landforms (i.e. marine terraces, valleys, cliffs). Successively younger marine sediments and terraces lie at progressively lower altitudes in both Messenia and Eastern Lakonia, demonstrating that both Peninsulae underwent relative marine regression during the last 1.6 Ma. This suggests that there was a common background control over marine and subaerial sedimentation and landscape evolution in both Peninsulae during the Quaternary. This control was relative sea level change, involving long term regression due to land uplift, operating over the time scale of the entire Quaternary (ca. 1.6 Ma) and glacio-eustatic sea level cyclicity. The latter operated in cycles of varying frequency: Two cycles of ca. 800 ka, corresponding to 3^{rd}-order Sequences Q1, Q2, at least four cycles of ca. 100-200 ka, and at least three cycles of ca. 1-30 ka were recognised. A further control operating over both Peninsulae was climate; this influenced subaerial processes and, in consequence, relief formation and facies of

suaberial sediments and soils. Climatic influence in marine sedimentation is also identified, in the form of warm fauna in deposits of 'warm' "Tyrrhenian" highstands (e.g. *Strombus bubonius* and associated fauna) and coral-algal reefs.

- **Local controls:** Differences in the altitude and number of marine terraces, as well as the facies and the number of subaerial depositional units, within each peninsula and between the two Peninsulae are attributed to the operation of local factors. The main local factor was active faulting, that, by controlling the gradient of the relief, influenced the deposition of alluvial fans and related sediments. The larger areal extent of Pleistocene fanglomerates in the Eastern Lakonia Peninsula is attributed to its more closely spaced fault pattern, compared to the Messenia Peninsula. In the Messenia Peninsula, early Pleistocene deltaic sediments were commonly fed by transverse drainage that locally followed ENE-WSW transfer faults. Local extensional faulting also controlled some offshore deposition, in both Peninsulae, notably of early Pleistocene offshore sediments within narrow asymmetrical grabens. As a result, on an outcrop scale, the preserved sediments mainly document the interplay between the effects of regional tectonic uplift, glacio-eustatic sea level change, climate and local extensional faulting.

Sediment architecture in relation to sea level change

- Each shallow-marine depositional unit is interpreted as a transgressive-regressive 'sequence'. Proximal parts of these units commonly overlie marine ravinement surfaces (formed from wave action during transgression). From bottom to top, depositional units commonly begin with aggradational to retrogradational, fining-up facies, deposited in an environment of progressively decreasing energy ('transgressive systems tract'), correlated with sea level rise. These are followed by progradational, coarsening-up facies, deposited in an environment of progressively increasing energy ('highstand systems tract'), correlated with shoreline progradation during sea level highstand and the early stages of sea level fall. These two parts of the unit are commonly separated by downlap surfaces, defined by the contact of coarser-grained, progradational clinoforms above, with finer-grained, poorly stratified sands and silts below.

- In both Peninsulae, shallow-marine units, are covered by subaerial deposits (alluvia and soils), locally filling channels and associated relief, eroded into shallow-marine sediments. Subaerial deposits (mainly channel, bar and interfluvial facies) exhibit aggradational, to progradational, geometries up-section. These are interpreted as

'lowstand systems tracts', deposited during Pleistocene lowstands and the early stages of sea level rise, after a sea level drop that triggered erosion of the valleys. Alluvial fan progradation probably required climatic conditions of seasonal rainfall, as also suggested by the intercalation of alluvial sediments and arid paleosols (caliche). 'Lowstand' alluvia are intercalated with late Pleistocene marine units (highstand deposits) in the Eastern Lakonia Peninsula.

- Alluvial deposits correlated with sea level highstands (early Pleistocene and Eutyrrhenian) are less widespread. These come above shoreline deposits in relative conformity (e.g. early Pleistocene terrace in both the Messenia and Eastern Lakonia Peninsulae), or can be correlated altimetrically with a marine terrace further distally (e.g. "Eutyrrhenian" in the Eastern Lakonia Peninsula). By contrast with the previous type of 'lowstand alluvia', alluvia correlated with highstands generally exhibit more distal characteristics (i.e. good sorting, clast-supported fabric, finer grain size, association with marginal marine facies). These sediments were probably deposited as a result of the seaward shift of backshore environments during highstands and the early stages of sea level fall.

Petrology and diagenesis

- In both Peninsulae, the main microfacies present within shallow-marine sediments comprise detrital carbonates, commonly with a high terrigenous content (i.e. lithic grainstone and packstone, peloidal packstone, foraminiferal wackestone), siliciclastics (i.e. calcareous sandstone, conglomerate) and bioconstructed carbonates (i.e. red algal framestone, coral-red algal bafflestone, blue-green algal bindstone).

- The terrigenous content of the shallow-marine sediments is systematically higher in the Eastern Lakonia Peninsula, possibly reflecting bedrock lithology (widespread outcrops of "Phyllite Series") and more widespread alluviation, triggered by closely spaced normal faulting (see above).

- The diagenetic evolution of shallow-marine sediments, in both Peninsulae, is distinguished into the following sequences:

1) Active marine phreatic zone $\Rightarrow$ (marine vadose zone) $\Rightarrow$ (freshwater phreatic zone) $\Rightarrow$ freshwater vadose zone.

2) Active marine phreatic zone ⇒ stagnant marine phreatic zone ⇒ freshwater phreatic zone ⇒

freshwater vadose zone.

3) Stagnant marine phreatic zone ⇒ freshwater phreatic zone ⇒ freshwater vadose zone.

From the above, the diagenetic sequences (1) and (3) are commonly present in the middle and upper

parts of depositional sequences, whereas sequence (2) characterises lags near the base of depositional sequences. The diagenetic sequences (1) and (3) exemplify a transition of the sediment

from a submarine depositional environment to a subaerial environment, during and after emergence

(i.e. relative sea level fall). The diagenetic sequence (2) exemplifies a transition of the sediment from

a high to a low energy submarine environment, during transgression (i.e. relative sea level rise).

- Palaeosols developed on shallow-marine sediments and alluvia are of the caliche type, suggesting that a semiarid climate prevailed in the Southern Peloponnese during some periods of the Pleistocene. Many of these semiarid periods coincided with sea level lowstands, as shown by intercalation of caliche with alluvial sediments (see above). Caliche types present in the Messenia and Eastern Lakonia Peninsulae include hardpan, platy, chalky, nodular caliche and *rhizocretion* paleosols.

- Besides climate, the age and lithology of the host sediment also controlled the development of caliche. Mature caliche types (hardpan and platy caliche) are generally absent from late Pleistocene sediments, but widespread on early Pleistocene sediments. Nodular caliche is present in fine-grained facies of early to middle Pleistocene host rock. Rhizocretion paleosols developed in shallow-marine sediments, aeolianite and alluvia of middle and late Pleistocene age.

Plio-Quaternary Evolution

- The Plio-Quaternary sedimentary and tectonic evolution of the Messenia and Eastern Lakonia Peninsulae is divided into the following stages:

1) Pliocene: In the Early Pliocene, NNW-SSE normal faulting in the eastern part of the Messenia Peninsula led to formation of grabens that accommodated offshore sedimentation during the Pliocene. The central and NW parts of the peninsula were emergent during the Pliocene and subaerial deposition was taking place. Large parts of the peninsula were drained by NNW-SSE oriented streams, partly controlled by ENE-WSW faulting. NNW-SSE faulting affected NW Messenia in the Late Pliocene and offshore deposition took place in grabens. The Late Pliocene pediment was eroded in emergent parts of the peninsula. So far, no marine sediments of Pliocene age have been identified in the Eastern Lakonia Peninsula. Pliocene sediments are mainly alluvial fans, partly controlled by normal faulting. Subaerial erosion led to the formation of dry, V-shaped valleys (that fed the fan systems) and the Late Pliocene pediment.

2) Early Pleistocene Transgression: Sea level rise (cycle 3.10) led to marine transgression over large parts of both Peninsulae and the deposition of sequences MQ1, LQ1 in Messenia and Eastern Lakonia, respectively. Continuing faulting controlled deposition in narrow grabens. In NW Messenia, NNW-SSE faulting and relative sea level change led to the establishment of a transverse, mainly E-W drainage, that eventually captured older, NNW-SSE oriented streams. Higher-order sea level cyclicity within cycle 3.10 led to deposition of 4^{th}- or higher-order units within sequences MQ1, LQ1. Regional uplift was taking place at the same time, leading to the formation of the first Pleistocene marine terraces.

3) Middle Pleistocene Regression: Sea level drop, probably the combined effect of the Riss lowstand and regional uplift, resulted in emergence and erosion of cliffs and valleys in both Peninsulae (maximum relief: 120 m, in Messenia). This surface of erosion formed the boundary between sequences MQ1, LQ1 and MQ2, LQ2 in Messenia and Eastern Lakonia, respectively. In the Eastern Lakonia Peninsula, alluvial fan progradation was probably influenced by seasonal rainfall and normal faulting. In the Messenia Peninsula, alluvial sediments possibly bypassed the (present) coastal zone and were deposited offshore. A semitropical climate, with high rainfall, is indicated in the Messenia Peninsula by the development of middle Pleistocene siliceous soils.

4) Middle Pleistocene Transgression: Sea level rise (cycle 3.11) resulted in transgression and the deposition of sequences MQ2 and LQ2 in Messenia and Eastern Lakonia, respectively. A combination of higher-order sea level cyclicity and regional uplift resulted in the formation of middle Pleistocene marine terraces.

5) Late Pleistocene Transgressions-Regressions: Fourth- and higher-order sea level cyclicity within cycle 3.11 resulted into formation of at least two late Pleistocene marine terraces ("Eutyrrhenian", "Neotyrrhenian"), in both Peninsulae, during highstands. Lowstands were marked by incision, alluvial fan progradation, soil formation and diagenesis. Normal faulting continued locally in both Peninsulae. The late Pleistocene culminated in sea level fall, correlated with the Last Glacial Maximum lowstand.

6) Holocene: Sea level rise during the last 10 ka led to the transgression of large part of the latest Pleistocene coastline, whereas a succession of alluviation and incision episodes marked valleys eroded during late Pleistocene. Emergent marine abrasion platforms of Holocene age are present locally in both the Messenia and Eastern Lakonia Peninsulae. These reflect either a slightly higher than present sea level, ca. 7 ka ago, or seismic uplift, possibly in historical time, as in other parts of the Eastern Mediterranean.

- In the Messenia Peninsula, an east to west progression of graben formation through time is confirmed (see above). In the east (in the vicinity of the Messenian Gulf graben), subsidence rates were high enough to allow deposition of offshore sediments in Early Pliocene time, whereas in the west subsidence was delayed until latest Pliocene-early Pleistocene This migration of deformation towards the west through time is attributed to "roll-back" of the subducting North African plate (possibly accompanied with gravity spreading of the overriding crust), and reflects tectonic processes operating at the time scale of 3-3.5 Ma. In the Eastern Lakonia Peninsula, an absence of dated pre-Pleistocene sediments does not allow the timing of normal faulting to be assessed.

Comparison with other fore-arc areas

- The Plio-Quaternary tectonic and sedimentary evolution of the Messenia and Lakonia Peninsulae is comparable with that of other fore-arc areas in the Eastern and Central Mediterranean (Crete, Rhodes, Cyprus, Sicily). The fabric of the areas of study comprises faults parallel and perpendicular to the arc, as in Crete; such faults have accommodated the outward expansion of the Hellenic fore-arc, probably corresponding

with periods of trench 'roll-back'. However, Neogene to Quaternary compressional structures, described from Crete and Sicily, were not identified in the Southern Peloponnese. Also, normal faults active in the Southern Peloponnese during the Plio-Quaternary have throws considerably smaller than in the central and eastern parts of the Hellenic fore-arc (e.g. Crete, Rhodes) .

- In the Southern Peloponnese uplift began in the Late Pliocene, as in other areas of the Hellenic, Cyprus, and Tyrrhenian fore-arcs (Crete, Rhodes, Cyprus, Sicily). Plio-Quaternary sedimentation in all these fore-arc areas involved long term-regression, at a time scale of ca. 1.6-2 Ma, punctuated by higher-order transgressions-regressions, reflecting 200-100 and <20-30 ka cycles. This correlation suggests that, local differences in tectonic activity notwithstanding, the interplay between long-term regional uplift (isostatic) and shorter term glacio-eustatic sea level change was the major control of Pleistocene sedimentation and landscape evolution along the Hellenic, the Cypriot and the Tyrrhenian forearcs.

- In the Southern Peloponnese, as in Crete and Rhodes, Quaternary outcrops and landforms are fragmentary and discontinuous, developed on fault-bounded blocks with semi-independent evolution (see above). In the Messenia and Eastern Lakonia Peninsulae continuous outcrops and terraces are rarely preserved for distances >20-25 km along strike. This contrasts with southern Cyprus, where the continuity of landforms and sedimentary units is remarkable, and marine terraces, shallow-marine sediments and fanglomerates extent around the centre of uplift in Troodos. However, Plio-Pleistocene extension in Polis Graben and Pigia Half-graben in Cyprus resulted to deformation of marine terraces, as in the Southern Peloponnese.

9.2 SUGGESTIONS FOR FURTHER STUDY

- A limitation of the present study is the lack of absolute dating of Pleistocene sediments in the Messenia and Eastern Lakonia Peninsulae. Attempts at dating coral with U-series methods failed, due to complete recrystallisation of primary aragonite to low-Mg calcite in all samples collected from the Messenia and Eastern Lakonia Peninsulae (as shown by XRD analysis). Thermoluminesence methods, however, could be applied in the future to date shallow-marine sediments, aeolianites and alluvia, allowing a refinement of the Pleistocene-Holocene stratigraphy of the area.

- In this work, marine sediments of both Peninsulae are divided into two 3rd-order sequences, of early and middle-late Pleistocene age, respectively. The middle-late Pleistocene sequence is further subdivided into at least three higher-order sequences; however, a similar subdivision of the early Pleistocene sequence was not possible. This would require detailed mapping of sequence-bounding unconformities in selected areas of good exposure (e.g. Gargaliani area in NW Messenia and Glikovrisi-Elea area in Eastern Lakonia). Assuming correlation of 4th-order sequences with Pleistocene sea level cycles from published sea level curves (e.g. Imbrie et al., 1984; Martinson et al., 1984), subdivision of the early Pleistocene sequence into higher order units could allow an estimation of the time span covered by the early Pleistocene sequence. This would provide a better constraint for the timing of uplift and block faulting in the studied areas.

- A higher resolution of alluvial units could possibly be achieved by detailed mapping of areas with consecutive alluvial fans (e.g. Petalidhi-Paniperi area in Messenia, Ano Glikovrisi-Elea area in Eastern Lakonia). Such a study, coupled with thermoluminescence dating of fan deposits could yield a detailed stratigraphy of subaerial deposits in the Southern Peloponnese.

- More information about the style of Pliocene-Pleistocene deformation in the Messenia and Eastern Lakonia Peninsulae could be derived from morphotectonic analysis and the creation of DEM models, using the published topographical maps of the HAGS (1:50,000).

REFERENCES

Abbot, S.T., 1997. Mid-cycle condensed shellbeds from mid-Pleistocene cyclothems, New Zealand: implications for sequence architecture. *Sedimentology*, **44**, 805-824.

Adey, W.H., 1986. Coralline algae as indicators of sea-level. In Van de Plassche, O.(ed), *Sea-Level Research: a manual for the collection and the evaluation of data.* Geo Books, Norwich, 229-280.

AGIP Mineraria, 1957. *Foraminiferi Padani (Terziario e Quaternario). Atlante iconographico e distribuzione stratigraphica.* AGIP Mineraria, Milano.

Aharon, P., 1984. Implications of the coral reef record from New Guinea concerning the astronomical theory of ice ages. In Berger, A.L., Imbrie, J., Hays, J., Kukla, G., and Saltzman, B. (eds), *Milankovitch and climate: understanding the response to astronomical forcing.* Reidel, Dordrecht, 379-389.

Aharon, P., and Chappell, J., 1986. Oxygen isotopes, sea level changes and the temperature history of a coral reef environment over the last 105 years. *Palaeogeography, Palaeoclimatology, Palaeoecology*, **56**, 337-379.

Ahnert, F., 1998. *Introduction to Geomorphology.* Arnold, London, 352 p.

Aissaoui, D.M., and Purser, B.H., 1983. Nature and origins of internal sediments in Jurassic limestones of Burgundy (France) and Fnoud (Algeria). *Sedimentology*, **30**, 273-284.

Alexandersson, T., 1969. Recent littoral and sublittoral high-Mg calcite lithification in the Mediterranean. *Sedimentology*, **12**, 47-61.

Alexandersson, T., 1972. Mediterranean beachrock cementation: marine precipitation of Mg-calcite. In Stanley, D.J.(ed), *The Mediterranean Sea: a natural sedimentation laboratory.* Dowden, Hutsinson and Ross Inc, Stroudsburg, Pennsylvania, 203-223.

Amorosi, A., Barbieri, M., Castorina, F., Colalongo, M.L., Pasini, G.,Vaiani, S.C., 1998. Sedimentology, micropalaeontology, and strontium isotope dating of a lower-middle Pleistocene marine succession ("Argille Azzure") in the Romagna Apennines, northern Italy. *Bolletino della Società Geologica Italiana*, **117**, 789-806.

Angelier, J., Gigout, M., and Hogrel, M.-Th., 1976. A propos de gisement Tyrrhenien d'Arvi (Crete): carte stratigraphique, faune, esquisse paleoecologique. *Annales Geologiques des Pays Helleniques*, **28**, 471-488.

Angelier, J., Lyberis, N., Le Pichon, X., Barrier, E., and Huchon, P., 1982. The tectonic development of the Hellenic arc and the sea of Crete: A synthesis. *Tectonophysics*, **86**, 159-196.

Armijio, R., Lyon-Caen, H., and Papanastasiou, D., 1991. A possible normal-fault rupture for the 446 BC Sparta earthquake. *Nature*, **351**, 137-139.

Armijio, R., Lyon-Caen, H., and Papanastasiou, D., 1992. East-West extension and Holocene normal fault scarps in the Hellenic arc. *Geology*, **20**, 491-494.

Arvidson, R., Becker, R., Shanabrook, A., Luo, W., Sturchio, N., Sultan, M., Lotfy, Z., Mahmood, A.M., and El Alfy, Z., 1994. Climatic, eustatic, and tectonic controls on Quaternary deposits and landforms, Red Sea coast, Egypt. *Journal of Geophysical Research*, **99**, 12,175-12,190.

Bard, E., Hamelin, B., and Fairbanks, R.G., 1990. U-Th ages obtained by mass spectrometry in corals from Barbados: sea level during the past 130 000 years. *Nature*, **345**, 405-410.

Bard, E., Jouannic, C., Hamelin, P., Pirazzoli, P., Arnold, M., Faure, G., Sumosusastro, P., and Syaefudin, 1996. Pleistocene sea levels and tectonic uplift based on dating of corals from Sumba Island, Indonesia. *Geophysical Research Letters*, **23**, 1473-1476.

Bassiakos, I.E., 1993. *Dating of fossils from caves and speleothems: Evidence from Electron Spin Resonance (E.S.R.) technique, the study of underground karst morphology and the relevant radiometric and geological conditions in speleoenvironments of Dyros, Mani.* Unpublished PhD Thesis, University of Athens.

Bathurst, R.G.C., 1975. *Carbonate sediments and their diagenesis.* Elsevier Publishing Company, Amsterdam, 658 p.

Bauer, B., 1980. Drainage density - An intergrative measure of the dynamics and the quality of watersheds. *Zeitscrift fur Geomorphologie N. F.*, **24**, 261-272.

Beach, D.K., 1995. Controls and effects of subaerial exposure on cementation and development of secondary porosity in the subsurface of Great Bahama Bank. In Budd, D.A., Saller, A.H., and Harris, P.M. (eds), Unconformities and porosity in carbonate strata. *American Association of Petroleum Geologists Memoir*, **63**, 1-33.

Bellas, S.M., Keupp, H., and Frydas, D., 1998. Sequence-stratigraphic analysis and biostratigraphy of NW Crete Island (Greece): The Neogene Kastelli Kissamou Basin as a case study. *Workshop on Deep Drilling Project in the Forearc of the Hellenic Arc, Crete, Abstracts*, 14.

Bellotti, P., Chiocchini, U., Castorina, F., Tolomeo., L., 1996. Le unità clastiche plio-pleistoceniche tra Monte Mario (città di Roma) e la costa tirrenica presso Focene: alcune osservazioni sulla stratigrafia sequenziale. *Bolletino del Servizio Geologico d'Italia*, **113**, 3-24.

Berckhemer, H., 1978. Some aspects of the evolution of marginal seas deduced from observations in the Aegean region. In Closs, H., Roeder, D., and Shmidt, K., (eds), *Alps, Apennines, Hellenides. Geodynamic investigations along geotraverses by an international group of geoscientists.* Inter-Union Commission on Geodynamics, Scientific Report, **No. 38**, E. Schweizerbart'she Verlagsbuchhandlung, Stuttgart, 527-529.

Berckhemer, H., and Kowalczyc, G., 1978. Post-Alpine geodynamics of the Peloponnesos. In Closs, H., Roeder, D., and Shmidt, K., (eds), *Alps, Apennines, Hellenides. Geodynamic investigations along geotraverses by an international group of geoscientists.* Inter-Union Commission on Geodynamics, Scientific Report, **No. 38**, E. Schweizerbart'she Verlagsbuchhandlung, Stuttgart, 519-522.

Berné, S., Lerocolais, G., Marsset, T., Bourillet, J.E., and DeBatist, M., 1998. Erosional offshore sand ridges and lowstand shorefaces. Examples from tide- and wave-dominated environments of France. *Journal of Sedimentary Research*, **68**, 540-555.

Berner, R.A., 1981. New geochemical classification of sedimentary environments.*Journal of sedimentary Petrology*, **51**, 359-365.

Blank-Vernet, L., 1969. Contribution a l'etude des foraminiferes de Méditerranée.Relations entre la microfaune et le sediment. Biocoenoses actuelles, thanatocoenoses pliocènes at quaternaires. *Extrait du Recueil des Travaux de la Station Marine d'Encoume*, **64-48**, 281 p.

Blatt, H., 1982. *Sedimentary Petrology*. W.H. Freeman and Company, San Francisco, 565 p.

Bonifay, E., 1975. L' "Ère quaternaire": définition, limites et sudbivision sur la base de la chronologie méditerranéenne. *Bulletin du Societè Géologique de France*, (7), **17**, 380-393.

Bottema, S., 1995. The Younger Dryas in the Eastern Mediterranean. *Quaternary Science Reviews*, **14**, 883-891.

Buttler, R.W.H., and Grasso M., 1993. Tectonic controls on base-level variations and depositional sequences within thrust-top and foredeep basins: examples from the Neogene thrust belt of central Sicily. *Basin Research*, **5**, 137-151.

Buttler, R.W.H., Grasso, M., and Linkorish, H., 1995. Plio-Quaternary megasequence geometry and its tectonic controls within the Maghrebian thrust belt of south-central Sicily. *Terra Nova*, **7**, 171-178.

Büttner, D., and Kowalczyk, G., 1978. Late Cenozoic stratigraphy and paleogeography of Greece - a review. In Closs, H., Roeder, D., and Schmidt, K. (eds), *Alps, Apennines, Hellenides. Geodynamic investigations along geotraverses by an international group of geoscientists*. Inter-Union Commission on Geodynamics, Scientific Report, **No. 38**, E. Schweizerbart'sche Verlagsbuchhandlung, Struttgart, 494-501.

Butzer, K.W., 1980. Holocene alluvial sequences: Problems of dating and correlation. In Cullingford, R.A., Davidson, D.A., and Lewin, J. (eds.), *Timescales in Geomorphology*. John Willey & Sons, Chichester, 131-142.

Caputo, R., 1995. Evolution of orthogonal sets of coeval extension joints. *Terra Nova*, **7**, 479-490.

Casten, U., and Makris, J., 1998. Crustal structure of the Hellenic Subduction Zone around Crete based on gravity modelling. *Workshop on Deep Drilling Project in the Forearc of the Hellenic Arc, Crete, Abstracts*, 7.

Chappell, J., 1974. Geology of coral terraces, Huon Peninsula, New Guinea: A study of Quaternary tectonic movements and sea-level cahanges. *Geological Society of America Bulletin*, **85**, 553-570.

Chappell, J., and Shackleton, N.J., 1986. Oxygen isotopes and sea-level. *Nature*,**324**, 137-140.

Chaumillon, E, and Mascle, J., 1995. Variation laterale des fronts de deformation de la Ridge méditarrannéene**. *Bulletin de la Societé géologique de France*, **166**, 463-478.

Choquette, P.W., and Pray, L.C., 1970. Geologic nomeclature and classification of porosity in sedimentary carbonates. *The American Association of Petroleum Geologists Bulletin*, **54**, 207-250.

Cimerman, F., and Langer, M., 1991. Mediterranean foraminifera. *Slovenska Academia Znanosti in Umetnosti, Razred za Naravoslovne Vede*, **30**, 118p.

Collela, A., 1988. Pliocene-Holocene fan deltas and braid deltas in the Crati Basin, southern Italy: a consequence of varying tectonic conditions. In Nemec, W., and Steel, R.J. (eds), *Fan deltas: Sedimentology and Tectonic Settings*. Blackie, London, 50-74.

Collier, R.E.Ll., 1990. Eustatic and tectonic controls upon Quaternary coastal sedimentation in the Corinth Basin, Greece. *Journal of the Geological Society, London*, **147**, 301-314.

Collier, R.E.Ll., and Dart, C.J., 1991. Neogene to Quaternary rifting, sedimentation, and uplift in the Corinth Basin, Greece. *Journal of the Geological Society, London*, **148**, 1049-1065.

Collier, R.E.L., Leeder, M.R., Rowe, P.J., and Atkinson, T.C., 1992. Rates of tectonic uplift in the Corinth and Megara basins, central Greece. *Tectonics*, **11**, 1159-1167.

Coudray, J., and Montaggioni, L., 1986. The diagenetic products of marine carbonates as sea-level indicators. In Van de Plassche, O.(ed), *Sea-Level Research: a mannual for the collection and the evaluation of data*. Geo Books, Norwich, 311-360.

Dalrymple, R.W., 1992. Tidal depositional systems. In Walker, R.G., and James, N.P. (eds), *Facies models. Response to sea level change*. Geological Association of Canada, Ontario, 195-218.

Daly, R.A., 1934. *The changing World of the Ice Age*. Yale University Press, New Haven, 271 p.

Davidson, D.A., 1980. Erosion in Greece during the first and second millenia BC. In Cullingford, R.A., Davidson, D.A., and Lewin, J. (eds.), *Timescales in Geomorphology*. John Willey & Sons, Chichester, 143-158.

Defontaines, B., and Chorowicz, J., 1991. Principles of drainage basin analysis from multisource data: Application to the structural analysis of the Zaire Basin. *Tectonophysics*, **194**, 237-263.

Deffontaines, B., Lee, J.-C., Angelier, J., Carvalho, J., and Rudant, J.-P., 1994. New geomorphic data on the active Taiwan orogen: A multisource approach. *Journal of Geophysical Research*, **99**, 20,243-20,266.

Degnan, P.J., and Robertson, A.H.F., 1994. Early Tertiary melange in the Peloponnese (Southern Greece) formed by subduction-accretion processes. *Bulletin of the Geological Society of Greece*, **30**, 93-107.

Degnan, P.J., and Robertson, A.H.F., 1998. Mesozoic-early Tertiary passive margin evolution of the Pindos ocean (NW Peloponnese, Greece). *Sedimentary Geology*, **117**, 33-70.

Dermitzakis, M., 1972. Pleistocenic deposits and old strandlines in the Peninsula of Gramboussa, in relation to the recent tectonic movements of Crete Island. *Annales Geologiques des Pays Helleniques*, 205-240.

Dermitzakis, M., and Theodoropoulos, D., 1974. Study of beach-rocks in the Aegean Sea. Observations on occurences in SE Crete, Rhodes, and Metopi. *Annales Geologiques des Pays Helleniques*, **26**, 275-305.

Dermitzakis, M.D., Georgiades-Dikeoulia, E., Koskeridou, E., and Triantaphyllou, M.V., 1993/95. The presence of a Pliocene outcrop in Chryssi Island (SE Crete). *Annales Geologiques des Pays Helleniques*, **36**, 351-385.

Dewey, J.F., and Sengör, A.M., 1979. Aegean and surrounding regions: complex multiplate and continuum tectonics in a convergent zone. *Geological Society of America Bulletin*, **90**, 84-92.

Di Grande, A., Grasso, M., Lentini, F., and Scamarda, G., 1976. Facies e stratigrafia dei depositi pliocenici tra Leonforte e Centuripe (Sicilia centro-orientale). *Bolletino della Società Geologica Italiana*, **95**, 1319-1345.

Doutsos, T., and Piper, D.J.W., 1990. Listric faulting, sedimentation, and morphological evolution of the Quaternary eastern Corinth rift, Greece: First stages of continental rifting. *Geological Society of America Bulletin*, **102**, 812-829.

Doutsos, T., and Poulimenos, G., 1992. Geometry and kinematics of active faults and their seismotectonic significance in the western Corinth-Patras rift (Greece). *Journal of Structural Geology*, **14**, 689-699.

Doutsos, T., Kontopoulos, N., and Poulimenos, D., 1987. The Corinth-Patras rift as the initial stage of continental fragmentation behind an active island arc (Greece). *Basin Research*, **1**, 177-190.

Dreghorn, W., 1978. Landforms of Cyprus. *Madem Tetkik ve Arama Enstitüsü, Ankara, Special Publications*, **172**, 222 p.

Duermejier, C.E., Krijgsman, W., Langereis, C.G., and Ten Veen, J.H., 1998. Post-early Messinian counterclockwise rotations on Crete: implications for Late Miocene to Recent kinematics of the southern Hellenic arc. *Tectonophysics*, **298**, 177-189.

Dufaure, J.-J., 1965. Problemes de neotectonique dans le Peloponnese. *Revue de Geographie Physique et de Geologie Dynamique (2)*, **8**, 235-252.

Dufaure, J.-J., 1969. Nivaux d' abrasion marine quaternaire deformes a la peripherie du Peloponnese, Grece. *3e Congres, INQUA, Resummes des communications*, 193.

Dufaure, J.-J., 1977. Neotectonique et morphogenese dans une peninsule Mediterraneenne: Le Peloponnese. *Revue de Geographie Physique et de Geologie Dynamique (2)*, **19**, 27-58.

Dufaure, J.-J., 1984. Distribution des mouvements de terrain dans un espace Mediterraneen instable (Peloponnese, Grece). *Documents, B.R.G.M.*, **83**, 507-516.

Dunham, R.J., 1962. Classification of carbonate rocks according to depositional texture. In Ham, W.E. (ed), Classification of Carbonate rocks, *American Association of Petroleum Geologists, Memoir*, **1**, 108-121.

El-Asmar, H.M., 1997. Quaternary isotope stratigraphy and paleoclimate of coral reef terraces, Gulf of Aqaba, South Sinai, Egypt. *Quaternary Science Reviews*, **16**, 911-924.

El Moursi, M., Hoang, C.T., El Fayoumy, L.F., Hegab, O., Faure, H., 1994. Pleistocene evolution of the Red Sea coastal plain, Egypt: Evidence from Uranium-Series dating of emergent reef terraces. *Quaternary Science Reviews*, **14**, 345-359.

Esteban, M., and Klappa, C.F., 1983. Subaerial exposure environment. In Scholle, P.A., Bebout, B.G., and Moore, C.H. (eds), Carbonate Depositional Environments. *American Association of Petroleum Geologists Memoir*, **33**, 1-54.

Faccenna, C., Nalpas, T., Brun, J.-P., Davy, P., and Bosi, V., 1995. The influence of pre-existing thrust faults on normal fault geometry in nature and in experiments. *Journal of Structural Geology*, **17**, 1139-1149.

Faugeres, L., Zamani, A., and Sabot, V., 1987/88. Analyse morphogenetique de l' escarpement de la cote occidentale de Crete, du Cap Gramvoussa ay Cap Krios a Palaeohora. *Annales Geolologiques des Pays Helleniques*, **33**, 1-21.

Fassoulas, C., 1988. Kinematic analysis of the Heraclion Basin bounding faults. *Workshop on Deep Drilling Project in the Forearc of the Hellenic Arc, Crete, Abstracts*, 28.

Fassoulas, C., Kilias, A., and Mountrakis, D., 1994a. New data about the pre-Oligocene structural evolution of Crete (Greece). *Bulletin of the Geological Society of Greece*, **30**, 67-81.

Fassoulas, C., Kilias, A., and Mountrakis, D., 1994b. Postnappe stacking extension of high-pressure/low-temperature rocks in the isalnd of Crete, Greece. *Tectonics*, **13**, 127-138.

Fernandez-Gonzalez, M., Frydas, D., Guernet, C., et Mathieu, R., 1994. Foraminifères et ostracodes du Pliopleistocène de la région de Patras (Grèce). Intérêt stratigraphique et paléogéographique. *Revista Española de Micropaleontologia*, **26**, 89-108.

FitzPatrick, E.A., 1971. *Pedology. A systematic approach to soil science.* Oliver & Boyd, Edinburgh, 306 p.

Flemming, N.C., 1968a. Derivation of Pleistocene marine chronology from morphometry of erosion profiles. *Journal of Geology*, **76**, 280-296.

Flemming, N.C., 1968b. Holocene earth movements and eustatic sea level change in the Peloponnese. *Nature*, **217**, 1031-1032.

Flemming, N.C., 1972. Eustatic and tectonic factors in the relative vertical displacement of the Aegean coast. In Stanley, D.J., (ed), *The Mediterranean Sea: A natural sedimentation laboratory.* Dowden, Hutchinson, and Ross Inc., Stroudsburg, Pennsylvania, 189-201.

Flemming, N.C., 1978. Holocene eustatic changes and coastal tectonics in the northeast Mediterranean: implications for models of crustal consumption. *Philosophical Transactions of the Royal Society, London*, Series A, **289**, 405-458.

Flemming, N.C., and Woodworth, P.L., 1988. Monthly mean sea levels in Greece during 1969-1983 compared to relative vertical land movements measured over different timescales. *Tectonophysics*, **148**, 59-72.

Flügel, E., 1982. *Microfacies Analysis of Limestones*. Springer-Verlag, Berlin, 631 p.

Folk, R.L., 1974a. *Petrology of Sedimentary Rocks.* Hemphill Publsishing Co., Austin, Texas, 159p.

Folk, R.L., 1974b. The natural history of crystalline calcium carbonate: effect of magensium content and salinity. *Journal of sedimentary Petrology*, **44**, 40-53.

Franseen, E.K., Goldstein, R.H., and Farr, M.R., 1998. Quantitative controls on location and architecture of carbonate depositional sequences: Upper Miocene, Cabo de Gata region, SE Spain. *Journal of Sedimentary Research*, **68**, 283-298.

Frydas, D., 1993. Über die Nannoplankton-Stratigraphie des Pliozäns und unteren Pleistozäns des SE-Peloponnes, Griechenland. *N. Jb.Geol. Paläont. Mh.*, **H 4**, 227-238.

Frydas, D., 1998. Biostratigrpahical research in Late Neogene deposits of the Chania Area, Crete. *Workshop on Deep Drilling Project in the Forearc of the Hellenic Arc, Crete, Abstracts*, 23-27.

Frydas, D., and Bellas, S., 1994. Plankton stratigraphy and some remarks on the Globorotalia evolutionary trends from the Plio-Pleistocene sections of southwest Peloponnesus, Greece. *Micropalaeontology*, **40**, 322-336.

Frydas, D., Kontopoulos, N., Stamatopoulos, L., Guernet, C., and Voltagio, M., 1995. Middle-Late Pleistocene sediments in the northwestern Peloponnesus, Greece. A combined study of biostratigraphical, radiochronological and sedimentological results. *Berliner geowiss. Abh.*, **E 16**, 589-605.

Fuller, I.G., Macklin, M.G., Lewin, J., Passmore, D.G., Wintle, A.G., 1998. River response to high-frequency climate oscillations in southern Europe over the past 200 kyr. *Geology*, **26**, 275-278.

Fytikas, M., Innocenti, F., Manetti, P., Mazzuoli, R., Peccerillo, A., and Villari, L., 1984. Tertiary to Quaternary evolution of volcanism in the Aegean region. In Roberston, A.H.F. and Dixon, J.E.D. (eds), Geological evolution of the Eastern Mediterranean. *Geological Society, London, Special Publication*, **17**, 687-699.

Fytrolakis, N., 1971. Geologische Untersuchungen im Provinz von Pylias (Messenien-Peloponnes). *Annales Geologiques des Pays Helleniques*, **23**, 57-122.

Fytrolakis, N., 1991. Contribution to the knowledge of the neotectonic structure of the Gerolimenas-Mezapou Peninsula (Mani). *Bulletin of the Geological Society of Greece*, **25**, 39-56.

Galanopoulos, A.G., 1947. Die Seismitzität von Messenien. *Annales Geologiques des Pays Helleniques*, **1**, 38-59.

Georgiades-Dikeoulia, E., 1984. Paleoenvironmental observations based on the Pliocene marine megafaunal assemblages of Crete Island. *Annales Géologiques des pays Helléniques*, **32**, 79-85.

Given R.K., and Wilkinson, B.H., 1985. Kinetic control of morphology, composition and mineralogy of abiotic sedimentary carbonates. *Journal of sedimentary Petrology*, **55**, 109-119.

Glover, C.P., and Robertson, A.H.F., 1998a. Role of regional extension and uplift in the Plio-Pleistocene evolution of the Aksu Basin, SW Turkey. *Journal of the Geological Society, London*, **155**, 365-387.

Glover, C.P., and Robertson, A.H.F., 1998b. Neotectonic intersection of the Aegean and Cyprus tectonic arcs: extesnional and strike-slip faulting in the Isparta Angle, SW Turkey. *Tectonophysics*, **298**, 103-132.

Goudie, A.S., 1983. Calcrete. In Goudie, A.S., and Pye, K. (eds.), *Chemical sediments: precipitates and residua in the near surface-environment*. Academic Press, London, 93-131.

Goy, J.L., and Zazo, C., 1986. Synthesis of the Quaternary in the Almeria littoral neotectonic activity and its morphological features, western Betics, Spain. *Tectonophysics*, **130**, 259-270.

Grasso, M., and Pedley, H.M., 1988. The sedimentology and development of the Terravecchia Formation carbonates (upper Miocene) of north central Sicily: possible eustatic influences on facies development. *Sedimentary Geology*, **57**, 131-149.

Greensmith, J.T., and Tucker, E.V., 1986. Compaction and consolidation. In Van de Plassche, O.(ed), *Sea-Level research: a manual for the collection and the evaluation of data*. Geo Books, Norwich, 591-603.

Hageman, J., 1979. Benthic foraminiferal assemblages from Plio-Pleistocene open bay to lagoonal sediments of the Western Peloponnesus (Greece). *Utrecht Micropaleontological Bulletin*, **20**, 171p.

Haq, B.U., Hradenbol, J., and Vail, P.R., 1988. Mesozoic and Cenozoic chronostratigraphy and eustatic cycles. In Wilgus, C.K., Hastings, B.S., Kendall, C.G.St.C., Posamentier, H.W., Ross, C.A., and Van Wagoner, J.C. (eds), Sea-level changes: an integrated approach. *Society of Economic Paleontologists and Mineralogists, Special Publication*, **42**, 71-108.

Hanken, N-M., Bromley, R.G., and Miller, J., 1996. Plio-Pleistocene sedimentation in coastal grabens, north-east Rhodes, Greece. *Geological Journal*, **31**, 271-296.

Hansen, K.S., 1999. Development of a prograding carbonate wedge during sea level fall: Lower Pleistocene of Rhodes, Greece. *Sedimentology*, **46**, 559-576.

Harjes, H.-P., and Vafidis, A., 1998. Seismicity in the accretionary complex of the Hellenic Subduction Zone around western Crete. *Workshop on Deep Drilling Project in the Forearc of the Hellenic Arc, Crete, Abstracts*, 8.

Harland, W.B., Cox, A.V., Llewellyn, P.G., Pickton, C.A.G., Smith, A.G., and Watters, R., 1982. *A Geologic Time Scale.* Cambridge University Press, 131 p.

Hatzfeld, D., Pedotti, G., Hatzidimitriou, P., Panagiotopoulos, D., Scordilis, M., Drakopoulos, I., Makropoulos, K., Delibasis, N., Latousakis, I., Baskoutas, J., and Frogneaux, M., 1989. The Hellenic subduction beneath the Peloponnesus: first results from a microearthquake study. *Earth and Planetary Science Letters*, **93**, 289-291.

Hatzfeld, D., Pedotti, G., Hatzidimitriou, P., and Makropoulos, K., 1990. The strain pattern of the western Hellenic arc deduced from a microearthquake survey. *Geophysical Journal International*, **101**, 181-202.

Hayward, A.B., Robertson, A.H.F., and Scoffin, T.P., 1996. Miocene patch reefs from a Mediterranean marginal terrigenous setting in southwest Turkey. In Franseen, E., Esteban, M., Ward, W., and Rouchy, J.-M. (eds.), *Models for carbonate stratigraphy from Miocene reef complexes of the Mediterranean region.* Society of Economic Paleontologists and Mineralogists, Concepts in Sedimentology and Paleontology, **5**, 317-332.

Hopley, D., 1986a. Beachrock as a sea-level indicator. In Van de Plassche, O.(ed), *Sea-Level research: a manual for the collection and the evaluation of data*. Geo Books, Norwich,157-174.

Hopley, D., 1986b. Corals and reefs as indicators of paleo-sea levels, with special reference to the Great Barrier Reef. In Van de Plassche, O.(ed), *Sea-Level Research: a mannual for the collection and the evaluation of data*. Geo Books, Norwich, 195-228.

Hottinger, L., Halicz, E., and Reiss, Z., 1993. Recent froraminifera from the Gulf of Aqaba, Red Sea. *Slovenska Academia Znanosti in Umetnosti, Razred za Naravoslovne Vede*, **33**, 199p.

Howard, A.D., 1967. Drainage analysis in geologic interpretaion: a summation. *The American Association of Petroleum Geologists Bulletin*, **51**, 2246-2259.

Howell, J., and Fitzsimmons, R., 1997. *An introduction to clastic sequence stratigraphy.* Bristish Sedimentology Research Group, Short Course notes.

Jackson, J., and McKenzie, D., 1983. The geometrical evolution of normal fault systems. *Journal of Structural Geology*, **5**, 471-482.

Jackson, J.A., King, G., and Vita-Finzi, C., 1982a. The neotectonics of the Aegean: an alternative view. *Earth and Planetary Science Letters*, **61**, 303-318.

Jackson, J.A., Gagnepain, J., Houseman, G., King, G.C.P., Papadimitriou, P., Soufleris, C., and Virieux, J., 1982b. Seismicity, normal faulting, and the geomorphogical development of the Gulf of Corinth (Greece): the Corinth earthquakes of February and March 1981. *Earth and Planetary Science Letters*, **57**, 377 - 397.

Jackson, J., Haines, J., and Holt, W., 1992. The horizontal velocity field in the deforming Aegean Sea region, determined from the moment tensors of earthquakes. *Journal of Geophysical Research*, **97**, 17,657-17,684.

Jacobschagen, V., Richter, D., Makris, J., Bachmann, G.H., Giese, P., and Risch, H., 1978. Alpidic development and structure of the Peloponnesus. In Closs, H., Roeder, D., and Schmidt, K. (eds), *Alps, Apennines, Helenides. Geodynamic investigations along geotraverses by an international group of geoscientists*. Inter-Union Commission on Geodynamics, Scientific Report, **No. 38**. E. Schweizerbart'sche Verlagsbuchhandlung, Stuttgart, 415 - 423.

Jardine, W.G., 1986. Determination of altitude, in Van de Plassche, O.(ed), *Sea-Level research: a manual for the collection and the evaluation of data*. Geo Books, Norwich, 569-590.

Julia, R., 1983. Travertines. In Scholle, P.A., Bebout, B.G., and Moore, C.H. (eds), Carbonate Depositional Environments. *American Association of Petroleum Geologists Memoir*, **33**, 64-72.

I.G.E.Y., 1970. *Papadianika-Neapolis-Potamos-Ag. Nikolaos (Voion) Sheet (1:50,000).* Athens.

I.G.M.E., 1980a. *Filiatra Sheet (1:50,000)*. Athens.

I.G.M.E., 1980b. *Koroni - Pylos - Skhiza Sheet (1:50, 000)*. Athens.

I.G.M.E., 1980c. *Mavrovounion-Areopolis-Gerolimin Sheet (1 : 50,000)*. Athens.

I.G.M.E., 1984. *Molai Sheet (1;50,000)*. Athens.

Imbrie, J., 1985. A theorectical framework for the Pleistocene ice ages. *Journal of the Geological Society, London*, **142**, 417-432.

Imbrie, J., and Imbrie, J.M., 1980. Modeling the climatic response to orbital variations. *Science*, **207**, 943-953.

Imbrie, J., Hayes, J.D., Martinson, D.G., MacIntyre, A., Mix, A., Morley, J.J., Pisias, N.G., Prell, W., and Shackleton, N.J., 1984. The orbital theory of the Pleistocene climate: support form a revised chronology of the marine δO16 record. In Berger, A., Imbrie, J., Hayes, J.D., Kukla, G., and Saltzman, B. (eds), *Milankovitch and Climate*, Hingham, Massachusetts, 209-305.

Jacobschangen, V., Richter, D., Makris, J., Bachmann, G.H., Giese, P., and Risch, H., 1978. Alpidic development and structure of the Peloponnesus. In Closs, H., Roeder, D., and Schmidt, K. (eds), *Alps, Apennines, Helenides. Geodynamic investigations along geotraverses by an international group of geoscientists*. Inter-Union Commission on Geodynamics, Scientific Report, **No. 38.** E. Schweizerbart'sche Verlagsbuchhandlung, Stuttgart, 415-423.

James, N.P., 1983. Reef Environment. In Scolle, P.A., Bebont, D.G., and Moore, C.H. (eds), Carbonate Depositional Environments. *American Association of Petroleum Geologists Memoir*, **33**, 345-440.

Kambouroglou, E., 1989. *Eretria. Paleogeographic and geomorphologic evolution during the Holocene. Environment and ancient sites.* Ph.D. thesis, University of Athens, Municipality of Eretria, Eretria, 243 p.

Kastens, K.A., Breen, N.A., and Cita, M.B., 1993. Progressive deformation on an evaporite-bearing accretionary complez: SeaMARC 1, SeaBeam, and piston-core observations from the Mediterranean Ridge. *Marine Geophysical Research*, **14**, 249-298.

Kastens, K., and Mascle., J., 1990. The geological evolution of the Tyrrhenian Sea: An introduction to the scientific results of ODP Leg 107: College Station, Texas. *Proceedings of the Ocean Drilling Program, Scientifica Results*, **107**, 3-26.

Keller, E.A., and Pinter, 1996. *Active Tectonics. Earthquakes, uplift and landscape.* Prentice Hall, New Jersey, 338 p.

Kelletat, D., 1991. The 1550 BP tectonic event in the Eastern Mediterranean as a basis for assessing the intensity of shore processes. In Paskoff, R.P., and Kelletat, D. (eds), Geomorphology and Geoecology. Coastal dynamics and environments. *Zeitschrift für Geomorphologie, Supplementband*, **81**, 181-194.

Kelletat, D., Kowalczyk, G., Schroder, B., and Winter K.-P., 1976. A synoptic view on the neotectonic development of the Peloponnesian coastal regions. *Zeitschrift der Deutsen Geologischen Gesellschaft*, **127**, 447-465.

Kelletat, D., Kowalczyk, G., Schroder, B., and Winter K.-P., 1978. Neotectonics in the Peloponnesian coastal regions. In Closs, H., Roeder, D., and Schmidt, K., (eds), *Alps, Apennines, Hellenides. Geodynamic investigations along geotraverses by an international groupof geoscientists*. Inter-Union Commission on Geodynamics Scientific Report, **No. 38.** E. Schweizerbart'sche Verlagsbuchhandlung, Struttgart, 512-518.

Kennett, J.P., 1982. *Marine Geology*, Prentice Hall, New Jersey, **p.

Keraudren, B., 1970. Les formations Quaternaires marines de la Grece. (Premiere Partie). *Bulletin du Musee d' Anthropologie Prehistorique, Monaco*, **16**, 4-148.

Keraudren, B., 1971. Les formations Quaternaires marines de la Grece (Deuxieme Partie). *Bulletin du Musee d' Anthropologie Prehistorique, Monaco*, **17**, 87-169.

Keraudren, B., and Sorel, D., 1987. The terraces of Corinth (Greece)- A detailed record of eustatic sea-level variations during the last 500,000 years. *Marine Geology*, **77**, 99-107.

Klappa, C.F., 1979. Calcified filaments in Quaternary calcretes: organo-mineral interactions in the subaerial vadose environment. *Journal of Sedimentary Petrology*, **43**, 387-400.

Kopf, A., Robertson, A.H.F., Screaton, E.S., Mascle, J., Parkes, R.J., Fouchet,J.P., De Lange, G.J., Stöckhert, B., and Sakellariou, D., 2000. Backstop hydrogeology of a wide accretionary complex south of Crete, Eastern Mediterranean Sea. ODP Proposal 555, *ODP Drilling Prospectus for FY2002-2003*, JOIDES Office, Kiel, Vol. **5**.

Kopp, K.-O., 1978. Stratigraphic and tectonic sequence of Crete. In Closs, H., Roeder, D., and Schmidt, K. (eds), *Alps, Apennines, Hellenides. Geodynamic investigations along geotraverses by an international group of geoscientists*. Inter-Union Commission on Geodynamics Scientific Report, **No. 38**, E. Schweizerbart'sche Verlagsbuchhandlung, Struttgart, 439-442.

Kowalczyk, G., Winter, K.-P., Steinich, G., und Reisch, L., 1992. Jungpleistozäne Strandterrassen in Südost-Lakonien (Peloponnes, Griechenland). *Schriftenreiche für Geowissenschaften*, **1**, 72 p.

Koufos, G., Syrides, G., Koliadimou, K., 1989. A new Pleistocene mammal locality from Macedonia (Greece). Contribution to the study of Villafrancian (Villafrangian) in Central Macedonia. *Bulletin of the Geological Society of Greece*, **23**, 113-124.

Kourampas, N., and Robertson, A.H.F., 2000. Controls on Plio-Quaternary sedimentation within an active fore-arc region: Messenia Peninsula, SW Peloponnese, Greece. In Panayides, I., and Xenophontos, C. (eds), *Proceedings of the Third International Conference on the Geology of the Eastern Mediterranean*, in press.

Koutsouveli, A., 1987. *Etude stratigraphique des formations pliocenes et pleistocenes en Messenie Occidentale (peloponnes, Grece)*. These de Doctorat, Universitat d' Aix-Marseille II, 162 p.

Kraft, J.C., Aschenbrenner, S.E., and Rapp, G., Jr., 1975. Late Holocene paleogeography of the coastal plain of the gulf of Messenia, Greece, and its relationships to archaeological settings and coastal change. *Geological Society of America Bulletin*, **86**, 1191 - 1208.

Kraft, J.C., Aschenbrenner, S.E., and Rapp, G., Jr., 1977. Paleogeografic reconstructions of coastal Aegean archaeological sites. *Science*, **195**, 941-947.

Kronberg, P., and Günther, R., 1978. Crustal fracture pattern of the Aegean region. In Closs, H., Roeder, D., and Schmidt, K. (eds), *Alps, Apennines, Hellenides. Geodynamic investigations along geotraverses by an international group of geoscientists*. Inter-Union Commission on Geodynamics Scientific Report, **No. 38**, E. Schweizerbart'sche Verlagsbuchhandlung, Struttgart, 522-526.

Kumar, N., and Sanders, J.E., 1976. Characteristics of shoreface strom deposits: modern and ancient examples. *Journal of Sedimentary Petrology*, **46**, 145-172.

Kump, L.R., and Hine, A.C., 1986. Ooids as sea-level indicators. In Van de Plassche, O.(ed), *Sea-Level Research: a mannual for the collection and the evaluation of data*. Geo Books, Norwich, 175-193.

Labeyrie, L.D., Duplessy, J.-C., and Blanc, P.L., 1987. Variations in mode of formation and temperature of ocean deep waters over the past 125,000 years. *Nature*, **327**, 477-482.

Lambeck, K., 1995. Late Pleistocene and Holocene sea-level change in Greece and south-west Turkey: a separation of eustatic, isostatic, and tectonic contributions. *Geophysical Journal International*, **122**, 1022-1044.

Land, L.S., 1970. Phreatic versus vadose meteoric diagenesis of limestones: evidence for a fossil water-table. *Sedimentology*, **14**, 175-185.

Leeder, M.R., Seger, M.J., and Stark, C.P., 1991. Sedimentation and tectonic geomorphology adjacent to major active and inactive normal faults, southern Greece, *Journal of the Geological Society, London*, **148**, 331-343.

Leeder, M.R., and Jackson, J.A., 1993. The interaction between normal faulting and drainage in active extensional basins, with examples from the western United States and central Greece. *Basin Research*, **5**, 79-102.

Leithold, E.L., and Bourgeois, J., 1984. Characteristics of coarse-grained sequences deposited in nearshore, wave-dominated environments-examples from the Miocene of south-west Oregon. *Sedimentology*, **31**, 749-775.

Lekkas, E., Logos, E., Danamos, G., Fountoulis, I., and Adamopoulou, E., 1991. Macroseismic observations after the earthquake of October 16th, 1988, in Kyllini peninsula (NW Peloponnesos, Greece). *Bulletin of the Geological Society of Greece*, **25**, 313-328.

Lentini, F., Carbone, S., Catalano, S., Di Stefano, A., Cargano, C., Romeo, M., Strazzulla, S., and Vinci, G., 1995. Sedimentary evolution of basins in mobile orogenic belts: examples from the Tertiary sequences of the Peloritani Mts. (NE Sicily). *Terra Nova*, **7**, 161-170.

Le Pichon, X., and Angelier, J., 1979. The Hellenic Arc and Trench system: a key to the neotectonic evolution of the Eastern Mediterranean area. *Tectonophysics*, **60**, 1-42.

Leydecker, G., Berckhemer, H., and Delibassis, N., 1978. A study of the seismicity in the Peloponnesos region by precise hypocenter determinations. In Closs, H., Roeder, D., and Scmidt, K., (eds), *Alps, Apennines, Hellenides. Geodynamic investigation along geotraverses by an international group of geoscientists*. Inter-Union Commission on Geodynamics, Scientific Report, **No 38**. E. Schweizerbart'sche Verlagsbuchhanlung, Struttgart, 406-410.

Lickorish, W.H., and Buttler, R.W.H., 1996. Fold amplification and parasequence stacking patterns in syntectonic shoreface carbonates. *Geological Society of America Bulletin*, **108**, 966-977.

Loeblich, A.R.Jr., and Tappan, H., 1988. *Foraminifera genera and their classification* (and plate volume). Van Nostrand Reinhold, New York, 970p.

Longman, M.W., 1980. Carbonate diagenetic textures from nearsurface diagenetic environments, *The American Association of Petroleum Geologists Bulletin*, **64**, 461-487.

Lyberis, N., Angelier, J., Barrier, E., and Lallemant, S., 1982. Active deformation of a segment of arc: the strait of Kythira, Hellenic arc, Greece. *Journal of Structural Geology*, 4, 299-311.

Lyberis, N., and Bizon, G., 1981. Signification structuralle des Iles Strophades dans la Marge Hellenique. *Marine Geology*, **39**, M57-M69.

Lyon-Caen, H., Armijo, R., Drakopoulos, J., Baskoutas, J., Delibassis, N., Gaulton, R., Kouskouna, V., Latoussakis, J., Makropoulos, K., Papadimitriou, P., Papanastasiou, d., and Pedotti, G., 1988. The 1986 Kalamata (south Peloponnesus) earthquake: detailed study of a normal fault, evidences for East-West extension in the Hellenic Arc. *Journal of Geophysical Research*, 93 (B12), 14,967-15,000.

Makris, J., 1978. A geophysical study of Greece based on deep seismic sounding, gravity, and magnetics. In Closs, H., Roeder, D., and Schmidt, K., (eds), *Alps, Apennines,Hellenides. Geodynamic investigation along geotraverses by an international group of geoscientists*. Inter-Union Commission on Geodynamics, Scientific Report, **No 38**. E. Schweizerbart'sche Verlagsbuchhandlung, Struttgart, 349-401.

Makris, J., 1985. Geophysics and geodynamic implications for the evolution of the Hellenides. In Stanley, D.J., and Wesel, F.-C. (eds), *Geological Evolution of the Mediterranean Basin. Raimondo Selli Commemorative Volume*. Springer-Verlag, New York, 231-248.

Makris, J., and Egloff, F., 1998. Crustal thickness and tectonic deformation of the Hellenides. *Workshop on Deep Drilling Project in the Forearc of the Hellenic Arc, Crete, Abstracts*, 6.

Mann, A.W., and Horwitz, R.C., 1979. Groundwater calcrete deposits in Australia: some observations from western Australia. *Journal of the Geological Society of Australia*, **26**, 293-303.

Marcopoulou-Diakantoni, A., 1975. Les plio-pleistocènes Echinides de la région de Neapolis Voion (Péloponnèse). *Annales Géologiques des Pays Helléniques*, **29**, 436-449.

Marcopoulou-Diacantoni, A., Mirkou, M.R., Mariolakos, I., and Fountoulis, I., 1991. Stratigraphic and paleoecological observations on the post-alpine sediments at the area of Filiatra (Messenia, Peloponnesus) and their neotectonic explanation. *Bulletin of the Geological Society of Greece*, **25**, 593-688.

Mariolakos, I., 1975. Thoughts and view points on certain problems of the geology and tectonics of Peloponnesus. *Annales Geologiques de Pays Helleniques*, **27**, 215-313.

Mariolakos, I., Papanicolaou, D., and Lagios, E., 1985. A neotectonic geodynamic model of Peloponnesus based on morphotectonics, repeated gravity measurements, and seismicity. *Geologische Jachrbuch*, **B50**, 3-17.

Mariolakos, I., Fountoulis, I., Logos, E., and Lozios, S., 1989. Surface faulting caused by the Kalamata (Greece) earthquakes (13.9.86). *Tectonophysics*, **163**, 197-293.

Mariolakos, I., Lekkas, E., Danamos, G., Logos, E., Fountoulis, I., and Adamopoulou, E., 1991. Neotectonic evolution of the Kyllini peninsulla (NW. Peloponnesus). *Bulletin of the Geological Society of Greece*, **25**, 163-176.

Mariolakos, I., Badekas, I., Fountoulis, I., and Theocharis, D., 1994. Reconstruction of the early Pleistocene paleoshore and peleorelief of SW Peloponnesus area. *Bulletin of the Geological Society of Greece*, **30**, 297-304.

Mariolakos, I., Foutnoulis, I., and Kranis, H., 1997. Paleoseismic events recorded in Pleistocene sediements in the area of Kalamata (Peloponnesos, Greece). *Journal of Geodynamics*, **24**, 241-247.

Martin, L., Suguio, K., and Flexor, J.- M., 1986. Shell middens as a source for additional information in Holocene shoreline and sea-level reconstruction: examples from the coast of Brazil. In Van de Plassche, O.(ed), *Sea-Level Research: a manual for the collection and the evaluation of data*. Geo Books, Norwich, 503-521.

Martindale, W., 1976. *Calcareous encrusting organisms of the Recent and Pleistocene reefs of Barbados, West Indies*. Unpublished Ph.D. thesis, University of Edinburgh, 141 p.

Martini, M., 1971. Standard Tertiary and Quaternary calcareous nannoplankton zonation. *Proceedings, II Planktonic Conference, Rome*, 739-785.

Martinson, D.G., Pisias, N.G., Hays, J.D., Imbrie, J., Moore, T.C., and Shackleton, N.J., 1987. Age dating and the orbital theory of the ice ages: development of a high resolution 0 to 300,000 year chronostratigraphy. *Quaternary Research*, **27**, 1-29.

Massari, F., 1997. High-frequency cycles within Pleistocene forced-regressive conglomerate wedges (Bradanic area, southern Italy) filling collapse scars. *Sedimentology*, **44**, 939-958.

Mascle, J., Le Quellec, P., Leite, O., and Jongsma, D., 1982. Structural sketch of the Hellenic continental margin between the western Peloponnesus and eastern Crete. *Geology*, **10**, 113-116.

Meijer, P., 1995. Dynamics of active continental margins: the Andes and the Aegean region. *Geologica Ultraiectina*, **130**, 218 p.

Meulenkamp, J.E., de Mulder, E.F.J., and Van de Weerd, A., 1972. Sedimentary history and paleogeography of the Late Cenozoic of the island of Rhodes. *Zeitschrift für Deutche Geologische Gesellschaft*, **123**, 541-553.

Meulenkamp, J.E., Wortel, M.J.R., Van Wamel, W.A., Spakman, W., and Hoogerduyn Strating, E., 1988. On the Hellenic subduction zone and the geodynamic evolution of Crete since the late Middle Miocene. *Tectonophysics*, **146**, 203-215.

Meulwnkamp, J.E., van der Zwaan, G.J., and van Wamel., W.A., 1994. On Late Miocene to Recent vertical motions in the Cretan segment of the Hellenic Arc. *Tectnophysics*, **234**, 53-72.

Migòn, P., 1993. Geomorphological characteristics of mature fault-generated range fronts, Sudetes Mts., south-western Poland. *Zeitschrift für Geomorphologie*, Suppl. Bd. **94**, 223-241.

Milton, N.J., and Emery, D., 1996. Outcrop and well data. In Emery, D., and Myers, K.J. (eds), *Sequence stratigraphy*, Blackwell Science, Oxford, 61-79.

Mörner, N.-A., 1976. Eustasy and geoid changes. *The Journal of Geology*, **84**, 123-151.

Mörner, N.-A., 1987. Models of global sea-level changes. In Tooley, M.J., and Shennan, I. (eds), *Sea-level Changes*. The Institute of British Geographers Special Publications Series, **20**, Basil Blackwell, Oxford, 332-355.

Multer, H.G., 1971. *Field guide to some carbonate rock environments. Florida Keys and western Bahamas.* Fairleigh Dickinson University, Madison, New Jersey, 158 p.

Murray, J.W., 1973. *Distribution and ecology of living benthic Foraminiferids.* Heinemann Educational Books, London, 274 p.

Myers, K.J. and Milton, N.J., 1996. Concepts and principles of sequence stratigraphy. In Emery, D., and Myers, K.J. (eds), *Sequence stratigraphy*, Blackwell Science, Oxford, 11-41.

Myrow, P.M., and Southard, J.B., 1996. Tempestite deposition. *Journal of Sedimentary Research*, **66**, 875-887.

McCallum, J.E., 1989. *Sedimentology and Tectonics of the Plio-Pleistocene of Cyprus.* Unpublished Ph.D. thesis, University of Edinburgh, 263 p.

McCallum, J.E., and Robertson, A.H.F., 1990. Pulsed uplift of the Troodos massif - evidence from the Plio-Pleistocene Mesaoria Basin. In Morre E.M. et al. (eds.), *Ophiolites-Oceanic crustal analogues. Proceedings, International Symposium "Troodos 1987"*, Geological Survey Department, 217-230.

McCallum, J.E., and Robertson, A.H.F., 1995. Sedimentology of two fan-delta systems in the Pliocene-Pleistocene of the Mesaoria Basin, Cyprus. *Sedimentary Geology*, **98**, 215-244.

McIntyre, J., Nance, R.D., and Smith, G., 1994. Neotectonic uplift rate of the mount Olympus, Greece, and the Quaternary sedimentary history of its eastern piedmont. *Bulletin of the Geological Society of Greece*, **30**, 251-260.

McKenzie, D., 1978. Active tectonics of the Alpine-Himalayan belt: the Aegean and surrounding regions. *Geophysical Journal of the Royal Astronomical Society*, **55**, 217-254.

Neev, D., Bakler, N., and Emery, K.O., 1987. *Mediterranean coasts of Israel and Sinai. Holocene tectonism from geology, geophysics, and archaeology.* Taylor & Francis, New York, Philadelphia, London, 130 p.

Nemec, W., and Postma, G., 1993. Quaternary alluvial fans in southwestern Crete sedimentation processes and geomorphic evolution. *International Assossiation of Sedimentologists, Special Publication,* **17**, 235-276.

Nicolich, P., 1998. Seismic images of the Ionian Basin and its margins. *Workshop on Deep Drilling Project in the Forearc of the Hellenic Arc, Crete, Abstracts*, 16.

Ollier, C.D., and Pain, C.F., 1988. Morphotectonics of Papua-new Guinea. *Zeitschrift für Geomorphologie, Supplementband*, **69**, 1-16.

Orton, G.J., and Reading, H.G., 1993. Variability of deltaic processes in terms of sediment supply, with particular emphasis on grain size. *Sedimentology*, **40**, 475-512.

Ota, Y., 1984. Marine terraces and active faults in Japan with special reference to co-seismic events. In Morisawa, M., and Hack, J.T.(eds), *Tectonic Geomorphology. Proceedings of the 15th Annual Binghampton Geomorphology Symposium, September 1984*. Urwin Hyman, Boston, 345-366.

Ouchi, S., 1985. Response of alluvial rivers to slow active tectonic movement. *Geological Society of America Bulletin*, **96**, 504-515.

Palmentola, G., 1994. Glacial features and snow-line trend during the last glacial age on the Albanian and Greek mountains. *Bulletin of the Geological Society of Greece*, **30**, 262-268.

Papanikolaou, D., Chronis, G., and Metaxas, Ch., 1994. Neotectonic structure of the Argolic Gulf. *Bulletin of the Geological Society of Greece*, **30**, 305-316.

Papapetrou-Zamanis, A., 1971. Dépôt du Tyrrhénien dans la côte septentrionale de l'île de Crète. *Annales Géologiques des Pays Hélleniques*, **23**, 301-307.

Papazachos, B.C., 1991. Active tectonic forces in the Aegean area. *Bulletin of the Geological Society of Greece*, **25(3)**, 195-204.

Paraskevaidis, Il., 1961. Uber die geologie des östlichen Asterussia gebirges auf der Insel Kreta. *Annales Géologiues des Pays Helléniques*, **12**, 139-152.

Pavlides, S.B., 1993. Active faulting in multi-fractured seismogenis areas; examples from Greece. In Stewart, I., Vita-Finzi, C., and Owen, L. (eds), Neotectonics and active faulting. *Zeitschrift für Geomorphologie, Supplementband*, **94**, 41-55.

Pavlides, S.B., Zouros, N.C., Chatzipetros, A.A., Kostopoulos, D.S., and Mountrakis, D.M., 1995. The 13 May 1995 western Macedonia, Greece (Kozani Grevena) earthquake; preliminary results. *Terra Nova*, 7, 544-549.

Payne, A.S., and Robertson, A.H.F., 1995. Neogene supra-subduction zone extension in the Polis graben system, west Cyprus. *Journal of the Geological Society, London*, **152**, 613-628.

Pedley, H.M., 1996a. Miocene reef distributions and their associations in the central Mediterranean region: an overview. In Franseen, E., Esteban, M., Ward, W., and Rouchy, J.-M. (eds.), *Models for carbonate stratigraphy from Miocene reef complexes of the Mediterranean region*. Society of Economic Paleontologists and Mineralogists, Concepts in Sedimentology and Paleontology, **5**, 73-87.

Pedley, H.M., 1996b. Miocene reef facies of the Pelagian region (central Mediterranean). In Franseen, E., Esteban, M., Ward, W., and Rouchy, J.-M. (eds.), *Models for carbonate stratigraphy from Miocene reef complexes of the Mediterranean region*. Society of Economic Paleontologists and Mineralogists, Concepts in Sedimentology and Paleontology, **5**, 247-259.

Pedley, H.M., and Grasso, M., 1993. Controls on faunal and sediment cyclicity within the Tripoli and Calcare di Base basins (Late Miocene) of central Sicily. *Palaeogeography, Palaeoclimatology, Palaeoecology*, **105**, 247-259.

Pemberton, S.G., MacEachen, J.A., and Frey, R.W., 1992. Trace fossil facies models: Environmental and allostratigraphic significance. In Walker, R.G., and James, N.P. (eds), *Facies models. Response to sea level change*. Geological Association of Canada, St. John's, Newfoundland, 47-72.

Perry, C.T., 1997. Biofilm-related calcification and constructive micritic envelopes: a criterion for the recognition of ancient grass-bed environments? *BSRG, 36th Annual Meeting, Abstract Volume*, 83.

REFERENCES

Petrochilos, J., 1953. Sur l' histoire du Quaternaire de la presqu'ile de Mani (Peloponnese). *Premier Congres International de Speleologie, Paris, Extrait des publications du Congres*, **2 (1)**, 4p.

Petrochilou, A., 1965. Le fleuve souterrain de Glyphada en Peloponnèse No 25. *Collogue International de Speleologie*, 62-77.

Pinter, N., and Gardner, T.W., 1989. Construction of a polynomial model of glacio-eustatic fluctuation: Estimating paleo-sea levels continuously through time. *Geology*, **17**, 295 - 298.

Piper, D.J., Stamatopoulos, L., Poulimenos, G., Doutsos, T., and Kontopoulos, N., 1990. Quaternary history of the Gulfs of Patras and Corinth, Greece. *Zeitschrift für Geomorphologie*, **34**, 451-458.

Pirazzoli, P.A., 1986a. Marine notches. In Van de Plassche, O.(ed), *Sea-Level Research: a manual for the collection and the evaluation of data*. Geo Books, Norwich, 361-400.

Pirazzoli, P.A., 1986b. The Early Byzantine tectonic paroxysm. *Zeitschrift für Geomorphologie, Supplementband*, **62**, 31-49.

Pirazzoli, P.A., 1987. Sea-level changes in the Mediterranean. In Tooley, M.J., and Shennan, I. (eds), *Sea-level Changes*. The Institute of British Geographers Special Publications Series, 20, Basil Blackwell, Oxford, 152-181.

Pirazzoli, P.A., 1991. *World atlas of Holocene sea-level changes*. Elsevier oceanography series, 58, Elsevier, Amsterdam, 300 p.

Pirazzoli, P.A., Thommeret, J., Thommeret, Y., Laborel, J., and Montaggioni, L.F., 1982. Crustal block movements from Holocene shorelines: Crete and Antikythera (Greece). *Tectonophysics*, **86**, 27-43.

Pirazzoli, P.A., Montaggioni, L.F., Saliege, J.F., Seconzac, G., Thommeret, Y., and Vergnaud - Grazzini, C., 1989. Crustal block movements from Holocene shorelines: Rhodes Island (Greece). *Tectonophysics*, **170**, 89-114.

Pirazzoli, P.A., Stiros, S.C., Arnold, M., Laborel, J., Laborel-Deguen, F., Papageorgiou, S., 1994. Episodic uplift deduced from Holocene shorelines in the Perachora Penninsula, Corinth area, Greece. *Tectonophysics*, **229**, 201-209.

Plaziat, J.-C., Reyss, J.-L., Choukri, A., Orszag-Sperber, F., Baltzer, F., et Purser, B.H., 1998. Mise en évidence, sur la côte récifale d'Egypte, d'une régression interrompant brièvement le plus haut niveau du Dernier Interglaciaire (5e): un nouvel indice de variations glacio-eustatiques à haute fréquence au Pléistocène? *Bulletin de la Societè géologique de France*, **169**, 115-125.

Poole, A.J., 1992. *Sedimentology, neotectonics and geomorphology related to tectonic uplift and sea-level change: Quaternary of Cyprus*. Unpublished Ph.D. thesis, University of Edinburgh.

Poole, A., and Robertson, A.H.F., 1991. Quaternary uplift and sea-level change at an active plate boundary. Cyprus. *Journal of the Geological Society, London*, **148**, 909-921.

Poole, A., and Robertson, A., 1998. Pleistocene fanglomerate deposition related to uplift of the Troodos Ophiolite, Cyprus. In Robertson, A.H.F., Emeis, K.-C., Richter, C., and Camerlenghi, A. (eds), *Proceedings of the Ocean Drilling Program, Scientific Results*, **160**, 545-566.

Poole, A., and Robertson, A.H.F., 2000. Quaternary marine terraces and aeolianites in coastal south and West Cyprus: implications for regional uplift and sea-level change. In Panayides I., and Xenophontos, C. (eds), *Proceedings of the Third International Conference on the Geology of the Eastern Meditaerranean*, in press.

Postma, G., 1990. Depositional architecture and facies of river and fan deltas: a synthesis. In Collela, A., and Prior, D.B. (eds), Coarse-grained deltas. *Special Publication, International Association of Sedimentologists*, **40**, 13-27.

Postma, G., and Nemec, W., 1990. Regressive and transgressive sequences in a raised Holocene gravelly beach, southwestern Crete. *Sedimentology*, **37**, 907-920.

Poulimenos, G., Zelilidis, A., Kontopoulos, N., and Doutsos, T., 1993. Geometry of trapezoidal fan deltsas and their relationschip to extensional faulting along the south-western active margins of the Corinth rift, Greece. *Basin Research*, **5**, 179-192.

Psarianos, P, 1961. Der einfluss der epirogenen bewegungen auf die morphologie der insel Kreta. *Annales Geologiques des Pays Helleniques*, **12**, 129-138.

Psilovikos, A.A., and Vavliakis, E.G., 1982/83. The problem of planation surfaces in the area of the Serbomacedonian and Rila-Rhodope Masses. *Bulletin of the Geological Society of Greece*, **16**, 3-16.

Purser, B.H., 1980. Sédimentation et diagenèse des carbonates néritiques récents. *Editions Technip*, 1, 159-344.

Purser, B.H., Barrier, P., Montenant, F., Orszag-Sperber, P., Ott d'Estevou, P., Plaziat, J.-C., and Philobbos, E., 1998. Carbonate and siliciclastic sedimentation in an active tectonic setting: Miocene of the north-western Red Sea rift, Egypt. In Purser, B.H., and Bosence, D.W.J. (eds), *Sedimentation and Tectonics of Rift Basins: Red Sea-Gulf of Aden*. Chapman & Hall, London, 239-270.

Pye, K.A., 1983. Red beds. In Goudie, A.S., and Pye, K. (eds.), *Chemical sediments: precipitates and residua in the near surface environment*. Academic Press, London, 227-263.

Reading, H.G., and Collinson, J.D., 1996. Clastic coasts. In Reading, H.G. (ed), *Sedimentary environments: Processes, facies, and stratigraphy*. Blackwell, Oxford, 125-142.

Rehaul, J.P., Moussat, E., and Fabbri, A., 1987. Structural evolution of the Tyrrhenian back-arc basin. *Marine Geology*, **74**, 123-150.

Reineck, H.E., and Singh, I.B., 1980. *Depositional sedimentary environments*. Springer-Verlag, Berlin, 549 p.

Reinson, G.E., 1992. Transgressive barrier island and estuarine systems. In Walker, R.G., and James, N.P. (eds), *Facies models. Response to sea level change*. Geological Association of Canada, Ontario, 179-194.

Reynolds, A.D., 1996. Paralic successions. In Emery, D., and Myers, K.J. (eds), *Sequence stratigraphy*, Blackwell Science, Oxford, 134-177.

Richards, M.T., 1996. Fluvial systems. In Emery, D., and Myers, K.J. (eds), *Sequence stratigraphy*, Blackwell Science, Oxford, 111-133.

Riedl, H., 1977. Die Formenelemente im Bereiche des arkadischen Zentralzuges und des westarkadischen Gebirges auf der Peloponnes (Griechenland). *Annales Géologiques des Pays Helléniques*, **29**, 209-225.

Riedl, H., unter Mitarbeit von Mariolakos, I., Papanikolaou, D., und Sabot., V., 1982. Die altflachenentwicklung der Kykladen. Die altflächenentwicklung der Kykladen. *Annales Géologiques des pays Helléniques*, **31**, 191-250.

Roberts, S., and Jackson, J., 1991. Active normal faulting in central Greece: an overview. In Roberts, A.M., Yielding, G., and Freeman, B. (eds), The geometry of normal faults. *Geological Society Special Publication No 56*, 125-142.

Robertson, A.H.F., 1998. Tectonic significance of the Eartosthenes Seamount: a continental fragment in the process of collision with a subduction zone in the eastern Mediterranean (Ocean Drilling Program Leg 160). *Tectonophysics*, **298**, 63-82.

Robertson, A.H.F., and Woodcock, N.H., 1986. The role of the Kyrenia Range Lineament, Cyprus, in the geological evolution of the eastern Mediterranean area. *Philosophical Transactions of the Royal Society, London*, **A 317**, 141-177.

Robertson, A., and Grasso, M., 1995a. Later Tertiary-Quaternary Meditarranean tectonics and palaeo-environments-an introduction. *Terra Nova*, **7**, 112-113.

Robertson, A.H.F., and Grasso, M., 1995b. Overview of the late Tertiary-Recent tectonic and palaeo-environmental development of the Mediterranean region. *Terra Nova*, **7**, 114-127.

Robertson, A.H.F., and Kopf, A., 1998. Tectonic setting and processes of mud volcanism on the Mediterranean Ridge accretionary complex: evidence from Leg 160. In Robertson, A.H.F., Emeis, K.-C., Richter, C., and Camerlengi, A. (eds), *Proceedings of the Ocean Drilling Program, Scientific Results*, **160**, 665-680.

Robertson, A.H.F., Emeis, K.-C., Richter, C. et al (Scientific Participants of Leg 160), 1995. Evidence of collisional processes associated with ophiolite obduction in the Eastern Mediterranean: Results from Ocean Drilling Program Leg 160. *GSA TODAY*, **5**, 213, 219-221.

Rotstein, Y., 1985. Tectonics of the Aegean Block: Rotation, side-arc collision and crustal extension. *Tectonophysics*, **117**, 117-137.

Ruddiman, W.F., and Raymo, M.E., 1988. Northern hemisphere climate regimes during the past 3 Ma: possible tectonic connections. *Philosophical Transactions of the Royal Society of London*, **B318**, 411-430.

Sauvage, J., 1979. Le Prépléistocène en Grèce centrale et mèridionale: corrélations palynologiques et faunistiques, comparaisons avec l'Italie. *Quaternaria*, **20**, 165-173.

Seger, M., and Alexander, J., 1993. Distribution of Plio-Pleistocene and Modern coarse-grained deltas south of the Gulf of Corinth, Greece. *International Association of Sedimentologists, Special Publication,* **20**, 37-48.

Shackleton, N.J., 1987. Oxygen isotopes, ice volume and sea level. *Quaternary Science Reviews*, **6**, 183-190.

Smith, G., Nance, R.-D., and Genes, A., 1994. A re-evaluation of the extemt of Pleistocene glaciation in the mount Olympus region, Greece. *Bulletin of the Geological Society of Greece*, **30**, 115-123.

Spadini, G., and Podlachikov, Y., 1996. Spacing of consecutive normal faulting in the lithosphere. A dynamic model of for rift axis jumping (Tyrrhenian Sea). *Earth and Planetary Science Letters*, **144**, 21-34.

Stamatopoulos, L., and Kontopoulos, N., 1994. Geomorphology and evolution of the region between Lapa and Eleotopos, northwestern Peloponnesus (Greece). *Il Quaternario*, **7**, 537-544.

Stamatopoulos, L., Voltaggio, M., and Kontopoulos, N., 1994. $230^{Th}/238U$ Dating of Corals from Tyrrhenian marine deposits and the Paleogeographic Evolution of the Western Peloponnesus (Greece). *Münster. Forsch. Geol. Paläont.*, **76**, 345-352.

Stiros, S.C., 1993. Kinematics and deformation of central and southwestern Greece from historical triangulation data and implications for the active tectonics of the Aegean. *Tectonophysics*, **220**, 283-300.

Stiros, S.C., 1988. Archaeology - A tool to study active tectonics. *Eos*, **69(50)**, 1633-1639.

Stiros, S.C., 1986. Geodetically controled taphrogenesis in back-arc environments : three examples from central and northern Greece. *Tectonophysics*, **130**, 281-288.

Stiros, S.C., Arnold, M., Pirazzoli, P.A., Laborel, J., Laborel, F., and Papageorgiou, S., 1992. Historical co-seismic uplift on Euboea Island, Greece. *Earth and Planetary Science Letters*, **108**, 109-117.

Stokes, M., and Muther, A.E., 2000. Responce of Plio-Pleistocene alluvial systems to tectonically induced base-level changes, Vera Basin, SE Spain. *Journal of the Geological Society, London*, **157**, 303-316.

Streif, H., 1978. Stratigraphy and tectonics of Late Cenozoic rocks in Western Peloponnese. In Closs, H., Roeder, D., and Schmidt, K., (eds), *Alps, Apennines,Hellenides. Geodynamic investigation along geotraverses by an international group of geoscientists*. Inter-Union Commission on Geodynamics Scientific Report No38. E. Schweizerbart'sche Verlagsbuchhandlung, Struttgart, 501-502.

Suc, J.-P., 1984. Origin and evolution of the Mediterranean vegetation and climate in Europe. *Nature*, **307**, 429-432.

Symeonidis, N.K, 1969. Stratigraphisch-Palaontologische Untersuchungen über die Neogenablagerungen von Lakonien, insbesondere der Gebite von Neapolis (Eparchia Epidaurus-Limira) und gegenüber liegenden Insel Elaphonisos. *Annales Géologiques des Pays Helléniques*, **21**, 531-553.

Taylor, J.C.M., and Illing, L.V., 1969. Holocene intertidal calcium carbonate cementation, Qatar, Persian Gulf. *Sedimentology*, **12**, 69-107.

Taymaz, T., 1998. On the Hellenic Trench Subduction Zone: Earthquake square mechanisms in the Hellenic Trench near Crete. *Workshop on Deep Drilling Project in the Forearc of the Hellenic Arc, Crete, Abstracts*, 9.

Taymaz, T., Jackson, J., and McKenzie, D., 1991. Active tectonics of the north and central Aegean Sea. *Geophysical Journal International*, **106**, 433 - 490.

Ten Veen, J.H., 1998. Neogene Outer-Arc Evolution in the Cretan Segment of the Hellenic Arc: Tectonic, Sedimentary and Geodynamic Reconstructions. *Geologica Ultraiectina*, **160**, 192p.

Theodoropoulos, D., 1973. Geologische und Morphologische Beobachtungen im Gebiet von Neapolis (Sud-Peloponnes). *Annales Geologiques de Pays Helleniques*, **25**, 445-466.

Torelli, L., Grasso, M., Mazzoldi, C., and Peis, D., 1998. Plio-Quaternary tectonic evolution and structure of the Catania foredeep, the northern Hyblean Plateau and the Ionian shelf (SE Sicily). *Tectonophysics*, **298**, 209-221.

Tucker, M.E., 1991. *Sedimentary Petrology. An introduction to the origin of sedimentary rocks*. Blackwell Science, Oxford, 260 p.

Tucker, M.E., 1982. *The field description of sedimentary rocks*. John Willey and Sons, London, 112 p.

Tucker, M.E., and Wright, V.P., 1990. *Carbonate Sedimentology*. Blackwell Scientific Publications, Oxford, 482 p.

Van Andel, T.H., Perissoratis, C., and Rondoyanni, T., 1993. Quaternary tectonics of the Argolicos Gulf and adjacent basins, Greece. *Journal of the Geological Society, London*, **150**, 529-539.

Van Wagoner, J.C., Posamentier, H.W., Mitchum, R.M., Vail, P.R., Sarg, J.F., Loutit, T.S., and Hardenbol, J., 1988. An overview of the fundamentals of sequence stratigraphy and key definitions. In Wilgus, C.K., Hastings, B.S., Kendall, C.G.St.C., Posamentier, H.W., Ross, C.A., and Van Wagoner, J.C. (eds), Sea-level changes: an integrated approach. *Society of Economic Paleontologists and Mineralogists, Special Publication*, **42**, 39-45.

Vavliakis, E.G., 1981. *Morphologische und morphogenetische Untersuchungen der Abtragungschflächen, Karstformen, Glazial- und Periglazialformen des Menikion-Gebirges (Ostmakedonien, Griechenland)*. Scientific Annales, Faculty of Physical and Mathematical Sciences, University of Thessaloniki, **19**, Suppl. **24**., **p.

Ten Veen, J.H., and Meijer, 1998. Late Miocene to Recent tectonic evolution of Crete (Greece): geological observations and model analysis. *Tectonophysics*, **298**, 191-208.

Verginis, S., und Nagl, H., 1982. Ein Landschaftökologischer vegleich von hochgebirgen am beispiel der Nordpeloponnes und der Nockberge. *Annales Géologiques des pays Helléniques*, **31**, 251-270.

Vita-Finzi, C., 1987. C14 deformation chronologies in coastal Iran, Greece and Jordan. *Journal of the Geological Society, London*, **144**, 553-560.

Vittori, J., Got, H., Mascle, J., and Mirabile, L., 1981. Emplacement of the recent sedimentary cover and processes of deposition on the Matapan trench margin (Hellenic Arc). *Marine Geology*, **41**, 113-135.

Vittori, J., Brambati, A., Got, H., Le Quellec, P., Mascle, J., Mezzadri, G., et Monaco, A., 1980. Alimentation des fosses de subduction de l' Arc hellenique au Sud de Peloponnese. *Bulletin de la Societe Geologique de France*, **22**, 707-711.

Wali, A.M.A., Brookfield, M.E., and Schreiber, B.C., 1994. The depositional environment and diagenetic evolution of the coastal ridges of northwestern Egypt. *Sedimentary Geology*, **90**, 113-136.

Walker, R.G., and Plint, A.G., 1992. Wave- and strom-dominated shallow marine systems. In Walker, R.G., and James, N.P. (eds), *Facies models. Response to sea level change.* Geological Association of Canada, Ontario, 219-238.

Weingartner, H., and Hejl., E., 1994. The relief generation of Thassos and the first attempt of fission-track dating in Northern Greece. *Bulletin of the Geological Society of Greece*, **30**, 307-312.

Williams, M.A.J., Dunkerley, D.L., De Deckker, P., Kershaw, A.P., and Stokes, T.J., 1993. *Quaternary Environments*. Edward Arnold, London, 329 p.

Wilson, J.L., 1974. Characteristics of carbonate platform margins. *Bulletin of the American Association of Petroleum Geologists*, **58**, 810-824.

Wilson, J.L., 1975. *Carbonate facies in geologic history*. Springer-Verlag, New York, 471 p.

Wilson, P.A., and Dickson, J.A.D., 1996. Radiaxial calcite: Alteration product of and petrographic proxy for magnesian calcite marine cement. *Geology*, **24**, 945-948.

Woodworth, P.L., 1993. Sea level changes, in Warrick, R.A., Barrow, E.M., and Wigley, T.M.L. (eds), *Climate and sea level change: Observations, projections and implications*. Cambridge University Press, Cambridge, 379-391.

Wright, V.P., Platt, N.H., and Wimbledon, W.A., 1988. Biogenic laminar calcretes: evidence of root-mat horizons in paleosols. *Sedimentology*, **35**, 603-620.

Zachariasse, W.J., 1975. Planktonic foraminiferal biostratigraphy of the Late Neogene of Crete (Greece). *Utrecht Micropaleontological Bulletins*, **11**, 171p.

Zamani, A., 1979. Contribution to the interpretation of the formation and development of the landfroms of Meteora. *Annales Géologiques des Pays Helléniques*, **30**, 281-290.

Zelilidis, A., 1988. *Post-Miocene evolution of the SW Peloponnese.* Unpublished Ph.D thesis, University of Patras, 282p.

Zelilidis, A., and Doutsos, T., 1992. An interference pattern of neotectonic faults in the southwetern part of the Hellenic forearc basin, Greece. *Zeitschrift der deutsche geologische Gesselschaft*, **143**, 95-105.

Zelilidis, A., and Frydas, D., 1994. Paleogeographical and stratigrpahical evolution in the southwestern Peloponnesus, Greece. Münster Forsch. Geol. Paläont., 76, 255-262.

Zelilidis, A., and Kontopoulos, N., 1996. Significance of fan deltas without toe-sets within rift and piggy-back basins: examples from the Corinth graben and the Mesohellenic trough, Central Greece. *Sedimentology*, **43**, 253-262.

Zelilidis, A., and Kontopoulos, N., 1999. Plio-Pleistocene alluvial architecture in marginal extensional narrow sub-basins: examples from southwest Greece. *Geological Magazine*, **136**, 1-22.

Zelilidis, A., Kontopoulos, N., Avramidis, P., and Piper, D.J.W., 1998. Tectonic and sedimentological evolution of the Pliocene-Quaternary basins of Zakynthos Island, Greece: case study of the transition from compressional to extensional tectonics. *Basin Research*, **10**, 393-408.

A.1.1) Messenia Peninsula

Samples	Lithology	Location	Inferred Age
1) Garg 1	Packstone	Gargaliani	early Pleistocene
2) Garg 2	-//-	-//-	-//-
3) Garg 3	Grainstone	-//-	-//-
4) G4/*	Mud	Gargaliani Road Cut	-//-
5) G4/A	-//-	-//-	-//-
6) G4/B1	-//-	-//-	-//-
7) G4/B2	Sand	-//-	-//-
8) G4/B3	Silt	-//-	-//-
9) G4/B4	Pecten sp.	-//-	-//-
10) G4/B5	Silt	-//-	-//-
11) GB4/5	granular conglomerate	-//-	-//-
12) Rom 1	Laminated sandstone	Romanos	Neotyrrhenian
13) Rom 2	-//-	-//-	-//-
14) Rom 3	-//-	-//-	-//-
15) Rom 4	-//-	-//-	-//-
Rom'1	-//-	-//-	-//-
Rom'2	algal boundstone	-//-	-//-
Rom'3	Sandstone	-//-	-//-
Rom'4	algal boundstone crust and Cladocora caespitosa	-//-	-//-
Rom'5	Beachrock	-//-	Holocene
Rom'5*	algal boundstone	-//-	middle Pleistocene or Eutyrrhenian (?)
Rom'6	-//-	-//-	-//-
Rom'7	Glycimeris sp., Arca sp.	-//-	Neotyrrhenian
Rom'8	vermetid crust	-//-	Holocene
Rom'9	-//-	-//-	-//-
16) Mar 1	Molluscan grainstone	Marathopolis	Neotyrrhenian
17) Mar 2	Molluscan grainstone	Marathopolis	Neotyrrhenian
18) Mar 7	red caliche hardpan	Marathopolis	late Pleistocene
19) M→G1	Packstone	Old Rd from Marathopolis to Gargaliani	middle Pleistocene
20) M→G2	Packstone	-//-	-//-
21) M→G3	Grainstone	-//-	-//-
22) M→G4	hardpan caliche	Gargaliani Cliff, near "Xenon Hotel"	Pliocene
23) M→G5	Cemented breccia	-//-	-//-
25) M→G 6	-//-	-//-	-//-
26) M→G7	-//-	-//-	-//-
27) M→G8	red hardpan caliche	-//-	-//-
28) Lag 1	Rhodolithic packstone	Laghouvardhos Coast	Eutyrrhenian
29) Lag 2	Calichified packstone	N cape of Laghouvardhos Coast	-//-
30) Lag 3	lithic packstone	Valta, Ayios Yeorghios Chapel	early Pleistocene
31) Lag 4	silty sand and mollusc fauna	Laghouvardhos Rema	Eutyrrhenian (?)
32) Lag 5	well sorted grainstone	-//-	-//-
33) Lag 6	well sorted sandstone	-//-	-//-
34) Lag 7	muddy palaeosol	-//-	late Pleistocene-Holocene (?)
35) Lag 8	tectonic gouge	-//-	?

Appendix 1: List of samples

36) Lag 9	Conglomerate	Rd from Gargaliani to Filiatra	middle Pleistocene
37) Lag 10	silty sand with pectenidae	Laghouvardhos Rema	Eutyrrheinian (?)
38) Lag 11	Silt	-//-	-//-
39) Lag 12	coarse grained sandstone	-//-	-//-
40) Lag 13	Sand	-//-	-//-
24) GRC21	red caliche	Gargaliani Road Cut	early Pleistocene
25) Chondr 1	Grainstone	Hondhrovouni (Gargaliani)	Late Pliocene-early Pleistocene (?)
26) Chondr 2	silty sand with pectenidae	-//-	-//-
27) Chondr 3	Packstone	-//-	-//-
28) Chondr 4	terra rossa	-//-	Pleistocene
29) Chondr 5	Flowstone	-//-	-//-
30) OCQ 1	Limestone breccia	Hill opposite Hondhrovouni Quarry	Tertiary
31) OCQ 2	matrix-supported conglomerate	-//-	early Pleistocene
32) OCQ 3	Silt	-//-	-//-
33) OCQ 4	pebbly silt	-//-	-//-
3) OCQ 5	fine grained calcareous sandstone	-//- (N part)	-//-
35) OCQ 6	coarse grained calcareous sandstone	-//-	-//-
36) OCQ 7	coral	-//-	-//-
37) OCQ 8	Grainstone	-//-	-//-
38) GQ 5	Reworked terra rossa	Gargaliani Quarry	late Pleistocene
39) GQ 6	Packstone with Ostrea sp., Pecten sp.	-//-	early Pleistocene
40) GQ 7	Packstone	-//-	-//-
41) GQ 8	Packstone	-//-	-//-
Fil 1	algal boundstone	Rd from Filiatra to Kiparissia	middle Pleistocene
Fil 2	-//-	Rd from Marathopolis to Filiatra	-//-
Lim 1	algal boundstone	Limenari coast	-//-
Lim 2	-//-	-//-	-//-
Lim 3	-//-	-//-	-//-
Lim 4	-//-	-//-	-//-
Lim 5	-//- (calichified)	-//-	-//-
Lim 6	-//-	-//-	-//-
Lim 7	-//-	-//-	-//-
Lim 8	-//-	-//-	-//-
Lim 9	-//-	-//-	-//-
Lim 10	-//-	-//-	-//-
Lim 11	Cladocora caespitosa	-//-	-//-
Lim 12	Fauna	-//-	-//-
Lim13	algal boundstone	Rd from Limenari to Filiatra	-//-
Lim 14	-//-	-//-	-//-
Fi→Ch1	matrix-supported conglomerate	Rd from Filiatra to Hristiani	early Pleistocene
Fi→Ch2	silty sandstone	-//-	-//-
Fi→Ch3	Flowstone	-//- (Prophitis Ilias Hill)	Pliocene (?)
Fi→Ch4	terra rossa	-//-	Pleistocene
Fi→Ch5	Flowstone	-//-	Pliocene
Fi→Ch6	-//-	-//-	-//-
Fi→Ch7	Sandstone	-//-	early Pleistocene

Appendix 1: List of samples

Fi→Ch8	Flowstone	-//-	Pliocene
P.I.1	-//-	-//-	Pliocene-Pleistocene (?)
P.I.2	hardpan caliche	-//-	early Pleistocene
P.I.3	Flowstone	-//-	Pliocene-Pleistocene (?)
P.I.4	red caliche hardpan	-//-	Pleistocene
P.I.5	pale caliche hardpan	-//-	-//-
P.I.6	Fanglomerate	-//-	early Pleistocene (?)
P.I.7	pale caliche hardpan	-//-	Pleistocene
P.I.8	-//-	-//-	-//-
Ma 3a,b	Ostrea sp1, Ostrea sp2	Mati Beach	Neotyrrhenian
Ma 5	Sandstone	-//-	-//-
Ma 6	granular conglomerate	-//-	-//-
Ma 7	muddy intraclast	-//-	-//-
Ma 8	Grainstone clast	-//-	middle Pleistocene (?) (reworked in the Neotyrrhenian terrace)
Ma 13	cross-laminated conglomerate	-//-	Neotyrrhenian
Ma→Vr1	silt and Cladocora caespitosa	Coastal cliff from Mati to Vromoneri	early Pleistocene
Ma→Vr2	chalky caliche	-//-	early-middle Pleistocene
Ma→Vr3	Silt	-//-	early Pleistocene
Ma→Vr4	algal boundstone	-//-	Eutyrrhenian
Ma→Vr5	Beachrock	-//-	Holocene
Ma→Vr6	-//-	-//-	-//-
Ma→Vr7	algal boundstone and Cladocora caespitosa	Vromoneri Coast	Eutyrrhenian
P.I.'1	Calcareous sand	Tragana	early Pleistocene
P.I.'2	pebbly silt	-//-	-//-
Tra 1	silty sand and fauna	-//-	-//-
Tra 2	fauna (mollsucs)	-//-	-//-
Petr 1	aeolian grainstone	Petrohori Village	late Pleistocene
Voidok 1	-//-	Voidokilia	-//-
Voidok 2	Grainstone	-//-	Eutyrrhenian
Voidok 3	-//-	-//-	-//-
Voidok 4	Laminated caliche	-//-	late Pleistocene
Voidok 5	Mudstone (flysch)	-//-	Oligocene
Pb 1	terra rossa	Petrohori Beach	latest Pleistocene
Pb 2	aeolian grainstone	-//-	-//-
Py 1	Mud	Pylos Port	early Pleistocene
Py 2	Recrystallised Lithophaga sp. Shells	Rd from Pylos to Kalamata	middle Pleistocene (?)
Py 3	bored pebbles	-//-	-//-
Py3*	Calichified calcareous mudstone	Pylos Castle	early Pleistocene
Py 4	algal packstone	-//-	-//-
Py→Me1	Conglomerate with calcareous sandstone matrix	Rd from Pylos to Methoni, near Mesohori	-//-
Py→Me2	algal boundstone	-//-	-//-
Py→Me3	lithic grainstone	-//-	-//-
Py→Me5	Grainstone	Palionero	-//-
Py→Me6	Lithophaga-bored pebbles	-//-	-//-
Fin 1	Sandstone	-//-	Eutyrrhenian
Me 1	Grainstone	Rd from Pylos to Methoni, near Ayios Athanassios	early Pleistocene

Appendix 1: List of samples

		Church	
Me 2	-//-	-//-	-//-
Me 3	pale caliche hardpan	-//-	early-middle (?) Pleistocene
Me 4	-//-	-//-	-//-
Me 5	Scree	-//-	Pleistocene
Me 6	Limestone with 'bird's eye' fabric	-//-	Eocene
Me 7	-//-	-//-	-//-
Me 8	-//-	-//-	-//-
Ko 1	Alluvium	Koroni Castle	late Pleistocene
Ko 7	Ostrea sp. lag	-//-	Eutyrrhenian
Ko 8	granular conglomerate	-//-	-//-
Ko 9	Packstone	-//-	-//-
Ko 10	Grainstone	-//-	-//-
Ko 11	mollusc fauna	-//-	-//-
Ko 12	Cladocora caespitosa	-//-	-//-
Ko 12	Mud	-//-	Early Pliocene
Ko 14	Conglomerate	Ayios Yeorghios, S of Koroni	early Pleistocene
Ko 15	-//-	-//-	-//-
Ko 16	-//-	-//-	-//-
Voun 1	bivalves, gastropods	Vounaria	Pliocene (?)
Kb 4	Rhodolithic packstone	Kombi Coast	middle Pleistocene or Eutyrrhenian
Chra 1	Sandstone	Hrani Coast	Pleistocene (?)
Chra 2	-//-	-//-	-//-
Chra 3	sandy silt	-//-	-//-
Chra 4	-//-	-//-	-//-
Pani 1	Flowstone	Paniperi	Pliocene (?)
Rhizom 1	well sorted sand	Rhizomilos	Late Pliocene
Rhizom 2	-//- (and Ostrea sp.)	-//-	-//-
Rhizom 3	-//-	-//-	-//-
Rhizom 4	chalky caliche	-//-	Pleistocene
Rhizom 5	well sorted pebbly sand	-//-	Late Pliocene
FiRe 1	Conglomerate	Filitrino Rema	Eutyrrhenian
Kyp 1	Grainstone/packstone	Kiprarissia Coast	-//-
Ma→Vr*1	Mud	Mati Coast	Early Pleistocene
Ma*2	Grainstone	Mati Coast	Middle Pleistocene
Ma*3	Sand	Mati Coast	Early Pleistocene
Meso*1	Sand	Mesohori	Early Pleistocene
Garg*1	Packstone	Gargaliani	Early Pleistocene
Garg*2	silty sand	Gargaliani	Early Pleistocene
Pyrg*1	Mud	Pirghos	Early Pleistocene (?)
Pyrg*2	caliche nodules	Pirghos	Pleistocene
Koum*1	Lacustrine marl	Rd from Koumarou to Kalamata	Pliocene (?)
Koum*2	caliche nodules	Rd from Koumarou to Kalamata	Pleistocene
Koum*3	fluvial sand	Rd from Koumarou to Kalamata	Pliocene (?)
MSN1	algal packstone	Mesohori	early Pleistocene
MSN2	algal packstone	Mesohori	early Pleistocene
MSN3	algal boundstone	Mesohori	early Pleistocene
MSN4	terra rossa	Mesohori	Pleistocene
MSN5	Calcareous sandstone	Mesohori	early Pleistocene
MSN6	Mud	Pylos Port	early Pleistocene

Appendix 1: List of samples

MSN7	pebbly mud	Pylos Port	early Pleistocene
MSN8	algal boundstone	Filiatrino Rema	early Pleistocene
MSN9	Mud	Filiatrino Rema	early Pleistocene
MSN10	granular conglomerate	Filiatrino Rema	Eutyrrhenian
MSN11	Mud	Filiatrino Rema	early Pleistocene
MSN12	fluvial sandstone	Rd from Filiatra to Valta	early Pleistocene
MSN13	fluvial sandstone	Rd from Filiatra to Valta	early Pleistocene
MSN14	fluvial sandstone	Rd from Filiatra to Valta	early Pleistocene
MSN15	Cladocora caespitosa	Laghouvardhos Coast	Eutyrrhenian

A.1.2) Eastern Lakonia Peninsula

Sample	Lithology	Location	Inferred Age
Kok*1	red alluvia	Kokkinia	late Pleistocene
Kok*5	pebbly silt (alluvial)	-//-	-//-
Kok*6	Burrows	-//- (Mourtitsa Rema)	early Pleistocene
Kok*7	Laminated silt-mud	-//-	-//-
Kok*8	-//-	-//-	-//-
Kok*9	-//-	-//-	-//-
Kok*15	sandy silt	-//-	-//-
Kok 10crd	Pectenidae	-//-	-//-
Kok 11crd	fine-grained silty sand	-//-	-//-
Kok 12crd	caliche nodules	-//-	Pleistocene
Kok 13crd	Laminated silt	-//-	early Pleistocene
Kok 14crd	caliche nodules	-//-	Pleistocene
Kok 16crd	Granular conglomerate	-//-	middle Pleistocene
Kok17crd	-//-	-//-	-//-
Kok 18crd	-//-	-//-	-//-
Kok 19crd	sandstone	-//-	-//-
Kok 20crd	pebbly sandstone	-//-	-//-
Kok 21crd	calichified silt	-//-	early Pleistocene
Kok 22crd	chalky caliche	-//-	Pleistocene
Kok 23crd	mud	-//-	early Pleistocene
Kok 24crd	fine-grained sand	-//-	-//-
Kok 25crd	red silt	-//-	late Pleistocene
Kok 26crd	stone tool	-//-	-//-
Kok 27crd	packstone with pectenidae	-//-	early to early-middle Pleistocene
Kok 28crd	algal packstone	-//-	-//-
Kok 29crd	sandstone (matrix in conglomerate)	-//-	early Pleistocene
Kok 30crd	calcareous sandstone	Between Ano Glykovrisi and Elea	early to early-middle Pleistocene
Kok 31a,b crd	sandstone	Dhiakos Hill	early Pleistocene
Kok 32crd	calcareous sandstone	-//-	-//-
Kok 33crd	-//-	-//-	-//-
Kok 34crd	bivalve fauna	-//-	-//-
Kok 35crd	calcareous sandstone	-//-	-//-
Kok 36crd	cross-laminated sandstone	Kambourani Rema	middle Pleistocene
Kok 37crd	siltstone	-//-	-//-
Kok 38crd	bivalve lag	-//-	-//-
Kok 39crd	mud	-//-	-//-
Kok 40crd	silt	-//-	-//-
Kok 41crd	mud	-//-	-//-
Kok 42crd	fine-grained sandstone	-//-	-//-
Kok 43crd	bivalves	-//-	-//-
Kok 45crd	coral-bafflestone	-//-	Eutyrrhenian
Kok 46crd	calichified clay	-//-	early Pleistocene
Kok 47crd	bivalves	-//-	Eutyrrhenian
Kok 48crd	grainstone	-//-	Neotyrrhenian
Kok 49crd	packstone	-//-	Eutyrrhenian
Kok 50crd	carbonated wood	-//-	middle Pleistocene
Kok 51crd	bioturbated sandstone	-//-	-//-
Kok 52crd	sandy silt	-//-	-//-
Kok 53crd	packstone	-//-	-//-

Appendix 1: List of samples

Kok 36cg	algal-coral packstone	-//-	Eutyrrheian
Kok 37cg	bivalves	-//-	-//-
Kok 38cg	silt matrix	Exit from Molai to Pakia	late Pleistocene
Kok 39cg	calcareous sandstone	Dhiakos	early Pleistocene
Kok 40cg	lithic tools (?)	Kokkinia	late Pleistocene-Holocene (?)
Kok 41cg	pebbly sand	Kambrourani Rema	middle Pleistocene
Kok 42cg	silt	-//-	-//-
Kok 43cg	Cladocora caespitosa bafflestone	-//-	Eutyrrhenian
Kok 44cg	silty sand	Mourtitsa Rema	early Pleistocene
Kok 45cg	calcareous sandstone	-//-	early to early-middle Pleistocene
Kok 46cg	lithic tool (?)	-//-	late Pleistocene
Kok 47cg	sand	-//-	early to early-middle Pleistocene
Kok 48cg	-//-	-//-	-//-
Kok 49cg	fauna from sandy beds	-//-	-//-
Kok 50cg	red silt from alluvia	-//-	middle or late Pleistocene
Ele*1	sandstone	Elea Coast	Eutyrrhenian
Ele*2	conglomerate	-//-	Holocene (Versilian)
Ele*3	algal crust	-//-	-//-
Ele*4	aeolian grainstone	-//-	latest Pleistocene
Ele*5	Spondylous gaederopous	-//-	Neotyrrhenian
Ele*6	cross-laminated sandstone	-//-	-//-
Ele 1	algal packstone	Kambourani Rema	Eutyrrhenian
Ele 2	well sorted sand	-//-	middle Pleistocene
Ele 3	bivalves	-//-	-//-
Ele 4	coral-bafflestone	-//-	Eutyrrhenian
Ele 5a,b	mud	-//-	early Pleistocene
Ele 6	chalky caliche	-//-	middle Pleistocene
Ele *	lithic tool from red alluvia	-//-	late Pleistocene
Plyt 1	grainstone	Plitra	middle Pleistocene
Plyt 3	grainstone	-//-	-//-
Plyt*4	mud	-//-	early Pleistocene
Plyt*5	grainstone	-//-	Eutyrrhenian
Plyt*6	algal boundstone	-//-	middle Pleistocene
Plyt*7	nodular caliche	-//-	Pleistocene
Plyt*8	grainstone	-//-	middle Pleistocene
Plyt*9	algal boundstone	-//-	-//-
Plyt*10	grainstone slab encrusted by red algae	-//-	-//-
Plyt*11	Cladocora caespitosa	-//-	middle Pleistocene or Eutyrrhenian
Plyt*12	grainstone	-//-	middle Pleistocene
Plyt*13	nodular caliche	-//-	Pleistocene
Plyt*14	grainstone	-//-	middle Pleistocene
Plyt*15	pebbly grainstone	-//-	-//-
Plyt*16	conglomerate	-//-	-//-
Plyt*17	-//-	-//-	-//-
Plyt*18	granular conglomerate	-//-	-//-
Plyt*19	algal boundstone	-//- (limestone quarry)	early-middle Pleistocene
Plyt*20	grainstone	-//-	-//-
Plyt*21	cemented soil mantle	Katsikoros	Late Pliocene (?)
AKor*1	calichified calcareous sandstone	Ano Koroghonas	early Pleistocene

Appendix 1: List of samples

AKor*2	grainstone	-//-	-//-
AKor*3	conglomerate	-//-	-//-
AKor*4	Ostrea sp. bank	-//-	-//-
AyAp*1	algal grainstone	Ayii Apostoli Coast	Eutyrrhenian
AyAp*2	bioturbated sand	-//-	early or middle Pleistocene (?)
MeSpi*1	calcareous sandstone	Meghali Spilia	early Pleistocene
MeSpi*2	-//-	-//-	-//-
MeSpi*3	sandstone	-//-	-//-
MeSpi*4	Planolite burrows in sandstone	-//-	-//-
MeSpi*5	sandstone	-//-	-//-
Monemv*1	sandstone with Rhizocretion bioturbation	Quarry S of Monemvasia	late Pleistocene (?)
Monemv*2	algal packstone	ca. 1.5 km S of Monemvasia	Eutyrrhenian (?)
Neap*1	hardpan caliche	Oros	Pleistocene
Neap*2	-//-	-//-	-//-
Neap*3	-//-	-//-	-//-
Neap*4	pebbly sandstone	Neapolis Coast	late Pleistocene
Neap*5	grainstone	-//-	-//-
Neap*6	-//-	-//-	-//-
Neap*7	conglomerate	-//-	-//-
Neap*8	rhodolithic grainstone	-//-	-//-
Neap*9	root-bioturbated	-//-	-//-
Vigl*1	grainstone	Viglaphia	middle Pleistocene
Vigl 2	pebbly rhodolithic grainstone	-//-	late Pleistocene
Vigl 3	silty sandstone	-//-	-//-
Vigl 4	silty sandstone	-//-	-//-
Vigl 5	well sorted sandstone	-//-	-//-
Vigl 6	Cladocora casespitosa, bryozoa	-//-	-//-
Vigl 7	bivalves, rhodoliths	-//-	-//-
Vigl 9	silty sandstone	-//-	early Pleistocene
Vigl 10	pebbly sandstone	-//-	-//-
AyMar*1	sandstone with imbricated bivalve shells	Ayia Marina	middle Pleistocene
AyMar 2	-//-	-//-	-//-
AyMar 3	algal bindstone	-//-	Holocene
AyMar 4	sandstone	-//-	middle or late Pleistocene
AyMar 5	hardpan caliche	-//-	-//-
AyMar 6	cross-bedded sandstone	-//-	-//-
AyMar 7	fine-grained sandstone		middle Pleistocene (?)
AyMar 8	-//-	-//-	-//-
AyMar 9	-//-	-//-	-//-
AyMar 11	obsidian tool	Prophitis Ilias	Holocene (Neolithic)
AyMar 12	sandstone matrix form conglomerate	-//-	early Pleistocene
AyMar 13	rhizocretion caliche	-//-	middle-late Pleistocene
AyMar 14	bivalves, irregular echinoids	-//-	early Pleistocene
AyMar 15	obsidian tools	Ayia Marina	Holocene (Neolithic)
AyMar 16	sandstone	Prophitis Ilias	middle-late Pleistocene
AyMar 17	sandstone	-//-	early Pleistocene
AyMar 18	conglomerate with angular clasts	-//-	-//-

Appendix 1: List of samples

AyMar 19	karstified calcareous sandstone	-//-	-//-
AyMar 20	hardpan caliche	-//-	-//-
AyMar 21	bioclastic sandstone	-//-	-//-
AyMar 22	sandstone and corals	-//-	middle Pleistocene
AyMar 23	coarse-grained sandstone	-//-	-//-
AyMar 24	fauna	-//-	-//-
AyMar 25	medium-grained sandstone	-//-	-//-
AyMar 26	fine-grained sand	-//-	-//-
AyMar 27	quartzite tool (?)	-//-	Late Pleistocene-Holocene
AyMar 28	pebbly sand	Prophitis Iias Port	early Pleistocene
AyMar 29	beachrock	Limni	Holocene
AyMar 30	irregular echinoid	Korakas	early Pleistocene
AyMar 31	rhodolithic pebbly sandstone	-//-	-//-
AyMar 32	sandstone-rudstone	-//-	early-middle Pleistocene (?)
AyMar 33	calcareous sandstone	Limnakia	Eutyrrhenian
AyMar 34	Cladocora caespitosa	-//-	-//-
AyMar 35	conglomerate	-//-	Neotyrrhenian
AyMar 36	sand and fauna	-//-	early Pleistocene
TaRe*1	breccia	Tasou Rema	Pliocene
TaRe*2	conglomerate	-//-	-//-
TaRe*3	caliche hardpan	-//-	-//-
TaRe*4	-//-	-//-	-//-
TaRe 5	red pebbly silt	-//-	middle Pleistocene
TaRe 6	pebbly silty sand	-//-	-//-
TaRe 7	pebbly silt with bivalves	-//-	-//-
TaRe 8	clay with carbonised plants	-//-	-//-
TaRe 9	silt (matrix of conglomerate)	-//-	-//-
TaRe 10	clay	-//-	-//-
TaRe 11	silt	-//-	-//-
TaRe 12	pebbly calcareous sandstone	-//-	Eutyrrhenian
TaRe 13	-//-	-//-	-//-
TaRe 14	sandy silt with nodules	-//-	-//-
TaRe 15	calcareous sandstone	-//-	-//-
TaRe 16	terrace clast reworked into fanglomerates	-//-	middle Pleistocene
TaRe 17	Cladocora caespitosa	-//-	Eutyrrhenian
TaRe 18	sandstone	-//-	-//-
TaRe 19	pebbly rhodolithic grainstone	-//-	Neotyrrhenian
TaRe 20	silt	-//-	Eutyrrhenian
TaRe 21	granular grainstone	-//-	-//-
TaRe 22	rhodolithic sandstone with Ostrea banks	-//-	-//-
TaRe 23	-//-	-//-	-//-
TaRe 24	coral bafflestone	-//-	middle Pleistocene (?)
TaRe 25	silt	-//-	-//-
TaRe 26	Cladocora caespitosa colonies	-//-	-//-
TaRe 27	Ostrea bank	-//-	-//-

Appendix 1: List of samples

TaRe 28	calichified pebbly silt	-//-	-//-
PaMo*1	coarse sand	Palaea Monemvasia	Pleistocene
Kast*1	conglomerate	1 km N of Kastella	late Pleistocene (Eutyrrhenian ?)
Kast*2	pebbly grainstone	-//-	-//-
Glyko 1	weathered volcaniclastics	Panayia, Ano Glikovrisi	Permian
Glyko 2	hardpan caliche	-//-	Pliocene (?)
Glyko 3	-//-	-//-	-//-
Glyko 4	conglomerate	Kambourani-Maganeika	early Pleistocene
Glf 1	pebbly silt	Glifadha	early Pleistocene (?)
Glf 2	silty sand	-//-	-//-
Glf 3	hardpan caliche	-//-	Pleistocene
Glf 4	reworked pebble	-//-	early Pleistocene
Glf 5	sand	-//-	-//-
Glf 6	pebbly sand	-//-	-//-
Glf 7	sandstone (matrix of conglomerate)	-//-	-//-
Glf 8	laminated sandstone	-//-	-//-
Glf 9	sandstone	-//-	-//-
Glf 10	calichified silt	-//-	-//-
Glf 11	caliche	-//-	-//-
Glf 12	flowstone	Dhiakos Hill	Pliocene
Glf 14	lithic grainstone	-//-	early Pleistocene
Glf 15	-//-	-//-	-//-
Glf 16	pissolithic caliche	Milia	Pleistocene
Glf 17	pissoliths	-//-	-//-
Glf 18	laminated caliche	-//-	-//-
Glf 19	cemented caliche	-//-	-//-
Glf 20	fluvial conglomerate	Dhiakos Hill	early Pleistocene (?)
BoRe 1	bivalves	Kambourani Rema	middle Pleistocene
BoRe 2	packstone	-//-	Eutyrrhenian
BoRe 3	silt	-//-	middle Pleistocene
BoRe 4	lithic packstone	Bozas Rema Coast	-//-
BoRe 5	bivalves and gatsropods	-//-	-//-
BoRe 6	silty sand	-//-	-//-
BoRe 7	mould of articulated bivalve	-//-	-//-
BoRe 8	red silt	-//-	-//-
BoRe 9	-//-	-//-	-//-
BoRe 10	caliche hardpan	-//-	early-middle Pleistocene
BoRe 11	grainstone	-//-	Eutyrrhenian
BoRe 12	silty mud	-//-	middle Pleistocene
BoRe 13	cemented breccia	-//-	Late Tertiary
BoRe 14	conglomerate	-//-	Eutyrrhenian
BoRe 15	conglomerate, sandstone, rhodolithic packstone with Strombus bubonius	-//-	-//-
BoRe 16	cemented soil mantle	-//-	Pliocene (?)
BoRe 17	red fanglomerate	-//-	late Pleistocene
BoRe 18	rhodolithic packstone	-//-	Eutyrrhenian
BoRe 19	Murex sp. reworked into fanglomerate	-//-	late Pleistocene
BoRe 20	grainstone	-//-	Eutyrrhenian
BoRe 21	coral-bafflestone (Cladocora caespitosa)	-//-	-//-
BoRe 22	caliche hardpan	-//-	Pleistocene (?)

Appendix 1: List of samples

BoRe 23	gastropod moulds	-//-	middle Pleistocene
BoRe 24	silty sand	-//-	-//-
BoRe 25	lithic tool (?)	-//-	Neolithic (?)
BoRe 26	yellow palaeosol	-//-	Late Tertiary
BoRe 27	grainstone	-//-	
Pa→De 1	cemented conglomerate	Havalas, Rd form Pappadhianika to Dhaemonia	Late Pliocene or early Pleistocene
Pa→De 2	red siltstone matrix form cemented conglomerate	-//-	-//-
Pa→De 3	pebbly sandstone	Assopos	early Pleistocene
Dem 1	fine-grained sandstone	Dhaemonia	-//-
Dem 2	grainstone	-//-	-//-
Dem 3	fine-grained sand	-//-	-//-
Dem 4	silt	Ayia Marina Chapel, Dhaemonia Coast	-//-
Dem 5	pebbly silt	-//-	-//-
Dem 6	mud with scaphopods	-//-	-//-
Dem 7	bivalves, scaphopods, bryozoa	-//-	-//-
Dem 8	grainstone	-//-	middle Pleistocene (?)
Dem 9	sandstone	-//-	early Pleistocene
Dem 10	lithic tools (?)	Dhokali Rema	Holocene
Dem 11	laminated sand (fluvial)	-//-	Eutyrrhenian
Dem 12	mud	Ayia Marina Chapel, Dhaemonia Coast	early Pleistocene
Dem 13	sandy silt	-//-	-//-
Dem 14	fossil beds	-//-	-//-
Dem 15	-//-	-//-	-//-
Dem 16	mud	-//-	-//-
Dem 17	-//-	-//-	-//-
Dem 18	molluscs	-//-	Eutyrrhenian
Dem 19	grainstone	-//-	-//-
Dem 20	molluscs	-//-	early Pleistocene
Dem 21	mud	-//-	-//-
Dem 22	-//-	-//-	-//-
Dem 23	-//-	-//-	-//-
Dem 24	fauna	-//-	-//-
Dem 25	-//-	-//-	-//-
Dem 26	-//-	-//-	-//-
Dem 27	-//-	-//-	-//-
Dem 28	-//-	-//-	-//-
Dem 29	-//-	-//-	-//-
Dem 30	-//-	-//-	Eutyrrhenian
Arch 1	pebbly sand	Arhangelos	middle Pleistocene
Arch 2	rhodolithic grainstone	-//-	late Pleistocene
Arch 3	bivalves	-//-	-//-
AyNik 1	cemented scree	Ayios Nikolaos	Late Pliocene (?)
AyNik 2	pebbly red silt	-//-	-//-
AyNik 3	-//-	-//-	-//-
AyNik 4	fanglomerate	-//-	early Pleistocene
AyNik 5	terra rossa	-//-	late Pleistocene (?)
AyNik 6	fluvial conglomerate	Dhokali Rema	early Pleistocene
Elik 1	cemented breccia	Pyrghos tou Phonia	Pliocene
Elik 2	-//-	-//-	-//-
Elik 3	pebbly sandstone	-//-	early Pleistocene

Appendix 1: List of samples

Elik 4	bioturbated sandstone	-//-	-//-
Elik 5	fine-grained sandstone	-//-	-//-
Elik 6	hardground	-//-	-//-
Elik 7	silty sand	-//-	-//-
Elik 8	bioturbated sandstone	-//-	-//-
Elik 9	aeolian grainstone	Martahias (Elika Coast)	-//-
Xif 1	sand	Psiphia Coast	middle Pleistocene
Xif 2	rhodolithic sandstone	-//-	Eutyrrhenian
Xif 3	granular conglomerate	-//-	-//-
Xif 4	Ostrea sp. bank	-//-	-//-
Xif 5	Ostrea sp.	-//-	middle Pleistocene
Xif 6	Cladocora caespitosa	-//-	-//-
Xif 7	ceramic fragments	-//-	Holocene (Historical)
Xif 8	red silt	-//-	late Pleistocene
Xif 9	lithic tool (?)	-//-	-//-
Xif 10	silty pebbly sand	Psiphia, "Estatorion ta Melitzanankia"	middle Pleistocene
Xif 11	sand	-//-	-//-
Xif 12	concretions from sand beds	-//-	-//-
Xif 13	-//-	-//-	-//-
CaPa 1	sandstone	"Camping Paradise", Monemvasia	Neotyrrhenian

a: Messenia Peninsula

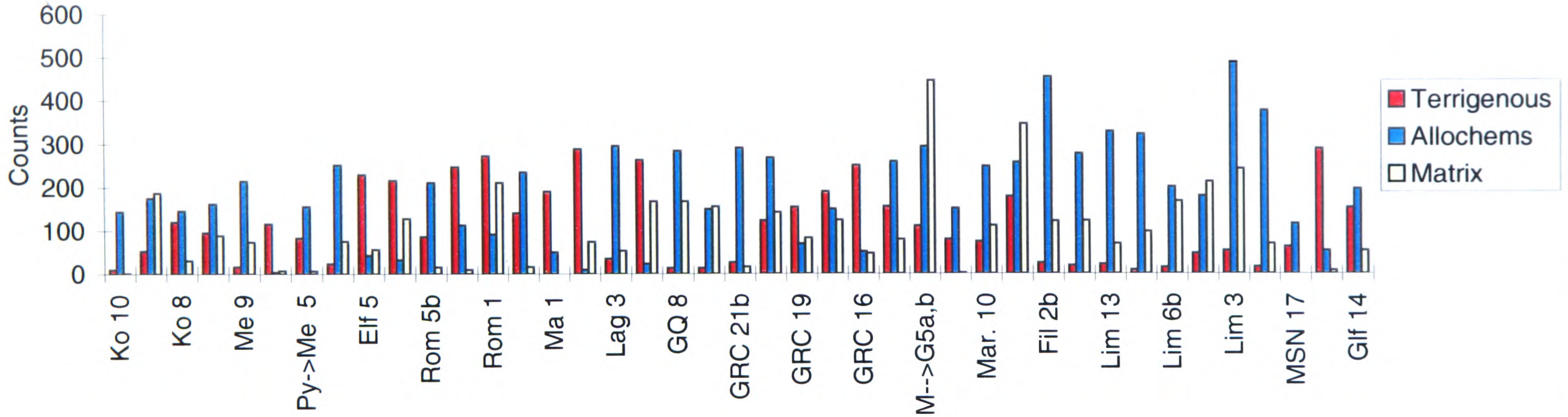

b: Lakonia

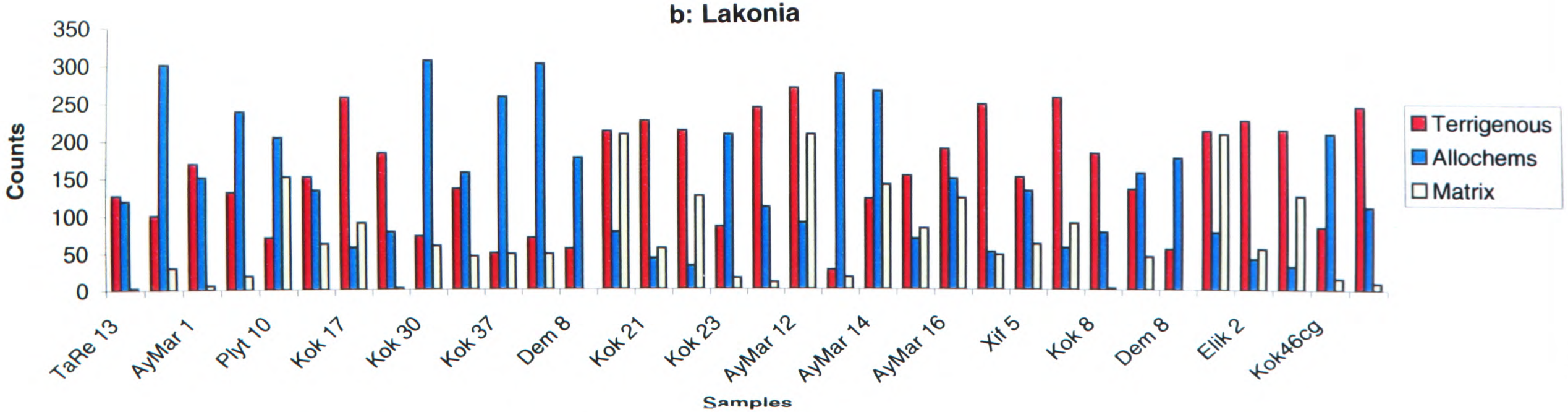

Tatatata

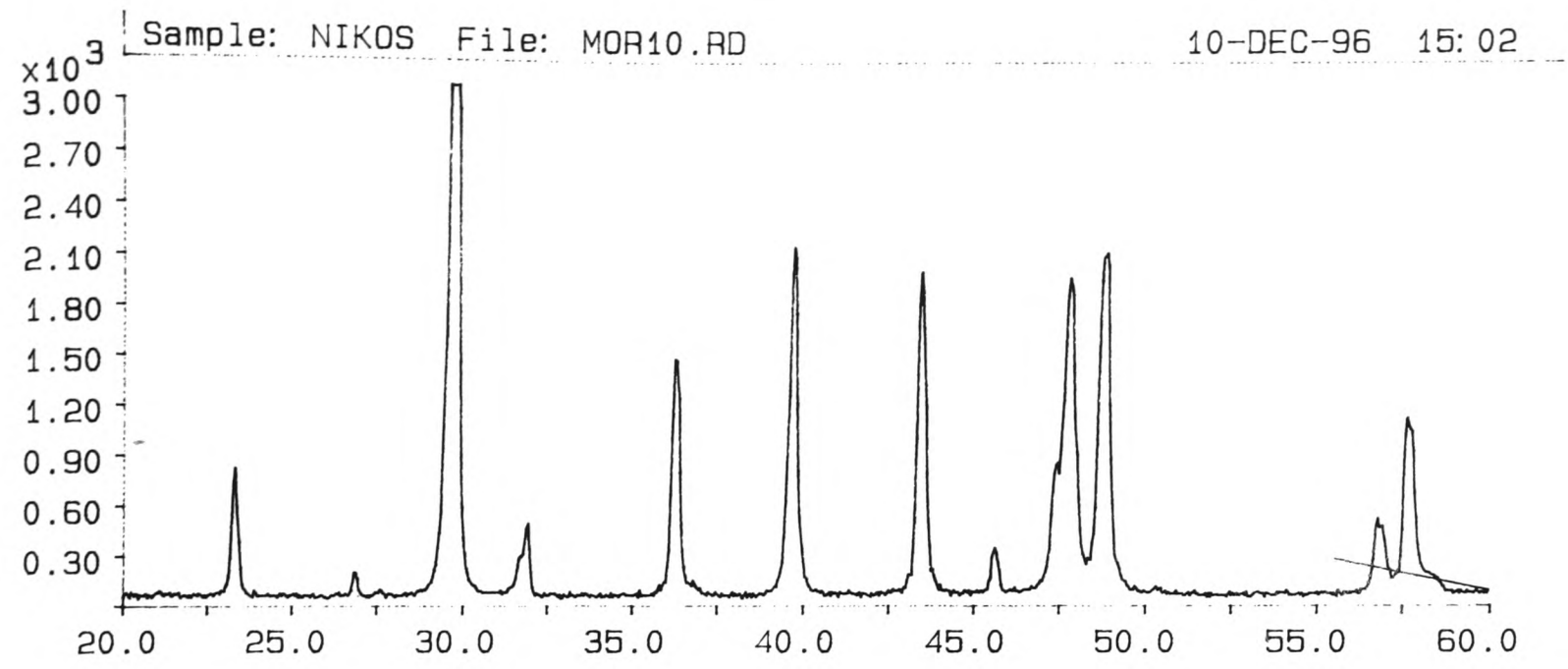
Sample: NIKOS File: MOR10.RD
10-DEC-96 15:02
x10 3
3.00
2.70
2.40
2.10
1.80
1.50
1.20
0.90
0.60
0.30
20.0 25.0 30.0 35.0 40.0 45.0 50.0 55.0 60.0

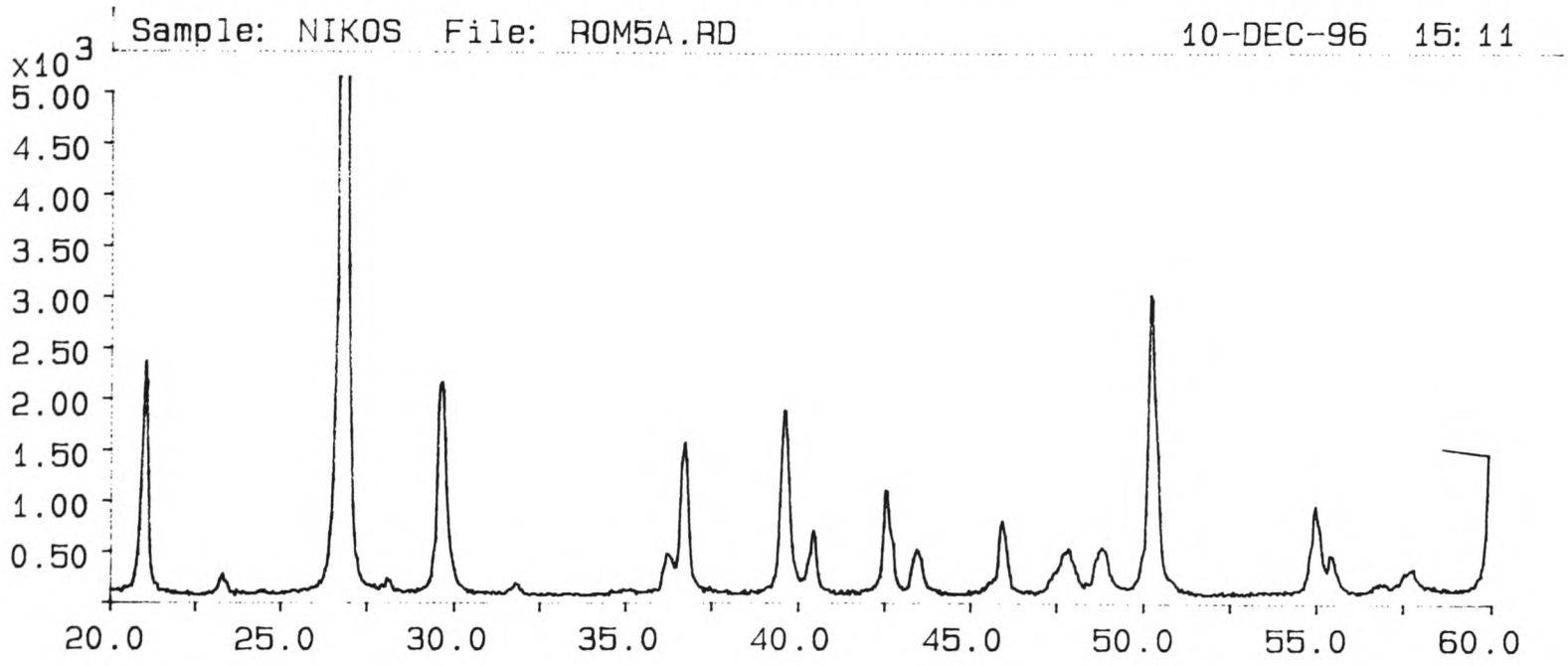
Sample: NIKOS File: ROM5A.RD
10-DEC-96 15:11
x10 3
5.00
4.50
4.00
3.50
3.00
2.50
2.00
1.50
1.00
0.50
20.0 25.0 30.0 35.0 40.0 45.0 50.0 55.0 60.0

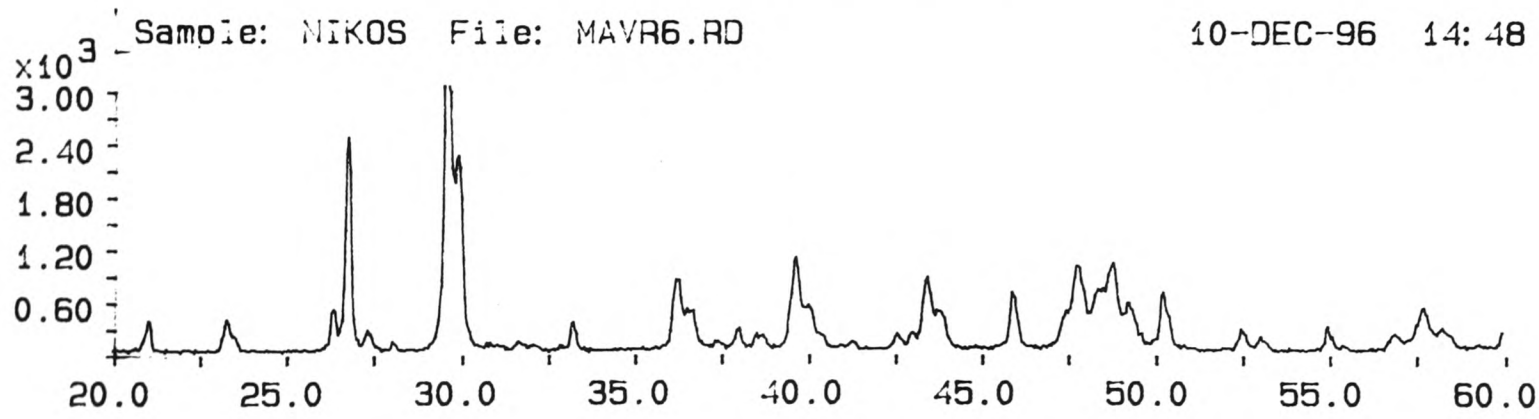
Sample: NIKOS File: MAVR6.RD
10-DEC-96 14:48
x10 3
3.00
2.40
1.80
1.20
0.60
20.0 25.0 30.0 35.0 40.0 45.0 50.0 55.0 60.0

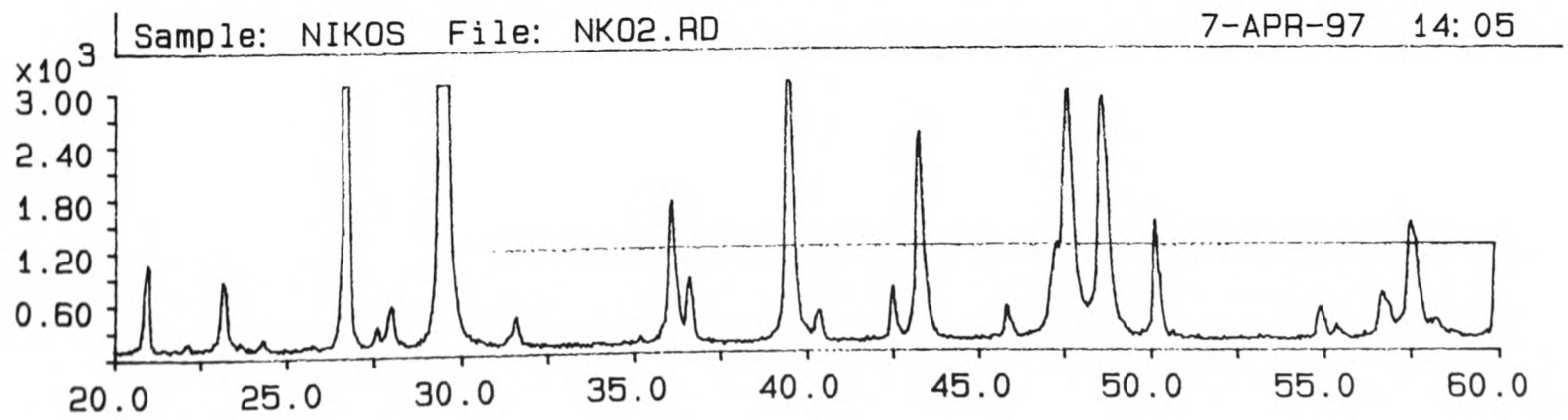
Sample: NIKOS File: NK02.RD
7-APR-97 14:05
x10 3
3.00
2.40
1.80
1.20
0.60
20.0 25.0 30.0 35.0 40.0 45.0 50.0 55.0 60.0

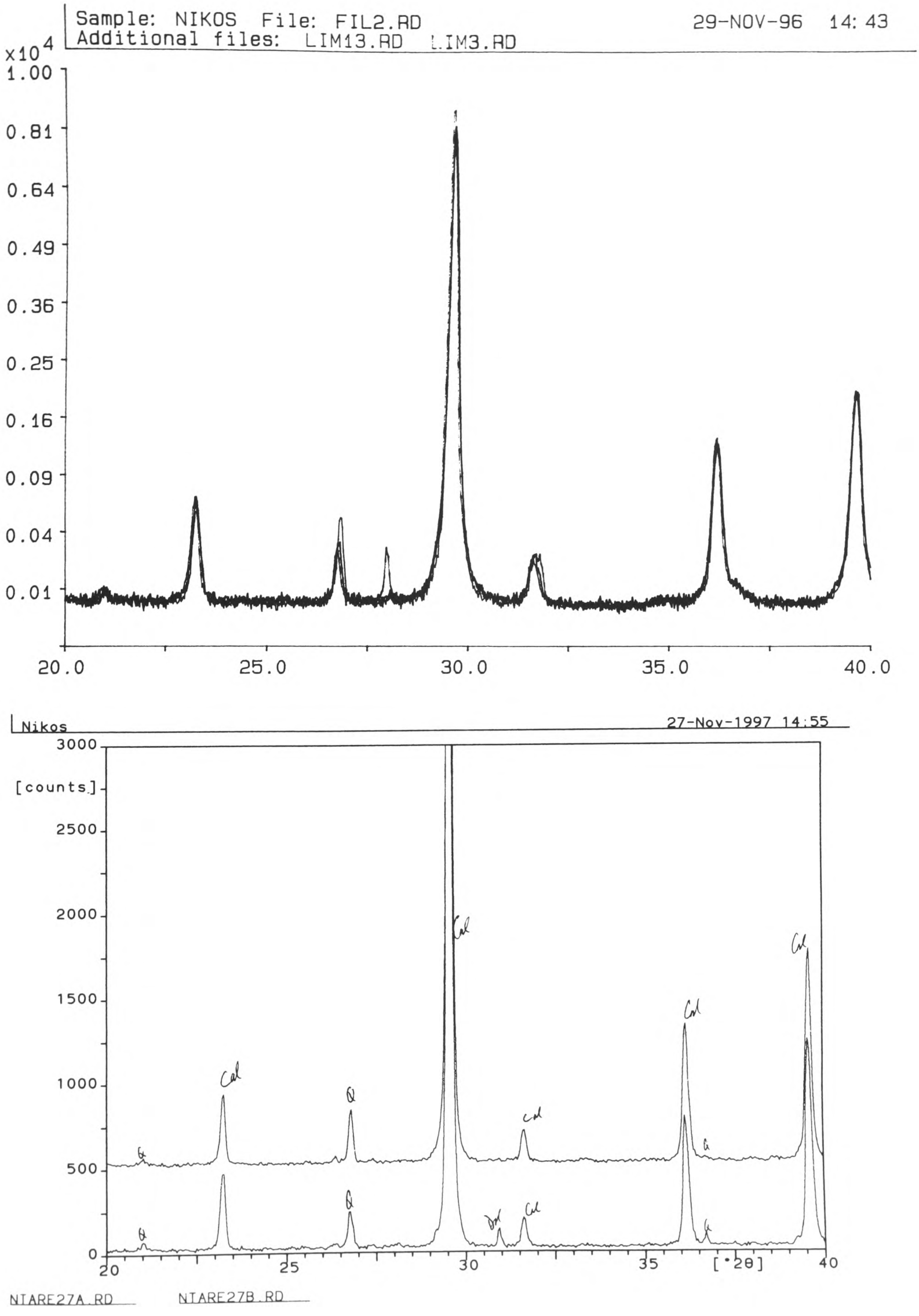
Sample: NIKOS File: FIL2.RD
29-NOV-96 14:43
Additional files: LIM13.RD LIM3.RD
x10 4
1.00
0.81
0.64
0.49
0.36
0.25
0.16
0.09
0.04
0.01
20.0
25.0
30.0
35.0
40.0
Nikos
27-Nov-1997 14:55
[counts]
3000
2500
2000
1500
1000
500
0
20
25
30
35
[°2θ]
40
Cal
Q
NIARE27A.RD
NIARE27B.RD

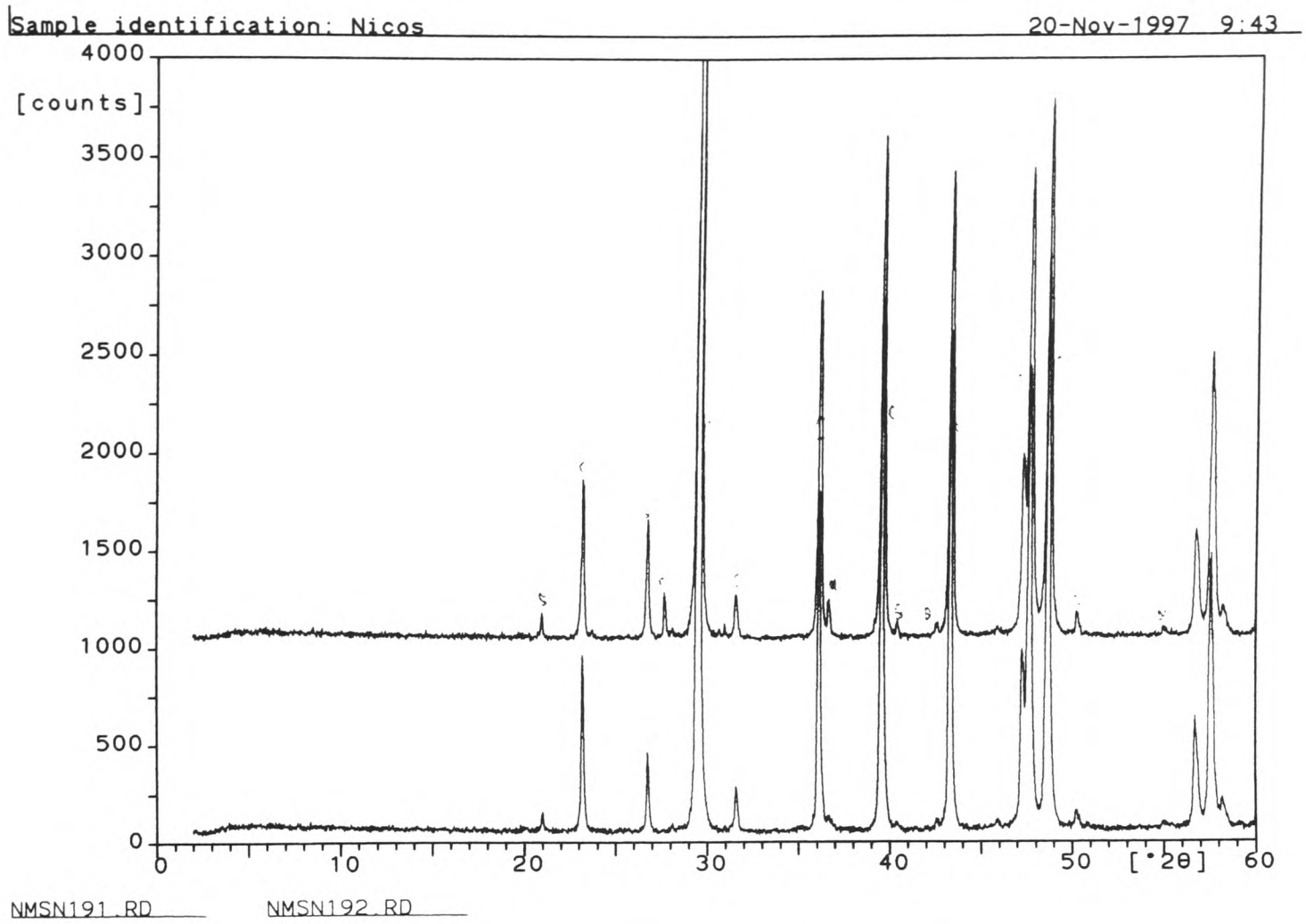
Sample identification: Nicos
20-Nov-1997 9:43
[counts]
4000
3500
3000
2500
2000
1500
1000
500
0
0
10
20
30
40
50
[°2θ]
60
NMSN191.RD
NMSN192.RD

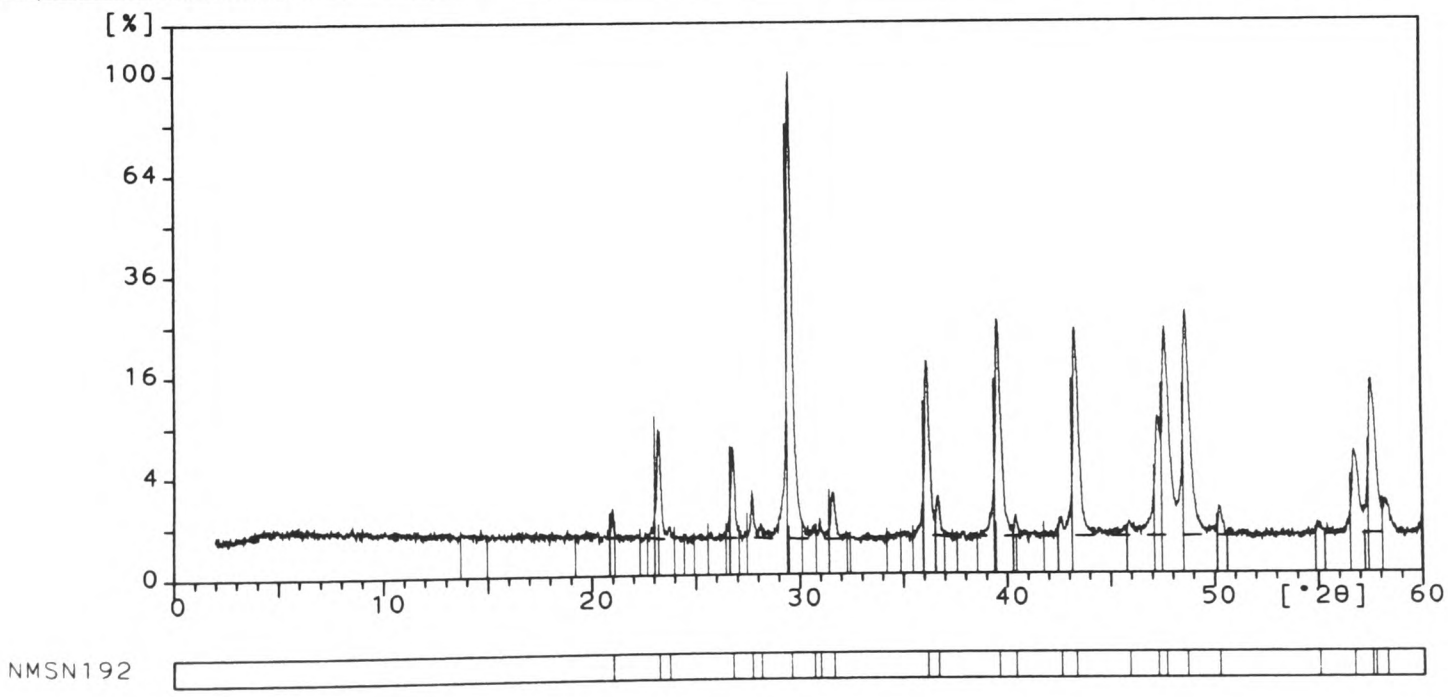
Sample ident.: nicos
20-Nov-1997 9:49
[%]
100
64
36
16
4
0
0
10
20
30
40
50
[°2θ]
60
NMSN192

Appendix 3: XRD results

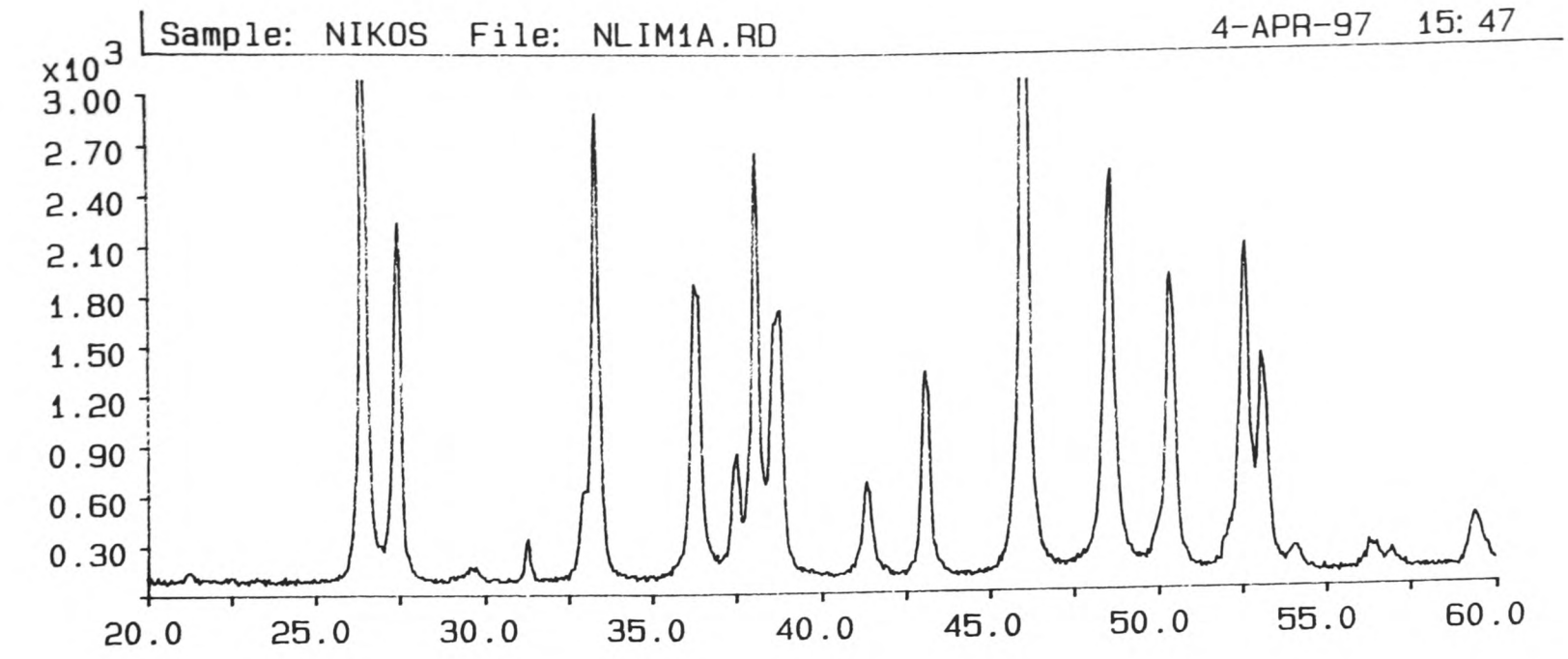

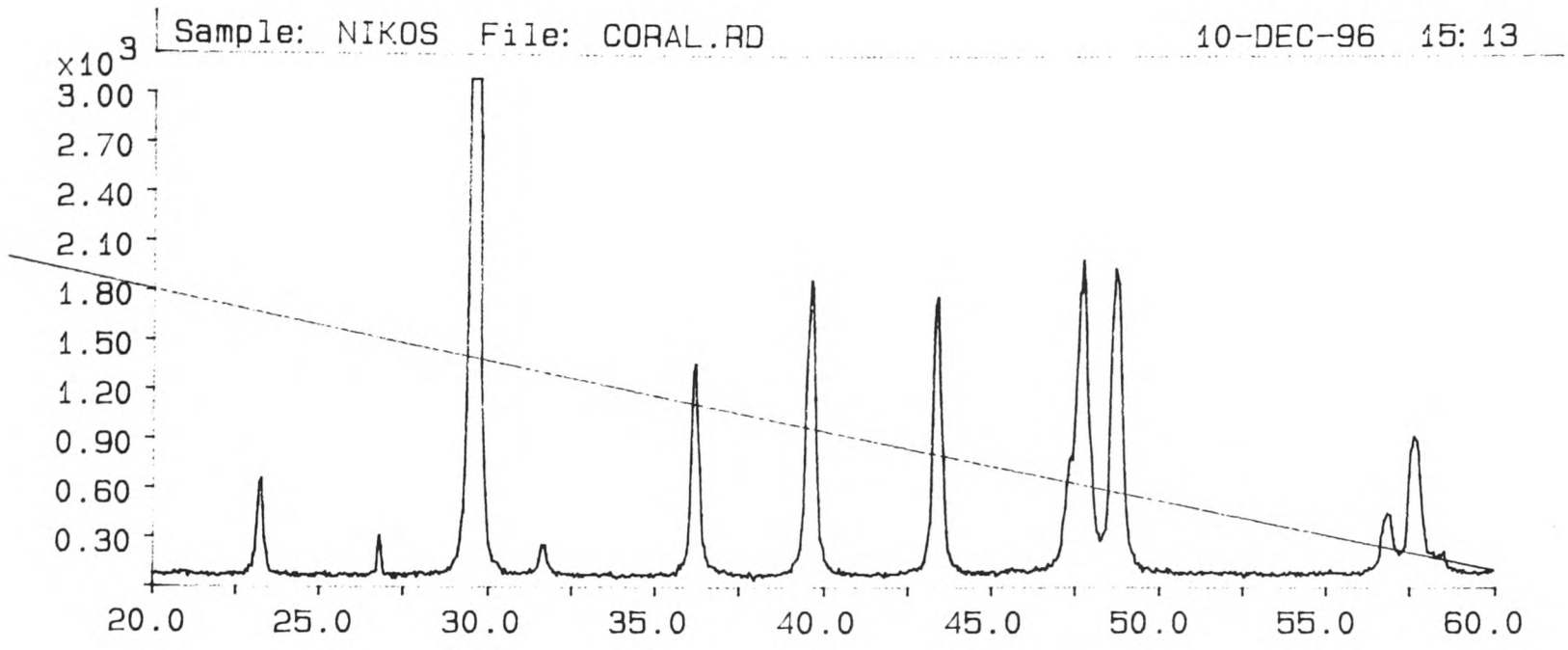

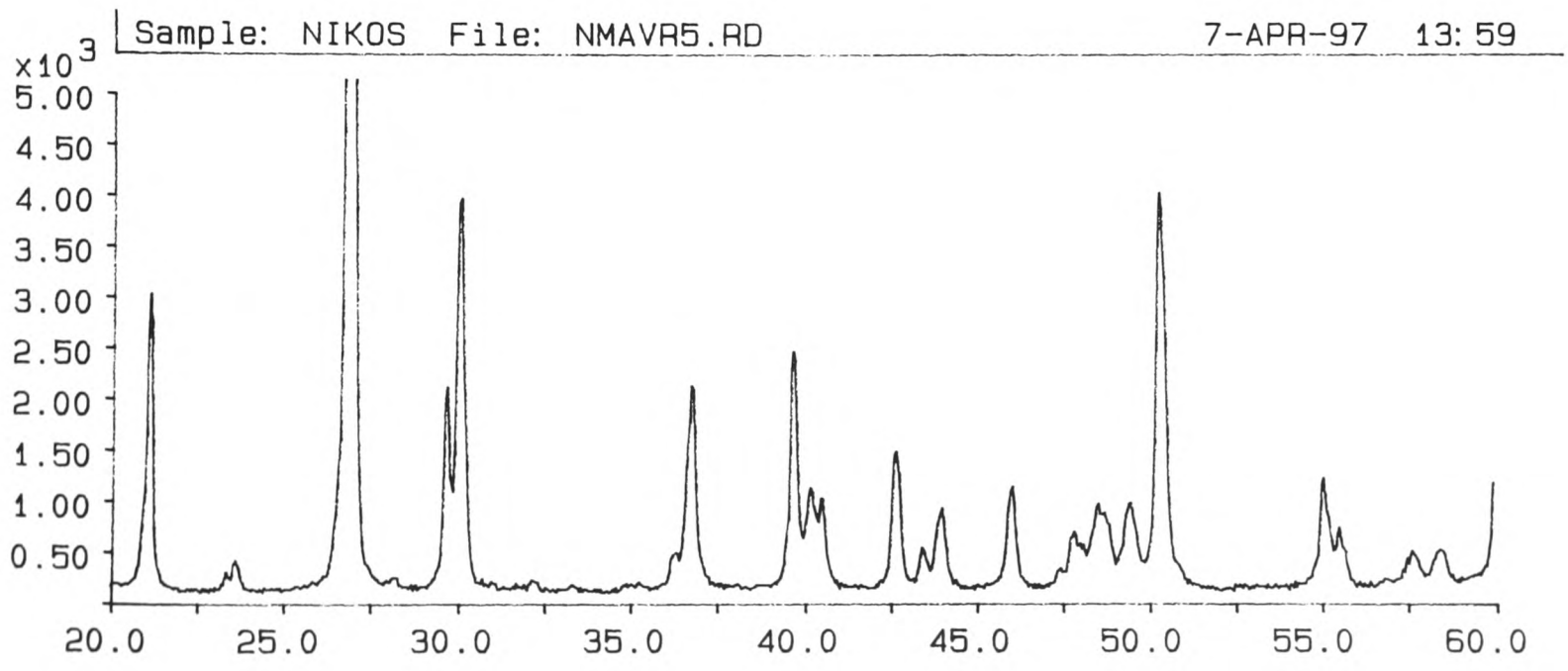

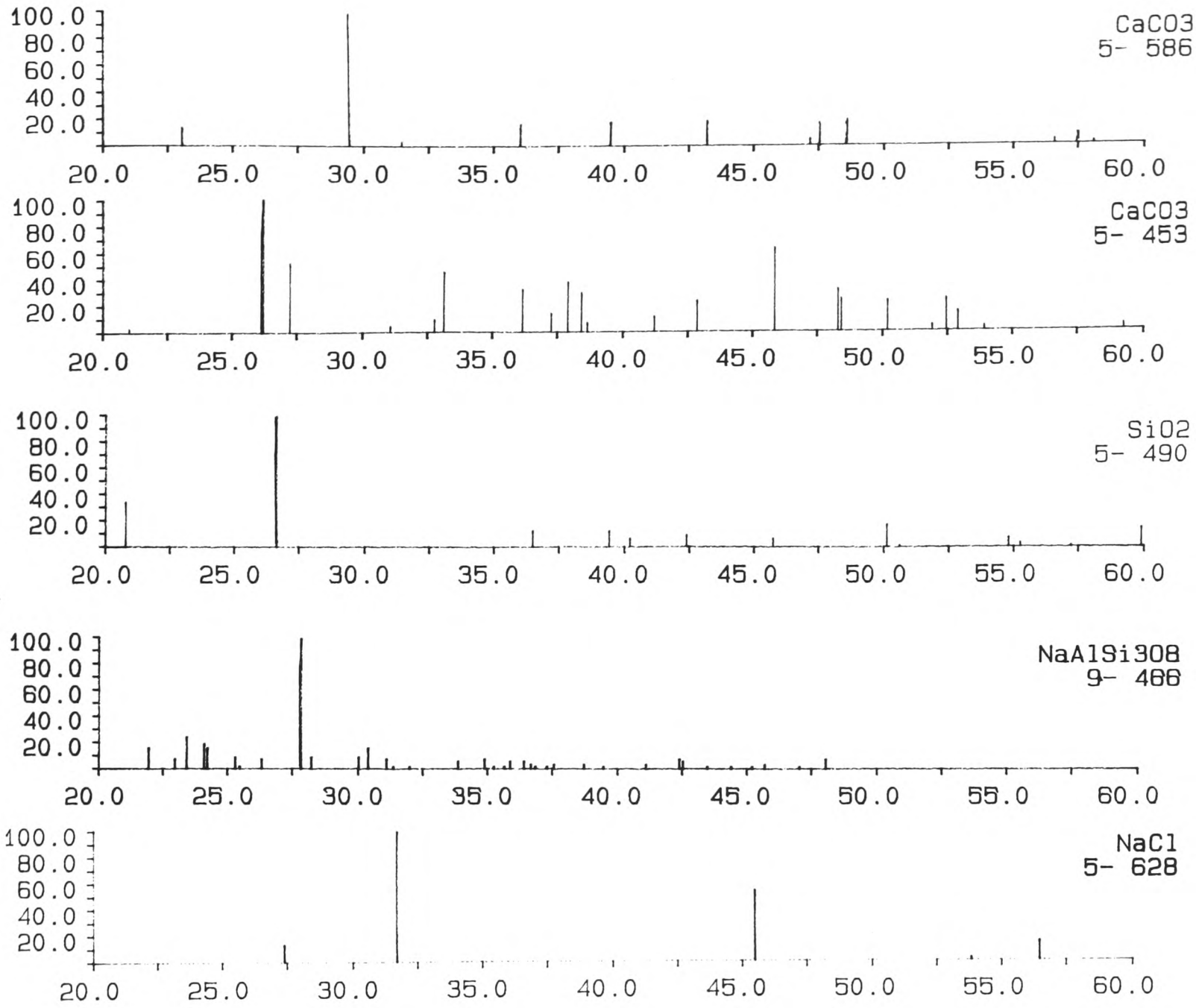

The main minerals identified in Quaternary sediments from the Southern Peloponnese

Controls on Plio-Quaternary sedimentation within an active fore-arc region: Messenia Peninsula (SW Peloponnese), S. Greece

N. Kourampas and A.H.F. Robertson
Department of Geology and Geophysics, University of Edinburgh,
West Mains Road, Edinburgh, EH9 3JW, U.K.

Abstract

Plio-Quaternary sedimentation in the Messenia Peninsula, SW Peloponnese (Greece), was dominated by the interplay between progressive tectonic uplift and global eustatic sea level change. Additional modifying controls were localised uplift of the footwalls and hangingwalls of extensional faults, climatic change and normal (autocyclic) sedimentary processes. Nine regionally correlated marine Plio-Quaternary sequences resulted from marine transgression and coastline/delta progradation during sea level highstands. Fluvial incision, cliff formation and local alluvial fan progradation took place mainly during sea level falls and lowstands.

Pliocene (ca. 5.5-1.6 Ma) transgressive marine sediments were deposited on a faulted Neogene topography. Early to middle Pleistocene (Calabrian, ca. 1.6-0.9 ka) shallow-marine sediments began with offshore marls (NN 19 biochronozone), coarsening upwards into shoreface - foreshore carbonates/deltaic sands. Syn- and post-depositional faulting occurred, at scales ranging from regional fault-bounded blocks, ca. 20-30 km across, to outcrop-scale faults and joints. In relatively gentle uplifted areas the highest Pleistocene terrace is overlain by siliceous soils. By contrast, strongly-faulted areas were marked by enhanced clastic run-off, with alluvial fans prograding over previous units during a lowstand at the beginning of the late Pleistocene (between Sicilian and Eutyrrhenenian). Sicilian (ca. 200 ka, or older) and Eutyrrhenian (ca. 120 ka) shoreface-foreshore carbonates occur seawards of older terraces as a result of progressive tectonic uplift. The Neotyrrhenian terrace (ca. 80-100 ka), at still lower elevations, is separated from the Eutyrrhenian terrace by a distinct unconformity. Local latest Pleistocene alluvial fans occur in the vicinity of major normal faults. Versilian vermetid encrustations formed in the Holocene, ca. 6 ka ago, or even later. Active regional uplift and local fault-controlled subsidence continued during Holocene time.

The entire sedimentary record from Early Pliocene onwards was influenced by the effects of regional northward subduction beneath the Peloponnese. This resulted in a combination of regional tectonic uplift (underplating and subduction dip changes?) and extension (southwestward "roll-back"). As a result, the Messenia Peninsula developed as two large uplifted horst blocks within a wider area of active extension.

Introduction

The purpose of this paper is to describe well exposed Plio-Quaternary (early Pliocene to Holocene) shallow-marine and terrestrial sediments from coastal areas of the Messenia Peninsula, SW Peloponnese, Greece and to interpret them in terms of potential controls, including regional tectonic uplift, global eustatic sea level change, uplift and subsidence related to local faulting, climate and autocyclic (normal) sedimentary processes. Previous work in the area focused on the geomorphology of terraces (Kelletat *et al.*, 1976; Mariolakos *et al.*, 1994), the sedimentology and the neotectonics of selected areas (Zelilidis, 1988; Zelilidis *et al.*, 1988, Zelilidis and Doutsos, 1992). In this study we adopt an *integrated* approach, drawing on the sedimentology and structural evidence, in addition to geomorphology, to deduce the Plio-Quaternary geological history of the region. This supplements the present data base for the Aegean arc (e.g. Gulf of Corinth; Collier, 1990; Doutsos and Piper, 1990, and Crete; Meulenkamp *et al.*, 1994). The results provide constraints on regional tectonic processes, notably the timing of extension related to southward retreat ("roll-back") of the Aegean subduction zone. The results also allow instructive comparisons with Quaternary Mediterranean marine terrace systems elsewhere, including Cyprus (Poole and Robertson, 1991; this volume).

Regional plate tectonic setting

The Messenia Peninsula forms part of the forearc of the northward-dipping Aegean subduction system (e.g. McKenzie, 1978; Le Pichon and Angelier, 1979; Fig. 1). This area is situated ca. 60 km NE of the western segment of the Hellenic Trench (Ionian trenches). To the west lies the westerly extension of the Mediterranean Ridge, interpreted as an accretionary prism created by subduction of deep-sea sediments of the African plate beneath the Eurasian plate (Kastens *et al.*, 1993; Chaumillon and Mascle, 1995, Robertson and Kopf, 1998). In keeping with this regional trend, compression apparently continued until the end of Early Pliocene time within a few kilometres offshore from the W Peloponnese (e.g. Strophades Islands; Lyberis and Bizon, 1981; L.H. Royden, pers. comm., 1998), but later in the Plio-Quaternary the plate boundary shifted to the Mediterranean Ridge further offshore (Kastens *et al.*, 1993; Chaumillon and Mascle, 1995; Robertson and Kopf, 1998).

During the Plio-Quaternary, the Messenia Peninsula underwent regional uplift, as part of the Peloponnese as a whole (Duffaure, 1977; Kelletat *et al.*, 1976). This uplift is thought to relate to underplating of the overriding Eurasian plate margin by buoyant accreted sediments (Le Pichon and Angelier, 1979), or result from changes in the angle of underthrusting of the Peloponnese

From Panayides, I., Xenophontos, C. and Malpas, J., (eds), 2000, Proceedings of the Third International Conference on the Geology of the Eastern Mediterranean.

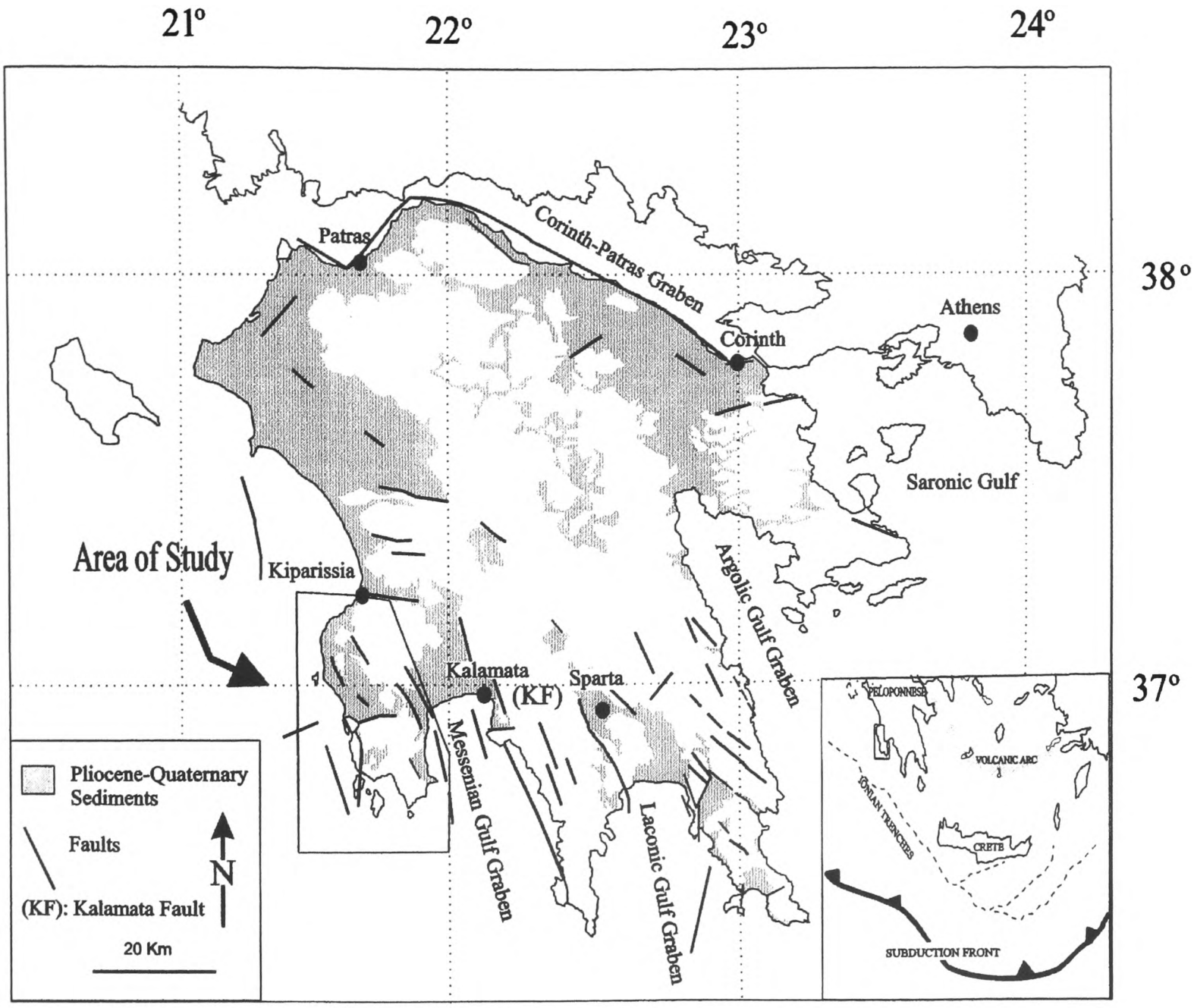

Figure 1. Outline map of the Peloponnese, Greece, showing the main neotectonic structures mentioned in the text and the location of the study area. Inset: Location in relation to the Ionian trench, part of the South Aegean arc system.

by the subducting slab (Berkchemer and Kowalczyk, 1978; Hatzfeld *et al.*, 1989), or both processes. Normal faulting, related to generally E-W extension in the western segment of the Aegean Arc (Armijio *et al.*, 1979; Lyon-Caen *et al.*, 1988), is superimposed on regional uplift of the Peloponnese. Today, the area remains seismically active (e.g. Galanopoulos, 1947), as shown by the 1986 Kalamata earthquake (Hatzfeld *et al.*, 1990).

Local geological setting

The basement of the Messenia Peninsula (Fig. 2) comprises the southerly extension of the westerly nappe units of the Mesozoic-Tertiary Hellenides (Jacobschagen *et al.*, 1978). These are, first, the Tripolis zone, exposed locally as Eocene nummulitic limestone and Late Eocene-Oligocene turbidites, and interpreted as part of the Mesozoic-Early Tertiary continental margin of the Apulian microcontinent. Secondly, there are ribbon-radiolarites, thin-bedded pelagic limestones and turbiditic sandstones/ limestones of the Pindos zone, representing far-traveled thrust sheets derived from the former Neotethys ocean to the (present) east (Fytrolakis, 1971; I.G.M.E., 1980 a,b). In the Messenia Peninsula, the Pindos zone is thrust over the Tripolis zone, such that the frontal thrust in the west now forms a prominent NNW-SSE trending tectonic lineament (Pindos Thrust); this also provides a backdrop to the study area in the north (Fig. 2). Compression on the Neotethyan thrust system ended by Mid-Miocene time (Jacobschagen *et al.*, 1978; Mariolakos *et al.*, 1994), ushering in the Neotectonic phase that is the subject of this paper.

Neotectonic structure

The Messenia Peninsula is characterised by several mappable sets of fault trends (Fig. 2). These are indicated on the I.G.M.E. map (1980 a,b), supplemented by regional and local mapping and collection of outcrop-scale kinematic data on fault orientation,

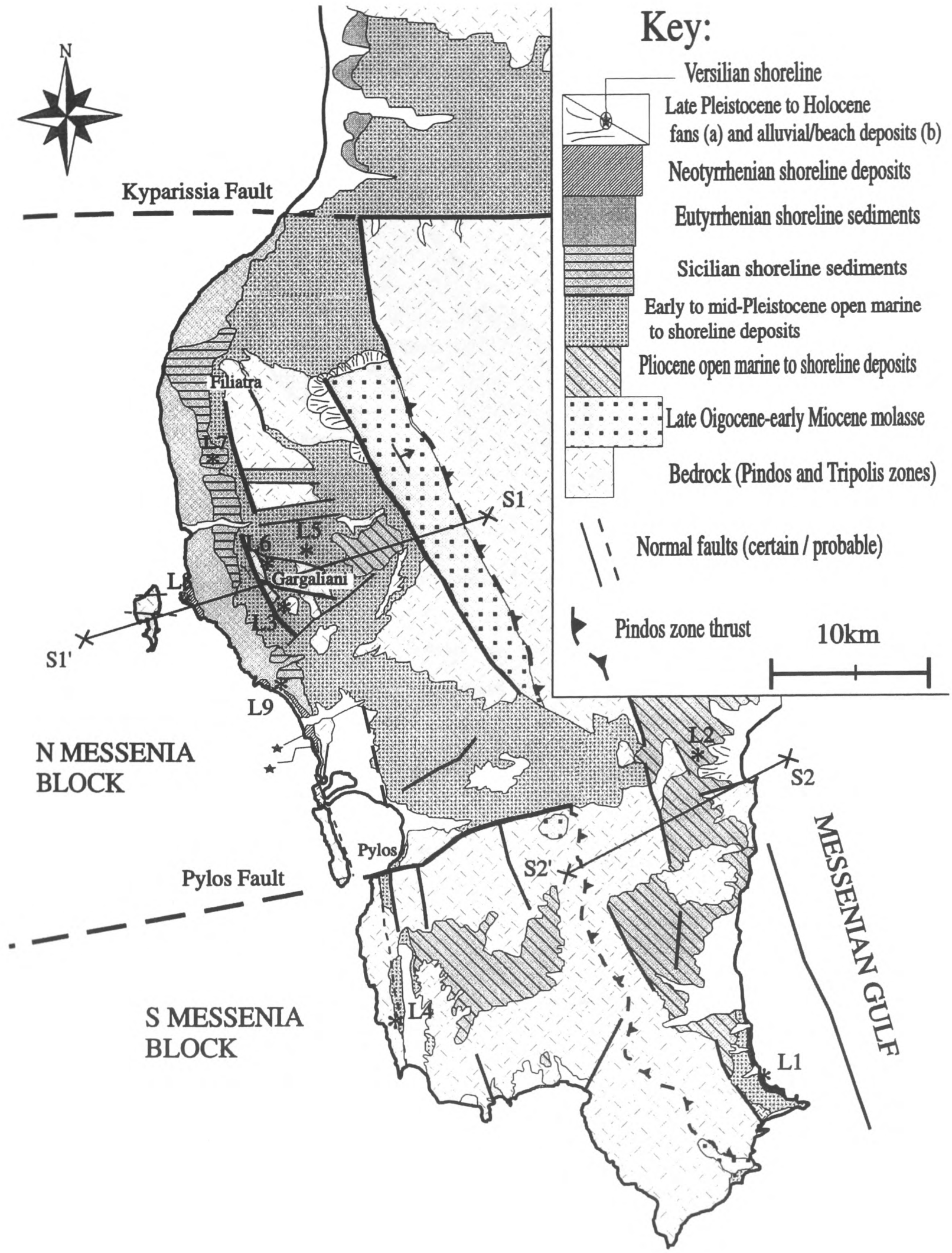

Figure 2. Outline tectonic map of the Messenia Peninsula, SW Peloponnese. Note the subdivision of the area into two tectonic blocks, N Messenia and S Messenia, by a combination of N-S and E-W faults. These faults partly re-activate pre-exiting tectonic lineaments and developed to accommodate the growing regional curvature of the SW Aegean arc. L1-L9: Positions of the logs discussed in the text.

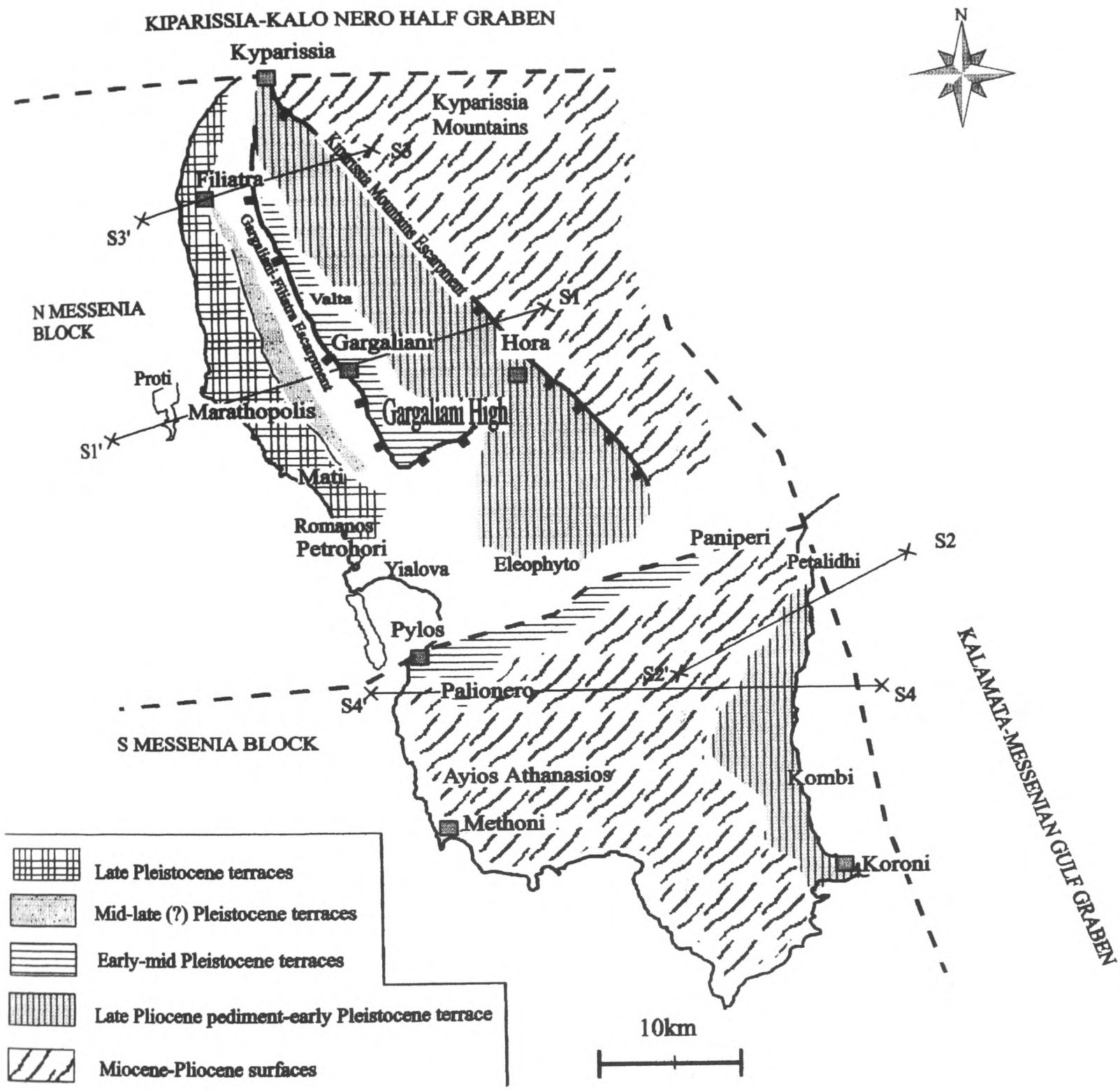

Figure 3. Outline map of the geomorphology of the Messenia Peninsula, also showing locations mentioned in the text. Five generations of relief are distinguished, from Miocene to late Pleistocene.

displacement and sense of movement (Zelilidis, 1988; Zelilidis and Doutsos, 1992; N. Kourampas, unpublished data). The main fault trends are as follows:

1) *NNW-SSE faults.* These long parallel faults, with the greatest observed cumulative throw (up to 120 m for the Gargaliani-Filiatra fault), are oriented parallel to the regional strike of pre-existing Neotethyan structures (thrusts, fold-axes), and are also parallel to a major graben within the Kalamata-Messenia Gulf to the east (Figs. 2, 3). The major NNW-SSE fault trends are inferred to re-activate zones of weakness within the Neotethyan basement, possibly including early Mesozoic rift-related structures. However, there is no evidence of reactivation of the major NNW-SSW Neotethyan Pindos thrust front as a Plio-Quaternary extensional lineament.

2) *ENE-WSW (to E-W) faults (e.g. Kyparissia and Pylos Faults).* These faults divide the Messenia Peninsula into two contrasting tectono-morphological blocks, bounded by the Kyparissia Fault to the north and the Pylos Fault to the south (see below). The large ENE-WSW faults (e.g. Pylos Fault) are seen as major transverse structures related to cross-strike segmentation of the Neogene Aegean arc (although these too might reactivate older Neotethyan structures). Within the N Messenia Block the dominant NNW-SSE fault trend is offset by E-W to ENE-WSW trending faults, up to 5-7 km long (e.g.

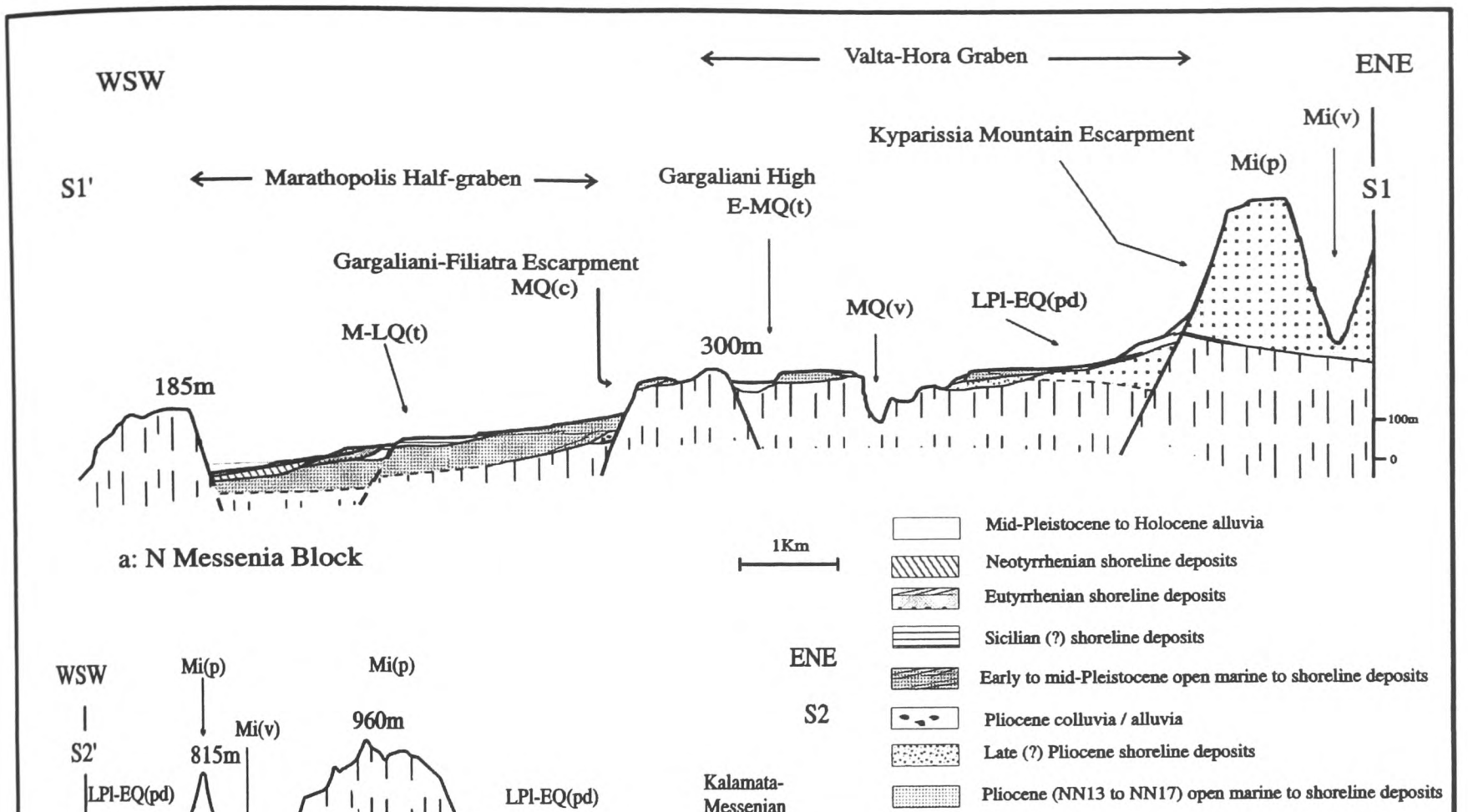

Figure 4. Representative cross sections of **a,** the N Messenia Block, and **b,** the S Messenia Block (see Figs. 2, 3 for locations of sections). **a,** Section in N Messenia from the Kyparissia mountain front westwards. Note the horst-graben topography; **b,** Section in S Messenia. Note the fault-controlled topography stepping down to the Kalamata-Messenian Gulf Graben. Both areas are dissected into horsts and grabens that generally step downwards towards the coast. Older sediments are generally preserved at higher altitudes.

between Filiatra and Gargaliani; Figs. 2, 3). In addition, there are many smaller (1-2 km) "transverse" faults that cut both Plio-Pleistocene sediments and bedrock, accommodating local extensional stress variations.

3) *NNE-SSW faults (average strike: 15°).* These are the commonest outcrop-scale faults in early to mid-Pleistocene sediments. Most of these faults are too small to show on a regional map of the area (Fig. 2). Faults on this trend also occur within longer NNW-SSE *en echelon* systems, often associated with earthquake activity (e.g. Kalamata Fault further E; Lyon-Caen *et al.*, 1988; Fig. 1). These NNE-SSW faults can be related to Quaternary-Recent extension of the SW Hellenic Arc (Armijio *et al.*, 1992; Lyon-Caen *et al.*, 1988; Hatzfeld *et al.*, 1990). The seismically active NNE-SSW faults apparently constitute the youngest fault-population in the area (Zelilidis and Doutsos, 1988).

Geomorphological-tectonic segments

The Messenia Peninsula can be subdivided, on the basis of relative altitude, structural, geomorphological and stratigraphic features, into two segments on a scale of 30-40 kms, termed the North Messsenia Block and the South Messenia Block (Figs. 2, 3). In addition, both blocks are segmented into grabens and half-grabens on a 5-7 km-scale (Fig. 4). The two blocks are separated by the important Pylos Fault, across which the sedimentary record differs markedly. Segmentation on this large scale (comparable to the depth of the seismogenic layer of the crust), is known elsewhere, including central Greece (Roberts and Jackson, 1991).

The N Messenia Block extends from the Kyparissia Mountains at 1200 m ASL in the east, to alluvial plain/lagoonal areas in the west, and then offshore (Figs. 1, 2, 3). The Kyparissia and Pylos Faults are its northern and southern boundaries. This

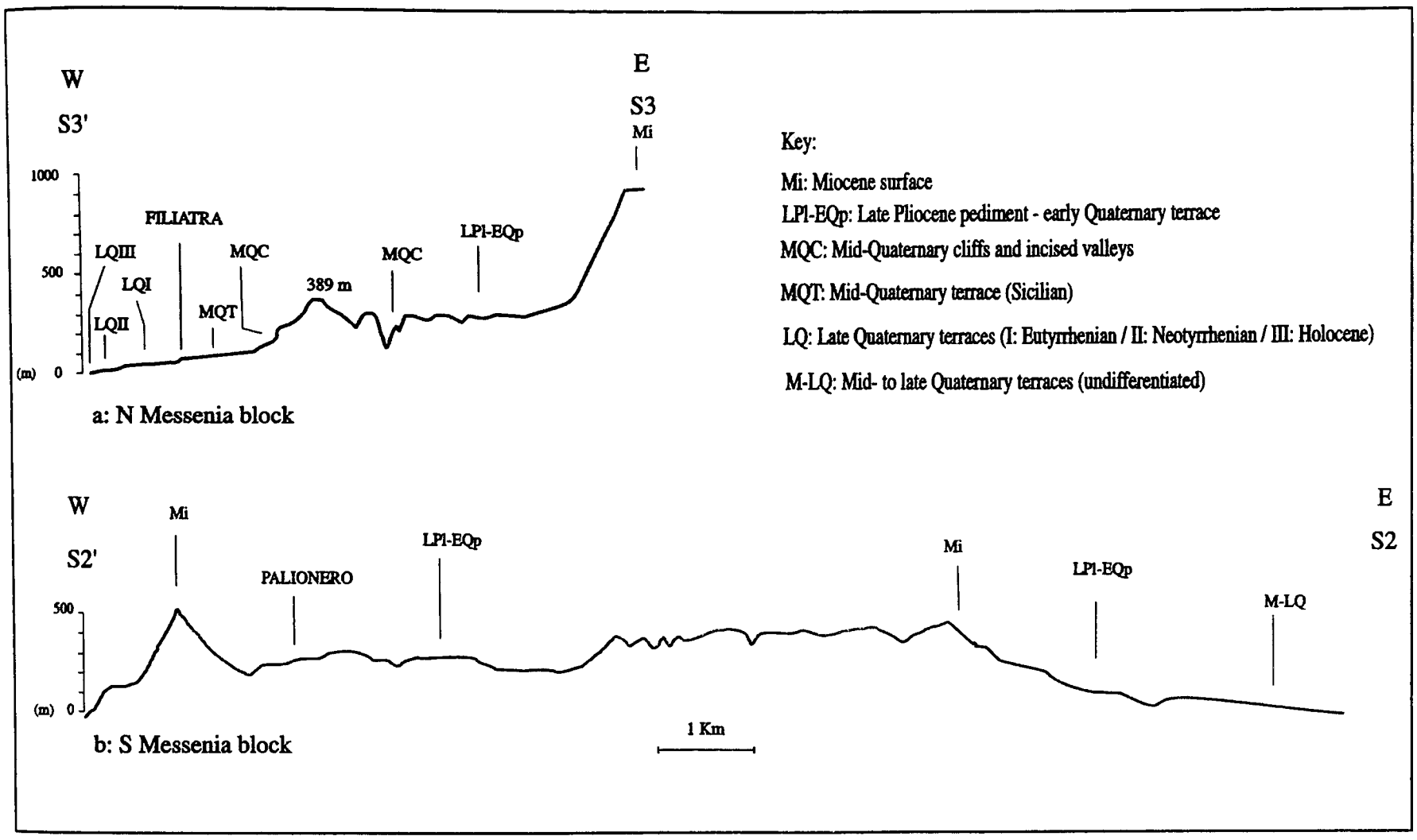

Figure 5. Topographic profiles of: **a,** the N Messenian Block and **b,** the S Messenian Block. Inland, the topography is mainly fault controlled, whereas near the coast marine terraces predominate. See Figure 3 for locations of profiles.

block has an extensive Late Oligocene-Miocene to Holocene sediment cover (Fytrolakis, 1971; I.G.M.E., 1980a). Sediments are preserved within small horsts and grabens (average width 6.5 km), stepping down towards the coast (Fig. 4a).

The S Messenia Block is less strongly uplifted than the N Messenia Block and is tilted to the SE, causing submergence in this direction (Kelletat *et al.*, 1976). The maximum height of preserved Quaternary sediments is ca. 200 m ASL, compared to ca. 340 m ASL in the N Messenia Block. Although erosional terraces are common, associated Quaternary sediments are relatively scarce in the southern block. The western part of the S Messenia Block is characterised by a southward continuation of the horst-graben topography further north. By contrast, the eastern part of the block is characterised by NNW-SSE to N-S, down-to-the east normal faulting, which preserves younger Pleistocene sediments at progressively lower altitudes (Fig. 4b). The S Messenia Block terminates in the east against major N-S submarine scarps with offsets of several hundred metres, marking the western margin of a large graben occupied by the Messenian Gulf (Mascle *et al.*, 1982; Figs. 1, 2, 3).

Age constraints

Up to five pre-Pleistocene erosion surfaces (without sediments) and seven Quaternary (Late Pliocene, Pleistocene and Holocene) terraces (with sediments) are identified within the N Messenia Block (Figs. 4, 5), representing the maximum number of terraces found in the S Peloponnese. Terraces and sediments associated with the S Messenia Block are less well developed and, thus, difficult to correlate (Fig. 4b, 5b). Nevertheless, the Pliocene stratigraphy is well preserved in the S Messenia Block.

During this study, Early Pleistocene sediments were dated biostratigraphically (identifications by D. Frydas, Patras University). Also Pliocene to Early Pleistocene sediments were correlated with adjacent dated sequences (Berckhemer and Kowalczyk, 1978; Frydas, 1990; Frydas and Bellas, 1994). Attempts at U-series dating of solitary corals were unsuccessful, as all the material collected was recrystallised to calcite. However, we are able to correlate two Late Pleistocene marine terraces with the classic "Eutyrrhenian" and "Neotyrrhenian" substages of the "Tyrrhenian" sea level cycle (Bonifay, 1975), as determined in the Peloponnese (Keraudren, 1970, 1971; Kelletat *et al.*, 1976; Kowalczyk *et al.*, 1992) and other areas of the Mediterranean (e.g. Sicily, Calabria, Cyprus). In addition, an uplifted shoreline of Holocene age is correlated with the "Versilian" stage of the classical Mediterranean chronostratigraphy (Keraudren, 1970, 1971; Bonifay, 1975). Correlations are based on relative altitude, geomorphology, lateral extent and detailed sedimentary facies.

In an attempt to further constrain the age of Pliocene to

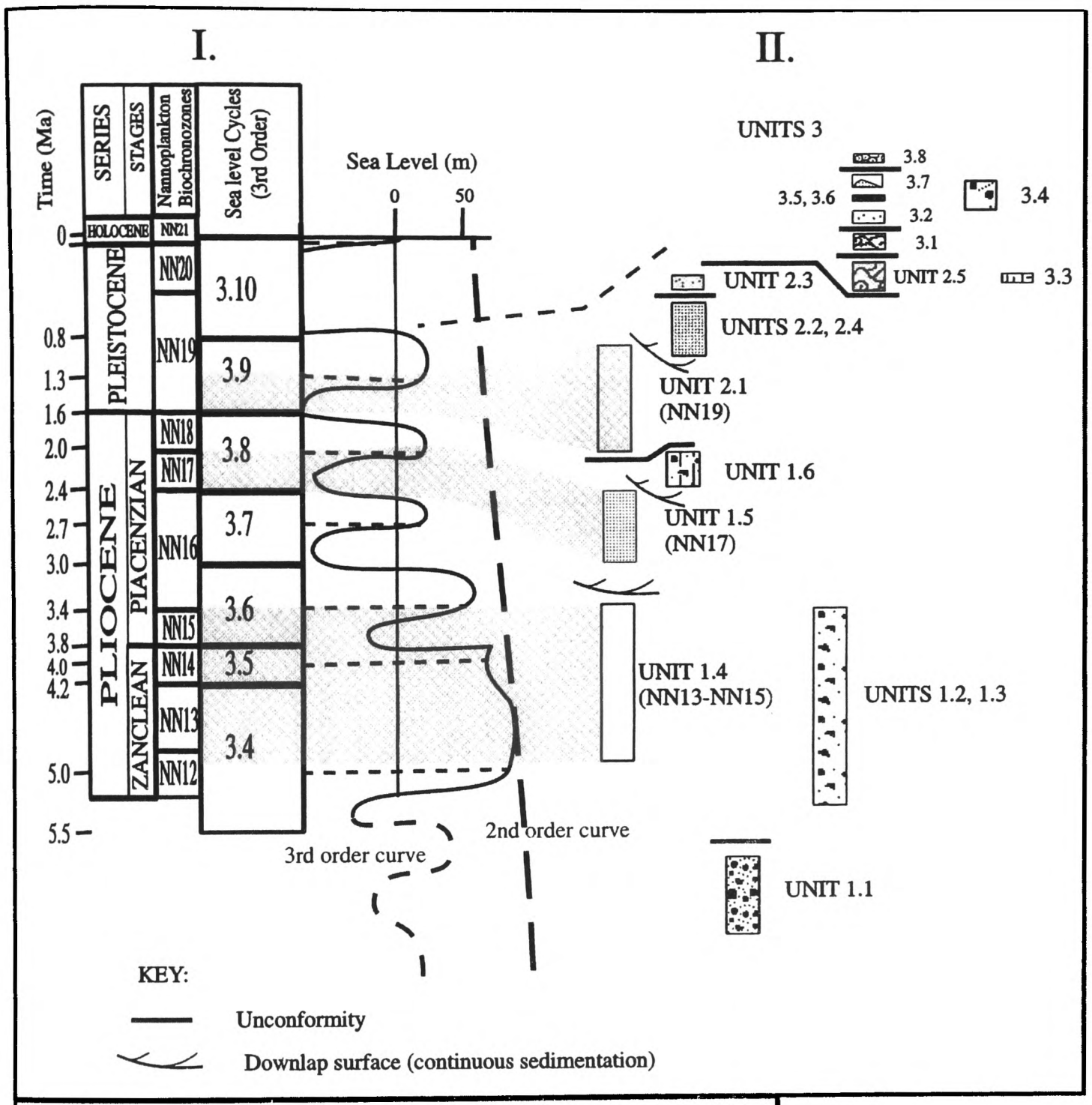

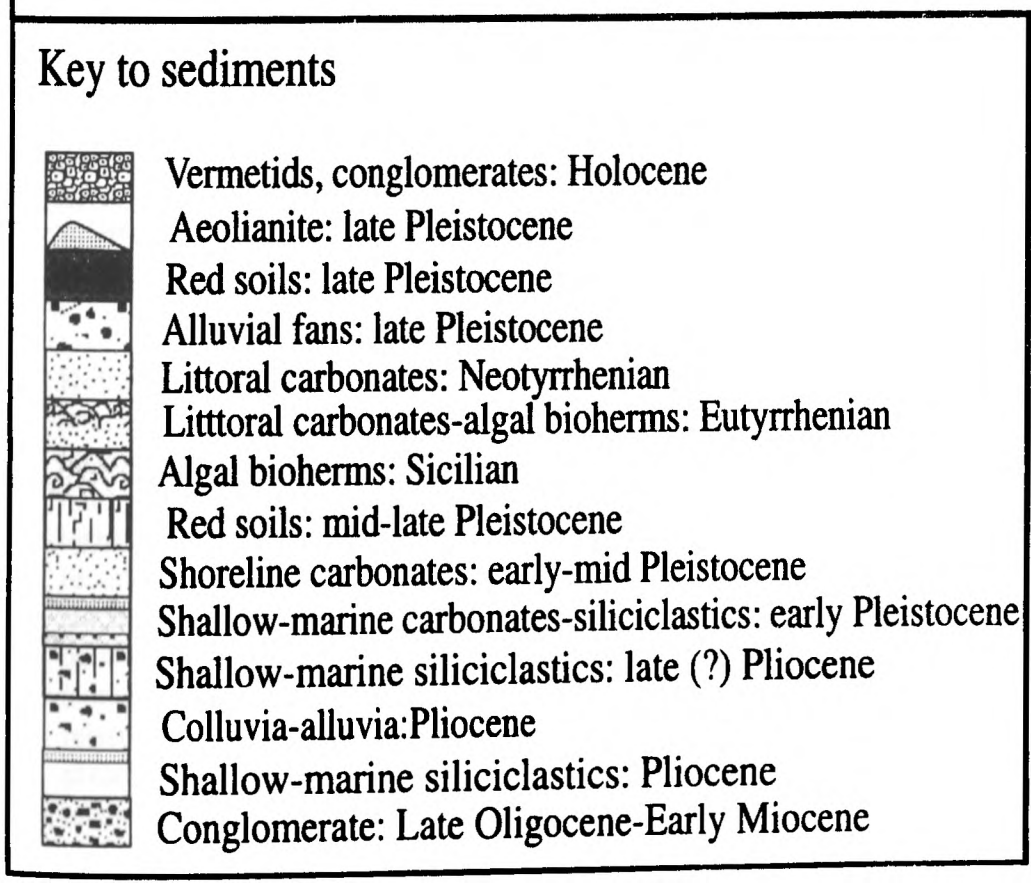

Figure 6A. Plio-Quaternary time scale (the last 5.5 Ma). I) Global eustatic sea level curves (a: third-order cycles; b: second-order cycle), mainly constructed from oxygen isotope stratigraphy and correlated with nannoplankton biochronozones (Haq *et al.*, 1988); ii) Simplified logs of sedimentary successions from Messenia. Maximum intact sequences are shown as log segments. Correlation with the eustatic sea level curve is based on nannofossil dating for the Pliocene-early Pleistocene (Frydas, 1990; pers. comm., 1998; Frydas and Bellas, 1994). Transgressive-regressive shallow-marine sequences of Pliocene to early Pleistocene age correlate with third-order eustatic highs of the global sea level curve.

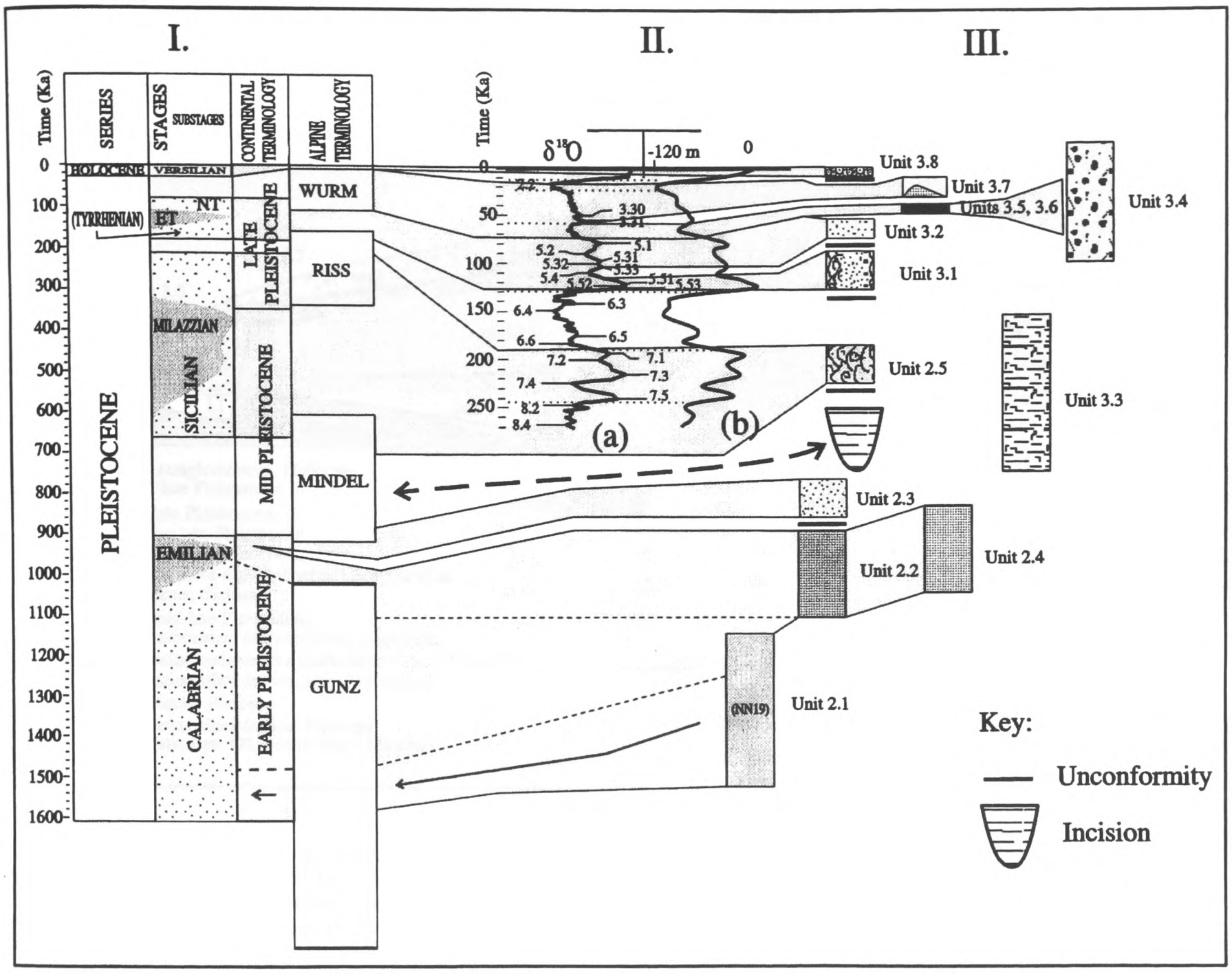

Figure 6B. Late mid-Pleistocene-Holocene time scale (270 ka). A Pleistocene stratigraphic scheme (modified from Bonifay, 1975) is shown on the left (I). The begining of the Pleistocene is set at 1600 ka. The easily identifiable "Versilian", "Eutyrrhenian"/"Neotyrrhenian" terraces in (III) (Units 3.8, 3.1 and 3.2, respectively) are correlated with the high-resolution oxygen-isotope curve (II a; Martinson et al., 1987) and the corresponding eustatic sea level curve (II b; Imbrie et al., 1984). In addition, the terraces between the dated early Pleistocene (Unit 2.1) and correlated "Eutyrrhenian"/"Neotyrrhenian" terraces (i.e. late "Calabrian"/"Sicilian": Units 2.1 to 2.5; see III) are assumed to relate to intervening eustatic highs (column I), although with major uncertainties owing to the presence of unresolved, multiple eustatic sea level highs. Key to sediments as in Figure 6A.

Holocene sediments and terraces we have adopted a sequence-stratigraphic approach (Fig. 6 a,b). Regionally extensive maximum flooding surfaces and unconformities observed in the field are interpreted to relate to global eustatic sea level highstands and lowstands, respectively. The marine sedimentary record can, thus, be tentatively linked to a relatively well constrained global sea level history, despite the paucity of palaeontological and geochronological data. Terrestrial deposits (some of which may be diachronous) can also be subdivided relative to underlying and overlying marine horizons, where present, but absolute ages are poorly constrained, especially inland, away from intercalated marine horizons.

Nine depositional sequences from the Messenia Peninsula can be correlated with sea level cycles of third-or higher-order on the basis of available field and biostratigraphic evidence. The dated Early Pliocene-early Pleistocene marine sequences (Frydas, 1990; pers. comm., 1998; Frydas and Bellas, 1994) can be directly correlated with third-order cycles of the global eustatic sea level curve of Haq *et al.* (1988), as shown in Fig. 6a. This allows identification of three third-order sequences, spanning Early Pliocene-early Pleistocene (sea level cycles 3.4-3.9 *sensu* Haq *et al.*, 1988). The part of the succession younger than early Pleistocene (ca. 1000-800 ka) is resolved into five terraces, belonging entirely to the third-order cycle 3.10 (Fig. 6a).

The five terraces younger than early Pleistocene are assigned

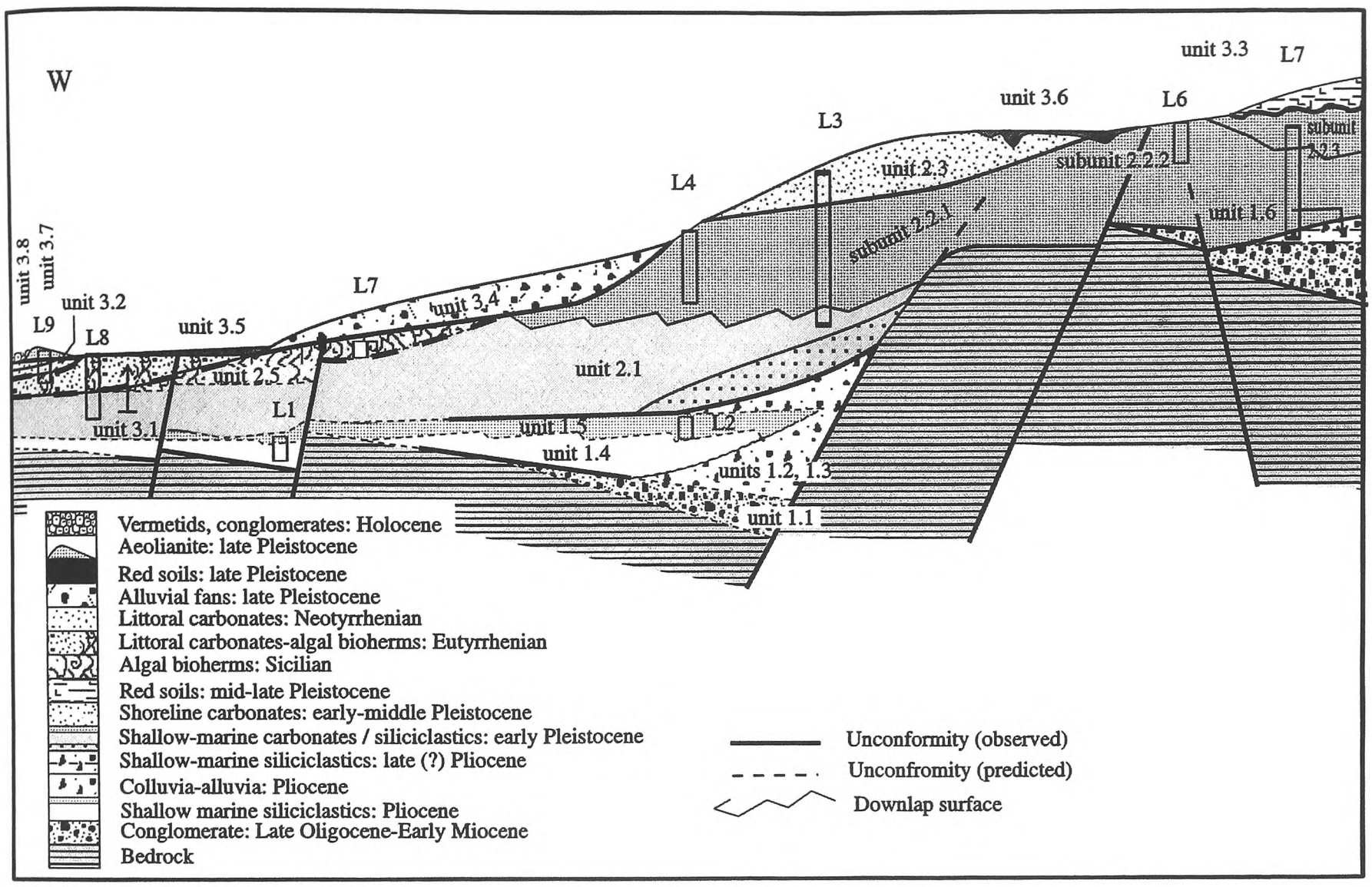

Figure 7. Tectonic-stratigraphic diagram showing the relative positions of the Plio-Pleistocene units discussed in this paper. The figure illustrates the relationships of each of the units described and is not intended as an accurate cross-section, as the logs are projected onto a simplified E-W traverse (approximate horizontal scale: ca. 7 km across). The figure is mainly applicable to the North Messenia Block where the stratigraphy is more complete than in the South Messenia Block. Individual logs are shown in detail in subsequent figures.

provisional ages, as follows (Fig. 6b): Both the late Pleistocene marine terraces identified as "Eutyrrhenian" and "Neotyrrhenian" can be correlated with the fourth-order isotopic stage 5 (Last Interglacial) in the global eustatic sea level curve, constructed from oceanic oxygen isotope evidence (Imbrie *et al.*, 1984, Martinson *et al.*, 1987). Following this correlation, each of these terraces corresponds to a higher-order substage within the fourth order isotopic stage 5 (*sensu* Martinson *et al.*, 1987). Given the lack of absolute dating of these two terraces in the Messenia Peninsula, correlation with particular substages is arbitrary. Nevertheless, we favour correlation of the "Eutyrrhenian" with the isotopic substage 5.5 and the "Neotyrrhenian" with the isotopic substages 5.3+5.1 for the following reasons: 1) The "Eutyrrhenian" is traditionally defined as the "transgressive maximum" of the "Tyrrhenian" (Last Interglacial) sea level cycle (Bonifay, 1975). According to isotopic evidence, this transgressive maximum took place at ca. 120 ka BP, during isotopic substage 5.5, when the eustatic sea level probably exceeded the present by a few metres (Imbrie *et al.*, 1984; Labeyrie *et al.*, 1987). 2) The "Neotyrrhenian" is traditionally defined as the later part of the "Tyrrhenian" (Last Interglacial) sea level cycle, when fourth-order sea level fall was punctuated by short-lived sea level highstands (Bonifay, 1975). Isotopic evidence suggests that the later part of isotopic stage 5 (Last Interglacial) was punctuated by higher-order sea level cyclicty. The isotopic substages 5.3 (ca. 100 ka) and 5.1 (ca. 80 ka) correspond to higher order highstands during a period of falling sea level (Labeyrie *et al.*, 1987; Martinson *et al.* 1987; Fig. 6b), conforming with the definition of the "Neotyrrhenian" substage (Bonifay, 1975). The presence of both substages 5.3 and 5.1 in the Messenia Peninsula cannot be proved without geochronological evidence. However, field evidence suggests that the "Neotyrrhenian" terrace comprises two stacked marine sequences separated by soil (see Fig. 7 and below). The "Versilian" terrace, above the two "Tyrrhenian" (Last Interglacial) terraces, can be correlated with a higher-order sea level highstand after the Last Glacial Maximum, but before the eustatic sea level reached its present-day level (Bonifay, 1975). Geochronological evidence from the western Mediterranean (Gulf of Lions, France; Labeyrie *et al.*, 1976) and the Red Sea (Plaziat *et al.*, 1996) suggests that a sea level highstand occurred at ca. 5-7 ka. Alternatively, this "Versilian" deposit could be correlated with coastal features of historic age (1700-1500 a) all along the Aegean Arc (from Antikythera to Crete), S Turkey,

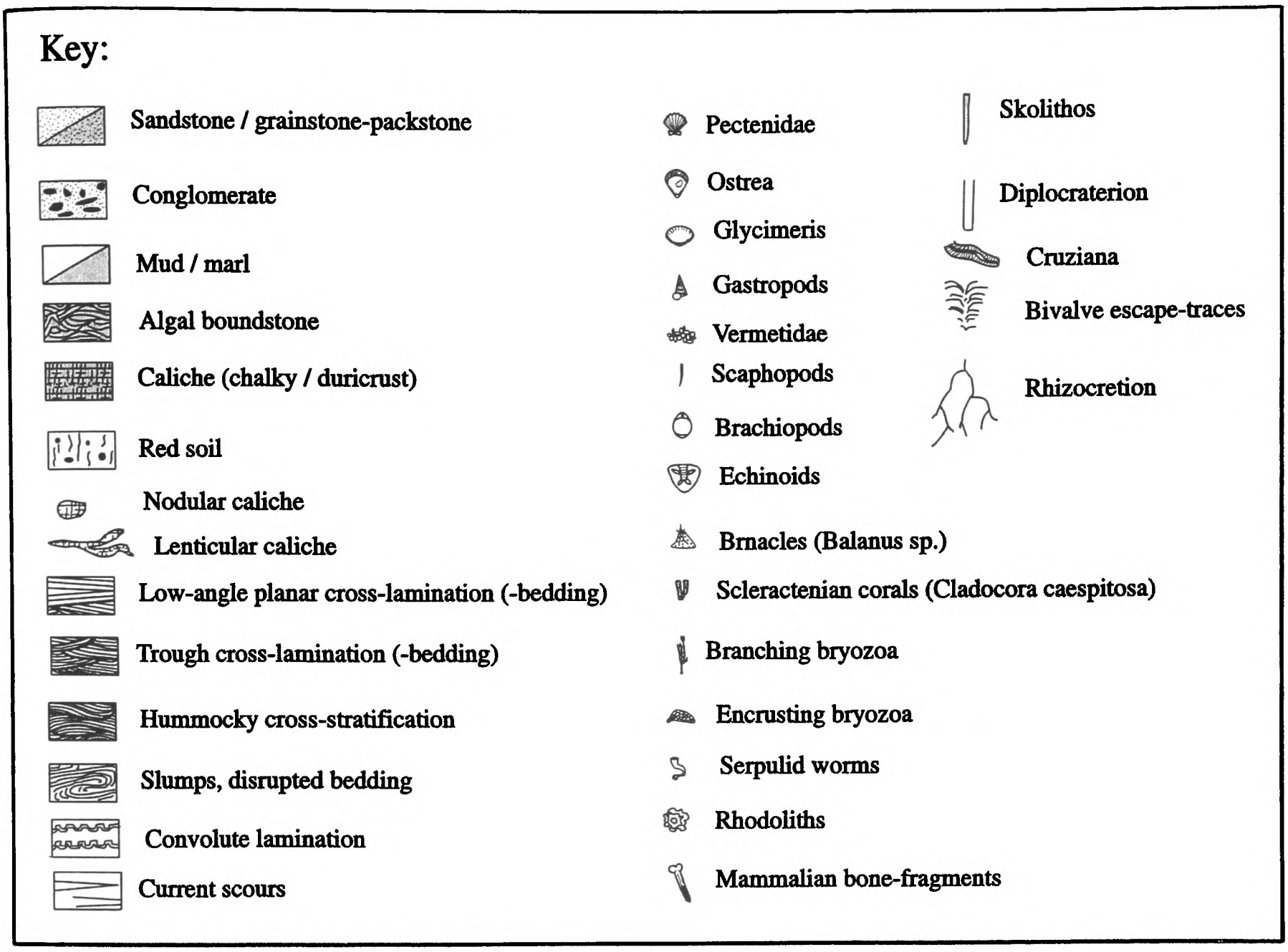

Figure 8. A. Key to measured logs in this paper.

Syria and Israel, that were uplifted as a result of a regional tectonic event ca. 1530-1550 years ago ("Early Byzantine tectonic paroxysm") (Pirazzoli, 1986, 1987; Kelletat, 1991).

The two remaining marine terraces (Units 2.3 to 2.5) are tentatively correlated with early to mid- and mid-Pleistocene eustatic highstands, respectively, although with marked uncertainty in view of multiple highstands within the latter. The first marine terrace topographically above the "Eutyrrhenian" (Unit 2.5) is attributed to the multiple "Sicilian" highstand, which, according to the classical chronostratigraphic scheme (Bonifay, 1975), spans the time from ca. 450-ca. 200 ka (Fig. 6b). This period includes several fourth-order eustatic cycles (up to three according to Imbrie *et al.*, 1984 and Imbrie, 1980); the latest of the above cycles corresponds to isotopic stage 7, with a transgressive maximum at ca. 210 ka (sensu Martinson *et al.*, 1987; Fig. 6b). Field evidence also suggests that in the Messenia Peninsula the "Sicilian" terrace comprises more than one amalgamated marine sequence (Fig. 7 and below), but ages remain uncertain. A further terrace (Unit 2.5), unconformably overlying the early Pleistocene (late "Calabrian") terrace, could correspond to any isotopic stage prior to stage 7, possibly including higher-order "intra-Calabrian" sea level cyclicity. The second alternative is favoured on the basis of field evidence suggesting that that terrace predates a major pre-Late Pleistocene phase of cliff cutting (Figs. 6b, 7). Assuming that the latter feature corresponds to the "Mindel" sea level lowstand (Bonifay, 1975), this terrace is probably late Early Pleistocene (latest "Calabrian") in age. Finally, Unit 2.4 from southern Messenia is younger than the lower "Calabrian" Unit 2.1, dated biostratigraphically. This unit could thus be correlated with either of the upper "Calabrian" Units 2.2 or 2.3 in N Messenia. The first alternative is favoured on the basis of similar facies, sedimentary architecture and stratigraphic position.

Using a sequence-stratigraphic approach, constrained by available micropalaeontological data, we are thus able to correlate the Pliocene to Holocene sequences in Messenia with stages in the classical Mediterranean Pleistocene stratigraphy (Bonifay, 1975). In the North Messenia block, where the

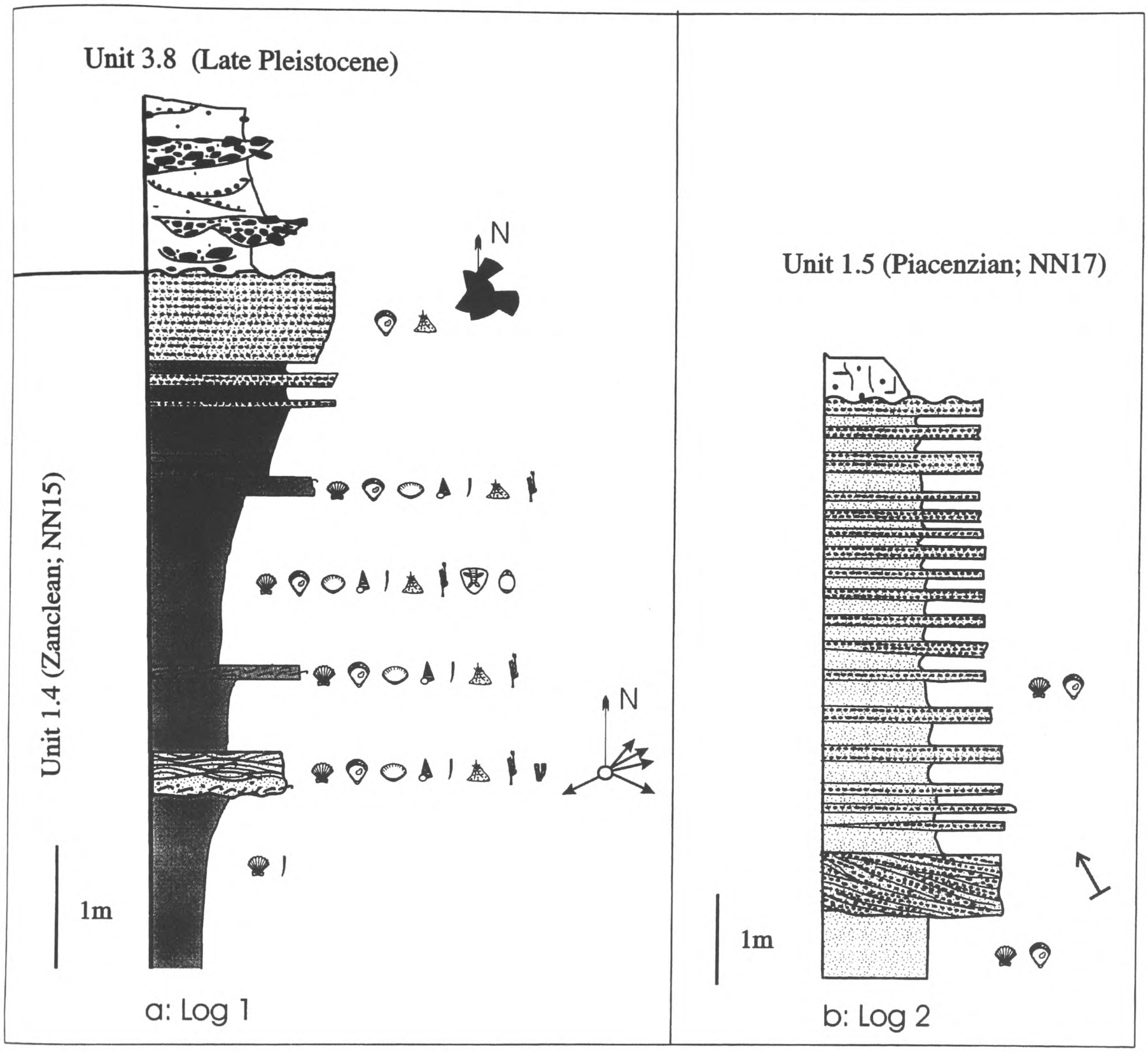

Figure 8 B. Representative sedimentary logs of Pliocene and younger sequences (logs 1 & 2): **a,** Early Pliocene shallow-marine sediments (Zanclean; Unit 1.4), unconformably overlain by late Pleistocene alluvia (Unit 3.4); note palaeocurrent data; Kombi; grid reference: KORONI -0375 0825. **b,** Early to Late Pliocene (Zanclean-Piacenzian; Unit 1.5) from Rhizomilos; MELIGALAS -0410 -2870 (see Figures 2, 3 for locations).

Pleistocene stratigraphic record is more complete, six successive fourth-(or higher) order depositional sequences correlate with marine terraces, located at progressively lower elevations. Our correlation suggests a minimum uplift rate of ca. 0.1 m/ka since the "Eutyrrhenian" (last ca. 120 ka), assuming constant uplift rate. The minimum uplift rate since the end of the "Calabrian" (last ca. 900 ka) was between 0.23-0.33 m/ka, depending on the correlation of the "Sicilian" terrace with mid-Pleistocene isotopic stages. These rates are similar to the radiometrically constrained minimum uplift rate in the Corinth area, N Peloponnese (ca. 0.3m/ka; Collier, 1990).

Stratigraphy of Messenia

We now go on to describe and interpret the Pliocene-Pleistocene sedimentary successions of Messenia, based on individual outcrop relations. A striking feature of the Messenia Peninsula is the presence of the well-developed flight of marine terraces

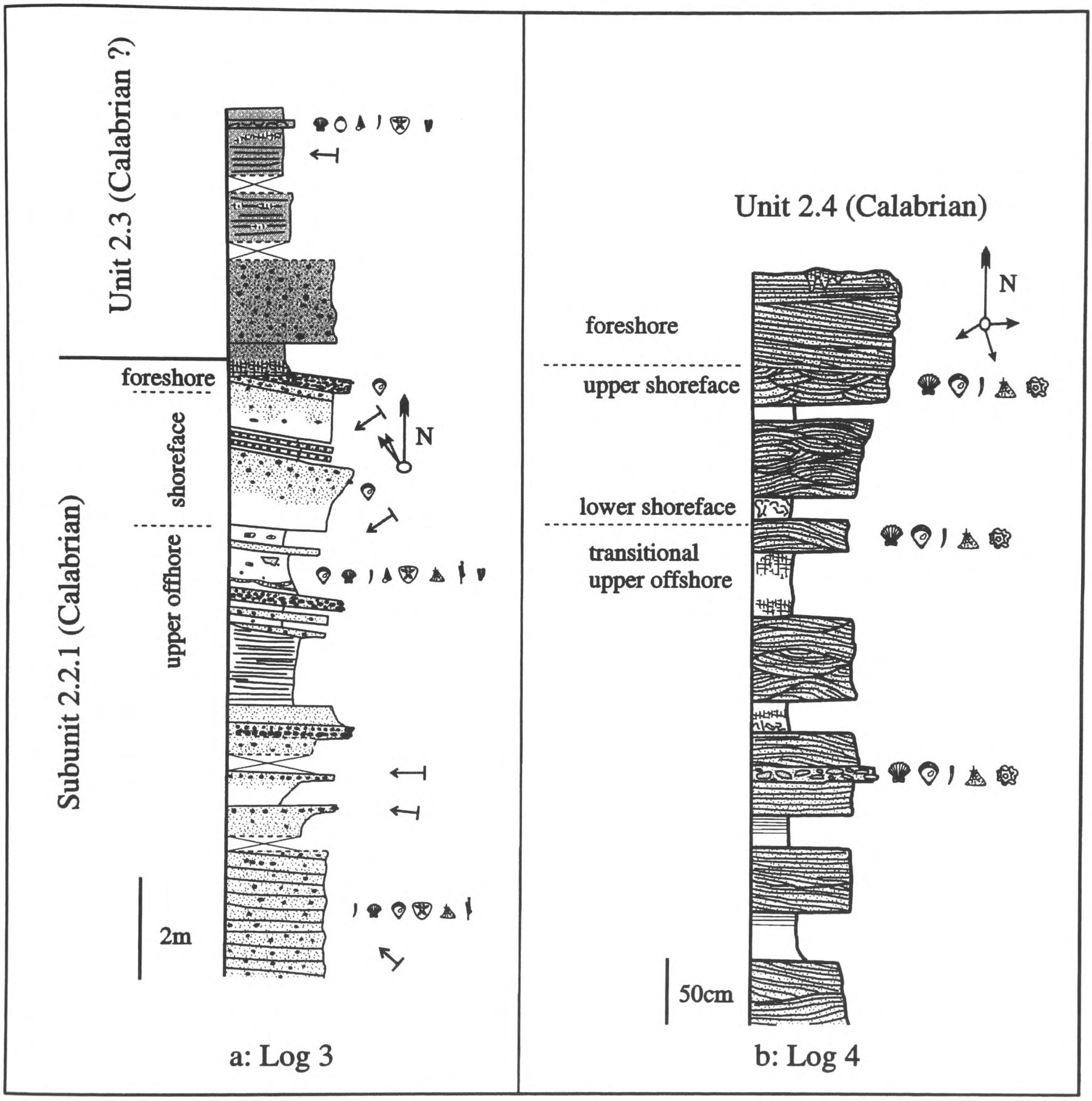

Figure 9. Representative sedimentary logs of early (to middle ?) Pleistocene sequences (logs 3 & 4): **a,** Subunit 2.2.1 (Calabrian) overlain unconformably by Unit 2.3 (upper Calabrian ?), Gargaliani; FILIATRA 1460 -2265. This section may indicate intra-Calabrian sea level cyclicity. Alternatively, the Unit 2.3 may correspond to some (early) mid-Pleistocene sea level highstand; **b,** Unit 2.4, Ayios Athanassios; PYLOS -2485 0980 (see Figures 2, 3 for locations). Palaeocurrent evidence is included from Unit 2.4.

along the western coastal area (Kelletat *et al.*, 1976; Zelilidis, 1988) (Fig. 5a). Kelletat *et al.* (1976) recognised up to eleven Pleistocene terraces, whereas during this study we mapped up to six Pleistocene-Holocene terraces, all with preserved shallow-marine sediments, at least locally. In addition, correlative coastal (e.g. lagoonal) and non-marine (terrestrial) sediments are locally present. Within individual areas, local short successions (generally tens of metres or less) can be recognised, based on sedimentary facies and the identification of unconformities/ disconformities (Fig. 7). These local successions contain a sufficient number of distinctive features to allow lateral correlation of Plio-Quaternary marine sediments throughout the Messenia Peninsula. Such correlations must take account of proximal-distal facies variation within single depositional packages.

A relative stratigraphy was erected for the entire area, including twenty informal units, correlated with third- and fourth-order sea level cycles, as discussed above (Figs. 2, 7). In addition, we recognise various sub-units representing fourth-, or higher-order cycles, that could not be resolved, or lateral facies variations within a given chronostratigraphic unit. Each of the units is shown on a schematic tectono-stratigraphic diagram (Fig. 7), most applicable to the North Messenia Block. Representative measured sedimentary logs for the marine units are shown on Figures 8.b, 9, 10, 12. The key to all of the logs is in Fig. 8.a.

Pre-Pleistocene sedimentary sequences

Unit 1.1 (Late Oligocene-Early Miocene ?): conglomerate

Successions are dominated by well cemented, clast-supported, polymict conglomerates that exhibit east-dipping tabular cross-bedding. These conglomerates contain well-rounded, mostly rod-shaped, imbricate clasts of basement lithologies (limestone, turbiditic sandstone, radiolarian chert and pelagic limestone), in a matrix of medium- to coarse-grained sandstone. This unit, >200m thick, crops out widely west of the Kyparissia Mountain Escarpment. A typical section is exposed a few kilometres E of Hora, towards Kalamata (Figs. 2, 3). This exposure was mapped by Fytrolakis (1971) as the uppermost, most proximal facies of the Tripolis zone "flysch", of Late Oligocene? age. Alternatively, I.G.M.E. (1980 a,b) mapped this sedimentary unit ("Messenian Conglomerate") as Late Oligocene to Early Miocene, affected by "Late-orogenic folding". This unit was also correlated with the "Late Miocene (or older)" *"Rahes Formation"* of the "Kyparissia-Kalo Nero Basin" by Fountoulis and Moraiti (1994). Reconnaissance during this study suggests that this conglomeratic unit represents fluvial clastic sediments deposited within a flexural foreland during, or soon after, the latest stage of thrusting (Late Oligocene?-Early Miocene) of the Pindos zone over the Tripolis zone foreland. This unit was subaerially exposed, eroded and peneplanated, probably during the Late Miocene.

Unit 1.2 (Pliocene?): fluvial conglomerate

This unit, with a maximum exposed thickness of only 1-2 m, consists of local outcrops of well indurated, clast-supported, polymict conglomerates, set in a red siltstone matrix. Individual clasts (3-7 cm) are commonly rod-shaped. The best exposure is seen within a N-S trending palaeovalley on the road from Pylos to Methoni (near the village of Palioneron; S Messenia; Fig. 3). This unit is unconformably overlain by shallow-marine sediments of inferred early to mid-Pleistocene age (Unit 2.4; see later; Fig. 7).

Interpretation: The conglomerate is interpreted as the infill of a pre-Pleistocene fluvial channel with N-S drainage.

Unit 1.3 (Late Pliocene?): breccia

This unit is composed of well cemented, red, monomict limestone breccias that crop out locally at ca. 210 m ASL, parallel to a prominent NW-SE-trending escarpment, near Gargaliani (Fig. 3). The breccia includes marine fossils (bivalves, corals) and reworked clasts of grainstone/packstone and is unconformably overlain by early to mid-Pleistocene shallow-marine sediments (Unit 2.2; see below; Fig. 7).

Interpretation: The red breccias are interpreted as colluvium, partly resulting from weathering and erosion of earlier marine terrace(s) developed along the margins of an elevated area ("Gargaliani High"), west of the Gargaliani-Filiatra escarpment. Where locally exposed, these sediments are strongly jointed, but not faulted. Exposure is insufficient to determine whether, or not, the Gargaliani-Filiatra fault escarpment was active during, as well as after accumulation of this unit. The age of the breccias could correspond to one of the sea level lowstands prior to the early Pleistocene deposition of Unit 2.1.

Unit 1.4 (Early Pliocene; Zanclean): shallow marine sandstone-mud

The upper part of this unit is well exposed in SE Messenia, in coastal cliffs north of Koroni (Fig. 8.2, log 1). This unit comprises very bioturbated medium- to thick-bedded, muddy sandstones (0.50-1.50 m thick), alternating with beds (10-20 cm thick) composed of imbricate shells and shell fragments, set in a muddy matrix (Fig. 11 b). A high-density fauna includes mud-dwelling bivalves, commonly still articulated and in life position, together with some gastropods. The shell-rich beds are sharp-based, locally with an undulating microrelief (1-3 cm). The lower parts of individual beds consist of imbricated shells set in a muddy matrix, coarsening upwards into fine, micaceous, laminated silty sandstone, with local symmetrical ripples and scattered shells. The microfauna of this unit were described by Frydas (1990).

Interpretation: This facies is interpreted as a storm-influenced upper offshore environment, with shell beds prograding over muds, deposited below the fair weather wave-base. Previously, some sections of Unit 1.4 were dated as Early Pliocene (Koutsouveli, 1987) and correlated with the NN13, NN14 and NN15 biochronozones (sensu Martini 1971), spanning the entire Early Pliocene (Zanclean) (Frydas, 1990). This unit correlates with sea level cycles 3.4, 3.5 and 3.6 *sensu* Haq *et al.* (1986) (ca. 5.0-3.4 Ma) (Fig. 6a). No sequence boundaries that could allow further subdivision were observed in the field. No equivalent unit is found in N Messenia; however, lower Zanclean (NN13 sensu Martini, 1971) deposits are known in the

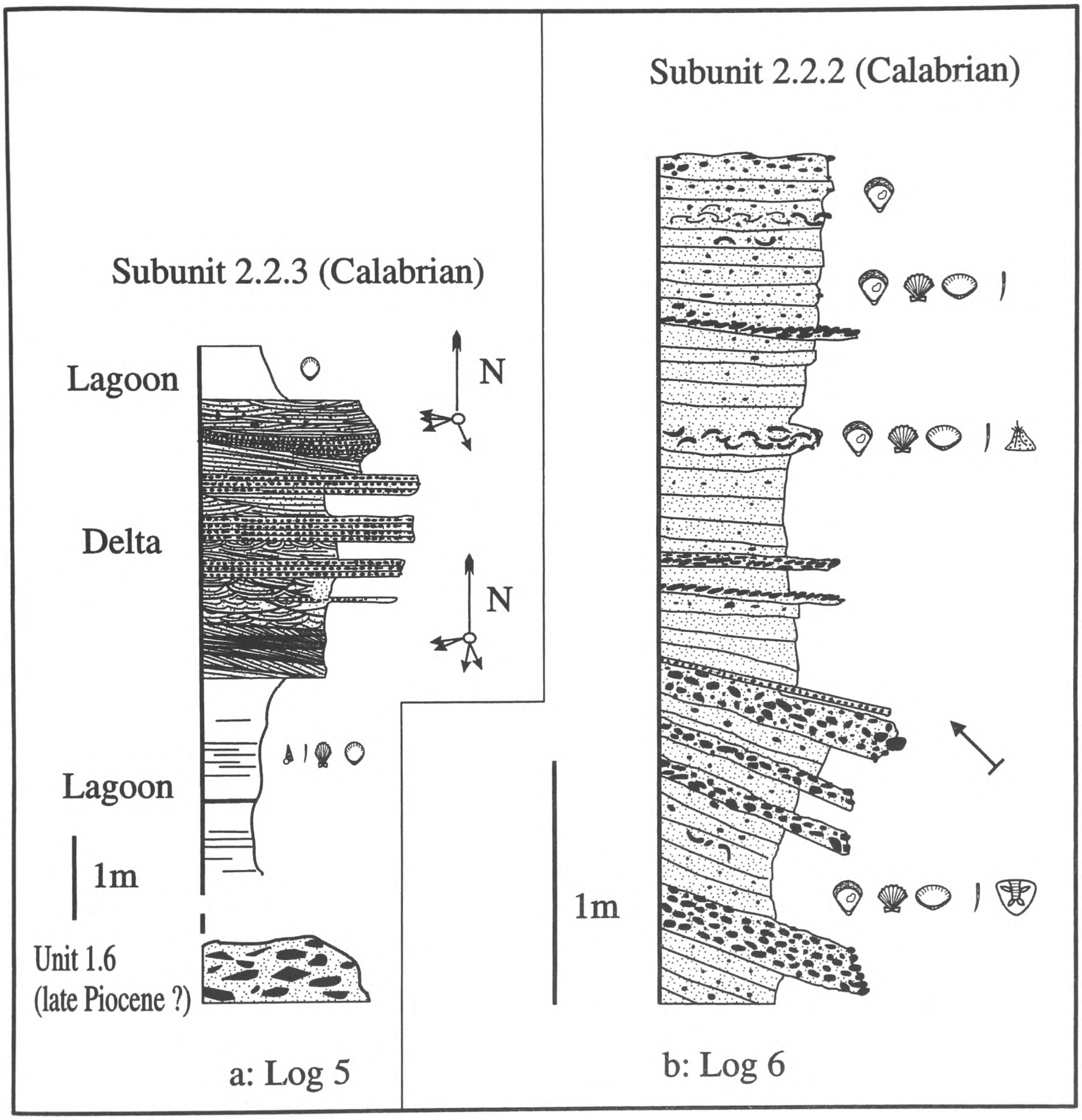

Figure 10. Representative sedimentary logs of Late (?) Pliocene-early Pleistocene sequences (logs 5 & 6): **a,** Shallow-marine Unit 1.6 (possibly Late Pliocene) overlain unconformably by marginal marine Subunit 2.2.3 (Early Pleistocene); road from Gargaliani to Valta; FILIATRA 1600 -2020. **b,** Subunit 2.2.2 (Early Pleistocene) from Gargaliani; FILIATRA 1450 -2045 (see Figures 2, 3 for locations).

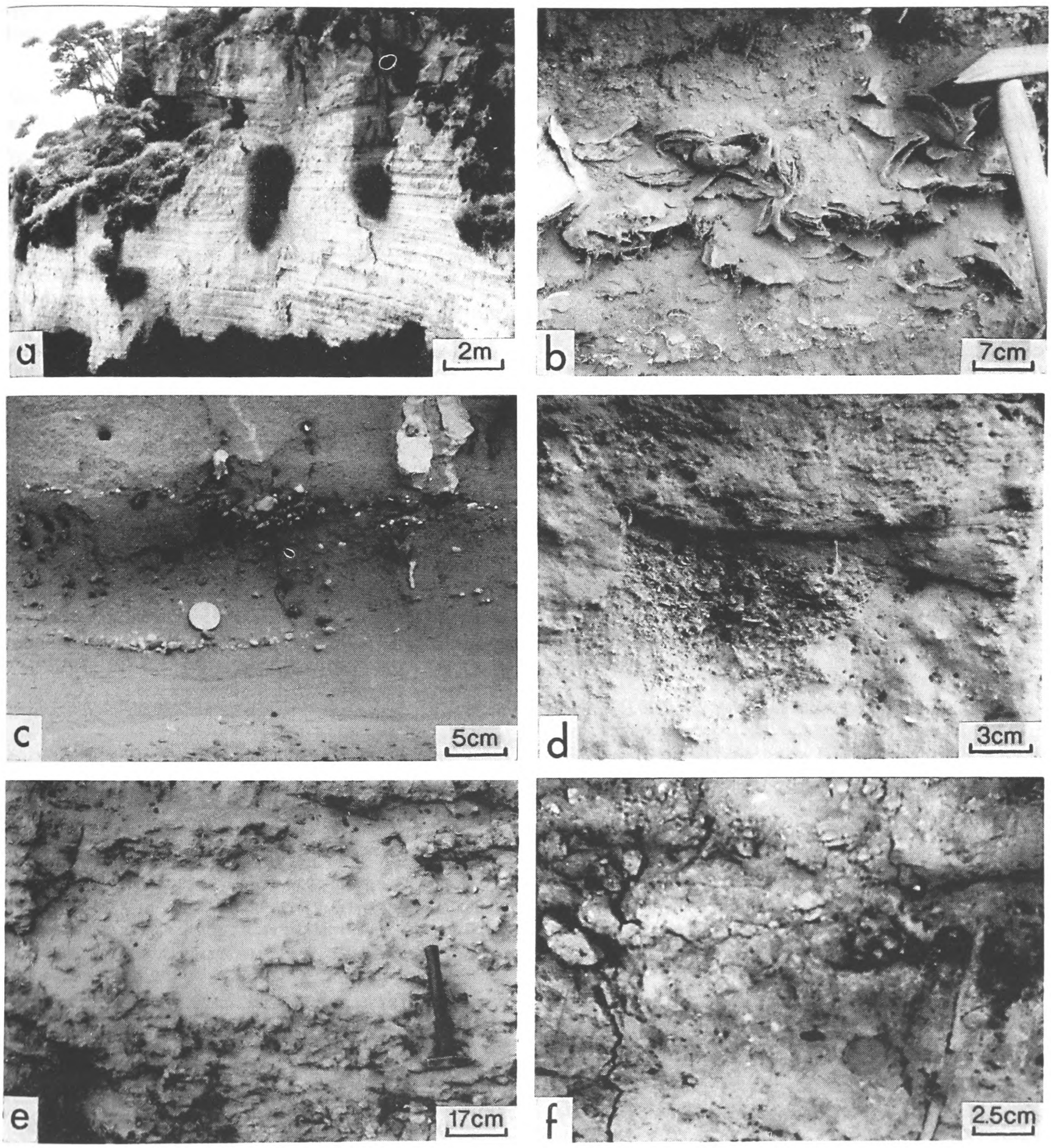

Figure 11. Field photographs of Late Pliocene-early Pleistocene sequences in Messenia. **a,** Early Pliocene (Zanclean) marls (tempestites?) (Unit 1.4), unconformably overlain by Pleistocene grainstone (shoreline sediments). Note ravinement surface between the two units (above the bushes); Koroni Castle, S Messenia; **b,** Early Pliocene, inferred storm deposit made up of a bivalve/gastropod lag. Note shell imbrication; Unit 1.4, Kombi coast, S Messenia; **c,** Early Pleistocene silty sand with small pebble-filled scours, associated with hummocky cross-stratification (tens of cm scale); pebbles show normal and reverse grading; Subunit 2.2.1, near Gargaliani, NW Messenia; **d,** Deeper scour in early Pleistocene calcareous mud, infilled with skeletal lag (scaphopod, coral and bivalve fragments), near Gargaliani, Subunit 2.2.1); **e,** Bioturbated (*Thalassinoides*), slightly nodular carbonate mud from near base of Pleistocene (NN19); Unit 2.1, Pylos Port; **f,** *Skolithos* burrow (right) and bivalve mould (left) within upper shoreface/foreshore calcareous sandstone/granular conglomerate; Topsets of regressive Unit 2.4, Palionero, S Messenia.

Kyparissia-Kalo Nero half-graben, north of the studied area (Fountoulis and Moraiti, 1994).

Unit 1.5 (Early-Late Pliocene; Zanclean-Piacenzian): shallow-marine conglomerate-sand

This unit comprises trough cross-stratified, matrix- to clast-supported polymict conglomerate and sand, well exposed near Rhizomilos village (Zelilidis, 1988; Figs. 2, 3, Fig. 8.2 , log 2). The exposed base of the sequence consists of tangential bedsets (50 cm thick) composed of well-sorted, fine sand and conglomerate, dipping N/NE at 18-22°. Clasts are well-rounded and can be correlated with lithologies of the Pindos zone (e.g. chert, pelagic limestone, turbiditic sandstone). The sequence passes upwards into polymict conglomerates with low-angle, N/NE dipping, tabular beds, alternating with well-sorted, tabular-planar beds of well-sorted yellow sand, up to 20 cm thick, with a shallow-water fauna of bivalves and benthic foraminifera (Table 1). An erosion surface above Unit ca 1.5 is located at 60 m ASL.

Interpretation: Trough cross-bedded conglomerates near the base correspond to distributory channel-fill, whilst alternating conglomerates and sands above represent prograding delta-front deposits. Frydas and Bellas (1994) correlated sediments from the same locality (10-20 m N) with the NN17 biochronozone (*sensu* Martini, 1971) of the Late Pliocene, Piacenzian stage (ca. 3.4-3.0 Ma). In sequence stratigraphic terms, Unit 1.5 can be attributed to the highstand systems tract of sea level cycle 3.6 *sensu* Haq *et al.* (1986; Fig. 6a). In the Kyparissia-Kalo Nero Basin, NW of the area of study, sediments equivalent to the Early Pliocene Unit 1.4 (see above) are capped by fluvial conglomerate, of inferred Late Pliocene age (Fountoulis and Moraiti, 1994). The deltaic conglomerates of Unit 1.5 could represent more distal counterparts of these fluvial conglomerates further north.

Unit 1.6 (Late (?) Pliocene): sandstone-conglomerate

This is a well cemented, extensively karstified unit, only 2-3 m thick, that crops out on the road near the exit from Gargaliani towards Valta (Figs. 2, 3). It consists of well-sorted lithic greywacke, containing numerous grains of radiolarian chert of Pindos zone origin (Figs, 2, 10 a, log 5). There are also interbeds of clast- or matrix-supported conglomerate, with well-rounded clasts, correlated with Tripolis limestone. A shallow-marine (infra-littoral) fauna of bivalves and foraminifera (Table 1) are present. This deposit is unconformably overlain by Unit 2.2 (Figs. 8, 10 a).

Interpretation: This is interpreted as a clastic shoreline deposit, adjacent to a deltaic system. The interpretation is based on the circum-littoral benthic foraminiferal fauna, the presence of terrigenous sediment and proximity to the Kyparissia Mountain front. There is no direct age evidence. However, the relatively high altitude (ca. 300 m ASL) and well cemented diagenetic state are suggestive of a Pliocene age. Similar, well-cemented conglomerates separate Early Pliocene and early Pleistocene shallow-marine sediments in the Kyparissia-Kalo Nero half-graben further north (Fountoulis and Moraiti, 1994). Unit 1.6 probably represents a more distant, submarine equivalent of this latter, probably Late Pliocene unit.

Early to mid-Pleistocene sediments

Unit 2.1 (Early Pleistocene; "Lower Calabrian"): bioturbated mud

This unit comprises parallel-bedded carbonate muds, rich in planktic and benthic foraminifera and exhibiting extensive *Thalassinoides* bioturbation (Fig. 11 e). Typical outcrops are seen in cliffs (<10 m high) above Pylos port in W Messenia (Figs 2, 3). Rich microfauna of benthic and planktic foraminifera are present (Table 1). Facies equivalents in NW Messenia (near Filiatrino Rema) are represented by marl with shallow-marine foraminifera, including *Hyalinea balthica* and *Globorotalia truncatulinoides,* together with mollusks and bryozoa (Marcopoulou-Diakantoni *et al.*, 1991).

Interpretation: The benthic foraminiferal fauna present in the succession (including *Uvigerina peregrina*), suggest deposition within the offshore, below 90 m (Blanc-Vernet, 1969; Murray, 1973; Amorosi *et al.*, 1998), thus making this unit the deepest early Pleistocene facies known in the Messenia Peninsula. Nannoplankton identification by D. Frydas (pers. comm., 1998) suggests that these sediments belong to the NN19 biochronozone, *sensu* Martini (1971), of early Pleistocene, "Calabrian" age (ca. 1600-900 ka). This unit can, thus, be correlated with the transgressive part of eustatic cycle 3.9 *sensu* Haq et al. (1988; Fig. 6a), corresponding to the "Emilian" substage in the classical chronostratigraphy (Bonifay, 1975). Nannoplankton within similar facies in the Kyparissia-Kalo Nero half-graben further north (*"Miros Formation"*) were also assigned to the NN19 biochronozone (Fountoulis and Moraiti, 1994). Unit 2.1 was deposited in a narrow asymmetrical offshore graben, defined by NNW-SSE normal faulting (Fig. 2). No indications of syn-depositional faulting were found; however, the unit is cut by antithetic faults, suggesting a long-history of fault movement.

Unit 2.2 Early to mid-Pleistocene ("Upper Calabrian")

This unit comprises a very extensive, overall transgressive-regressive sequence in NW Messenia (e.g. near Gargaliani; Figs. 2, 3). The transgressive base of the sequence is exposed only locally, as clast-supported polymict conglomerate forming steep clinoforms. These are deposited directly on bedrock and cemented colluvia/breccia (Unit 1.3) along the Gargaliani-Filiatra escarpment (Figs. 3, 7). The regressive part of the sequence is widely exposed near the western margin of the Gargaliani-Filiatra High further E (Figs. 2, 3, 4 a, 7). Details of the individual subunits are as follows:

Subunit 2.2.1: lithic packstone to pebbly-silty calcareous sandstone (Figs. 2, 9 a, log 3).

This sequence consists of foresets of lithic packstone to pebbly-silty calcareous sandstone, alternating with bioturbated mud. A typical outcrop (180-240 m ASL) occurs ca. 300 m S of Gargaliani, where a fining-upwards, then coarsening-upwards trend is observed. The lower beds are rich in carbonate skeletal grains, whilst the terrigenous content increases upwards. The uppermost beds comprise well-sorted, matrix-free, coarse-grained sandstone to granular conglomerate, with very well-

rounded pebbles, alternating with laminated calcareous sandstone. Foresets (10-40 cm thick) dip WNW at 7-18° (Fig 9 a, log 3). Individual beds are commonly sharp-based, normally graded (low in the sequence), or coarsen upwards to pebbly sandstone/matrix-supported conglomerate. Disc- and rod-shaped clasts are relatively common in the upper parts of the sequence. Pebbles, including rounded, bored limestone, are correlated with the Tripolis zone basement, whereas angular granule-sized grains of red chert were derived from the Pindos zone. A small proportion of the calcareous sandstone clasts were reworked from older terraces located around the periphery of the Gargaliani High (e.g. Unit 1.6). A shallow-marine fauna of mollusks, bryozoa, barnacles and echinoids are present, locally forming shell beds. Bioclast density decreases upwards and the uppermost, terrigenous-rich beds contain only a few thick-shelled macrofossils (e.g. *Ostrea* sp.).

Associated muddy units (up to 2.20 m thick) contain a diverse fauna of non-abraded bivalves, together with moderately abraded and fragmented barnacles, gastropods, corals, echinoids and bryozoa. The sediment is commonly well mixed as a result of bioturbation. Sharp-based, coarse, shelly sandstone beds, with a dense and diverse fauna of thin-shelled bivalves and scaphopods (<1-2 cm in size) occur in the upper parts of the muddy intervals. Most of the bivalve shells are convex side upwards; some are imbricated. Triangular scours (ca. 7 cm wide x ca. 5 cm deep) are infilled with well-sorted, very coarse, bioclastic sand (largely scaphopod fragments) (Fig. 11 d). A diverse microfauna is present in the muddy intervals (Table 1).

Interpretation: This overall shallowing-up sequence is interpreted as prograding deltaic/inner shelf deposits. The benthic microfauna are of mixed shallow-marine bathyal origin (Blanc-Vernet, 1969; Murray, 1973; Amorosi et al., 1998), probably indicating deposition in the upper bathyal zone, but is not age diagnostic. Delta-influenced clinoforms prograded into a shallow sea west of the Gargaliani-Filiatra escarpment. Clinoform progradation was interrupted by periods of lower-energy, finer-grained muddy deposition. Accumulation of sand-size sediment was influenced by longshore drift, as indicated by NNW-SSE palaeocurrents parallel to the inferred palaeo-shoreline (Fig. 9 a). Muddy sediments accumulated below the fair-weather wave base, but above storm-wave base, as indicated by palaeo-water depth, storm-wave scouring (Fig. 11 c) and pervasive bioturbation. Terrigenous-rich foresets high in the sequence are interpreted as lower shoreface deposits, probably in a deltaic/clastic shoreline setting. The pebble content probably reflects storm-wave reworking of beach deposits: rod-and blade-shaped pebbles are common in the lower beach zone (Reading and Collision, 1996). The uppermost, laminated, matrix-free sandstone/conglomerate is interpreted as an upper shoreface-foreshore deposit.

Subunit 2.2.2: matrix-supported conglomerate (Figs. 7, 10 b, log 6)

This subunit comprises steep, matrix-supported conglomerate foresets dipping at 30° to the W/WNW, passing upwards into lower-angle (ca. 8-10°), poorly sorted pebbly sand, well exposed in quarries ca. 1 km N of Gargaliani (ca. 270-290 m ASL). The contact between steep foresets and gentle topsets is transitional, with a gradual decrease in dip. The bedset geometry is sigmoidal; individual bedset-bounding surfaces can be traced from fore- to topsets in single longitudinal sections. Bounding surfaces are locally truncated by reactivation surfaces. The sediment is poorly sorted and strongly bimodal, with both medium-grained sand and pebbles/granules. Pebbles include well-rounded, heavily bored limestone and chert, correlated with Tripolis and Pindos zone lithologies, respectively. Fauna include barnacles, mollusks, scaphopods and benthic foraminifera. Rich accumulations of articulated *Ostrea* sp. occur as banks within topsets units.

Interpretation: This subunit is interpreted as a proximal, shallow marine equivalent of the prograding offshore/coastal unit above (Subunit 2.2.1) that accumulated behind (east of) the Gargaliani-Filiatra escarpment. A proximal delta-front/delta-top setting (of partly Gilbert type), is inferred from the terrigenous nature, sedimentary structure and poor sorting (Orton and Reading, 1993). The characteristic sigmoidal architecture and presence of reactivation surfaces indicate wave influence (Colella, 1988).

Subunit 2.2.3: heterogeneous terrigenous sediments (Figs. 7, 10 a, log 5)

This begins with dark grey, sandy, relatively homogenous mud, with local sub-horizontal lamination. A typical outcrop is located E (inland) of the two subunits described above, where it unconformably overlies Late(?) Pliocene sediments (Unit 1.6) at an altitude of 280-290 m ASL. This mud is spectacularly fossiliferous, with a very dense and diverse macrofauna, including gastropods (e.g. *Cerithids*), bivalves, scaphopods, occasional arthropod remnants and carbonised sea-grass, all in excellent state of preservation. Gastropods outnumber bivalves, but the relative abundance of the latter increases upwards. Many of the bivalve shells are still articulated. The microfauna exclusively consist of benthic foraminifera and ostracods (Table 1).

The mudstone is succeeded by brown marl with a very high-density, monospecific macrofauna of *Cardium edule* and an oligospecific microfauna, including *Ammonia tepida* (Table 1). Well-sorted, matrix-free, fine quartzose sand sharply overlies the brown marl. Sedimentary structures in this sand include millimetre-scale festoon and tangential ripple cross-lamination, planar cross-lamination, symmetrical and asymmetrical ripples and reactivation surfaces that define larger-scale ripple sets. Palaeocurrent directions are both WSW (offshore) and N and S (shore-parallel) (Fig. 10 a, log 5). Bioturbation is restricted to a few *Skolithos*-like burrows. The sand is succeeded by alternating planar cross-beds (3-7 cm thick) of conglomerate and well-sorted, ripple cross-laminated sand. The basal beds of this interval consist of coarsening-upward, matrix-supported conglomerate, passing into well-sorted, trough cross-laminated sand, with planar, clast-supported, normally graded and imbricated conglomerate towards the top. Maximum clast size increases upwards from 1 to 7 cm. The clasts (Tripolis limestone and Pindos chert) are moderately-rounded, commonly disc- and rod-shaped. Planar bedsets dip NNW at ca. 10°. Imbrication,

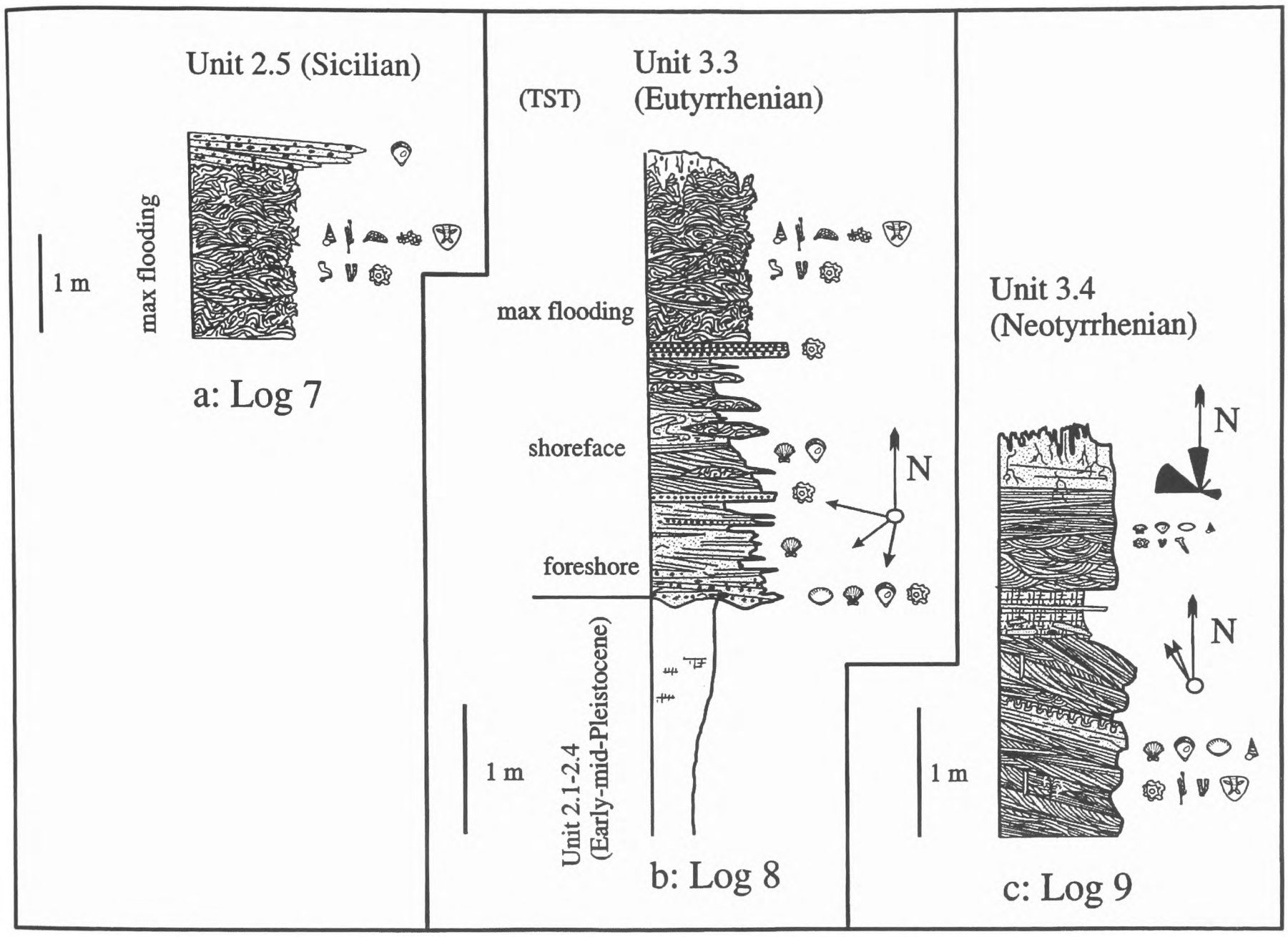

Figure 12. Representative sedimentary logs of mid-late Pleistocene sequences (logs 7, 8, 9); **a,** Sicilian (Unit 2.5) from near Filiatra; FILIATRA 1185 - 1645. The sharp contact between the algal bioherm below and the detrital sediment above may reflect high order intra-Sicilian sea level cyclicity (see also Figures 6b III, 7 b I) **b,** Eutyrrhenian (Unit 3.1), unconformably over early (to mid ?) Pleistocene (Units 2.1-2.3), from Mati Coast; FILIATRA 1475 - 2730. Note the gradual development of algal bioherms up the sequence. **c,** Neotyrrhenian (Unit 3.2); Note palaeocurrent data; from Marathopolis; FILIATRA 0960 -2265 (see Figures 2, 3 for locations).

ripple cross-lamination and trough cross-bedding indicate a WNW direction of transport. Above this, brown mud intervals (1.5-2 m), similar to the mud lower in the succession, contains a monospecific fauna of *Cardium edule*.

Interpretation: The lower parts of the sequence (grey mud with a mixed *Cerithid* gastropod and bivalve fauna) was deposited in a low-energy, shallow-marine environment of reduced salinity, as indicated by the presence of hyposaline species (e.g. A. *tepida*) (Fernandez-Gonzalez *et al.*, 1994; Amorosi *et al.*, 1998). Oxygen depletion below the sediment-water interface is suggested by excellent preservation of organic matter (Pemberton *et al.*, 1992). The low-diversity benthic fauna may reflect stressful ecological conditions. The most probable setting is a lagoon behind a barrier, but with an open-marine connection in view of the fully marine macrofauna present. The upward incoming of the dominantly brackish mollusk *Cardium edule* may indicate brackish-water conditions in a more restricted lagoonal environment. The overlying coarsening-upward sand/conglomerate intervals are interpreted as a Gilbert-type delta (*"Hjulström-type"* delta of Postma, 1990) that prograded into the lagoon. The overall sequence is interpreted as progradational, with an increase in the thickness of deltaic facies toward the top, representing a proximal equivalent of more westerly offshore units discussed above (Subunits 2.2.1 and 2.2.2) (Fig. 7).

The prograding sediments of Unit 2.2. probably correspond to a prominent highstand systems tract over the maximum flooding deposits of Unit 2.1 (inferred Calabrian, ca. 1600-800

ka; Fig. 6b). A late Calabrian age (ca. 1300-800 ka) is, thus, plausible, corresponding to the later, highstand part of eustatic cycle 3.10 sensu Haq *et al.* (1986) (Fig. 6a). A similar age was assigned to sediments elsewhere in N and in S. Messenia by Frydas (1990).

Unit 2.3 (Lower Pleistocene ?): shallow-marine carbonates (Fig. 2, 7, 9a, log 3)

This unit rests on a sharp erosional surface at the top of Unit 2.2.1, near Gargaliani, at about 280 m ASL. It begins with packstone/wackestone that accumulated on the previous unit with a minor erosional relief (5-10 cm). This sequence passes upwards into coarser-grained bioclastic packstone/grainstone, with a few intervals of fine-grained carbonate. Scoured surfaces are overlain by pebbly lags. The lower, fine-grained parts of the sediment are very porous and almost unconsolidated, with widespread bivalve-moldic porosity after small bivalves and gastropods. The preserved fauna are restricted to small fragments of thin-shelled bivalves. The upper, coarser-grained beds are parallel bedded (20-45 cm thick) and dip to the SSW (190-200°) at ca. 10°. The sediment is very bioclastic, with abundant (but not age diagnostic) fragments of mollusks, gastropods, echinoids, brachiopods, scaphopods and coral. Common bioturbation includes vertical burrows (7-9 cm long x 2 cm deep).

Interpretation: This unit accumulated in a current- or wave-swept shallow-marine setting. Assuming that the directly underlying sediments (Unit 2.2, Fig. 7) are of upper "Calabrian" age, Unit 2.3 could record high-frequency (fourth-order) "intra-Calabrian" sea level cyclicity, within the third-order sea level cycle 3.9 (Haq *et al.*, 1988; Fig. 6b). This interpretation is further supported by the fact that a prominent cliff of inferred early mid-Pleistocene age (Gargaliani-Filiatra Escarpment) postdates the deposition of Unit 2.3. However, a possible early mid-Pleistocene age (beginning of the sea level cycle 3.10) cannot be excluded.

Unit 2.4 (Early-Middle Pleistocene ?): shallow-marine carbonates-siliciclastics (Fig. 2, 9b, log. 4)

Calcareous mudstone at the base grades upwards into grainstone/packstone with occasional algal boundstone bioherms and low-angle, trough cross-laminated calcareous sandstone. The Unit crops out in the S Messenia block, over Pliocene(?) subaerial sediments (e.g. Unit 1.2) and bedrock. Good exposures are seen along the road from Pylos to Methoni in S Messenia (e.g. Palioneron, Ayios Athanassios; Figs. 2, 3). Locally (Palioneron), this unit was deposited on the hangingwall of a NNW-SSE normal fault (with ca. 60 m of minimum accumulated Quaternary throw). A coarsening-upward sequence drapes a fluvial channel incised into pre-Quaternary fluvial conglomerate (Unit 1.2). The upper parts of Unit 2.4 comprise planar cross-laminated calcareous sandstone/conglomerate, with well-rounded and bored Tripolis limestone pebbles, together with bivalves and worm-burrows (Fig. 11 f). Further inland, toward the NNW-SSE fault, the sediment passes upwards into clast-supported, bouldery conglomerate with a calcareous siltstone matrix. Clasts are very well-rounded, commonly spherical, including *Lithophaga*-bored bedrock limestone boulders and a few, commonly discoidal, chert pebbles. Post-depositional faulting with a N-S strike and a throw of ca. 20 m is coupled with intense jointing.

Elsewhere, in S Messenia (e.g. Ayios Athanasios; Figs. 3, 9 b, log. 4) the sequence begins with intensively karstified and calcified calcareous mudstone/siltstone, deposited above a ravinement surface on Tripolis limestone. This facies contains a poorly preserved microfauna (Table 1). Up-sequence, beds of sharp-based, hummocky cross-stratified calcareous sandstone, or lithic packstone/grainstone alternate with calcareous mudstone. This is followed by coarse calcareous sandstone with, first, trough cross-bedding, then low-angle planar cross-lamination, accompanied by an increase in bed-thickness and degree of amalgamation. Mollusks, scaphopods, barnacles, red and green algae and diverse foraminifera (Table 1) are abundant in sandstones and grainstones. Many bioclasts are micritised, or surrounded by micritic envelopes. The benthic foraminifera in upper levels are of mixed shallow marine/upper bathyal type (Blanc-Vernet, 1969; Murray, 1973).

Interpretation: The first-mentioned sequence (Palionero; Fig. 3) is interpreted as a transition through the following environments: upper offshore (lower mudstone with storm-deposited packstone interbeds), middle-upper shoreface (trough cross-laminated sandstone), and then upper shoreface/foreshore (planar cross-laminated sandstone), probably all indicative of overall coastal progradation. The conglomerate facies close to the fault-scarp is interpreted as a rocky foreshore deposit, probably resulting from wave-reworking of scarp colluvium.

The second sequence (Ayios Athanasios, Figs 3, 9 b, log. 4) is interpreted to reflect a transition from shallow marine, to coastal, environments, as above. Most of the carbonate grains originated as micritised allochems, probably derived from *Thalassia* banks (Perry, 1997). The high content of *Textulariidae*, together with the presence of *Lagenidae*, probably indicate a water depth of >50 m (Blanc-Vernet, 1969; Murray, 1973). The mixing of shallow-marine and upper bathyal benthic foraminifera is suggestive of storm conditions. The trough cross-bedding in the upper parts of the sequence is attributed to storm-generated bar and trough morphology in the foreshore-upper shoreface zone (Kumar, 1976; Reading and Collinson, 1996).

Unit 2.4 is in the same relative stratigraphic position (and probably of the same age) as Unit 2.2 in the N Messenia Block and is, therefore, interpreted as corresponding to the highstand of early Pleistocene (upper "Calabrian") age, prograding over more basinal (maximum flooding) facies of lower "Calabrian" age, represented by Unit 2.1 (Figs. 6b, 7).

Unit 2.5: ("Sicilian"?): boundstone and clastic sediments (Figs. 2, 4a, 7, 12a, log. 7)

This unit crops out between Gargaliani and Filiatra (Figs. 2, 3), forming a prominent 30-60 m ASL terrace surface in the N Messenia block. Its contact with the earlier Pleistocene units is not visible. Unit 2.5 consists of extensively karstified and bioeroded red algal boundstone, passing up into a thin interval of lithic grainstone and conglomerate. Algal limestone below is separated from clastic sediments above by a sharp surface (with

centimetre-scale erosional relief). The limestone facies includes porous algal boundstone, rhodolithic rudstone and packstone. Typical encrusting organisms are crustose coralline algae, bryozoa, foraminifera and gastropods, with a lower abundance of articulating coralline algae. Diverse non-encrusting benthic foraminifera occur, in addition (Table 1). Erect bryozoa taxa are also present, together with a few ostracods and common rhodoliths. *Polychaetae* worm burrows are common in wackestones. *Cladocora caespitosa* corals are locally abundant, either as *in situ* colonies, or as fragments in coral-mollusk lags. Mollusks comprise bivalves and gastropods (including *Astrea rugosa*), while echinoids are very common. The overlying grainstone is matrix-free, with well-rounded grains, derived mainly from the Pindos zone.

Interpretation: This boundstone lithofacies is interpreted as an algal reef deposited in the high-energy shoreface zone, away from fluvial influence (James, 1983; Poole and Robertson, 1991; this volume). The benthic assemblage indicates shallow-marine deposition. The gastropod *Astrea rugosa* is a common component of 'warm' Mediterranean faunas during interglacial periods (Keraudren, 1970, 1971; Poole and Robertson, 1991; this volume). The unit is correlated with the mid-Pleistocene "Sicilian" stage (Bonifay, 1975), since it is younger than the early mid-Pleistocene cliffs (Gargaliani-Filiatra Escarpment), but older than the "Eutyrrhenian", further west (Fig. 7). The overlying matrix-free grainstone is interpreted as a foreshore deposit. The succession probably records "intra-Sicilian" sea level cyclicity (of fourth- or higher-order; see Fig. 6 b), with an erosive relief on the algal boundstone resulting from relatively short-lived emergence, prior to resumed sea level rise and progradation of lithic grainstone.

Late Pleistocene-Holocene

Unit 3.1 ("Eutyrrhenian"): littoral carbonates (Figs. 2, 4a, 7, 12 b, log 8)

This unit, extensively developed in N Messenia (Figs. 2, 4 a), can be split into a mixed clastic-carbonate lower part and a carbonate, to terrigenous upper part.

This sequence overlies a relatively smooth (but locally undulating) ravinement surface, cut into offshore muds of Unit 2.1, or Tripolis zone bedrock (mainly sandstone), as seen in NW Messenia (Mati-Vromoneri coast; Figs. 2, 3, 7). The unit begins with oligomict, poorly-sorted, clast-supported, intraformational conglomerate (including slab-shaped clasts of calcareous sandstone), or with polymict conglomerate with well-rounded, disc- and rod-shaped clasts of Tripolis limestone, Pindos zone-derived chert and calcareous sandstone, with abraded bivalve shells. Relatively well-sorted, fine sand with pectenidae is succeeded by an alternation of well-sorted, medium-bedded calcareous sand with low-angle planar cross-lamination and small, mound-shaped red algal bioherms (20-60 cm across x30cm -2m high). Lamination is commonly disrupted by load-structures, slumps and other liquefaction features. A poorly-expressed cyclicity was observed, with cemented, laminated calcareous sandstone alternating with well-sorted, trough cross-laminated, uncemented sand. A gradual transition from calcareous sand, to fine sand with reactivation surfaces and longitudinal scours was commonly observed. SW (offshore)-directed palaeocurrents are indicated from measurements of cross-bedding (Fig. 12 b, log 8). The discontinuous, red algal bioherms comprise closely bound boundstone and packstones with a high content of entrapped terrigenous grains. In general, the boundstone becomes more abundant and closely-spaced, to locally amalgamated upwards. The sequence is capped by latest Pleistocene terra rossa and caliche of Unit 3.6 (see below). Sediments of this unit are cut by closely-spaced, NNW-SSE faults, with throws ca. 3-5m (Fig 13 e).

Interpretation: This sequence is interpreted as part of the "Eutyrrhenian" marine transgression (isotopic stage 5.5; ca. 120 ka; Imbrie *et al.*, 1987; Martinson *et al.*, 1987; Fig. 6 b) The uneven ravinement surface with the coarse clasts and intraclasts is interpreted as a buried plunge step on a palaeo-foreshore (Dabrio *et al.*, 1990). The calcareous sandstone is interpreted as beachrock that underwent storm-reworking and redeposition as lags. Slump and liquefaction events were probably triggered by syn-sedimentary seismic activity, consistent with ubiquitous faulting. The terrigenous composition indicates shoreline reworking and redeposition of fluvially derived sediment. The overlying finer-grained sand is indicative of high-energy upper shoreface sediments, marked by offshore-directed scour structures. Above this, the algal bioherms required high-energy conditions and low clastic sediment input to form (James, 1983), possibly controlled by autocyclic (i.e. "normal" sedimentary) processes. However, the dominance of algal bioherms high in the succession probably reflects maximum flooding conditions, when deltas were in retreat, as also inferred for "Tyrrhenian" equivalent in southern Cyprus (Poole and Robertson, 1991; this volume).

Unit 3.2 ("Neotyrrhenian"): mainly littoral carbonates (Figs. 2, 4a, 7, 12c, log 9)

This unit is dominated by shallow-marine carbonates with a distinctive intercalation of red palaeosol. This unit was mapped as "Neotyrrhenian" by Kelletat *et al.* (1976) in N Messenia, but depositional terraces of this age were not identified in S Messenia during this study. Where exposed (near Marathopolis; Fig. 3), the unit unconformably overlies the "Eutyrrhenian" (Unit 3.1).

The lower part of the unit consists of steep (ca. 30-32°) planar-tabular bedsets of rhodolitic grain/packstone (30-100 cm thick) dipping to the WSW. Prograding clinoforms are internally cross-laminated with normally graded, tangential cross-laminae (0.2-3 cm thick). Measured palaeocurrents are mainly offshore, but shore-parallel trends were also noted (Fig. 12 c, log 9). The uppermost beds consist of calcirudite with large (up to 7 cm) fossil fragments, clasts of bedrock limestone (<3 cm in size), algal boundstone (derived from unit 3.2) and tabular intraclasts of matrix-free grainstone. The fauna include bivalves, gastropods, large asymmetrical echinoids (in life-position), solitary corals and rhodoliths (up to 3 cm in diameter). Foraminifera are mainly benthic forms of shoreline habitat and a few non-age-diagnostic planktic taxa (Table 1). The sediment is intensively bioturbated, with *Cruziana*, *Diplocraterion* and

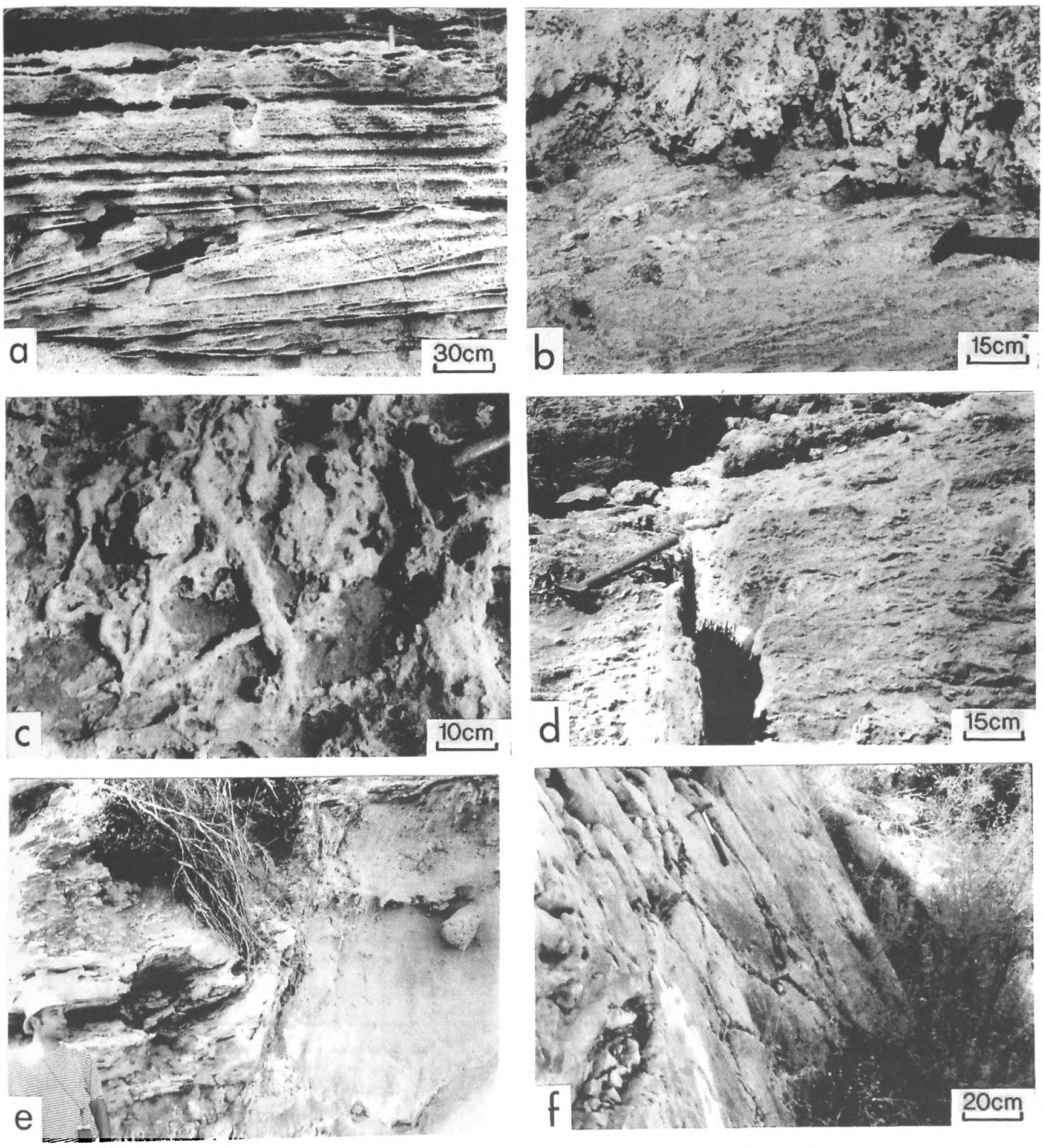

Figure 13 Field photographs of late Pleistocene sequences in Messenia. **a,** Sigmoidal bedsets in calcareous sandstone (prograding shoreface sandwave), overlain by low-angle cross-bedded aeolianite (foreshore), Neotyrrhenian terrace, Unit 3.2, Romanos, NW Messenia; **b,** Bioturbated grainstone (with sub-horizontal bedding traces), Neotyrrhenian (Unit 3.2), unconformably overlain by thin soil (dark patch to left of hammer), in turn overlain by aeolianite with subvertical root traces; correlated with the latest Pleistocene eustatic sea level lowstand (Unit 3.7); Marathopolis, NW Messenia; **c,** Rhizocretion (root) network within red calichified soil; post-Neotyrrhenian; same location as **b; d,** Extensional joints affecting Neotyrrhenian shallow-marine grainstone and latest Pleistocene soils/aeolianite; the extensional joints are lined with hard caliche (pale). The joints overlie extensional faults through bedrock that cut an offshore island on strike. Marathopolis coast, opposite Proti Island, NW Messenia; **e,** Normal fault (NNW-SSE) throws early Pleistocene offshore carbonate mud (right), against the preserved unconformity between the above carbonate muds (lower left) and overlying Eutyrrhenian well-bedded sandstone (upper left); Mati coast; NW Messenia; **f,** Major slickensided scarp marking the Pylos Fault, a major boundary between the N and S Messinia Blocks.

Table 1. Benthic and planktic foraminifera fauna of Plio-Pleistocene marine successions from the Messenia Peninsula.

	UNITS												
Foraminifera	1.5	1.6	2.1	2.2 .1	2.2 .2	2.2 .3	2.3	2.4	2. 5	3. 1	3. 2	3. 8	**Environment**
Ammonia becarii	+	+		+	+	+	+	+	+	+	+		**15-<100m, high energy, normal-slightly hyposaline, coastal lagoons (1, 2)**
A. tepida						+							**10-30 m, hyposaline, fluvial runoff (1, 2, 4)**
A. spp.			+		+		+	+	+				
Angulogerina angulosa			+										
Asterigerinata mamila			+	+	+		+		+	+			
Brizalina spathulata			+										
Br. spp.			+										
Bulimina marginata			+										**60-150m, oxygen deficiency, fluvial runoff (1, 2)**
Bl. spp.			+										**>20m (4)**
Carpenteria utricularis									+				
Cassidulina crassa			+										
Cibicides lobatulus	+		+	+	+		+	+	+	+			
C. refulgens			+	+	+		+			+			
C. ungerianus-pseudungerianus	+		+										
C. spp.								+			+		
Discorbis sp.		+		+			+	+		+			
Elphidium aculeatum			+										
E. advenum			+	+									
E. complanatum			+	+									
E. crispum	+	+		+	+	+	+	+	+	+			**10-75 m, commonly epiphytic (1, 2, 3)**
E. jenseni				+									
E. macellum	+			+	+					+			**10-75 m, commonly epiphytic (1, 2, 3, 4)**
E. spp.	+	+			+	+	+	+	+	+	+		
Glandulina sp.			+										
Globocassidulina subglobosa			+										
Hanzawaia sp.			+										
Homotrema rubrum									+	+			
Lagena orbignyana			+										
other Lagenidae								+					
Nonion depressulum				+									**10-40 m, normal-**

													slightly hyposaline (1)
N. incrassatum				+									
Nonionella sp.			+										
Planorbulina mediterranensis			+						+	+			**infralittoral, epiphytic (2, 4)**
Planulina ariminensis			+										
Quinqueloculina spp.									+	+	+		**infralittorla, epiphytic (1, 2, 4)**
Reophacidae									+				
Reussella spinulosa			+										
Robertina bradyii			+										**infralittoral. epiphytic (2, 4)**
Rosalina utricularis									+				**infralittoral, epiphytic (2, 4)**
Sphaeroidina bulloides			+										
Spiroloculina sp.									+	+	+		**infralittoral, epiphytic (2, 4)**
Textularia saggitula			+										**>50m, inner shelf (3)**
T. spp.			+					+	+				**-//- (3)**
Triloculina sp.									+	+	+		
Uvigerina meditarranea			+										**>90 m , rich in organic matter (1, 2, 3)**
Valvulineria bradyana				+									
Globigerina bulloides			+										
G. falconensis			+										
G. venezuellana (*)				+									
Globigerinella aequilaterallis			+	+									
Globigerinoides ruber			+								+		**warm water (2)**
Gb. obliqus extremus			+										**-//- (2)**
Neogloboquadrina humerosa			+	+									**-//- (2)**
Orbulina universa			+										**-//- (2)**
Globigerinidae		+						+	+		+		
Globorataliidae								+	+				

Amorosi et al., 1998: (1)
Blanc-Vernet, 1969:(2)
Fernandez-Gonzales et al., 1994:(3)
Murray, 1973:(4)

(*): Derived from bedrock.

Skolithos burrows (i.e. *Cruziana* ichnofacies; see Pemberton *et al.*, 1992), and also bivalve escape-traces. The relative abundance of mollusks, rhodoliths, trace fossils and matrix decreases towards the top of the unit.

The red soil layer consists of sandy-pebbly caliche (hardpan) that overlies the littoral grainstones with a marked erosional relief (Fig. 13 b). Numerous slab-shaped, angular intraclasts (<60 cm long) were derived from the directly subjacent calcarenite. *Rhizocretion* bioturbation is abundant (Fig. 13 c). Elsewhere, this red interval consists of multiple caliche crusts, alternating with layers of normal- or reverse-graded, calcified grainstone, up to three cm-thick.

Above the caliche comes trough cross-laminated grainstone and shell concentrates (2.5-3 m thick) with bivalves, gastropods, a few rhodoliths, *Cladocora caespitosa* fragments and rare mammalian bone fragments. Shells are mostly convex side-upwards. Almost horizontal trough cross-bedded bedsets (up to 20 cm thick) exhibit internal trough and festoon cross-lamination (0.2-3 cm thick). Individual laminae are normal- and reverse-graded. Current directions, determined from imbricated bivalves and trough cross-lamination, are both WNW (offshore) and NNE (shore-parallel) (Fig. 12 c). Low-angle planar cross-lamination predominates higher up, with laminae dipping to both offshore and onshore directions. Locally, along the Marthopolis coast (Fig. 3) the red soil is directly overlain by small *in situ* colonies of *Cladocora caespitosa.*

Interpretation: The lower part of this unit is interpreted to reflect progradation of shoreface sand-waves over quiet, shoreface areas stabilised by *Thalassia.* The tabular calcarenite intraclasts in the uppermost bedsets are interpreted as beachrock clasts, reworked by storms from the foreshore. This unit is, therefore, thought to represent transgression during the "Neotyrrhenian" sea level cycle (Fig. 6 b). This lower part is correlated with the substage 5.3 of the isotopic stage 5 (Last Interglacial; ca. 100 ka; Martinson *et al.*, 1987; Fig.6 b). Above, the red soil interval indicates subaerial exposure and soil formation during an "intra-Neotyrrhenian" sea level fall, possibly corresponding to the substage 5.2 (ca. 90 ka; Martinson *et al.*, 1987). The multiple caliche crusts may record storm-induced(?) backshore deposition (i.e. autocyclic effects). Alternatively, they could reflect very high-order sea level cyclicity during the substage 5.2 lowstand. The overlying upper interval is interpreted as a barrier located in a middle to upper shoreface, to foreshore setting. This feature developed during a resumed latest Pleistocene sea level rise, that possibly corresponded to substage 5.1 (ca. 80 ka; Martinson *et al.*, 1987; Fig. 6 b). Well sorted peloidal grainstone with spherical, blue-green algae/microbia-encrusted grains is locally preserved ca.4-5 m onshore from the above facies. As this occurs at the same elevation this sediment is interpreted as a small restricted lagoon behind a coastal barrier. Further S (Romanos; Fig 3), this unit is represented by siliciclastic foreshore-backshore facies (Fig. 13 a).

Alternatively, the above stratigraphy could reflect even higher-order, intra-substage sea level variation at thousands of years-time scale (e.g. the multiple substage 5.3.3+5.3.1 *sensu* Martinson et al., 1987).

Unit 3.3 (mid- to late Pleistocene ?): palaeosols

The unit comprises purple-red siliceous soil overlying detrital carbonates and sandstones of Unit 2.2 (Fig. 7). The siliceous content mainly consists of angular, corroded grains of red chert of Pindos zone origin. This unit is widely exposed in NW Messenia on an elevated relatively level area west of the Kyparissia Mountain front.

Interpretation: This unit is interpreted as an extensively hydrolysed krasnozerm soil, locally reworked into sandier, arenosol facies (*sensu* FitzPatrick, 1971). Its formation was probably favoured by a relatively flat topography. Extensively hydrolysed soils are formed in wet, to dry, tropical conditions of mean annual temperature, ideally >25°C, associated with a vegetation ranging from semi-deciduous forest to savannah (FitzPatrick, 1971). Identical palaeosols further north, in the Kyparissia-Kalo Nero Basin *("Kalo Nero Formation")* post-date early Pleistocene sediments, and are overlain by calcarenites of probable "Tyrrhenian" age (Fountoulis and Moraiti, 1994).

Unit 3.4 (Mid- to late Pleistocene): fluvial conglomerate (Figs. 2, 4b, 8b, log 1)

Red, clast-supported fluvial conglomerates form a number of fluvial terraces, well exposed on the E coast of S Messenia (Paniperi-Petalidi and Koroni areas; Figs. 3, 8.2, log 1). In the Kombi area (Fig. 3), the upper part of this clastic unit comprises fluvial conglomerates, inferred overbank deposits and reworked terra rossa that post-date apparent equivalents of littoral carbonates Unit 3.1 (see above). In NW Messenia, this clastic unit is restricted to Profitis Ilias Hill near Filiatra, and also to the Eleophyton-Iklena area, discussed previously (Zelilidis, 1988; ZeliIidis *et al.*, 1988). This unit unconformably overlies sediments equivalent to Units 2.4, 2.5, or older, and was assigned a mid- to late Pleistocene age by Fytrolakis (1971) and I.G.M.E. (1980 b), although it is probably diachronous.

Unit 3.5 (Latest Pleistocene): terra rossa

This unit consists of terra rossa, often associated with chalky caliche. It covers "Neotyrrhenian" shallow-marine sediments (Unit 3.2 in NW Messenia (Marathopolis and Petrohori; Fig. 3). The unit is considered to be a time equivalent of the upper parts of Unit 3.4 (Fig. 7).

Unit 3.6 (Late Pleistocene ?): terra rossa

This unit comprises a karstic cavity-fill in the topsets of Subunit 2.2.2, as seen in and around Gargaliani Quarry (Fig. 3). It consists of reworked sandy terra rossa with bovine and micro-mammal bone fragments and lithic tools. Fluvial reworking is indicated by the nature of grading, pebble and fossil imbrication. This deposit may also be Holocene.

Unit 3.7 (Latest Pleistocene): aeolianite (Figs. 7, 12 c, log 9)

"Neotyrrhenian" sediments (Unit 3.2) are overlain by well-sorted, fine to medium-grained, trough cross-laminated, or massive grainstone, extensively calichified, with *Rhizocretion*

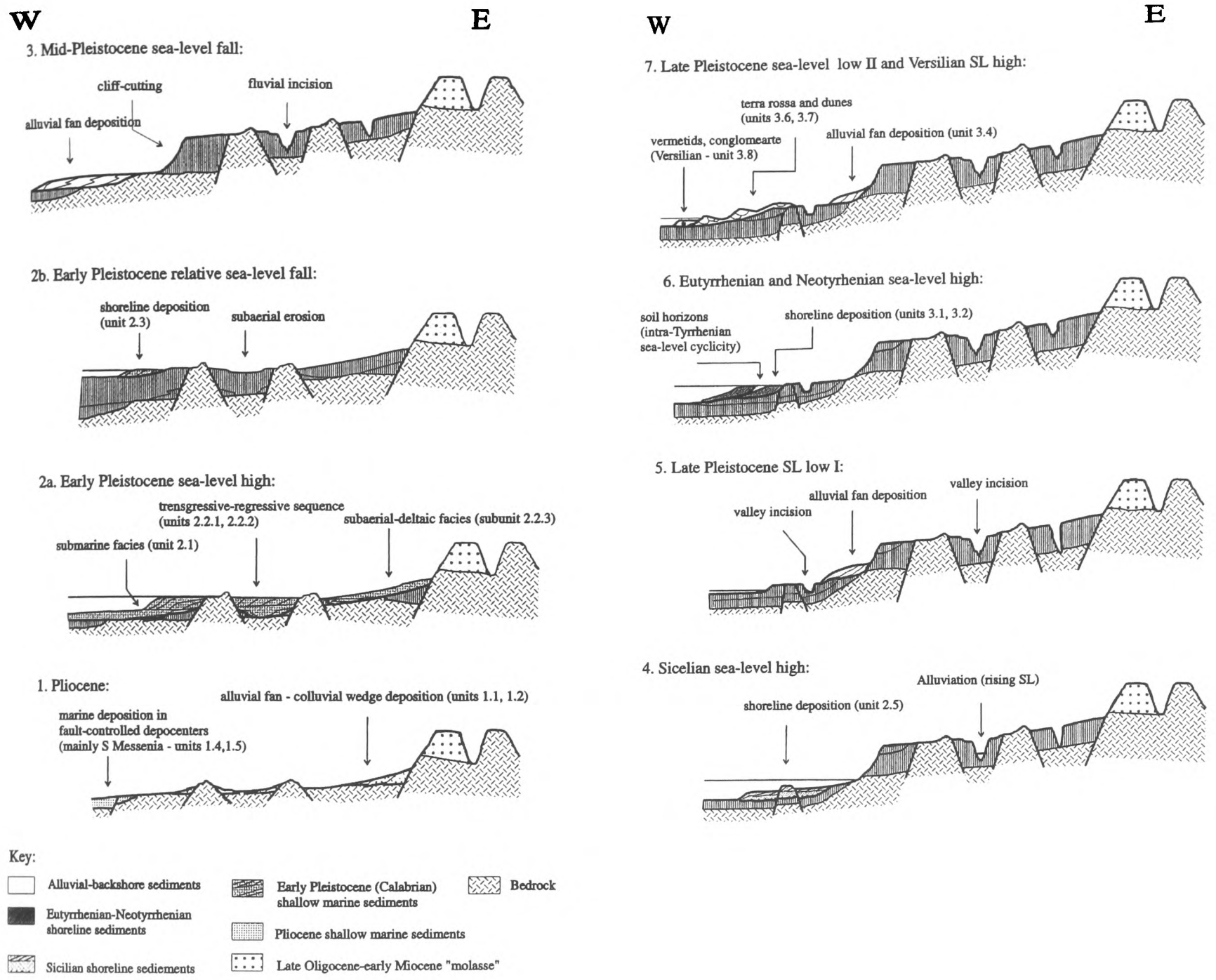

Figure 14. Interpretative cross-sections showing the recognisable stages in the Pliocene-Holocene development of the Messenia Peninsula. These are applicable mainly to the N Messenia Block, where the sedimentary record is nearly complete. The dominant control on sedimentation was regional tectonic uplift, with marine terraces and associated shallow-marine sediments being related to marine transgressions and eustatic sea level highs. Additional accommodation space was mainly provided by localised subsidence along the hanging walls of extensional faults that are inferred to have remained mainly collectively active. See text for details.

(Fig. 13 b). This unit is interpreted as aeolianite, probably derived by reworking of sand from an exposed offshore shelf during the Last Glacial Maximum sea level low stand (Fig. 6 b). Deep solution wells penetrate this sediment to below present-day sea level, suggesting that the water table fell beneath present-day levels, as expected during sea level lowstands (assuming no significant tectonic subsidence during the Holocene).

Unit 3.8 ("Versilian" or younger ?): bioconstructions

Vermetid bioconstructions (*"trottoires"*) occur at ca. 1-1.5 m ASL along the coast of NW Messenia (Romanos coast; Figs. 2, 3, 7), associated with an abrasion platform cut into "Neotyrrhenian" sediments (Unit 3.2). This unit can be attributed to the "Versilian" highstand, of Holocene age, as elsewhere in Greece (e.g. Keraudren, 1970, 1971). The age of this high-order highstand is radiometricaly constrained at ca. 5-7 ka (e.g. Red Sea; Plaziat *et al.*, 1996). Alternatively, this unit could be correlated with other similar foreshore deposits of the Aegean Arc (Crete), S Turkey (Alanya), Syria, Lebanon and Israel (Pirazzoli, 1986, 1987; Kelletat, 1991). Radiometric dating of these deposits suggests that they were uplifted ca. 1550-1530 years ago, as a result of a tectonic event of regional significance (*"Early Byzantine tectonic paroxysm"*; Pirazzoli, 1986). Holocene beachrocks occur locally in NW Messenia a few centimetres above present sea level, but still within the intertidal zone (<20-30 cm). Their present position is interpreted as resulting from localised uplift, probably fault-controlled.

Unit 3.9: Modern sediments

Modern sedimentation is represented by beaches, active and inactive dunes, ephemeral lagoons, fluvial sediments and various soils (Fig. 2). Present-day sedimentation is mainly controlled by a combination of climate and the inherited geomorphic setting of particular areas, largely fault-controlled.

Discussion: Plio-Quaternary tectonic-sedimentary evolution

We recognise eleven main stages in the post-Miocene depositional/tectonic history of the Messenia Peninsula, as follows:

1) Pliocene (Fig. 14a.1)

Following 'late orogenic' compressional tectonics in Late Oligocene-Early Miocene time, a long period of Miocene subaerial erosion culminated in peneplanation, followed by valley incision. Normal faulting into the two tectonic-geomorphological blocks (N Messenia and S Messenia Blocks) probably began by this time, with activation of ENE-WSW to E-W faults, transverse to the inherited Neotethyan tectonic grain. These transverse faults were active by Late Miocene-Early Pliocene time, as shown by evidence from the Kyparissia-Kalo Nero half graben further north (Fountoulis and Moraiti, 1994). In SE Messenia, NNW-SSE faults that bound the Messenian Gulf graben were clearly active in Early Pliocene, controlling deposition of offshore sediments (Unit 1.4, Figs, 2, 4b, 7). By contrast, in W Messenia, west of the Kyparissia Mountain front, colluvial wedges (Unit 1.2) and fluvial conglomerates (Unit 1.1) accumulated. This suggests that although extensional faulting was already taking place in W Messenia in Pliocene times, the subsidence rate was inadequate to allow marine transgression. In NW Messenia, the earliest reported marine sediments, of latest Pliocene (late Piacenzian) age (Frydas, 1990), are associated with fault activity within NNW-SSE to N-S grabens and half-grabens (e.g. Gargaliani-Filiatra half-graben; see also Zelilidis and Doutsos, 1992).

2) Early to mid-Pleistocene (Fig. 14a.2)

Relative sea level rise, starting in the Early Pliocene in SE Messenia, culminated in extensive progradation of shallow-marine clinoforms (e.g. Unit 2.2) over offshore mud, now preserved mainly within narrow, NNW-SSE to N-S grabens (e.g. Unit 2.1, Pylos). The rate of fault-induced basinal subsidence was locally high enough to allow deposition of offshore facies at water depths of >90 m. These facies represent the maximum marine transgression during the early Pleistocene ("Emilian" *sensu* Bonifay, 1975) and shoreline progradation during the subsequent highstand (sea level cycle 3.9 *sensu* Haq *et al.*, 1988). Mixed detrital carbonate/terrigenous clinoforms developed away from areas of fluvial input (e.g. Subunit 2.2.1), whereas deltaic sands/conglomerates were deposited close to river mouths (e.g. Subunit 2.2.2). Areas of high fluvial discharge commonly coincided with the ENE-WSW to E-W transverse fault lineaments that were exploited by drainage transverse to the regional N-S tectonic grain. Brackish lagoonal and braided stream deposits (e.g. Subunit 2.2.3) correspond to back-barrier settings that prograded over shoreline sediments. This was followed by relative sea level fall that allowed cliff-cutting and fluvial incision of marine sediments and bedrock. This relative sea level fall may be explained as high-order, "intra-Calabrian" sea level cyclicity. Resumed relative sea-level rise during the late early (to mid-?) Pleistocene then resulted in deposition of detrital carbonate shoreline clinoforms (e.g. Unit 2.3) over a ravinement surface cut into "Calabrian" shoreline to offshore facies.

3) Mid-Pleistocene lowstand (Fig. 14a.3)

Important relative sea level fall took place during mid-Pleistocene time. In NW Messenia, a major cliff (Gargaliani Escarpment; Figs. 3, 4b) separates early/mid(?) Pleistocene from mid- and late Pleistocene terraces. The minimum magnitude of relative sea level fall in that area equals the height of the cliff (ca. 120 m). Relative sealevel fall probably resulted from combination of eustatic sea level fall, regional uplift and possibly footwall uplift related to the Gargaliani-Filiatra fault (assuming that the latter was active). The regional extent of cliffs and incised valleys, together with the observation that pre- and post-cliff marine terraces are relatively closely-spaced, suggest that much of the Quaternary uplift of the Messenia Peninsula took place after the early Pleistocene, prior to, or during, this phase of major downcutting. Assuming a late middle Pleistocene age for the succeeding "Sicilian" terrace (i.e. correlated with oxygen-isotopic stage 7), a long time interval (~ 400-500 ka) separates the early and late Pleistocene marine terraces.

The above inferred mid-Pleistocene lowstand corresponds to the "Mindel" sea level fall (beginning of the mid-Pleistocene) in Bonifay's (1975) chronostratigraphic scheme (Fig. 6b). However, final (present day) incision could be the cumulative effect of downcutting during both the "Mindel" and the "Riss" (begining of the late Pleistocene) lowstands. Karstic dissolution of early Pleistocene carbonates and further freshwater diagenesis/pedogenesis took place during this stage. Alluvial fans, related to the intense downcutting, probably bypassed the present coastal zone and were deposited further offshore. Two notable exceptions are alluvial fans preserved on the flanks of the Kalamata-Messenian Gulf Graben (Paniperi-Petalidhi; Figs. 2, 3, 4b), and associated with a small graben elsewhere (Eleophyton graben; Zelilidis and Doutsos, 1992). Some of the older/higher fanglomerates of Unit 3.4 (diachronous?) may correspond to meet the mid-Pleistocene low stand. Reworked terra rossa of Unit 3.5 was deposited at this time, or later. Fanglomerate deposition probably indicates a climate characterized by strongly seasonal rainfall.

4) "Sicilian" (Fig. 14b.4)

During the "Sicilian" stage (*sensu* Bonifay, 1975, Fig 6 b), the sea level rose to the level of the piedmont west of the Gargaliani-Filiatra escarpment (40-60 m ASL at present). Algal boundstone bioherms were deposited (e.g. Unit 2.5), probably recording maximum transgression and delta retreat. "Intra-Sicilian" relative sea level cyclicity is suggested by erosional contact of underlying algal boundstones and prograding detrital shoreline

sediments; the latter were probably formed during a later "Sicilian" highstand. Pronounced sea level cyclicity during the mid-Pleistocene is suggested by correlation with oxygen-isotope curves (Imbrie *et al.*, 1987; Martinson *et al.*, 1987; Fig 6b).

5) "Sicilian-Tyrrhenian" Lowstand (Fig. 14b.5)

The sea level fell after the "Sicilian" (at about 180 ka), triggering fluvial incision and cliff cutting. U-shaped meanders were entrenched into "Sicilian" algal boundstone in the N Messenia Block (e.g. middle reaches of the Lagouvardos gorge). This stage, associated with subaerial diagenesis and calichification of the previous marine deposits, possibly corresponds to the isotopic stage 6 lowstand (ca. 180-130 ka; Martinson *et al.*, 1987), equivalent to the "Riss" lowstand, *sensu* Bonifay (1975) (Fig. 6 b).

6) "Eutyrrhenian" (Fig. 14b. 6)

During the "Eutyrrhenian" (isotopic stage 5.5; ca. 120 ka; Martinson *et al.*, 1987), the sea level rose again, to the level of ca. 20 m ASL (present altitude). In the N Messenia block, sediments corresponding to the "Eutyrrhenian" marine transgression (Unit 3.1) were deposited over a ravinement surface cut into offshore facies of early (or mid ?) Pleistocene age. The lower part of the transgressive sequence is characterised by detrital sediments (terrigenous or carbonates, according to proximity to fluvial discharge), whereas algal bioherms characterise higher parts, interpreted as a maximum flooding horizon. The highstand is characterized by clinoforms of detrital carbonates/conglomerates, locally capped by deltaic to fluvial deposits. By contrast, with the exception of the coast N of Koroni (Fig. 2, 3), no unambiguous "Eutyrrhenian" deposits were found in the S Messenia Block (c.f. Kelletat *et al.*, 1976).

7) Late Pleistocene Lowstand I (Fig. 14b. 6)

Sea level fell after the "Eutyrrhenian" and valley incision and cliff-cutting took place (substage 5.4; ca. 110 ka; Martinson *et al.*, 1987). Alluvial fan progradation probably occurred in NE areas of the S Messenia Block (e.g. lower/younger fans of Unit 3.4), representing an area of intense normal faulting along the uplifting flanks of the Messenian Gulf graben. Elsewhere, alluvial fan progradation was minimal. Intense calichification of "Eutyrrhenian" carbonates, accompanied by karstic dissolution and cementation took place during this first "post-Eutyrrhenian" lowstand.

8) "Neotyrrhenian" (Fig. 14b. 6)

Sea level rose again during the "Neotyrrhenian" (substages 5.3+5.1; ca. 100-80 ka; Martinson *et al.*, 1987) and detrital sediments were deposited over a karstified and bio-eroded relief of previous "Eutyrrhenian" deposits in NW Messenia (Unit 3.2). Only very proximal sediments are exposed (upper shoreface to foreshore). Higher order, "intra-Neotyrrhenian", sea level cyclicity is possibly indicated by thin caliche horizons intercalated with shallow-marine sediments. Tectonic activity was locally intense, as indicated by dense jointing of "Neotyrrhenian" deposits (Fig. 13. d). Extensional joints follow well established trends in the bedrock and demonstrate that "Neotyrrhenian" / post-"Neotyrrhenian" tectonic activity involved reactivation of older, buried extensional faults. By contrast, in S Messenia, low (1-5 m ASL) marine abrasion platforms without sediment may not be of "Neotyrrhenian" age Despite their low altitude, these could, instead, reflect diminished uplift (or even subsidence), leaving older Pleistocene terraces near (or below) sea level in this area.

9) Late Pleistocene Lowstand II (Fig. 14b.7)

Sea level fell again after the "Neotyrrhenian" and during the Last Glacial Maximum lowstand, resulting in further valley incision, cliff-cutting and karstic dissolution (isotopic stages 4 and 2; ca. 60-12 ka, respectively; Martinson *et al.*, 1987; equivalent to the "Würm" lowstand, *sensu* Bonifay, 1975). Alluvial fan progradation was restricted to areas of inferred active normal faulting, coinciding with major tectonic boundaries (e.g. lowest/youngest parts of diachronous Unit 3.4). Elsewhere, in most parts of the peninsula, red terra rossa soils, locally associated with chalky caliche horizons, covered a karstified relief of "Neotyrrhenian" and older sediments (e.g. Unit 3.5). Emergence of inner shelf areas during the maximum regression exposed uncemented littoral carbonate sand that was reworked into sand dunes (e.g. Unit 3.6) that drape "Neotyrrhenian" foreshore facies and terra rossa attributed to Late Pleistocene Lowstand II (Units 3.1, 3.5). A similar model was proposed for late Pleistocene aeolianites in southern Cyprus (Poole and Robertson, 1991; this volume).

Aeolianites are widespread along the exposed western coast of the Messenia Peninsula, facing the open Ionian Sea, but are almost absent from the eastern coast, facing the Messenian Gulf. Palaeowind directions from inferred late "Pleistocene lowstand II" aeolianites (Fig. 12b, log 8) are generally eastwards, similar to the present-day prevailing wind direction. Co-existence of calichification with subsurface karstic dissolution is suggestive of a semi-arid climate, with alternating wet/dry periods. Rainfall possibly increased towards the end of this period to early Holocene (prior to the maximum of the Holocene transgression in the "Versilian"), allowing deep solution holes in coastal aeolianite to penetrate deeper that the present sea level.

10) "Versilian" (Fig. 14b.7)

Eustatic sea level rose after the Last Glacial Maximum, reaching the present, or a slightly higher level at ca. 6 ka (Kraft *et al.*, 1975; Labeyrie *et al.*, 1976; Kambouroglou, 1989; Plaziat *et al.*, 1996). As a result, cemented Pleistocene deposits were transgressed and subjected to marine abrasion and bioerosion (e.g. Romanos and Petrohori coasts). A short-lived marine transgression/regression event in the Kalamata-Messenian Gulf Graben (Pamissos Plain) at around this time (Kraft *et al.*, 1975) can be attributed either to the "Versilian" sea level cycle, or to local tectonic subsidence. Deposits formed during the short-lived "Versilian" sea level high were either vermetid bioconstructions (e.g. Romanos coast, Figs. 2, 3), or pebbly-beach sediments deposited on a ravinement surface over aeolianite of the latest Pleistocene lowstand stage (e.g. Petrohori coast). These deposits

could also be of an even younger (historical ?) age, uplifted during the *"Early Byzantine tectonic paroxysm"* (*sensu* Pirazzoli, 1986).

11) Later Holocene to Recent

Since regional relative sea level change after the "Versilian" is well documented (e.g. Kraft *et al.*, 1975), local deviations from the regional sea level curve is assumed to relate to faulting (Flemming, 1968, 1978), combined with the effects of possible regional isostatic readjustment after the last glaciation (Lambeck, 1995). The Messenia Peninsula has been constantly inhabited since Neolithic times and human activity has influenced geomorphic and sedimentary processes. An example of noticeable geomorphic change in the peninsula since Mycaenean times is the ca. 3 km of delta/flood-plain progradation in the S part of the NW Messenia Block (Yialova area) (Fig. 3).

Conclusions

1. The Plio-Pleistocene sedimentary and geomorphological record of the Messenia Peninsula, SW Peloponnese, is very well preserved, shedding light on the tectonic-sedimentary evolution of a forearc area adjacent to the Ionian subduction zone, along the western part of the Hellenic arc. The results supplement observations from an area between the better known Corinth-Patras and Cretan areas to the north and south, respectively.

2. The Messenia Peninsula is characterised by dominant NNW-SSE faults parallel to the pre-existing, Neotethyan tectonic grain of the region, cut by ENE-WSW (to E-W) transverse faults. Later stage (Pleistocene) small faults are mainly orientated NNE-SSW (some probably being still active) and may relate to anticlockwise rotation of the principal axis of extension, as the southward curvature of the Aegean arc increased during Plio-Quaternary time.

3. The Messenia Peninsula is divided into two tectonic-geomorphic blocks, the N Messenia Block and the S Messenia Block, on the basis of elevation, structure, stratigraphy and geomorphology. The two blocks are separated by the NNW-SSE Pylos Fault. The N Messenia Block, is the more elevated and retains a relatively complete Pleistocene stratigraphy as compared with to the southern block which is subdued and dips beneath the sea to the south. Both blocks are flanked by an extensional forearc to the west, whilst the southern block is bordered by the Messenia Gulf graben to the east. On a regional scale, the Messenia Peninsula, thus, represents, a large segmented horst within a regionally extending area.

4. The Plio-Quaternary marine sediments are dated using nannofossils for the Pliocene-early Pleistocene time interval. In addition, late Pleistocene sediments are correlated with the well known "Eutyrrhenian" (isotopic stage 5.5; ca. 120 ka) and "Neotyrrhenian" (isotopic stages 5.3+5.1? ca. 100-80 ka) deposits elsewhere in Greece and other Mediterranean areas (e.g. Cyprus). A sequence-stratigraphic approach, involving correlation of successive marine terraces with known, dated, global sea level highs, is used to infer possible ages for the "Calabrian" and "Sicilian" stages (although with uncertainties resulting from unresolved multiple sea level highs).

5. Within the N Messenia Block six main Quaternary (Pleistocene-Holocene) terraces with overlying shallow marine sediments are present (Early Pleistocene (<200-340 m), late Early (to mid ?) Pleistocene (ca. 240 m), "Sicilian" (40-60 m), "Eutyrrhenian" (15-25 m), "Neotyrrhenian" (2-4 m) and "Versilian" (0.2-1.5 m). Some of the marine successions are backed by correlative non-marine (e.g. lagoonal), to terrestrial deposits.

6. Within the N Messenia Block younger marine terraces occur at successively lower levels. This implies that at time scales of the order of 1-2 Ma (Late Pliocene to Holocene) regional tectonic uplift, punctuated by glacio-eustatic sea level change, exercised the dominant control over shallow-marine sedimentation. On the time scale of the last 1 Ma the uplift rate (if assumed to be constant) ranges from 0.33-0.23 m/ka, comparable with that inferred for the Gulf of Corinth region further north (ca. 0.3 m /ka; Collier, 1990).

7) Local extensional faulting controlled some deposition (notably of early Pleistocene offshore sediments within narrow asymmetrical grabens). As a result, on an outcrop scale, the preserved sediments mainly document the interplay between the effects of regional tectonic uplift, glacio-eustatic sea level change and footwall uplift (or hangingwall subsidence) related to local extensional faults.

8) On a regional scale, an east to west progression of graben formation through time is confirmed. In the east (vicinity of Messenian Gulf graben), subsidence rates were high enough to allow deposition of offshore sediments in Early Pliocene time, whereas in the west subsidence was delayed until latest Pliocene-early Pleistocene time. This migration of deformation towards the west through time is attributed to "roll-back" of the subducting North African plate (possibly accompanied with gravity spreading of the overriding crust).

Acknowledgments

We thank D. Frydas and S. Tsaila, University of Patras, for identifying calcareous nannoplankton and foraminifera, respectively. S. Tsaila is also thanked for hospitality and guidance. Vasilis Panayiotou's assistance in the field during the summer of 1998 is gratefully acknowledged, as is Selen Etingi's assistance with drafting the figures. N. Kourampas was funded by the Greek State Scholarships Foundation (I.K.Y. - grant no.77069.07.3: "Geodynamic Evolution during the Quaternary"). The second author thanks Edinburgh University for financial assistance to carry out fieldwork. J. E. Dixon provided a thought-provoking review of the initial draft. T. Doutsos and an anonymous reviewer are thanked for constructive comments.

References

Amorosi, A., Barbieri, M., Castorina, F., Colalongo, M.L., Pasini, G. and Vaiani, S.C., 1998, Sedimentology, micropalaeontology, and strontium-isotope dating of a lower-middle Pleistocene marine succession ("Argille Azzure") in the Romagna Apennines, northern Italy: *Bolletino della Societa Geologica Italiana*, vol. 117, p. 789 - 806.

Armijio, R., Lyon-Caen, H., and Papanastasiou, D., 1992, East - West

extension and Holocene normal fault scarps in the Hellenic Arc: *Geology*, vol. 20, p. 491 - 494.

Arvidson, R., Becker, R., Shanabrock, A., Luo, W., Sturchio, N., Sultan, M., Lofty, Z., Mahmood, A.M., and El Alfy, Z., 1994, Climatic, eustatic, and tectonic controls on Quaternary deposits and landforms, Red Sea coast, Egypt: *Journal of Geophysical Research*, vol. 99, p. 12,175-12,190.

Berckhemer, H. and Kowalczyk, G., 1978, Post-Alpine geodynamics of the Peloponnesos, *in* Closs, H., Roeder, D. and Shmidt, K., eds., Alps, Apennines, Hellenides. Geodynamic investigations along geotraverses by an international group of geoscientists: *Inter-Union Commission on Geodynamics Scientific Report*, No. 38, Stuttgart, p. 519-522.

Blanc-Vernet, L., 1969, Contribution a l'étude des formanifères de Méditerranée. Relations entre la microfaune et le amiment. Biocoenoses actuelles, thanatocoenoses pliocènes at quaternaires: *Extrait du Recueil des Travaux de la Station Marine d'Encoume*, vol. 64-48, 281 p.

Bonifay, E., 1975, L' "Ere quaternaire" : definition, limites et subdivision sur la base de la chronologie mediterraneénne: *Bulletin de la Societé géologique de France*, vol. 17, p. 380-393.

Buttler, R.W.H., Grasso, M., and Linkorish, H., 1995, Plio-Quaternary megasequence geometry and its tectonic controls within the Maghrebian thrust belt of south-central Sicily: *Terra Nova*, vol. 7, p. 171-178.

Chaumillon, E. and Mascle, J., 1995, Variation laterale des fonts de deformation de la Ridge mediterraneénne (Méditerraneé oriental): *Bulletin de la Societé géologique de France*, vol. 166, p. 463-478.

Colella, A., 1988, Pliocene-Holocene fan deltas and braid deltas in the Crati Basin, southern Italy: a consequence of varying tectonic conditions *in* Nemec, W., and Steel, R.J., eds., *Fan deltas: Sedimentology and Tectonic Settings*: Blackie, London, p. 50-74.

Collier, R.E.Ll., 1990, Eustatic and tectonic controls upon Quaternary coastal sedimentation in the Corinth Basin, Greece: *Journal of the Geological Society*, London, vol. 147, p. 301-314.

Doutsos, T. and Piper, D., 1990, Listric faulting, sedimentation and morphological evolution of the Quaternary eastern Corinth rift as the initial stage of continental fragmentation behind an island arc (Greece): *Basin Research*, vol. 1, p. 177-190.

Duffaure, J.-J., 1977, Néotectonique et morphogenèse dans une péninsule Méditerranéenne: Le Péloponnèse: *Revue de Géographie Physique et de Géologie Dynamique (2)*, vol. 19, p. 27-58.

Fernandez-Gonzalez, M., Frydas, D. Guernet, D., and Mathieu, R., 1994, Foraminifères et ostracodes du Pliopleistocène de la région de Patras (Grèce). *Intérèt stratigraphique et paléogéographique: Revista Espanola de Micropaleontologia*, vol. 26, p. 89-108.

FitzPatrick, E.A., 1971, Pedology. *A systematic approach to soil science*: Oliver & Boyd, Edinburgh, 306 p.

Flemming, N.C.A., 1968, Holocene earth movements and eustatic sea level change in the Peloponnese: *Nature*, vol. 217, p. 1031-1032.

Flemming, N.C.A., 1978, Holocene eustatic changes and coastal tectonics in the northeast Mediterranean: implications for models of crustal consumption: *Philosophical Transactions of the Royal Society, London*, Series A., vol. 289, p. 405-458.

Fountoulis, I. and Moraiti, E., 1994, Sedimentation, paleogeography, and neotectonic interpretation of post-alpine deposits in the Kyparissia-Kalo Nero Basin: *Bulletin of the Geological Society of Greece*, vol. 30, p. 323-336.

Frydas, D., 1990, Plankton-Stratigraphie des Pliozäns und unteren Pleistozäns der SW-Peloponnes, Griechenland: *Newsletter on Stratigraphy*, vol. 23, p. 91-108.

Frydas, D., and Bellas, S., 1994, Plankton stratigraphy and some remarks on the Globorotalia evolutionary trends from the Plio-Pleistocene sections of southwest Peloponnesus, Greece: *Micropalaeontology*, vol. 40, p. 322 - 336.

Frydas, D. Kontopoulos, N., Stamatopoulos, L., Guernet, C., and Voltaggio, M., 1995, Middle-Late Pleistocene sediments in the northwestern Peloponnessus, Greece. A combined study of biostratigraphical, radiochronological and sedimentological results, *Berliner geowissenschaft Abhandlungen*, vol. 16, p. 589-605.

Fytrolakis, N., 1971, Geologische Untersuchungen im Provinz von Pylias (Messenien - Peloponnes): *Annales Géologiques des Pays Helléniques*, vol. 23, p. 57-122.

Galanopoulos, A.G., 1947. Die Seismitzität von Messenien: *Annales Géologiques des Pays Helléniques*, vol. 1, p. 38-59.

Haq, B.U., Hardenbol, J. and Vail, P.R., 1988, Mesozoic and Cenozoic chronostratigraphy and eustatic cycles, *in* Wilgus, C.K., Hastings, B.S., Kendall, C.G.St.C., Posamentier, H.W., Ross, C.A. and Van Wagoner, J.C., eds., Sea-level changes: an integrated approach: *Society of Economic Paleontologists and Mineralogists, Special Publication*, No. 42, p. 71-108.

Hatzfeld, D., Pedotti, G., Hatzidimitriou, P., and Makropoulos, K., 1990, The strain pattern of the western Hellenic arc as deduced from a microearthquake survey: *Geophysical Journal International*, vol. 101, p. 181-202.

Hatzfeld, D., Pedotti, G., Hatzidimitriou, P., Panagiotopoulos, D., Scordilis, M., Drakopoulos, I., Makropoulos, K., Delibasis, N., Latousakis, I., Baskoutas, J. and Frogneaux, M., 1989, The Hellenic subduction beneath the Peloponnesus: first results from a microearthquake study: *Earth and Planetary Science Letters*, vol. 93, p. 289-291.

I.G.M.E., 1980a, *Filiatra Sheet* (1:50,000), Athens.

I.G.M.E., 1980b, *Koroni-Pylos-Skhiza Sheet* (1:50,000), Athens.

Imbrie, J., 1980, A theretical framework for the Pleistocene ice ages: *Journal of the Geological Society*, London, vol. 142, p. 417-432.

Imbrie, J., Hayes, J.D., Martinson, D.G., MacIntyre, A., Mix, A., Morley, J.J., Pisias, N.G., Prell, W. and Shackleton, N.J., 1984, The orbital theory of the Pleistocene climate: support from a revised chronology of the marine δO16 record, *in* Berger, A., Imbrie, J., Hayes, J.D., Kukla, G. and Saltzman, B., eds, *Milankovitch and Climate*, Hingham, Massachussets, p. 209-305.

Imbrie, J., and Imbrie, J.M., 1980, Modeling the climatic response to orbital variations: *Science*, vol. 207, p. 943-953.

Jacobschagen, V., Richter, D., Makris, J., Bachmann, G.H., Giese, P. and Risch, H., 1978, Alpidic development and structure of the Peloponnesus, *in* Closs, H., Roeder, D., and Schmidt, K., eds., Alps, Apennines, Helenides. Geodynamic investigations along geotraverses by an international group of geoscientists: *Inter-Union Commission on Geodynamics Scientific Report*, No. 38, Stuttgart, p. 415-423.

James, N.P., 1983, Reef Environment, *in* Scholle, P.A., Bebont, D.G., and Moore, C.H., eds, Carbonate Depositional Environments: *American Association of Petroleum Geologists Memoir*, No. 33, p. 345-440.

Kambouroglou, E., 1989, Eretria. Paleogeographic and geomorphologic evolution during the Holocene. Environment and ancient settlements, *PhD thesis*, University of Athens: Municipality of Eretria, 234 p.

Kastens, K.A., Breen, N.A. and Cita, M.B., 1993, Progressive deformation on an evaporite-bearing accretionary complex: SeaMARC 1, SeaBeam, and piston-core observations from the Mediterranean Ridge: *Marine Geophysical Research*, vol. 14, p. 249-298.

Kelletat, D., 1991, The 1550 BP tectonic event in the Eastern Mediterranean as a basis for assessing the intensity of shore processes, *in* Paskoff, R.P., and Kelletat, D., eds., Geomorphology and Geoecology. Coastal dynamics and environments: *Zeitschrift für Geomorphologie, Supplementband*, vol. 81, p. 181-194.

Kelletat, D., Kowalczyk, G., Schroeder, B. and Winter K.-P., 1976, A synoptic view on the neotectonic development of the Peloponnesian coastal regions: *Zeitschrift der Deutschen Geologischen Gesellschaft*, vol. 127, p. 447-465.

Keraudren, B., 1970, Les formations Quaternaires marines de la Grèce. (Première Partie): *Bulletin du Musée d'Anthropologie Préhistorique de Monaco*, vol. 16, p. 4-148.

Keraudren, B., 1971, Les formations Quaternaires marines de la Grèce (Deuxième Partie): Bulletin du *Musée d'Anthropologie Préhistorique de Monaco*, vol. 17, p. 87-169.

Kowalczyk, G., Winter, K.-P., Steinich, G. and Reisch, L., 1992, Jungpleistozäne Strandterrassen in Südost-Lakonien (Peloponnes, Griechenland): *Schriftenreihe für Geowissenschaften*, vol. 1, p. 1-72.

Koutsouveli, A., 1987, Etude stratigraphique des formations pliocènes et pleistocènes en Messenie Occidentale (Peloponnèse, Grèce): *Thése de Doctorate*, Université d' Aix-Marseille II, 162 p.

Kraft, J.C.A., Aschenbrenner, S.E. and Rapp, G., Jr., 1975, Late Holocene paleogeography of the coastal plain of the gulf of Messenia, Greece, and its relationships to archaeological settings and coastal change: *Geological Society of America Bulletin*, vol. 86, p. 1191-1208.

Kumar, N. and Sanders, J.E., 1976, Characteristics of shoreface storm deposits: modern and ancient examples: *Journal of Sedimentary Petrology*, vol. 46, p. 145-172.

Labeyrie, L.D., Duplessy, J.-C. and Blanc, P.L., 1987, Variations in mode of formation and temperature of oceanic deep waters over the past 125,000 years: *Nature*, vol. 327, p. 477-482.

Lambeck, K., 1995, Late Pleistocene and Holocene sea-level change in Greece and south-west Turkey: a separation of eustatic, isostatic, and tectonic contributions: *Geophysical Journal International*, vol. 122, p. 1022-1044.

Le Pichon, X. and Angelier, J., 1979. The Hellenic Arc and Trench system: a key to the neotectonic evolution of the Eastern Mediterranean area: *Tectonophysics*, vol. 60, p. 1-42.

Lyberis, N., Angelier, J., Barrier, E., and Lallemant, S., 1982, Active deformation of a segment of arc: the strait of Kythira, Hellenic arc, Greece: *Journal of Structural Geology*, vol. 4, p. 299-311.

Lyberis, N., and Bizon, G., 1981, Signification structural des 'Iles Strophades dans la Marge Hellénique: *Marine Geology*, vol. 39, p. M57-M69.

Lyon-Caen, H., Armijo, R., Drakopoulos, J., Baskoutas, J., Delibassis, N., Gaulton, R., Kouskouna, V., Latoussakis, J., Makropoulos, K., Papadimitriou, P., Papanastasiou, D. and Pedotti, G., 1988, The 1986 Kalamata (south Peloponnesus) earthquake: detailed study of a normal fault, evidences for East - West extension in the Hellenic Arc: *Journal of Geophysical Research*, vol. 93, p. 14,967-15,000.

Makris, J., 1985, Geophysics and geodynamic implications for the evolution of the Hellenides, in Stanley, D.J., and Wesel, F.-C.A., eds., *Geological Evolution of the Mediterranean Basin. Raimondo Selli Commemorative Volume*: Springer-Verlag, New York, p. 231-248.

Marçopoulou-Diacantoni, A., Mirkou, M.R., Mariolakos, I. and Fountoulis, I., 1991, Stratigraphic and paleoecological observations on the post-alpine sediments at the area of Filiatra (Messenia, Peloponnesus) and their neotectonic explanation: *Bulletin of the Geological Society of Greece*, vol. 25, p. 593-688.

Mariolakos, I., Badekas, I., Fountoulis, I. and Theocharis, D., 1994. Reconstruction of the early Pleistocene paleoshore and pelorelief of the SW Peloponnesos area: *Bulletin of the Geological Society of Greece*, vol. 30/2, p. 297-304.

Martini, M, 1971, Standard Tertiary and Quaternary calcareous nannoplankton zonation: *Proceedings, II Planktonic Conference*, Rome, p. 739-785.

Martinson, D.G., Pisias, N.G., Hays, J.D., Imbrie, J., Moore, T.C., and Shackleton, N.J., 1987, Age dating and the orbital theory of the ice ages: development of a high resolution 0 to 300,000 year chronostratigraphy: *Quaternary Reasearch*, vol. 27, p. 1-29.

Mascle, J., Le Quellec, P., Leite, O., and Jongsma, D., 1982, Structural sketch of the Hellenic continental margin between the western Peloponnesus and eastern Crete: *Geology*, vol. 10, p. 113-116.

Meulenkamp, J.E., van der Zwaan, G.J. and van Wamel, W.A., 1994, On Late Miocene to Recent vertical motions in the Cretan segment of the Helleninc Arc: *Tectonophysics*, vol. 234, p. 53-72.

McKenzie, D., 1978, Active tectonics of the Alpine-Himalayan belt: the Aegean and surrounding regions: *Geophysical Journal of the Royal Astronomical Society*, vol. 55, p. 217-254.

Murray, J.W., 1973, *Distribution and ecology of living benthic Formaniferids*: Heinemann Educational Books, London, 274 p.

Myers, K.J., and Milton, N.J., 1996, Concepts and principles of sequence stratigraphy: in Emery, D., and Myers, K.J., eds., *Sequence Stratigraphy*: Blackewell, Oxford, p. 11-41.

Orton, G.J., and Reading, H.G., 1993, Variability of deltaic processes in terms of sediment supply, with particular emphasis on grain size: *Sedimentology*, vol. 40, p. 475-512.

Pemberton, S.G., MacEachern, J.A., and Frey, R.W., 1992, Trace fossil facies models: Environmental and allostratigraphic significance, in Walker, R.G., and James N.P., eds., *Facies models. Response to sea level change*: Geological Association of Canada, St. John's, Newfoundalnd, p. 47-72.

Perry, C.T., 1997, Biofilm-related calcification and constructive micrite envelopes: a criterion for the recognition of ancient grass-bed environments?: BSRG, 36th *Annual Meeting, Abstract Volume*, p. 83.

Pirazzoli., P.A., 1986, The Early Byzantine tectonic paroxysm: *Zeitschrift für Geomorphologie, Supplementband*, vol. 62, p. 31-49.

Pirazzoli, P., 1987, Sea-level changes in the Mediterranean, *in* Tooley, M.J. and Shennan, I., eds, *Sea-level changes*: The Institute of British Geographers, Special Publications, Series 20: Blackwell, Oxford, p. 152-181.

Plaziat, J.-C., Reyss, J.-L., Choukri, A., Orszag-Sperber, F., Baltzer, F. and Purser, B.H., 1998, Mise en évidence, sur la cτte récifale d'Egypte, d'une régression interrompant brièvement le plus haut niveau du Dernier Interglaciaire (5e): un nouvel indice des variations glacio-eustatiques ὐ haute fréquence au Pléistocène?: *Bulletin de la Societé géologique de France*, vol. 169, p. 115-125.

Poole A. and Robertson, A.H.F., 1991, Quaternary uplift and sea-level

change at an active plate boundary, Cyprus: *Journal of the Geological Society*, London, vol. 148, p. 909-921.

Poole A. and Robertson, A.H.F., 2000, Quaternary marine terraces and aeolianites in coastal South and West Cyprus: implications for regional uplift and sea-level change: this volume.

Postma, G., 1990, Depositional architecture and facies of river and fan deltas: a synthesis, *in* Colella, A., and Prior, D.B., eds., Coarse-grained deltas: *Special Publication, International Association of Sedimentologists*, No.10, p. 13-27.

Reading, H.G. and Collinson, J.D., 1996. Clastic coasts, *in* Reading, H.G., ed., *Sedimentary environments: Processes, facies and stratigraphy*: Blackwell, Oxford, p. 154-231.

Roberts, S. and Jackson, J., 1991, Active normal faulting in central Greece: an overview, *in* Roberts, A.M., Yielding, G. and Freeman, B., eds., The geometry of normal faults: *Geological Society Special Publication*, No.56, p. 125-142.

Robertson, A.H.F. and Kopf, A., 1998, Tectonic setting and processes of mud volcanism on the Mediterranean Ridge accretionary complex: evidence from Leg 160: *in* Robertson, A.H.F., Emeis, K.-C., Richter, C., and Camerlenghi, A., eds., *Proceedings of the Ocean Drilling Program, Scientific Results*, vol. 160, p. 665-680.

Zelilidis, A., 1988, Post-Miocene evolution of the NW. Peloponnese: *unpublished Ph.D thesis*, University of Patras, 282 p.

Zelilidis, A. and Doutsos, T., 1992, An interference pattern of neotectonic faults in the southwestern part of the Hellenic Forearc Basin, Greece: *Zeitschrift der deutschen geologischen Gesselschaft*, vol. 143, p. 95-105.

Zelilidis, A., Kontopoulos, N. and Doutsos, T., 1988, Geosection across the Neogene and Quaternary of the SW Peloponnese: *Bulletin of the Geological Society of Greece*, vol. 20/2, p. 149-166.

A.GLIKOVRISI
HORST B
ANO GLIKOVRISI
B1
E
915
847
A
MOLAI
5.18b
F
C
Molai Fault
D
D1
E1
MOLAI GRABEN
PAKTIA
KOKKINIA
5.8a
5.8b
A1
Mourtitsa R.
C1
5.11b
5.11c
5.11d
5.6
DHIAKOS
Kambourani R.
5.11a
ELEA
F1
AYIOS IOANNIS
Tasou R.
EPIDHAVROS LIMIRA
Stravorrema R.
5.13
ASOPOS
PAPPADHIANIKA
Boza R.
KAMBOS
G1
4.7
5.18a
AYIOS DIMITRIOS
MONEMVASIA
PLITRA
KATSIKOROS
H
ANO KOROGONAS
4.10
Dakali R.
G
5.17
5.8c
5.14a
5.9b
DHAEMONIA H1
5.9a
PSIPHIA
5.16
ARHANGELOS
FLIKA

M2: TECTONIC MAP OF THE EASTERN LAKONIA PENINSULA

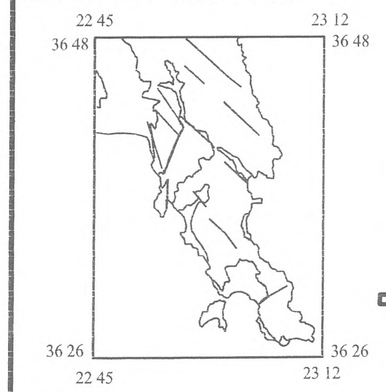

Pleistocene alluvia

Pliocene-Pleistocene shallow marine sediments

Tethyan bedrock

Normal faults
mapped
probable

Logs refered to in text

Sections refered to in text


ANO KOROGONAS
4.10
Dokati R.
5.17
5.8c
5.14a
5.9b
DHAEMONIA H1
5.9a
PSIPHIA
5.16
ARHANGELOS
ELIKA
Sfendilagadho R.
5.14c
MARATHIAS
Platanistos R.
Vathanandrea R.
Houlekares R.
Hiralkas R.
Karsses R.
NEAPOLIS GRABEN
VIGLAPHIA
NEAPOLIS
LAHI
PALIOKASTRO
5.14b
AYIOS NIKOLAOS
LIMNAKIA
5.15
KORAKAS
AYIA MARINA
CAPE MALEAS
PROPHITIS ILIAS
5.10